

**C-H ACTIVATION OF HYDROCARBONS BY TUNGSTEN ALKYLIDENE AND  
RELATED COMPLEXES**

by

**CRAIG S. ADAMS**

B. Sc. (Hons), McMaster University, 1996

A THESIS SUBMITTED IN PARTIAL FULFILLMENT OF  
THE REQUIREMENTS FOR THE DEGREE OF  
DOCTOR OF PHILOSOPHY

in

THE FACULTY OF GRADUATE STUDIES  
(Department of Chemistry)

We accept this thesis as conforming  
to the required standard

THE UNIVERSITY OF BRITISH COLUMBIA

October 2001

© Craig S. Adams, 2001

In presenting this thesis in partial fulfilment of the requirements for an advanced degree at the University of British Columbia, I agree that the Library shall make it freely available for reference and study. I further agree that permission for extensive copying of this thesis for scholarly purposes may be granted by the head of my department or by his or her representatives. It is understood that copying or publication of this thesis for financial gain shall not be allowed without my written permission.

Department of CHEMISTRY

The University of British Columbia  
Vancouver, Canada

Date OCTOBER 3<sup>rd</sup>, 2001

## Abstract

Thermolysis of  $\text{Cp}^*\text{W}(\text{NO})(\text{CH}_2\text{C}_6\text{H}_5)(\text{CH}_2\text{CMe}_3)$  (**2**) in various solvents generates neopentane and benzylidene  $\text{Cp}^*\text{W}(\text{NO})(=\text{CHC}_6\text{H}_5)$  (**B**) in situ. Complex **B** activates the C-H bonds of alkane solvents to yield alkene or allyl hydride complexes, and activates arene solvents to yield aryl or benzyl derivatives. The basic mechanistic features of the formation and reactivity of **B**, and the scope of **B**'s activation chemistry are very similar to those of the previously-studied neopentylidene  $\text{Cp}^*\text{W}(\text{NO})(=\text{CHCMe}_3)$  (**A**) derived from  $\text{Cp}^*\text{W}(\text{NO})(\text{CH}_2\text{CMe}_3)_2$  (**1**). However, the product distributions derived from the activation of substituted arenes by **B** are more abundant in the aryl products over the benzyl products than those obtained from **A** (toluene, *p*-xylene). Likewise, the aryl regioisomer distributions obtained from **B** favour the meta isomer over other isomers, more so than those obtained from **A** ( $\alpha,\alpha,\alpha$ -trifluorotoluene, toluene).

The mechanism of the thermal chemistry of **1** and **2** is re-examined for the possible involvement of hydrocarbon intermediates in the formation of the activation products. The observation of H/D scrambling in  $\text{Cp}^*\text{W}(\text{NO})(\text{CD}_2\text{CMe}_3)_2$  (**1-d<sub>4</sub>**) prior to neopentane elimination indicates that hydrocarbon intermediates do exist on the reaction coordinate. The near-unity values of the KIEs measured for benzene, tetramethylsilane and mesitylene indicate that the key step in the C-H activation of these substrates is coordination to the metal center, rather than substrate C-H bond scission.

An in-depth experimental and theoretical investigation of the activation of toluene reveals that the aryl vs benzyl product distributions are controlled by the relative energetics of substrate coordination in two different fashions to the metal center. In contrast, the aryl regioselectivity is controlled by the relative energies of the aryl products. The product distributions obtained from the activation of other substituted arenes are controlled by these same factors, but with variations that depend on the substrate and the alkylidene complex utilized.

The alkylidene systems can potentially be used to convert alkanes into homoallylic alcohols, via the allyl hydride products of C-H activation. Strategies for developing related Cp'M(NO)-based systems (Cp' = Cp or Cp\*; M = Mo, W) are also described, along with preliminary investigations into the activation chemistry derived from CpMo(NO)(CD<sub>2</sub>CMe<sub>3</sub>)<sub>2</sub> and Cp\*W(NO)(CH<sub>2</sub>CMe<sub>3</sub>)(η<sup>3</sup>-1,1-Me<sub>2</sub>-C<sub>3</sub>H<sub>3</sub>).

**Table of Contents**

Abstract	ii
Table of Contents	iv
List of Tables	xvi
List of Figures	xvii
Abbreviations	xxi
Acknowledgements	xxiii

**CHAPTER 1. Intermolecular C-H Activation of Hydrocarbons by Soluble Metal**

<b>Complexes</b>	<b>1</b>
1.1 Introduction	2
1.1.1 An Overview of Organometallic Chemistry	2
1.1.2 An Overview of Organometallic C-H Activation of Hydrocarbons	3
1.1.3 Types of Organometallic C-H Activation Systems	4
1.1.4 Types of Organometallic Hydrocarbon C-H Activations Mediated by Soluble Metal Complexes	5
1.1.4.1 Hydrocarbon C-H Activation by Oxidative Addition to a Soluble Metal Complex	5
1.1.4.2 Hydrocarbon C-H Activation by M-C $\sigma$ -Bond Metathesis with a Soluble Metal Complex	7
1.1.4.3 Hydrocarbon C-H Activation by Addition to the M=NR Linkages of Soluble Metal Imido Complexes	9

1.1.5 Soluble Metal Complexes that Convert Hydrocarbons Into Functionalized Organic Chemicals	10
1.1.6 A New Mode of Organometallic Hydrocarbon C-H Bond Activation: Addition of R-H to the M=CHR Linkages of Soluble Metal Alkylidene Complexes	13
1.1.7 Alkane and Arene C-H Activation by $\text{Cp}^*\text{W}(\text{NO})(=\text{CHCMe}_3)$ ( <b>A</b> ): The Discovery and Preliminary Investigations	15
1.1.8 Alkane and Arene C-H Activation by $\text{Cp}^*\text{W}(\text{NO})(=\text{CHCMe}_3)$ ( <b>A</b> ): Subsequent Investigations	20
1.1.8.1 Kinetic Studies on, and The Proposed General Mechanism for, C-H Activation Derived from <b>1</b>	20
1.1.8.2 Activation of Alkane Substrates	22
1.1.8.3 Activation of Methyl-Substituted Arene Substrates	22
1.2 Outline of This Thesis	25
1.3 Format of This Thesis	28
1.4 References and Notes	30
<b>CHAPTER 2. Investigations Into The Thermal Chemistry of <math>\text{Cp}^*\text{W}(\text{NO})(\text{CH}_2\text{C}_6\text{H}_5)(\text{CH}_2\text{CMe}_3)</math></b>	<b>37</b>
2.1 Introduction	38
2.2 Results and Discussion	38

2.2.1 Synthesis and Characterization of Complex <b>2</b>	38
2.2.1.1 Synthesis of Complex <b>2</b>	39
2.2.1.2 Properties of Complex <b>2</b>	40
2.2.2 Thermolysis of <b>1</b> in Toluene Revisited	41
2.2.3 Thermolysis of <b>2</b> in Toluene	45
2.2.4 A Note on the Thermolyses Conditions for <b>1</b> and <b>2</b>	45
2.2.5 Trapping of the Reactive Benzylidene Complex	47
2.2.6 Solid-State Molecular Structure of Complex <b>2.4a</b>	48
2.2.7 Comparison of Mechanistic Features of the Neopentylidene and Benzylidene Systems: Thermolysis of Complex <b>2</b> in Benzene and Benzene- <i>d</i> <sub>6</sub>	50
2.2.8 Comparison of Scope of Substrate Activation Mediated by <b>A</b> and <b>B</b> : Thermolysis of <b>2</b> in Alkanes	52
2.2.8.1 Thermolysis of <b>2</b> in Tetramethylsilane and in Cyclohexane/ <i>PM</i> e <sub>3</sub>	52
2.2.8.2 Thermolysis of <b>2</b> in Methylcyclohexane	53
2.2.8.3 Thermolysis of <b>1</b> in Methylcyclohexane Revisited	55
2.2.9 Summary of the Comparisons of the Neopentylidene and Benzylidene Systems Presented Thus Far	56
2.2.10 Thermolysis of <b>2</b> in <i>m</i> -Xylene	57
2.2.11 Thermolysis of <b>2</b> in <i>o</i> - and <i>p</i> -Xylene	59

2.2.12	The Solid-State Molecular Structure of Complex <b>2.12</b>	60
2.2.13	Thermolysis of <b>2</b> in Mesitylene	62
2.2.14	Thermolysis of <b>2</b> in $\alpha,\alpha,\alpha$ -Trifluorotoluene	63
2.2.15	Thermolyses of <b>1</b> in <i>p</i> -Xylene, Mesitylene and $\alpha,\alpha,\alpha$ -Trifluorotoluene Revisited	65
2.2.15.1	Thermolysis of <b>1</b> in <i>p</i> -Xylene	65
2.2.15.2	Thermolysis of <b>1</b> in Mesitylene	67
2.2.15.3	Thermolysis of <b>1</b> in $\alpha,\alpha,\alpha$ -Trifluorotoluene	67
2.2.16	Trends in the Activation of Arenes Substrates	68
2.3	Epilogue	71
2.4	Experimental Procedures	72
2.4.1	General Methods.	72
2.4.2	Reagents	74
2.4.3	NMR assignments	74
2.4.4	Preparation of $\text{Cp}^*\text{W}(\text{NO})(\text{CH}_2\text{C}_6\text{H}_5)(\text{CH}_2\text{CMe}_3)$ ( <b>2</b> )	75
2.4.5	Monitoring the Thermolysis of <b>1</b> in Toluene by $^1\text{H}$ NMR spectroscopy	75
2.4.6	Preparative Thermolyses of <b>2</b> in Hydrocarbon Solvents: General Comments	76
2.4.7	Preparation of $\text{Cp}^*\text{W}(\text{NO})(\text{CH}_2\text{C}_6\text{H}_5)(\text{C}_6\text{H}_4\text{-3-Me})$ ( <b>2.2a</b> ),	

$\text{Cp}^*\text{W}(\text{NO})(\text{CH}_2\text{C}_6\text{H}_5)(\text{C}_6\text{H}_4\text{-4-Me})$ ( <b>2.2b</b> )	77
2.4.8 Preparation of $\text{Cp}^*\text{W}(\text{NO})(=\text{CHC}_6\text{H}_5)(\text{PMe}_3)$ ( <b>2.4a-b</b> )	78
2.4.9 Preparation of $\text{Cp}^*\text{W}(\text{NO})(\text{CH}_2\text{C}_6\text{H}_5)(\text{C}_6\text{H}_5)$ ( <b>2.5</b> ) and $\text{Cp}^*\text{W}(\text{NO})(\text{CHDC}_6\text{H}_5)(\text{C}_6\text{D}_5)$ ( <b>2.5-d<sub>6</sub></b> )	79
2.4.10 Kinetic Studies of the Thermolysis of <b>1</b> and <b>2</b> in Benzene- <i>d</i> <sub>6</sub>	80
2.4.11 Thermolysis of <b>2</b> in Alkanes: General Comments	80
2.4.12 Preparation of $\text{Cp}^*\text{W}(\text{NO})(\text{CH}_2\text{C}_6\text{H}_5)(\text{CH}_2\text{SiMe}_3)$ ( <b>2.6</b> )	81
2.4.13 Preparation of <b>2.4a-b</b> and $\text{Cp}^*\text{W}(\text{NO})(\eta^2\text{-cyclohexene})(\text{PMe}_3)$ ( <b>1.3</b> )	81
2.4.14 Preparation of $\text{Cp}^*\text{W}(\text{NO})(\eta^3\text{-C}_7\text{H}_{11})(\text{H})$ ( <b>1.5</b> and <b>2.7</b> ) from <b>1</b> and <b>2</b>	81
2.4.15 Thermolysis of <b>1</b> and <b>2</b> in Xylenes, Mesitylene and $\alpha,\alpha,\alpha$ - Trifluorotoluene: General Comments	82
2.4.16 Preparation of $\text{Cp}^*\text{W}(\text{NO})(\text{CH}_2\text{C}_6\text{H}_5)(\text{C}_6\text{H}_3\text{-3,5-Me}_2)$ ( <b>2.8</b> ) and $\text{Cp}^*\text{W}(\text{NO})(\text{CH}_2\text{C}_6\text{H}_5)(\text{CH}_2\text{C}_6\text{H}_4\text{-3-Me})$ ( <b>2.9</b> )	83
2.4.17 Independent Preparation of <b>2.9</b> via Metathesis	84
2.4.18 Preparation of $\text{Cp}^*\text{W}(\text{NO})(\text{CH}_2\text{C}_6\text{H}_5)(\text{C}_6\text{H}_3\text{-3,4-Me}_2)$ ( <b>2.10</b> ) and $\text{Cp}^*\text{W}(\text{NO})(\text{CH}_2\text{C}_6\text{H}_5)(\text{CH}_2\text{C}_6\text{H}_4\text{-2-Me})$ ( <b>2.11</b> )	84
2.4.19 Preparation of $\text{Cp}^*\text{W}(\text{NO})(\text{CH}_2\text{C}_6\text{H}_5)(\text{C}_6\text{H}_3\text{-2,5-Me}_2)$ ( <b>2.12</b> ) and $\text{Cp}^*\text{W}(\text{NO})(\text{CH}_2\text{C}_6\text{H}_5)(\text{CH}_2\text{C}_6\text{H}_4\text{-4-Me})$ ( <b>2.13</b> )	85
2.4.20 Preparation of $\text{Cp}^*\text{W}(\text{NO})(\text{CH}_2\text{C}_6\text{H}_5)(\text{CH}_2\text{C}_6\text{H}_3\text{-3,5-Me}_2)$ ( <b>2.14</b> )	86

2.4.21	Preparation of $\text{Cp}^*\text{W}(\text{NO})(\text{CH}_2\text{C}_6\text{H}_5)(\text{C}_6\text{H}_4\text{-3-CF}_3)$ ( <b>2.15a</b> ) and $\text{Cp}^*\text{W}(\text{NO})(\text{CH}_2\text{C}_6\text{H}_5)(\text{C}_6\text{H}_4\text{-4-CF}_3)$ ( <b>2.15b</b> )	87
2.4.22	Thermolysis of <b>1</b> in <i>p</i> -Xylene, Mesitylene and $\alpha,\alpha,\alpha$ -Trifluorotoluene	88
2.4.23	X-ray Diffraction Analyses of <b>2.4a</b> , <b>2.12</b> and <b>2.14</b>	88
2.5	References and Notes	90
<b>CHAPTER 3. Investigations Into The Mechanism of the C-H Bond Activation</b>		
<b>Chemistry Derived from Complexes 1 and 2</b>		<b>96</b>
3.1	Introduction	97
3.2	Results and Discussion	104
3.2.1	Known Strategies For Detecting Hydrocarbon Complexes	104
3.2.2	Thermolysis of <b>1-d<sub>4</sub></b> in Tetramethylsilane: NMR Analysis	104
3.2.3	Thermolysis of <b>1-d<sub>4</sub></b> in Benzene- <i>d</i> <sub>6</sub> : NMR Analysis	106
3.2.4	Thermolysis of <b>1-d<sub>4</sub></b> in Tetramethylsilane and Benzene- <i>d</i> <sub>6</sub> : GC/MS Analysis	107
3.2.5	Spectroscopic Monitoring of the Thermolysis of <b>1-d<sub>4</sub></b> in Benzene	108
3.2.6	Explanation of The Results: Hydrocarbon Complexes are Intermediates on the Reaction Coordinate for Alkylidene Complex Formation	110
3.2.7	An Aside: The True Magnitude of the KIE for $\alpha$ -H Neopentane Elimination for Complex <b>1</b> vs Complex <b>1-d<sub>4</sub></b>	113

3.2.8 Implications of the Existence of Hydrocarbon Complexes on the General Mechanism of C-H Bond Activation by <b>A</b> and <b>B</b>	114
3.2.9 Measurement of Intermolecular KIEs for Activation of Tetramethylsilane, Benzene and Mesitylene	116
3.2.10 The Questionable Intermediacy of the Alkylidene Complexes <b>A</b> and <b>B</b>	120
3.3 Epilogue	123
3.4 Experimental Procedures	124
3.4.1 General Methods	124
3.4.2 Reagents	124
3.4.3 Characterization Data for <b>1-d<sub>4</sub></b>	124
3.4.4 Thermolyses of <b>1-d<sub>4</sub></b> in Tetramethylsilane, Benzene, and Benzene- <i>d</i> <sub>6</sub> : General Comments	124
3.4.5 Preparation of Cp*W(NO)(CH <sub>syn</sub> DCMe <sub>3</sub> )(CH <sub>2</sub> SiMe <sub>3</sub> ) ( <b>3.1-d<sub>1</sub></b> ) and Cp*W(NO)(CH <sub>2</sub> CMe <sub>3-d<sub>x</sub></sub> )(CH <sub>2</sub> SiMe <sub>3</sub> ) ( <b>3.1'-d<sub>x</sub></b> )	125
3.4.6 Preparation of Cp*W(NO)(CD <sub>2</sub> CMe <sub>3</sub> )(Ph- <i>d</i> <sub>5</sub> ) ( <b>3.2-d<sub>7</sub></b> ) and Cp*W(NO)(CHD <sub>syn</sub> CMe <sub>3-d<sub>y</sub></sub> )(Ph- <i>d</i> <sub>5</sub> ) ( <b>3.2'-d<sub>y</sub></b> )	125
3.4.7 Preparation of Cp*W(NO)(CH <sub>syn</sub> DCMe <sub>3</sub> )(Ph- <i>h</i> <sub>5</sub> ) ( <b>3.2-d<sub>1</sub></b> ) and Cp*W(NO)(CH <sub>2</sub> CMe <sub>3-d<sub>x</sub></sub> )(Ph- <i>h</i> <sub>5</sub> ) ( <b>3.2'-d<sub>x</sub></b> )	126
3.4.8 GC/MS Analysis of Organic Volatiles	126

3.4.9 Measurement of Intermolecular KIEs: General Comments	126
3.4.10 Determination of the KIEs for <b>1</b> in Benzene/Benzene- $d_6$ and Tetramethylsilane/Tetramethylsilane- $d_{12}$	127
3.4.11 Determination of the KIE for <b>2</b> in Benzene/Benzene- $d_6$	127
3.4.12 Determination of the KIE for <b>2</b> in Mesitylene/Mesitylene- $d_{12}$	128
3.5 References and Notes	129
<b>CHAPTER 4. Rationalizing the C-H Activation Chemistry Derived From Complexes 1 and 2</b>	<b>135</b>
4.1 Introduction	136
4.2 Results and Discussion	136
4.2.1 Case 1: Activation of Toluene	136
4.2.1.1 The Nature of the Product Distributions	137
4.2.1.2 The Mechanism of Aryl Product Regioisomerization	141
4.2.1.3 The Nature of The Arene Complex in Aryl Ligand Isomerizations	144
4.2.1.4 Aryl Regioisomerizations in Benzyl Aryl Complexes	146
4.2.1.5 The Nature of the Aryl vs Benzyl Product Distributions Revisited.	147
4.2.1.6 Theoretical Investigations into Toluene Activation by CpW(NO)(=CH <sub>2</sub> )	151

4.2.1.6.1 Benzyl and Aryl Products of Toluene C-H Activation	151
4.2.1.6.2 Intermediate Hydrocarbon Complexes	152
4.2.1.6.3 Transition States for Benzyl and Aryl C-H bond Cleavage.	154
4.2.1.6.4 The Theoretical Reaction Coordinate For Toluene Activation	156
4.2.1.7 Explanation of the Product Selectivities For Benzylidene- and Neopentylidene-Mediated Activations of Toluene	160
4.2.2 Case 2. C-H Activation of Xylenes	161
4.2.2.1 The Nature of the Product Distributions	163
4.2.2.2 Interpretation of Aryl vs Benzyl Product Selectivity	165
4.2.2.3 Rationalizing The Differences between Aryl vs Benzyl Product Distributions Derived From <b>A</b> and <b>B</b>	167
4.2.3 Case 3. C-H Activation of Mesitylene	167
4.2.4 Case 4. Activation of $\alpha,\alpha,\alpha$ -Trifluorotoluene By <b>A</b>	169
4.2.4.1.1. The Nature of the Product Distribution	169
4.2.4.1.2. The Origin of Meta vs Para Aryl Product Selectivity	170
4.2.5 Case 5: Activation of $\alpha,\alpha,\alpha$ -Trifluorotoluene By <b>B</b>	171
4.2.5.1.1 Nature of Product Distribution	172
4.2.5.1.2 Interpretation of Product Selectivity	173

4.3	Epilogue	174
4.4	Experimental Procedures	177
4.4.1	General	177
4.4.2	Reagents	177
4.4.3	Preparation of Cp*W(NO)(CH <sub>2</sub> C <sub>6</sub> H <sub>5</sub> )(C <sub>6</sub> H <sub>4</sub> -2-Me) ( <b>2.2c</b> )	178
4.4.4	Kinetic Studies of the Isomerization of <b>2.1c</b> and <b>2.2c</b>	178
4.4.5	Preparation of Cp*W(NO)(CH <sub>2</sub> CMe <sub>3</sub> )(C <sub>6</sub> D <sub>5</sub> ) ( <b>4.1-d<sub>5</sub></b> )	179
4.4.6	Preparation of Cp*W(NO)(CH <sub>2</sub> C <sub>6</sub> H <sub>5</sub> )(C <sub>6</sub> D <sub>5</sub> ) ( <b>4.2-d<sub>5</sub></b> )	179
4.4.7	Thermolysis of Complexes <b>4.1-d<sub>5</sub></b> and <b>4.2-d<sub>5</sub></b>	180
4.4.8	Theoretical Calculations using the DFT approach	181
4.4.9	Thermolysis of Complexes <b>1.7</b> , <b>2.8</b> , <b>2.9</b> and <b>2.12</b>	181
4.4.10	Kinetic Studies of the Isomerizations of <b>2.15a-b</b> and <b>2.17a-b</b>	182
4.5	References and Notes	183
<b>CHAPTER 5. Towards the Development of Alkylidene and Related Complexes as Reagents for The Conversion of Alkanes Into Functionalized Chemicals</b>		<b>187</b>
5.1	Introduction	188
5.2	Results and Discussion	191
5.2.1	The Conversion of Allyl Ligands into Functionalized Organic Compounds	191

5.2.2 Proposed Method for the Conversion of Acyclic Alkanes and Alkyl-Substituted Cycloalkanes Into Homoallylic Alcohols Via Alkylidene-Mediated C-H Activation	193
5.2.3 The Utilization of Other Alkylidene Complexes of the Type $\text{Cp}'\text{M}(\text{NO})(=\text{CHR})$ for Alkane Activations and Functionalizations	195
5.2.3.1 The C-H Activation of Hydrocarbons by $\text{CpMo}(\text{=CHCMe}_3)$	196
5.2.3.2 Towards the Use of CpMo Alkylidene Complexes and Other $\text{Cp}'\text{M}(\text{NO})(=\text{CHR})$ Complexes for Alkane C-H Activation and Functionalization Reactions	202
5.2.4 Alternatives to $\text{Cp}'\text{M}(\text{NO})$ Alkylidene-Based C-H Activation and Functionalization of Alkanes	205
5.2.5 Towards Alkane Functionalizations Using Complexes <b>1.1</b> , <b>5.8</b> and <b>5.9</b>	209
5.3 Epilogue	211
5.4 Experimental Procedures	212
5.4.1 General Methods	212
5.4.2 Reagents	212
5.4.3 Preparation of $\text{CpMo}(\text{NO})(\text{CHD}_{\text{anti}}\text{CMe}_3)(\text{CH}_2\text{C}_6\text{H}_3\text{-3,5-Me}_2)(\mathbf{5.4-d}_1)$	212
5.4.4 Thermolysis of $\text{Cp}^*\text{W}(\text{NO})(\text{CH}_2\text{CMe}_3)(\text{CH}_2\text{SiMe}_3)$ ( <b>1.4</b> ) in Tetramethylsilane	213

5.4.5 Synthesis of $(1,1\text{-Me}_2\text{-C}_3\text{H}_3)_2\text{Mg}\cdot x(\text{dioxane})$	213
5.4.6 Synthesis of $\text{Cp}^*\text{W}(\text{NO})(\text{CH}_2\text{CMe}_3)(\eta^3\text{-}1,1\text{-Me}_2\text{-C}_3\text{H}_3)$ ( <b>5.9</b> )	214
5.4.7 Preparation of $\text{Cp}^*\text{W}(\text{NO})(\text{C}_6\text{H}_5)(\eta^3\text{-}1,1\text{-Me}_2\text{-C}_3\text{H}_3)$ ( <b>5.10</b> )	216
5.4.8 Thermolysis of <b>5.9</b> in Benzene- $d_6$ : Kinetic Studies and the Preparation of $\text{Cp}^*\text{W}(\text{NO})(\text{C}_6\text{D}_5)(\eta^3\text{-}1,1\text{-Me}_2\text{-allyl-}d_1)$ ( <b>5.10-<math>d_6</math></b> )	216
5.4.9 X-ray Diffraction Analysis of <b>5.10</b>	217
5.5 References and Notes	218
<b>Appendix A. Tables of Bond Distances, Angles and Fractional Atomic Coordinates for the Structurally Characterized Complexes Described in this Thesis</b>	<b>226</b>
<b>Appendix B. Plots of Kinetic Data and Corresponding Regression Analyses for the Systems Studied Kinetically in this Thesis</b>	<b>244</b>
<b>Appendix C. Optimized Geometries, Z-Matrices and Energies Calculated by DFT Methods for Toluene Activation by Methylidene C</b>	<b>250</b>

## List of Tables

<b>Table 2.1.</b> Relative Aryl vs Benzyl Product Distributions Obtained from the Thermolysis of <b>1</b> and <b>2</b> in Methyl-Substituted Arene Solvents	69
<b>Table 2.2.</b> Relative Distributions of Meta and Para Aryl Regioisomers from the Thermolyses of <b>1</b> and <b>2</b> in Toluene and $\alpha,\alpha,\alpha$ -Trifluorotoluene	69
<b>Table 3.1.</b> Average Relative Intensities of Mass Spectral Peaks Derived From Neopentane	108
<b>Table 3.2.</b> Calculated Distributions of Neopentane Isotopomers Generated During the Thermolyses of <b>1-d<sub>4</sub></b>	108
<b>Table 3.3.</b> Product Ratios for Activation of Protio vs Deuterio Substrates by <b>A</b> and <b>B</b>	118
<b>Table 4.1.</b> Calculated Energies for the Aryl and Benzyl Products of C-H Bond Activation by <b>C</b>	157
<b>Table 4.2.</b> Calculated Energies for the Optimized Hydrocarbon Intermediates from Coordination of Toluene to Alkylidene Fragment <b>C</b>	157
<b>Table 4.3.</b> Calculated Energies for the Transition States Corresponding to Aryl and Benzyl Product Formation	158

## List of Figures

- Figure 1.1.** Two different views of the stereochemistry about the methylene linkages of **1.4** as determined from the conformation exhibited in its solid-state molecular structure. 19
- Figure 2.1.** Qualitative diagram of the metal-based LUMO (top), and the  $\eta^2$ -benzyl and  $\eta^1$ -benzyl/ $\alpha$ -agostic conformations (bottom), of **2**. 41
- Figure 2.2.** ORTEP plot of the solid-state molecular structure  $\text{Cp}^*\text{W}(\text{NO})(=\text{CHC}_6\text{H}_5)(\text{PMe}_3)$  (**2.4a**) with 50% probability ellipsoids. 49
- Figure 2.3.** ORTEP plot of the solid-state molecular structure of  $\text{Cp}^*\text{W}(\text{NO})(\text{CH}_2\text{C}_6\text{H}_5)(\text{C}_6\text{H}_3\text{-2,5-Me}_2)$  (**2.12**) with 50% probability ellipsoids. 61
- Figure 2.4.** ORTEP plot of the solid-state molecular structure of  $\text{Cp}^*\text{W}(\text{NO})(\text{CH}_2\text{C}_6\text{H}_5)(\text{CH}_2\text{C}_6\text{H}_3\text{-3,5-Me}_2)$  (**2.14**) with 50% probability ellipsoids. 64
- Figure 3.1.** Qualitative free energy vs reaction coordinate diagram of the purported abstraction mechanism for the C-H activation chemistry derived from the amido complexes of Ti and Zr. 98
- Figure 3.2.** Qualitative depiction of the origin of product selectivity for the activation of toluene by the imido complexes of Ti and Zr under conditions of thermodynamic control. 99
- Figure 3.3.** Qualitative depiction of the origin of product selectivity for the activation of toluene by the imido complexes of Ti and Zr under conditions of kinetic control. 100

- Figure 3.4.** A qualitative representation of the free energy vs reaction coordinate diagram for the proposed abstraction mechanism for substrate C-H activation derived from **1** and **2**. 101
- Figure 3.5.**  $^2\text{H}\{^1\text{H}\}(\text{C}_6\text{H}_6)$  NMR spectra from the thermolysis of **1-d<sub>4</sub>** in benzene-*h*<sub>6</sub> over 90 h at 70 °C (the asterisk denotes the solvent peak). 109
- Figure 3.6.** A possible qualitative free energy vs reaction coordinate diagram for the activation chemistry of **1** and **2** with C-H bond scission as the rate-limiting step, using the activation of an alkane substrate (R-H) via complex **1** as an illustrative example. 115
- Figure 3.7.** The proposed qualitative free energy vs reaction coordinate diagram for the activation chemistry derived from **1** and **2**, using the activation of an alkane substrate (R-H) via complex **1** as an illustrative example. 119
- Figure 3.8.** The alternative qualitative free energy vs reaction coordinate diagram with interchange-dissociation of neopentane as the rate-limiting step in the substrate activation process, using the activation of an alkane substrate (R-H) via complex **1** as an illustrative example. 121
- Figure 4.1.** Plot of conversion of **4.1-d<sub>5</sub>** to **4.1'-d<sub>5</sub>** vs time for the approach to equilibrium at 70°C (■ = **4.1-d<sub>5</sub>**, ▲ = **4.1'-d<sub>5</sub>**). 143
- Figure 4.2.** A qualitative depiction of the free energy vs reaction coordinate diagram for the activation of toluene, using intermediate **A** as the reactive alkylidene species. 149
- Figure 4.3.** A qualitative depiction of the free energy vs reaction coordinate diagram for the activation of toluene, using  $\sigma$ -**A** as the reactive alkylidene species. 150

- Figure 4.4.** Optimized geometries of (a) the benzyl product derived from  $sp^3$  C-H bond activation of toluene, and (b) the para aryl product derived from  $sp^2$  C-H bond activation of toluene. 152
- Figure 4.5.** Optimized geometries and selected bond distances (Å) and angles (°) of, (a) the hydrocarbon intermediate **D**, (b) the representative (meta, anti) intermediates **E**, and (c) the para intermediate **E'**. 155
- Figure 4.6.** Optimized geometries of the transition states for (a)  $sp^3$  C-H bond activation, and (b) para  $sp^2$  C-H bond activation. 156
- Figure 4.7.** Free-energy profiles of the intermediates, transition states and products of toluene activation by methylidene **C** as determined by DFT calculations. 159
- Figure 4.8.** A qualitative representation of the free energy vs reaction coordinate diagram for the activation of xylenes by **A** and **B**, using **A** and *p*-xylene as an illustrative example. 166
- Figure 4.9.** A qualitative representation of the free energy vs reaction coordinate diagram for the activation of mesitylene by **A** and **B**, using **A** as an illustrative example. 168
- Figure 4.10.** Plot of conversion of **2.17a** to **2.17b** vs time for the approach to equilibrium at 70°C (■ = **2.17a**, ▲ = **2.17b**). 170
- Figure 4.11.** A qualitative representation of the free energy vs reaction coordinate diagram the activation of  $\alpha,\alpha,\alpha$ -trifluorotoluene by **A**. 171
- Figure 4.12.** A qualitative representation of the free energy vs reaction coordinate

diagram for the activation of  $\alpha,\alpha,\alpha$ -trifluorotoluene by **B**.

174

**Figure 5.1.** A qualitative representation of the general free energy vs reaction coordinate for alkane C-H activation derived from **5.1**.

201

**Figure 5.2.** ORTEP plot of the solid-state molecular structure of  $\text{Cp}^*\text{W}(\text{NO})(\text{C}_6\text{H}_5)(1,1\text{-Me}_2\text{-C}_3\text{H}_3)$  (**5.10**) with 50% probability ellipsoids.

208

## List of Abbreviations

The following abbreviations are employed in this Thesis.

°	degree (of angle or temperature)	Cp*	$\eta^5$ -C <sub>5</sub> Me <sub>5</sub> , pentamethyl Cp
$\alpha$	the position once removed from a reference point (i.e. a metal center)	Cp'	Cp or Cp*
A(t)	absorbance at time t	$\delta$	chemical shift in ppm
A(0)	initial absorbance	d	doublet or day(s)
Å	angstrom, 10 <sup>-10</sup> m	D, <i>d</i>	<sup>2</sup> H, deuterium, deuteron
anal	analysis	DFT	density-functional theory
Ar	aryl ligand	$\Delta$	heat, or a difference in two states
atm	atmosphere(s)	EI	electron impact
$\beta$	the position twice removed from from a reference point	$\eta$	hapto, denotes ligand hapticity
br	broad (spectral)	Et <sub>2</sub> O	diethyl ether
<sup>t</sup> Bu	tert-butyl	<sup>19</sup> F	fluorine-19
Bzl	benzyl, CH <sub>2</sub> C <sub>6</sub> H <sub>5</sub>	g	gram(s)
°C	degrees Celsius	<i>G</i>	Gibb's free energy
<sup>13</sup> C	carbon-13	$\gamma$	the position thrice removed from a reference point
<sup>13</sup> C{ <sup>1</sup> H}	proton-decoupled <sup>13</sup> C	h	hours(s)
cal	calorie	<sup>1</sup> H	hydrogen, proton
calcd	calculated	<i>H</i>	enthalpy
cm <sup>-1</sup>	wavenumbers	HMQC	heteronuclear multiple quantum coherence
COSY	correlation spectroscopy	<i>h</i> $\nu$	irradiation
Cp	$\eta^5$ -C <sub>5</sub> H <sub>5</sub> , cyclopentadienyl	Hz	hertz (s <sup>-1</sup> )

IR	infrared	$\nu$	stretching frequency
$J$	coupling constant	$o$	ortho
${}^nJ_{AB}$	n-bond J between atoms A and B	ORTEP	Oak Ridge Thermal Ellipsoid Program
$k_n$	rate constant for the nth elementary step	Oxl	2-Me-benzyl, $\text{CH}_2\text{C}_6\text{H}_4$ -2-Me
$k_{\text{obs}}$	observed rate constant	${}^{31}\text{P}$	phosphorus-31
K	degree Kelvin	$\text{P}^+$	parent molecular ion
$K_{\text{eq}}$	equilibrium constant	$p$	para
KIE	kinetic isotope effect	Ph	phenyl, $\text{C}_6\text{H}_5$
L	ligand or litre	ppm	parts per million
LUMO	lowest unoccupied molecular orbital	Pxl	4-Me-benzyl, $\text{CH}_2\text{C}_6\text{H}_4$ -4-Me
m	multiplet	q	quartet
$m$	meta	R	hydrocarbyl ligand
$m/z$	mass-to-charge ratio	$R^2, R1$	residuals (statistics)
Me	methyl, $\text{CH}_3$	s	singlet, strong (spectral) or second(s)
Mes	mesityl, $\text{CH}_2\text{C}_6\text{H}_3$ -2,5-Me <sub>2</sub>	t	triplet or time (s)
mg	milligram(s)	$t_{1/2}$	half-life
mL	millilitre(s)	T	temperature
mmol	millimole(s)	THF	tetrahydrofuran
mol	mole	TMS	trimethylsilyl, $\text{SiMe}_3$
MS	mass spectrum	Tol	tolyl, $\text{C}_6\text{H}_4$ -CX <sub>3</sub> (X=H, F)
Mxl	3-Me-benzyl, $\text{CH}_2\text{C}_6\text{H}_4$ -3-Me	UV-vis	ultraviolet-visible
NMR	nuclear magnetic resonance	VT	variable temperature
NOE	nuclear Overhauser effect	w	weak (spectral)
Npt	neopentyl, $\text{CH}_2\text{CMe}_3$	Xyl	dimethyl aryl ligand, $\text{C}_6\text{H}_3$ -Me <sub>2</sub>

## Acknowledgements

Several individuals deserve recognition for their contributions to the successful completion of the research described in this Thesis. First and foremost, my thanks go to Peter Legzdins for his continual guidance, support, and wisdom, and for the occasional reminders about the important things in life. Many thanks to past members of the Legzdins research group, including Eric “Dancing” Janciu for helping me stay sane and crazy at the same time, Steve McNeil for the mentorship and for letting me hijack his brain repeatedly and not minding, Brett Sharp for his sharp wit that kept us all loose, Sean Lumb and Jamie Daff for their help, Canadian- and British-style, Rob Poe, Elizabeth Tran, and Kevin Smith for his endless ideas, advice and enthusiasm. Many thanks to the current group members for their good humour and lab camaraderie: Stephen Ng, Sonya Cohen, Bryan Chan and Dr. Kenji Wada, and especially Trevor “Tasty T” Hayton for being Mr. Dependable and for broadening my musical and linguistical horizons.

Marietta Austria, Liane Darge, and Nick Burlinson deserve recognition for their invaluable assistance in helping me record some of the the NMR data presented in this Thesis. Likewise, I thank Brian Patrick for the solid-state X-ray crystallographic determinations, and Marshall Lapawa for recording mass spectral data presented in this Thesis. Many thanks to Peter Borda for his diligence and excellence in conducting the elemental analyses. Thanks also to Steve Rak, Brian Ditchburn, Zoltan Germann, Ron Marwick, Jason Gozjolko, and the rest of the UBC Chemistry Mechanical and Electronic Services Departments for their skills and help over the years. Finally, Dr. Fryzuk and Dr.

Storr deserve my thanks for their aid in revising this Thesis.

Thanks go to Carrie Rogers, Sam Johnson, Emily Crowe and all the other friends that I have shared time with in Vancouver.

Anne and Dave Adams for giving me a great start in this world and for the support and pick-me-ups when I needed them.

Scott Adams for being a hunky brother and for the friendship and outdoor adventures.

Dave and Leigh Dobson for their endless energy, for taking an interest, and for bringin' up the next one....

Last but definitely not least, to my wife, Heather. What can I say without filling endless pages, except for "Keep on snorkeling".

To life, in all its shapes and colours.....

## CHAPTER 1

# Intermolecular C-H Activation of Hydrocarbons by Soluble Metal Complexes

---

<b>1.1</b>	<b>Introduction .....</b>	<b>2</b>
<b>1.2</b>	<b>The Outline of This Thesis .....</b>	<b>25</b>
<b>1.3</b>	<b>Format of This Thesis.....</b>	<b>28</b>
<b>1.4</b>	<b>References and Notes.....</b>	<b>30</b>

---

## 1.1 Introduction

This Thesis deals exclusively with the organometallic C-H activation chemistry exhibited by a specific type of metal complex. Consequently, it is pertinent to begin with brief overviews of organometallic chemistry and the field of organometallic C-H activation research.

### 1.1.1 An Overview of Organometallic Chemistry<sup>1,2</sup>

Organometallic chemistry, as the name suggests, bridges the gap between organic and inorganic chemistry. A compound is traditionally classified as organometallic if it contains both a metal component and an organic component, and if it has at least one metal-carbon bond within it. Organometallic compounds can be grouped in three broad classes according to the Periodic Table of Elements: the main-group organometallics (s-block and p-block metals, as well as Group 12 d-block metals), the transition-metal organometallics (Groups 3-11 of the d-block) and the lanthanide and actinide organometallics (f-block).

There are many fields of organometallic chemical research, ranging from those concerned with the fundamentals aspects of bonding interactions between metal atoms and ions, to applications in biochemistry and materials science.<sup>1</sup> However, the largest and most general field of organometallic chemical research concerns the activation and transformation of small molecules.<sup>1</sup> Perhaps the most prominent small-molecule transformation involving organometallic complexes is the polymerization of terminal alkenes, such as ethene and propene.<sup>3</sup> The resulting polyolefin products are subsequently

shaped and molded into common plastic items like grocery bags, milk jugs, and automotive parts.

### 1.1.2 An Overview of Organometallic C-H Activation of Hydrocarbons

Another small molecule transformation involving organometallic complexes is the so-called “organometallic” C-H activation of hydrocarbons.<sup>4,5</sup> The transformation specifically involves the cleavage of a carbon-hydrogen (C-H) bond of a hydrocarbon substrate by a metal or metal-containing species to yield an organometallic product.<sup>6</sup> The significance of this chemistry is made apparent by the following facts:

1. Hydrocarbon C-H bonds are generally difficult to break due to the high bond strengths, low bond polarity, and low acidity and basicity.<sup>7</sup> For example, saturated hydrocarbons, or alkanes, have traditionally been considered to be chemically inert, since the C-H bonds of alkanes do not react with other common organic reagents unless under specific, and usually forcing, conditions.<sup>4</sup> For instance, temperatures of  $>900$  °C are required before aliphatic C-H bonds spontaneously cleave to form radicals that can be converted into other chemicals.
2. Metal atoms and ions can readily cleave the C-H bonds of alkanes, and other hydrocarbon substrates such as arenes, to form organometallic products. These reactions usually occur under moderate to mild conditions, sometimes even at temperatures well below 0 °C.<sup>8</sup> In addition, the regioselectivities of the C-H bond activations are opposite to those obtained from radical-based activation methods (i.e. the general reactivity trend is  $1^\circ > 2^\circ \gg 3^\circ$   $sp^3$  C-H bonds for alkanes, and aromatic  $sp^2 >$  benzylic  $sp^3$  C-H bonds for toluene).<sup>7</sup>

3. Hydrocarbons are the primary feedstocks of the chemical industry. However, few methods exist for the conversion of the most abundant hydrocarbons, the alkanes, into more useful organic chemicals with high chemoselectivity (i.e. only one type of product is formed).<sup>7,9,10</sup>
4. The formation of an organometallic compound via the C-H bond activation of a hydrocarbon can be viewed as the first step in the conversion of the hydrocarbon into a functionalized organic molecule. Given the unique regioselectivities exhibited during the activation, metal-based systems that can selectively form an organometallic derivative by alkane C-H activation may provide new routes for the conversion of alkanes into other organic chemicals.

For these reasons, the discovery and development of metal-based systems that can mediate the organometallic C-H activation of hydrocarbon substrates continue to be pursued.

### **1.1.3 Types of Organometallic C-H Activation Systems**

Several types of metal-based systems are known to effect organometallic hydrocarbon C-H activations, including those that feature metal atoms in the gas phase, those that feature metal atoms on the surfaces of solids, and those that feature metal atoms that are part of inorganic or organometallic complexes that are soluble in organic solvents including hydrocarbons. The latter type of metal-based systems is particularly amenable to detailed investigations of the activation chemistry, and consequently, a great deal has been learned about hydrocarbon C-H activations mediated by these types of complexes. In addition, certain soluble metal complexes have been developed to effect

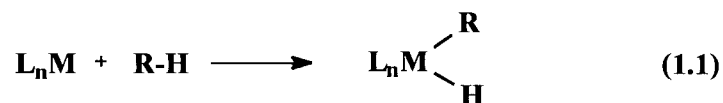
the conversion of alkane substrates into other functionalized chemicals. Details of these matters are provided in the following two sections.

#### 1.1.4 Types of Organometallic Hydrocarbon C-H Activations Mediated by Soluble Metal Complexes

Soluble metal complexes typically activate hydrocarbons by one of three modes of C-H bond scission: oxidative addition, M-C  $\sigma$ -bond metathesis or M=NR addition.<sup>7</sup> The general characteristics of these modes are described below, along with pertinent details of the activation chemistry of representative systems within each class.

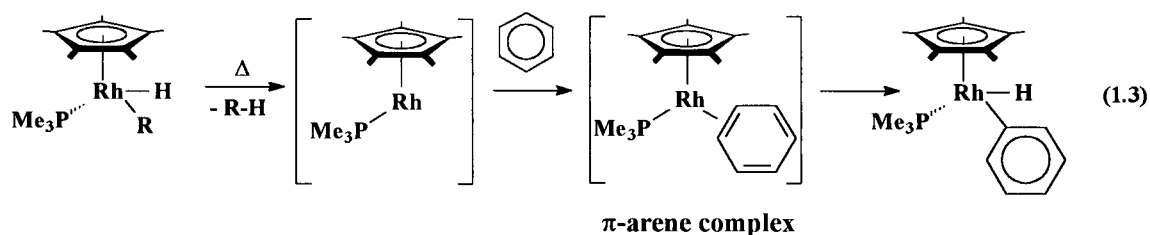
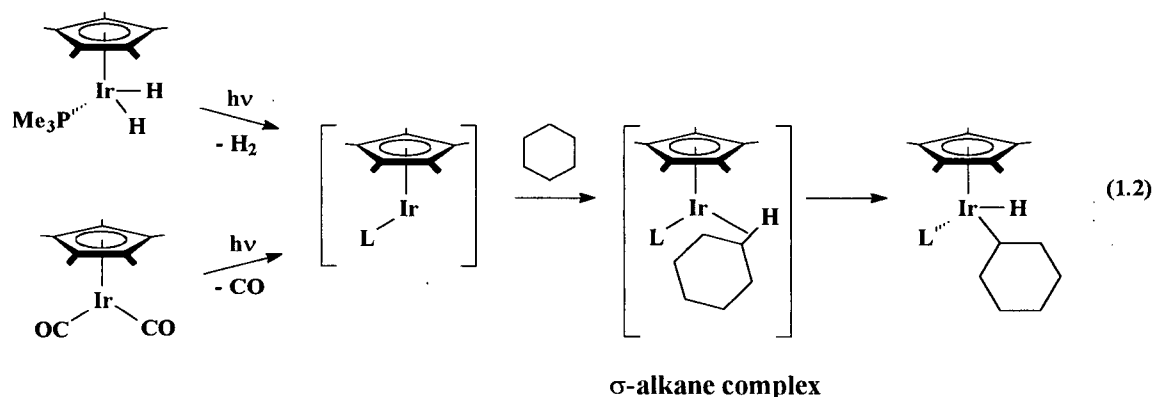
##### 1.1.4.1 Hydrocarbon C-H Activation by Oxidative Addition to a Soluble Metal Complex

Oxidative addition was the first mode of organometallic C-H activation to be identified.<sup>11</sup> The general transformation involves the reaction of an unsaturated metal fragment ( $L_nM$ ) with a molecule of the hydrocarbon solvent (R-H) to generate an organometallic product in which the metal atom has been inserted into one of the C-H bonds of the substrate (eq 1.1). It is called oxidative addition due to the fact that the reaction increases the formal oxidation state at the metal center by two. The metal center in the reactive fragment must contain d-electrons, which typically means that oxidative addition is limited to low-valent mid- to -late transition metals.



Numerous soluble metal complexes are known to activate hydrocarbons by this mechanism, including those containing Ir,<sup>12,13,14</sup> Rh,<sup>15,16,17</sup> Pt,<sup>10,18</sup> Fe,<sup>19</sup> Re,<sup>20</sup> Os,<sup>21</sup> and

W<sup>22,23</sup> metal centers. The most prominent and well-studied oxidative addition systems are those containing the Cp\*M(L) (Cp\* =  $\eta^5\text{-C}_5\text{Me}_5$ ; M = Ir, Rh) reactive fragment (eqs 1.2 and 1.3).<sup>12,13,15</sup> The C-H activation chemistry was first discovered for Cp\*Ir complexes by Graham (L = CO) and Bergman (L = PMe<sub>3</sub>) in 1982,<sup>12</sup> but has been expanded to include a variety of related species.



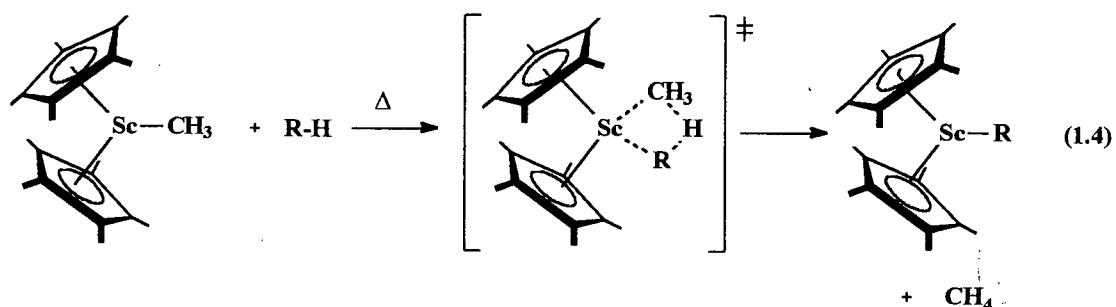
Oxidative addition C-H activation reactions are usually not direct processes, as depicted in eq 1.1. Rather, these transformations can involve intermediate hydrocarbon complexes, namely  $\sigma$ -alkane complexes in the case of alkanes (eq 1.2), and  $\pi$ -arene complexes in the case of arenes (eq 1.3). When more than one type of C-H bond is present within a hydrocarbon substrate, the reactions typically generate the organometallic products associated with the activation of the stronger and/or most accessible bond within the molecule (i.e.  $1^\circ > 2^\circ \gg 3^\circ$   $\text{sp}^3$  C-H bonds for alkane substrates; aromatic  $\text{sp}^2 >$  benzylic  $\text{sp}^3$ , and meta, para  $>$  ortho aromatic  $\text{sp}^2$  C-H bonds

for toluene). However, the relative magnitudes and the factors responsible for these product selectivities depend on the metal fragment employed and the reaction conditions. For example, the  $\text{Cp}^*\text{Ir}(\text{PMe}_3)$  system is less selective than the corresponding Rh system when activating the same substrate under similar conditions.<sup>17</sup> When the  $\text{Cp}^*\text{Ir}(\text{PMe}_3)$  reactive fragment is generated in hydrocarbon solvents at low temperatures (i.e.  $< -45$  °C) by photolysis of the dihydride precursor, the C-H activation process is effectively irreversible and the formation of the activation products is under kinetic control.<sup>11</sup> Since the rate-determining step in the two-step activation process is the formation of the hydrocarbon complex intermediates, the relative product distribution is determined by the relative rates of substrate coordination to the metal center. In contrast, when the reactive fragment is generated thermally, or photochemically at higher temperatures, C-H activation becomes reversible and product equilibration occurs with sufficient reaction time. The observed product distribution in this case is formed under thermodynamic control and is dependent upon the relative thermodynamic energies of the organometallic products themselves.

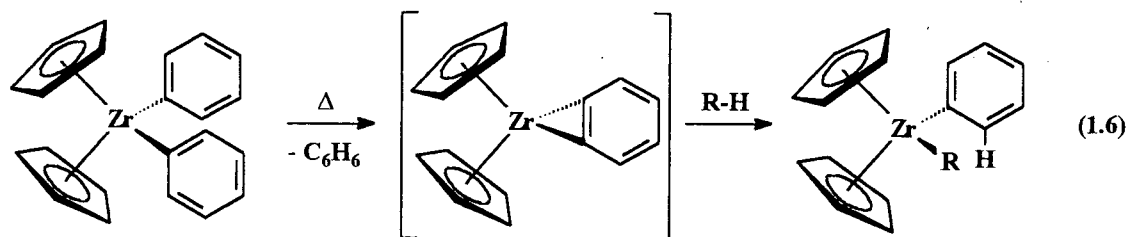
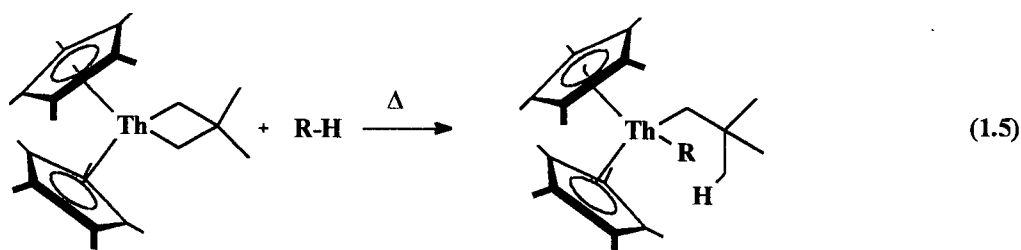
#### 1.1.4.2 Hydrocarbon C-H Activation by M-C $\sigma$ -Bond Metathesis with a Soluble Metal Complex

The second type of intermolecular hydrocarbon C-H activation mediated by soluble metal complexes is known as  $\sigma$ -bond metathesis. The reaction still results in the formation of a metal-carbon bond, but the H atom of the hydrocarbon substrate ends up on a ligand-based carbon acceptor atom rather than the metal center. One class of reagents in this category is the  $\text{Cp}^*_2\text{M}(\text{R}')$  complexes, such as the scandocene complex in eq 1.4.<sup>24</sup> Direct attack on R-H by the complex via a four-centered transition state results

in "metathesis" of the M-C bonds. Similar reactivity has been observed for the yttrium<sup>25</sup> and lutetium<sup>26</sup> analogues.



A related set of complexes involves those that effect C-H activation by  $\sigma$ -bond metathesis at a hydrocarbyl ligand that is attached to the metal center through more than one M-C bond, such as a metallacyclic ligand (eq 1.5)<sup>27</sup>, a benzyne ligand (eq 1.6)<sup>28</sup>, or an  $\eta^2$ -alkyne ligand.<sup>29</sup> In these cases, the acceptor carbon remains within the complex once the C-H bond is cleaved.

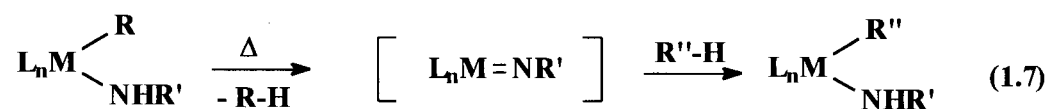


In the systems in eqs 1.4-1.6, the products generally form according to the same general trend as observed for oxidative addition reactions (e.g aryl > benzyl products for

toluene,  $1^\circ > 2^\circ$  alkyls for alkanes). Intermediate hydrocarbon complexes may be also present in some of these systems, given the changes in some product distributions on longer reaction times,<sup>24,28</sup> and given the results of substrate labeling experiments.<sup>29</sup> However, unlike the  $\text{Cp}^*\text{Ir}(\text{PMe}_3)(\text{H})_2$  oxidative addition system, the initial product distributions are controlled by rate-determining C-H bond scission. Thus, the principle factors that govern the product selectivities in these systems are the strength and/or the s-character of the C-H bonds (i.e.  $\text{sp}^2 > \text{sp}^3$ ), and steric interactions in the four-centered metathesis transition state.

#### 1.1.4.3 Hydrocarbon C-H Activation by Addition to the $\text{M}=\text{NR}$ Linkages of Soluble Metal Imido Complexes

Transient, thermally-generated transition-metal imido complexes are also capable of activating C-H bonds. As shown in equation 1.7, the overall reaction is similar to those in eqs 1.4-1.6, with the H atom of the hydrocarbon substrate being transfer to the  $\alpha$ -N atom of the imido ligand.



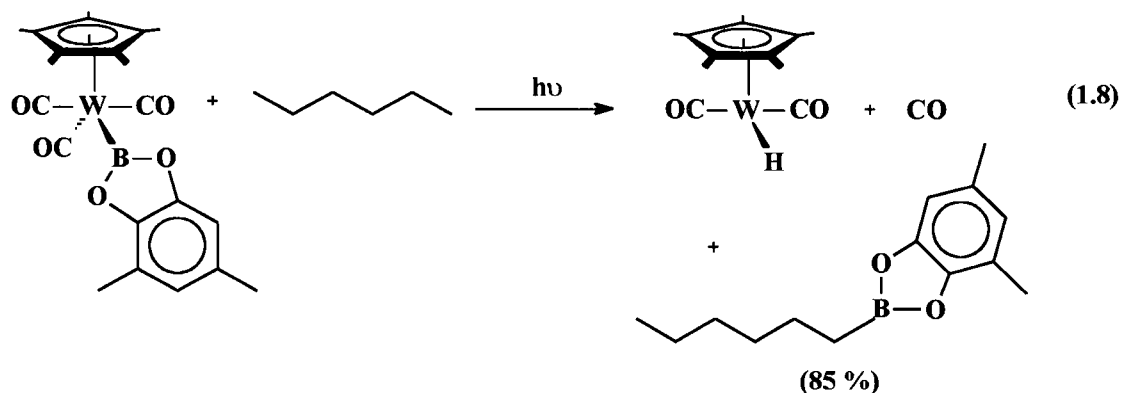
Specific members of this class of compounds include those derived from  $\text{Cp}_2\text{Zr}(\text{R})(\text{NH}^t\text{Bu})$  ( $\text{Cp} = \eta^5\text{-C}_5\text{H}_5$ ;  $\text{R} = \text{alkyl}$ ),<sup>30</sup>  $(\text{X})_2\text{M}(\text{R})\text{NHSi}^t\text{Bu}_3$  ( $\text{M} = \text{Ti}$ ,  $\text{X} = \text{OSi}^t\text{Bu}_3$ ;  $\text{M} = \text{Zr}$ ,  $\text{X} = \text{NHSi}^t\text{Bu}_3$ ;  $\text{R} = \text{alkyl}$ ,  $\text{aryl}$ ),<sup>31</sup>  $(^t\text{Bu}_3\text{Si}(\text{H})\text{N}=\text{M}(\text{R})(\text{NHSi}^t\text{Bu}_3)_2$  ( $\text{M} = \text{V}^{32}$ ,  $\text{Ta}^{33}$ ), and  $(^t\text{Bu}_3\text{Si}(\text{H})\text{N}=\text{W}(\text{R})(\text{NHSi}^t\text{Bu}_3)_2$ .<sup>34</sup> In the well-characterized Ti, Zr and Ta systems, the products again typically form according to the same general trend (e.g

aryl > benzyl products for toluene, 1° > 2° alkyls for alkanes). Intermediate substrate hydrocarbon complexes may or may not be present on the C-H activation reaction coordinate. Yet, as in the metathesis systems described above, these intermediates, if present, do not influence the activation chemistry since rate-determining step in substrate activation is C-H bond scission. Thus, initial product distributions are linked to the relative transition state energies for C-H bond scission, which in turn depend primarily on the ground state energies of the product complexes. Product distributions formed after equilibration via reversible C-H activation are likewise determined by the product energies. The mechanistic features of these particular systems are discussed in more detail in Chapter 3.

#### **1.1.5 Soluble Metal Complexes that Convert Hydrocarbons Into Functionalized Organic Chemicals**

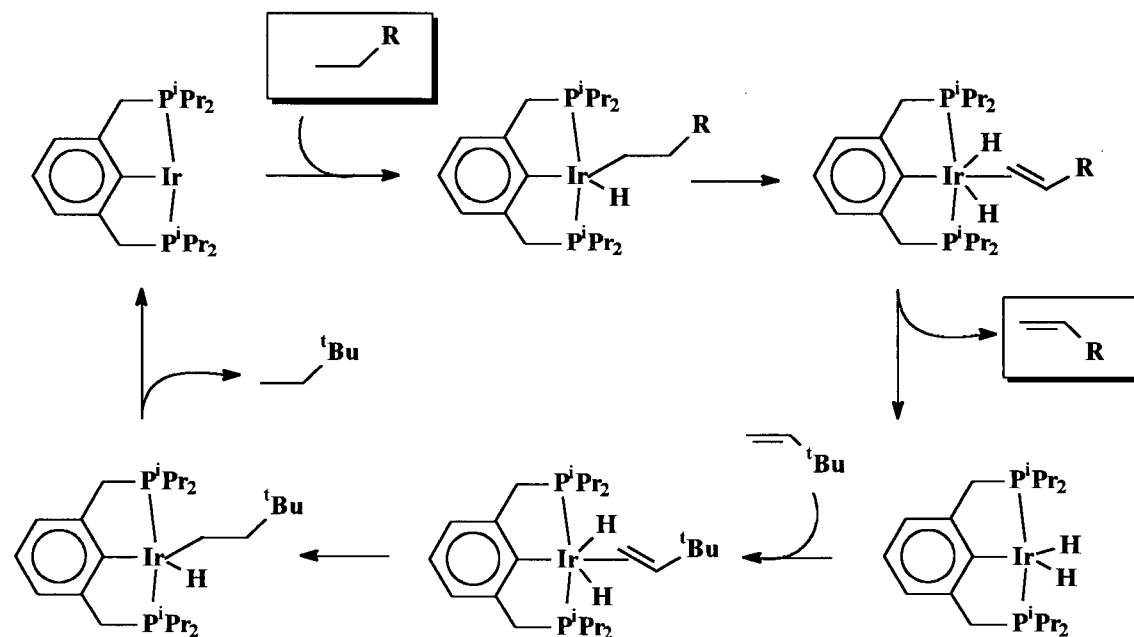
In addition to being amenable to detailed studies of the C-H activation process, some systems featuring reactive soluble metal complexes have been developed to activate and transform hydrocarbons, particularly alkanes, into functionalized chemicals. For example, Waltz and Hartwig have developed a series of metal boryl complexes that transforms alkanes into alkylboronate esters.<sup>35</sup> A representative transformation employing a tungsten boryl complex is shown in eq 1.8. The key step in the process is believed to be oxidative addition of the alkane to the dicarbonyl derivative of the tungsten complex. The resulting alkyl boryl complex then undergoes reductive elimination to form the functionalized organic product, which can be converted into a variety of other organic compounds by standard synthetic methodologies. Recent advances have resulted

in the catalytic conversion of alkanes to alkylboronate esters using similar organometallic reagents.<sup>36</sup>



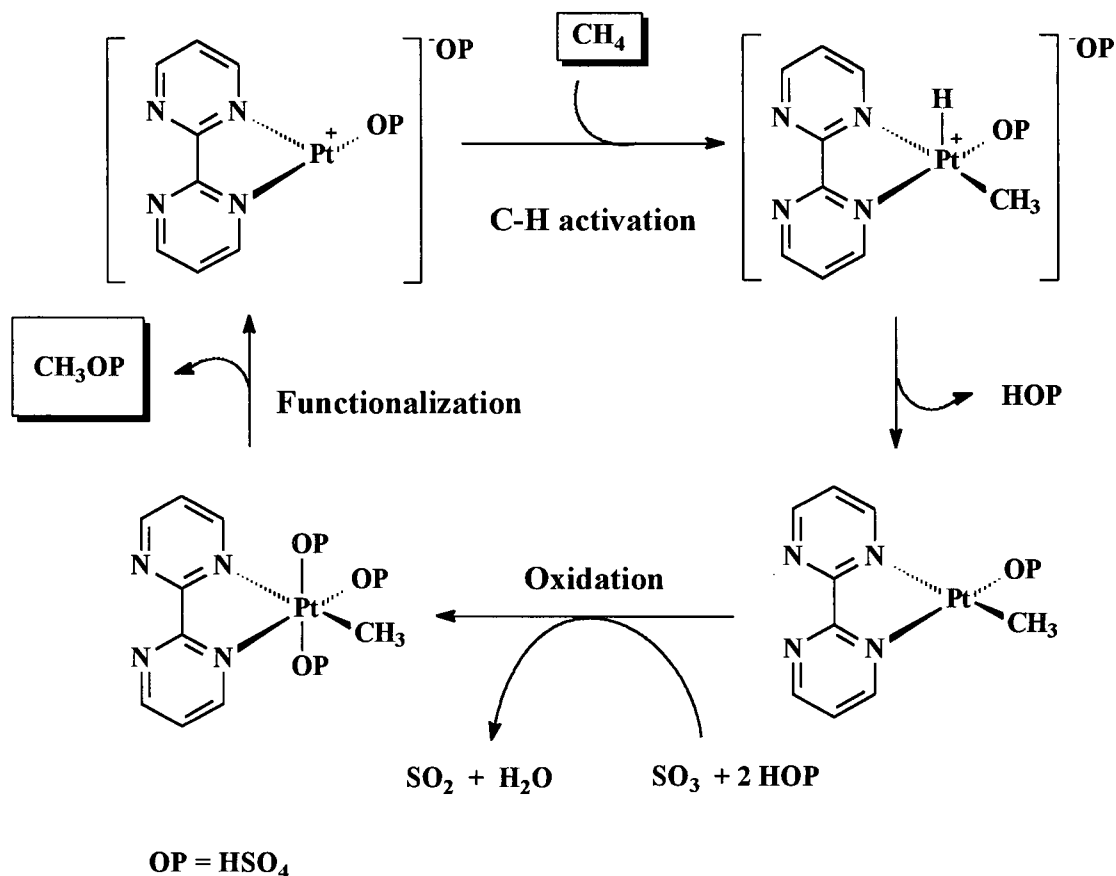
Several other systems employing soluble metal complexes can also mediate the catalytic conversion of alkanes to functionalized organic molecules via organometallic intermediates.<sup>37</sup> One notable example is the catalytic iridium-based alkane-to-alkene dehydrogenation system developed by Jensen, Goldman and co-workers (Scheme 1.1).<sup>38</sup> Here, terminal alkanes are first activated by oxidative addition to form an alkyl hydride complex. Since this complex is coordinatively and electronically unsaturated,<sup>1</sup> a second C-H activation event, namely  $\beta$ -H elimination, generates a dihydride alkene complex. Dissociation of the alkene from the metal center yields the desired functionalized organic moiety. A sacrificial alkene molecule such as *t*-butylethylene is then used to regenerate the iridium catalyst by the reverse of the alkane functionalization process. By this so-called transfer dehydrogenation, a number of different alkanes may be efficiently converted to their terminal alkene derivatives.

Scheme 1.1



Another notable example is the system being developed by Periana et al. at Catalytica Corporation for the industrial-scale direct catalytic conversion of methane to methanol (Scheme 1.2).<sup>39</sup> It is believed to involve the oxidation addition of methane to a cationic Pt(II) complex to form a platinum methyl intermediate.<sup>10</sup> This organometallic complex is then converted by the boiling sulfuric acid solvent into methyl bisulfate, which yields methanol upon hydrolysis. If this, or a similar, process can be made to be efficient and economically viable, it would be a boon to both the chemical industry and the energy industry, since methanol is a common chemical feedstock and a better fuel source than methane, but is expensive to produce by current indirect methods.<sup>40</sup>

Scheme 1.2



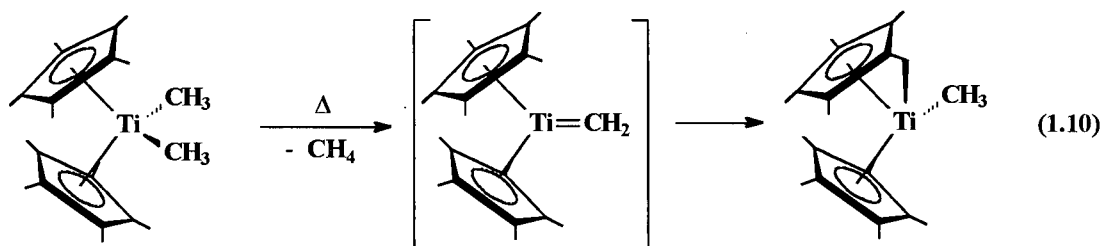
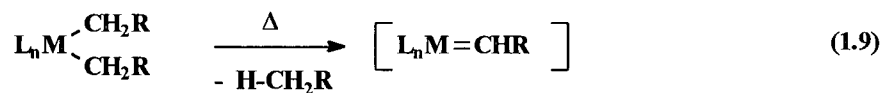
### 1.1.6 A New Mode of Organometallic Hydrocarbon C-H Bond Activation:

#### Addition of R-H to the M=CHR Linkages of Soluble Metal Alkylidene

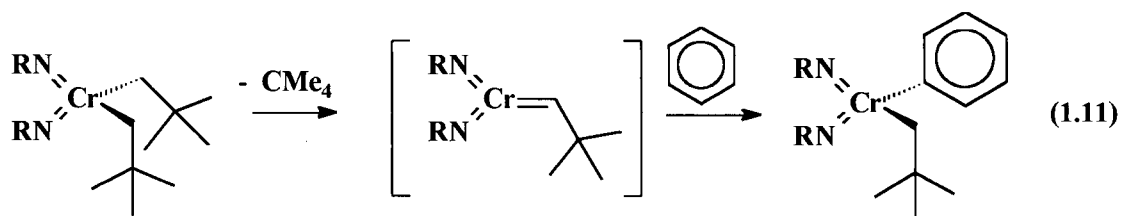
#### Complexes

After over twenty years of research, it was noted in early 1995 that there was a curious absence of one particular mode of intermolecular C-H activation by soluble metal complexes, namely the addition of hydrocarbon C-H bonds to the M=C linkage of an alkylidene complex.<sup>7</sup> In stark contrast, the microscopic reverse of this process, namely the  $\alpha$ -H elimination of hydrocarbon (eq 1.9) was well known,<sup>41</sup> and that there had been

the activation of a methyl group of the Cp\* ligand by the methyldiene intermediate shown in eq 1.10.



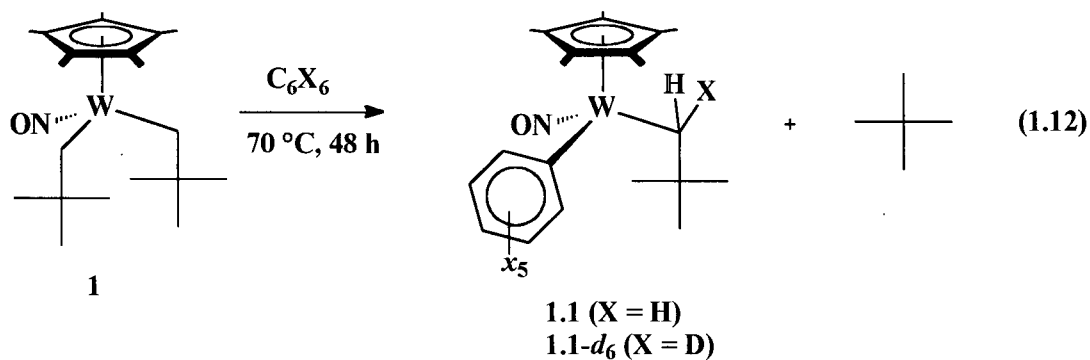
In the following three years, four systems were reported to effect intermolecular hydrocarbon activation by this mode of C-H bond scission. In each system, the reactive species is a neopentylidene complex generated thermally in situ from a *cis*-bis(neopentyl) precursor by  $\alpha$ -H elimination of neopentane ( $\text{R} = \text{CMe}_3$  in eq 1.9). The neopentylidene complexes generated from  $(2,6\text{-}i\text{-Pr}_2\text{C}_6\text{H}_3\text{N})_2\text{Cr}(\text{CH}_2\text{CMe}_3)_2$  (eq 1.11)<sup>43</sup> and  $\text{Cp}'_2\text{Ti}(\text{CH}_2\text{CMe}_3)_2$  ( $\text{Cp}' = \text{Cp}$  or  $\text{Cp}^*$ )<sup>44</sup> in this manner activate a C-H bond of benzene to afford the corresponding phenyl neopentyl complexes. There is also strong evidence for the activation of alkane and arene C-H bonds by a transient neopentylidene complex during the thermal decomposition of  $\text{Ti}(\text{CH}_2\text{CMe}_3)_4$ .<sup>45</sup>



Finally, members of this research group reported that the thermolysis of  $\text{Cp}^*\text{W}(\text{NO})(\text{CH}_2\text{CMe}_3)_2$  (**1**) under modest conditions ( $70\text{ }^\circ\text{C}$ , 40-48 h) leads to the formation of the reactive alkylidene intermediate,  $\text{Cp}^*\text{W}(\text{NO})(=\text{CHCMe}_3)$  (**A**), which subsequently activates the C-H bonds of both alkane and arene solvents. Details of the initial discovery of, and subsequent investigations into, this chemistry are presented in the next two sections.

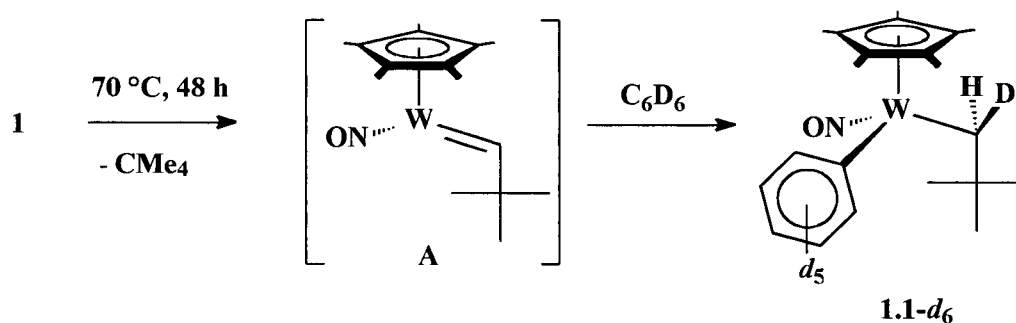
### 1.1.7 Alkane and Arene C-H Activation by $\text{Cp}^*\text{W}(\text{NO})(=\text{CHCMe}_3)$ (**A**): The Discovery and Preliminary Investigations

The discovery of the C-H activation chemistry derived from **1** occurred during the final stages of thesis work conducted by Kevin Ross of this group.<sup>46</sup> He noted that the thermolysis of **1** in benzene for 48 h at  $70\text{ }^\circ\text{C}$  led to the formation and isolation of the aryl neopentyl complex  $\text{Cp}^*\text{W}(\text{NO})(\text{CH}_2\text{CMe}_3)(\text{C}_6\text{H}_5)$  (**1.1**). A similar experiment in benzene- $d_6$  revealed the formation of free neopentane (detected by  $^1\text{H}$  NMR spectroscopy) as well as  $\text{Cp}^*\text{W}(\text{NO})(\text{CHDCMe}_3)(\text{C}_6\text{D}_5)$  (**1.1- $d_6$** ), which features exclusive deuterium incorporation at only one of the two methylene positions of the neopentyl ligand (eq 1.12).

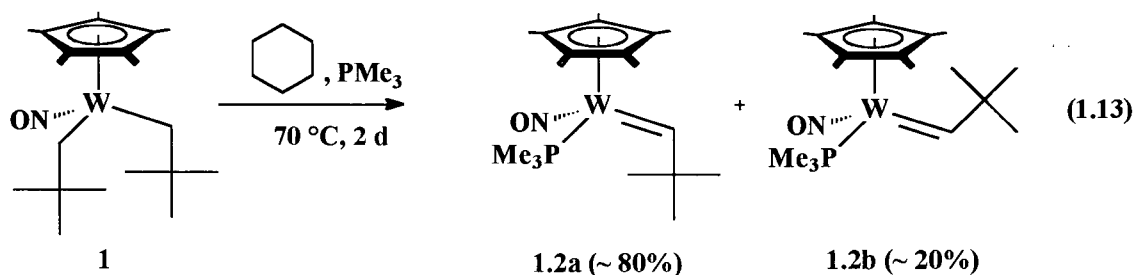


Incorporation of deuterium at the methylene position is only consistent with the addition of C-D across the M=C linkage of an intermediate alkylidene complex. Moreover, the stereoselective nature of the incorporation is consistent with 1,2-cis addition of C-D across the M=C linkage of only one of the two possible isomers of this neopentylidene complex. Although no experimental proof was obtained at the time, Dr. Ross suggested that the most likely reactive intermediate was the 16e neopentylidene complex, **A**, in which the alkylidene <sup>t</sup>Bu group is “antichinal” (i.e. pointing away) to the Cp\* ligand, rather than “synchinal” (pointing towards it) (Scheme 1.3).

**Scheme 1.3**

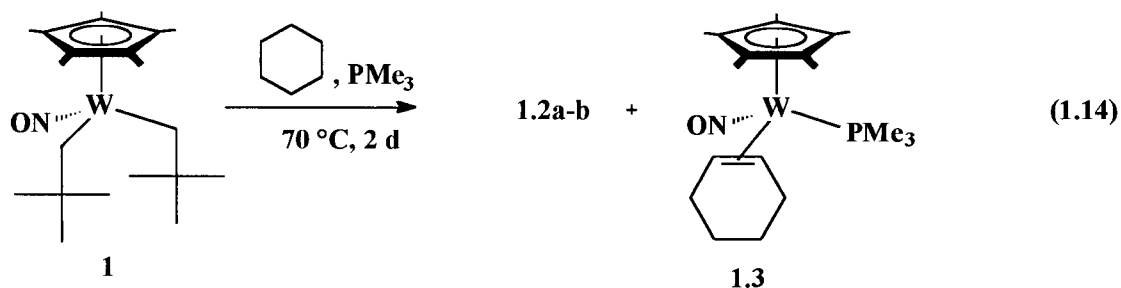


Subsequent work on the thermal chemistry of **1** was conducted by Elizabeth Tran of this group.<sup>47,48,49</sup> Evidence was obtained for the formation of a transient alkylidene complex from **1** via the thermolysis of **1** in neat trimethylphosphine. Two products were observed in the final reaction mixture, namely the anti- and synchinal isomers of Cp\*W(NO)(=CHCMe<sub>3</sub>)(PMe<sub>3</sub>) (**1.2a-b**) in a ~ 4:1 ratio (eq 1.13). The solid-state molecular structure of the major isomer **1.2a** was established to be that of the phosphine-trapped form of the purported antichinal neopentylidene intermediate **A**.



Shortly thereafter, a startling discovery was made when the trapping experiments were conducted with  $\text{PMe}_3$  in cyclohexane. The thermolysis of **1** in cyclohexane in the presence of a large excess of  $\text{PMe}_3$  (i.e.  $> 50$  equiv) yields the  $\text{PMe}_3$ -trapped alkylidene complexes **1.2a-b** as expected. However, as the relative amount of  $\text{PMe}_3$  is decreased, a third product forms, namely  $\text{Cp}^*\text{W}(\text{NO})(\eta^2\text{-cyclohexene})(\text{PMe}_3)$  (**1.3**) (eq 1.14):

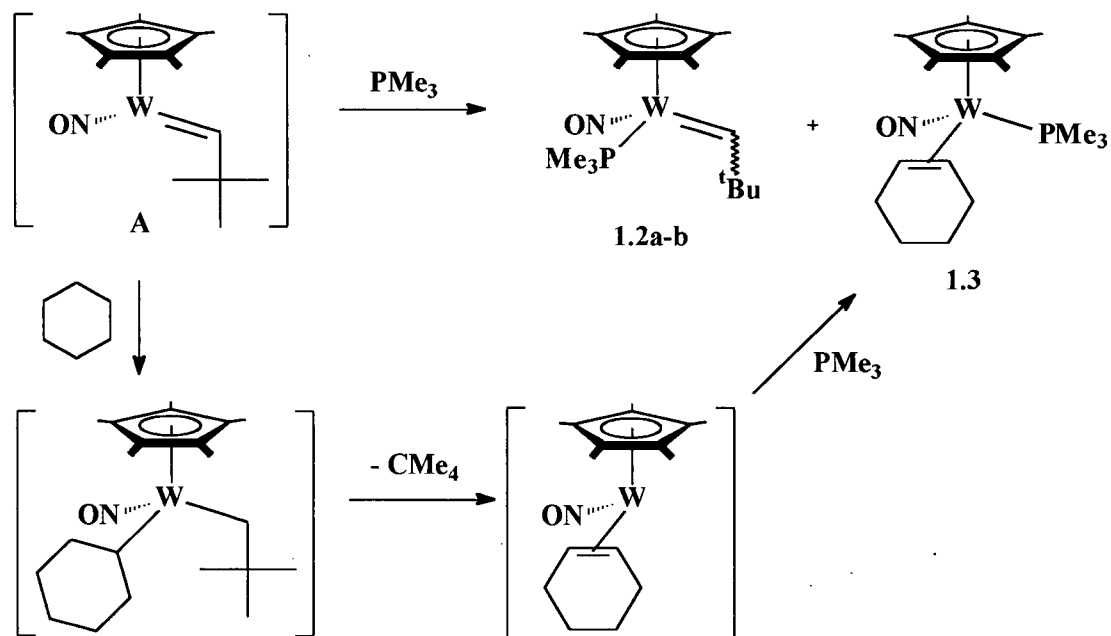
Complex **1.3** is the major product formed under “dilute” conditions (i.e.  $\leq 12$  equiv of  $\text{PMe}_3$ ) and, accordingly, was successfully isolated and fully characterized. The reaction shown in eq 1.14 was the first clear example of intermolecular C-H activation of an alkane substrate by a metal alkylidene complex.<sup>47</sup>



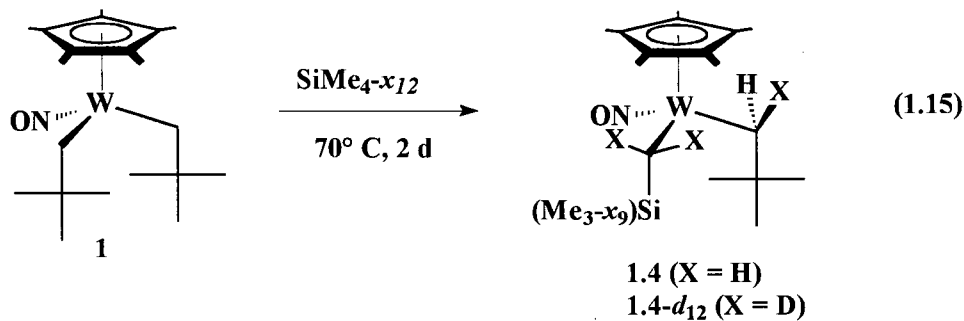
The purported mechanism for the formation of **1.3** involves initial C-H activation of cyclohexane mediated by **1**, followed by a second C-H bond activation, namely  $\beta$ -H elimination of neopentane (Scheme 1.4). Notably, the reaction results in the net conversion of cyclohexane to cyclohexene by dehydrogenation, although the alkene

remains coordinated to the metal center. The majority of organometallic C-H activation systems do not permit such transformations of the alkyl ligands after the initial C-H activation event.<sup>7</sup>

**Scheme 1.4**



The initial investigation into the activation chemistry exhibited by this system included another aliphatic substrate, tetramethylsilane, and its perdeuterio analogue, tetramethylsilane- $d_{12}$ .<sup>47</sup> Specifically, it was found that the thermolyses of **1** in these solvents generate the respective products of C-H and C-D activation, namely  $\text{Cp}^*\text{W}(\text{NO})(\text{CH}_2\text{CMe}_3)(\text{CH}_2\text{SiMe}_3)$  (**1.4**), and  $\text{Cp}^*\text{W}(\text{NO})(\text{CHDCMe}_3)(\text{CD}_2\text{Si}(\text{CD}_3)_3)$  (**1.4- $d_{12}$** ), in very high yield ( $\sim 97\%$ ) (eq 1.15).



Deuterium is incorporated in **1.4-*d*<sub>12</sub>** at only one of the two methylene positions of the neopentyl ligand. This position was identified by solution <sup>1</sup>H-<sup>1</sup>H NOE NMR and solid-state X-ray crystallographic studies<sup>48</sup> of **1.4** to be the synclinal methylene position (*H<sub>syn</sub>*), rather than the anticlinal position (*H<sub>anti</sub>*) (Figure 1.1). The incorporation of deuterium at this position is consistent with the exclusive 1,2-cis C-H activation by the anticlinal alkylidene isomer **A**, as originally proposed by K. Ross.



**Figure 1.1.** Two different views of the stereochemistry about the methylene linkages of **1.4** as determined from the conformation exhibited in its solid-state molecular structure. The syn- and anticlinal positions are defined with respect to the other W-C alkyl linkage in the molecule.

### 1.1.8 Alkane and Arene C-H Activation by Cp\*W(NO)(=CHCMe<sub>3</sub>) (A):

#### Subsequent Investigations

At the time, the C-H activation system featuring neopentylidene **A** was the only one of the four reported systems that could activate both arene and alkane substrates to yield isolable and well-defined organometallic products. Hence, our research group was provided with the opportunity to conduct the first in-depth investigation into the C-H activation of alkanes and arenes by a soluble metal alkylidene complex. In that regard, E. Tran subsequently conducted a kinetic study of the activation process and surveyed the C-H activation of select alkane and arene substrates. Highlights of the results of these efforts are presented below.

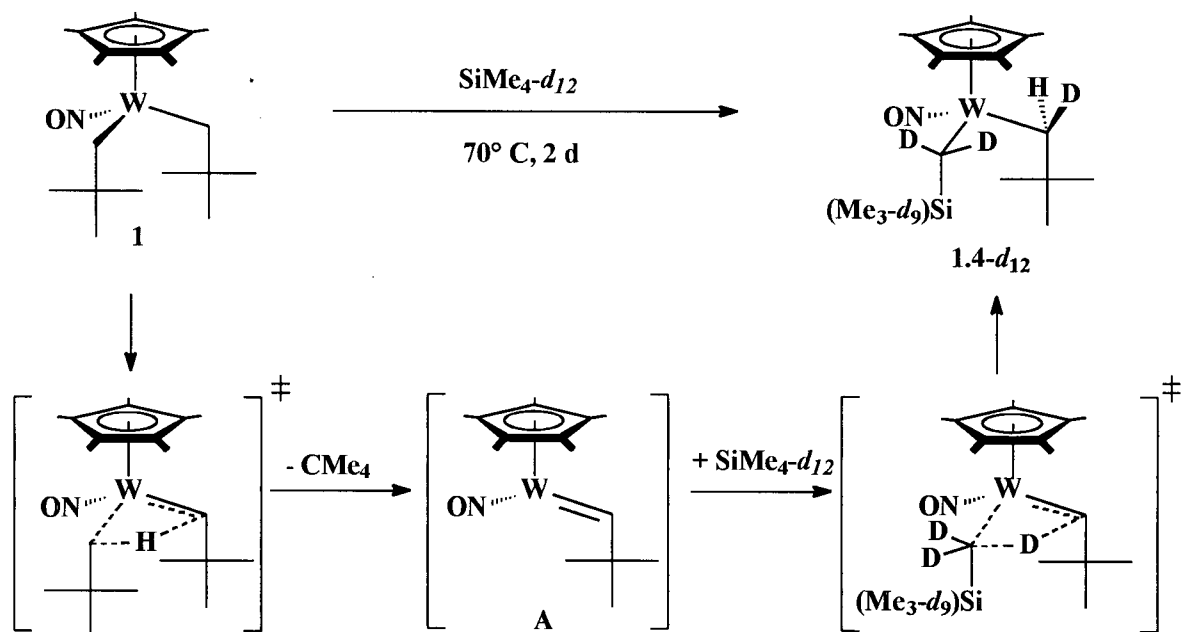
#### 1.1.8.1 Kinetic Studies on, and the Proposed General Mechanism for, C-H

##### Activation Derived from **1**

The thermolysis of **1** was monitored over > 3.5 half-lives by UV-vis spectroscopy in cyclohexane solutions containing an excess of PMe<sub>3</sub> (e.g. 300 equiv).<sup>49</sup> The reaction exhibits first-order kinetics for the loss of **1** over the temperature range of 71 - 98 °C (i.e.  $k_{\text{obs}} = 5.3 \times 10^{-5} \text{ s}^{-1}$  at 72 °C). An Eyring plot of these data afforded the activation parameters  $\Delta H^\ddagger = 28(2) \text{ kcal mol}^{-1}$  and  $\Delta S^\ddagger = 1(3) \text{ cal mol}^{-1} \text{ K}^{-1}$ . Other kinetic analyses in hydrocarbon solvents in the absence of PMe<sub>3</sub> also exhibit first-order dependence on **1** with similar rate-constants.<sup>48</sup> A comparison of the rates of the PMe<sub>3</sub>-trapping of **1** vs Cp\*W(NO)(CD<sub>2</sub>CMe<sub>3</sub>)<sub>2</sub> (**1-d<sub>4</sub>**) at 91 °C by UV-visible spectroscopy yields a relative ratio of 2.4(2) in favour of **1**.<sup>49</sup> This was assigned as the kinetic isotope effect for direct  $\alpha$ -elimination of neopentane.

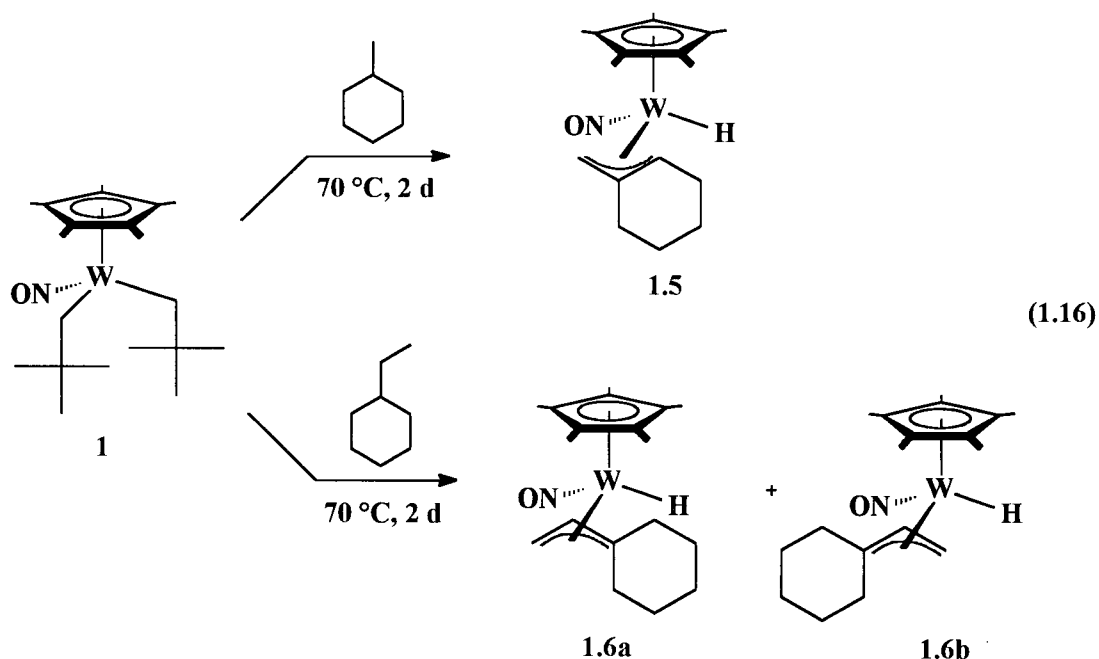
Taken together, these data are consistent with the thermal decomposition of **1** by a rate-determining intramolecular  $\alpha$ -H bond scission process. When combined with the labeling studies in benzene and tetramethylsilane, the mechanism for the activation chemistry derived from **1** has the following characteristics (1) rate-limiting intramolecular  $\alpha$ -H elimination of neopentane to form the reactive anticlinal alkylidene complex (2) 1,2-cis addition of R-H across the W=C linkage of the alkylidene complex. Consequently, a simple two-step  $\alpha$ -abstraction mechanism was proposed, involving anticlinal neopentylidene intermediate **A** and concerted 1,2-cis C-H bond addition to the M=C linkage.<sup>50</sup> The purported mechanism is illustrated in Scheme 1.5 for the activation of deuterated tetramethylsilane.

**Scheme 1.5**



### 1.1.8.2 Activation of Alkane Substrates

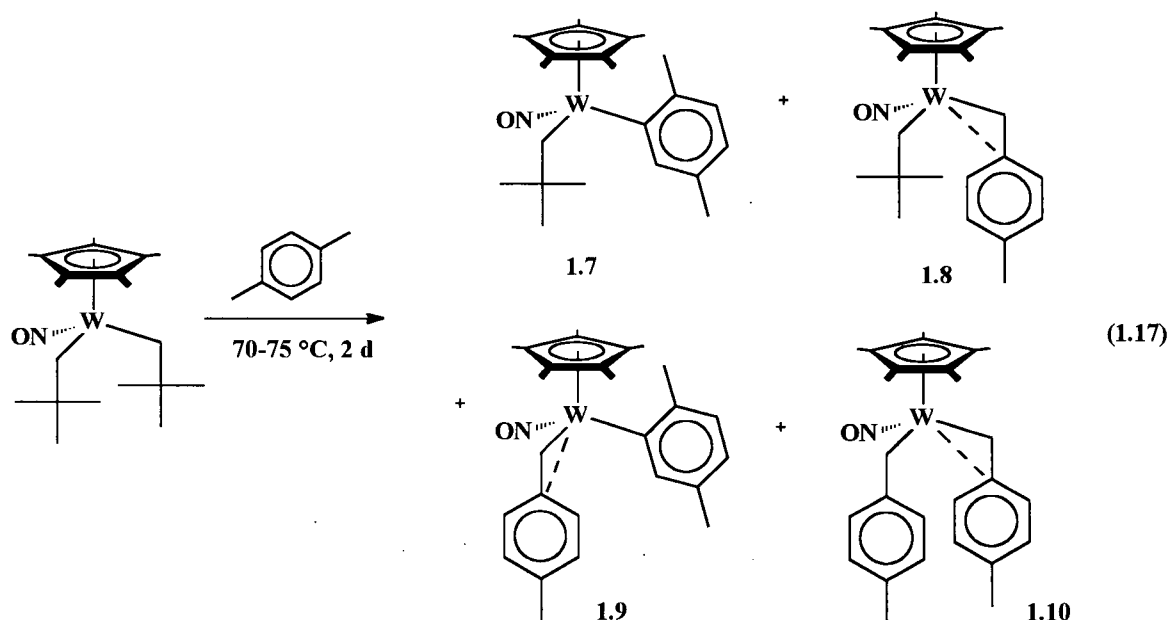
Two different modes of reactivity were found for the activation of alkanes by this system. The thermolysis of **1** in a cycloalkane solvent in the presence of  $\text{PMe}_3$  was found to generate **1.2a-b** and the corresponding  $\text{PMe}_3$ -trapped alkene complexes,<sup>48</sup> as observed with cyclohexane (eq 1.14). In contrast, the thermolysis of **1** in an alkyl-substituted alkane such as methylcyclohexane,<sup>49</sup> or an acyclic alkane such as pentane,<sup>48</sup> in the presence or absence of  $\text{PMe}_3$  was found to generate the corresponding terminal allyl hydride complexes, such as **1.5** and **1.6a-b**, via an additional C-H activation event (eq 1.16). These investigations established that the transformation of alkane substrates into coordinated dehydrogenated derivatives is a general phenomenon for this system.



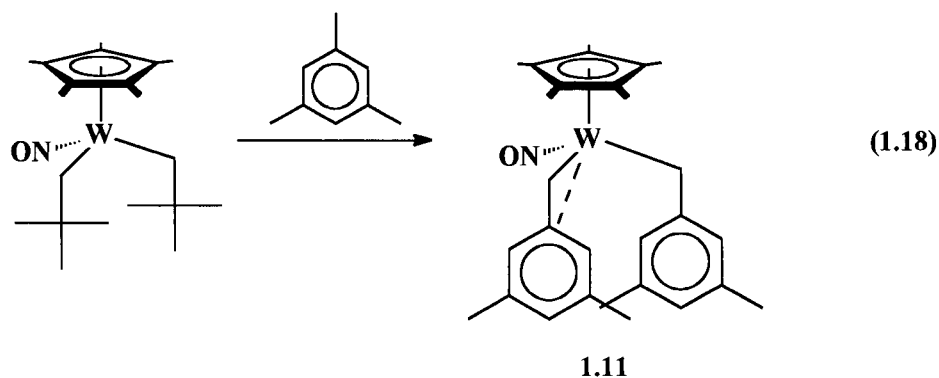
### 1.1.8.3 Activation of Methyl-Substituted Arene Substrates

The thermolysis of **1** in methyl-substituted arenes, such as toluene,<sup>49</sup> *p*-xylene and mesitylene<sup>48</sup> generated some unexpected results. In each case, products of the activation

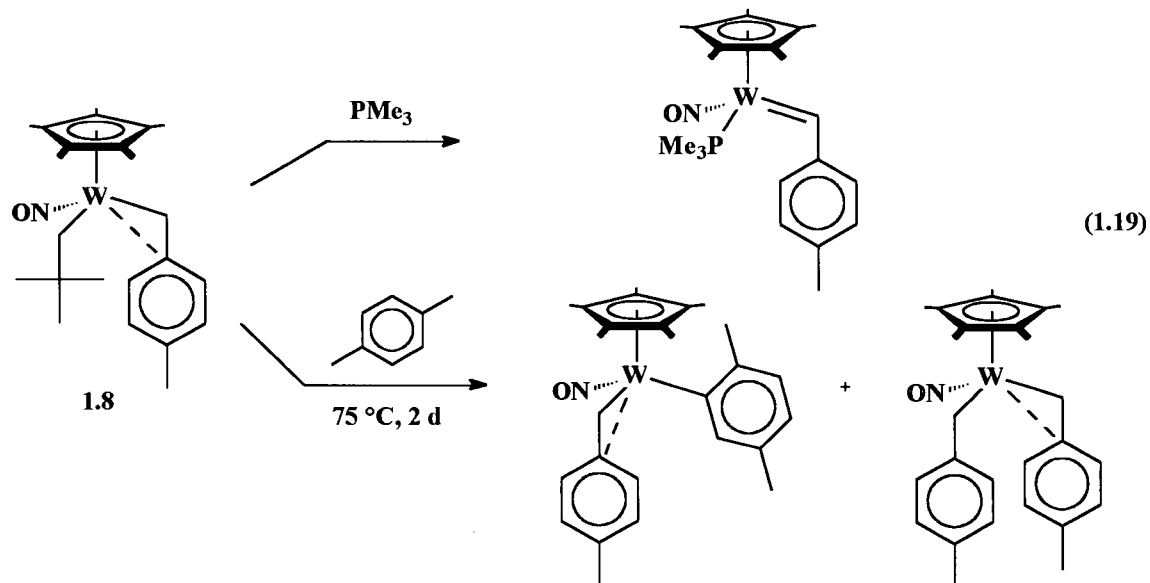
of one and/or *two* substrate molecules were observed in the final product mixture. For example, the thermolysis of **1** in *p*-xylene leads to the formation of four products (eq 1.17). The first two complexes, **1.7** and **1.8**, are the aryl and benzyl products derived from the activation of an  $sp^2$  and  $sp^3$  C-H bond of one *p*-xylene molecule, respectively. The other two complexes, **1.9** and **1.10**, are derived from the activation of two *p*-xylene molecules.



In comparison, the thermolysis of **1** in mesitylene (eq 1.18) leads only to one product containing two C-H activated substrate molecules, namely  $Cp^*W(NO)(CH_2C_6H_3-3,5-Me_2)_2$  (**1.11**).



These results suggest that the activation of the  $sp^3$  C-H bonds of methyl-substituted arenes by **A** leads to the formation of complexes of the general type  $Cp^*W(NO)(CH_2CMe_3)(CH_2Ar)$  which are thermally sensitive. These complexes then undergo  $\alpha$ -H elimination of neopentane to generate the corresponding benzylidene analogues of **A**, namely  $Cp^*W(NO)(=CHAr)$ , that subsequently activate solvent C-H bonds. In support of this conclusion, two of the benzyl neopentyl products, namely  $Cp^*W(NO)(CH_2CMe_3)(CH_2Ar)$  ( $Ar = C_6H_5$  (**2**) and  $Ar = CH_2C_6H_4-4-Me$  (**1.8**)) were prepared and thermolysed in  $PMe_3$  as well as the parent arene solvent (toluene for **2**,<sup>49</sup> *p*-xylene for **1.8**<sup>48</sup>). The thermolyses in  $PMe_3$  lead to the isolation of the  $PMe_3$ -trapped alkylidene complexes,  $Cp^*W(NO)(=CHAr)(PMe_3)$ , which were isolated and characterized spectroscopically. The thermolyses in the parent solvent lead to the formation of the respective aryl and benzyl activation products as predicted. The results for **1.8** are detailed in eq 1.19.



From these investigations, it became apparent that the chemistry effected by neopentylidene **A** was not unique. In fact, an entire family of benzylidene analogues of **A** seemed to be readily available from the thermolysis of the respective benzyl neopentyl precursor complexes.

## 1.2 Outline of This Thesis

In light of the novelty of the activation chemistry initiated by neopentylidene **A**, a study of the activation chemistry of a representative benzylidene system was clearly warranted. In addition, using the research conducted on other systems as a guide, several issues regarding the activation chemistry exhibited by both types of alkylidene systems remained to be addressed. These included (1) probing the mechanism of C-H activation for the possible existence and significance of hydrocarbon intermediates in the activation of arene and alkane substrates, (2) accurately quantifying the product selectivities for substrates in which more than one type of C-H bond is present, and identifying the factors that control these selectivities, and (3) assessing the potential of these or related systems

for development as reagents for the conversion of hydrocarbons into functionalized organic chemicals. This Thesis describes work conducted on all four of these topics.

Chapter 2 begins with the investigation of the thermal chemistry of a representative benzyl neopentyl complex and its benzylidene derivative, namely  $\text{Cp}^*\text{W}(\text{NO})(\text{CH}_2\text{C}_6\text{H}_5)(\text{CH}_2\text{CMe}_3)$  (**2**) and  $\text{Cp}^*\text{W}(\text{NO})(=\text{CHC}_6\text{H}_5)$  (**B**). The benzylidene and neopentylidene systems are compared with respect to the basic mechanistic features of the activation process, as well as the scope and the selectivity of arene and alkane C-H activation. These investigations reveal that the kinetics of formation and the general nature of the reactive alkylidene species are very similar, and that the benzylidene system activates alkane substrates to yield the same alkene or terminal allyl hydride complexes as the neopentylidene system. However, while the activation of toluene by benzylidene **B** yields the same types of aryl and benzyl products as neopentylidene **A**, the resulting distribution of organometallic products is significantly different. Moreover, the activation of toluene is identified to be the one instance where a range of products is formed from the activation of different C-H bonds within the molecule. Consequently, the remainder of Chapter 2 concerns the activation of other substituted arenes by both systems with the goal of quantifying the respective product selectivities and identifying trends between them. This work reveals that the product distributions obtained from the benzylidene system are consistently more abundant in the aryl products than those obtained from the neopentylidene system in the same solvent (toluene, *p*-xylene). Likewise, in the activations of  $\alpha,\alpha,\alpha$ -trifluorotoluene and toluene, the aryl regioisomer distributions obtained from **2** favour the meta isomer over the para and ortho isomers, more so than the distributions obtained from **1**. Finally, for both systems, the

organometallic products associated with the activation of the stronger and most accessible bond within the arene molecule are generally formed preferentially, with some moderation by the steric and electronic nature of the substituent(s) in the arene substrate.

A detailed understanding of the mechanism of the activation process was required to determine the origin of these trends and to identify the factors responsible for the observed product selectivities. In that regard, Chapter 3 describes the reinvestigation of the mechanism of thermal chemistry of both **1** and **2** directed at evaluating the possible involvement of hydrocarbon intermediates in the formation of the activation products. The results of this investigation indicate that hydrocarbon intermediates do exist on the reaction coordinate for C-H activation, and do influence the outcome of the activation process. In particular, the key step in the activation of benzene, tetramethylsilane and mesitylene is found to be coordination to the metal center, rather than scission of the substrate C-H bond as originally thought.

With the key mechanistic features of the activation process successfully resolved, additional work could be conducted to rationalize the rest of the activation chemistry reported in Chapter 2. In that regard, Chapter 4 focuses on explaining the activation of the substituted arenes, beginning with an in-depth experimental and theoretical investigation of the activation of toluene. These investigations reveal that the aryl vs benzyl product distributions are controlled by the relative energetics of the coordination of the substrate in two different fashions to the metal center. In contrast, the aryl regioselectivity is controlled by the relative energies of the aryl products themselves. The product distributions obtained from the activation of other substituted arenes are

controlled by these same factors, namely substrate coordination and the energy of the activation products, but with variations that depend on the substrate and the alkylidene complex utilized. In the end, the factors that control the product distributions are found to be highly dependent on the substrate, the activated products and the alkylidene complex employed. Furthermore, the trends in the observed product selectivities do not result from a simple correlation to the relative activated product energies as in the imido systems mentioned earlier in this Chapter.

The final Chapter of this Thesis is concerned with assessing the utility of the alkylidene systems as reagents for the conversion of alkanes into other functionalized chemicals. In particular, a potentially viable and novel application of the activation chemistry mediated by the neopentylidene system to the field of organic syntheses is presented. In addition, new alternative alkylidene systems related to the neopentylidene and benzylidene systems discussed in Chapter 2-4 are presented, systems that may be more amenable to the proposed alkane functionalization application. Finally, a general strategy is described for the development of other, related non-alkylidene C-H activation systems that can potentially be used to effect alkane functionalization in alternative fashions.

### **1.3 Format of This Thesis**

This Thesis is formatted with Chapters 2 through 5 possessing five major sections. If X is the chapter number, then the Sections appear as X.1 Introduction, X.2 Results and Discussion, X.3 Epilogue, X.4 Experimental Procedures, and X.5 References and Notes. Subsections of these categories are numbered using legal outlining

procedures, e.g. X.1.1, X.1.2, X.1.2.1, X.1.3, etc. Compounds  $\text{Cp}^*\text{W}(\text{NO})(\text{CH}_2\text{CMe}_3)_2$  (**1**) and  $\text{Cp}^*\text{W}(\text{NO})(\text{CH}_2\text{CMe}_3)(\text{CH}_2\text{C}_6\text{H}_5)$  (**2**) and the respective alkylidene complexes  $\text{Cp}^*\text{W}(\text{NO})(=\text{CHCMe}_3)$  (**A**) and  $\text{Cp}^*\text{W}(\text{NO})(=\text{CHC}_6\text{H}_5)$  (**B**) are defined as such throughout this thesis. All other compounds discussed elsewhere in this Thesis are defined by the Chapter and sequence in which they are mentioned, e.g. in Chapter X, compounds appear as X.1, X.2 etc. and are referred to as X.1, X.2, etc. in subsequent chapters. Schemes, Tables, Figures and Equations are similarly sequenced and referenced. The standard experimental methodologies employed during the research described in this Thesis are outlined in detail in Chapter 2, Section 2.4.1

#### 1.4 References and Notes

- (1) Crabtree, R. H. *The Organometallic Chemistry of the Transition Metals*, 3<sup>rd</sup> ed.; Wiley and Sons: Toronto, ON, 2001.
- (2) Also see: (a) Collman, J. P.; Hegedus, L. S.; R. Norton, J.R.; Finke, R. G. *Principles and Applications of Organotransition Metal Chemistry*, 2<sup>nd</sup> ed.; University Science: Mill Valley, CA, 1987. (b) Shriver, D. F.; Atkins, P.; Langford, C. H. *Inorganic Chemistry*, 2<sup>nd</sup> ed.; Freeman and Co.: New York, NY, 1994; Chapters 10, 16. (c) Butler, I. S.; Harrod, J. F. *Inorganic Chemistry Principles and Applications*; Benjamin/Cummings Publishing: Don Mills, ON, 1989; Chapter 22.
- (3) For a lead reference, see: Bochmann, M. E. *J. Chem. Soc., Dalton Trans.* **1996**, 255-270.
- (4) Shilov, A. E.; Shul'pin, G. B. *Activation and Catalytic Reactions of Saturated Hydrocarbons in the Presence of Metal Complexes*; Kluwer Academic Publishers: Dordrecht, The Netherlands, 2000.
- (5) *Activation and Functionalization of Alkanes*; Hill, C. L., Ed.; Wiley-Interscience: New York, NY, 1989.

- (6) It should be noted that not all hydrocarbon C-H activation reactions involving organometallic complexes directly form an organometallic complex when the C-H bond is cleaved. Rather, the C-H activation reaction can be mediated through a ligand of a metal complex, or is promoted by the complex via the formation of a non-metallic reactive species. However, these types of organometallic reactions lie outside the scope of this Thesis. For details, see reference 4.
- (7) Arndtsen, B. A.; Bergman, R. G.; Mobley, T. A.; Peterson, T. H. *Acc. Chem. Res.* **1995**, *28*, 154-162.
- (8) For example, C-H activation of cyclohexane can be effected at 163-193 K by photolytically-generated Cp\*Rh(CO). For details, see: Schultz, R. H.; Bengali, A. A.; Tauber, M. J.; Weiller, B. H.; Wasserman, E. P.; Kyle, K. R.; Moore, C. B.; Bergman, R. G. *J. Am. Chem. Soc.* **1994**, *116*, 7369-7377.
- (9) Crabtree, R. H. *Chem. Rev.* **1995**, *95*, 987-1007.
- (10) Stahl, S. S.; Labinger, J. A.; Bercaw, J. E. *Angew. Chem., Int. Ed.* **1998**, *37*, 2180-2192.
- (11) Jones, W. D. in reference 5; Chapter 4.
- (12) (a) Janowicz, A. H.; Bergman, R. G. *J. Am. Chem. Soc.* **1983**, *105*, 3929-3939.  
(b) Hoyano, J. K.; Graham, W. A. G. *J. Am. Chem. Soc.* **1982**, *104*, 3723-3725.

- (13) Peterson, T. H.; Golden, J. T.; Bergman, R. G. *J. Am. Chem. Soc.* **2001**, *123*, 455-462, and references therein.
- (14) Crabtree, R. H.; Mihelcic, J. M.; Quirk, J. M. *J. Am. Chem. Soc.* **1982**, *104*, 107-113.
- (15) (a) Ghosh, C. K.; Graham, W. A. G. *J. Am. Chem. Soc.* **1987**, *109*, 4726-4727. (b) Jones, W. D.; Feher, F. J. *Acc. Chem. Res.* **1989**, *22*, 91-100. (c) Jones, W. D.; Hessel, E. T. *J. Am. Chem. Soc.* **1993**, *115*, 554-562.
- (16) (a) Price, R. T.; Andersen, R. A.; Muetterites, E. L. *J. Organomet. Chem.* **1989**, *376*, 407-417. (b) Wang, C.; Ziller, J. W.; Flood, T. C. *J. Am. Chem. Soc.* **1995**, *117*, 1647-1648.
- (17) Periana, R. A.; Bergman, R. G. *Organometallics* **1984**, *3*, 508-510.
- (18) (a) Shilov, A.E.; Shteinman, A.A. *Coord. Chem. Rev.* **1977**, *24*, 97. (b) Kushch, L. A.; Lavrushko, V. V.; Misharin, Y. S.; Moravsky, A. P.; Shilov, A. E. *Nouv. J. Chem.* **1983**, *7*, 729.
- (19) Baker, M. V.; Field, L. D. *J. Am. Chem. Soc.* **1987**, *109*, 2825-2826.
- (20) (a) Bergman, R. G.; Seidler, P. F.; Wenzel, T. T. *J. Am. Chem. Soc.* **1985**, *107*, 4358-4359. (b) Jones, W. D.; Rosini, G. P.; Maguire, J. A. *Organometallics* **1999**, *18*, 1754-1760.

- (21) Harper, T. G. P.; Shinomoto, R. S.; Deming, M. A.; Flood, T. C. *J. Am. Chem. Soc.* **1988**, *110*, 7915-7916.
- (22) Berry, M.; Elmitt, K.; Green, M. L. H. *J. Chem. Soc., Dalton Trans.* **1979**, 1950-1958.
- (23) Martin, D. T. Ph.D. Dissertation, University of British Columbia, 1984.
- (24) Thompson, M. E.; Baxter, S. M.; Bulls, R.; Burger, B. J.; Nolan, M. C.; Santarsiero, B. D.; Schaefer, W. P.; Bercaw, J. E. *J. Am. Chem. Soc.* **1987**, *109*, 203-219.
- (25) Booij, M.; Deelman, B.-J.; Duchateau, R.; Postma, D. S.; Meetsma, A.; Teuben, J. H. *Organometallics* **1993**, *12*, 3531-3540.
- (26) Watson, P. L.; Parshall, G. W. *Acc. Chem. Res.* **1985**, *18*, 51-56.
- (27) (a) Bruno, J. W.; Smith, G. M.; Marks, T. J.; Fair, C. K.; Schultz, A. J.; Williams, J. M. *J. Am. Chem. Soc.* **1986**, *108*, 40-56. (b) Fendrick, C. M.; Marks, T. J. *J. Am. Chem. Soc.* **1986**, *108*, 425-437.
- (28) (a) Erker, G.; *J. Organomet. Chem.*, **1977**, *134*, 189-202. (b) England, A. F.; Burns, C. J.; Buchwald, S. L. *Organometallics* **1994**, *13*, 3491-3495.

- (29) For details of this system, see Section 5.2.4 , as well as: Debad, J. D.; Legzdins, P.; Lumb, S. A.; Rettig, S. J.; Batchelor, R. J.; Einstein, F. W. B. *Organometallics* **1999**, *18*, 3414-3428.
- (30) (a) Walsh, P. J.; Hollander, F. J.; Bergman, R. G. *Organometallics* **1993**, *12*, 3705-3723. (b) Lee, S. Y.; Bergman, R. G. *J. Am. Chem. Soc.* **1995**, *117*, 5877-5878.
- (31) (a) Schaller, C. P.; Cummins, C. C.; Wolczanski, P. T. *J. Am. Chem. Soc.* **1996**, *118*, 591-611. (b) Bennett, J. L.; Wolczanski, P. T. *J. Am. Chem. Soc.* **1997**, *119*, 10696-10719.
- (32) With, J.; Horton, A. D. *Angew. Chem., Intl. Ed. Engl.* **1993**, *32*, 903-905.
- (33) Schaller, C. P.; Wolczanski, P. T. *Inorg. Chem.* **1993**, *32*, 131-144.
- (34) Schaefer, D. F. II; Wolczanski, P. T. *J. Am. Chem. Soc.* **1998**, *120*, 4881-4882.
- (35) Waltz, K. M.; Hartwig, J. F. *Science* **1997**, *277*, 211-213.
- (36) Chen, H.; Schlecht, S.; Semple, T. C.; Hartwig, J. F. *Science* **2000**, *287*, 1995-1998.
- (37) For more examples, see references 4, 7 and 10.
- (38) Liu, F.; Pak, E. B.; Singh, B.; Jensen, C. M.; Goldman, A. S. *J. Am. Chem. Soc.* **1999**, *121*, 4086-4087.

- (39) Periana, R. A.; Taube, D. J.; Gamble, S.; Taube, H.; Satoh, T.; Fujii, H. *Science* **1998**, *280*, 560-564.
- (40) For details on the quest for efficient and direct methods of methane-to-methanol conversion, see reference 9.
- (41) Schrock, R. R. *Acc. Chem. Res.* **1979**, *12*, 98-104.
- (42) (a) Vilardo, J. S.; Lockwood, M. A.; Hanson, L. G.; Clark, J. R.; Parkin, B. C.; Fanwick, P. E.; Rothwell, I. P. *J. Chem. Soc., Dalton Trans.* **1997**, 3353-3362 and references therein. (b) McDade, C.; Green, J. C.; Bercaw, J. E. *Organometallics* **1982**, *1*, 1629-1634. (c) Bulls, A. R.; Schaefer, W. P.; Serfas, M.; Bercaw, J. E. *Organometallics* **1987**, *6*, 1219-1226. (d) van Doorn, J. A.; van der Heijden, H.; Orpen, A. G. *Organometallics* **1994**, *13*, 4271-4277. (e) Duncalf, D. J.; Harrison, R. J.; McCamley, A.; Royan, B. W. *J. Chem. Soc., Chem. Commun.* **1995**, 2421-2422.
- (43) Coles, M. P.; Gibson, V. C.; Clegg, W.; Elsegood, M. R. J.; Porrelli, P. A. *J. Chem. Soc., Chem. Commun.* **1996**, 1963-1964.
- (44) van der Heijden, H.; Hessen, B. *J. Chem. Soc., Chem. Commun.* **1995**, 145-146.
- (45) Cheon, J.; Rogers, D. M.; Girolami, G. S. *J. Am. Chem. Soc.* **1997**, *119*, 6804-6813.
- (46) Ross, K. J. Ph. D. Dissertation, University of British Columbia, 1994.

- (47) Tran, E.; Legzdins, P. *J. Am. Chem. Soc.* **1997**, *119*, 5071-5072.
- (48) Tran, E.; Legzdins, P., unpublished observations.
- (49) Adams, C. S.; Legzdins, P.; Tran, E. *J. Am. Chem. Soc.* **2001**, *123*, 612-624.
- (50) Tran, E., personal communication, 2000.

## CHAPTER 2

### Investigations Into The Thermal Chemistry of



---

2.1	Introduction .....	38
2.2	Results and Discussion.....	38
2.3	Epilogue .....	71
2.4	Experimental Procedures .....	72
2.5	References and Notes.....	90

---

## 2.1 Introduction

The first goal of the research described in this Thesis was to study the C-H activation chemistry derived from a representative benzyl neopentyl complex,  $\text{Cp}^*\text{W}(\text{NO})(\text{CH}_2\text{Ar})(\text{CH}_2\text{CMe}_3)$ . Several congeners could have been selected, but the complex that was ultimately chosen was the simplest member of the family, namely  $\text{Cp}^*\text{W}(\text{NO})(\text{CH}_2\text{C}_6\text{H}_5)(\text{CH}_2\text{CMe}_3)$  (**2**). Preliminary investigations by E. Tran had already demonstrated that complex **2** is readily synthesized, is thermally unstable, and forms the corresponding benzylidene derivative,  $\text{Cp}^*\text{W}(\text{NO})(=\text{CHC}_6\text{H}_5)$  (**B**) in situ (Section 1.1.8.3). Complex **B**, in turn, is isolable as the base-stabilized  $\text{PMe}_3$  complex and activates the C-H bonds of toluene. This Chapter begins by expanding on these investigations to further explore the reactivity of **1** and **2** in toluene and confirm the formation of **B** from **2**.

## 2.2 Results and Discussion

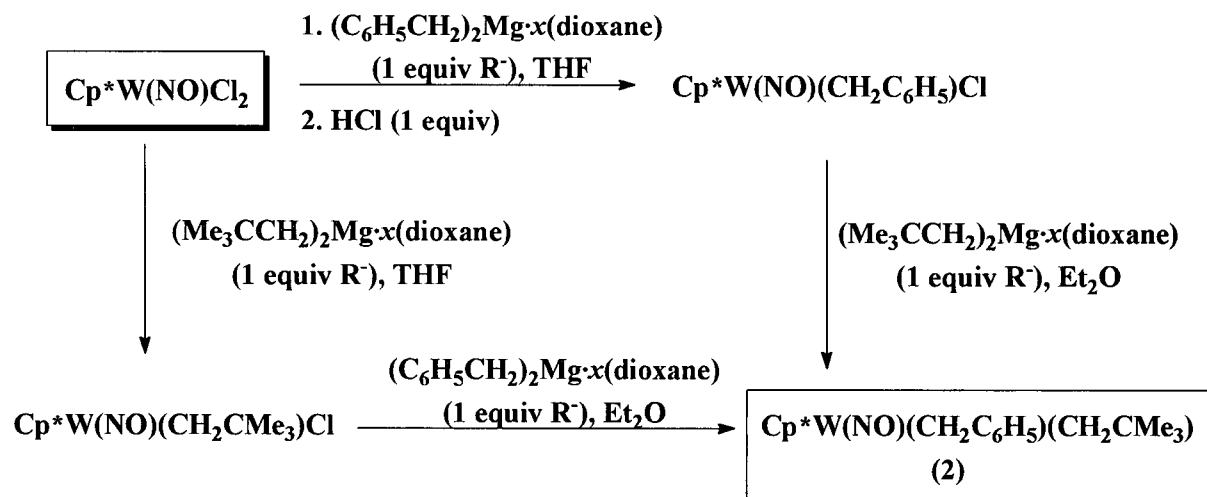
### 2.2.1 Synthesis and Characterization of Complex 2

The original synthesis of **2**<sup>1</sup> was conducted using synthetic methods that are well established in our research group. However, since the preparation of **2** is representative of the preparation of related compounds in this Thesis, the details of this methodology will be reviewed briefly. In addition, complex **2** has several noteworthy characteristics that are relevant to the ensuing discussions in Chapters 2-5.

### 2.2.1.1 Synthesis of Complex 2

The general method employed for the synthesis of hydrocarbyl complexes of the type  $\text{Cp}'\text{W}(\text{NO})(\text{R})(\text{R}')$  ( $\text{Cp}' = \text{C}_5\text{H}_5$  (Cp) or  $\text{Cp}^*$ ;  $\text{R} = \text{R}' = \text{alkyl, aryl, benzyl}$ ) is a sequential alkylation of the dichloro complex,  $\text{Cp}^*\text{W}(\text{NO})\text{Cl}_2$ , using ethereal solvents and  $\text{R}_2\text{Mg}\cdot x(\text{dioxane})$  reagents.<sup>2,3</sup> Both  $\text{Cp}^*\text{W}(\text{NO})(\text{CH}_2\text{CMe}_3)\text{Cl}^2$  and  $\text{Cp}^*\text{W}(\text{NO})(\text{CH}_2\text{C}_6\text{H}_5)\text{Cl}^4$  monohalide complexes can be readily synthesized, providing two possible synthetic routes to **2** (Scheme 2.1). However, the preparation of  $\text{Cp}^*\text{W}(\text{NO})(\text{CH}_2\text{CMe}_3)\text{Cl}$  involves only one synthetic step, so this route to **2** has been employed. Alkylation of  $\text{Cp}^*\text{W}(\text{NO})(\text{CH}_2\text{CMe}_3)\text{Cl}$  by  $(\text{C}_6\text{H}_5\text{CH}_2)_2\text{Mg}\cdot x(\text{dioxane})$  in  $\text{Et}_2\text{O}$  on a 0.5 to 1.5 g scale generates **2** as an orange microcrystalline powder in 70-85 % yield after recrystallization from  $\text{Et}_2\text{O}/\text{hexanes}$ .

**Scheme 2.1**



### 2.2.1.2 Properties of Complex 2

The properties of **2** are consistent with those reported for other benzyl complexes of the type  $\text{Cp}'\text{W}(\text{NO})(\text{CH}_2\text{C}_6\text{H}_5)(\text{R})$  ( $\text{R} = \text{aryl, alkyl, benzyl}$ ).<sup>4,5</sup> It can be handled in air for short periods of time without any visible signs of decomposition. Its IR spectrum exhibits a strong absorbance at  $1538\text{ cm}^{-1}$  attributable to the stretching frequency of a terminal NO linkage. Its  $^1\text{H}$  NMR spectrum exhibits a typical ABXY pattern of doublets attributable to the diastereotopic methylene H atoms of the two hydrocarbyl ligands. The doublets for the benzyl moiety occur at lower field ( $\delta$  2.22 and 2.98) than those of the neopentyl ligand ( $\delta$  -2.35 and 2.20) and have a smaller  $^2J_{\text{HH}}$  coupling constant (8.5 vs 13.4 Hz). The large chemical shift difference between the resonances for the methylene protons of the neopentyl ligand and the negative resonance for the synclinal methylene proton are features typical of alkyl benzyl and mixed alkyl complexes of the  $\text{Cp}'\text{M}(\text{NO})$  fragment.<sup>4,5,6</sup> A notable feature of the  $^{13}\text{C}\{^1\text{H}\}$  NMR spectrum of **2** is the chemical shift of the resonance due to the ipso carbon of the benzyl ligand ( $\delta$  113) which lies well below that of most benzyl ligands ( $\delta > 140$ ). The low chemical shift is indicative of a bonding interaction between the ipso carbon and the major lobe of the metal-based LUMO that lies between the two hydrocarbyl ligands.<sup>7</sup> The  $\eta^2$ -benzyl linkage is present in the solid-state molecular structures of numerous related benzyl congeners (vide infra).<sup>4,5</sup> In solution, however, the  $\eta^2$  interactions in these benzyl complexes are not static. In the case of **2**, variable-temperature gated  $^{13}\text{C}\{^1\text{H}\}$  NMR spectroscopy has revealed that the  $\eta^2$ -benzyl conformation is in equilibrium with another, in which there appears to be an agostic bond<sup>8</sup> between the synclinal methylene C-H bond of the

neopentyl ligand and the metal-based LUMO (Figure 2.1).<sup>6</sup> Such  $\alpha$ -agostic interactions have been detected in several other neopentyl complexes, both in solution and in solid state, the latter having been confirmed by a neutron diffraction analysis.<sup>6</sup> Thus, at room and higher temperatures, complex **2** is rapidly exchanging between these two conformations, with the equilibrium favouring the  $\eta^2$ -benzyl conformation.

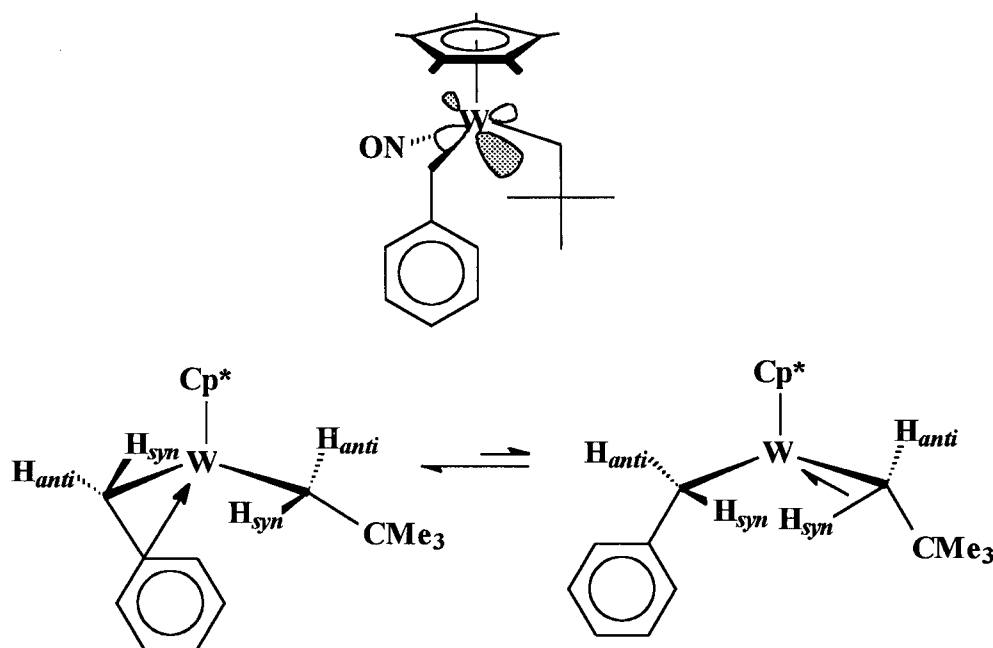
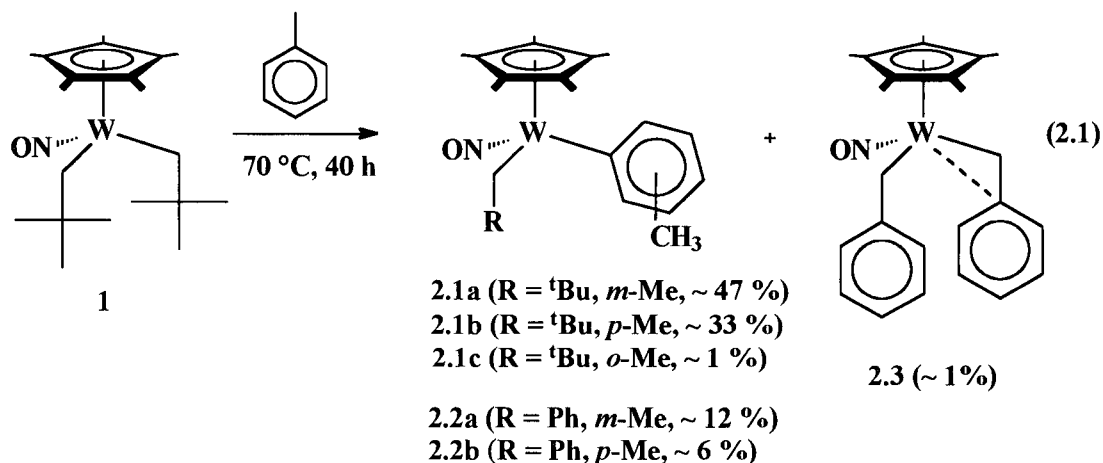


**Figure 2.1.** Qualitative diagram of the metal-based LUMO (top), and the  $\eta^2$ -benzyl and  $\eta^1$ -benzyl/ $\alpha$ -agostic conformations (bottom), of **2**. Note that the complexes on the bottom are rotated about the Cp\* ligand to place the NO ligand behind W, and that the NO ligand is not shown for clarity.

### 2.2.2 Thermolysis of **1** in Toluene Revisited

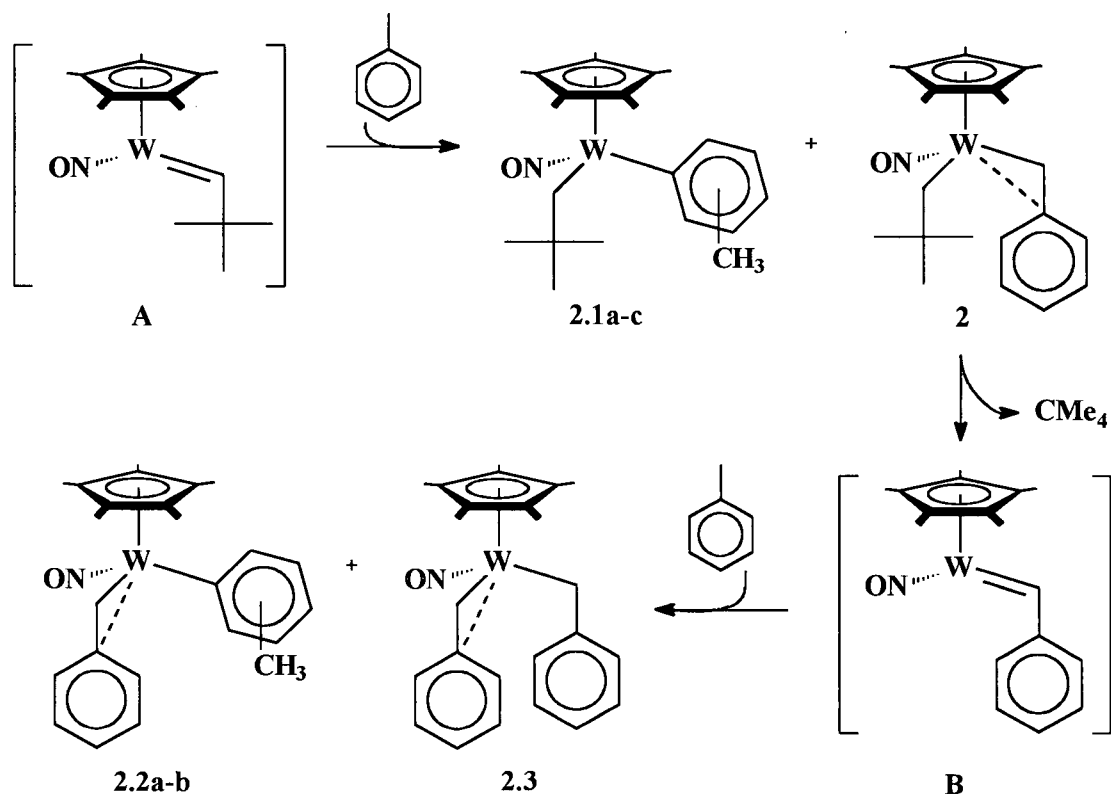
According to previous observations, the thermolysis of **1** in toluene should lead to the formation of **2** via  $sp^3$  C-H bond activation of toluene by **A**. Moreover, **2** is thermally

sensitive and leads to formation of products from the net activation of two molecules of toluene, namely  $\text{Cp}^*\text{W}(\text{NO})(\text{CH}_2\text{C}_6\text{H}_5)(\text{R})$  ( $\text{R} = \text{C}_6\text{H}_4\text{-Me}$  or  $\text{CH}_2\text{C}_6\text{H}_5$ ). To confirm that this process is indeed occurring, the thermolysis of **1** in toluene has been conducted for several days at 70 °C on a sufficient scale to permit monitoring the progress of the reaction by periodic sampling of the reaction mixture. The  $^1\text{H}$  NMR spectroscopic data for the samples obtained from the first 15h of the thermolysis reveal that all four products of the C-H activation of toluene by **A** are formed initially. Specifically, these are the meta and para aryl neopentyl complexes  $\text{Cp}^*\text{W}(\text{NO})(\text{CH}_2\text{CMe}_3)(\text{C}_6\text{H}_4\text{-3-Me})$  (**2.1a**) and  $\text{Cp}^*\text{W}(\text{NO})(\text{CH}_2\text{CMe}_3)(\text{C}_6\text{H}_4\text{-4-Me})$  (**2.1b**) as major products, the ortho aryl neopentyl complex  $\text{Cp}^*\text{W}(\text{NO})(\text{CH}_2\text{CMe}_3)(\text{C}_6\text{H}_4\text{-2-Me})$  (**2.1c**) as a trace product, and **2**. Complexes **2.1a-c** have all been characterized previously.<sup>2,9,10</sup> As the thermolysis progresses, the signals for **2** disappear as those for three new products appear in the  $^1\text{H}$  NMR spectra. The two major products are the meta and para aryl benzyl complexes,  $\text{Cp}^*\text{W}(\text{NO})(\text{CH}_2\text{C}_6\text{H}_5)(\text{C}_6\text{H}_4\text{-3-Me})$  (**2.2a**) and  $\text{Cp}^*\text{W}(\text{NO})(\text{CH}_2\text{C}_6\text{H}_5)(\text{C}_6\text{H}_4\text{-4-Me})$  (**2.2b**), while the minor product is the previously reported bis(benzyl) complex  $\text{Cp}^*\text{W}(\text{NO})(\text{CH}_2\text{C}_6\text{H}_5)_2$  (**2.3**).<sup>4</sup> After 40 h, all of **1** and **2** have been consumed. Integration of appropriate signals in the 40 h  $^1\text{H}$  NMR spectrum reveals that the respective neopentyl and benzyl aryl products **2.1a-b** and **2.2a-b** are present in a 4.3(2):1 ratio (95% confidence limit (CI)), with meta isomers (**2.1a**, **2.2a**) favouring the corresponding para isomers (**2.2b**, **2.2b**) by the respective ratios of 1.45(8):1 and 2.0(2):1. Using these integrations as a basis, the other two products, **2.1c** and **2.3**, were each determined to comprise ~ 1 % of the total activated products, thus yielding the relative product distribution shown in equation 2.1.



Monitoring the thermolysis of **1** in toluene for an additional 24 h past the endpoint of typical thermolysis experiments (64 h total) reveals no significant changes in the ratio of the activated products. This result indicates that the product distribution is essentially fixed after 40 h, and that, once formed, the neopentyl aryl products **2.1a-c** do not convert to the benzyl aryl and bis(benzyl) products **2.2a-b** and **2.3** at any appreciable rate (e.g. by isomerization to **2** and the subsequent formation of **B**). Hence, based on the  $\alpha$ -abstraction mechanism described in Chapter 1, it appears that the products of toluene activation are indeed formed by the process illustrated in Scheme 2.2.

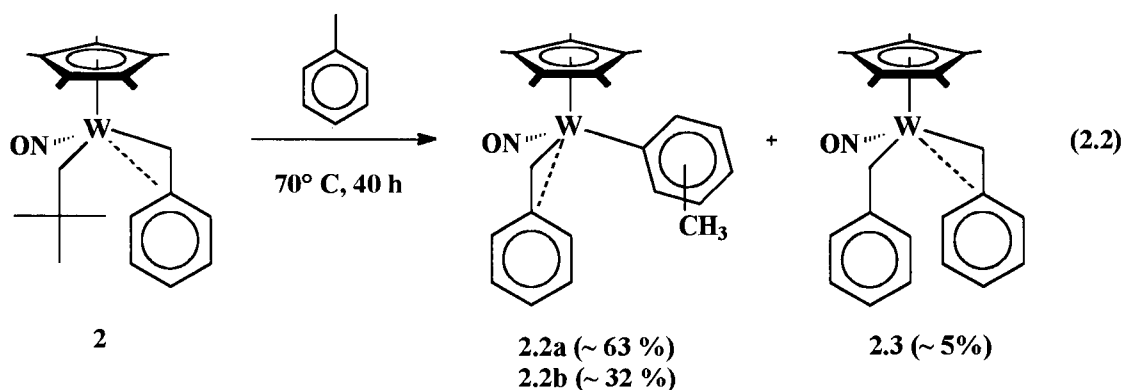
Scheme 2.2



It should be noted that after the mixture was heated for an additional 24 h, product decomposition was observed, as indicated by the appearance of a small cluster (~ 5 - 10 %) of new Cp\* signals in the  $^1\text{H}$  NMR spectrum. These signals gradually increase in intensity upon prolonged heating of the mixture. While several processes could cause this decomposition, it may be noted that the related neopentyl phenyl complex,  $\text{Cp}^*\text{W}(\text{NO})(\text{CH}_2\text{CMe}_3)(\text{C}_6\text{H}_5)$  (**1.1**), decomposes in arene solvents at elevated temperatures through loss of neopentane (110 °C, 6 h).<sup>11</sup> The major products in the thermolysis mixture **2.1a-b** likely undergo the same process, but more slowly under these thermal conditions.

### 2.2.3 Thermolysis of 2 in Toluene

Thermolysis of independently prepared **2** in toluene for 40 h at 70 °C cleanly generates the same aryl and benzyl products of toluene activation observed from the reaction of **1** in toluene, namely **2.2a-b** and **2.3**. The product distribution is also the same, within error, as judged by integration of signals in the  $^1\text{H}$  NMR spectrum of the final reaction mixture (**2.2a** : **2.2b** = 1.97(11):1 and **2.2a-b** : **2.3** = 18.6(1.2):1) (eq 2.2). The product of ortho  $\text{sp}^2$  C-H bond activation, namely  $\text{Cp}^*\text{W}(\text{NO})(\text{CH}_2\text{C}_6\text{H}_5)(\text{C}_6\text{H}_4\text{-2-Me})$  (**2.2c**), was not observed. Complex **2.2a** can be isolated as a crystalline solid from this reaction mixture in adequate yield (25%), and its spectral characteristics are indeed those of the meta isomer. Complex **2.2b** can only be further characterized spectroscopically in the crude reaction mixture, but its spectral features are fully consistent with it being the para isomer. Both **2.2a** and **2.2b** possess  $\eta^2$ -benzyl ligands characterized by the ipso carbon resonances at  $\delta \sim 114$  in their  $^{13}\text{C}$  NMR spectra.



### 2.2.4 A Note on the Thermolyses Conditions for 1 and 2

Heating the thermolysis mixture generated from **2** in toluene for prolonged periods ( $\geq 48$  h), or conducting the experiment at higher temperatures ( $\geq 75$  °C), results

in the partial decomposition of the C-H activation products. Similar results were obtained when conducting the thermolyses of **2** in other solvents. The decomposition could also be observed during the independent thermolysis of purified products in their parent solvent.

It would appear, then, that the C-H activation products derived from **1** or **2** can exhibit some degree of thermal instability, thereby suggesting that the temperature and time of thermolysis are factors to consider when conducting these experiments. Product decomposition becomes a particularly important issue in the situations when the relative distributions of the C-H activated products need to be determined: decomposition of only some of the activated products in the final reaction mixture will skew the product yields towards the most stable products and cause any assessment of the relative yield to become inaccurate when compared to the relative yields actually obtained by the C-H bond activation event. Given this problem, the thermolysis conditions were fixed for both complexes **1** and **2** at temperature = 70 °C, and time = 40 h. The latter condition is a convenient time period for the reaction, since the 40 h period fits well into the workweek. More importantly, nearly all thermolyses conducted under these conditions generated final reaction mixtures whose NMR spectra show < 5 % residual **1** or **2**, and < 5 % decomposition products. When desired, relative product distributions could then be determined by integration of appropriate signals in the <sup>1</sup>H NMR spectrum of the product mixtures and can be considered to be accurate assessments of the actual relative yield of each product as initially formed from **A** or **B**, within the errors associated with the specific integrations.

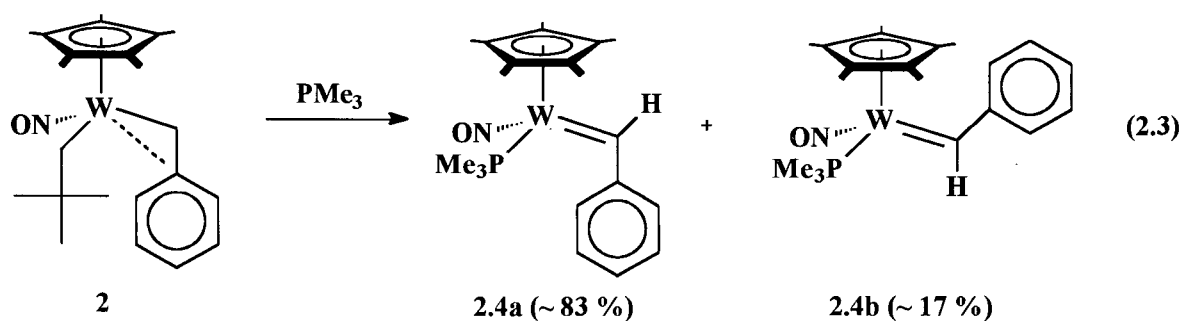
### 2.2.5 Trapping of the Reactive Benzylidene Complex

Intermediate **B** has previously been isolated in base-stabilized form as the  $\text{PMe}_3$  adduct, namely  $\text{Cp}^*\text{W}(\text{NO})(=\text{CHC}_6\text{H}_5)(\text{PMe}_3)$  (**2.4a**).<sup>1</sup> However, at that time, complex **2.4a** was only characterized to confirm its formulation, and the stereochemistry as well as other structural features of the complex were not deduced. In addition, the related reaction of **1** with  $\text{PMe}_3$ ,<sup>9</sup> as well as that of a molybdenum analogue of **1**,  $\text{CpMo}(\text{NO})(\text{CH}_2\text{CMe}_3)_2$ ,<sup>12</sup> both generate two isomeric phosphine-trapped alkylidene complexes, the major isolable one with the alkylidene R substituent anticlinal to the  $\text{Cp}^*$  ligand and the minor with the synclinal orientation.<sup>13</sup>

To ascertain whether **2.4a** is in fact the anticlinal isomer and to determine if an isomer of **2.4a** is formed, the thermolysis of **2** has been conducted in THF in the presence of excess  $\text{PMe}_3$  (~ 130 equiv). Analysis of the final reaction mixture by NMR spectroscopy does reveal the presence of two alkylidene complexes, assigned as **2.4a** and **2.4b** in a ~ 5:1 ratio (eq 2.3). Complex **2.4a** can be isolated as an orange crystalline solid by recrystallization of the crude reaction mixture in THF/hexanes (52% yield), and its NMR properties are consistent with the data obtained previously. Notable features are the high-field NMR resonances for the benzylidene proton ( $\delta$  12.01,  $^1J_{\text{HP}} = 3.8$  Hz) and the benzylidene carbon ( $\delta$  261.2,  $^2J_{\text{CP}} = 9$  Hz) which are diagnostic values for alkylidene linkages.<sup>14</sup> The observation of NOE enhancements between the  $\text{Cp}^*$  ring and the benzylidene H atom as detected by  $^1\text{H}$ - $^1\text{H}$  NOE difference spectroscopy suggests an anticlinal orientation of the  $\text{Cp}^*$  and Ph groups in **2.4a**. Complex **2.4b** can be characterized spectroscopically in the final reaction mixture. It also exhibits diagnostic

benzylidene resonances for the benzylidene  $\alpha$ -H ( $\delta$  13.70) and  $\alpha$ -C ( $\delta$  262.5) atoms.

Moreover, the  $^1\text{H}$ - $^1\text{H}$  NOE spectroscopic features of **2.4b** are consistent with it being the synclinal geometric isomer of **2.4a**. Thus, the stereochemistry and relative distribution of the  $\text{PMe}_3$ -trapped complexes of **B** are the same as those reported for **1** and the molybdenum analogue. In addition, while **2.4a-b** do not interconvert at room temperature on the NMR timescale (as indicated by the lack of magnetization transfer during the NOE experiments), the complexes do interconvert upon prolonged heating at elevated temperatures. Specifically, complex **2.4a** forms a mixture of **2.4a-b** when heated in benzene- $d_6$  (16 h, 80 °C), as detected by  $^1\text{H}$  NMR spectroscopy. The interconversion of alkylidene isomers by rotation around the  $\text{M}=\text{C}$  bond is a common phenomenon.<sup>15</sup>



### 2.2.6 Solid-State Molecular Structure of Complex 2.4a

A single crystal of **2.4a** has been subjected to an X-ray crystallographic analysis to confirm its stereochemistry, as well as to determine the metrical parameters of the benzylidene linkage.<sup>16</sup> The resulting ORTEP diagram is shown in Figure 2.2. The overall geometry of **2.4a** is best described as a three-legged piano stool and is similar to

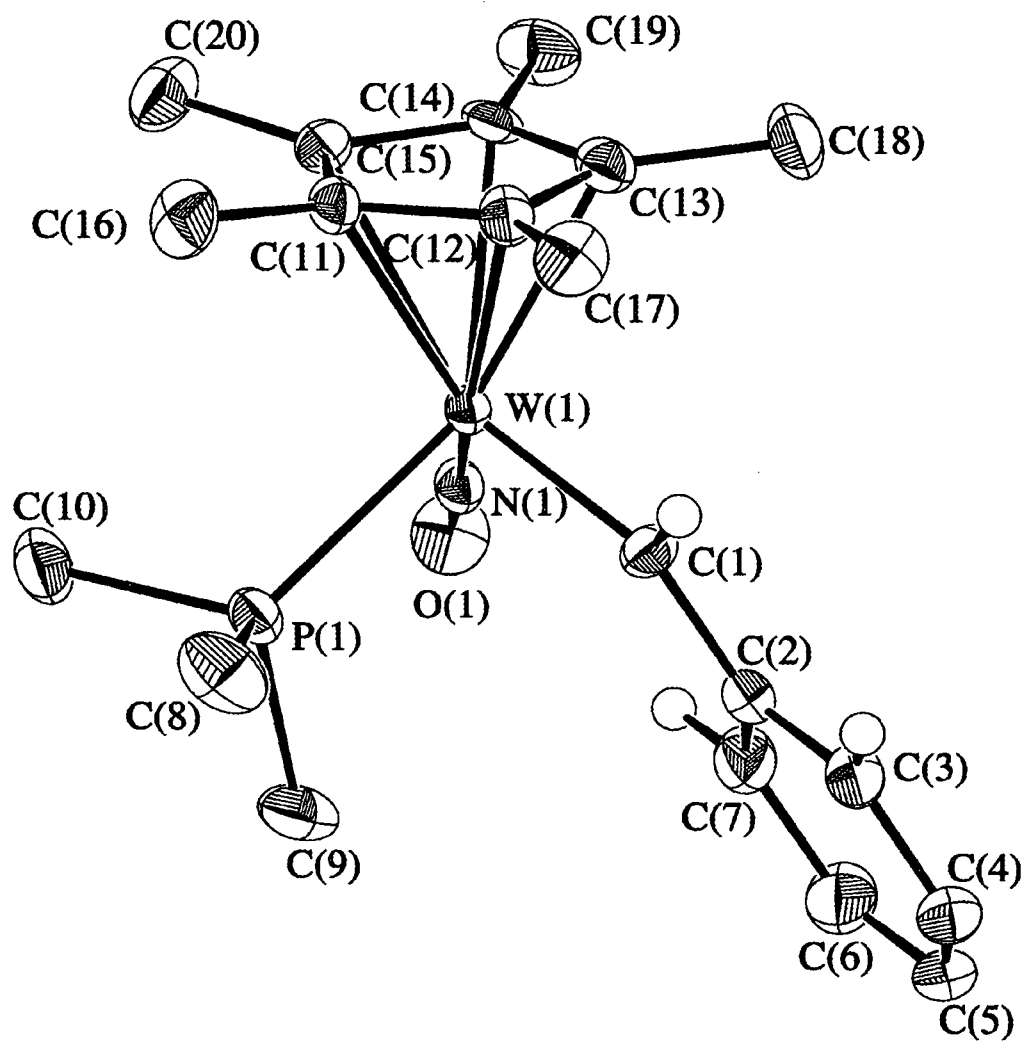


**Figure 2.2.** ORTEP plot of the solid-state molecular structure

$\text{Cp}^*\text{W}(\text{NO})(=\text{CHC}_6\text{H}_5)(\text{PMe}_3)$  (**2.4a**) with 50% probability ellipsoids. Selected bond lengths ( $\text{\AA}$ ) and angles ( $^\circ$ );  $\text{W}(1)\text{-C}(1) = 1.975(3)$ ,  $\text{N}(1)\text{-O}(1) = 1.244(6)$ ,  $\text{W}(1)\text{-N}(1)\text{-O}(1) = 178.1(3)$ ,  $\text{W}(1)\text{-C}(1)\text{-C}(2) = 137.2(2)$ ,  $\text{W}(1)\text{-C}(1)\text{-C}(2)\text{-C}(3) = -171.3(3)$ ,  $\text{N}(1)\text{-W}(1)\text{-(C1)-C}(2) = -8.3(4)$ .

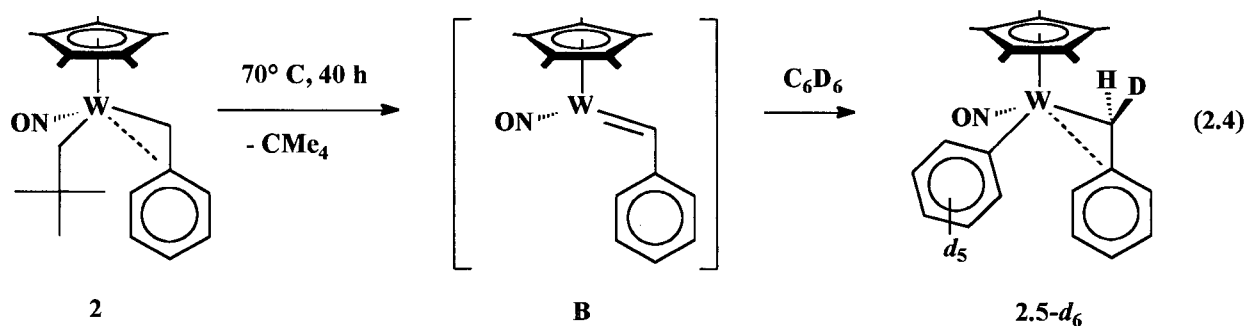
that of its neopentylidene analogue. The benzylidene linkage has a short W=C bond (1.975(3) Å) and an obtuse W-CH-R bond angle (137.2(2)°), typical of tungsten alkylidene complexes in general.<sup>17</sup> In addition, there is a nearly planar N(1)-W(1)-C(1)-C(2) grouping (-8.3(4)°), consistent with the maximization of the synergic  $\pi$ -bonding between the  $\pi$ -donor alkylidene and  $\pi$ -acceptor NO ligands.<sup>13,18</sup> The phenyl group of the benzylidene ligand is indeed anticlinal to the Cp\* group, consistent with the preferred conformation of several other isostructural alkylidene complexes.<sup>19</sup> Finally, a structural feature unique to benzylidene linkages is the planar alignment of the phenyl and W=C moieties (W(1)-C(1)-C(2)-C(3) = 171.3(3)°) which is indicative of conjugation of the alkylidene and phenyl  $\pi$ -systems.<sup>19</sup>

### 2.2.7 Comparison of Mechanistic Features of the Neopentylidene and Benzylidene Systems: Thermolysis of Complex **2** in Benzene and Benzene-*d*<sub>6</sub>

With the formation of benzylidene **B** from **2** firmly established, the general features of the benzylidene and neopentylidene systems can be compared. With regards to the mechanism, it has previously been determined that the activation process derived from **1** proceeds via (1) rate-limiting intramolecular  $\alpha$ -H elimination of neopentane to form the anticlinal alkylidene complex, and (2) 1,2-cis addition of R-H across the W=C linkage of the alkylidene complex. To see if the benzylidene system is the same or different with respect to these mechanistic features, complex **2** has been thermolysed in benzene and benzene-*d*<sub>6</sub>.

In benzene, the benzyl phenyl complex Cp\*W(NO)(CH<sub>2</sub>C<sub>6</sub>H<sub>5</sub>)(C<sub>6</sub>H<sub>5</sub>) (**2.5**) forms via sp<sup>2</sup> C-H bond activation as anticipated. Complex **2.5** exhibits two doublet resonances

at  $\delta$  2.14 and 3.41 in its  $^1\text{H}$  NMR spectrum for the syn- and anticlinal methylene protons of the benzyl ligand respectively, as determined by NOE difference spectroscopy. Thermolysis of **2** in benzene- $d_6$  under these conditions cleanly forms  $\text{Cp}^*\text{W}(\text{NO})(\text{CHDC}_6\text{H}_5)(\text{C}_6\text{D}_5)$  (**2.5- $d_6$** ), in which a deuterium resonance is observed at  $\delta$  2.15 in the  $^2\text{H}\{^1\text{H}\}$  NMR spectrum. The exclusive incorporation of the label at the synclinal position of the neopentyl ligand is consistent with the cis addition of C-H (C-D) across the  $\text{M}=\text{C}$  linkage of an anticlinal benzyldiene intermediate (eq 2.4). Hence, the stereochemistries of the reactive alkylidene intermediates derived from **1** and **2** are the same.



Similarly, the side-by-side monitoring the rates of reaction of **2** and **1** in benzene- $d_6$  over 15 h at 72.0 °C by  $^1\text{H}$  NMR spectroscopy reveals that both **1** and **2** decompose by first-order processes and eliminate neopentane, with respective rate constants of  $4.6(1) \times 10^{-5} \text{ s}^{-1}$  for **1** ( $R^2 = 0.999$ ) and  $4.9(1) \times 10^{-5} \text{ s}^{-1}$  for **2** ( $R^2 = 0.999$ ) (see Appendix B for plots of the data). The rate constants are very similar to each other ( $k_2/k_1 = 1.07$ ), as well as to that of **1** in cyclohexane/ $\text{PMe}_3$  at 72 °C ( $5.3 \times 10^{-5} \text{ s}^{-1}$ ). These results are fully consistent with the formation of benzyldiene **B** from **2** by the same intramolecular  $\alpha$ -H cleavage process that generates neopentylidene **A** from **1**.

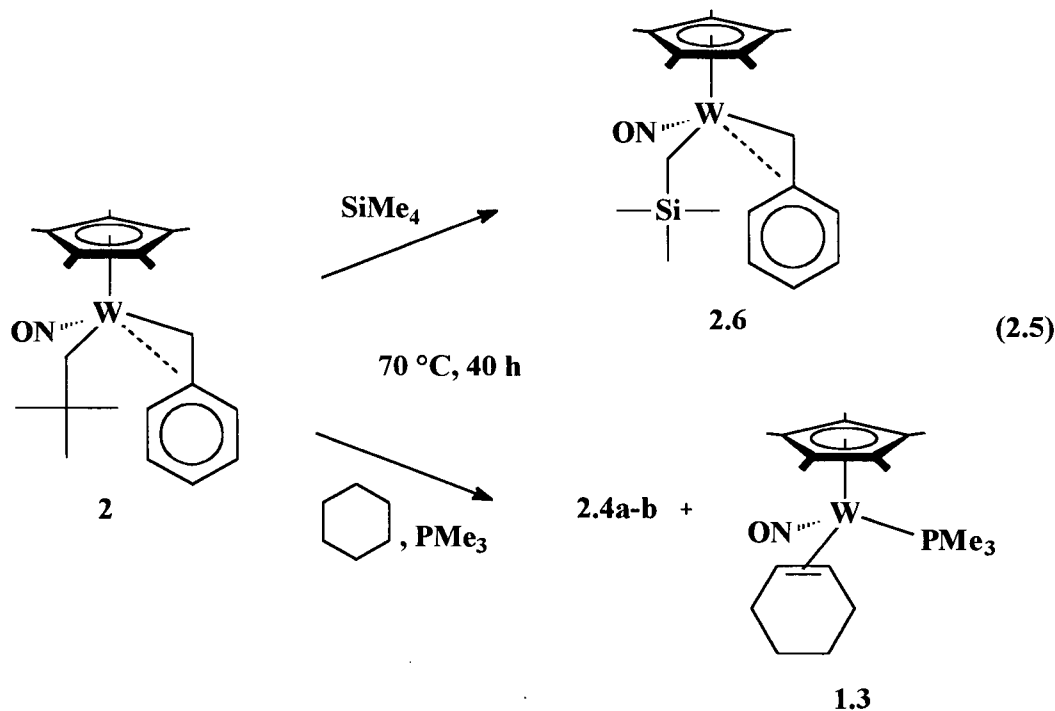
## 2.2.8 Comparison of Scope of Substrate Activation Mediated by A and B:

### Thermolysis of 2 in Alkanes

In terms of the scope of the activation chemistry, the work described in Section 2.2.3 has established that benzyldiene **B** can activate the  $sp^2$  and  $sp^3$  C-H bonds of toluene to yield the corresponding aryl and benzyl complexes. However, it has not yet been demonstrated that the activation ability of **B** encompasses alkane substrates as well. In the C-H activation literature, there are indeed examples of complexes that activate the C-H bonds of arenes to yield isolable products, but do not activate the aliphatic  $sp^3$  C-H bonds of alkane substrates.<sup>20</sup> To see if benzyldiene **B** is similarly limited in its C-H activation ability, complex **2** has been thermolysed in three representative aliphatic substrates, as described below.

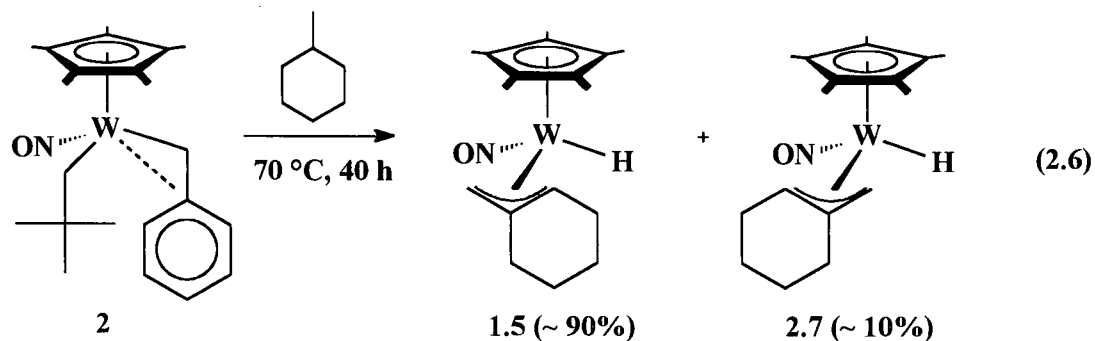
#### 2.2.8.1 Thermolysis of 2 in Tetramethylsilane and in Cyclohexane/ $PMe_3$

The thermolysis of **2** in neat tetramethylsilane (at 70 °C for 40 h) yields the  $Cp^*W(NO)(CH_2C_6H_5)(CH_2SiMe_3)$  (**2.6**) in ~ 95% yield as judged by  $^1H$  NMR spectroscopy (eq 2.5). Complex **2.6** is the product of C-H activation of tetramethylsilane and has been prepared previously by other means.<sup>4</sup> Likewise, the thermolysis of **2** in cyclohexane in the presence of  $PMe_3$  (~ 20 equiv) generates  $Cp^*W(NO)(\eta^2\text{-cyclohexene})(PMe_3)$  (**1.3**) via  $2^\circ$   $sp^3$  C-H bond activation, in addition to the alkylidene complexes **2.4a-b** (**1.3** : **2.4a-b**  $\cong$  1 : 10). Hence, it appears that **B** can activate both the  $1^\circ$  and  $2^\circ$   $sp^3$  C-H bonds of aliphatic substrates.



### 2.2.8.2 Thermolysis of 2 in Methylcyclohexane

Thermolysis of **2** in methylcyclohexane results in the formation of two principal activation products in a 9(1):1 ratio. A plethora of additional, but weak, signals is also observed in the Cp\* and aromatic regions of the  $^1\text{H}$  and  $^{13}\text{C}\{^1\text{H}\}$  NMR spectra (< 10 % as judged by  $^1\text{H}$  NMR) (eq 2.6).



The major product is the previously characterized allyl hydride complex,  $\text{Cp}^*\text{W}(\text{NO})(\eta^3\text{-C}_7\text{H}_{11})(\text{H})$  (**1.5**), which contains a terminal *cis, endo*- $\eta^3$ -allyl linkage (see Section 1.1.8.2). The identity of the minor product (**2.7**) has been resolved by gated- $^{13}\text{C}$   $\{^1\text{H}\}$  NMR and NOE spectroscopic analyses of the reaction mixture. For comparison, **1.5** exhibits a high-field,  $\text{sp}^3$ -like resonance for the exocyclic allyl carbon that is *cis* to the NO ligand ( $\delta$  41.3 (t,  $^1J_{\text{CH}} = 155$  Hz,  $\text{CH}_2$ )), and low-field,  $\text{sp}^2$ -like resonances for the endocyclic allyl carbons ( $\delta$  80.0 (d,  $^1J_{\text{CH}} = 148$  Hz, CH), 121.1 (s, C)). These spectral features are typical of allyl ligands attached to the  $\text{Cp}'\text{M}(\text{NO})(\text{L})$  ( $\text{L} = 2\text{e}$  donor) and  $\text{Cp}'\text{M}(\text{NO})(\text{X})$  ( $\text{X} = 1\text{e}$  donor) fragments, since the  $\pi$ -acceptor NO ligand induces a  $\eta^3 \rightarrow \sigma$ - $\pi$  distortion in which the allyl carbons *trans* to the NO linkage adopt  $\text{sp}^2$ -like characteristics.<sup>18a,21</sup> This distortion is also evident in the solid-state molecular structure of **1.5**.<sup>9</sup> NOE difference spectroscopy on complex **1.5** reveals a *cis* arrangement of the hydride ligand and the allyl CH atom in solution, consistent with the structure depicted in eq 2.6.

For the minor allyl hydride product **2.7**, two resolvable signals can be attributed to its allyl carbons in the gated- $^{13}\text{C}\{^1\text{H}\}$  NMR spectrum, based on the magnitude of the coupling constants ( $\delta$  49.7 (t,  $^1J_{\text{CH}} = 155$ ) and 62.8 (d,  $^1J_{\text{CH}} = 146$ )). The triplet and doublet resonances are only consistent with an exocyclic allyl ligand, thereby identifying **2.7** as one of three terminal allyl isomers of **1.5**. By NOE difference spectroscopy, the allyl  $\text{CH}_2$  group and the hydride ligand are *cis* to each other, suggesting that complex **2.7** is either the *exo* or *endo trans*- $\eta^3$ -allyl isomer. Unfortunately, the *exo* or *endo* configuration of **2.7** could not be conclusively established by the NOE experiments, but

given the steric bulk of the cyclohexyl ring, **2.7** is most likely the trans, endo isomer as shown in equation 2.6. A small amount of spin-saturation transfer is observed between the allyl CH atoms of **1.5** and **2.7** in the NOE difference spectra, thus indicating that **1.5** and **2.7** interconvert on the NMR timescale at room temperature, likely by rotation around the terminal C-C bond of an unobserved  $\eta^1$ -allyl intermediate.<sup>22</sup> The rapid interconversion of the allyl products in solution indicates that the product distribution is under thermodynamic control.

### 2.2.8.3 Thermolysis of **1** in Methylcyclohexane Revisited

Curiously, a second allyl hydride product was not reported for the original thermolysis of **1** in methylcyclohexane,<sup>1</sup> despite the fact that **1.5** is in equilibrium with **2.7** when obtained from **2**. To probe this discrepancy, complex **1** has been thermolysed again in methylcyclohexane under the same conditions as **2** (70 °C, 40 h). Not surprisingly, the resulting <sup>1</sup>H NMR spectrum reveals the same relative distribution of allyl hydride products **1.5** and **2.7** (9(1):1 ratio). The formation of both **1.5** and **2.7** from **1** is also consistent with the reported results of the thermolysis of **1** in other alkanes such as pentane and ethylcyclohexane for which minor allyl hydride products were noted to be present in the final product mixture.<sup>1</sup> Notably, the spectrum obtained from **1** contains is cleaner (> 95% conversion to **1.5** and **2.7**) as determined by the lack of additional peaks in the Cp\* region. This result implies that the additional trace products observed from the thermolysis of **2** in this solvent result from either inefficient activation of methylcyclohexane by **B**, or from the subsequent inefficient dehydrogenation of the resulting cyclohexylmethyl ligand by  $\beta$ -H elimination of toluene. Consequently,

complex **1** would appear to be the reagent of choice for conducting the activations of acyclic alkanes and alkyl-substituted cycloalkanes.

### 2.2.9 Summary of the Comparisons of the Neopentylidene and Benzylidene Systems Presented Thus Far

Taken together, the results in Sections 2.2.2 to 2.2.8 indicate that there are few differences between the benzylidene and neopentylidene systems. There appear to be no significant differences in the basic mechanistic features of the formation and reactivity of the alkylidene intermediates **A** and **B**. Likewise, there are no discernable differences in the range of alkane and arene substrates that can be activated by **A** and **B**. The similarities in the scope of the activation chemistry of the benzylidene and neopentylidene systems is in sharp contrast to the related  $\text{Cp}_2\text{Ti}=\text{NR}$  system, where the replacement of an alkyl R substituent with an aryl substituent renders the imido complex unreactive towards hydrocarbons.<sup>23</sup>

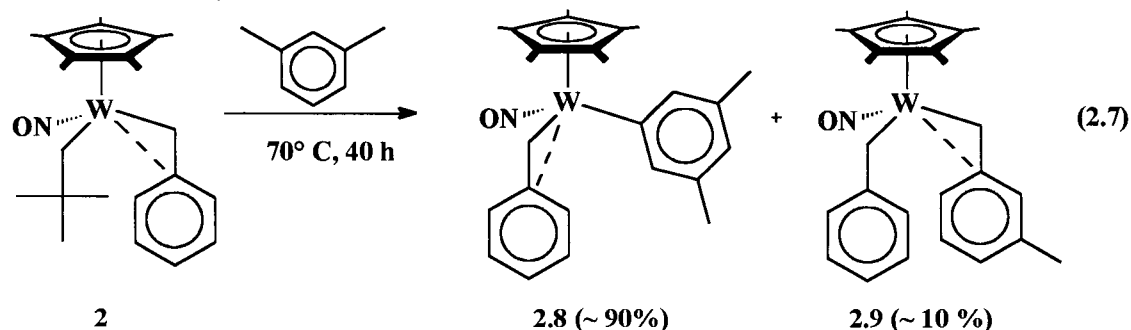
In terms of individual substrates, there appear to be no significant differences in the types of products obtained from alkane activation by **B** vs **A**, although, for reasons stated above, the novel triple C-H activation of alkane substrates such as methylcyclohexane is mediated more cleanly by the neopentylidene system. Significant differences are apparent, however, in the relative product selectivities for the activation of toluene of **B** vs **A**. In both cases, the aryl products of  $\text{sp}^2$  C-H bond activation are formed preferentially over the benzyl products of  $\text{sp}^3$  C-H bond activation, but the ratios of aryl vs benzyl products are not the same. The ratio of aryl vs benzyl products from toluene activation by **A** is 4.2(3):1,<sup>24</sup> which is much smaller than that obtained from toluene

activation by **B** (18.6(1.2):1). Likewise, the distribution of aryl regioisomers derived from toluene activation by **A** and **B** both favour the meta and para isomers. Yet, the distribution obtained from **A** significantly favours the para isomer (meta : para = 1.45(8):1), while the distribution obtained from **B** is the statistical meta: para distribution of 2:1 (1.97(11):1). Moreover, the ortho aryl complex is observed as a trace product in the activation mediated by **A**, but is not observed in the activation mediated by **B**.

In addition to these differences, the activation of toluene in both cases generates different organometallic products derived from the activation of more than one type of C-H bond within the molecule. Hence, it would appear that studying the activation of substituted arenes provides a means to quantify the relative product distributions for substrates containing more than one type of C-H bond, and thus a means to identify the factors that control these distributions. To that end, both **1** and **2** have been thermolysed in other selected arene solvents, as described below.

### 2.2.10 Thermolysis of **2** in *m*-Xylene

Thermolysis of **2** in *m*-xylene for 40 h at 70 °C results in the formation of two products, namely  $\text{Cp}^*\text{W}(\text{NO})(\text{CH}_2\text{C}_6\text{H}_5)(\text{C}_6\text{H}_3\text{-3,5-Me}_2)$  (**2.8**) and  $\text{Cp}^*\text{W}(\text{NO})(\text{CH}_2\text{C}_6\text{H}_5)(\text{CH}_2\text{C}_6\text{H}_4\text{-3-Me})$  (**2.9**), in > 95% overall yield as determined by  $^1\text{H}$  NMR spectroscopy (eq 2.7). Two independent thermolyses were conducted to assess the reproducibility of the experiments; the product ratios obtained (9.1(5):1 and 9.4(5):1 (95% CI)) are statistically the same. No signals for any additional C-H activation products were detected in the  $^1\text{H}$  NMR spectrum obtained from either experiment.



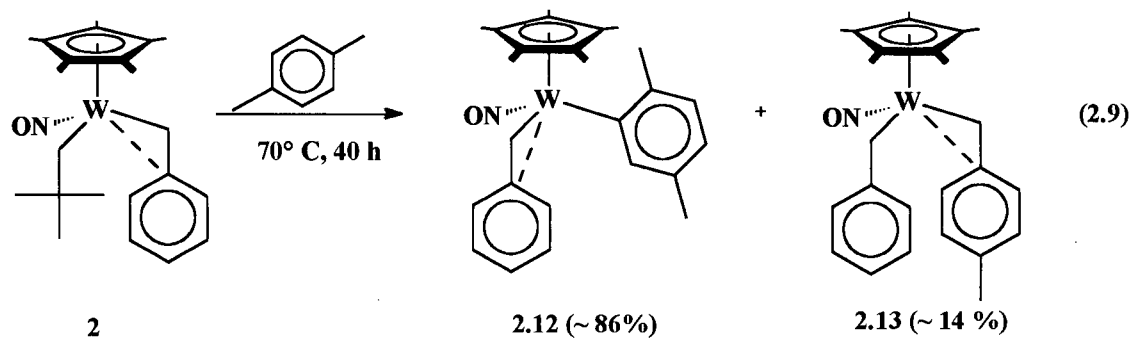
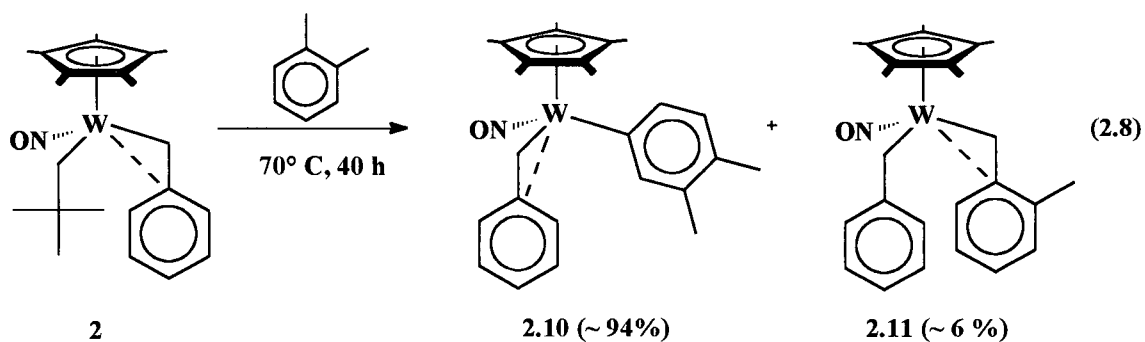
The major product is the aryl benzyl complex **2.8** derived from  $sp^2$  C-H bond activation of a solvent molecule. It has been isolated by crystallization from 3:1  $\text{Et}_2\text{O}$ /hexanes in sufficient yield (29 %) to permit full characterization. Its  $^1\text{H}$  NMR spectrum exhibits a distinct  $^1\text{H}$ - $^1\text{H}$  coupling pattern in the aromatic region that conclusively identifies it as the 3,5-dimethyl aryl isomer. The signal for the ortho H protons is a broad hump (21 Hz at half-height), rather than a distinct doublet, and is the farthest downfield of the aromatic signals ( $\delta$  6.29). Similar features have been observed for the ortho H protons in other alkyl aryl complexes (vide infra).<sup>10</sup> The ipso carbon resonance in its  $^{13}\text{C}\{^1\text{H}\}$  NMR spectrum ( $\delta$  114.8) is indicative of an  $\eta^2$ -benzyl ligand.

The minor product of the thermolysis, **2.9**, is derived from  $sp^3$  C-H bond activation of *m*-xylene, as identified by spectroscopic analysis of the final reaction mixture. It has diagnostic resonances for the ABXY methylene doublets, plus a coupling pattern in the aryl region consistent with a (3-methyl)benzyl ligand. Complex **2.9** has also been prepared independently by metathesis from  $\text{Cp}^*\text{W}(\text{NO})(\text{CH}_2\text{C}_6\text{H}_5)\text{Cl}$  to confirm these assignments. The most notable spectral features of **2.9** are the two distinct ipso carbon resonances in the  $^{13}\text{C}\{^1\text{H}\}$  NMR spectrum ( $\delta$  113.9 and 142.3), and the pair of methylene resonances with the lowest chemical shifts that correlate to the benzyl ligand

rather than the (3-methyl)benzyl ligand. These features indicate that, in solution on average, the more electron-rich substituted benzyl ligand is attached in an  $\eta^2$  fashion to the metal center (vide infra).<sup>4,5</sup>

### 2.2.11 Thermolysis of **2** in *o*- and *p*-Xylene

Similar results are obtained from the thermolysis of **2** in *o* and *p*-xylene. In *o*-xylene, the aryl and benzyl products of *o*-xylene activation, namely  $\text{Cp}^*\text{W}(\text{NO})(\text{CH}_2\text{C}_6\text{H}_5)(\text{C}_6\text{H}_3\text{-3,4-Me}_2)$  (**2.10**) and  $\text{Cp}^*\text{W}(\text{NO})(\text{CH}_2\text{C}_6\text{H}_5)(\text{CH}_2\text{C}_6\text{H}_4\text{-2-Me})$  (**2.11**), form in a 14.6(4):1 ratio (eq 2.8). In *p*-xylene, the aryl and benzyl activation products  $\text{Cp}^*\text{W}(\text{NO})(\text{CH}_2\text{C}_6\text{H}_5)(\text{C}_6\text{H}_3\text{-2,5-Me}_2)$  (**2.12**) and  $\text{Cp}^*\text{W}(\text{NO})(\text{CH}_2\text{C}_6\text{H}_5)(\text{CH}_2\text{C}_6\text{H}_4\text{-4-Me})$  (**2.13**) are detected in a 6.2(4):1 ratio (eq 2.9).



The minor benzyl products of solvent activation **2.11** and **2.13** are readily identified in the final reaction mixture by the ABXY doublets from the methylene hydrogen atoms in the  $^1\text{H}$  NMR spectra. The aryl products **2.10** and **2.12** can be isolated by crystallization in adequate yield (30-40 %) and have been fully characterized. The regiochemistries of the aryl ligands in **2.10** and **2.12** are readily identified by the distinct coupling patterns in the aromatic region of the respective  $^1\text{H}$  NMR spectra. Both **2.10** and **2.12** have features similar to **2.8**, namely  $\eta^2$ -benzyl ligands and broadened, downfield resonances for the ortho H atoms of the aryl ligands. Of note, complex **2.12** also exhibits a broadened signal for one of the methyl groups of the *p*-xylyl ligand, as well as a broadened signal for the synclinal methylene H atom of the benzyl ligand. The related neopentyl complex,  $\text{Cp}^*\text{W}(\text{NO})(\text{CH}_2\text{CMe}_3)(\text{C}_6\text{H}_3\text{-2,5-Me}_2)$  (**1.7**), exhibits even broader features for its *p*-xylyl ligand in its  $^1\text{H}$  NMR spectrum.<sup>1</sup> VT NMR analysis of **1.7** has demonstrated that the room temperature spectrum is actually a time-averaged spectrum of two interconverting isomers related by rotation about the M-C bond of the *p*-xylyl ligand. Presumably, the broadened features of **2.8**, **2.10** and **2.12** are induced by a similar rapid interconversion at room temperature.

### 2.2.12 The Solid-State Molecular Structure of Complex 2.12

The solid-state molecular structure of **2.12** has been determined by X-ray crystallography.<sup>25</sup> The resulting ORTEP is shown in Figure 2.3. An obvious structural feature of the three-legged piano-stool structure is the  $\eta^2$ -benzyl ligand, which is characterized by a short W-C<sub>ipso</sub> bond distance (W(1)-C(2) = 2.554(4)) and the acute W-C-C<sub>ipso</sub> bond angle (W(1)-C(1)-C(2) = 86.4(3)). Another interesting feature of the structure is the preferred orientation and metrical parameters of the *p*-xylyl ligand. The

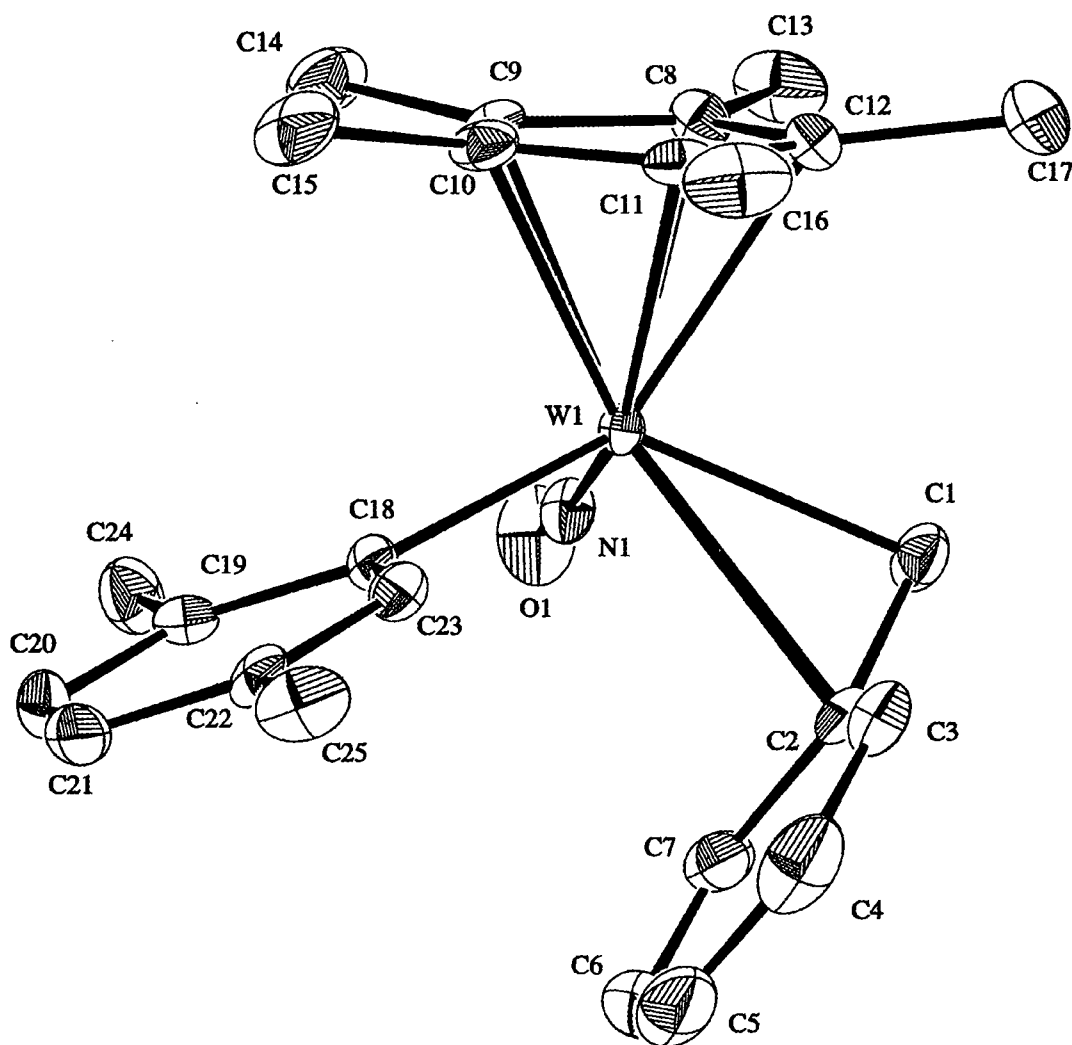
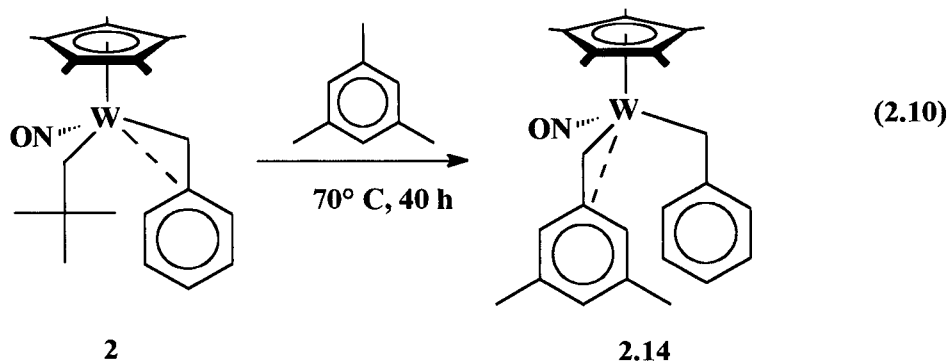


**Figure 2.3.** ORTEP plot of the solid-state molecular structure of  $\text{Cp}^*\text{W}(\text{NO})(\text{CH}_2\text{C}_6\text{H}_5)(\text{C}_6\text{H}_3\text{-2,5-Me}_2)$  (**2.12**) with 50% probability ellipsoids. Selected bond lengths ( $\text{\AA}$ ) and angles ( $^\circ$ );  $\text{W}(1)\text{-C}(1) = 2.191(4)$ ,  $\text{W}(1)\text{-C}(2) = 2.554(4)$ ;  $\text{W}(1)\text{-C}(18) = 2.181(3)$ ,  $\text{N}(1)\text{-O}(1) = 1.224(4)$ ,  $\text{W}(1)\text{-N}(1)\text{-O}(1) = 169.3(3)$ ,  $\text{W}(1)\text{-C}(1)\text{-C}(2) = 86.4(3)$ ,  $\text{C}(18)\text{-W}(1)\text{-C}(2) = 124.7(1)$ ,  $\text{N}(1)\text{-W}(1)\text{-C}(18) = 98.6(1)$ ,  $\text{W}(1)\text{-C}(18)\text{-C}(19) = 128.2(2)$ ,  $\text{W}(1)\text{-C}(18)\text{-C}(23) = 115.5(3)$ ,  $\text{N}(1)\text{-W}(1)\text{-C}(18)\text{-C}(19) = -23.3(4)$ ,  $\text{W}(1)\text{-C}(18)\text{-C}(23)\text{-C}(22) = -179.0(3)$ .

W-C-C bond angle to the ortho carbon is distorted from the expected bond angle of  $120^\circ$  ( $128.2(2)^\circ$ ). This conformation places the ortho methyl group *cis* to the NO ligand ( $\text{N}(1)\text{-W}(1)\text{-C}(18)\text{-C}(19) = -23.3(4)^\circ$ ), even though the *trans* orientation has the largest gap between the three legs of the piano-stool molecule ( $\text{C}(18)\text{-W}(1)\text{-C}(2) = 124.7(1)^\circ$  vs  $\text{N}(1)\text{-W}(1)\text{-C}(18) = 98.6(1)^\circ$ ). The same conformation and distortions of the *p*-xylyl linkage are present in the solid-state molecular structure of the related neopentyl *p*-xylyl complex, **1.7**.<sup>26</sup> Similar *cis*-NO conformations and M-C bond distortions ( $\text{M-C-C}_{ortho} = \sim 130^\circ$ ) are also observed for the *o*-tolyl ligands in the solid-state molecular structures of the complexes  $\text{CpW}(\text{NO})(\text{C}_6\text{H}_4\text{-2-Me})(\text{C}_6\text{H}_4\text{-3-Me})$ ,<sup>27</sup>  $\text{Cp}^*\text{W}(\text{NO})(\text{CH}_2\text{CMe}_3)(\text{C}_6\text{H}_4\text{-2-Me})$ ,<sup>10</sup>  $\text{Cp}^*\text{W}(\text{NO})(\text{C}_6\text{H}_4\text{-2-Me})_2$  and  $\text{Cp}^*\text{Mo}(\text{NO})(\text{C}_6\text{H}_4\text{-2-Me})_2$ .<sup>3</sup> A common mode of decomposition of several of these aryl products is the formation of an aryne complex by  $\beta$ -H elimination.<sup>11,27</sup> The solid-state structures of all of these complexes provide a clue as to why this is so. The obtuse angle to the ortho methyl carbon places the  $\beta$ -H linkage in close proximity to the metal center, even when there is an  $\eta^2$ -benzyl ligand interacting with the metal-centered LUMO.

### 2.2.13 Thermolysis of **2** in Mesitylene

The thermolysis of **2** in mesitylene ( $70^\circ\text{C}$ , 40h) results in the formation of only one C-H activation product, namely  $\text{Cp}^*\text{W}(\text{NO})(\text{CH}_2\text{C}_6\text{H}_5)(\text{CH}_2\text{C}_6\text{H}_3\text{-3,5-Me}_2)$  (**2.14**) in > 95 % yield (eq 2.10). The other possible C-H activation product, namely the aryl benzyl isomer of **2.14** derived from  $\text{sp}^2$  C-H bond activation, is not observed even at early conversions (i.e. at 15 h).



Complex **2.14** exhibits spectral features typical of the mixed benzyl complexes reported above. Interestingly, the  $^1\text{H}$  and  $^{13}\text{C}\{^1\text{H}\}$ NMR data indicate that the bulky mesityl ligand is the ligand that is  $\eta^2$  on average in solution. This observation is supported by the solid-state molecular structure of **2.14**.<sup>28</sup> The ORTEP plot of the structure (Figure 2.4) clearly shows an  $\eta^2$ -mesityl ligand, with a bonding contact between the ipso carbon to the metal center ( $\text{W}(1)\text{-C}(2) = 2.391(4) \text{ \AA}$ ), and an acute  $\text{W-C-C}_{\text{ipso}}$  bond angle ( $83.7(2)^\circ$ ).

From these data as well as from the data for **2.9**, it appears that the methyl-substituted benzyl ligand is attached in an  $\eta^2$  fashion in mixed benzyl complexes of the type  $\text{Cp}^*\text{W}(\text{NO})(\text{CH}_2\text{Ar})(\text{CH}_2\text{Ar-Me}_x)$ , despite the increase in steric congestion at the metal center. Presumably then, the controlling factor is the increased electron-donor capability of the more electron-rich substituted phenyl ring.

#### 2.2.14 Thermolysis of **2** in $\alpha,\alpha,\alpha$ -Trifluorotoluene

Thermolysis of **2** in  $\alpha,\alpha,\alpha$ -trifluorotoluene cleanly generates two aryl products, namely the meta and para isomers  $\text{Cp}^*\text{W}(\text{NO})(\text{CH}_2\text{C}_6\text{H}_5)(\text{C}_6\text{H}_4\text{-3-CF}_3)$  (**2.15a**) and

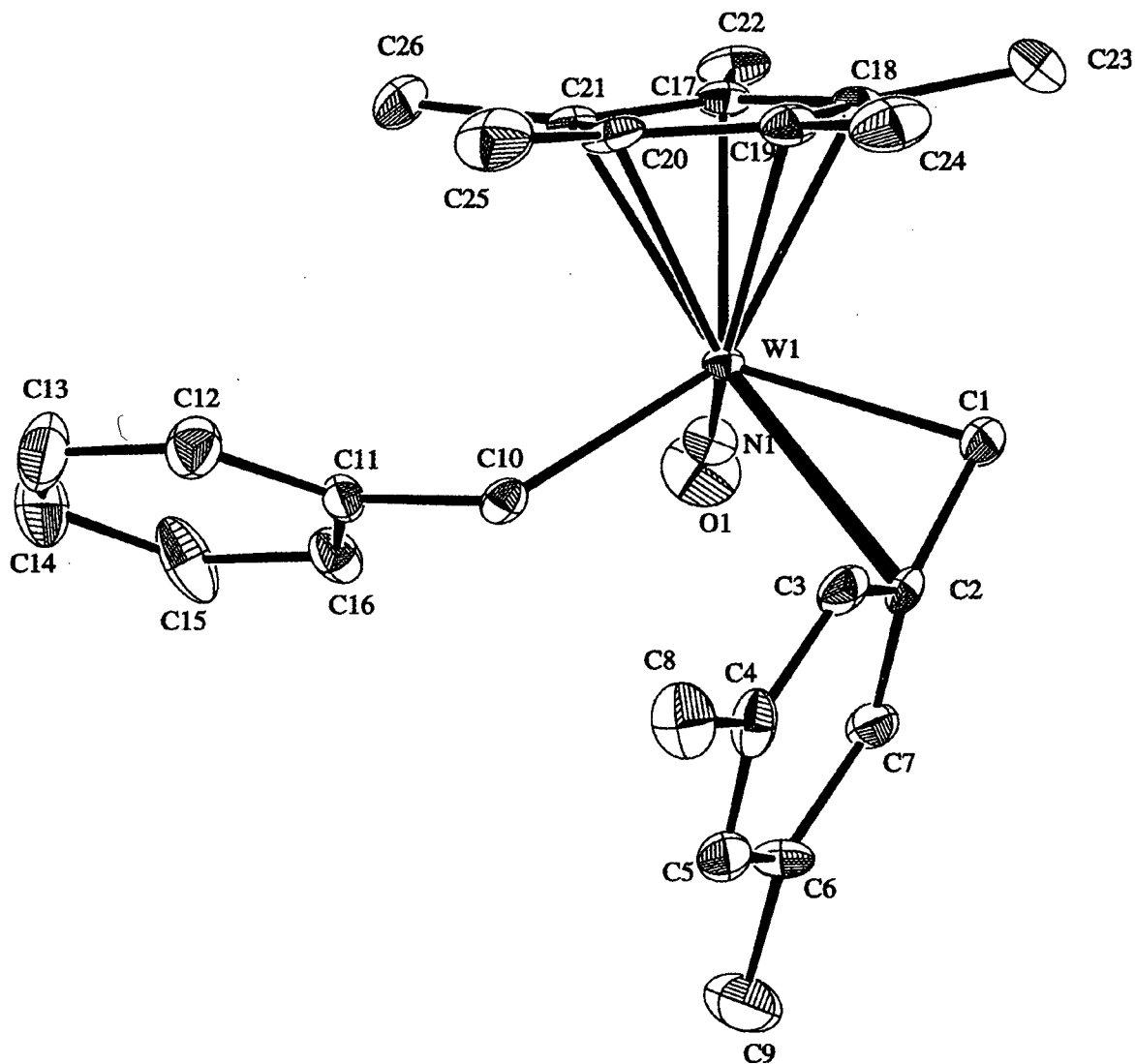


**Figure 2.4.** ORTEP plot of the solid-state molecular structure of

$\text{Cp}^*\text{W}(\text{NO})(\text{CH}_2\text{C}_6\text{H}_5)(\text{CH}_2\text{C}_6\text{H}_3\text{-}3,5\text{-Me}_2)$  (**2.14**) with 50% probability ellipsoids.

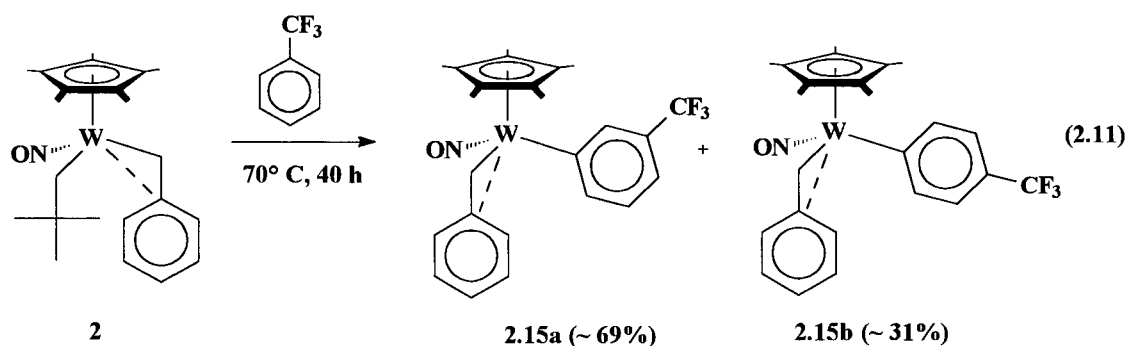
Selected bond lengths ( $\text{\AA}$ ) and angles ( $^\circ$ );  $\text{W}(1)\text{-C}(1) = 2.181(4)$ ,  $\text{W}(1)\text{-C}(2) = 2.391(4)$ ;

$\text{W}(1)\text{-C}(10) = 2.225(4)$ ;  $\text{N}(1)\text{-O}(1) = 1.231(4)$ ,  $\text{C}(1)\text{-C}(2) = 1.467(6)$ ,  $\text{C}(10)\text{-C}(11) =$

$1.500(5)$ ,  $\text{W}(1)\text{-N}(1)\text{-O}(1) = 170.4(3)$ ,  $\text{W}(1)\text{-C}(10)\text{-C}(11) = 83.7(2)$ ,  $\text{W}(1)\text{-C}(10)\text{-C}(11) =$

$120.1(3)$ .

$\text{Cp}^*\text{W}(\text{NO})(\text{CH}_2\text{C}_6\text{H}_5)(\text{C}_6\text{H}_4\text{-4-CF}_3)$  (**2.15b**) in a 2.27(3):1 ratio (eq 2.11). The isomers can be isolated as a crystalline mixture (39% yield) and are again readily distinguished by distinctive patterns in the aromatic region of the  $^1\text{H}$  NMR spectrum. The other spectral features of **2.15a-b** are consistent with the other benzyl aryl complexes reported previously. No evidence was obtained for the formation of the ortho isomer or products from C-F activation.



### 2.2.15 Thermolyses of **1** in *p*-Xylene, Mesitylene and $\alpha,\alpha,\alpha$ -Trifluorotoluene

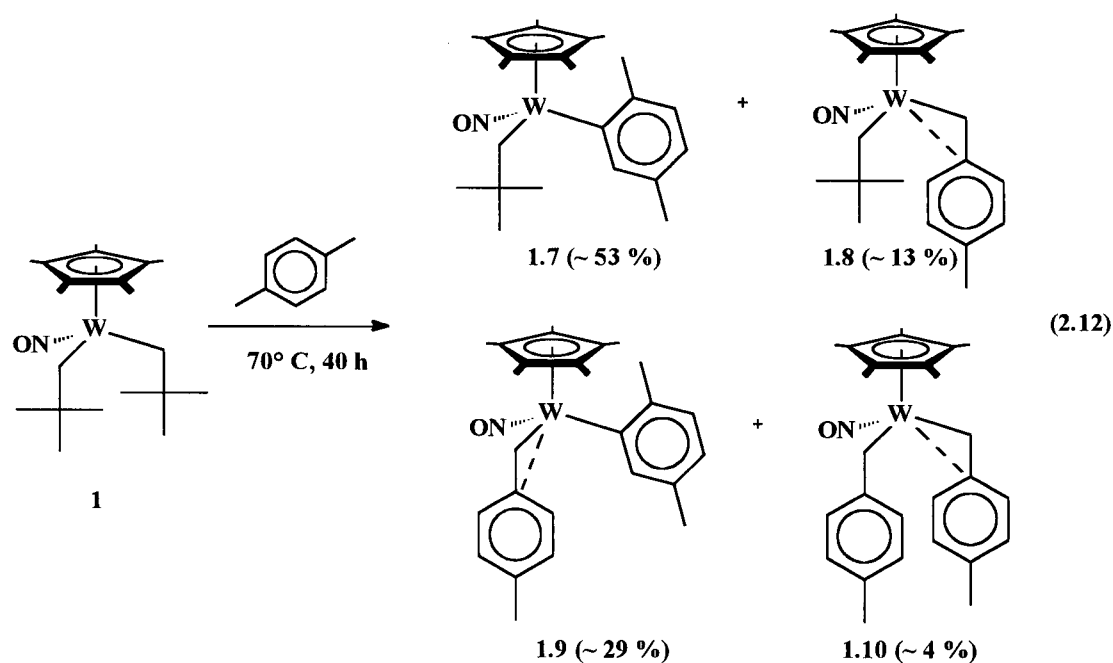
#### Revisited

For accurate comparisons of the activated product distributions derived from **1** and **2**, the thermolyses of **1** in *p*-xylene, mesitylene and  $\alpha,\alpha,\alpha$ -trifluorotoluene were repeated under the standardized thermolysis conditions (70 °C, 40 h).

#### 2.2.15.1 Thermolysis of **1** in *p*-Xylene

Monitoring by  $^1\text{H}$  NMR spectroscopy indicates that thermolysis of **1** in *p*-xylene for 40 h at 70 °C generates four products (eq 2.12). The major products are the aryl products from  $\text{sp}^2$  C-H bond activation of *p*-xylene, namely the neopentyl aryl complex **1.7** and the benzyl aryl complex  $\text{Cp}^*\text{W}(\text{NO})(\text{CH}_2\text{C}_6\text{H}_4\text{-4-Me})(\text{C}_6\text{H}_4\text{-2,5-Me}_2)$  (**1.9**). The

minor products are the benzyl complexes derived from  $sp^3$  C-H bond activation of *p*-xylene, namely  $Cp^*W(NO)(CH_2CMe_3)(CH_2C_6H_4-4-Me)$  (**1.8**), and  $Cp^*W(NO)(CH_2C_6H_4-4-Me)_2$  (**1.10**). All have been previously characterized.<sup>1,4</sup> The product ratio was estimated to be as follows: **1.7**: **1.8**: **1.9**: **1.10** = 1.81(9): 0.44(5): 1.0: 0.15(2).

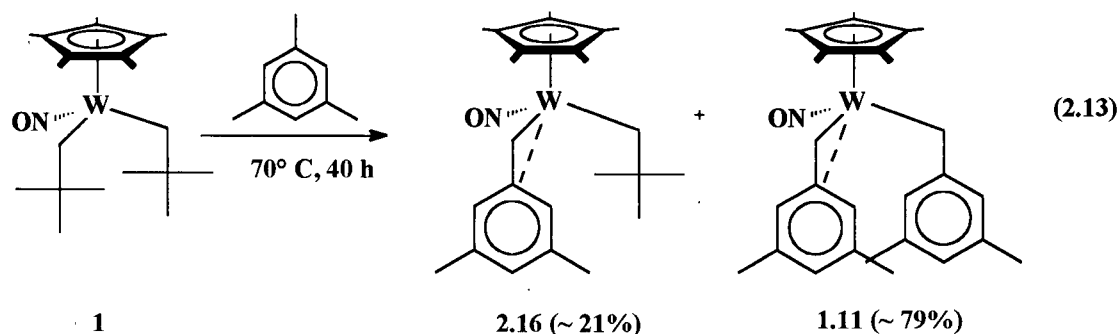


Stopping the thermolysis after 15 h reveals that **1.8** is present in larger amounts than either **1.9** or **1.10**. This observation is consistent with the chemistry reported in Section 1.1.8.3 (eq 1.17), namely that **1.9** and **1.10** form via thermal decomposition of **1.8** to the *p*-xylidene complex,  $Cp^*W(NO)(=CH_2C_6H_4-4-Me)$  which then activates a second molecule of *p*-xylene.<sup>1</sup> Interestingly, the ratio of aryl vs benzyl products of *p*-xylene activation derived from **1.8** (**1.9**: **1.10** = 6.6(9):1) is the same as that derived from **2** within error (**2.12**: **2.13** = 6.2(4):1). It thus appears that the presence of a para methyl group on the phenyl ring of the reactive alkylidene intermediate exerts little influence on

the outcome of the activation chemistry. This is confirmed by the independent thermolyses of **1.8** in other arene solvents, which show no significant differences in the distributions of aryl and benzyl activation products compared to **2**.<sup>1,29</sup>

### 2.2.15.2 Thermolysis of **1** in Mesitylene

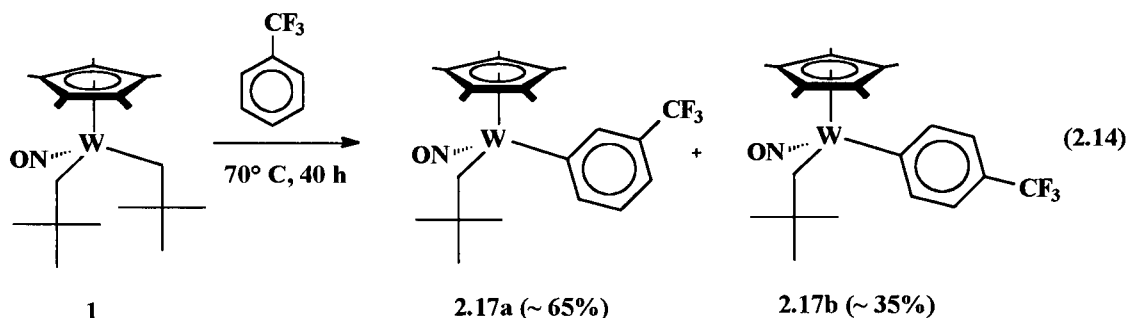
Thermolysis of **1** in mesitylene for 40 h at 70 °C results in formation of two C-H activation products, Cp\*W(NO)(CH<sub>2</sub>CMe<sub>3</sub>)(CH<sub>2</sub>C<sub>6</sub>H<sub>3</sub>-3,5-Me<sub>2</sub>) (**2.16**) and Cp\*W(NO)(CH<sub>2</sub>C<sub>6</sub>H<sub>3</sub>-3,5-Me<sub>2</sub>)<sub>2</sub> (**1.11**)<sup>1</sup> in a 3.6(4): 1 ratio (eq 2.13). Stopping the thermolysis at 15 h shows instead a ~ 2:1 ratio in favour of **2.16**, thereby indicating that **2.16** also thermally decomposes to generate **1.11**. Presumably, heating for longer or at higher temperature results in complete conversion to **1.11**, as originally reported (see Section 1.1.8.3, eq 1.18). There is no evidence for the formation of aryl C-H activation products in either of the <sup>1</sup>H NMR spectra.



### 2.2.15.3 Thermolysis of **1** in $\alpha,\alpha,\alpha$ -Trifluorotoluene

Thermolysis of **1** in  $\alpha,\alpha,\alpha$ -trifluorotoluene cleanly generates two products in a 1.85(5):1 ratio (eq 2.14). The spectral properties match those of

$\text{Cp}^*\text{W}(\text{NO})(\text{CH}_2\text{CMe}_3)(\text{C}_6\text{H}_4\text{-3-CF}_3)$  (**2.17a**) and  $\text{Cp}^*\text{W}(\text{NO})(\text{CH}_2\text{CMe}_3)(\text{C}_6\text{H}_4\text{-4-CF}_3)$  (**2.17b**) respectively.<sup>1</sup>



### 2.2.16 Trends in the Activation of Arenes Substrates

The relative product distributions obtained from the thermolysis of **1** and **2** in the selected arene solvents can be collected together in two tables, one summarizing the distributions of aryl vs benzyl C-H activation products (Table 2.1), the other summarizing the distributions of aryl regioisomers.

As anticipated, both tables reveal some statistically significant differences in the product distributions obtained from **1** vs **2**. First, the distributions obtained from **2** are consistently more abundant in the aryl products than those obtained from **1** in the same solvent (toluene, *p*-xylene). Likewise, in the activations of  $\alpha,\alpha,\alpha$ -trifluorotoluene and toluene, the aryl regioisomer distributions obtained from **2** favour the meta isomer over the para and ortho isomers, more so than the distributions obtained from **1**. These results confirm that the alkylidene substituent can be an important factor in directing the C-H bond activation of substituted arenes.

**Table 2.1.** Relative Aryl vs Benzyl Product Distributions Obtained from the Thermolysis of **1** and **2** in Methyl-Substituted Arene Solvents

Reagent	Solvent	Relative Product Ratio (aryl : benzyl)
<b>2</b>	toluene	18.6(1.2) : 1
<b>2</b>	<i>o</i> -xylene	14.6(4) : 1
<b>2</b>	<i>m</i> -xylene	9.3(7) : 1 <sup>a</sup>
<b>2</b>	<i>p</i> -xylene	6.2(4) : 1
<b>2</b>	mesitylene	0 : 100
<b>1</b>	toluene	4.2(3) : 1 <sup>b</sup>
<b>1</b>	<i>p</i> -xylene	1.14(7) : 1 <sup>c</sup>
<b>1</b>	mesitylene	0 : 100

<sup>a</sup> average and uncertainty (95% CI) from two independent experiments

<sup>b</sup> ratio from integrals for **2.1a-c**: (**2.2a-b** + **2.3**)

<sup>c</sup> ratio from integrals for **1.7** : (**1.8** + **1.9** + **1.10**)

**Table 2.2.** Relative Distributions of Meta and Para Aryl Regioisomers from the Thermolyses of **1** and **2** in Toluene and  $\alpha,\alpha,\alpha$ -Trifluorotoluene

Reagent	Solvent	Relative Product Ratio (meta : para)
<b>2</b>	toluene	1.97(11):1
<b>1</b>	toluene	1.45(8): 1 <sup>a</sup>
<b>2</b>	$\alpha,\alpha,\alpha$ -trifluorotoluene	2.27(3): 1
<b>1</b>	$\alpha,\alpha,\alpha$ -trifluorotoluene	1.85(6) : 1

<sup>a</sup> the ortho tolyl isomer is also present in ~ 1 % abundance relative to the meta and para isomers combined

Tables 2.1 and 2.2 also reveal several other interesting trends in the product distributions. The trends with respect to aryl vs benzyl product distributions in Table 2.1 are as follows:

1. For both **1** and **2**, the aryl products are preferred over the benzyl products (toluene, xylenes), unless the aryl bonds of the substrate are flanked by two ortho methyl groups (mesitylene).
2. Increased steric shielding of the  $sp^2$  C-H bonds by ortho methyl groups correlates with subtle shifts of the product distribution toward the benzyl products (aryl vs benzyl products obtained from **2**: *o*-xylene > *m*-xylene > *p*-xylene).

The notable trends in the aryl product regioselectivities in Table 2.2 are:

3. Meta and para aryl products are formed preferentially over ortho aryl products
4. Only the least sterically-congested aryl regioisomers are formed in the activations of *o*-xylene and *m*-xylene.
5. In the activations of  $\alpha,\alpha,\alpha$ -trifluorotoluene vs toluene, both distributions exhibit a small shift towards the meta isomer upon replacement of  $CH_3$  with the  $CF_3$  group.

These data indicate that the product or product(s) associated with activation of the stronger and most accessible C-H bond within the arene molecule, is (are) formed

preferentially, with some moderation by the steric and electronic nature of the arene substituent(s). This characteristic is reminiscent of those found for the activation of hydrocarbons by other types of soluble metal complexes (see Section 1.1.4).

### 2.3 Epilogue

In this Chapter, the C-H activation chemistry derived from a representative benzyl neopentyl complex **2** has been shown for the most part to be very similar to that of the bis(neopentyl) congener **1**. The characteristics that are common to both systems include the rate of formation and the nature of the reactive alkylidene species, the scope of alkane and arene substrates that can be activated, and the type of products that can be formed from these substrates. The benzylidene and neopentylidene systems also exhibit the same selectivity for the products formed from alkane substrates, but exhibit markedly different product selectivities for the activation of substituted arenes. In particular, the product distributions obtained from the benzylidene system are consistently more abundant in the aryl products than those obtained from the neopentylidene system in the same solvent (toluene, *p*-xylene). Likewise, in the activations of  $\alpha,\alpha,\alpha$ -trifluorotoluene and toluene, the aryl regioisomer distributions obtained from **2** favour the meta isomer over the para and ortho isomers, more so than the distributions obtained from **1**. The activation of these arene substrates has further revealed a general preference for formation of the product(s) associated with activation of the stronger and most accessible C-H bond within the arene molecule, with some moderation by the steric and electronic nature of the arene substituent(s). It now remains to be determined exactly how these selectivities, and

trends between them, arise during the activation of these substrates by the alkylidene complexes **A** and **B**.

## 2.4 Experimental Procedures

### 2.4.1 General Methods

The methodologies described in this Section apply to the entire Thesis. All reactions and subsequent manipulations involving organometallic reagents were performed under anaerobic and anhydrous conditions either under high vacuum or an atmosphere of pre-purified Ar or N<sub>2</sub>. Purification of inert gases was achieved by passing them first through a column containing MnO and then a column of activated 4Å molecular sieves. Conventional glovebox and vacuum-line Schlenk techniques were utilized throughout.<sup>30</sup> The gloveboxes utilized were Innovative Technologies LabMaster 100 and MS-130 BG dual-station models equipped with freezers maintained at -30 to -35 °C. Many reactions were performed in a thick-walled bomb, here defined as a glass vessel possessing a Kontes greaseless stopcock and a side-arm inlet for vacuum-line attachment. Small-scale reactions and NMR spectroscopic analyses were conducted in J. Young NMR tubes, which were also equipped with a Kontes greaseless stopcock.

All solvents were dried with appropriate drying agents under N<sub>2</sub> or Ar atmospheres and distilled prior to use, or were directly transferred under vacuum from the appropriate drying agent. Hydrocarbon solvents, their deuterated analogues, Et<sub>2</sub>O and PMe<sub>3</sub> were dried and distilled from Na or Na/benzophenone ketyl. Tetrahydrofuran was distilled from molten potassium, dichloromethane and chloroform were distilled from calcium hydride, and  $\alpha,\alpha,\alpha$ -trifluorotoluene was distilled from P<sub>2</sub>O<sub>5</sub>.

All IR samples were prepared as Nujol mulls sandwiched between NaCl plates and recorded on an ATI Mattson Genesis Series FT-IR spectrometer. All NMR spectra were recorded at room temperature unless otherwise noted.  $^1\text{H}$  NMR spectra were recorded on Bruker AC-200 (200 MHz), Bruker AV-300 (300 MHz), Bruker AV-400 (400 MHz) or Bruker AMX-500 (500 MHz) instruments.  $^2\text{H}\{^1\text{H}\}$  NMR spectra were recorded on Varian XL-300 (46 MHz), Bruker AV-400 (61 MHz) or Bruker AMX-500 (77 MHz) instruments.  $^{13}\text{C}\{^1\text{H}\}$  spectra were recorded on Bruker AC-200 (50 MHz), Varian XL-300 or Bruker AV-300 (75 MHz), Bruker AMX-400 or AV-400 (100 MHz), or Bruker AMX-500 (125 MHz) instruments.  $^{31}\text{P}$  NMR spectra were recorded on the Bruker AC 200 instrument, while  $^{19}\text{F}$  NMR were recorded on the AV-300 machine. All chemical shifts are reported in ppm and all coupling constants are reported in Hz.  $^1\text{H}$  NMR spectra are referenced to the residual protio-isotopomer present in a particular solvent.  $^2\text{H}\{^1\text{H}\}(\text{C}_6\text{H}_6)$  NMR spectra are referenced to residual  $\text{C}_6\text{H}_5\text{D}$  (7.15 ppm) while  $^{13}\text{C}$  NMR spectra are referenced to the natural abundance carbon signal of the solvent employed.  $^{19}\text{F}$  and  $^{31}\text{P}$  NMR spectra are referenced to external  $\text{CF}_3\text{COOH}$  (0.0 ppm) and  $\text{P}(\text{OMe})_3$  in  $\text{C}_6\text{D}_6$  (141.0 ppm), respectively. Where appropriate,  $^1\text{H}$ - $^1\text{H}$  COSY,  $^1\text{H}$ - $^1\text{H}$  NOEDS,  $^1\text{H}$ - $^{13}\text{C}$  HMQC,  $^{13}\text{C}$  APT, homonuclear decoupling, and gated  $^{13}\text{C}\{^1\text{H}\}$  experiments were carried out to correlate and assign  $^1\text{H}$  and  $^{13}\text{C}$  signals. Ms. M. T. Austria, Ms. L. K. Darge and Dr. N. Burlinson of the UBC Department of Chemistry NMR facilities assisted in recording some of the spectra. Low-resolution mass spectra (EI, 70 eV) were recorded by the staff of the UBC Chemistry Mass Spectrometry Laboratory on a Kratos MS50 spectrometer utilizing the direct-insertion sample introduction method. All elemental analyses were performed by Mr. P. Borda at the

Department of Chemistry at UBC. X-ray crystallographic analyses were performed by Dr. B. O. Patrick of the UBC X-ray Crystallography Laboratory.

### 2.4.2 Reagents

The  $R_2Mg \cdot x(\text{dioxane})$  ( $R = \text{CH}_2\text{CMe}_3, \text{CH}_2\text{C}_6\text{H}_5, \text{CH}_2\text{C}_6\text{H}_4\text{-3-Me}$ ) alkylating reagents<sup>3</sup> and the complexes  $\text{Cp}^*\text{W}(\text{NO})(\text{R})(\text{X})$  ( $R = \text{CH}_2\text{CMe}_3, X = \text{Cl}, \text{CH}_2\text{CMe}_3$  (**1**)) were prepared according to published procedures.<sup>2,6</sup>  $\text{Cp}^*\text{W}(\text{NO})(\text{CH}_2\text{C}_6\text{H}_5)\text{Cl}$  was prepared by the published procedure,<sup>4</sup> except that a stoichiometric amount of 1.0 M HCl in  $\text{Et}_2\text{O}$  was used to effect protonolysis rather than an atmosphere of HCl gas. Complexes  $\text{Cp}^*\text{W}(\text{NO})(\text{CH}_2\text{C}_6\text{H}_5)(\text{CH}_2\text{CMe}_3)$  (**2**) and  $\text{Cp}^*\text{W}(\text{NO})(\text{CH}_2\text{C}_6\text{H}_5)(\text{CH}_2\text{C}_6\text{H}_4\text{-3-Me})$  (**2.9**) were prepared in a similar fashion as **1**, with pertinent synthetic and characterization details reported below.

### 2.4.3 NMR assignments

The following format has been used to help identify peaks in the NMR spectra: xxx ppm (multiplicity, coupling constant(s), relative number of atoms, Ligand Ligand-Part<sub>regio/stereochemistry</sub>). Ligands were abbreviated as follows: Npt = neopentyl,  $\text{CH}_2\text{CMe}_3$ ; TMS = trimethylsilyl,  $\text{SiMe}_3$ ; Ph = phenyl,  $\text{C}_6\text{H}_5$ ; Tol = tolyl,  $\text{C}_6\text{H}_4\text{-CX}_3$  ( $X = \text{H}, \text{F}$ ),  $\text{C}_5\text{H}_4\text{-Me}$ ; Bzl = benzyl,  $\text{CH}_2\text{C}_6\text{H}_5$ ; Xyl = dimethyl aryl,  $\text{C}_6\text{H}_3\text{-Me}_2$ ; Pxl = 4-Me-benzyl,  $\text{CH}_2\text{C}_6\text{H}_4\text{-4-Me}$ ; Mxl = 3-Me-benzyl,  $\text{CH}_2\text{C}_6\text{H}_4\text{-3-Me}$ ; Oxl = 2-Me-benzyl,  $\text{CH}_2\text{C}_6\text{H}_4\text{-2-Me}$ ; Mes = mesityl,  $\text{CH}_2\text{C}_6\text{H}_3\text{-2,5-Me}_2$ ; Ar = ambiguous or generic aryl ligand. Part of the ligand may be identified by italics if otherwise ambiguous (i.e.  $\text{CH}_{\text{syn}}\text{H}$ ). Subscripts for specific portions of a ligand are as follows: *syn*, *anti* for syn and anticlinal methylene

H atoms; *ortho*, *meta*, *para*, *ipso* for positions on an aryl ring; *aryl* if the position is not known; *s* for H<sub>syn</sub>, *a* for H<sub>anti</sub> and *c* for H<sub>c</sub> in allyl complexes.

#### 2.4.4 Preparation of Cp\*W(NO)(CH<sub>2</sub>C<sub>6</sub>H<sub>5</sub>)(CH<sub>2</sub>CMe<sub>3</sub>) (2)

Complex **2** was prepared via the reaction of Cp\*W(NO)(CH<sub>2</sub>CMe<sub>3</sub>)Cl (1.0 g, 2.2 mmol) and (C<sub>6</sub>H<sub>5</sub>CH<sub>2</sub>)<sub>2</sub>Mg·x(dioxane) (0.34 g, 2.2 mmol R<sup>-</sup>) in Et<sub>2</sub>O (10 mL). The crude residue was extracted with 4:1 Et<sub>2</sub>O/hexanes (3 x 15 mL), and the mixture was filtered through Celite (1 x 0.7 cm) supported on a frit. Concentration and cooling of the mother liquor – 30 °C over a period of several days afforded **2** in several crops (890 mg, 79 %). IR (cm<sup>-1</sup>) 1538 (s, ν<sub>NO</sub>). MS (LREI, m/z, probe temperature 150 °C) 511 [P<sup>+</sup>, <sup>184</sup>W]. <sup>1</sup>H NMR (400 MHz, C<sub>6</sub>D<sub>6</sub>) δ -2.35 (d, <sup>2</sup>J<sub>HH</sub> = 13.4, 1H, Npt CH<sub>syn</sub>H), 1.16 (s, 9H, CMe<sub>3</sub>), 1.54 (s, 15H, C<sub>5</sub>Me<sub>5</sub>), 2.20 (d, <sup>2</sup>J<sub>HH</sub> = 13.4, 1H, Npt CH<sub>anti</sub>H), 2.22 (d, <sup>2</sup>J<sub>HH</sub> = 8.5, 1H, Bzl CH<sub>syn</sub>H), 2.98 (d, <sup>2</sup>J<sub>HH</sub> = 8.5, 1H, Bzl CH<sub>anti</sub>H), 6.89 (m, 4H, Bzl H<sub>ortho</sub>, H<sub>meta</sub>), 7.31 (t, <sup>3</sup>J<sub>HH</sub> = 7.3, 1H, Bzl H<sub>para</sub>). <sup>13</sup>C{<sup>1</sup>H} NMR (50 MHz, CDCl<sub>3</sub>) δ 10.4 (C<sub>5</sub>Me<sub>5</sub>), 33.8 (CMe<sub>3</sub>), 38.4 (CMe<sub>3</sub>), 51.7 (CH<sub>2</sub>), 64.0 (CH<sub>2</sub>) 109.2 (C<sub>5</sub>Me<sub>5</sub>), 113.3 (Bzl C<sub>ipso</sub>), 127.3, 129.2, 131.8 (Bzl C<sub>aryl</sub>). Anal. Calcd. for C<sub>22</sub>H<sub>33</sub>NOW: C, 51.67; H, 6.50, N, 2.74. Found: C, 51.74; H, 6.50; N, 2.82.

#### 2.4.5 Monitoring the Thermolysis of 1 in Toluene by <sup>1</sup>H NMR spectroscopy

A bomb was charged with **1** (150 mg, 0.305 mmol), toluene (10.0 mL) and a magnetic stir bar. The bomb was heated and stirred in an oil-bath set at 70(2) °C. At select time intervals (8, 15, 40, 64 h, 80 h), the bomb was removed from the bath and a 1.0 mL aliquot was removed from the bomb. The aliquots were dried in vacuo and the

residue was dissolved in  $C_6D_6$  whereupon a  $^1H$  NMR spectrum was recorded. Relative product ratios at 40 h were determined from the average of multiple (at least five) integrations of select peaks of the same type (i.e.  $Cp^*$  signals,  $CH_2$  signals, etc.). The reported errors are standard errors in the mean and have been adjusted for sample size by multiplication of the appropriate Student t factor at the 95% confidence level.<sup>31</sup>

#### 2.4.6 Preparative Thermolyses of 2 in Hydrocarbon Solvents: General Comments

The preparations of new compounds via the thermolysis of **2** were conducted in the same manner: a bomb was charged with 75 –100 mg of **2**, a magnetic stir-bar and 4-5 mL of solvent. The solvent was either pipetted directly into the bomb from a storage bomb in a glovebox or vacuum transferred onto the powder on a vacuum line. The sealed bomb was then heated and stirred for 40 h in an oil-bath set at 70(2) °C. During this time, the colour of the solution remained either essentially unchanged (deep red-orange) or lightened to an orange or yellow colour, depending on the solvent employed. The bomb was removed from the bath and the solvent was removed in vacuo. The resulting residue was then dissolved in a suitable NMR solvent, and the desired NMR spectral data were obtained. The NMR solvent was then removed and the residue was redissolved in an appropriate solvent or solvent mixture for recrystallization. The solution was filtered through Celite supported on a frit, concentrated to the point of incipient crystallization, and the mixture was placed in a freezer at – 30-35 °C. The major product(s) were isolated as crystals from the mother liquor after a suitable period of time. The reported yields are not optimized. Minor products that could not be isolated by crystallization were characterized spectroscopically from the final reaction mixture. Average product

ratios were obtained from multiple (at least five) integrations of like signals in the  $^1\text{H}$  NMR spectrum of the final reaction mixture. The reported errors are standard errors in the mean and have been adjusted for sample size by multiplication of the appropriate Student t factor at the 95% confidence level.<sup>31</sup>

#### 2.4.7 Preparation of $\text{Cp}^*\text{W}(\text{NO})(\text{CH}_2\text{C}_6\text{H}_5)(\text{C}_6\text{H}_4\text{-3-Me})$ (2.2a),

#### $\text{Cp}^*\text{W}(\text{NO})(\text{CH}_2\text{C}_6\text{H}_5)(\text{C}_6\text{H}_4\text{-4-Me})$ (2.2b)

Complexes **2.2a-b** and **2.3** were prepared by thermolysis of **2** in toluene.

Complex **2.2a** was isolated as orange microcrystals (19 mg, 25 %) by crystallization from 4:1  $\text{Et}_2\text{O}$ /hexanes. Complex **2.2b** was characterized in the reaction mixture, while **2.3** was identified by comparison of its  $^1\text{H}$  NMR resonances to those previously reported.<sup>5</sup>

**2.2a:** IR ( $\text{cm}^{-1}$ ) 1562 (s,  $\nu_{\text{NO}}$ ). MS (LREI,  $m/z$ , probe temperature 150 °C) 531 [ $\text{P}^+$ ,  $^{184}\text{W}$ ], 501 [ $\text{P}^+$  - NO].  $^1\text{H}$  NMR (400 MHz,  $\text{C}_6\text{D}_6$ )  $\delta$  1.59 (s, 15H,  $\text{C}_5\text{Me}_5$ ), 2.19 (d,  $^2J_{\text{HH}} = 5.9$ , 1H, Bzl  $\text{CH}_{\text{syn}}\text{H}$ ), 2.20 (s, 3H, Tol Me), 3.46 (d,  $^2J_{\text{HH}} = 5.9$ , 1H, Bzl  $\text{CH}_{\text{anti}}\text{H}$ ), 6.56 (t,  $^3J_{\text{HH}} = 7.8$ , 2H, Bzl  $\text{H}_{\text{meta}}$ ), 6.82 (d,  $^3J_{\text{HH}} = 7.1$ , 1H, Tol  $\text{H}_{\text{ortho/para}}$ ), 6.89 (d,  $^3J_{\text{HH}} = 7.4$ , 2H, Bzl  $\text{H}_{\text{ortho}}$ ), 6.96 (d,  $^3J_{\text{HH}} = 7.1$ , 1H, Tol  $\text{H}_{\text{ortho/para}}$ ), 7.03 (t,  $^3J_{\text{HH}} = 7.1$ , 1H, Tol  $\text{H}_{\text{meta}}$ ), 7.10 (t,  $^3J_{\text{HH}} = 7.4$ , 1H, Bzl  $\text{H}_{\text{para}}$ ), 7.19 (s, 1H, Tol  $\text{H}_{\text{ortho}}$ ).  $^{13}\text{C}\{^1\text{H}\}$  NMR (75 MHz,  $\text{CDCl}_3$ )  $\delta$  10.60 ( $\text{C}_5\text{Me}_5$ ), 20.79 (Tol Me), 48.18 (Bzl  $\text{CH}_2$ ), 108.95 ( $\text{C}_5\text{Me}_5$ ), 113.57 (Bzl  $\text{C}_{\text{ipso}}$ ), 129.11, 132.07, 135.71 (Bzl  $\text{C}_{\text{aryl}}$ ), 125.05, 126.67, 128.25, 135.37, 138.7 (Tol  $\text{C}_{\text{aryl}}$ ), 172.4 (Tol  $\text{C}_{\text{ipso}}$ ). Anal. Calcd. for  $\text{C}_{24}\text{H}_{29}\text{NOW}$ : C, 54.25; H, 5.50; N, 2.64. Found: C, 54.34; H, 5.65; N, 2.70

**2.2b:**  $^1\text{H}$  NMR (400 MHz,  $\text{C}_6\text{D}_6$ )  $\delta$  1.60 (s, 15H,  $\text{C}_5\text{Me}_5$ ), 2.19 (d,  $^2J_{\text{HH}} = 5.9$ , 1H, Bzl  $\text{CH}_{\text{syn}}\text{H}$ ), 2.23 (s, 3H, Tol Me), 3.46 (d,  $^2J_{\text{HH}} = 5.9$ , 1H, Bzl  $\text{CH}_{\text{anti}}\text{H}$ ), 6.58 (t,  $^3J_{\text{HH}} = 7.8$ , 2H, Bzl  $\text{H}_{\text{meta}}$ ), 6.90 (d,  $^3J_{\text{HH}} = 7.4$ , 2H, Bzl  $\text{H}_{\text{ortho}}$ ), 6.92 (d,  $^3J_{\text{HH}} = 7.1$ , 2H, Tol  $\text{H}_{\text{meta/para}}$ ), 7.00 (d,  $^3J_{\text{HH}} = 7.1$ , 2H, Tol  $\text{H}_{\text{meta/para}}$ ), 7.10 (t,  $^3J_{\text{HH}} = 7.4$ , 1H, Bzl  $\text{H}_{\text{para}}$ ).

$^{13}\text{C}\{^1\text{H}\}$  NMR (75 MHz,  $\text{CDCl}_3$ )  $\delta$  10.68 ( $\text{C}_5\text{Me}_5$ ), 21.26 (Tol Me), 48.22 (Bzl  $\text{CH}_2$ ), 108.95 ( $\text{C}_5\text{Me}_5$ ), 113.59 (Bzl  $\text{C}_{\text{ipso}}$ ), 129.22, 132.09, 135.98 (Bzl  $\text{C}_{\text{aryl}}$ ), 128.08, 133.35, 139.2, (Tol  $\text{C}_{\text{aryl}}$ ), 168.4 (Tol  $\text{C}_{\text{ipso}}$ ).

#### 2.4.8 Preparation of $\text{Cp}^*\text{W}(\text{NO})(=\text{CHC}_6\text{H}_5)(\text{PMe}_3)$ (2.4a-b)

Complexes **2.4a-b** were prepared by the thermolysis of **2** (75 mg, 0.15 mmol) in THF (4 mL) and  $\text{PMe}_3$  (~ 20 mmol). Complex **2.4a** was isolated as yellow-orange blocks (38 mg, 52% yield) by crystallization from 1:2 THF/hexanes.

**2.4a:** IR ( $\text{cm}^{-1}$ ) 1527 (s,  $\nu_{\text{NO}}$ ). MS (LREI,  $m/z$ , probe temperature 150  $^\circ\text{C}$ ) 515 [ $\text{P}^+$ ,  $^{184}\text{W}$ ].  $^1\text{H}$  NMR (400 MHz,  $\text{C}_6\text{D}_6$ )  $\delta$  0.94 (d,  $^2J_{\text{HP}} = 9.0$ , 9H,  $\text{PMe}_3$ ), 1.88 (s, 15H,  $\text{C}_5\text{Me}_5$ ), 7.05 (t,  $^3J_{\text{HH}} = 7.3$ , 1H, Bzl  $\text{H}_{\text{para}}$ ), 7.37 (t,  $^3J_{\text{HH}} = 7.6$ , 2H, Bzl  $\text{H}_{\text{meta}}$ ), 8.06 (d,  $^3J_{\text{HH}} = 7.6$ , 2H, Bzl  $\text{H}_{\text{ortho}}$ ), 12.01 (d,  $^3J_{\text{HP}} = 3.8$ , 1H,  $\text{W}=\text{CH}$ ).  $^{13}\text{C}\{^1\text{H}\}$  NMR (75 MHz,  $\text{CDCl}_3$ )  $\delta$  11.2 ( $\text{C}_5\text{Me}_5$ ), 17.8 (d,  $^1J_{\text{CP}} = 34$ ,  $\text{PMe}_3$ ), 108.4 ( $\text{C}_5\text{Me}_5$ ), 125.6, 128.4, 128.6 (Bzl  $\text{C}_{\text{aryl}}$ ), 153.6 (d,  $^3J_{\text{CP}} = 3.3$ , Bzl  $\text{C}_{\text{ipso}}$ ), 262.5 (d,  $^2J_{\text{CP}} = 9.6$ ,  $\text{W}=\text{CH}$ ).  $^{31}\text{P}$  NMR (81 MHz,  $\text{C}_6\text{D}_6$ )  $\delta$  - 8.9 (s,  $^1J_{\text{PW}} = 445$  Hz). NOEDS (400 MHz,  $\text{C}_6\text{D}_6$ )  $\delta$  irrad. at 0.94, NOEs at 8.06, 12.01; irrad. at 1.88; NOE at 12.01. Anal. Calcd. for  $\text{C}_{20}\text{H}_{30}\text{NOPW}$ : C, 46.62; H, 5.87; N, 2.72. Found: C, 46.42; H, 5.69; N, 2.95.

**2.4b:**  $^1\text{H}$  NMR (400 MHz,  $\text{C}_6\text{D}_6$ )  $\delta$  1.08 (d,  $^2J_{\text{HP}} = 9.0$ , 9H,  $\text{PMe}_3$ ), 1.80 (s, 15H,  $\text{C}_5\text{Me}_5$ ), 7.05 (t,  $^3J_{\text{HH}} = 7.8$ , 1H, Bzl  $\text{H}_{\text{para}}$ ), 7.10 (t,  $^3J_{\text{HH}} = 7.8$ , 2H, Bzl  $\text{H}_{\text{meta}}$ ), 7.20 (d,  $^3J_{\text{HH}} = 7.8$ , 2H, Bzl  $\text{H}_{\text{ortho}}$ ), 13.70 (d,  $^3J_{\text{HP}} = 4.4$ , 1H, W=CH).  $^{13}\text{C}\{^1\text{H}\}$  NMR (75 MHz,  $\text{CDCl}_3$ )  $\delta$  11.0 ( $\text{C}_5\text{Me}_5$ ), 19.4 (d,  $^1J_{\text{CP}} = 34$ ,  $\text{PMe}_3$ ), 107.8 ( $\text{C}_5\text{Me}_5$ ), 124.8, 126.7, 127.9 (Bzl  $\text{C}_{\text{aryl}}$ ), 153.5 (d,  $^3J_{\text{CP}} = 2.5$ , Bzl  $\text{C}_{\text{ipso}}$ ), 259.7 (d,  $^2J_{\text{CP}} = 10.1$ , W=CH).  $^{31}\text{P}$  NMR (81 MHz,  $\text{C}_6\text{D}_6$ )  $\delta$  - 7.2 (s,  $^1J_{\text{PW}} = 482$  Hz). NOEDS (400 MHz,  $\text{C}_6\text{D}_6$ )  $\delta$  irradi. at 1.08, NOE at 13.70; irradi. at 1.80, NOE at 7.20.

#### 2.4.9 Preparation of $\text{Cp}^*\text{W}(\text{NO})(\text{CH}_2\text{C}_6\text{H}_5)(\text{C}_6\text{H}_5)$ (2.5) and

##### $\text{Cp}^*\text{W}(\text{NO})(\text{CHDC}_6\text{H}_5)(\text{C}_6\text{D}_5)$ (2.5- $d_6$ )

Compounds **2.5** and **2.5- $d_6$**  were prepared via the thermolysis of **2** in benzene and benzene- $d_6$  respectively and were isolated as red needles by crystallization from 4:1  $\text{Et}_2\text{O}$ /hexanes.

**2.5:** 46 mg (59 %). IR ( $\text{cm}^{-1}$ ) 1562 (s,  $\nu_{\text{NO}}$ ). MS (LREI, m/z, probe temperature 120 °C) 517 [ $\text{P}^+$ ,  $^{184}\text{W}$ ], 487 [ $\text{P}^+ - \text{NO}$ ].  $^1\text{H}$  NMR (400 MHz,  $\text{C}_6\text{D}_6$ )  $\delta$  1.53 (s, 15H,  $\text{C}_5\text{Me}_5$ ), 2.14 (d,  $^2J_{\text{HH}} = 6.4$ , 1H, Bzl  $\text{CH}_{\text{syn}}\text{H}$ ), 3.41 (d,  $^2J_{\text{HH}} = 6.4$ , 1H, Bzl  $\text{CH}_{\text{anti}}\text{H}$ ), 6.50 (t,  $^3J_{\text{HH}} = 7.8$ , 2H, Bzl  $\text{H}_{\text{meta}}$ ), 6.84 (d,  $^3J_{\text{HH}} = 7.6$ , 2H, Bzl  $\text{H}_{\text{ortho}}$ ), 6.9-7.3 (m, Bzl  $\text{H}_{\text{para}}$ , Ph H).  $^{13}\text{C}\{^1\text{H}\}$  NMR (100 MHz,  $\text{CDCl}_3$ )  $\delta$  10.5 ( $\text{C}_5\text{Me}_5$ ), 48.0 (Bzl  $\text{CH}_2$ ), 108.9 ( $\text{C}_5\text{Me}_5$ ), 113.2 (Bzl  $\text{C}_{\text{ipso}}$ ), 124.1, 127.0 (Ph  $\text{C}_{\text{aryl}}$ ), 129.1, 132.3, 135.7 (Bzl  $\text{C}_{\text{aryl}}$ ), 138.6 (Ph  $\text{C}_{\text{aryl}}$ ), 172.0 (Ph  $\text{C}_{\text{ipso}}$ ). Anal. Calcd. for  $\text{C}_{23}\text{H}_{27}\text{NOW}$ : C, 53.40; H, 5.26; N, 2.71. Found: C, 53.10; H, 5.36; N, 2.77. NOEDS (400 MHz,  $\text{C}_6\text{D}_6$ )  $\delta$  irradi. at 2.14, NOEs at 3.41 (s), 6.50 (w), 6.84 (s), 7.03 (Ph  $\text{H}_{\text{meta}}$ , w).

**2.5-*d*<sub>6</sub>**: (39 mg, 48% yield). IR (cm<sup>-1</sup>) 1562 (s, ν<sub>NO</sub>). MS (LREI, m/z, probe temperature 120 °C) 523 [P<sup>+</sup>, <sup>184</sup>W], 493 [P<sup>+</sup> - NO]. <sup>1</sup>H NMR (400 MHz, C<sub>6</sub>D<sub>6</sub>) δ 1.53 (s, 15H, C<sub>5</sub>Me<sub>5</sub>), 3.39 (br s, 1H, Bzl CH<sub>anti</sub>D), 6.50 (t, <sup>3</sup>J<sub>HH</sub> = 7.8, 2H, Bzl H<sub>meta</sub>), 6.84 (d, <sup>3</sup>J<sub>HH</sub> = 7.6, 2H, Bzl H<sub>ortho</sub>), 7.31 (t, <sup>3</sup>J<sub>HH</sub> = 7.3, 1H, Bzl H<sub>para</sub>). <sup>2</sup>H{<sup>1</sup>H} NMR (46 MHz, C<sub>6</sub>H<sub>6</sub>) δ 2.15 (br s, Bzl CHD<sub>syn</sub>), 7.1 (m, Ph D). <sup>13</sup>C{<sup>1</sup>H} NMR (100 MHz, CDCl<sub>3</sub>) δ 10.5 (C<sub>5</sub>Me<sub>5</sub>), 47.7 (t, <sup>1</sup>J<sub>CD</sub> = 22.5 Hz, Bzl CHD), 108.9 (C<sub>5</sub>Me<sub>5</sub>), 113.2 (Bzl C<sub>ipso</sub>), 129.1, 132.3, 135.7 (Bzl C<sub>aryl</sub>), 171.8 (Ph C<sub>ipso</sub>). <sup>13</sup>C resonances attributable to aryl C-D of the phenyl ligand were not observed. Anal. Calcd. for C<sub>23</sub>H<sub>21</sub>D<sub>6</sub>NOW:<sup>32</sup> C, 52.80; H/D, 5.20; N, 2.67. Found: C, 52.45; H/D, 4.99; N, 2.80.

#### 2.4.10 Kinetic Studies of the Thermolysis of **1** and **2** in Benzene-*d*<sub>6</sub>

These experiments were performed using a J. Young NMR tube charged with **1** or **2** (15 mg, 30 mmol) and 1 mL of a benzene-*d*<sub>6</sub> solution containing hexamethyldisilane (0.5 equiv, 15 mmol) as an internal integration standard. The thermolyses were conducted side-by-side in a VWR 1160A constant-temperature bath set at 72.0 °C, and the samples were removed at several intervals to record <sup>1</sup>H NMR spectra. The monitoring was performed for > 3.5 half-lives (15 h) and rate constants were calculated using linear regression methods from first-order plots of the loss of starting material vs time. See Appendix B for plots of the data.

#### 2.4.11 Thermolysis of **2** in Alkanes: General Comments

These experiments were conducted in a fashion similar to the thermolysis of **2** in toluene, but on smaller scale (30-50 mg of **2**) than for arenes since all of the activation

products, except for **2.7**, have been reported previously. Also, given the limited solubility of **2** in aliphatic solvents, sufficient solvent was added to dissolve **2** at room temperature. The resulting final reaction mixtures were analyzed by  $^1\text{H}$  and  $^{13}\text{C}\{^1\text{H}\}$  NMR spectroscopy and MS spectrometry.

#### 2.4.12 Preparation of $\text{Cp}^*\text{W}(\text{NO})(\text{CH}_2\text{C}_6\text{H}_5)(\text{CH}_2\text{SiMe}_3)$ (**2.6**)

Complex **2.6**<sup>4</sup> was prepared by the thermolysis of **2** (30 mg, 0.059 mmol) in tetramethylsilane (5 mL).

#### 2.4.13 Preparation of **2.4a-b** and $\text{Cp}^*\text{W}(\text{NO})(\eta^2\text{-cyclohexene})(\text{PMe}_3)$ (**1.3**)

Complexes **2.4a-b** and **1.3**<sup>33</sup> were prepared as a ~ 10:1 mixture from the thermolysis of **2** (50 mg, 0.098 mmol) in cyclohexane (5 mL) in the presence of  $\text{PMe}_3$  (~ 0.160 mmol, 20 equiv).

#### 2.4.14 Preparation of $\text{Cp}^*\text{W}(\text{NO})(\eta^3\text{-C}_7\text{H}_{11})(\text{H})$ (**1.5** and **2.7**) from **1** and **2**

Compounds **1.5** and **2.7** were prepared from the thermolysis of **2** (50 mg, 0.098 mmol) in methylcyclohexane (10 mL), as well as from the thermolysis of **1** (60 mg, 0.122 mmol) in methylcyclohexane (5 mL). Complexes **1.5** and **2.7** were characterized as a mixture.

MS (LREI,  $m/z$ , probe temperature 150 °C) 445 [ $\text{P}^+$ ,  $^{184}\text{W}$ ]. **1.5**<sup>9</sup>:  $^1\text{H}$  NMR (400 MHz,  $\text{C}_6\text{D}_6$ )  $\delta$  -0.73 (s,  $^1J_{\text{HW}} = 123$ , 1H, WH), 0.31 (br s, 1H, allyl  $\text{CH}_s\text{H}$ ), 1.39 (m, 1H,  $\text{C}_b\text{HH}$ ), 1.54 (m, 1H,  $\text{C}_a\text{HH}$ ), 1.71 (m, 1H,  $\text{C}_b\text{HH}$ ), 1.76 (s, 15H,  $\text{C}_5\text{Me}_5$ ), 1.84 (m, 1H,  $\text{C}_a\text{HH}$ ), 2.28 (br s, 1H, allyl  $\text{CH}_c$ ), 2.60 (m, 1H, allyl  $\text{CH}_d\text{H}$ ), 2.68 (m, 2H,  $\text{C}_c\text{HH}$ ,  $\text{C}_d\text{HH}$ ),

2.91 (q, 1H,  $^2J_{\text{HH}} = 7.9$ , C<sub>c</sub>HH), 2.97 (m, 1H, C<sub>d</sub>HH).  $^{13}\text{C}\{^1\text{H}\}$  (75MHz, C<sub>6</sub>D<sub>6</sub>)  $\delta$  10.7 (C<sub>5</sub>Me<sub>5</sub>), 22.1 (t,  $^1J_{\text{CH}} = 124$ , C<sub>a</sub>H<sub>2</sub>), 22.5 (t,  $^1J_{\text{CH}} = 126$ , C<sub>b</sub>H<sub>2</sub>), 28.8 (t,  $^1J_{\text{CH}} = 125$ , C<sub>c</sub>H<sub>2</sub>), 29.6 (t,  $^1J_{\text{CH}} = 126$ , C<sub>d</sub>H<sub>2</sub>), 41.3 (t,  $^1J_{\text{CH}} = 155$ , allyl CH<sub>2</sub>), 80.0 (d,  $^1J_{\text{CH}} = 148$ , allyl CH), 104.9 (C<sub>5</sub>Me<sub>5</sub>), 121.1 (s, allyl C). NOEDS (400 MHz, C<sub>6</sub>D<sub>6</sub>)  $\delta$  irradi. at -0.73, NOEs at 2.28, 2.97; irradi. at 0.31, NOEs at 2.28, 2.68; irradi. at 2.28, NOEs at -0.73, 0.31, 2.97; irradi. at 2.68, NOE at 0.31. 2.7:  $^1\text{H}$  NMR (400 MHz, C<sub>6</sub>D<sub>6</sub>)  $\delta$  -0.73 (s, 1H, WH), 0.48 (br s, 1H, allyl CHH), 1.75 (s, 15H, C<sub>5</sub>Me<sub>5</sub>), 2.61 (br s, 1H, allyl CH), 3.95 (m, 1H, allyl CHH), other resonances obscured.  $^{13}\text{C}\{^1\text{H}\}$  (75MHz, C<sub>6</sub>D<sub>6</sub>)  $\delta$  10.3 (C<sub>5</sub>Me<sub>5</sub>), 22.5, 23.0, 27.3, 29.6 (CH<sub>2</sub>), 49.7 (t,  $^1J_{\text{CH}} = 155$ , allyl CH<sub>2</sub>), 62.8 (d,  $^1J_{\text{CH}} = 146$ , allyl CH), 104.7 (C<sub>5</sub>Me<sub>5</sub>). The  $^{13}\text{C}$  resonance attributable to allyl C was not observed. NOEDS (400 MHz, C<sub>6</sub>D<sub>6</sub>)  $\delta$  irradi. at 3.95, NOEs at - 0.73, 0.48.

#### 2.4.15 Thermolysis of 1 and 2 in Xylenes, Mesitylene and $\alpha,\alpha,\alpha$ -Trifluorotoluene:

##### General Comments

For the thermolyses of 2 in these solvents, the same procedure outlined in Section 2.4.6 was used for preparation and isolation of the activated products. The thermolyses of 1 in these solvents were conducted on a much smaller scale (12-15 mg, 1.0 – 1.5 mL solvent), since, for the most part, the products have been previously characterized. For consistency, the thermolyses of 2 were repeated side-by-side with those involving 1 on the same small-scale thermolyses under identical conditions (70.0 °C, 40 h), and the resulting ratios of activated products derived from 1 and 2 were determined from  $^1\text{H}$  NMR spectra recorded on the same NMR machine.

### 2.4.16 Preparation of Cp\*W(NO)(CH<sub>2</sub>C<sub>6</sub>H<sub>5</sub>)(C<sub>6</sub>H<sub>3</sub>-3,5-Me<sub>2</sub>) (2.8) and

#### Cp\*W(NO)(CH<sub>2</sub>C<sub>6</sub>H<sub>5</sub>)(CH<sub>2</sub>C<sub>6</sub>H<sub>4</sub>-3-Me) (2.9)

Compounds **2.8** and **2.9** were prepared as a mixture from the thermolysis of **2** in *m*-xylene. Complex **2.8** was isolated as orange blocks (23 mg, 29 % yield) from 3:1 Et<sub>2</sub>O/hexanes.

**2.8:** IR (cm<sup>-1</sup>) 1559 (s, ν<sub>NO</sub>). MS (LREI, m/z, probe temperature 150 °C) 545 [P<sup>+</sup>, <sup>184</sup>W], 515 [P<sup>+</sup> - NO]. <sup>1</sup>H NMR (400 MHz, CD<sub>2</sub>Cl<sub>2</sub>) δ 1.80 (s, 15H, C<sub>5</sub>Me<sub>5</sub>), 2.06 (s, 6H, Xyl Me), 2.38 (d, <sup>2</sup>J<sub>HH</sub> = 6.0, 1H, Bzl CH<sub>syn</sub>H), 3.31 (d, <sup>2</sup>J<sub>HH</sub> = 6.0, 1H, Bzl CH<sub>anti</sub>H), 6.29 (br s, 2H, Xyl H<sub>ortho</sub>), 6.44 (s, 1H, Xyl H<sub>para</sub>), 6.80 (t, <sup>3</sup>J<sub>HH</sub> = 7.9, 2H, Bzl H<sub>meta</sub>), 6.93 (d, <sup>3</sup>J<sub>HH</sub> = 7.1, 2H, Bzl H<sub>ortho</sub>), 7.34 (t, <sup>3</sup>J<sub>HH</sub> = 7.5, 1H, Bzl H<sub>para</sub>). <sup>13</sup>C{<sup>1</sup>H} NMR (75 MHz, CD<sub>2</sub>Cl<sub>2</sub>) δ 10.6 (C<sub>5</sub>Me<sub>5</sub>), 20.7 (Xyl Me), 48.5 (Bzl CH<sub>2</sub>), 109.2 (C<sub>5</sub>Me<sub>5</sub>), 114.8 (Bzl C<sub>ipso</sub>), 126.5, 129.4, 131.8, 135.3, 135.9, 136.7 (Ar C<sub>aryl</sub>), 173.3 (Xyl C<sub>ipso</sub>). Anal. Calcd. for C<sub>25</sub>H<sub>31</sub>NO: C, 55.06; H, 5.72; N, 2.57. Found: C, 55.10; H, 5.80; N, 2.64.

**2.9:** <sup>1</sup>H NMR (400 MHz, CD<sub>2</sub>Cl<sub>2</sub>) δ -0.11 (d, <sup>2</sup>J<sub>HH</sub> = 9.9, 1H, Bzl CH<sub>syn</sub>H), 1.17 (d, <sup>2</sup>J<sub>HH</sub> = 7.9, 1H, Mxl CH<sub>syn</sub>H), 1.80 (Bzl CH<sub>anti</sub>H), 1.85 (s, 15H, C<sub>5</sub>Me<sub>5</sub>), 2.29 (s, 3H, Mxl Me), 2.66 (d, <sup>2</sup>J<sub>HH</sub> = 7.9, 1H, Mxl CH<sub>anti</sub>H), 6.45 (s, 1H, Mxl H<sub>ortho</sub>), 6.63 (d, <sup>3</sup>J<sub>HH</sub> = 7.5, 1H, Mxl H<sub>ortho</sub>), 6.85 (d, <sup>3</sup>J<sub>HH</sub> = 7.5, 2H, Bzl H<sub>ortho</sub>), 6.95 (t, <sup>3</sup>J<sub>HH</sub> = 7.5, 1H, Bzl H<sub>para</sub>), 7.02 (t, <sup>3</sup>J<sub>HH</sub> = 7.9, 2H, Bzl H<sub>meta</sub>), 7.10 (t, <sup>3</sup>J<sub>HH</sub> = 7.5, 1H, Mxl H<sub>meta</sub>), 7.42 (d, <sup>3</sup>J<sub>HH</sub> = 7.5, 1H, Mxl H<sub>para</sub>).

#### 2.4.17 Independent Preparation of 2.9 via Metathesis.

Complex **2.9** was also prepared via the reaction of  $\text{Cp}^*\text{W}(\text{NO})(\text{CH}_2\text{C}_6\text{H}_5)\text{Cl}$  (0.100 g, 0.21 mmol) and  $(3\text{-Me-C}_6\text{H}_4\text{CH}_2)_2\text{Mg}\cdot x(\text{dioxane})$  (0.037 g, 0.21 mmol  $\text{R}^+$ ) in THF (10 mL). The crude residue was extracted with 1:1  $\text{CH}_2\text{Cl}_2$ /hexanes (15 mL), and filtered through alumina (I) (1 x 0.7 cm) supported on a frit. Concentrating the solution followed by storage at  $-30\text{ }^\circ\text{C}$  overnight provided **2.9** as red blocks (85 mg, 74 %).

**2.9**: IR ( $\text{cm}^{-1}$ ) 1554 (s,  $\nu_{\text{NO}}$ ). MS (LREI, m/z, probe temperature  $150\text{ }^\circ\text{C}$ ) 545 [ $\text{P}^+$ ,  $^{184}\text{W}$ ], 515 [ $\text{P}^+ - \text{NO}$ ].  $^{13}\text{C}\{^1\text{H}\}$  NMR (75 MHz,  $\text{CD}_2\text{Cl}_2$ )  $\delta$  10.4 ( $\text{C}_5\text{Me}_5$ ), 21.2 (Mxl Me), 41.1, 43.8 ( $\text{CH}_2$ ), 108.2 ( $\text{C}_5\text{Me}_5$ ), 113.9 (br, Mxl  $\text{C}_{\text{ipso}}$ ), 124.9, 125.1, 127.9, 129.1, 130.0, 130.9, 133.0, 138.9, (Ar  $\text{C}_{\text{aryl}}$ ), 142.3 (Bzl  $\text{C}_{\text{ipso}}$ ). NOEDS (400 MHz,  $\text{CD}_2\text{Cl}_2$ )  $\delta$  irradi. at 2.66, NOEs at 1.17, 6.45, 6.63. Anal. Calcd. for  $\text{C}_{25}\text{H}_{31}\text{NOW}$ : C, 55.06; H, 5.72; N, 2.57. Found: C, 55.03; H, 5.88; N, 2.59.

#### 2.4.18 Preparation of $\text{Cp}^*\text{W}(\text{NO})(\text{CH}_2\text{C}_6\text{H}_5)(\text{C}_6\text{H}_3\text{-3,4-Me}_2)$ (**2.10**) and

#### $\text{Cp}^*\text{W}(\text{NO})(\text{CH}_2\text{C}_6\text{H}_5)(\text{CH}_2\text{C}_6\text{H}_4\text{-2-Me})$ (**2.11**)

Complexes **2.10-2.11** were prepared by thermolysis of **2** in *o*-xylene. Complex **2.10** was isolated as yellow-needles (28 mg, 30%) by recrystallization using 3:1  $\text{Et}_2\text{O}$ /hexanes.

**2.10**: IR ( $\text{cm}^{-1}$ ) 1549 (s,  $\nu_{\text{NO}}$ ). MS (LREI, m/z, probe temperature  $150\text{ }^\circ\text{C}$ ) 545 [ $\text{P}^+$ ,  $^{184}\text{W}$ ], 515 [ $\text{P}^+ - \text{NO}$ ].  $^1\text{H}$  NMR (400 MHz,  $\text{CD}_2\text{Cl}_2$ )  $\delta$  1.80 (s, 15H,  $\text{C}_5\text{Me}_5$ ), 2.02 (s, 3H, Xyl Me), 2.08 (s, 3H, Xyl Me), 2.35 (d,  $^2J_{\text{HH}} = 6.1$ , 1H, Bzl  $\text{CH}_{\text{syn}}\text{H}$ ), 3.31 (d,  $^2J_{\text{HH}} = 6.1$ , 1H, Bzl  $\text{CH}_{\text{anti}}\text{H}$ ), 6.25 (br s, 1H, Xyl  $\text{H}_{\text{ortho}}$ ), 6.62 (m, 2H, Xyl  $\text{H}_{\text{ortho}}$ , Xyl  $\text{H}_{\text{meta}}$ ), 6.80

(t,  $^3J_{\text{HH}} = 7.6$ , 2H, Bzl H<sub>meta</sub>), 6.92 (d,  $^3J_{\text{HH}} = 7.6$ , 2H, Bzl H<sub>ortho</sub>), 7.31 (t,  $^3J_{\text{HH}} = 7.6$ , 1H, Bzl H<sub>para</sub>).  $^{13}\text{C}\{^1\text{H}\}$  NMR (75 MHz, CD<sub>2</sub>Cl<sub>2</sub>)  $\delta$  10.7 (C<sub>5</sub>Me<sub>5</sub>), 18.9, 19.6 (Xyl Me), 48.6 (Bzl CH<sub>2</sub>), 109.2 (C<sub>5</sub>Me<sub>5</sub>), 115.0 (Bzl C<sub>ipso</sub>), 128.5, 129.4, 129.6, 131.9, 132.5, 134.6, 137.1, 139.9 (Ar C<sub>aryl</sub>), 170.3 (Xyl C<sub>ipso</sub>). Anal. Calcd. for C<sub>25</sub>H<sub>31</sub>NOW: C, 55.06; H, 5.72; N, 2.57. Found: C, 54.69; H, 5.55; N, 2.74.

**2.11:**  $^1\text{H}$  NMR (400 MHz, CD<sub>2</sub>Cl<sub>2</sub>)  $\delta$  - 0.98 (d,  $^2J_{\text{HH}} = 11.9$ , 1H, Bzl CH<sub>syn</sub>H), 1.22 (d,  $^2J_{\text{HH}} = 11.9$ , 1H, Bzl CH<sub>anti</sub>H), 1.70 (Oxl CH<sub>syn</sub>H), 1.85 (s, 15H, C<sub>5</sub>Me<sub>5</sub>), 1.99 (s, 3H, Oxl Me), 3.23 (d,  $^2J_{\text{HH}} = 6.1$ , 1H, Oxl CH<sub>anti</sub>H), 5.46 (d,  $^3J_{\text{HH}} = 7.3$ , 1H, Oxl H<sub>ortho</sub>), 6.65 (m, 1H, Oxl H<sub>meta</sub>), 7.15 (d,  $^3J_{\text{HH}} = 7.5$ , 1H, Oxl H<sub>meta</sub>), 7.45 (d,  $^3J_{\text{HH}} = 7.3$ , Bzl H<sub>ortho</sub>), 7.82 (t,  $^3J_{\text{HH}} = 7.5$ , 1H, Oxl H<sub>para</sub>), other signals for the benzyl ligand obscured. NOEDS (400 MHz, CD<sub>2</sub>Cl<sub>2</sub>)  $\delta$  irradiat. at - 0.98, NOE at 7.45.

**2.4.19 Preparation of Cp\*W(NO)(CH<sub>2</sub>C<sub>6</sub>H<sub>5</sub>)(C<sub>6</sub>H<sub>3</sub>-2,5-Me<sub>2</sub>) (2.12) and Cp\*W(NO)(CH<sub>2</sub>C<sub>6</sub>H<sub>5</sub>)(CH<sub>2</sub>C<sub>6</sub>H<sub>4</sub>-4-Me) (2.13)**

Compounds **2.12** and **2.13** were prepared from the thermolysis of **2** in *p*-xylene. Complex **2.12** was subsequently crystallized from 4:1 Et<sub>2</sub>O/hexanes as red needles (36 mg, 40% yield).

**2.12:** IR (cm<sup>-1</sup>) 1569 (s,  $\nu_{\text{NO}}$ ). MS (LREI, *m/z*, probe temperature 150 °C) 545 [P<sup>+</sup>, <sup>184</sup>W], 515 [P<sup>+</sup> - NO].  $^1\text{H}$  NMR (500 MHz, CDCl<sub>3</sub>)  $\delta$  1.81 (s, 15H, C<sub>5</sub>Me<sub>5</sub>), 1.96 (s, 3H, Xyl Me), 2.50 (br s, 3H, Xyl Me), 2.58 (br s, Bzl CH<sub>syn</sub>H), 3.35 (d,  $^2J_{\text{HH}} = 5.6$ , 1H, Bzl CH<sub>anti</sub>H), 5.34 (br s, 1H, Xyl H<sub>ortho</sub>), 6.50 (d,  $^3J_{\text{HH}} = 7.3$ , 1H, Xyl H<sub>meta/para</sub>), 6.81 (t,  $^3J_{\text{HH}} = 7.7$ , 2H, Bzl H<sub>meta</sub>), 6.87 (d,  $^3J_{\text{HH}} = 7.5$ , 1H, Xyl H<sub>meta/para</sub>), 7.07 (t,  $^3J_{\text{HH}} = 7.5$ , 1H,

Bzl H<sub>para</sub>), 7.11 (d,  $^3J_{\text{HH}} = 7.7$ , 2H, Bzl H<sub>ortho</sub>).  $^{13}\text{C}\{^1\text{H}\}$  NMR (75 MHz,  $\text{CDCl}_3$ )  $\delta$  10.4 ( $\text{C}_5\text{Me}_5$ ), 19.8, 27.6 (Xyl Me), 52.2 (br, Bzl  $\text{CH}_2$ ), 109.5 ( $\text{C}_5\text{Me}_5$ ), 120.0 (br, Bzl  $\text{C}_{\text{ipso}}$ ), 125.8, 128.2, 128.9, 130.8, 131.6, 134.0, 134.5, 146.5 (Ar  $\text{C}_{\text{aryl}}$ ), 178.8 (Xyl  $\text{C}_{\text{ipso}}$ ). Anal. Calcd. for  $\text{C}_{25}\text{H}_{31}\text{NO}$ : C, 55.06; H, 5.72; N, 2.57. Found: C, 55.24; H, 5.73; N, 2.80.

**2.13:**  $^1\text{H}$  NMR (500 MHz,  $\text{CDCl}_3$ )  $\delta$  0.03 (d,  $^2J_{\text{HH}} = 11.4$ , 1H, Bzl  $\text{CH}_{\text{syn}}\text{H}$ ), 1.39 (d,  $^2J_{\text{HH}} = 7.6$ , 1H, Pxl  $\text{CH}_{\text{syn}}\text{H}$ ), 1.54 (d,  $^2J_{\text{HH}} = 11.4$ , 1H, Bzl  $\text{CH}_{\text{anti}}\text{H}$ ), 1.80 (s, 15H,  $\text{C}_5\text{Me}_5$ ), 2.26 (s, 3H, Pxl Me), 2.86 (d,  $^2J_{\text{HH}} = 7.6$ , 1H, Pxl  $\text{CH}_{\text{anti}}\text{H}$ ), 6.69 (d,  $^3J_{\text{HH}} = 7.9$ , 2H, Pxl H<sub>ortho/meta</sub>), 6.94 (d,  $^3J_{\text{HH}} = 7.9$ , 2H, Pxl H<sub>ortho/meta</sub>), aromatic signals for the benzyl ligand obscured.

#### 2.4.20 Preparation of $\text{Cp}^*\text{W}(\text{NO})(\text{CH}_2\text{C}_6\text{H}_5)(\text{CH}_2\text{C}_6\text{H}_3\text{-3,5-Me}_2)$ (**2.14**)

Complex **2.14** was prepared as a red microcrystalline powder from the thermolysis of **2** in mesitylene. To obtain single crystals for X-ray crystallographic analysis, the residue was dissolved in 1:1  $\text{CH}_2\text{Cl}_2$ /hexanes (10 mL). The mixture was filtered through Celite supported on a glass frit (1 x 0.7 cm) and concentrated in vacuo to one-third of the original volume. Cooling of the solution to  $-30^\circ\text{C}$  for several days induced the crystallization of **2.14** as orange needles (22 mg, 27 % yield).

IR ( $\text{cm}^{-1}$ ) 1553 (s,  $\nu_{\text{NO}}$ ). MS (LREI, m/z, probe temperature  $150^\circ\text{C}$ ) 559 [ $\text{P}^+$ ,  $^{184}\text{W}$ ], 529 [ $\text{P}^+ - \text{NO}$ ].  $^1\text{H}$  NMR (400 MHz,  $\text{CD}_2\text{Cl}_2$ )  $\delta$  -0.62 (d,  $^2J_{\text{HH}} = 11.5$ , 1H, Bzl  $\text{CH}_{\text{syn}}\text{H}$ ), 1.48 (d,  $^2J_{\text{HH}} = 11.5$ , 1H, Bzl  $\text{CH}_{\text{anti}}\text{H}$ ), 1.54 (d,  $^2J_{\text{HH}} = 6.6$ , 1H, Mes  $\text{CH}_{\text{syn}}\text{H}$ ), 1.82 (s, 15H,  $\text{C}_5\text{Me}_5$ ), 2.27 (s, 6H, Mes Me), 2.92 (d,  $^2J_{\text{HH}} = 6.6$ , 1H, Mes  $\text{CH}_{\text{anti}}\text{H}$ ), 6.26 (s, 2H, Mes H<sub>ortho</sub>), 6.85 (d,  $^3J_{\text{HH}} = 7.5$ , 2H, Bzl H<sub>ortho</sub>), 6.89 (t,  $^3J_{\text{HH}} = 7.3$ , 1H, Bzl H<sub>para</sub>),

7.00 (t,  $^3J_{\text{HH}} = 7.5$ , 2H, Bzl  $\text{H}_{\text{meta}}$ ), 7.42 (s, 1H, Mes  $\text{H}_{\text{para}}$ ).  $^{13}\text{C}\{^1\text{H}\}$  NMR (75 MHz,  $\text{CD}_2\text{Cl}_2$ )  $\delta$  10.6 ( $\text{C}_5\text{Me}_5$ ), 21.0 (Mes Me), 39.3 ( $\text{CH}_2$ ), 43.8 ( $\text{CH}_2$ ), 108.1 ( $\text{C}_5\text{Me}_5$ ), 118.9 (Mes  $\text{C}_{\text{ipso}}$ ), 123.4, 127.7, 129.8, 130.9, 132.5, 139.5 (Ar  $\text{C}_{\text{aryl}}$ ), 148.4 (Bzl  $\text{C}_{\text{ipso}}$ ).  
 NOEDS (400 MHz,  $\text{CD}_2\text{Cl}_2$ )  $\delta$  irradi. at 2.92, NOEs at 1.54, 6.26; irradi. at 6.26, NOEs at 1.54, 2.27, 2.92. Anal. Calcd. for  $\text{C}_{26}\text{H}_{33}\text{NOW}$ : C, 55.93; H, 5.95; N, 2.50. Found: C, 55.63; H 5.86; N.2.56.

**2.4.21 Preparation of  $\text{Cp}^*\text{W}(\text{NO})(\text{CH}_2\text{C}_6\text{H}_5)(\text{C}_6\text{H}_4\text{-3-CF}_3)$  (2.15a) and  $\text{Cp}^*\text{W}(\text{NO})(\text{CH}_2\text{C}_6\text{H}_5)(\text{C}_6\text{H}_4\text{-4-CF}_3)$  (2.15b)**

Complexes **2.15a-b** were prepared by the thermolysis of **2** in  $\alpha,\alpha,\alpha$ -trifluorotoluene and co-crystallized as a  $\sim 12 : 1$  mixture from 2:1  $\text{Et}_2\text{O}$ /hexanes (43 mg, 39 % yield).

IR ( $\text{cm}^{-1}$ )  $\nu_{\text{NO}}$  1595. MS (LREI,  $m/z$ , probe temperature 150  $^\circ\text{C}$ ) 585 [ $\text{P}^+$ ,  $^{184}\text{W}$ ], 555 [ $\text{P}^+ - \text{NO}$ ].  $^1\text{H}$  NMR (400 MHz,  $\text{C}_6\text{D}_6$ ) **2.15a**:  $\delta$  1.52 (s, 15H,  $\text{C}_5\text{Me}_5$ ), 2.09 (d,  $^2J_{\text{HH}} = 5.8$ , 1H, Bzl  $\text{CH}_{\text{syn}}\text{H}$ ), 3.32 (d,  $^2J_{\text{HH}} = 5.8$ , 1H, Bzl  $\text{CH}_{\text{anti}}\text{H}$ ), 6.52 (t,  $^3J_{\text{HH}} = 7.9$ , 2H, Bzl  $\text{H}_{\text{meta}}$ ), 6.76 (d,  $^3J_{\text{HH}} = 7.3$ , 2H, Bzl  $\text{H}_{\text{ortho}}$ ), 6.92 (t,  $^3J_{\text{HH}} = 7.6$ , 1H, Tol  $\text{H}_{\text{meta}}$ ), 7.08 (t,  $^3J_{\text{HH}} = 7.3$ , 1H, Bzl  $\text{H}_{\text{para}}$ ), 7.16 (d,  $^3J_{\text{HH}} = 7.6$ , 1H, Tol  $\text{H}_{\text{para}}$ ), 8.0 (br d, 1H, Tol  $\text{H}_{\text{ortho}}$ ), other  $\text{H}_{\text{ortho}}$  singlet not observed. **2.15b**:  $\delta$  1.51 (s, 15H,  $\text{C}_5\text{Me}_5$ ), 2.11 (d,  $^2J_{\text{HH}} = 5.8$ , 1H, Bzl  $\text{CH}_{\text{syn}}\text{H}$ ), 3.33 (d,  $^2J_{\text{HH}} = 5.8$ , 1H, Bzl  $\text{CH}_{\text{anti}}\text{H}$ ), 6.44 (t,  $^3J_{\text{HH}} = 7.9$ , 2H, Bzl  $\text{H}_{\text{meta}}$ ), 6.73 (d,  $^3J_{\text{HH}} = 7.3$ , 2H, Bzl  $\text{H}_{\text{ortho}}$ ), 7.08 (t,  $^3J_{\text{HH}} = 7.3$ , 1H, Bzl  $\text{H}_{\text{para}}$ ); 7.21 (d,  $^3J_{\text{HH}} = 7.6$ , 2H, Tol  $\text{H}_{\text{ortho/meta}}$ ), other doublet obscured.  $^{13}\text{C}\{^1\text{H}\}$  NMR (75 MHz,  $\text{C}_6\text{D}_6$ ) **2.15a**:  $\delta$  10.3, 10.5 ( $\text{C}_5\text{Me}_5$ ), 47.3, 47.4 ( $\text{CH}_2$ ), 108.2, 108.3 ( $\text{C}_5\text{Me}_5$ ), 112.7 (Bzl  $\text{C}_{\text{ipso}}$  of **2.15a**), 112.8 (Bzl  $\text{C}_{\text{ipso}}$  of **2.15b**), 124.4 (q,  $^2J_{\text{CF}} = 38$ ,  $\text{CCF}_3$  of **2.15a**), 118.8, 121.3, 123.1, 129.1,

129.8, 132.5, 132.8, 133.9, 135.6, 135.9, 139.5, 144.9 (Ar C<sub>aryl</sub>), 168.7 (Tol C<sub>ipso</sub> of **2.15a**), 172.2 (Tol C<sub>ipso</sub> of **2.15b**), other signals for aryl carbons not observed. <sup>19</sup>F NMR (188 MHz, CDCl<sub>3</sub>): δ 13.98 (**2.15a**), δ 13.4 (**2.15b**). Anal. Calcd. for C<sub>24</sub>H<sub>26</sub>F<sub>3</sub>NOW: C, 49.25; H, 4.48; N, 2.39. Found: C, 48.86; H, 4.63; N, 2.38.

#### 2.4.22 Thermolysis of **1** in *p*-Xylene, Mesitylene and α,α,α-Trifluorotoluene

Thermolysis of **1** in these solvents for 40 h at 70 °C led to the formation of known compounds **1.7** - **1.10**, and **2.17a-b**<sup>1,4</sup> except for the case of mesitylene, when an additional product, Cp\*W(NO)(CH<sub>2</sub>CMe<sub>3</sub>)(CH<sub>2</sub>C<sub>6</sub>H<sub>3</sub>-3,5-Me<sub>2</sub>) (**2.16**), was observed.

**2.16**: <sup>1</sup>H NMR (400 MHz, CDCl<sub>3</sub>) δ -2.38 (d, <sup>2</sup>J<sub>HH</sub> = 13.7, 1H, Npt CH<sub>syn</sub>H), 0.77 (s, 9H, CMe<sub>3</sub>), 1.52 (d, <sup>2</sup>J<sub>HH</sub> = 13.7, 1H, Npt CH<sub>anti</sub>H), 1.92 (s, 15H, C<sub>5</sub>Me<sub>5</sub>), 2.22 (7H, Mes CH<sub>syn</sub>H, Mes Me), 3.04 (d, <sup>2</sup>J<sub>HH</sub> = 7.4, 1H, Mes CH<sub>anti</sub>H), 6.53 (s, 2H, Mes H<sub>ortho</sub>), 7.29 (s, 1H, Mes H<sub>para</sub>).

#### 2.4.23 X-ray Diffraction Analyses of **2.4a**, **2.12** and **2.14**

Data collection and structure solutions were conducted at the University of British Columbia by Dr. B. O. Patrick. All measurements were recorded at -93(1) °C on a Rigaku/ADSC CCD area detector using graphite-monochromated Mo K<sub>α</sub> radiation. Data sets were corrected for Lorentz and polarization effects. The solid-state structures were solved by direct methods or heavy-atom Patterson methods, expanded using Fourier techniques and refined by full-matrix least-squares methods. The non-hydrogen atoms were refined anisotropically while the hydrogen atoms were included, but not refined.

All calculations were performed using the *teXsan* crystallographic software package of Molecular Structure Corporation.<sup>34</sup>

## 2.5 References and Notes

- (1) Tran, E.; Legzdins, P., unpublished results.
- (2) Debad, J. D.; Legzdins, P.; Rettig, S. J.; Veltheer, J. E. *Organometallics* **1993**, *12*, 2714-2725.
- (3) Dryden, N. H.; Legzdins, P.; Rettig, S. J.; Veltheer, J. E. *Organometallics*, **1992**, *11*, 2583-2590.
- (4) Dryden, N. H.; Legzdins; Trotter, J.; Yee, V. C. *Organometallics* **1991**, *10*, 2857-2870.
- (5) Legzdins, P.; Jones, R. H.; Phillips, E. C.; Yee, V. C.; Trotter, J.; Einstein, F. W. B. *Organometallics* **1991**, *10*, 986-1002.
- (6) Bau, R. Mason, S. A.; Patrick, B. O.; Adams, C. S.; Sharp, W. B.; Legzdins, P. *Organometallics* (in press).
- (7) (a) Bursten, B. E.; Cayton, R. H. *Organometallics*, **1987**, *6*, 2004-2005. (b) Poli, R.; Smith, K. M. *Organometallics*, **2000**, *19*, 2858-2867.
- (8) An agostic bond is a weak covalent interaction between the two atoms in a  $\sigma$ -bond (i.e. a C-H bond) and a metal center. For details, see: Brookhart, M.; Green, M. L. H.; Wong, L.-L. *Prog. Inorg. Chem.* **1988**, *36*, 1-124.

- (9) Adams, C. S.; Legzdins, P.; Tran, E. *J. Am. Chem. Soc.* **2001**, *123*, 612-624.
- (10) Debad, J. D.; Legzdins, P.; Batchelor, R. J.; Einstein, F. W. B. *Organometallics*, **1993**, *12*, 2094-2102.
- (11) For details, see Section 5.2.4 as well as: Debad, J. D. Ph. D. Dissertation, University of British Columbia, 1994.
- (12) Legzdins, P.; Rettig, S. J.; Veltheer, J. E. *Organometallics* **1993**, *12*, 3575-3585.
- (13) Theoretical calculations have shown that the model complex CpW(NO)(PMe<sub>3</sub>)(=CH<sub>2</sub>) has syn- and anticlinal orientations of the methyldiene H's about the M=C bond with respect to the Cp\* ligand. For details, see: Smith, K. M.; Poli, R.; Legzdins, P. *Chem. Eur. J.* **1999**, *5*, 1598-1608.
- (14) Nugent, W. A.; Mayer, J. M. *Metal-Ligand Multiple Bonds*; Wiley: New York, 1988; Chapter 4.
- (15) Schofield, M. H.; Schrock, R. R.; Park, L. Y. *Organometallics* **1991**, *10*, 1844-1851.
- (16) Crystals of **2.4a** are monoclinic of space group P<sub>c</sub>(#7),  $a = 9.5066(3) \text{ \AA}$ ,  $b = 8.8989(2) \text{ \AA}$ ,  $c = 12.5831(3) \text{ \AA}$ ,  $\alpha = 90^\circ$ ,  $\beta = 104.8540(5)^\circ$ ,  $\gamma = 90^\circ$ . The structure was solved by heavy-atom Patterson methods. Full-matrix least-squares

- refinement procedures lead to  $R_1 = 0.016$  for 3836 observed reflections ( $I > 3\sigma(I)$ ). Full details of the crystallographic analysis are provided in Appendix A.
- (17) (a) Nugent, W. A.; Mayer, J. M. *Metal-Ligand Multiple Bonds*; Wiley: New York, 1988; Chapter 3. (b) Labinger, J. A.; Winter, M. J. in *Comprehensive Organometallic Chemistry II*, Abel, E. W.; Stone, F. G. A.; Wilkinson, G. Eds.; Elsevier Science Ltd: New York, 1995; Volume 5, Chapter 5, pp 311-315.
- (18) (a) Schilling, B. E. R.; Hoffman, R.; Faller, J. W. *J. Am. Chem. Soc.* **1979**, *101*, 592-598. (b) Gibson, V. C. *J. Chem. Soc., Dalton Trans.* **1994**, 1607-1618.
- (19) (a) Chan, M. C. W.; Cole, J. M.; Gibson, V. C.; Howard, J. A. K.; Lehmann, C.; Poole, A. D.; Siemeling, U. *J. Chem. Soc., Dalton Trans.* **1998**, 103-111. (b) Mashima, K.; Tanaka, Y.; Kaidzu, M.; Nakamura, A. *Organometallics* **1996**, *15*, 2431-2433. (c) Kiel, W. A.; Lin, G.; Constable, A. G.; McCormick, F. B.; Strouse, C. E.; Eisenstein, O.; Gladysz, J. A. *J. Am. Chem. Soc.* **1982**, *104*, 4865-4878.
- (20) For example, the alkylidene complex  $\text{Cp}_2\text{Ti}(=\text{CHCMe}_3)$ , which is generated thermally by neopentane elimination from  $\text{Cp}_2\text{Ti}(\text{CH}_2\text{CMe}_3)_2$ , readily activates the C-H bonds of benzene and *p*-xylene, but reacts with itself intramolecularly and/or decomposes when generated in alkane solvents. For details, see: van der Heijden, H.; Hessen, B. *J. Chem. Soc., Chem. Commun.* **1995**, 145-146.

- (21) (a) Greenhough, T. J.; Legzdins, P.; Martin, D. T.; Trotter, J. *Inorg. Chem.* **1979**, *11*, 3268-3270. (b) Adams, R. D.; Chodosh, D. F.; Faller, J. W.; Rosan, A. M. *J. Am. Chem. Soc.* **1979**, *101*, 2570-2578. (c) Faller, J. W.; Nguyen, J. T.; Ellis, W.; Mazzieri, M. R. *Organometallics* **1993**, *12*, 1434-1438. (d) Ipaktschi, J.; Mirzaei, F.; Demuth-Eberle, G.; Beck, J.; Serafin, M. *Organometallics* **1997**, *16*, 3965-3972.
- (22) Crabtree, R. H. *The Organometallic Chemistry of the Transition Metals*, 3<sup>rd</sup> ed. J. Wiley and Sons, Inc.: Toronto, ON, 2001.
- (23) Walsh, P. J.; Hollander, F. J.; Bergman, R. G. *Organometallics* **1993**, *12*, 3705-3723.
- (24) Calculation for **A**: (2.1a-c) : (2.2a-b + 2.3) = 4.2(3) : 1.
- (25) Crystals of **2.12** are triclinic of space group  $P\bar{1}$  (#2),  $a = 8.5023(9)$  Å,  $b = 8.6298(9)$  Å,  $c = 15.805(1)$  Å,  $\alpha = 74.510(2)^\circ$ ,  $\beta = 79.936(2)(4)^\circ$ ,  $\gamma = 74.797(3)^\circ$ . The structure was solved by Patterson methods. Full-matrix least-squares refinement procedures lead to  $R1 = 0.026$  for 3801 observed reflections ( $I > 3\sigma(I)$ ). Full details of the crystallographic analysis are provided in Appendix A.
- (26) Two distinct conformations are observed in the crystal lattice of **1.7**. Both have the ortho methyl group cis to the NO ( $34.0(10)$  and  $-25.3(12)^\circ$  dihedral angles to

- N) as well as distorted bond angles to the ortho ring carbon (129.6(10) and 129.6(8)°).
- (27) Sharp, W. B. Ph. D. Dissertation, University of British Columbia, 2001.
- (28) Crystals of **2.14** are monoclinic of space group  $P2_1/a$ (#14),  $a = 8.7551(5)$  Å,  $b = 27.187(1)$  Å,  $c = 9.7641(5)$  Å,  $\alpha = 90^\circ$ ,  $\beta = 102.254(4)^\circ$ ,  $\gamma = 90^\circ$ . The structure was solved by direct methods. Full-matrix least-squares refinement procedures lead to  $R1 = 0.027$  for 3870 observed reflections ( $I > 3\sigma(I)$ ). Full details of the crystallographic analysis are provided in Appendix A.
- (29) Thermolysis of **1.8** in toluene under standard conditions (70 °, 40 h) confirms the presence of three products of toluene C-H activation, namely the meta and para aryl products,  $\text{Cp}^*\text{W}(\text{NO})(\text{CH}_2\text{C}_6\text{H}_4\text{-4-Me})(\text{C}_6\text{H}_4\text{-3-Me})$  and  $\text{Cp}^*\text{W}(\text{NO})(\text{CH}_2\text{C}_6\text{H}_4\text{-4-Me})(\text{C}_6\text{H}_4\text{-4-Me})$ , and the benzyl product  $\text{Cp}^*\text{W}(\text{NO})(\text{CH}_2\text{C}_6\text{H}_4\text{-4-Me})(\text{CH}_2\text{C}_6\text{H}_5)$ . Integration of signals in the  $^1\text{H}$  NMR spectrum yields a product ratio of 64: 32: 4, which is the same, within error, as that obtained from the thermolyses of **2** under the same conditions (63: 32: 5).
- (30) Shriver, D. F.; Drezdon, M. A. *The Manipulation of Air-Sensitive Compounds*, 2<sup>nd</sup> ed.; Wiley-Interscience: New York, 1986.
- (31) Harris, D. C. *Quantitative Chemical Analysis* 2<sup>nd</sup>. Ed.; W. H. Freeman and Co.: New York, 1987, pp. 44-55.

- (32) Since the detection method used in the elemental analysis cannot distinguish between  $D_2O$  and  $H_2O$ , H/D abundances were calculated using  $1 D = 1 H$
- (33) Tran, E.; Legzdins, P. *J. Am. Chem. Soc.* **1997**, *119*, 5071-5072.
- (34) *teXsan: Structure Analysis Package*. Molecular Structure Corp.: The Woodlands, TX, 1985 and 1992.

## CHAPTER 3

### Investigations Into The Mechanism of the C-H Bond Activation Chemistry Derived from Complexes 1 and 2

---

3.1	Introduction.....	97
3.2	Results and Discussion .....	104
3.3	Epilogue .....	123
3.4	Experimental Procedures.....	124
3.5	References and Notes.....	129

---

### 3.1 Introduction

In the previous Chapter, several trends were observed in the product selectivities derived from the C-H activation of substituted arenes by benzylidene **B** and neopentylidene **A**. At first glance, it would seem that identifying the factors responsible for these trends is straightforward, due to the mechanistic work conducted on both alkylidene systems and the pioneering work conducted on the selectivity of hydrocarbon activations effected by certain metal imido complexes.

In detail, Wolczanski and co-workers have rigorously studied the C-H bond activation chemistry mediated by a series of reactive imido complexes derived from amido precursors, namely  $X_2M(R)NHR'$  ( $M = Ti, Zr; X = NHSi^tBu_3, OSi^tBu_3$ )<sup>1,2</sup> and  $(Si^tBu_3(H)N=)Ta(R)(NHR')_2$ <sup>3</sup> ( $R = \text{alkyl, aryl; } R' = Si^tBu_3$ ). The general mechanism is illustrated in Figure 3.1, using the  $M = Ti, Zr$  complexes as examples.

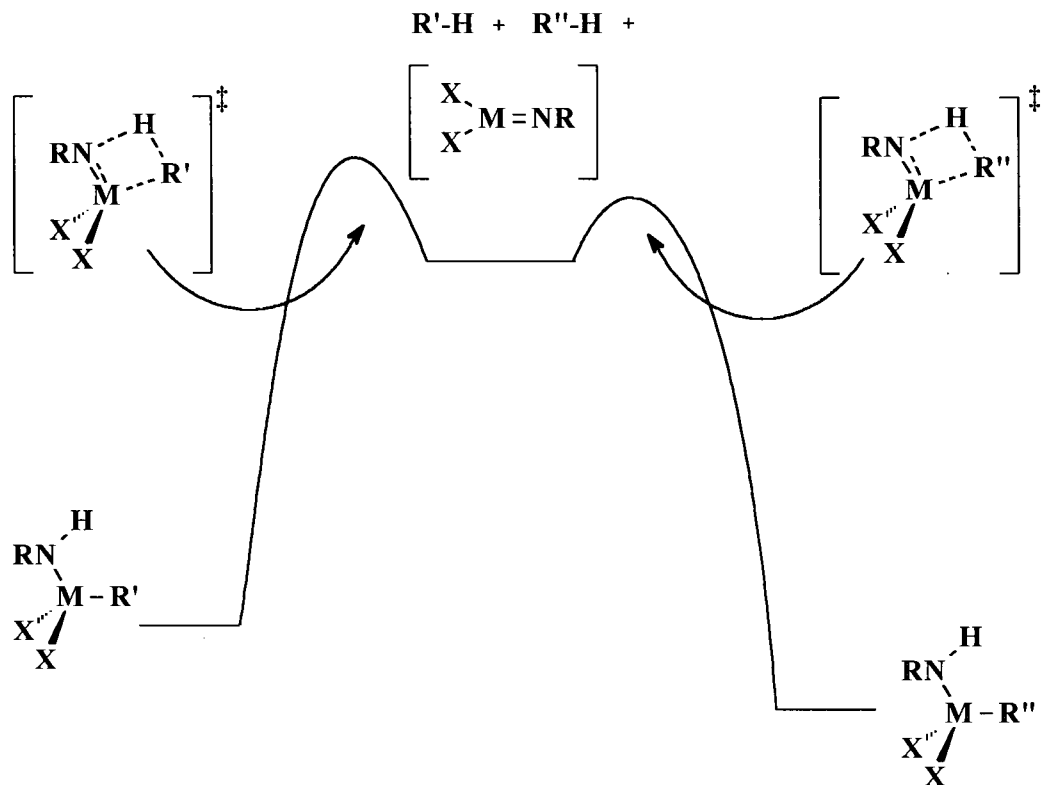


**Figure 3.1.** Qualitative free energy vs reaction coordinate diagram of the purported abstraction mechanism for the C-H activation chemistry derived from the amido complexes of Ti and Zr.

In these systems, the factors responsible for the product distributions obtained from the activation of a substrate containing more than one type of C-H bond, such as toluene, have been found to depend on the reaction conditions. In the first scenario, conditions are such that the activation of the substrate C-H bond is a reversible process (i.e. the products can revert back to the imido intermediate after the initial C-H bond scission event). In this instance, product formation is ultimately under thermodynamic control, and the observed equilibrium product distribution depends on the relative energies of the products themselves (i.e.  $\Delta\Delta G^\circ$  in Figure 3.2). Typically, the products of

activation of the stronger C-H bond are the most stable, with some moderation by steric effects. Hence, during the activation of toluene, the meta and para aryl products are formed preferentially over the ortho aryl and benzyl products.

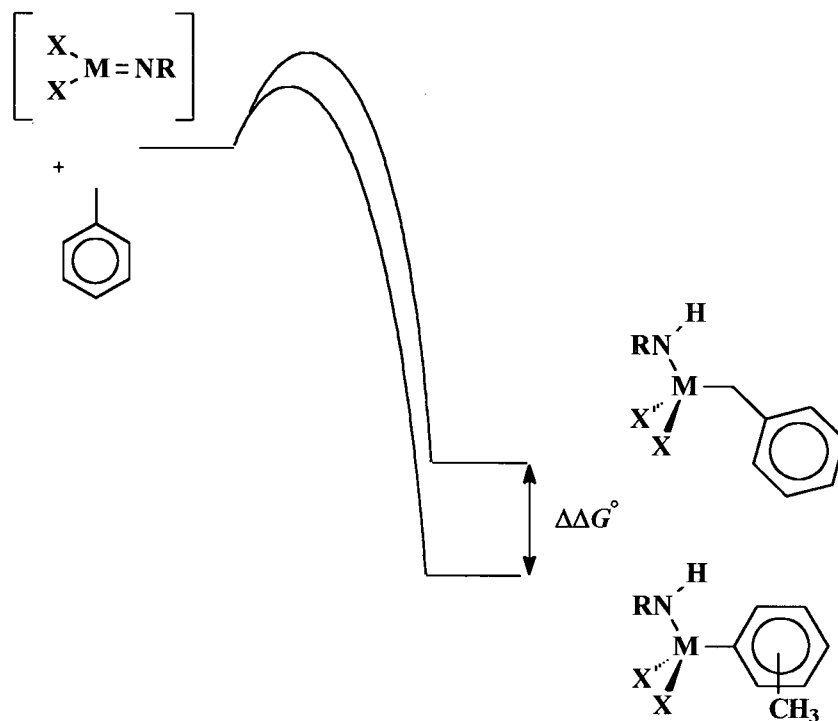


**Figure 3.2.** Qualitative depiction of the origin of product selectivity for the activation of toluene by the imido complexes of Ti and Zr under conditions of thermodynamic control.

In the second scenario, reaction conditions are such that the activation of the substrate C-H bond is irreversible (i.e. the products do not revert to the imido intermediate once formed). In this instance, product formation is under kinetic control, and the product distribution is determined by the relative transition-state energies for the cleavage of each type of C-H bond (i.e.  $\Delta\Delta G^\ddagger$  in Figure 3.3). Here again, the stronger C-H bonds are activated preferentially with some moderation by steric interactions in the

transition state. Hence, during the C-H activation of toluene under these conditions, the meta and para aryl products are again the preferred products over both ortho and benzyl derivatives. Note that the stronger bonds are broken faster due to the correlation of product energies with kinetic energy barriers, as explained by an extension of the Hammond Postulate.<sup>4</sup>

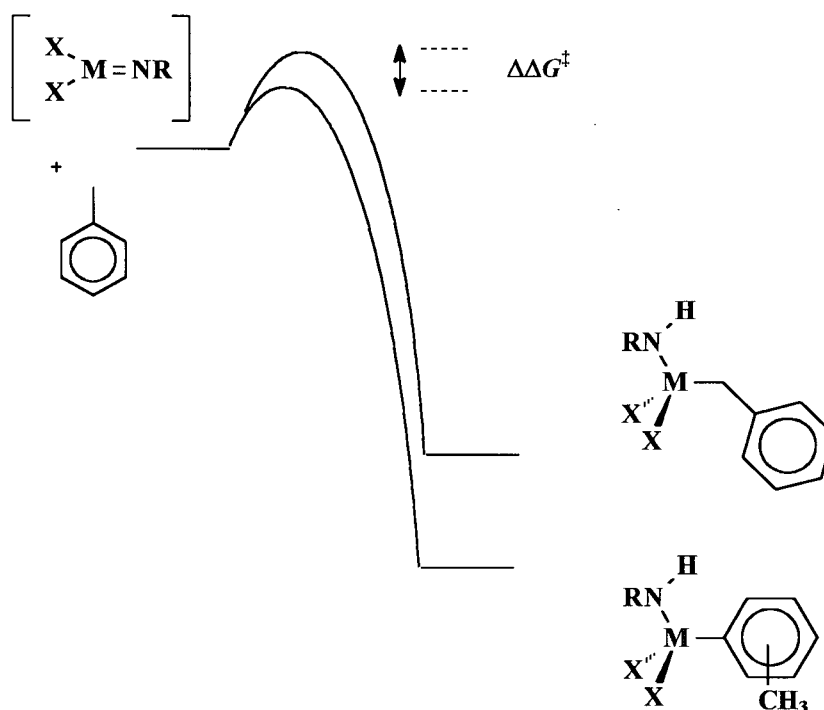


**Figure 3.3.** Qualitative depiction of the origin of product selectivity for the activation of toluene by the imido complexes of Ti and Zr under conditions of kinetic control.

Intriguingly, the general mechanism for the imido-mediated activation chemistry in Figure 3.1 is very similar to the proposed mechanism for the alkylidene-mediated activation chemistry derived from **1** (and **2**), as described in Section 1.1.8.1 and as illustrated in Figure 3.4.

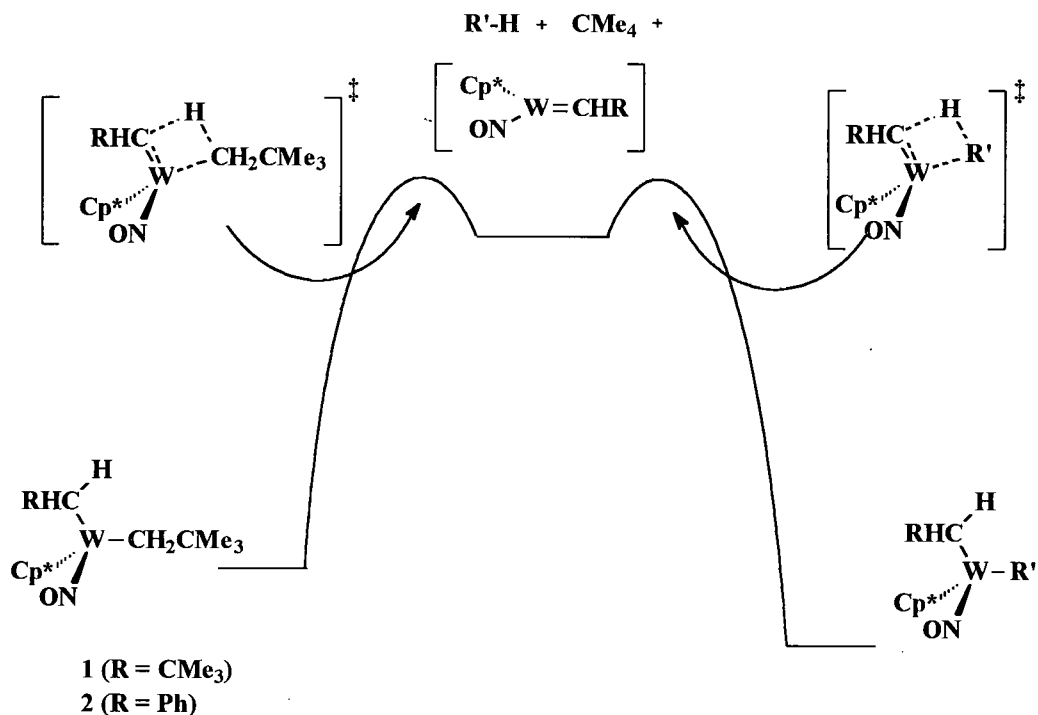


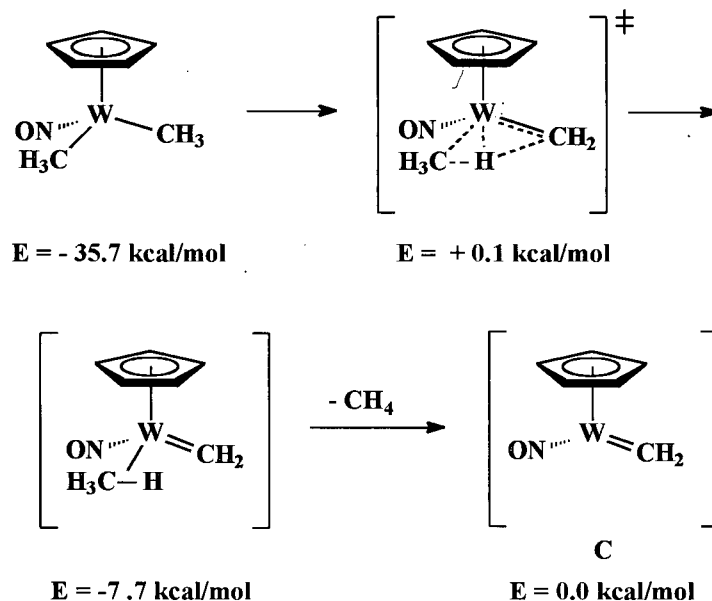
**Figure 3.4.** A qualitative representation of the free energy vs reaction coordinate diagram for the proposed abstraction mechanism for substrate C-H activation derived from **1** and **2**.

Hence, all that would appear to be required to explain the product selectivities reported in Chapter 2 is to determine whether or not substrate C-H bond scission is irreversible or reversible under the thermolysis conditions (i.e. 40 h at 70 °C). If substrate C-H bond scission is irreversible under these conditions, the formation of the products is under kinetic control and the observed product distribution is determined by the relative transition-state energies for cleavage of the various C-H bonds within the substrate. At the other extreme, if the C-H bond scission is reversible and rapid on the time-scale of the reaction (i.e. 40 h), the formation of the products is under thermodynamic control and the observed product distribution is determined by energy of the final products themselves.

An intermediate case is that C-H bond scission is reversible, but slow on the reaction time scale, so that the distributions observed at 40 h arise from a combination of both factors.

Unfortunately, the situation is not that straightforward: The purported  $\alpha$ -abstraction mechanism illustrated in Figure 3.4 *is not the only mechanism that fits the labeling and kinetic data reported in Section 1.1.8.1*. In fact, another valid and more complicated mechanism has been deduced by Poli and Smith from theoretical DFT calculations on the transformation of the model compound  $\text{CpW}(\text{NO})(\text{CH}_3)_2$  to the methylidene complex  $\text{CpW}(\text{NO})(=\text{CH}_2)$  (**C**).<sup>5</sup> These results indicate that the formation of the reactive alkylidene complex **C** does indeed begin with a metal-assisted, intramolecular  $\alpha$ -H abstraction with a late transition state in which M=C bond formation is essentially complete. Yet, a discrete hydrocarbon complex intermediate exists on the reaction coordinate after the  $\alpha$ -H abstraction, namely a methane  $\eta^2\text{-C,H}$   $\sigma$ -complex in which the methane remains coordinated to the metal center via one of its C-H bonds (Scheme 3.1).<sup>6</sup>

Scheme 3.1



The mechanism suggested by these calculations for **1** and **2** thus consists of rate-limiting  $\alpha$ -H abstraction from **1** or **2**, followed by neopentane elimination from a transient  $\sigma$ -neopentane complex to form the reactive alkylidene species **A** and **B**. By the Principle of Microscopic Reversibility,<sup>7</sup> the subsequent activation of the hydrocarbon substrates also involves formation of the respective hydrocarbon complexes prior to C-H bond addition to the M=C linkage. The mechanism is consistent with the kinetic and labeling data since the rate-determining step in the overall process still involves cleavage of an  $\alpha$ -H bond, and 1,2 cis addition of the substrate C-H (C-D) bond to the M=C linkage can still occur.

The presence of intermediate hydrocarbon complexes could significantly alter the interpretation of the activation chemistry derived from **1** and **2**. Consequently, this Chapter addresses whether or not hydrocarbon complexes exist as intermediates prior to

and after the formation of the reactive alkylidene species, and the role, if any, these intermediates play in the activation process.

## 3.2 Results and Discussion

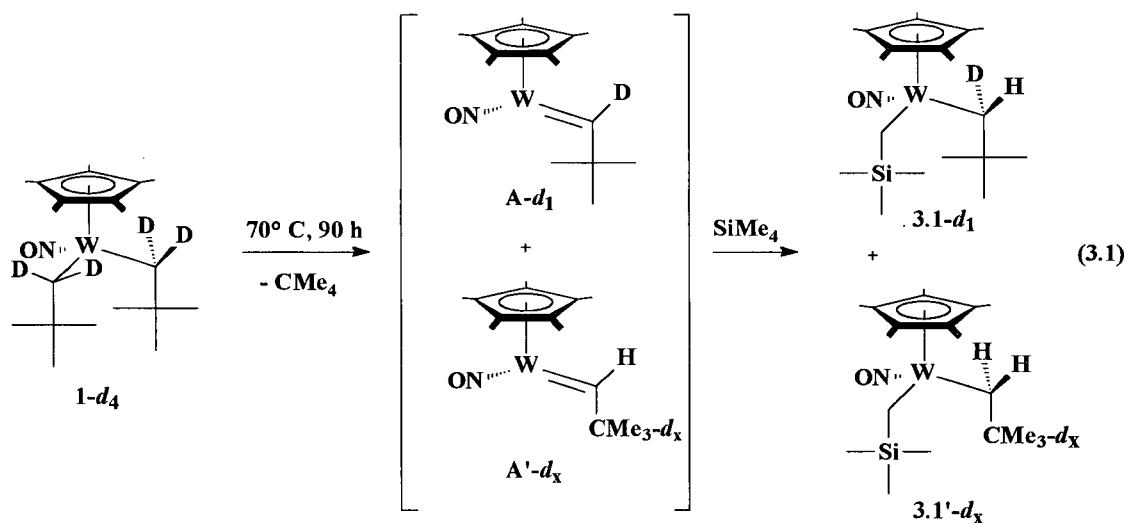
### 3.2.1 Known Strategies For Detecting Hydrocarbon Complexes

Hydrocarbon complexes have been observed directly by several spectroscopic methods, but specific conditions and/or special equipment are usually required to detect them.<sup>6</sup> Fortuitously, intermediate hydrocarbon complexes can also be detected indirectly via the observation of intramolecular H/D scrambling in the ligands involved in hydrocarbon elimination reactions.<sup>8,9</sup> This H/D scrambling strategy can be utilized here, since a suitable deuterated derivative, namely the  $\alpha$ -deuterated analog of **1**,  $\text{Cp}^*\text{W}(\text{NO})(\text{CD}_2\text{CMe}_3)_2$  (**1-d<sub>4</sub>**), can be synthesized.<sup>10</sup> If intermediate hydrocarbon complexes are being formed as suggested by Poli and Smith, then H/D scrambling should be observed between the neopentyl methylene and *t*-butyl positions of **1-d<sub>4</sub>** prior to neopentane elimination. To that end, complex **1-d<sub>4</sub>** has been thermolysed in representative aliphatic and aromatic solvents, and the results have been analyzed by NMR and GC/MS spectroscopic techniques.

### 3.2.2 Thermolysis of **1-d<sub>4</sub>** in Tetramethylsilane: NMR Analysis

Thermolysis of **1-d<sub>4</sub>** in tetramethylsilane at 70 °C for 90 h generates two products, as determined by NMR analysis of the resulting solid residue. The first product is  $\text{Cp}^*\text{W}(\text{NO})(\text{CH}_{\text{syn}}\text{DCMe}_3)(\text{CH}_2\text{SiMe}_3)$  (**3.1-d<sub>1</sub>**) (eq 3.1). Diagnostic features of **3.1-d<sub>1</sub>** in the  $^1\text{H}$  ( $\text{C}_6\text{D}_6$ ) NMR and  $^2\text{H}\{^1\text{H}\}$  ( $\text{C}_6\text{H}_6$ ) NMR spectra are the doublets attributable to the

syn- and anticlinal methylene protons of the trimethylsilylmethyl ligand, and the singlets arising from the syn- and anticlinal methylene proton and deuteron of the neopentyl ligand. Superimposed upon the spectral features of **3.1-d<sub>1</sub>** are those of the second product, namely Cp\*W(NO)(CH<sub>2</sub>CMe<sub>3-d<sub>x</sub></sub>)(CH<sub>2</sub>SiMe<sub>3</sub>) (**3.1'-d<sub>x</sub>**, 0 ≤ x ≤ 4 (vide infra)).<sup>11</sup> Diagnostic features of **3.1'-d<sub>x</sub>** are the two diastereotopic methylene doublets for the neopentyl ligand and a decrease in intensity of the combined *t*-butyl resonances relative to the Cp\* signal in the <sup>1</sup>H (C<sub>6</sub>D<sub>6</sub>) NMR spectrum. The latter feature is matched by the presence of a strong singlet in the *t*-butyl region in the <sup>2</sup>H{<sup>1</sup>H} (C<sub>6</sub>H<sub>6</sub>) NMR spectrum.



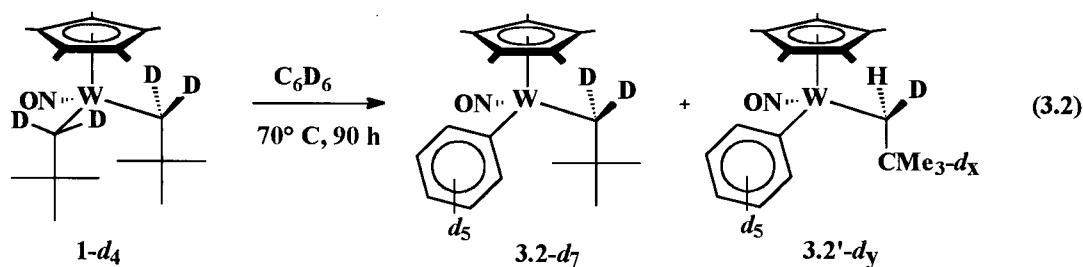
Complex **3.1-d<sub>1</sub>** is clearly formed via the C-H activation of tetramethylsilane by the  $\alpha$ -D neopentylidene complex derived from **1-d<sub>4</sub>**, namely Cp\*W(NO)(=CDCMe<sub>3</sub>) (**A-d<sub>1</sub>**). On the other hand, complex **3.1'-d<sub>x</sub>** is formed from substrate C-H bond activation by an  $\alpha$ -H alkylidene complex with deuterium in the *t*-butyl group, namely Cp\*W(NO)(=CHCMe<sub>3-d<sub>x</sub></sub>) (**A'-d<sub>x</sub>**). Complex **A'-d<sub>x</sub>**, in turn, is the expected result of H/D

exchange in the neopentyl ligands of **1-d<sub>4</sub>** prior to neopentane elimination.

Integration of appropriate signals in the <sup>1</sup>H (C<sub>6</sub>D<sub>6</sub>) NMR spectrum indicates that ~ 48% of the total product is **3.1'-d<sub>x</sub>**, thereby indicating that approximately half of **1-d<sub>4</sub>** undergoes H/D exchange during the thermolysis to form **A'-d<sub>x</sub>**. Moreover, on average, slightly less than three deuterium atoms are exchanged into the *t*-butyl group of **A'-d<sub>x</sub>** and **3.1'-d<sub>x</sub>** ( $x \cong 2.8$  in CMe<sub>3</sub>-d<sub>x</sub>).<sup>12</sup>

### 3.2.3 Thermolysis of **1-d<sub>4</sub>** in Benzene-d<sub>6</sub>: NMR Analysis

The thermolysis of **1-d<sub>4</sub>** in benzene-d<sub>6</sub> likewise generates products consistent with C-D activation by both **A-d<sub>1</sub>** and **A'-d<sub>x</sub>** (eq 3.2).



The <sup>2</sup>H{<sup>1</sup>H}(C<sub>6</sub>H<sub>6</sub>) NMR spectrum of the product mixture has unique signals attributable to Ph-D and D<sub>anti</sub> of Cp\*W(NO)(CD<sub>2</sub>CMe<sub>3</sub>)(Ph-d<sub>5</sub>) (**3.2-d<sub>7</sub>**) derived from **A-d<sub>1</sub>**. Additionally, there are overlapping resonances for D<sub>syn</sub> of **3.2-d<sub>7</sub>** and Cp\*W(NO)(CHD<sub>syn</sub>CMe<sub>3</sub>-d<sub>x</sub>)(Ph-d<sub>5</sub>) (**3.2'-d<sub>y</sub>**), as well as a *t*-butyl-D resonance for **3.2'-d<sub>y</sub>**. To match, there is a singlet resonance for H<sub>anti</sub> of **3.2'-d<sub>y</sub>** in the <sup>1</sup>H (C<sub>6</sub>D<sub>6</sub>) NMR spectrum. Integration of appropriate signals in the <sup>1</sup>H (C<sub>6</sub>D<sub>6</sub>) NMR spectrum reveals that the same amounts of H/D exchange are occurring, within error, in benzene-d<sub>6</sub> and in tetramethylsilane (i.e.  $y = x + 6$ ).

### 3.2.4 Thermolysis of 1- $d_4$ in Tetramethylsilane and Benzene- $d_6$ : GC/MS

#### Analysis

GC/MS spectrometry has been used to corroborate the results in Sections 3.2.2 and 3.2.3. The relative intensities of the *t*-butyl ion peaks in the  $m/z = 57$  to 61 portion of the mass fragmentation patterns formed by an 80 eV ionizing beam are known to reflect the relative composition of deuterated neopentanes in the volatile organics of thermolyses mixtures.<sup>13</sup> Each neopentane isotopomer that is present contributes to the intensity of the peaks at 57-61 according to the deuteration of the methyl groups and the presence of  $^{13}\text{C}$  isotopomers. Moreover, the fragmentation patterns derived from pure neopentane- $d_0$  through neopentane- $d_4$  have been experimentally determined and/or are calculable.<sup>13,14</sup> Thus, the isotopic composition of a volatile mixture of neopentanes can be determined by mathematical methods.

GC/MS analysis of the organic volatiles from both of the above reactions for 1- $d_4$  yields the observed patterns of *t*-butyl ion peaks collected in Table 3.1. The distributions clearly indicate that isotopomers in addition to neopentane- $d_3$  are being formed. Moreover, the 5x5 matrix analysis of the peak intensities estimates the composition in both cases to be primarily neopentane- $d_3$  and neopentane- $d_1$ , with small amounts of neopentane- $d_2$  and neopentane- $d_4$  (Table 3.2). Thus, the deuterium label is indeed being scrambled out of one of the neopentyl ligands prior to its elimination as neopentane. Note that the small negative values assigned to neopentane- $d_0$  are likely due to a combination of the assumptions that need to be made in the calculations (see Section 3.4.8) and the uncertainties in the average mass spectral intensities.

**Table 3.1.** Average Relative Intensities of Mass Spectral Peaks Derived From Neopentane.

sample	relative $m/z$ peak intensity				
	57	58	59	60	61
neopentane- $d_3$ <sup>a</sup>	33	1.47	0	100	4.4
from $1-d_4$ in tetramethylsilane	48.3	54.6	9.7	100	5.6
from $1-d_4$ in benzene- $d_6$	47.5	56.4	12.3	100	6.8

<sup>a</sup> reference 13

**Table 3.2.** Calculated Distributions of Neopentane Isotopomers Generated During the Thermolyses of  $1-d_4$ .

solvent	neopentane isotopomer distribution (%)				
	$d_0$	$d_1$	$d_2$	$d_3$	$d_4$
tetramethylsilane	(- 0.5)	31.6	4.9	63.3	0.6
benzene- $d_6$	(- 1.5)	31.8	6.4	61.8	1.6

### 3.2.5 Spectroscopic Monitoring of the Thermolysis of $1-d_4$ in Benzene

The results in Section 3.2.2-3.2.4 clearly support the notion that H/D exchange is occurring in the neopentyl ligands of  $1-d_4$  prior to neopentane elimination and activation of the solvent C-H (C-D) bonds. The H/D exchange process can also be observed directly via spectroscopic monitoring of the reactions of  $1-d_4$ .

For example, monitoring the thermolysis of  $1-d_4$  in benzene by  $^2\text{H}\{^1\text{H}\}(\text{C}_6\text{H}_6)$  NMR spectroscopy yields the spectra shown in Figure 3.5.

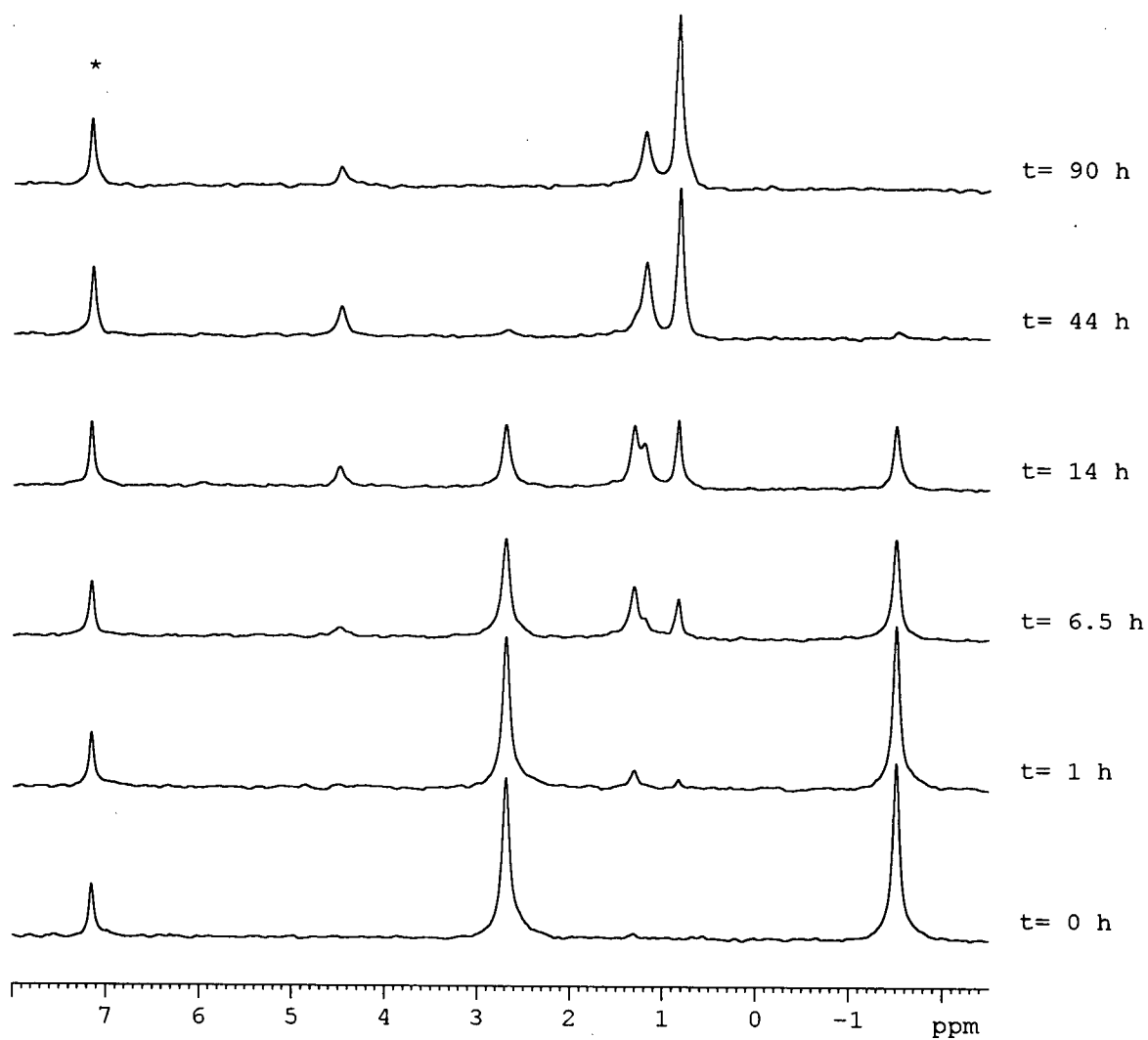


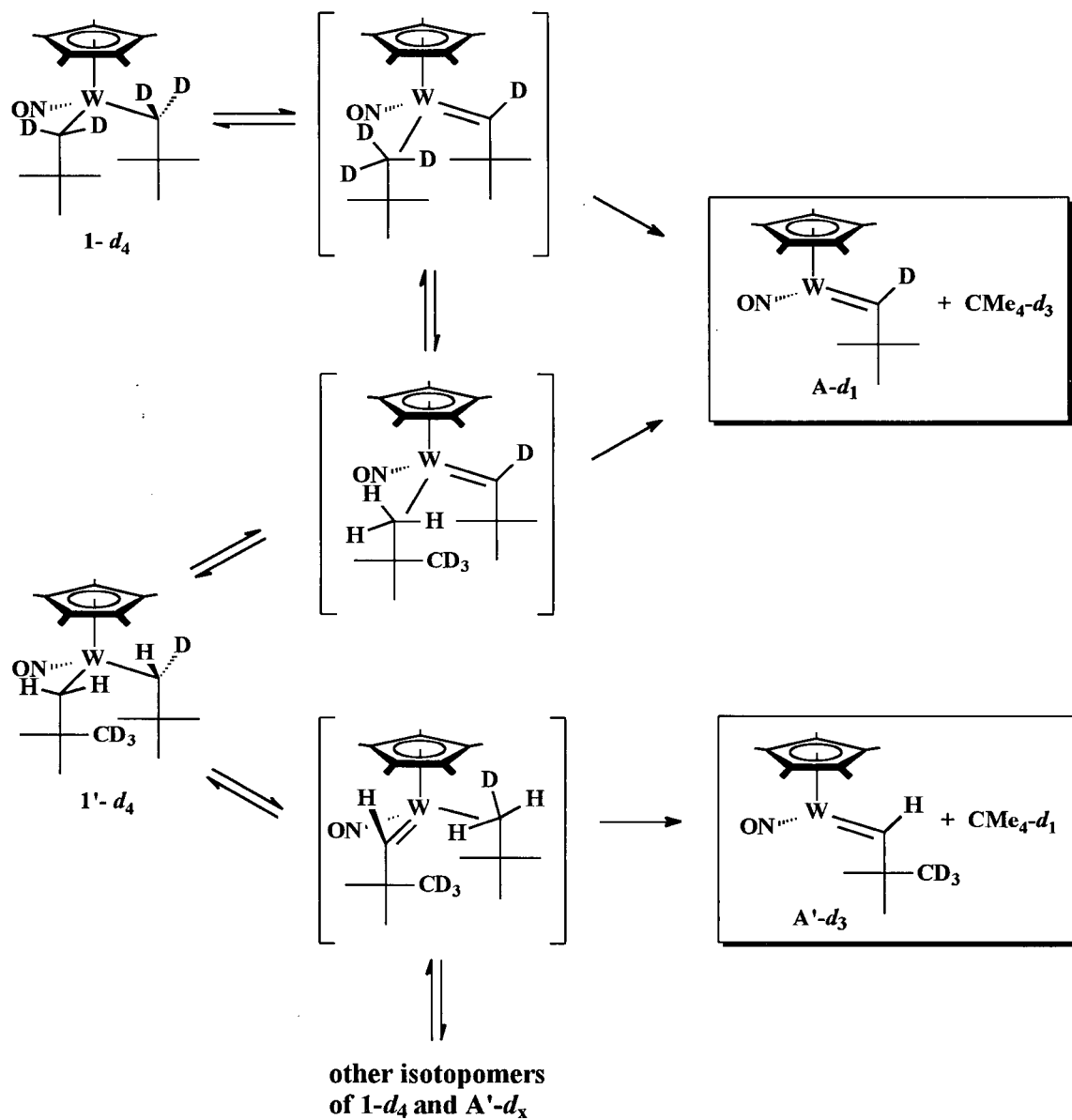
**Figure 3.5.**  $^2\text{H}\{^1\text{H}\}$  ( $\text{C}_6\text{H}_6$ ) NMR spectra from the thermolysis of  $1\text{-}d_4$  in benzene- $h_6$  over 90 h at  $70^\circ\text{C}$  (\* denotes the solvent peak).

Initially, a small resonance for deuterium in the *t*-butyl moiety of **1-*d*<sub>4</sub>** is observable at  $\delta$  1.30, along with the expected strong resonances from the deuterium label in the synclinal and anticlinal methylene positions at  $\delta$  - 1.51 and 2.69, respectively. After 1 h, however, the intensity of the signal at  $\delta$  1.30 increases noticeably while a new signal attributable to free deuterated neopentane is observed at  $\delta$  0.83. These spectral features are consistent with concomitant product formation and H/D exchange between the methylene positions and the *t*-butyl position of the neopentyl ligands. After 14 h, new signals are clearly visible for the  $D_{anti}$  ( $\delta$  4.49) and *t*-butyl-D moieties ( $\delta$  1.18) of the respective products of activation by **A**, namely  $Cp^*W(NO)(CH_{syn}DCMe_3)(Ph-h_5)$  (**3.2-*d*<sub>1</sub>**) and by **A'-*d*<sub>x</sub>**, namely  $Cp^*W(NO)(CH_2CMe_3-d_x)(Ph-h_5)$  (**3.2'-*d*<sub>x</sub>**). During the rest of the thermolysis, the signals for the starting material isotopomers decrease, while those of the products grow in, with no new signals being evident in the spectrum even after 90 h.<sup>15</sup>

### 3.2.6 Explanation of The Results: Hydrocarbon Complexes are Intermediates on the Reaction Coordinate for Alkylidene Complex Formation

All of the above results are consistent with the proposed intermediacy of  $\sigma$ -neopentane complexes, as shown in Scheme 3.2.

Scheme 3.2



$\alpha$ -D abstraction from  $1-d_4$  generates two types of  $\sigma$ -neopentane alkylidene complexes via exchange of  $\sigma$ -(C-H) and  $\sigma$ -(C-D) bonds. Elimination of neopentane from either  $\sigma$ -complex leads to  $\text{A-}d_1$ , while reversion of the abstraction leads to the reformation of  $1-d_4$  or to the formation of its H/D scrambled isotopomer,

$\text{Cp}^*\text{W}(\text{NO})(\text{CH}_{\text{syn}}\text{DCMe}_3)(\text{CH}_2\text{CMe}_3-d_3)$  ( $\mathbf{1}'-d_4$ ). A second abstraction event from  $\mathbf{1}'-d_4$  forms either  $\mathbf{A}-d_1$  or  $\mathbf{A}'-d_3$  depending on which neopentyl ligand undergoes C-H bond cleavage. Thus, upon neopentane elimination, neopentane- $d_1$  and - $d_3$  are generated as well as the C-H activation products of  $\mathbf{A}-d_1$  and  $\mathbf{A}'-d_3$ . After one or more additional generations of  $\sigma$ -neopentane complexes without neopentane elimination, other starting material isotopomers are produced from  $\mathbf{1}'-d_4$  in which the deuterium label is scrambled into the other positions of the neopentyl ligands. Upon elimination, these isotopomers can generate neopentane- $d_4$ , neopentane- $d_2$ , and neopentane- $d_0$ , as well as additional  $\alpha$ -H alkylidene intermediates  $\mathbf{A}'-d_0$ ,  $\mathbf{A}'-d_1$ ,  $\mathbf{A}'-d_2$  and  $\mathbf{A}'-d_4$ , which contain 0, 1, 2 or 4 deuterium atoms in the *t*-butyl group. However, even after repeated H/D exchange events, the formation of intermediates  $\mathbf{A}-d_1$  and  $\mathbf{A}'-d_3$ , and to a lesser extent  $\mathbf{A}'-d_1$ , remains statistically dominant. Thus, the average number of deuterium atoms incorporated into the *t*-butyl group remains close to three, while neopentane- $d_3$  and neopentane- $d_1$  are the dominant isotopomer by-products, as indeed observed experimentally.

The experimental data are inconsistent with all other mechanisms for the observed H/D exchange in the neopentyl ligands that are not on the reaction coordinate for formation of the alkylidene complexes from  $\mathbf{1}-d_4$ . For example, the lack of deuterium incorporation into the Cp\* methyl groups of the starting material isotopomers rules out H/D exchange via reversible formation of tucked-in Cp\*  $\sigma$ -neopentane complexes. Likewise, H/D exchange via reversible formation of metallacyclobutane  $\sigma$ -neopentane intermediates by  $\gamma$ -H abstraction would generate neopentane- $d_3$  and neopentane- $d_2$  as the

principal by-products. Finally, it is unlikely but possible that the H/D exchange is a bimetallic rather than a monometallic intramolecular process.<sup>9a,16</sup> However, the thermolysis of **1-d<sub>4</sub>** in benzene-*d*<sub>6</sub> at 70 °C at two different concentrations (15 mM and 75 mM) does not show any significant concentration effects on the rate of H/D exchange or product formation over the course of the reaction, observations consistent with an intramolecular process.

### 3.2.7 An Aside: The True Magnitude of the KIE for $\alpha$ -H Neopentane Elimination for Complex **1** vs Complex **1-d<sub>4</sub>**

The thermal decomposition of **1-d<sub>4</sub>** has been previously monitored by UV-visible absorbance spectroscopy and a first-order process was observed with a  $k_{\text{obs}}$  of  $2.01(1) \times 10^{-4} \text{ s}^{-1}$  at 91 °C ( $R^2 = 0.9989$ ) (see Section 1.1.8.1).<sup>17</sup> Without evidence of the H/D exchange process from this methodology, this  $k_{\text{obs}}$  was equated to the rate constant for  $\alpha$ -D elimination of neopentane ( $k_{\text{elim}}(\text{D}_{\text{syn}})$ ) for pure **1-d<sub>4</sub>**, and the  $\alpha$ -H(D) isotope effect for neopentane elimination was reported as 2.4(2) (91 °C).

In light of the results in Sections 3.2.2-3.2.5, it is now apparent that the thermal decomposition of **1-d<sub>4</sub>** involves both direct elimination of neopentane from **1-d<sub>4</sub>** and H/D exchange to  $\text{H}_{\text{syn}}$  isotopomers that intrinsically eliminate neopentane faster than **1-d<sub>4</sub>**. In other words, the measured  $k_{\text{obs}}$  is in fact a composite of the rate constants for direct neopentane elimination from **1-d<sub>4</sub>** ( $k_{\text{elim}}(\text{D}_{\text{syn}})$ ) as well as for elimination from its  $\text{H}_{\text{syn}}$  isotopomers ( $k_{\text{elim}}(\text{H}_{\text{syn}})$ ). Thus, the actual value of  $k_{\text{elim}}(\text{D}_{\text{syn}})$  from pure **1-d<sub>4</sub>** is likely less

than  $2.0 \times 10^{-4} \text{ s}^{-1}$  at 91 °C and the value of 2.4 is an underestimation of the true isotope effect for  $\alpha$ -H neopentane elimination in this system.

### 3.2.8 Implications of the Existence of Hydrocarbon Complexes on the General Mechanism of C-H Bond Activation by A and B

Given that hydrocarbon complexes do exist prior to formation of the reactive alkylidene species, then the two-step abstraction mechanism originally proposed from the initial mechanistic data cannot be valid. However, at the same time, the correlation between the C-H activation chemistry mediated by alkylidenes **A** and **B**, and Wolczanski et al.'s explanation of this chemistry may still hold, providing that the general reaction coordinate is shaped like that shown in Figure 3.6 (i.e.  $\Delta G^\ddagger_1$  and  $\Delta G^\ddagger_4 > \Delta G^\ddagger_2$  and  $\Delta G^\ddagger_3$ ). Moving from left to right,  $\alpha$ -abstraction from the starting complex **1** (or **2**) is the rate-limiting step in the overall process. Dissociation of neopentane from the resulting  $\sigma$ -neopentane complex leads to the formation of the reactive alkylidene intermediate **A** (or **B**). From this point forward, the activation of the substrate occurs, beginning with coordination of the substrate, such as an alkane, to the metal center, followed by C-H bond scission of the aliphatic bond to generate the activated products. Note that of the two steps in the activation of the substrate, C-H bond scission is the rate-limiting one (i.e.  $\Delta G^\ddagger_4 > \Delta G^\ddagger_3$ ).<sup>18</sup>

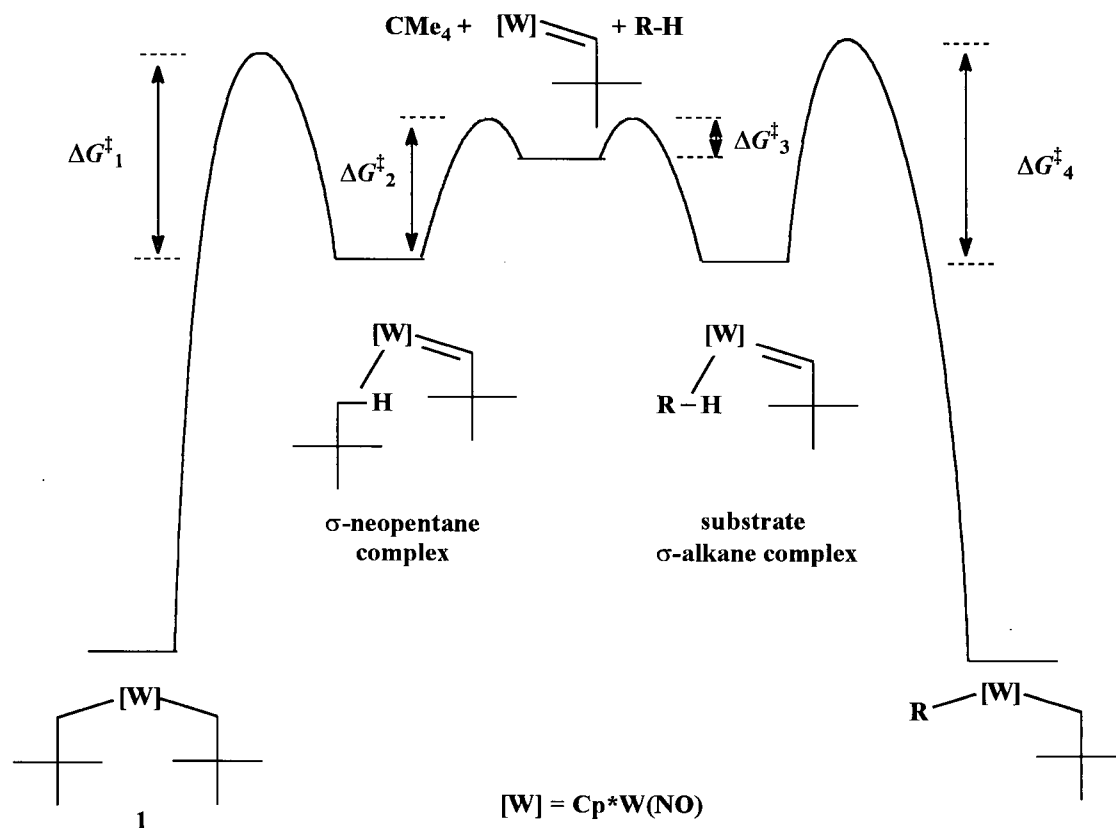


**Figure 3.6.** A possible qualitative free energy vs reaction coordinate diagram for the activation chemistry of 1 and 2 with C-H bond scission as the rate-limiting step, using the activation of an alkane substrate (R-H) via complex 1 as an illustrative example.

Figure 3.6 fits the explanation put forth by Wolczanski et al. for conditions under which the substrate C-H bond scission step is reversible, since the product distributions will still be ultimately determined by the relative energies of the products themselves. It will also apply for conditions in which the C-H bond scission step is irreversible, since the product distribution will still be determined by the relative transition state energies for C-H bond cleavage. In fact, Wolczanski et al. acknowledge that hydrocarbon

intermediates may also exist in their imido systems prior to C-H bond scission, and that the true reaction coordinates may resemble that in Figure 3.6, rather than the preferred concerted  $\alpha$ -abstraction mechanism drawn in Figure 3.1.<sup>1,2,3</sup> Whether or not Figure 3.6 is the correct reaction coordinate for the C-H activation chemistry resulting from **1** and **2** can be ascertained experimentally by measuring the intermolecular kinetic isotope effects (KIEs) for the activation of representative arene and aliphatic substrates.

### 3.2.9 Measurement of Intermolecular KIEs for Activation of Tetramethylsilane, Benzene and Mesitylene

The established method for measuring intermolecular KIEs involves thermolyses in 1:1 molar mixtures of a given substrate and its deuterated analog. Product ratios favouring the protio substrate will be observed if the reaction coordinate is like the one in Figure 3.6, as the distribution is controlled by the rate-determining cleavage of C-H vs C-D bonds. For example, Wolczanski et al. obtain KIE values of 9.0(6) and 29.4(35) for the activations of benzene/benzene- $d_6$  and methane/methane- $d_{12}$  by  $({}^t\text{Bu}_3\text{SiO})_2\text{Ti}=\text{NSi}{}^t\text{Bu}_3$ .<sup>19</sup> The isotope effects for rate-limiting substrate C-H (C-D) bond cleavage by other metal-complexes in a four-centered transition state are in the range of 3-6.<sup>20</sup> An important condition of the measurement of the KIEs is that solvents must be chosen in which the deuterio and protio activated products are formed irreversibly from one another under thermolysis conditions. If the activated products are not formed irreversibly, then the distribution of C-H and C-D activated products will reflect the thermodynamic stability of the respective products, rather than reflect the desired kinetic distribution.<sup>8b</sup>

Fortuitously, the activation of tetramethylsilane by **A** has been shown to be irreversible under the thermolysis conditions employed here: the product from thermolysis of **1** in tetramethylsilane- $d_{12}$ ,  $\text{Cp}^*\text{W}(\text{NO})(\text{CHDCMe}_3)(\text{CD}_2\text{SiMe}_3-d_3)$  (**1.4- $d_{12}$** ) does not form the protio analog  $\text{Cp}^*\text{W}(\text{NO})(\text{CH}_2\text{CMe}_3)(\text{CH}_2\text{SiMe}_3)$  (**1.4**) when thermolysed in tetramethylsilane- $h_{12}$  under standard thermolytic conditions (70 °C, 40 h).<sup>21</sup> Likewise, the activations of benzene by **A** and **B**, and mesitylene by **B**, are also irreversible, by similar tests of the thermal stability of the protio (or deuterio) activation products in the respective deuterio (or protio) solvents.

Hence, intermolecular KIEs have been determined for tetramethylsilane, benzene and mesitylene. In each case, complex **1** or **2** has been heated in a 1:1 molar mixture of the selected protio and deuterio solvent at 70 °C for 40 h, and the ratio of C-H and C-D activation products determined by integration of appropriate peaks in the resulting  $^1\text{H}$  NMR spectrum (Table 3.3). For instance, the thermolysis of **1** in a 1:1 molar mixture of tetramethylsilane- $h_{12}$  and tetramethylsilane- $d_{12}$  results in the formation of C-H and C-D activation products  $\text{Cp}^*\text{W}(\text{NO})(\text{CH}_2\text{CMe}_3)(\text{CH}_2\text{SiMe}_3)$  (**1.4**) and  $\text{Cp}^*\text{W}(\text{NO})(\text{CHD}_{syn}\text{CMe}_3)(\text{CD}_2\text{SiMe}_3-d_9)$  (**1.4- $d_{12}$** ) (eq 3.3). Integration of the  $\text{CH}_{anti}\text{H}$  doublet and  $\text{CH}_{anti}\text{D}$  singlets of **1.4** and **1.4- $d_{12}$** , respectively in the  $^1\text{H}$  NMR spectrum yields a 1.07(4):1 ratio at the 95% CI. Details of the other experiments and calculations are provided in Sections 3.4.9 to 3.4.12.

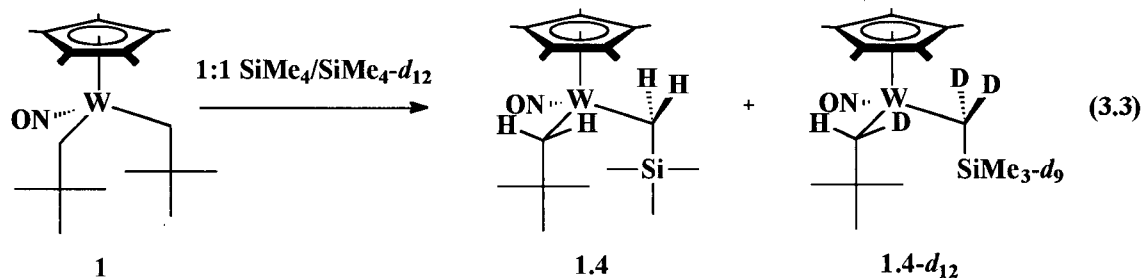


**Table 3.3.** Product Ratios for Activation of Protio vs Deuterio Substrates by **A** and **B**

Rea- gent	Solvent	Products	Products Ratio (C-H : C-D)
1	tetramethylsilane- <i>h</i> <sub>12</sub> / tetramethylsilane- <i>d</i> <sub>12</sub>	Cp*W(NO)(CH <sub>2</sub> CMe <sub>3</sub> )(CH <sub>2</sub> SiMe <sub>3</sub> ) ( <b>1.4</b> ) /Cp*W(NO)(CHD <sub>syn</sub> CMe <sub>3</sub> )(CD <sub>2</sub> SiMe <sub>3</sub> - <i>d</i> <sub>9</sub> ) ( <b>1.4-d</b> <sub>12</sub> )	1.07(4):1
1	benzene/benzene- <i>d</i> <sub>6</sub>	Cp*W(NO)(CH <sub>2</sub> CMe <sub>3</sub> )(C <sub>6</sub> H <sub>5</sub> ) ( <b>1.1</b> ) /Cp*W(NO)(CHD <sub>syn</sub> CMe <sub>3</sub> )(C <sub>6</sub> D <sub>5</sub> ) ( <b>1.1-d</b> <sub>6</sub> )	1.03(5):1
2	benzene/benzene- <i>d</i> <sub>6</sub>	Cp*W(NO)(CH <sub>2</sub> C <sub>6</sub> H <sub>5</sub> )(C <sub>6</sub> H <sub>5</sub> ) ( <b>2.5</b> ) /Cp*W(NO)(CHD <sub>syn</sub> C <sub>6</sub> H <sub>5</sub> )(C <sub>6</sub> D <sub>5</sub> ) ( <b>2.5-d</b> <sub>6</sub> )	1.17(19):1
2	mesitylene/ mesitylene- <i>d</i> <sub>12</sub>	Cp*W(NO)(CH <sub>2</sub> C <sub>6</sub> H <sub>5</sub> )(CH <sub>2</sub> C <sub>6</sub> H <sub>3</sub> -3,5-Me <sub>2</sub> ) ( <b>2.14</b> ) /Cp*W(NO)(CHD <sub>syn</sub> C <sub>6</sub> H <sub>5</sub> )(CD <sub>2</sub> C <sub>6</sub> D <sub>3</sub> - 3,5-Me <sub>2</sub> - <i>d</i> <sub>6</sub> ) ( <b>2.14-d</b> <sub>12</sub> )	1.06(15):1

The four product ratios in Table 3.3 are the intermolecular KIEs for substrates containing aliphatic sp<sup>3</sup>, aromatic sp<sup>2</sup> or benzylic sp<sup>3</sup> C-H vs C-D bonds. The near-unity values in all four cases indicate that **A** and **B** exhibit little preference for activating protio over deuterio substrates regardless of the C-H (C-D) bond type. This is clearly inconsistent with the reaction coordinate in Figure 3.6, in which protio substrate activation should be significantly favoured over deuterio substrate activation. Thus, it would appear that the alkylidene systems do not correlate to Wolczanski's imido systems

in any fashion whatsoever, and interpretations of the observed activation chemistry must be developed independently.

Fortuitously, the experimental KIE data can be fitted to two alternative reaction coordinates, one of which is depicted in Figure 3.7.

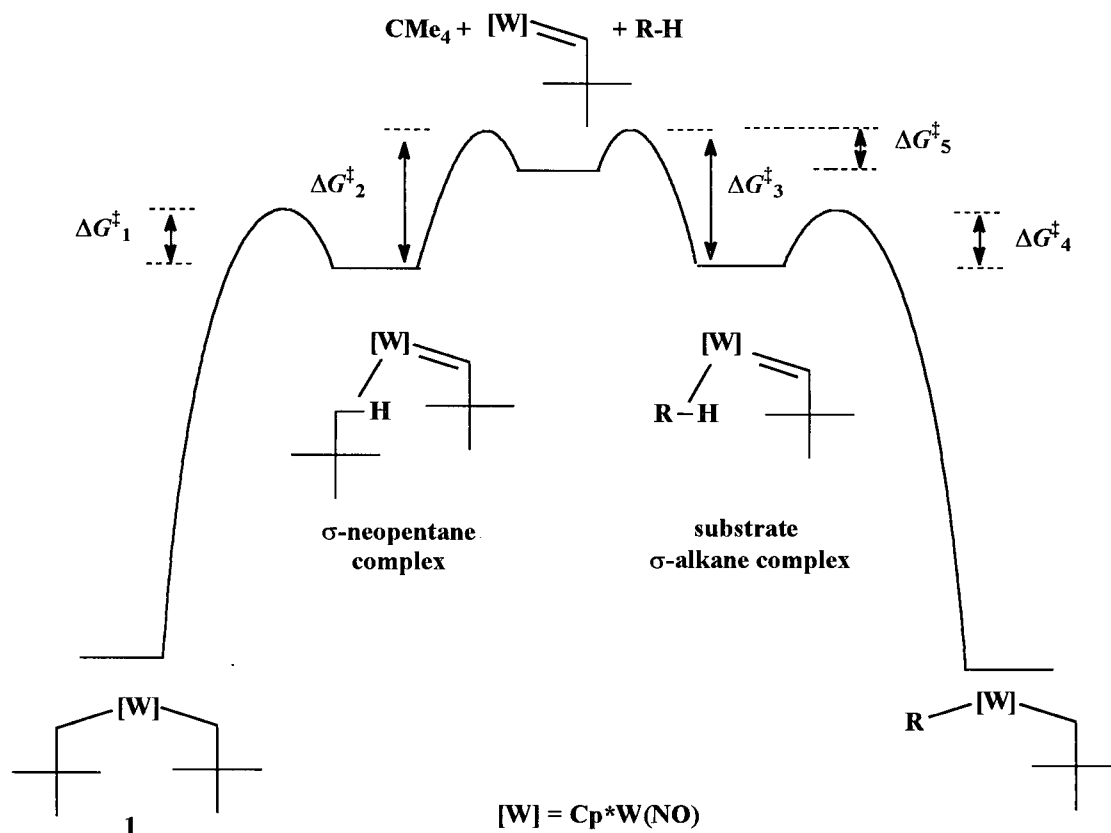


**Figure 3.7.** The proposed qualitative free energy vs reaction coordinate diagram for the activation chemistry derived from **1** and **2**, using the activation of an alkane substrate (R-H) via complex **1** as an illustrative example.

The key feature of Figure 3.7 is that the energy barrier to C-H bond scission from the substrate hydrocarbon complex is smaller than that for reversion back to the alkylidene intermediate (i.e.  $\Delta G^\ddagger_4 < \Delta G^\ddagger_3$ ). Thus, once a substrate is coordinated to the

alkylidene fragment, the activation of the C-H (C-D) bond is faster than exchange with the solvent. Hence, protio and deuterio substrates are not labile once activated. Moreover, providing that there is little energy difference between coordination of the protio vs deuterio substrates to the metal center ( $\Delta G^\ddagger_{5(\text{C-H})} \cong \Delta G^\ddagger_{5(\text{C-D})}$ ), the intermolecular KIEs will be small. Similarly-shaped reaction coordinates have been presented to account for the small intermolecular KIEs in the oxidative addition of alkane and arene to the thermally-generated  $\text{Cp}^*\text{Ir}(\text{PMe}_3)$  fragment and a related metallated derivative.<sup>22</sup>

### 3.2.10 The Questionable Intermediacy of the Alkylidene Complexes **A** and **B**

It is important to note that another reaction coordinate also fits the experimental data. To this point in this Thesis, it has been assumed that the alkylidene complexes **A** and **B** exist as discrete intermediates on the reaction coordinate. Indeed, **A** and **B** *must* be intermediates on the reaction coordinate for the proposed abstraction mechanism shown in Scheme 3.4. However, with hydrocarbon complex intermediates being present on the reaction coordinate, **A** and **B** do not have to exist as discrete entities. In fact, it is *unlikely* that **A** and **B** exist as discrete complexes, because there probably is not any significant barrier to solvation by the substrate, as there is depicted in Figure 3.7 ( $\Delta G^\ddagger_5$ ). The only instance in which a barrier to substrate solvation occurs is when **A** and **B** are internally solvated (or stabilized) by agostic interactions with either the  $\gamma$ - or  $\alpha$ -positions of the neopentylidene ligand, or a C-H bond of the  $\text{Cp}^*$  ligand.<sup>2,23</sup>

Consequently, the reaction coordinate in Figure 3.8 is also valid. In this instance, displacement of neopentane occurs via an interchange-dissociative mechanism,<sup>24</sup> rather than the dissociative mechanism pictured in Figure 3.7.<sup>25</sup> Thus, the discrimination

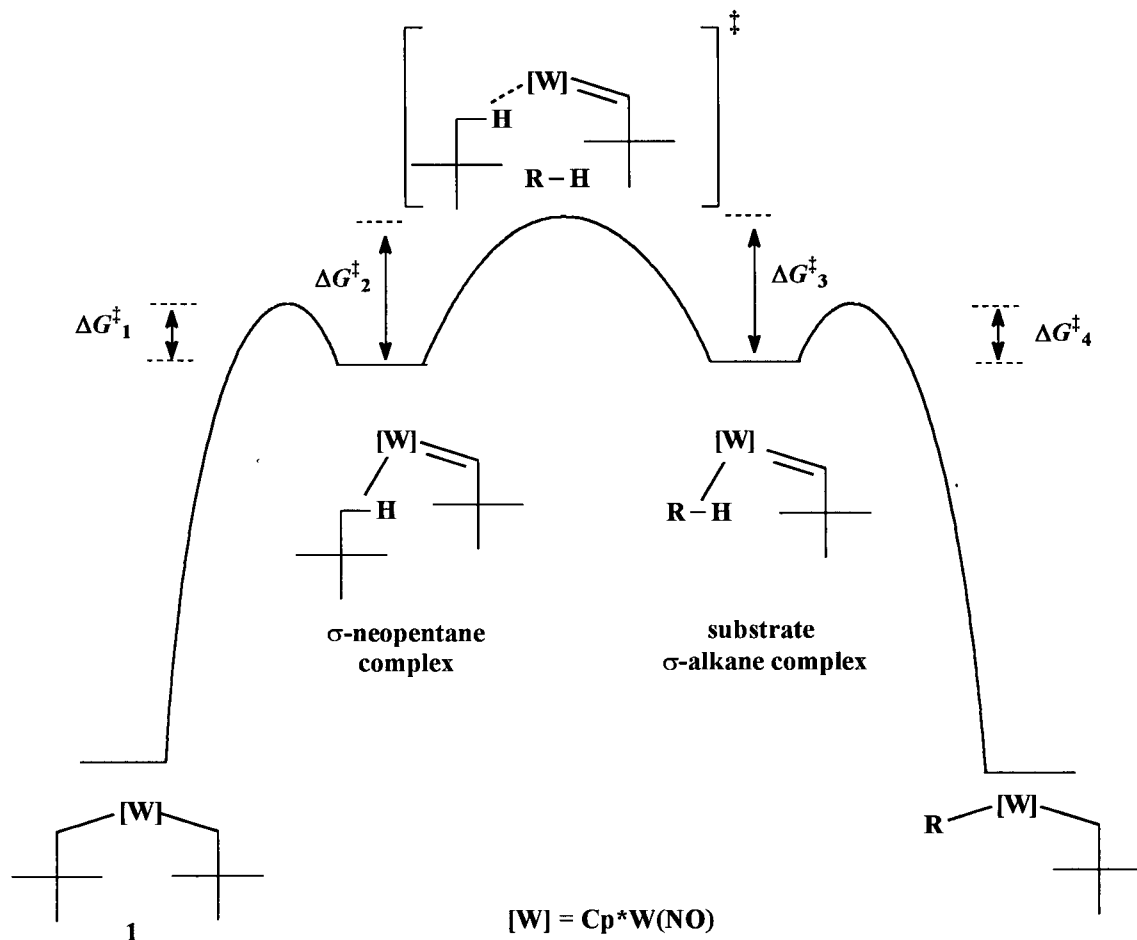


**Figure 3.8.** The alternative qualitative free energy vs reaction coordinate diagram with interchange-dissociation of neopentane as the rate-limiting step in the substrate activation process, using the activation of an alkane substrate (R-H) via complex **1** as an illustrative example.

between protio and deuterio substrates occurs via the relative transition-state energies for displacement of neopentane (i.e.  $\Delta G^\ddagger_{2(\text{C-H})} \cong \Delta G^\ddagger_{2(\text{C-D})}$ ) from the  $\sigma$ -neopentane complexes of **A** and **B**. The coordinate step is now effectively the rate-determining step in the

activation of the substrate. Again, little discrimination between protio and deuterio substrates will be observed providing that the differences in the transition-state energies for  $\sigma$ -(C,H) vs  $\sigma$ -(C,D) complex formation are small.

In the author's opinion, Figure 3.8 is most likely the correct representation of the reaction coordinate. However, at this stage of this Thesis, redefining the reactive alkylidene species from "intermediates **A** and **B**" to "the intermediate  $\sigma$ -complexes of **A** and **B**" creates several complications when discussing the activation chemistry derived from **1** and **2**. For example, since the reactive alkylidene intermediate may be the preceding  $\sigma$ -neopentane complex of **A** ( $\sigma$ -**A**), the phrase "activation of the substrate by **A** and **B**", as **A** and **B** are defined in Chapter 1, is no longer correct. Similarly, the phrase "the thermolysis of **1** and **2** generates **A** and **B**" is also no longer correct, since these species may not exist as discrete complexes. Moreover, all of the equations, schemes and figures to this point have utilized **A** and **B** as the reactive intermediates.

In addition to these technical issues, the intermediacy of **A** and **B** cannot be ruled out entirely due to the remote possibility of internal stabilization of the 16e species by agostic interactions. So, for the sake of simplicity, brevity, and the avoidance of any further confusion, intermediates **A** and **B** will be assumed to be the reactive alkylidene species in the remainder of the text, unless the differences in interpretations based on **A** and **B** vs  $\sigma$ -**A** and  $\sigma$ -**B** need to be explicitly stated or illustrated. It should be noted that the same decision has been made by other authors when faced with the same dilemma.<sup>1,2,22</sup> Note also, however, that in the future discussion of the chemistry derived from **1** and **2** outside of this Thesis, the following terminology should be used: (1) the

reactive alkylidene intermediates are complexes  $\text{Cp}^*\text{W}(\text{NO})(=\text{CHCMe}_3)$  and  $\text{Cp}^*\text{W}(\text{NO})(=\text{CHC}_6\text{H}_5)$ , or  $\text{Cp}^*\text{W}(\text{NO})(=\text{CHCMe}_3)(\sigma\text{-CMe}_4)$  and  $\text{Cp}^*\text{W}(\text{NO})(=\text{CHC}_6\text{H}_5)(\sigma\text{-CMe}_4)$ , and (2) that substrates coordinate to the reactive *fragments*  $\text{Cp}^*\text{W}(\text{NO})(=\text{CHCMe}_3)$  (**A**) and  $\text{Cp}^*\text{W}(\text{NO})(=\text{CHC}_6\text{H}_5)$  (**B**). The latter statement is unambiguous since the reactive fragments **A** and **B** may exist as discrete complexes or are the important part of the reactive  $\sigma$ -neopentane complexes.

### 3.3 Epilogue

Through labeling studies and intermolecular KIE measurements, the general mechanism of C-H activation derived from **1** and **2** have been shown to be fundamentally different from the general mechanism that was originally proposed. In particular, hydrocarbon complexes are present on the reaction coordinate prior to formation of the reactive alkylidene species and prior to substrate C-H bond scission. Moreover, the discriminating step in the activation of benzene, tetramethylsilane and mesitylene is the coordination of the substrate to the metal center in either intermediates **A** and **B**, or the preceding  $\sigma$ -neopentane complexes,  $\sigma\text{-A}$  and  $\sigma\text{-B}$ , and not the subsequent addition of the substrate C-H bond to the M=C linkage. The qualitative reaction coordinate for the activation of these substrates has thus been resolved to be either that shown in Figure 3.7 or in Figure 3.8. With these mechanistic details now resolved, completing the interpretation of the activation chemistry reported in Chapter 2 is now possible. Work conducted in this regard is described in the next Chapter.

### 3.4 Experimental Procedures

#### 3.4.1 General Methods

All reactions and subsequent manipulations were performed under anaerobic and anhydrous conditions using procedures described in Section 2.4.1. GC/MS analyses were performed on a Hewlett-Packard 6890 gas chromatograph with a HP-5MS column (30 M x 0.25 mm x 0.25  $\mu$ m) and a 5973N mass selective detector. An 80-eV ionizing beam was utilized.

#### 3.4.2 Reagents

The  $(\text{CD}_2\text{CMe}_3)\text{Mg}\cdot x(\text{dioxane})$  alkylating reagent and complex **1-*d*<sub>4</sub>** were prepared according to published procedures.<sup>10</sup>

#### 3.4.3 Characterization Data for **1-*d*<sub>4</sub>**

<sup>1</sup>H NMR (400 MHz, C<sub>6</sub>D<sub>6</sub>)  $\delta$  1.32 (s, 9H, CMe<sub>3</sub>), 1.47 (s, 15H, C<sub>5</sub>Me<sub>5</sub>). <sup>2</sup>H{<sup>1</sup>H} NMR (77 MHz, C<sub>6</sub>H<sub>6</sub>)  $\delta$  - 1.51 (br s, D<sub>syn</sub>), 2.69 (br s, D<sub>anti</sub>). Anal. Calcd. for C<sub>20</sub>H<sub>33</sub>D<sub>4</sub>NOW: C, 48.49; H/D<sup>26</sup>, 7.53; N, 2.83. Found: C, 48.80; H/D, 7.41; N, 2.85.

#### 3.4.4 Thermolyses of **1-*d*<sub>4</sub>** in Tetramethylsilane, Benzene, and Benzene-*d*<sub>6</sub>: General Comments

In each case, a J. Young NMR tube was charged with **1-*d*<sub>4</sub>** (12 mg, 0.024 mmol) and the appropriate solvent (0.8 mL). Two additional thermolyses were also conducted in benzene-*d*<sub>6</sub> at two different concentrations (6 mg and 30 mg in 0.80 mL of solvent), with hexamethyldisilane (2 mg, 0.014 mmol) added as an internal integration standard. The

thermolyses were conducted in a VWR 1160A constant-temperature bath set at 70.0 °C. The tubes were periodically removed to record  $^1\text{H}$  or  $^2\text{H}\{^1\text{H}\}$  NMR spectra at ambient temperature. After 90 h, the organic volatiles were separated *in vacuo* and were analyzed by GC/MS. The organometallic residue was analyzed further by  $^1\text{H}$  or  $^2\text{H}\{^1\text{H}\}$  NMR spectroscopies. Products were identified by comparison of the spectral data to those for the corresponding products of C-H and C-D activation from the thermolysis of **1** in protio and perdeuterio solvent (e.g. for tetramethylsilane, the data were compared to those exhibited by authentic  $\text{Cp}^*\text{W}(\text{NO})(\text{CH}_2\text{CMe}_3)(\text{CH}_2\text{SiMe}_3)$  (**1.4**) and  $\text{Cp}^*\text{W}(\text{NO})(\text{CH}_{\text{syn}}\text{DCMe}_3)(\text{CD}_2\text{SiMe}_3-d_9)$  (**1.4-d<sub>12</sub>**).<sup>17,21</sup>

#### 3.4.5 Preparation of $\text{Cp}^*\text{W}(\text{NO})(\text{CH}_{\text{syn}}\text{DCMe}_3)(\text{CH}_2\text{SiMe}_3)$ (**3.1-d<sub>1</sub>**) and $\text{Cp}^*\text{W}(\text{NO})(\text{CH}_2\text{CMe}_3-d_x)(\text{CH}_2\text{SiMe}_3)$ (**3.1'-d<sub>x</sub>**).

Complexes **3.1-d<sub>1</sub>** and **3.1'-d<sub>x</sub>** were prepared as a mixture from the thermolysis of **1-d<sub>4</sub>** in tetramethylsilane.  $^1\text{H}$  NMR (400 MHz,  $\text{C}_6\text{D}_6$ )  $\delta$  - 2.16 (overlapping dd and s, Npt  $\text{CH}_{\text{syn}}\text{H}$  and  $\text{CH}_{\text{syn}}\text{D}$ ), -1.29 (dd,  $^2J_{\text{HH}} = 12.0$ ,  $^4J_{\text{HH}} = 2.2$ , TMS  $\text{CH}_{\text{syn}}\text{H}$ ), 0.42 (s,  $\text{SiMe}_3$ ), 1.07 (d,  $^2J_{\text{HH}} = 12.0$ , TMS  $\text{CH}_{\text{anti}}\text{H}$ ), 1.35 (s,  $\text{CMe}_3$ ), 1.53 (s,  $\text{C}_5\text{Me}_5$ ), 3.28 (d,  $^2J_{\text{HH}} = 12.8$ , Npt  $\text{CH}_{\text{anti}}\text{H}$ ).  $^2\text{H}\{^1\text{H}\}$  NMR (61 MHz,  $\text{C}_6\text{H}_6$ )  $\delta$  1.25 (br s,  $\text{CMe}_3-d_x$ ), 3.23 (br s, Npt  $\text{CD}_{\text{anti}}\text{H}$ ).

#### 3.4.6 Preparation of $\text{Cp}^*\text{W}(\text{NO})(\text{CD}_2\text{CMe}_3)(\text{Ph}-d_5)$ (**3.2-d<sub>7</sub>**) and $\text{Cp}^*\text{W}(\text{NO})(\text{CHD}_{\text{syn}}\text{CMe}_3-d_x)(\text{Ph}-d_5)$ (**3.2'-d<sub>y</sub>**).

Complexes **3.2-d<sub>7</sub>** and **3.2'-d<sub>y</sub>** were prepared as a mixture from the thermolysis of **1-d<sub>4</sub>** in benzene- $d_6$ .  $^1\text{H}$  NMR (400 MHz,  $\text{C}_6\text{D}_6$ )  $\delta$  1.24 (s,  $\text{CMe}_3$ ), 1.53 (s,  $\text{C}_5\text{Me}_5$ ), 4.35

(br s,  $CH_{anti}D$ ).  $^2H\{^1H\}$  NMR (61 MHz,  $C_6H_6$ )  $\delta$  -2.01 (br s,  $CD_{syn}D$  and  $CD_{syn}H$ ), 1.18 (br s,  $CMe_3-d_x$ ), 4.34 (br s,  $CD_{anti}D$ ), 6.9-7.2 (Ph D).

#### 3.4.7 Preparation of $Cp^*W(NO)(CH_{syn}DCMe_3)(Ph-h_5)$ (3.2- $d_1$ ) and $Cp^*W(NO)(CH_2CMe_3-d_x)(Ph-h_5)$ (3.2'- $d_x$ ).

Complexes 3.2- $d_1$  and 3.2'- $d_x$  were prepared as a mixture from the thermolysis of 1- $d_4$  in benzene- $h_6$ .  $^1H$  NMR (400 MHz,  $C_6D_6$ )  $\delta$  -2.06 (br s,  $CH_{syn}D$ ), 1.26 (s,  $CMe_3$ ), 1.54 (s,  $C_5Me_5$ ), 4.49 (d,  $^2J_{HH} = 11.8$ ,  $CH_{anti}H$ ), 7.10 (m, Ph H), 7.70 (d,  $^3J_{HH} = 6.0$ , Ph H).  $^2H\{^1H\}$  NMR (61 MHz,  $C_6H_6$ )  $\delta$  1.22 (br s,  $CMe_3-d_x$ ), 4.50 (br s,  $CD_{anti}H$ ).

#### 3.4.8 GC/MS Analysis of Organic Volatiles

GC/MS spectra were recorded in triplicate. Average intensities were determined for neopentane fragment peaks 57 to 61. The neopentane isotopomer composition of each sample was then deduced by matrix methods as described by Girolami and coworkers,<sup>13</sup> using the experimental matrix coefficients for neopentane- $d_0$  to neopentane- $d_3$  under the assumption that all deuterium atoms reside on the same carbon. The coefficients for neopentane- $d_4$  were calculated assuming that  $(CD_3)(CH_2D)C(CH_3)_2$  was the only isotopomer present.

#### 3.4.9 Measurement of Intermolecular KIEs: General Comments

All experiments were conducted in a similar manner. A small reaction bomb was charged with 1 or 2 (12-15 mg), a stir-bar, and 3 mL of a 1.0:1.0 (v/v) mixture of benzene/benzene- $d_6$  or mesitylene/mesitylene- $d_{12}$ , or  $\sim$  2 mL of a 1.0:1.0 (mol/mol)

mixture of tetramethylsilane/tetramethylsilane- $d_{12}$ . After the stirred mixtures had been heated at 70(2) °C for 40 h in an oil-bath, the solvent was removed in vacuo and a  $^1\text{H}$  NMR ( $\text{C}_6\text{D}_6$ ) spectrum was recorded. KIE values were determined from the  $^1\text{H}$  NMR spectrum as described below. The reported errors are based on the standard errors in the mean and have been adjusted for sample size by multiplication of the appropriate Student  $t$  factor at the 95% confidence level.<sup>27</sup>

#### 3.4.10 Determination of the KIEs for **1** in Benzene/Benzene- $d_6$ and Tetramethylsilane/Tetramethylsilane- $d_{12}$

These KIEs are the average values obtained from multiple integrations of the fully resolved  $\text{CH}_{anti}\text{H}$  doublet and  $\text{CH}_{anti}\text{D}$  singlets of the products  $\text{Cp}^*\text{W}(\text{NO})(\text{CH}_2\text{CMe}_3)(\text{C}_6\text{H}_5)$  (**1.1**) to  $\text{Cp}^*\text{W}(\text{NO})(\text{CHD}_{syn}\text{CMe}_3)(\text{C}_6\text{D}_5)$  (**1.1- $d_6$** ), and  $\text{Cp}^*\text{W}(\text{NO})(\text{CH}_2\text{CMe}_3)(\text{CH}_2\text{SiMe}_3)$  (**1.4**) to  $\text{Cp}^*\text{W}(\text{NO})(\text{CHD}_{syn}\text{CMe}_3)(\text{CD}_2\text{SiMe}_3- $d_9$ )$  (**1.4- $d_{12}$** ). Two independent experiments were conducted for  $\text{C}_6\text{H}_6/\text{C}_6\text{D}_6$ , while the experiment in  $\text{SiMe}_4/\text{SiMe}_4- $d_{12}$$  was conducted only once.

#### 3.4.11 Determination of the KIE for **2** in Benzene/Benzene- $d_6$

The KIE was determined as follows: integration of the combined overlapping  $\text{H}_{anti}$  signals for the products  $\text{Cp}^*\text{W}(\text{NO})(\text{CH}_2\text{C}_6\text{H}_5)(\text{C}_6\text{H}_5)$  (**2.5**) and  $\text{Cp}^*\text{W}(\text{NO})(\text{CHD}_{syn}\text{C}_6\text{D}_5)(\text{C}_6\text{D}_5)$  (**2.5- $d_6$** ) vs the  $\text{H}_{syn}$  signal for **2.5** gave a relative ratio of 1.84(7):1 for (**2.5- $d_6$**  + **2.5**) vs **2.5**. Integration of  $\text{H}_{syn}$  vs  $\text{H}_{anti}$  for a sample of pure **2.5** recorded under identical spectrometer conditions yielded a value of 0.99(5):1. The ratio **2.5** to **2.5- $d_6$**  was then calculated to be 1.17(19):1

### 3.4.12 Determination of the KIE for 2 in Mesitylene/Mesitylene- $d_{12}$

The KIE was determined in similar manner as in 3.4.11, using the relative integrations of the 5 benzyl hydrogen atoms arising from both products  $\text{Cp}^*\text{W}(\text{NO})(\text{CH}_2\text{C}_6\text{H}_5)(\text{CH}_2\text{C}_6\text{H}_3\text{-3,5-Me}_2)$  (**2.14**) and  $\text{Cp}^*\text{W}(\text{NO})(\text{CHD}_{\text{syn}}\text{C}_6\text{H}_5)(\text{CD}_2\text{C}_6\text{D}_3\text{-3,5-Me}_2\text{-}d_6)$  (**2.14- $d_{12}$** ) vs the mesityl ortho singlet for **2.14** (4.9(3), (95% CI)), compared to the same ratio obtained for **2.14** (2.52(3)) under identical experimental/spectrometer conditions. The calculated ratio was thus 1.06(15).

### 3.5 References and Notes

- (1) Bennett, J. L.; Wolczanski, P. T. *J. Am. Chem. Soc.* **1997**, *119*, 10696-10719.
- (2) Schaller, C. P.; Cummins, C. C.; Wolczanski, P. T. *J. Am. Chem. Soc.* **1996**, *118*, 591-611.
- (3) Schaller, C. P.; Wolczanski, P. T. *Inorg. Chem.* **1993**, *32*, 131-144.
- (4) Briefly, when the reactions of two similar substrates proceed from a common intermediate by concerted processes with similar transition states, then the relative rates of the reactions will be proportional to the relative thermodynamic energies of the products. See: Connors, K. A. *Chemical Kinetics: The Study of Reaction Rates in Solution*; VCH Publishers: New York, NY, 1990; Chapter 5 and pp 371-375. Also see references 1-3 for illustrations.
- (5) Poli, R.; Smith, K. M. *Organometallics* **2000**, *19*, 2858-2867.
- (6) Hall, C.; Perutz, R. N. *Chem. Rev.* **1996**, *96*, 3125-3146.
- (7) The Principle of Microscopic Reversibility states that the forward and reverse reactions of a thermal process will follow the same path. Crabtree, R. H. *The Organometallic Chemistry of the Transition Metals*, 3<sup>rd</sup> ed; Wiley and Sons: Toronto, ON, 2001; pg. 177.

- (8) (a) Feher, F. J.; Jones, W. D. *J. Am. Chem. Soc.* **1984**, *106*, 1650-1663. (b) Jones, W. D.; Feher, F. J. *J. Am. Chem. Soc.* **1986**, *108*, 4814-4819. (c) Selmecky, A. D.; Jones, W. D.; Osman, R.; Perutz, R. N. *Organometallics* **1995**, *14*, 5677-5685. (d) Jones, W. D.; Hessel, E. T. *J. Am. Chem. Soc.* **1992**, *114*, 6087-6095. (e) Wick, D. D.; Reynolds, K. A.; Jones, W. D. *J. Am. Chem. Soc.* **1999**, *121*, 3974-3983. (f) Schaefer, D. F. II.; Wolczanski, P. T. *J. Am. Chem. Soc.* **1998**, *120*, 4881-4882. (g) Periana, R. A.; Bergman, R. G. Bergman, *J. Am. Chem. Soc.* **1986**, *108*, 7346-7355. (h) Stoutland, P. O.; Bergman, R. G. *J. Am. Chem. Soc.* **1988**, *110*, 5732-5744. (i) McGhee, W. D.; Bergman, R. G. *J. Am. Chem. Soc.* **1988**, *110*, 4246-4262. (j) Mobley, T. A.; Schade, C.; Bergman, R. G. *Organometallics*. **1998**, *17*, 3574-3587.
- (9) (a) Bullock, R. M.; Headford, C. E. L.; Hennessy, K. M.; Kegley, S. E.; Norton, J. E. *J. Am. Chem. Soc.* **1989**, *111*, 3897-3908. (b) Parkin, G.; Bercaw, J. E. *Organometallics* **1989**, *8*, 1172-1179. (c) Gould, G. L.; Heinekey, D. M. *J. Am. Chem. Soc.* **1989**, *111*, 5502-5504. (e) Gross, C. L.; Girolami, G. S. *J. Am. Chem. Soc.* **1998**, *120*, 6605-6606. (f) Chernega, A.; Cook, J.; Green, M. L. H.; Labella, L.; Simpson, S. J.; Souter, J.; Stephens, A. H. H. *J. Chem. Soc., Dalton Trans.* **1997**, 3225-3243.
- (10) Bau, R.; Mason, S. A.; Patrick, B. O.; Adams, C. S.; Sharp, W. B.; Legzdins, P. *Organometallics* (in press).

- (11) Throughout this Chapter, a “ ’ ” after a compound number is used to denote an isotopomer of the parent compound that is formed via intramolecular H/D exchange (i.e. **3.1-d<sub>1</sub>** and **3.1'-d<sub>1</sub>**).
- (12) The intensity of the  $CH_{anti}CMe_3$  signal of **3. 1'-d<sub>x</sub>** in the  $^1H$  ( $C_6D_6$ ) NMR spectrum is 48(2)% of the combined  $CH_{syn}HSiMe_3$  doublets for **3.1-d<sub>1</sub>** and **3. 1'-d<sub>x</sub>**, while the intensity of the  $^tBu$  resonance vs the  $Cp^*$  resonance in the  $^1H$  NMR spectrum is 85(2) % of the intensity for a fully protio  $^tBu$  moiety, as in the case of  $Cp^*W(NO)(CH_2CMe_3)(CH_2SiMe_3)$  (i.e. 0.66: 1.00 or  $\sim 9H : 15 H$ ). The average number of H atoms per  $^tBu$  group is thus  $(0.85*9 - (0.52*9))/0.48$  or 6.2. Therefore  $x$  in **3. 1'-d<sub>x</sub>** is approximately 2.8.
- (13) Cheon, J.; Rogers, D. M.; Girolami, G. S. *J. Am. Chem. Soc.* **1997**, *119*, 6804-6813.
- (14) For example, if one assumes that neopentane- $d_4$  has the composition  $(CH_3)_2C(CD_3)(CH_2D)$ , then the expected fragmentation should be  $(CH_3)_2C(CD_3)^+$  ( $m/z = 60$ ),  $(CH_3)_2C(CH_2D)^+$  ( $m/z = 58$ ), and  $(CH_3)C(CD_3)(CH_2D)^+$  ( $m/z = 61$ ) in a 1: 1 : 2 ratio. Also present will be peaks corresponding to the  $^{13}C$  satellites of each of these signals at  $m/z + 1$  of  $\sim 4.4$  % relative intensity of the  $m/z$  parent peak. Hence, the coefficients for  $m/z$  peaks 57-61 for pure  $(CH_3)_2C(CD_3)(CH_2D)$  are 0 : 48.9 : 2.15: 48.9 : 100.

- (15) As mentioned in Section 2.2.2, the protio-phenyl neopentyl complexes such as **3.2-*d*<sub>1</sub>** and **3.2'-*d*<sub>x</sub>** are sufficiently unstable towards β-H elimination of a second equivalent of neopentane under these conditions that the analysis of the neopentane isotopomer distribution from this reaction could not be included in Tables 3.1 and 3.2.
- (16) Booij, M.; Deelman, B-J.; Duchateau, R.; Postma, D. S.; Meetsma, A.; Teuben, J. H. *Organometallics* **1993**, *12*, 3531-3540.
- (17) Adams, C. S.; Legzdins, P.; Tran, E. *J. Am. Chem. Soc.* **2001**, *123*, 612-624.
- (18) It should be clarified that the relative displacement of the intermediates and products, as well as the relative peak heights and depth of the energy wells, in Figure 3.6 are not meant to be quantitative. True, the relative energies of the intermediates and transition states must be significantly higher than the starting material or products, given that H/D exchange in the thermolyses of **1-*d*<sub>4</sub>** is not observed until neopentane elimination is observed as well. However, the differences in the free energy barriers for C-H bond scission and neopentane dissociation, namely  $\Delta G^\ddagger_1$  and  $\Delta G^\ddagger_2$ , and  $\Delta G^\ddagger_3$  and  $\Delta G^\ddagger_4$ , cannot be as large as depicted given that H/D exchange and reversion back to starting material is competitive with neopentane formation in the thermolyses of **1-*d*<sub>4</sub>**.

- (19) Slaughter, L. M.; Wolczanski, P. T.; Klinckman, T. R.; Cundari, T. R. *J. Am. Chem. Soc.* **2000**, *122*, 7953-7975
- (20) Arndtsen, B. A.; Bergman, R. G.; Mobley, T. A.; Peterson, T. H. *Acc. Chem. Res.* **1995**, *28*, 154-162.
- (21) Tran, E.; Legzdins, P. *J. Am. Chem. Soc.* **1997**, *119*, 5071-5072.
- (22) Peterson, T. H.; Golden, J. T.; Bergman, R. G. *J. Am. Chem. Soc.* **2001**, *123*, 455-462.
- (23) For a review of agostic interactions, see: Brookhart, M.; Green, M. L. H.; Wong, L.-L. *Prog. Inorg. Chem.* **1988**, *36*, 1-124.
- (24) For a good illustration of the differences between these mechanisms and their associative counterparts, see: Cotton, F. A.; Wilkinson, G.; Gaus, P. L. *Basic Inorganic Chemistry*, 2<sup>nd</sup> ed. Wiley and Sons Inc.: Toronto, ON: 1987; pp 176-179.
- (25) Note that the other two possible mechanisms for exchange of neopentane for substrate, namely associative and interchange-associative mechanisms, can be ruled out. Both associative and intimate-associative mechanisms would require association of the substrate with the metal center prior to neopentane dissociation. However, this is not likely given the 18e nature of the  $\sigma$ -neopentane alkylidene

complexes. Moreover, the rate-constants for the thermolysis of **1** and **2**, as well the amounts of H/D exchange in the thermolyses of **1-d<sub>4</sub>**, do not show any significant solvent effects, which would be expected if the solvent is involved in the displacement of neopentane from the metal's coordination sphere.

- (26) Since the detection method used in the elemental analysis cannot distinguish between D<sub>2</sub>O and H<sub>2</sub>O, H/D abundances were calculated using 1 D = 1 H
- (27) Harris, D. C. *Quantitative Chemical Analysis* 2<sup>nd</sup>. Ed.; W. H. Freeman and Co.: New York, 1987; pp. 44-55.

## CHAPTER 4

### Rationalizing the C-H Activation Chemistry Derived From Complexes 1 and 2

---

4.1	Introduction.....	136
4.2	Results and Discussion .....	136
4.3	Epilogue .....	174
4.4	Experimental Procedures.....	177
4.5	References and Notes.....	183

---

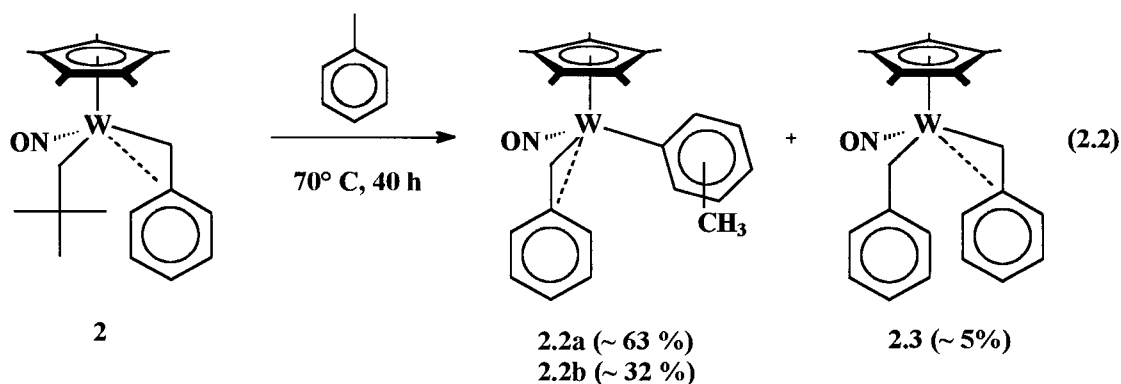
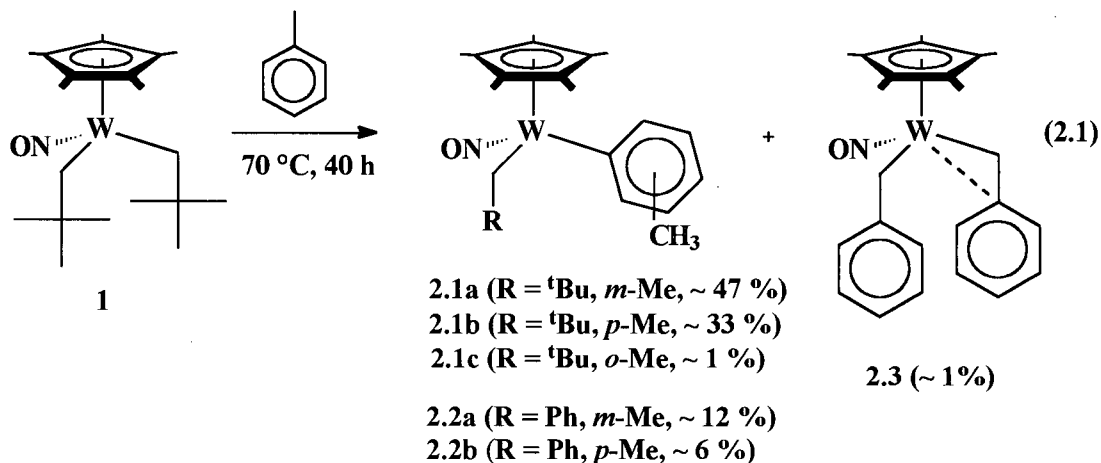
## 4.1 Introduction

In the previous Chapter, it was determined that hydrocarbon complexes are intermediates on the reaction coordinate for hydrocarbon activation mediated by alkylidenes **A** and **B**, and that the formation of these intermediates is the key step in the activation of benzene, tetramethylsilane and mesitylene. However, these substrates only contain one type of C-H bond, or only yield one type of organometallic product. Thus, it remains to be determined how the product selectivities and trends arise from the activation of the other substituted arenes reported in Chapter 2. Investigations into these matters are described in this Chapter, beginning with an in-depth examination of the activation of toluene.

## 4.2 Results and Discussion

### 4.2.1 Case 1: Activation of Toluene

As outlined in Sections 2.2.2, 2.2.3 and 2.2.16, the thermolysis of **1** and **2** in toluene leads to the formation of the respective aryl and benzyl products of  $sp^2$  C-H and  $sp^3$  C-H bond activation of toluene by **A** and **B**, as depicted in eq 2.1 and 2.2. These equations are reproduced below to help facilitate the ensuing discussion. Of note, the ratio of aryl vs benzyl products from toluene activation by **A** is 4.2(3):1, compared to 18.6(1.2):1 by **B**. Also, the distribution of the aryl regioisomers obtained from activation by **B** is the statistical meta: para distribution of 2:1 (1.97(11):1), whereas that obtained from activation by **A** is 1.45(8):1 and the ortho aryl activated product is observed as a trace product (~ 1% overall).



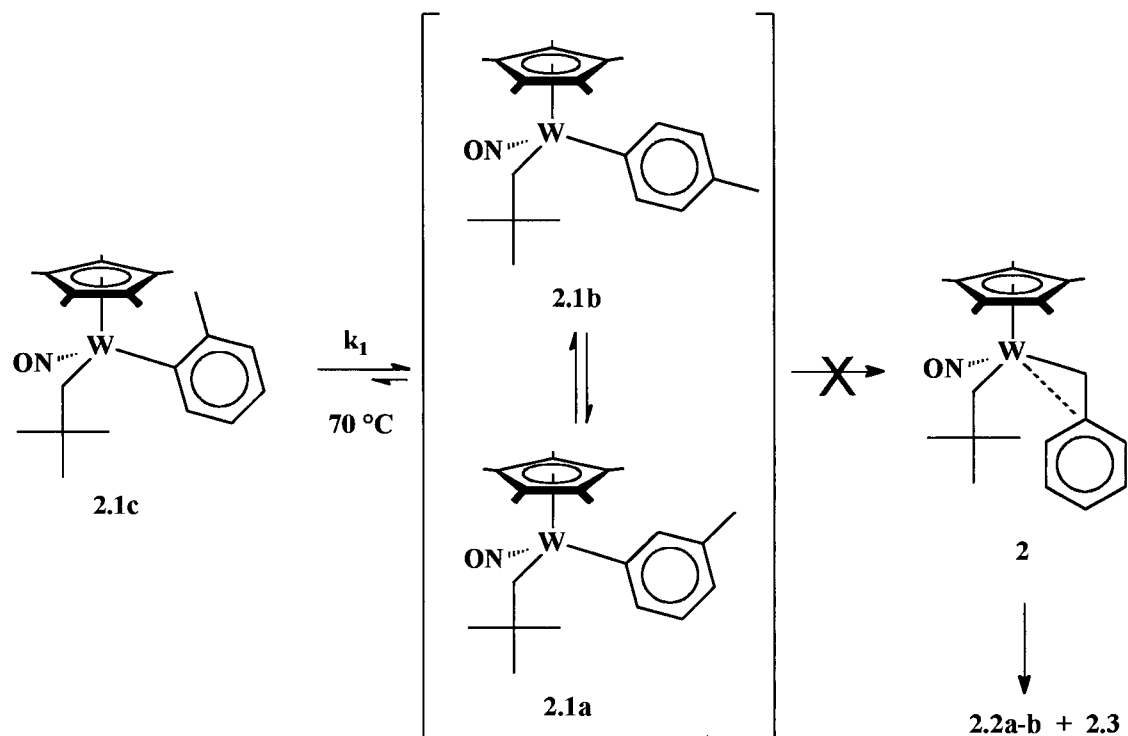
#### 4.2.1.1 The Nature of the Product Distributions

To determine the kinetic or thermodynamic nature of the toluene product distributions, three representative complexes were synthesized by metathetical methods: the *o*-tolyl neopentyl complex **2.1c**, the *o*-tolyl benzyl complex  $\text{Cp}^*\text{W}(\text{NO})(\text{CH}_2\text{C}_6\text{H}_5)(\text{C}_6\text{H}_4\text{-2-Me})$  (**2.2c**), and the bis(benzyl) complex **2.3**. Each was then heated independently in toluene at 70 °C for > 24 h. As anticipated, complex **2.3** is thermally robust and does not convert to the corresponding aryl benzyl products **2.2a-c**. Likewise, the *o*-tolyl complex **2.1c** does not convert to the benzyl complexes **2.3** or **2.2a-b** by isomerization to **2**, nor does **2.2c** isomerize to **2.3**. Thus, it would appear that the aryl and benzyl products of toluene C-H activation are formed separately and irreversibly

from **A** and **B** under the thermolysis conditions. In other words, the aryl vs benzyl product distributions are formed under kinetic control, and the magnitudes of these distributions reflect the intrinsic preferences for formation of the aryl products of toluene C-H activation from alkylidenes **A** and **B**, respectively.

Surprisingly, when thermolysed in toluene, **2.1c** does convert quantitatively to the same relative distribution of aryl isomers **2.1a-c** as observed during the thermolysis of **1** in toluene (~ 47 : 33 : 1) (Scheme 4.1). Monitoring the thermolysis of **2.1c** in benzene-*d*<sub>6</sub> at 70° C by <sup>1</sup>H NMR spectroscopy reveals that the isomerization is a rapid intramolecular process with **2.1a** and **2.1b** forming concomitantly. The conversion of **2.1c** to **2.1a-b** follows first-order kinetics ( $k_{\text{obs}} = 6.6(3) \times 10^{-4} \text{ s}^{-1}$ ,  $t_{1/2} = 18 \text{ min}$ ,  $R^2 = 0.993$ ) for ~ 120 min, after which time the equilibrium distribution of **2.1a-c** is attained. No resonances attributable to free toluene, **2.3** or **2.2a-b** are observed, even after prolonged heating for 40 h. Rather, **2.1a-c** slowly decompose to release free neopentane, presumably via reaction with benzene in the same manner as **1.1** (see Section 2.2.2).

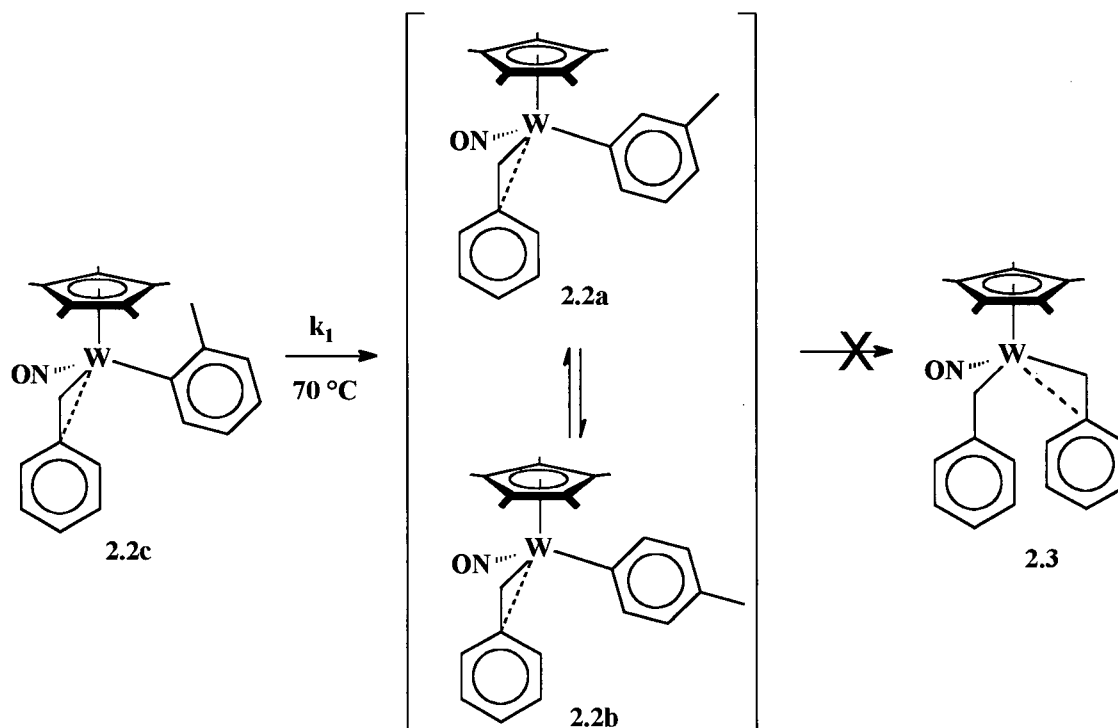
Scheme 4.1



Similar results are obtained with the *o*-tolyl benzyl complex **2.2c** (Scheme 4.2).

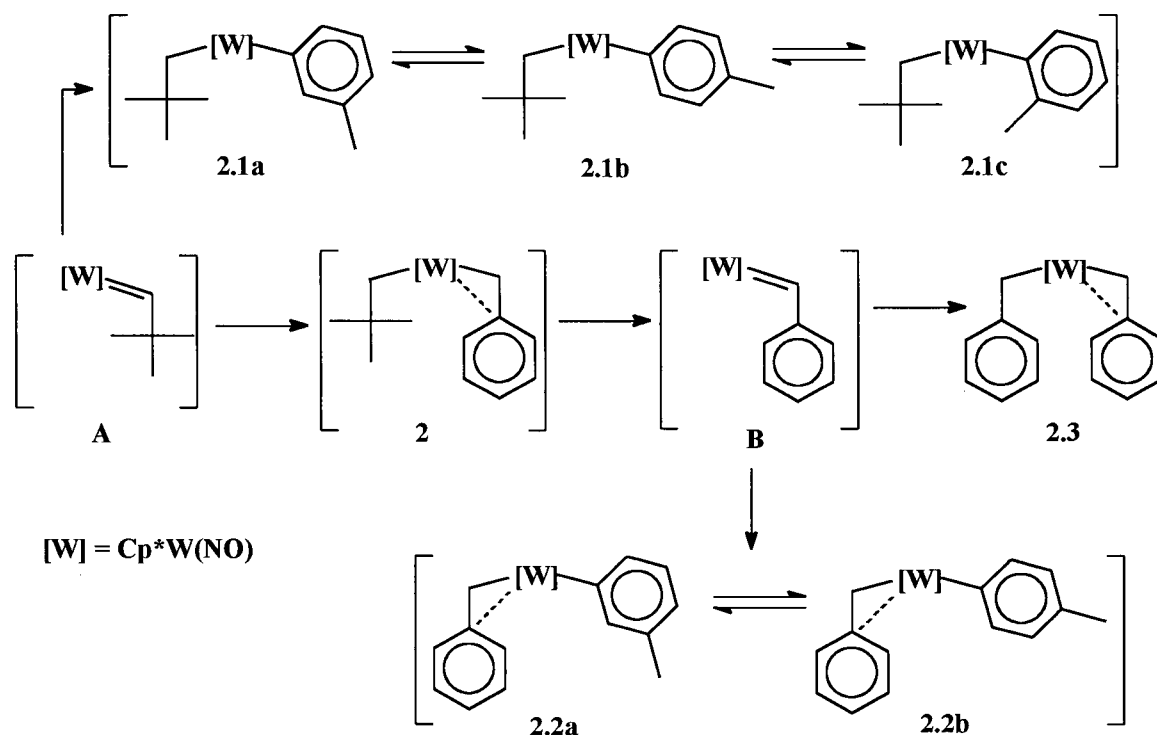
The thermolyses of **2.2c** in toluene and benzene- $d_6$  reveal a rapid and concomitant intramolecular isomerization to the 2:1 mixture of **2.2a** and **2.2b** observed from thermolysis of **2** in toluene ( $k_{\text{obs}} = 1.9(1) \times 10^{-4} \text{ s}^{-1}$ ,  $t_{1/2} = 61 \text{ min}$ ,  $R^2 = 0.999$  in benzene- $d_6$ ). Again, no resonances attributable to free toluene or the bis(benzyl) complex **2.3** are observed, even when **2.2c** is heated in benzene- $d_6$  and toluene at  $70\text{ }^\circ\text{C}$  for  $> 40 \text{ h}$ . Rather, as reported earlier, the complexes **2.2a-b** slowly decompose to a plethora of unidentified products (see Section 2.2.4).

Scheme 4.2



These results indicate that the two sets of aryl regioisomers **2.1a-c** and **2.2a-b** derived from the thermolyses of **1** and **2** in toluene are formed under thermodynamic rather than kinetic control. Thus, the relative distributions of aryl regioisomers *do not* arise from the intrinsic selectivity for the formation of the ortho, meta and para aryl products of toluene C-H activation from **A** and **B**, but instead arise from the relative thermodynamic stabilities of the respective aryl complexes. The interrelationship of the complexes derived from the thermolysis of **1** in toluene is shown in Scheme 4.3.

Scheme 4.3

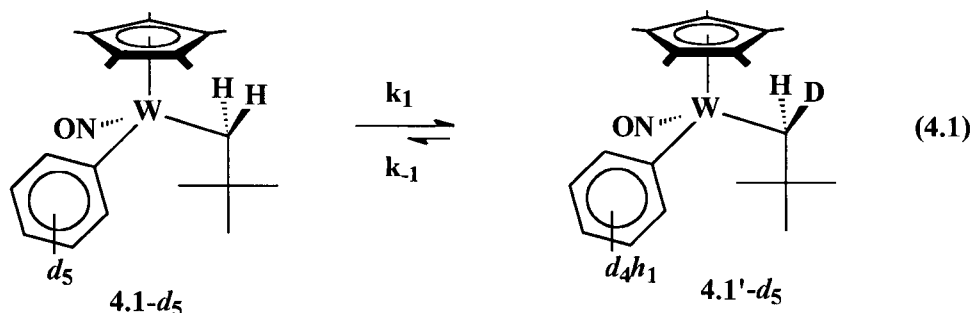


#### 4.2.1.2 The Mechanism of Aryl Product Regioisomerization

In order to isomerize as they do, the aryl products must be undergoing a rapid intramolecular H transfer process via an unobserved intermediate. An intriguing possibility based on the reaction coordinate for the activation of benzene is that the unobserved intermediate is a hydrocarbon complex formed by the coordination of toluene to **A** and **B**. In other words, the cleavage of the  $sp^2$  C-H bonds of toluene may be reversible. There are several precedents in other C-H activation systems in which the reversible formation of the hydrocarbon intermediates on the C-H activation reaction coordinate has been invoked to account for thermal rearrangements of activated products.<sup>1,2</sup> However, in this instance, several other intermediates not related to the C-H

activation of toluene by **A** and **B** could conceivably be involved in the intramolecular H-atom transfer. These include tucked-in Cp\*, metallacyclic, or aryne intermediates (see eqs 1.5, 1.6 and 1.10 for examples of these types of complexes).

To elucidate the mechanism operative in the aryl product isomerizations, the labeled neopentyl phenyl complex  $\text{Cp}^*\text{W}(\text{NO})(\text{CH}_2\text{CMe}_3)(\text{C}_6\text{D}_5)$  (**4.1-d<sub>5</sub>**) has been thermolysed in  $\text{C}_6\text{D}_6$  and  $\text{CD}_2\text{Cl}_2$  at 70 °C. Monitoring the thermolyses by  $^1\text{H}$  NMR spectroscopy over 5 h reveals a rapid, exclusive, and concomitant exchange of hydrogen and deuterium between the synclinal methylene position of the neopentyl ligand and all three aromatic positions of the phenyl ligand to yield  $\text{Cp}^*\text{W}(\text{NO})(\text{CHD}_{\text{syn}}\text{CMe}_3)(\text{C}_6\text{D}_4\text{H}_1)$  (**4.1'-d<sub>5</sub>**) (eq 4.1).



The rate of conversion is independent of the solvent, and free benzene is not detected during the experiment conducted in  $\text{CD}_2\text{Cl}_2$ . A non-linear least-square analysis of the data from the reaction in  $\text{CD}_2\text{Cl}_2$  (Figure 4.1) using an exponential approach to equilibrium kinetic model yields a calculated  $k_{\text{obs}}$  of  $3.6(2) \times 10^{-4} \text{ s}^{-1}$ . This corresponds to rate constants of  $3 \times 10^{-4} \text{ s}^{-1}$  for H transfer to the aryl ligand ( $k_1$ ) and  $9 \times 10^{-5} \text{ s}^{-1}$  for D transfer to the aryl ligand ( $k_{-1}$ ). The calculated  $K_{\text{eq}}$  of 3.0(3) for H incorporation into the

aromatic ring is less than the statistical  $K_{\text{eq}}$  of 5, a fact consistent with the preferential association of deuterium with the stronger aryl  $\text{sp}^2$  C-H/C-D bond.

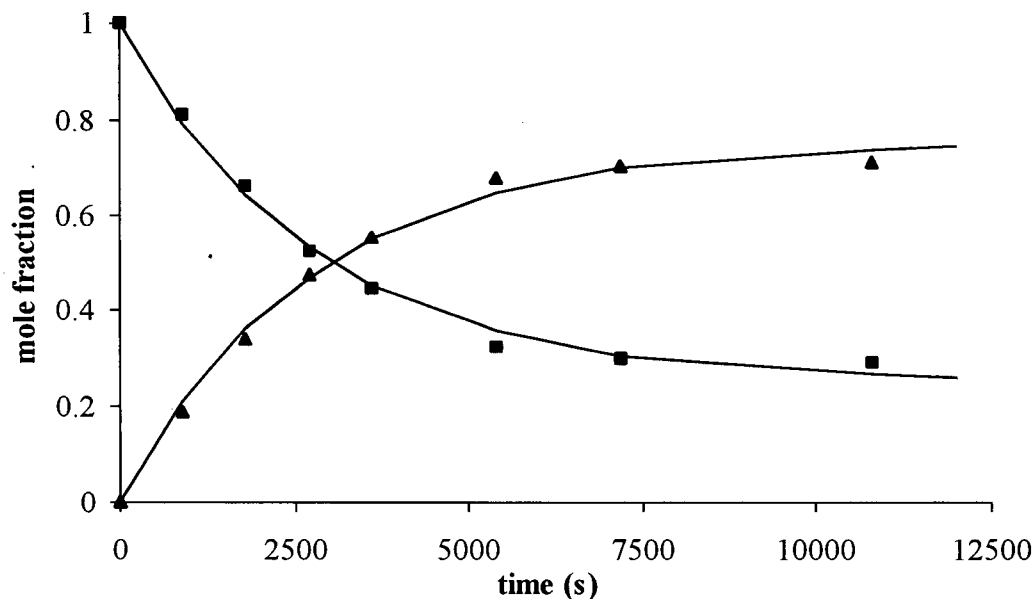
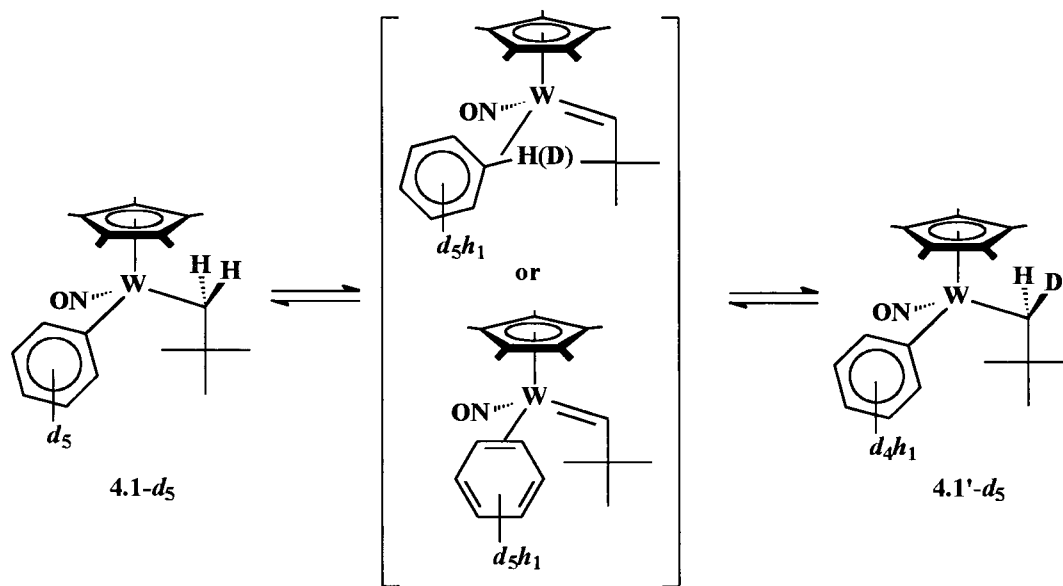


**Figure 4.1.** Plot of conversion of  $4.1\text{-d}_5$  to  $4.1'\text{-d}_5$  versus time for the approach to equilibrium at  $70^\circ\text{C}$  ( $\blacksquare = 4.1\text{-d}_5$ ,  $\blacktriangle = 4.1'\text{-d}_5$ ). The solid lines indicate a non-linear least-squares fit to an exponential decay to equilibrium.

The rapid and exclusive H/D exchange between the phenyl ring and the synclinal methylene position of the neopentyl ligand, and the lack of incorporation of deuterium into any other positions of  $4.1'\text{-d}_5$  even on prolonged thermolysis ( $> 40$  h), effectively rules out the involvement of benzyne, metallacyclic, or tucked-in  $\text{Cp}^*$  intermediates. On the other hand, the experimental data are fully consistent with reversible  $\text{sp}^2$  bond C-H (C-D) cleavage to the arene alkylidene complex on the C-H activation reaction coordinate, as illustrated in Scheme 4.4. Rapid interconversion of the arene complex to a

different rotamer will result in aryl ligand isomerization upon re-addition of the C-H bond across the M=C bond.

**Scheme 4.4**



#### 4.2.1.3 The Nature of The Arene Complex in Aryl Ligand Isomerizations

An unresolved issue regarding the observed aryl ligand isomerizations is the exact nature of the intermediate arene complex that is involved. Toluene can coordinate to the metal centers in **A** and **B** in one of three ways; through an  $sp^3$  C-H bond of the methyl group to form an  $\eta^2$ -(C,H) phenylmethane  $\sigma$ -complex, through an  $sp^2$  C-H bond of the phenyl ring to form an  $\eta^2$ -(C,H) methylbenzene  $\sigma$ -complex (or a  $\sigma$ -arene complex for short), or through the  $\pi$ -system of the phenyl ring to form an  $\pi$ -arene complex. The last two types of complexes, which are shown in Scheme 4.4, are possible intermediates for the aryl ligand isomerization since related complexes of both types are reportedly involved in similar aryl ligand isomerizations in other systems.<sup>3,4</sup> In one particular

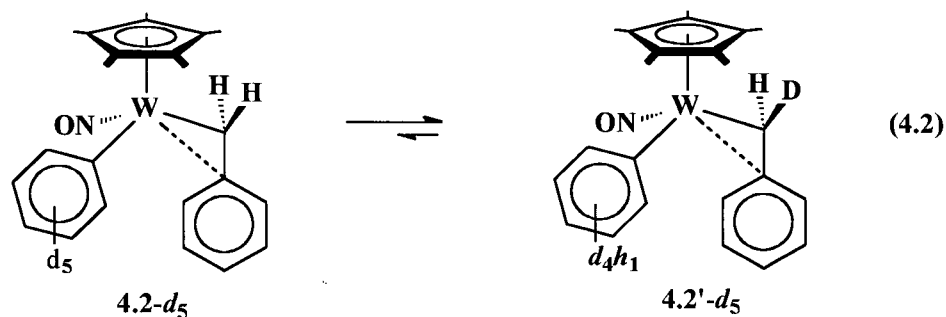
instance, the comparison of inter- and intramolecular kinetic isotope effects for benzene activation has identified which of the two possible types of intermediates is in fact present.<sup>5</sup> In detail, the intermolecular kinetic isotope effect for activation of molar mixtures of benzene/benzene-*d*<sub>6</sub> by Cp\*Rh(PMe<sub>3</sub>) is 1.0, while the intramolecular kinetic isotope effect for thermolysis in 1,3,5-benzene-*d*<sub>3</sub> is significantly larger at 1.4. The difference in the two KIE values indicates that hydrocarbon intermediates exist on the reaction coordinate for benzene activation, while the unity value for the intermolecular KIE suggests that the substrate C-H (C-D) bond is not involved in the substrate coordination step. Thus, these data support the formation of a  $\pi$ -arene intermediate rather than a  $\sigma$ -arene intermediate in the Rh system.

It would seem appropriate to apply a similar comparison of inter- and intramolecular KIEs to this system to determine the type of arene intermediates involved in alkylidene-mediated C-H activation. However, the usefulness of the comparison is obviated by the fact that the product ratios obtained from the thermolysis of **1** or **2** in 1,3,5-benzene-*d*<sub>3</sub> (70 °C, 40 h) will be thermodynamic and not kinetic in nature, due to the rapid intramolecular H/D exchange between the aryl and methylene positions of the ligands under the requisite thermolytic conditions. In other words, the measured intramolecular isotope effect is an equilibrium isotope effect, not a KIE, and as such would have no relation to ascertaining the nature of the hydrocarbon intermediate. An argument could be made that the near-unity intermolecular KIE values measured from the thermolysis of **1** and **2** in benzene/benzene-*d*<sub>6</sub> support the formation of  $\pi$ -arene intermediates. However, the intermolecular KIE for the activation of the molar mixture of tetramethylsilane-*h*<sub>12</sub> and tetramethylsilane-*d*<sub>12</sub> by **A** is also near-unity, even though the

C-H (C-D) bond must be involved in the substrate coordination in this instance. Clearly, neither arene coordination mode can be ruled out and the nature of the hydrocarbon intermediate involved in the formation and isomerization of the aryl products cannot be resolved by experimental methods in this instance.

#### 4.2.1.4 Aryl Regioisomerizations in Benzyl Aryl Complexes

The cleavage of arene substrate  $sp^2$  C-H bonds also appears to be reversible in the corresponding benzyl aryl complexes. Thermolysis of  $Cp^*W(NO)(CH_2C_6H_5)(C_6D_5)$  (**4.2-d<sub>5</sub>**) in  $C_6D_6$  at 70 °C results in exclusive synclinal methylene deuterium incorporation to yield  $Cp^*W(NO)(CHD_{syn}C_6H_5)(C_6D_4H_1)$  (**4.2'-d<sub>5</sub>**) (eq 4.2).<sup>6</sup>



Quantitative analysis of the exchange process in this case was prevented by the presence of overlapping resonances from contaminants in the original sample of **4.2-d<sub>5</sub>** (see Section 4.4.6). However, the initial rate of the exchange of **4.2-d<sub>5</sub>** does appear to be qualitatively slower than that of **4.1-d<sub>5</sub>**, a feature also seen in the isomerization of the related benzyl *o*-tolyl and neopentyl *o*-tolyl complexes **2.2c** and **2.1c**. A rationale for the difference in rates can be proposed based on the mechanism in Scheme 4.4 shown above. As mentioned in Section 2.2.1, the  $Cp^*M(NO)(R)(R')$  ( $Cp^* = Cp, Cp^*$ ;  $M = Mo, W$ ;  $R =$  benzyl;  $R' =$  alkyl, aryl, benzyl) complexes like **4.2-d<sub>5</sub>** and **2.2c** possess a stabilizing  $\eta^2$ -

benzyl interaction in the ground state.<sup>7</sup> However, the intramolecular transfer of an H atom between the benzyl and aryl ligands to reform the benzyldiene linkage requires the benzyl ligand to be  $\eta^1$ . The rates of H/D exchange and aryl ligand isomerization in the benzyl complexes are thus slowed by the equilibrium between the  $\eta^2$  and  $\eta^1$  benzyl conformations and/or a higher energy barrier to reformation of the  $\pi$ - or  $\sigma$ -arene complex of **B** from the ground-state of the aryl benzyl products.

#### 4.2.1.5 The Nature of the Aryl vs Benzyl Product Distributions Revisited.

The reversibility of  $sp^2$  C-H bond cleavage resolves another issue regarding the activation of toluene by **A** and **B**, namely the mechanism by which the aryl and benzyl C-H activation products of toluene are formed separately from one another. Given that hydrocarbon intermediates are present during the activation process, there are only two possible points at which the irreversible discrimination between aryl and benzyl products can occur: upon coordination of toluene, or upon cleavage of the  $sp^2$  and  $sp^3$  C-H bonds. The latter scenario can be ruled out. In this instance, discrimination between the aryl and benzyl products would have to arise from the relative energy barriers associated with  $sp^2$  vs  $sp^3$  C-H bond cleavage from a common hydrocarbon intermediate (e.g a  $\pi$ -arene complex), or from  $\pi$ - and/or  $\sigma$ - complexes that undergo rapid exchange. However, the rapid reformation of the  $\pi$ - or  $\sigma$ -arene complexes that are involved in substrate  $sp^2$  C-H bond scission means that the corresponding benzyl products of **2.2c** and **2.1c** should be formed during the thermolyses of the *o*-tolyl products **2.1c** and **2.2c** in toluene, in addition to formation of the meta and para regioisomers. This scenario is clearly inconsistent with the observed experimental results.

The point of discrimination between aryl and benzyl products must therefore be the coordination of toluene to the metal center (i.e. in intermediates **A** or **B**, or in the preceding  $\sigma$ -neopentane complexes of **A** or **B**). Moreover, *two distinct* types of hydrocarbon complexes must be formed for the pathways leading to aryl and benzyl products, either a  $\pi$ -arene or a  $\sigma$ -arene for aryl product formation, and a  $\eta^2$ -( $sp^3$ -C,H) phenylmethane  $\sigma$ -complex for benzyl product formation.<sup>8</sup> In addition, these two types of hydrocarbon complexes must not interconvert once formed, either by intramolecular isomerization or dissociation of toluene. Finally, the pathway leading to the  $\pi$ -arene/ $\sigma$ -arene complex must be kinetically preferred over that leading to the  $\sigma$ -phenylmethane complex, while the transition state energy for  $sp^2$  C-H bond scission is small enough to permit rapid, reversible aryl ligand isomerization. Only if these four conditions are satisfied can the aryl and benzyl products form independently whilst rapid and reversible  $sp^2$  C-H bond scission occurs.

The implied reaction coordinate for toluene activation by the reactive alkylidene complexes **A** and **B** is thus shown in Figure 4.2. Note, for simplicity, it is assumed that  $\pi$ -arene complexes are formed instead of  $\sigma$ -arene complexes along the pathway to formation of the aryl products (vide infra). Key features of Figure 4.2 are as follows:

1.  $\pi$ -arene coordination is kinetically preferred over  $\sigma$ -phenylmethane coordination (represented by  $\Delta\Delta G^\ddagger$ ), in keeping with the observed preference for aryl products.
2. From the  $\pi$ -arene complex, the energy barrier to  $sp^2$  C-H bond scission is smaller than both the barrier to substrate dissociation and reversion back to the free

alkylidene, and the barrier to exchange with the  $\sigma$ -phenylmethane complex (represented by the dashed curve).

- From the  $\sigma$ -phenylmethane complex, the energy barrier to  $sp^3$  C-H bond scission is also lower than the energy barriers for dissociation and exchange.

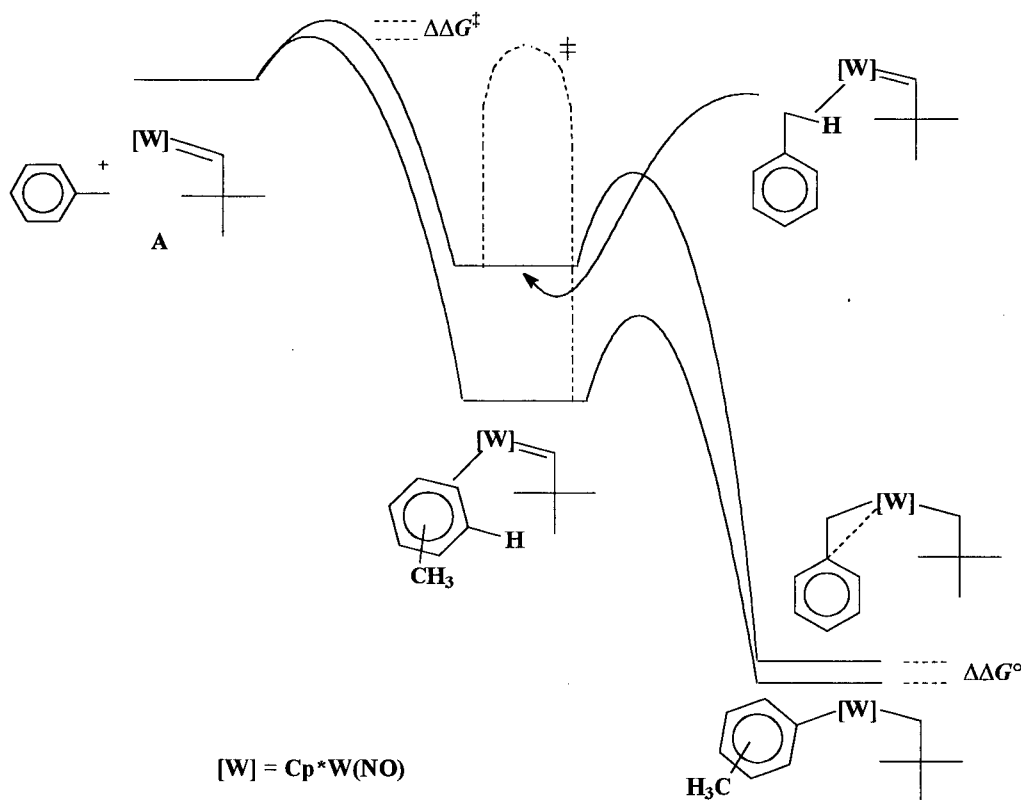


**Figure 4.2.** A qualitative depiction of the free energy vs reaction coordinate diagram for the activation of toluene, using intermediate **A** as the reactive alkylidene species.

Note that these last two features are also in keeping with the intermolecular KIEs measured for  $sp^2$  and  $sp^3$  C-H bond activations (see Section 3.2.9), which indicate substrate C-H bond scission is faster than substrate dissociation or hydrocarbon intermediate exchange. Note also that the observed lack of conversion of the benzyl-

activated product to its aryl isomers under thermolysis conditions may be assisted by the presence of the additional  $\eta^2$ -benzyl interaction that blocks access to the  $\eta^1$ -benzyl conformation required for reversion back to the  $\sigma$ -phenylmethane intermediate.

The alternative reaction coordinate for toluene activation by the  $\sigma$ -neopentane complexes of **A** and **B** is depicted in Figure 4.3. For the most part, the reaction coordinate is similar to that in Figure 4.2, with one key difference being that neopentane dissociation is rate-limiting and effectively irreversible. Hence, exchange of the  $\pi$ - or  $\sigma$ -arene and  $\sigma$ -phenylmethane complexes cannot occur by reversion back to  $\sigma$ -**A** or  $\sigma$ -**B**.

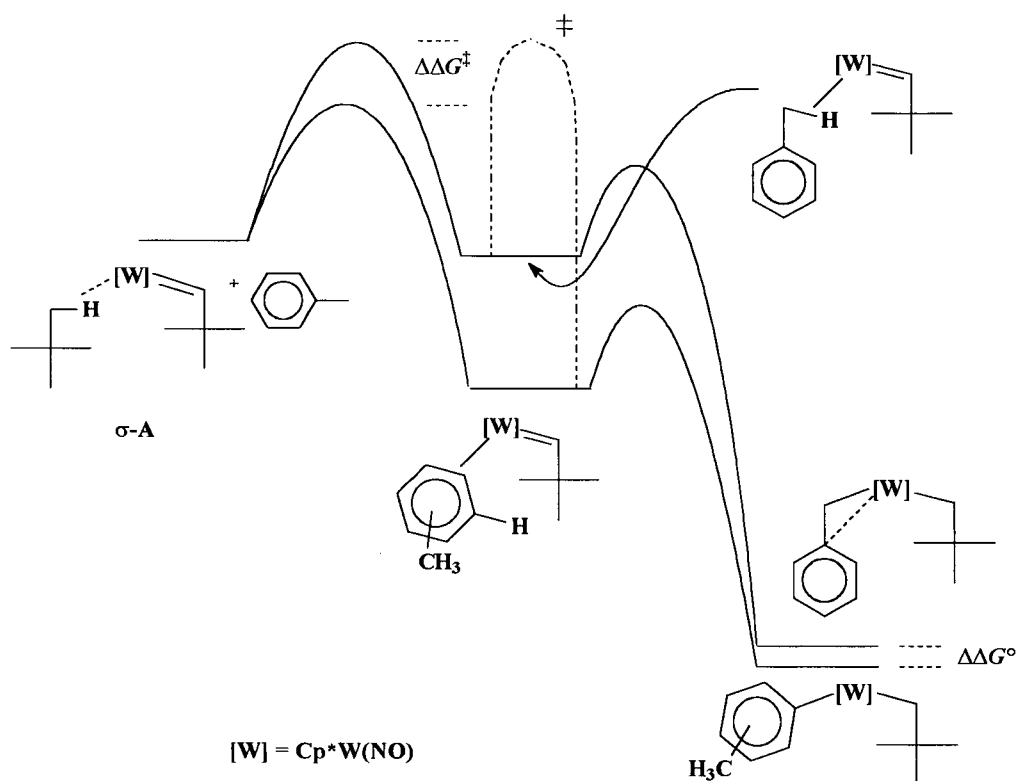


**Figure 4.3.** A qualitative depiction of the free energy vs reaction coordinate diagram for the activation of toluene, using  $\sigma$ -**A** as the reactive alkylidene species.

#### 4.2.1.6 Theoretical Investigations into Toluene Activation by $\text{CpW}(\text{NO})(=\text{CH}_2)$

To substantiate this interpretation of the toluene activation reaction coordinate, rudimentary theoretical DFT calculations have been conducted on the coordination and activation of toluene by an alkylidene complex. The calculations have been conducted in the manner employed by Poli and Smith, using  $\text{CpW}(\text{NO})(=\text{CH}_2)$  (**C**) as a simplified version of the alkylidene fragments **A** and **B** and the LANL2DZ basis set to minimize computational expense. Optimized geometries and the corresponding gas-phase free energies have been determined for various species involved in the activation process, as discussed below.

##### 4.2.1.6.1 Benzyl and Aryl Products of Toluene C-H Activation

The optimized geometry of the benzyl product of toluene activation by **C**, namely  $\text{CpW}(\text{NO})(\text{CH}_3)(\text{CH}_2\text{C}_6\text{H}_5)$ , is shown in Figure 4.4(a). Most notably, the benzyl ligand is coordinated in the expected  $\eta^2$  fashion. The optimized geometries of the regioisomeric aryl products have also been determined, and a representative structure is shown in Figure 4.4(b) (see Appendix C for pictures of all optimized complexes). A noteworthy feature of the aryl products is the distortion of one of the methyl C-H bonds ( $\text{W-C-H}^* = 103.7^\circ$  vs  $\text{W-C-H} = 113.9^\circ$ ), which is indicative of an  $\alpha$ -agostic interaction with the metal center. As mentioned in Chapter 2, such interactions have recently been detected by neutron diffraction analysis and spectroscopic methods in related  $\text{Cp}'\text{M}(\text{NO})(\text{R})(\text{R}')$  complexes ( $\text{R} = \text{hydrocarbyl}$ ,  $\text{R}' = \text{hydrocarbyl}$ , aryl, halide).<sup>9</sup>

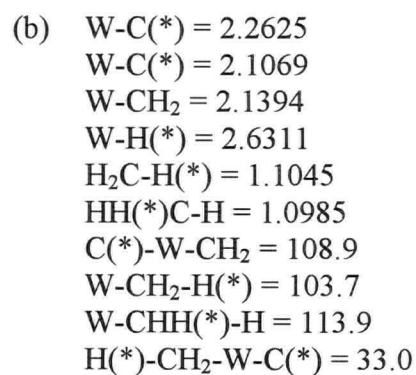
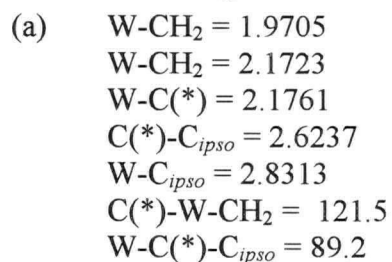
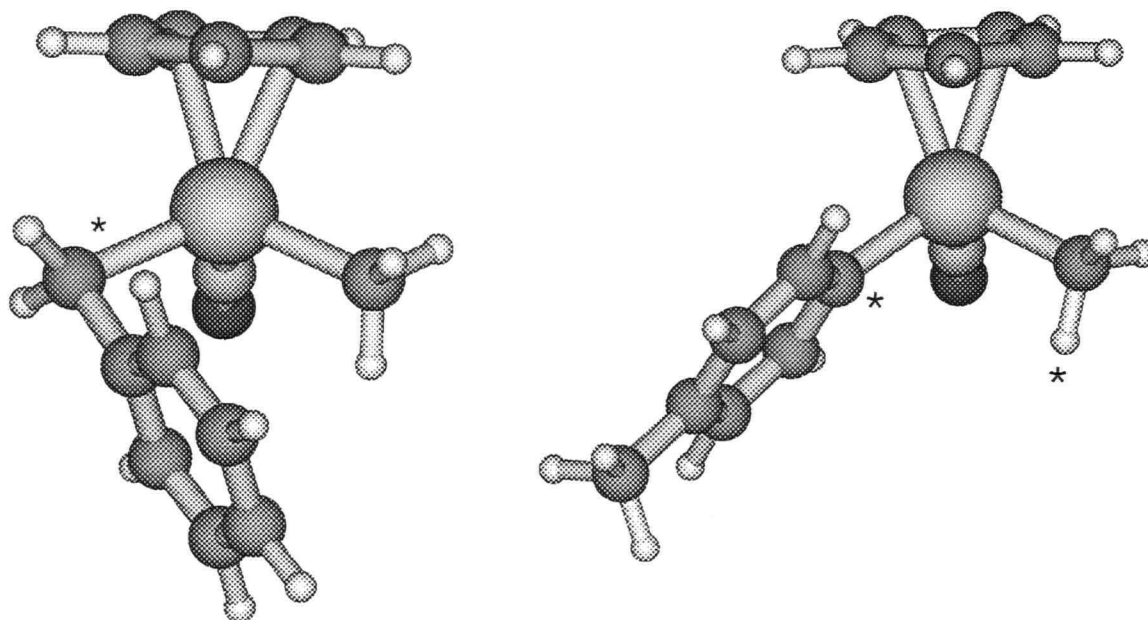


**Figure 4.4.** Optimized geometries of (a) the benzyl product derived from  $sp^3$  C-H bond activation of toluene, and (b) the para aryl product derived from  $sp^2$  C-H bond activation of toluene. In this instance, the asterisk denotes the C atoms of the new metal-carbon bond and the C-H agostic bond in (b).

#### 4.2.1.6.2 Intermediate Hydrocarbon Complexes

The placement of toluene in various orientations near the open coordination site of C results in two distinct classes of hydrocarbon complexes. Placement of one of the methyl C-H bonds close to the metal center in several orientations results in the  $\eta^2$ -(C,H)

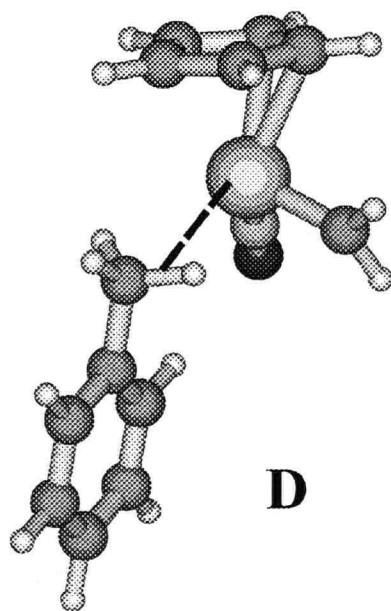
$\sigma$ -phenylmethane complex (**D**) upon geometry optimization (Figure 4.5(a)). Not surprisingly, the geometrical parameters of **D** are nearly identical to the corresponding  $\sigma$ -methane intermediate optimized by Poli and Smith and shown in Scheme 3.1.<sup>10</sup> Placement of toluene with the bulk of the arene ring being parallel to the NO-W=CH<sub>2</sub> plane of **C** (i.e. face on) and away from the Cp\* ring results in optimized structures of the type shown in Figure 4.5(b), namely **E**. Likewise, initial geometries with the arene ring perpendicular to the NO-W=CH<sub>2</sub> plane (i.e. edge-on), or face on with the bulk of the arene ring close to the Cp ligand result in geometry optimizations to arene complexes of the type shown in Figure 4.5(c) (**E'**). Type **E** complexes are readily described as  $\pi$ -arene complexes given the parallel arrangement of the arene ring and the W=CH<sub>2</sub> bond. At first glance, type **E'** complexes would appear to be bound in a  $\sigma$ -arene fashion through an sp<sup>2</sup> C-H bond, given the obtuse angles between the arene ring and the W=CH<sub>2</sub> bond and the close distance between the metal center and an aryl H atom. However, examination of the molecular orbitals of the para **E'** congener reveals that the bonding interaction between the metal center and the arene involves the  $\pi$ -orbitals of the aromatic ring and not the orbital of the closest sp<sup>2</sup> C-H bond. Thus, despite the different geometries, it appears that type **E'** complexes are also  $\pi$ -arene complexes and are interconvertible with type **E** complexes via simple rotation of the arene ring about the W- $\pi$  bond. It can be inferred from these results that  $\pi$ -arene complexes are the reactive intermediates in the formation of the aryl products, rather than  $\sigma$ -arene complexes.

The orientation of the methyl group in toluene has some influence on the optimized geometries of the  $\pi$ -complexes **E** and **E'**. For the most part, steric interactions

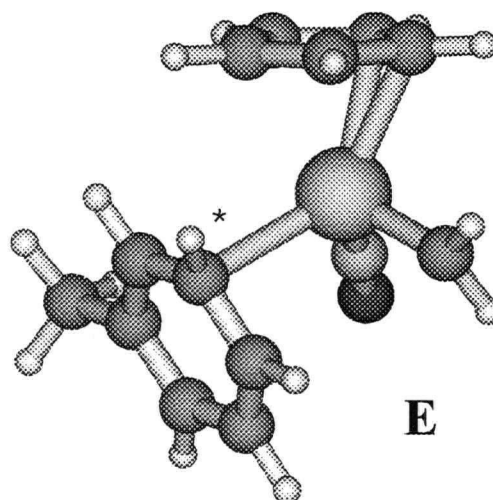
between the methyl group and the methylene linkage or Cp ring only induce mild geometric derivations from those shown in Figures 4.5(b) and 4.5(c). In some instances, however, these steric interactions are sufficient to prevent optimization of specific rotamers of both **E** and **E'**  $\pi$ -complexes.

#### 4.2.1.6.3 Transition States for Benzyl and Aryl C-H bond Cleavage.

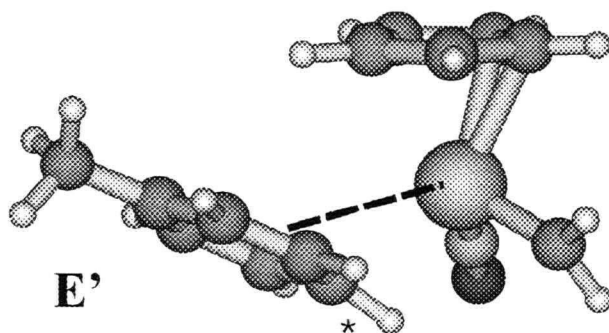
Transition states have been located for cleavage of both  $sp^3$  and  $sp^2$  C-H bonds (Figure 4.6). For  $sp^3$  C-H bonds, the transition state is a logical geometric successor to the  $\sigma$ -phenylmethane complex **D** as the  $\eta^2$ -bound C-H bond of **D** is being cleaved (Figure 4.6(a)). It is very similar geometrically to the transition state for methane C-H bond scission shown in Scheme 3.1, and is best described as a metal-assisted 1,2-cis addition of C-H to the M=C linkage. For  $sp^2$  C-H bonds, five different transition states were located for different orientations of the methyl group with respect to the activated bond. A representative structure for para aryl C-H bond activation is shown in Figure 4.6(b). All five transition states possess very similar geometries about the atoms involved in the C-H bond addition and are geometrically quite similar to the metal-assisted early transition state for  $sp^3$  C-H bond activation. One difference between the transition states for  $sp^2$  and  $sp^3$  C-H bond activations is that the incipient W-C bond from activation is significantly shorter for aryl activation (2.267 Å vs 2.396 Å). Finally, geometry optimization performed from representative  $sp^2$  C-H bond activation transition states results in optimization to the respective **E'**  $\pi$ - arene complex as a local minimum. Thus, the calculated transition states and the hydrocarbon  $\pi$ -complexes **E** and **E'** lie on the same reaction coordinate with no other intermediates lying between them. In other words, two



- (a) W-CH<sub>2</sub> = 1.9474  
 W-C(\*) = 2.7056  
 W-H(\*) = 2.0645  
 C(\*)-H(\*) = 1.1420  
 C(\*)-H = 1.0979  
 C(\*)-W-CH<sub>2</sub> = 102.4  
 W-C(\*)-C<sub>ipso</sub> = 130.5  
 H(\*)-CH<sub>2</sub>-W-C(\*) = 9.2



- (b) W-C(\*) = 2.8191  
 W-CH<sub>2</sub> = 1.9474  
 W-H(\*) = 3.1862  
 C(\*)-W-CH<sub>2</sub> = 80.4  
 W-C(\*)-C<sub>ortho</sub> = 89.0



- (c) W-C(\*) = 2.4918  
 W-CH<sub>2</sub> = 1.9473  
 W-H(\*) = 2.3663  
 CH<sub>2</sub>-H(\*) = 2.7835  
 C(\*)-H(\*) = 1.0996  
 C(\*)-W-CH<sub>2</sub> = 100.4  
 W-C(\*)-C<sub>methyl</sub> = 121.0

**Figure 4.5.** Optimized geometries and selected bond distances (Å) and angles (°) of, (a) the hydrocarbon complex **D**, (b) the representative (meta, anti) complex **E**, and (c) the para complex **E'**. In (b) and (c), the asterisk denotes the H and C atoms closest to the metal center.

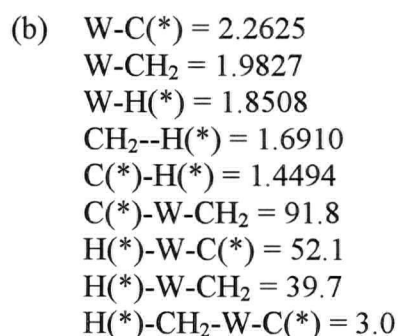
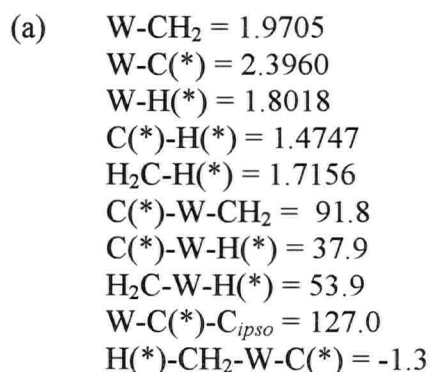
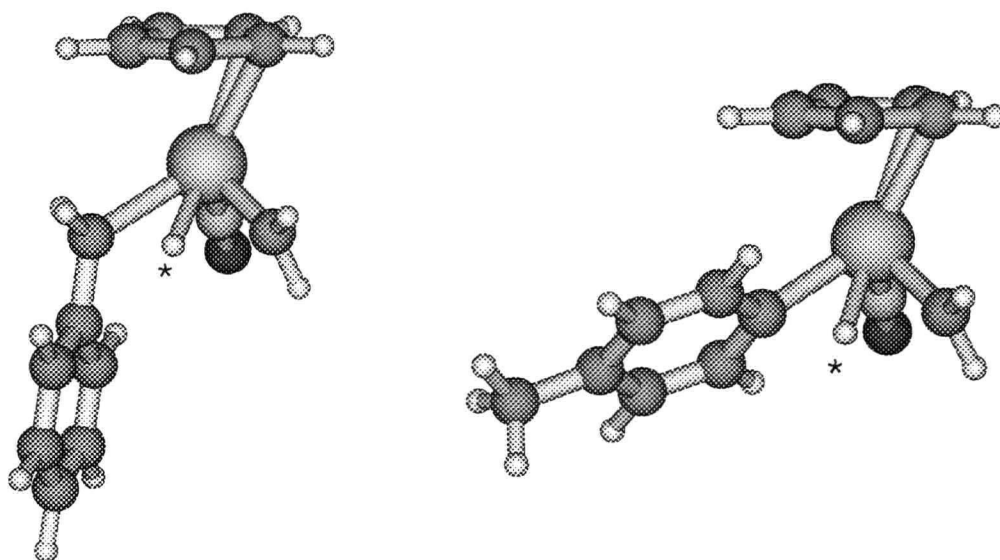


**Figure 4.6.** Optimized geometries of the transition states for (a)  $sp^3$  C-H bond activation, and (b) para  $sp^2$  C-H bond activation. In this instance, the asterisk denotes the H and C atoms of the C-H bond being cleaved.

distinct types of intermediates do indeed appear to lead to the aryl and benzyl products of toluene activation.

#### 4.2.1.6.4 The Theoretical Reaction Coordinate For Toluene Activation

The relative gas-phase free energies for the products, intermediates and transition states are collected Tables 4.1-4.3. Figure 4.7 depicts the relative displacement of these species on the reaction coordinate for toluene activation.

**Table 4.1.** Calculated Energies for the Aryl and Benzyl Products of C-H BondActivation by **C**

complex	orientation of methyl group <sup>a</sup>	relative energy (kcal/mol) <sup>b</sup>
CpW(NO)(CH <sub>3</sub> )(CH <sub>2</sub> C <sub>6</sub> H <sub>5</sub> )	-	3.7
CpW(NO)(CH <sub>3</sub> )(C <sub>6</sub> H <sub>4</sub> -CH <sub>3</sub> )	ortho, anti	3.6
	ortho, syn	4.7
	meta, syn	0.8
	para	0.0

<sup>a</sup> with respect to C(\*) in Figure 4.4(a) or (b) and the Cp-W bond. <sup>b</sup> with respect to *para*- CpW(NO)(CH<sub>3</sub>)(C<sub>6</sub>H<sub>4</sub>-4-CH<sub>3</sub>).

**Table 4.2.** Calculated Energies for the Optimized Hydrocarbon Intermediates fromCoordination of Toluene to Alkylidene Fragment **C**

complex	orientation of methyl group <sup>a</sup>	relative energy (kcal/mol) <sup>b</sup>
CpW(NO)(=CH <sub>2</sub> )(H-CH <sub>2</sub> C <sub>6</sub> H <sub>5</sub> ) ( <b>D</b> )	-	32.1
CpW(NO)(=CH <sub>2</sub> )(C <sub>6</sub> H <sub>5</sub> CH <sub>3</sub> ) ( <b>E</b> )	meta, syn	23.6
	para	22.9
	meta, anti	24.2
	ortho, anti	24.7
CpW(NO)(=CH <sub>2</sub> )(C <sub>6</sub> H <sub>5</sub> CH <sub>3</sub> ) ( <b>E'</b> )	ortho, syn	24.2
	meta, syn	24.2
	para	23.7
	ortho, anti	24.0

<sup>a</sup> ortho, meta and para are defined with respect to C(\*)-H(\*) in Figure 4.5(b) and 4.5(c), while synclinal and anticlinal are defined with respect to the W=CH<sub>2</sub> bond <sup>b</sup> with respect to *para*- CpW(NO)(CH<sub>3</sub>)(C<sub>6</sub>H<sub>4</sub>-4-CH<sub>3</sub>).

**Table 4.3.** Calculated Energies for the Transition States Corresponding to Aryl and Benzyl Product Formation.

complex	orientation of methyl group <sup>a</sup>	relative energy (kcal/mol) <sup>b</sup>
CpW(NO)(H <sub>2</sub> C•••H•••CH <sub>2</sub> C <sub>6</sub> H <sub>5</sub> )	-	41.8
CpW(NO)(H <sub>2</sub> C•••H•••C <sub>6</sub> H <sub>4</sub> -CH <sub>3</sub> )	ortho, anti	37.3
	ortho, syn	37.5
	meta, syn	33.0
	meta, anti	33.2
	para	32.7

<sup>a</sup> defined with respect to C(\*)-H(\*) in Figure 4.6(b) and the Cp-W bond. <sup>b</sup> with respect to *para*- CpW(NO)(CH<sub>3</sub>)(C<sub>6</sub>H<sub>4</sub>-4-CH<sub>3</sub>).

Given the simplistic basis set employed in the DFT calculations, the energies in Tables 4.1-4.3 and Figure 4.7 are semi-quantitative.<sup>11</sup> Nevertheless, the results of the calculations support the basic conclusion drawn from the experimental data: the C-H activation pathway leading to the aryl products through  $\pi$ -arene complexes is lower in energy than the pathway leading to the benzyl products via the  $\sigma$ -phenylmethane complex. Interestingly, the calculated potential energy barrier for the regioisomerization of the methyl *o*-tolyl complex CpW(NO)(CH<sub>3</sub>)(C<sub>6</sub>H<sub>4</sub>-2-Me) is 32.8-33.7 kcal/mol (298 K), which is reasonably close to the free energy for isomerization of the related neopentyl *o*-tolyl complex, Cp\*W(NO)(CH<sub>2</sub>CMe<sub>3</sub>)(C<sub>6</sub>H<sub>4</sub>-2-Me) complex (26 kcal/mol, 343 K) considering the limitations of the model system and the computational techniques employed.<sup>12</sup> Another notable feature is that the energies of the optimizable aryl regioisomers are very similar to that of the benzyl complex. This suggests that the well-

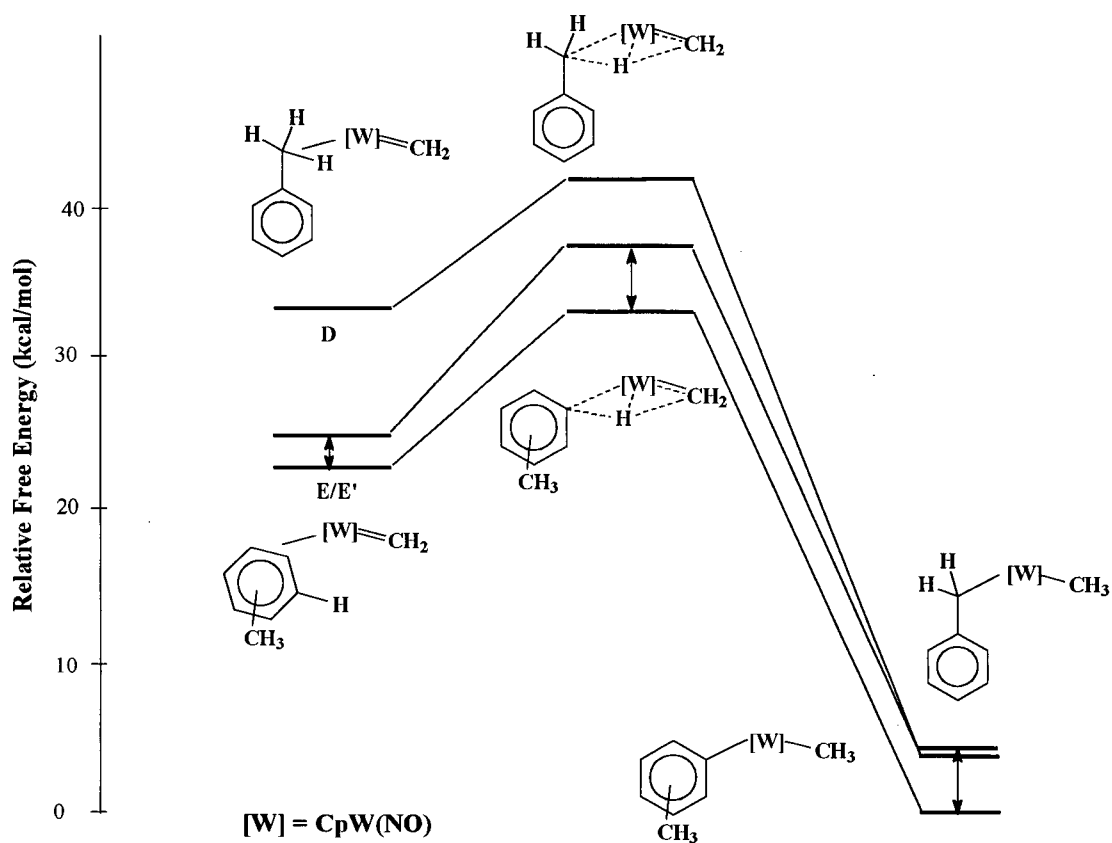


**Figure 4.7.** Free-energy profiles of the intermediates, transition states and products of toluene activation by methylenecyclopentadienyltungsten as determined by DFT calculations.

documented stability of the formally  $18e^-$  benzyl complexes

$Cp^*M(NO)(CH_2C_6H_5)(R')$  as compared to their  $16e^-$  aryl congeners<sup>13</sup> is a kinetic rather than a thermodynamic effect. A more detailed DFT investigation of the full reaction coordinate using more advanced theoretical methods to fully model both neopentylidene **A** and benzylidene **B** is required to confirm these observations and obtain quantitative theoretical data for the reaction coordinate.<sup>11</sup>

#### 4.2.1.7 Explanation of the Product Selectivities For Benzylidene- and Neopentylidene-Mediated Activations of Toluene.

Based on the experimental and theoretical data above, the reaction coordinates for toluene in Figures 4.2 and 4.3 appear to be valid qualitative depictions of the true reaction coordinates for toluene activation by alkylidene complexes **A/B** and  $\sigma$ -**A**/ $\sigma$ -**B**, respectively. In both Figures, the general preference for the formation of the aryl products from toluene C-H activation by the reactive alkylidene species arises from the faster formation of the  $\pi$ -arene complex over the  $\sigma$ -benzyl complex (i.e.  $\Delta\Delta G^\ddagger$  in Figures 4.2 and 4.3). In other words, the fact that the aryl products are formed preferentially is due to the link between the kinetics of  $\pi$ -arene complex formation and  $sp^2$  C-H bond cleavage. It would appear that in these systems, the intrinsic strengths of the C-H bonds are not significant factors in governing product selectivity under kinetically-controlled conditions.

The reaction coordinates in Figures 4.2 and 4.3 can also be used to explain the differences in the aryl vs benzyl product distributions obtained from the activation of toluene by **A** and **B**, respectively. For instance, the smaller ratio of aryl vs benzyl products observed for the activation mediated by **A** (4.2(3):1) compared to **B** (18.6(1.2):1) correlates to a smaller difference in the energy barriers for coordination of the  $\pi$ -arene and  $\sigma$ -phenylmethane complexes to **A** vs **B** (i.e.  $\Delta\Delta G^\ddagger$  in Figure 4.2). The smaller difference in transition state energies for **A** likely results from increased interactions between the methyl substituents of the incipient  $\pi$ -arene complex and the bulkier t-butyl substituent of **A** compared to the slimmer phenyl substituent of **B**. The  $\sigma$ -phenylmethane complexes leading to benzyl product formation from **A** and **B** would not

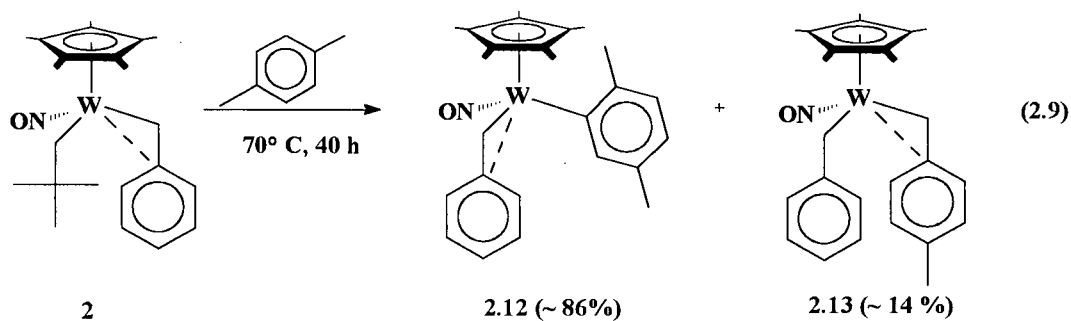
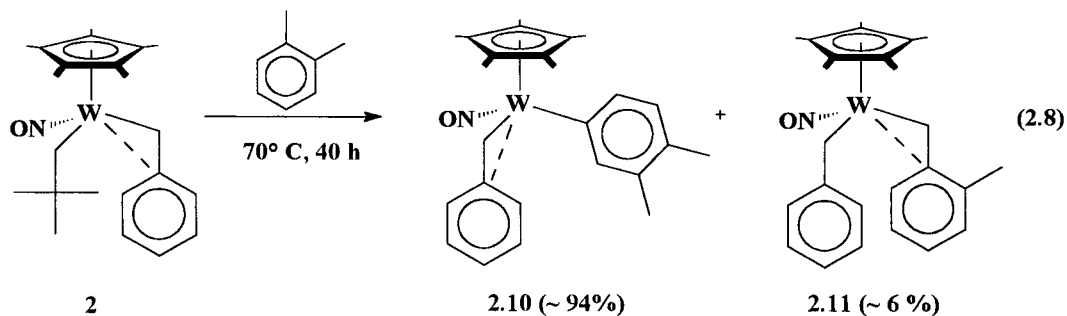
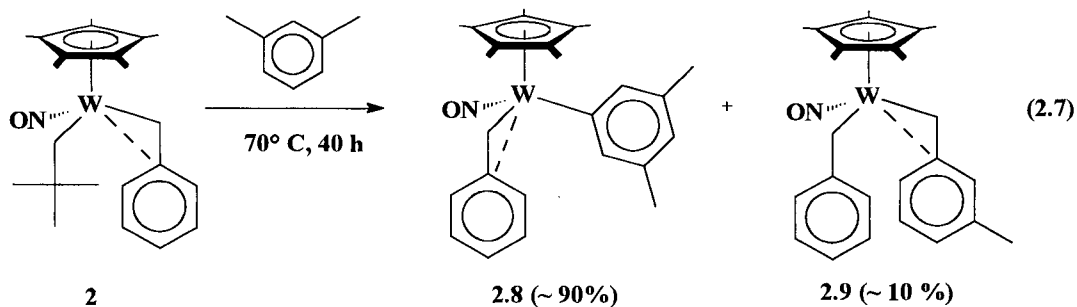
likely be affected by such steric interactions with the alkylidene substituent given the structure of complex **D** (vide supra).

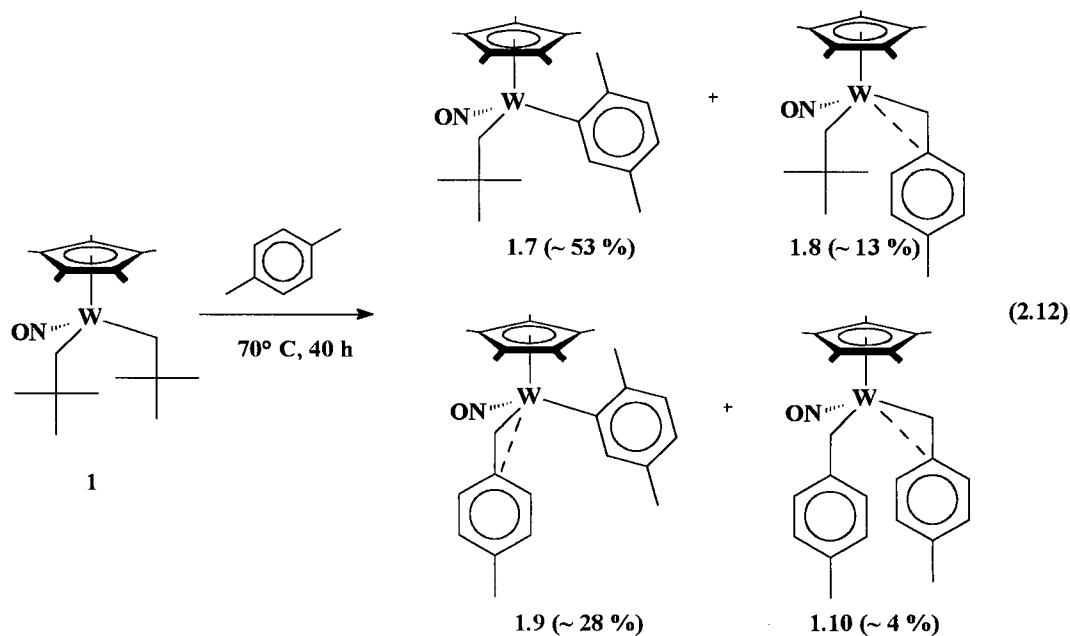
In contrast, the fact that the aryl products derived from toluene activation by **B** (1.97(11):1) are the statistical distribution of meta and para isomers, whereas the meta isomer is less favoured for the activations mediated by **A** (1.45(8):1), can now be attributed to the differences in the thermodynamic stability of the *m*-tolyl vs *p*-tolyl product complexes (i.e.  $\Delta G^\circ(\text{meta})$  vs  $\Delta G^\circ(\text{para})$  in Figure 4.2). Put simply, the meta isomer of the neopentyl tolyl complex derived from activation by **A** is destabilized relative to the para isomer for either steric or electronic reasons. Interestingly though, the neopentyl *o*-tolyl product from activation by **A** is evidently more stable than the benzyl *o*-tolyl product from activation by **B** relative to the respective meta and para isomers since the benzyl *o*-tolyl product is not observed in the thermodynamic distribution. This suggests that the steric interactions between the *o*-, *m*- and *p*-tolyl ligand and the alkylidene substituent are not the dominant factors in determining the overall stability of the products.

#### 4.2.2 Case 2. C-H Activation of Xylenes

Rationalizing the observed product distributions obtained from the activation of xylenes by **A** and **B** is more straight-forward than for toluene, since there is only one regioisomeric aryl product in each case. As described in Sections 2.2.10 through 2.2.12 and 2.2.15.1 and as summarized in Table 2.1, the aryl products of xylene C-H activation are always formed preferentially in the cases of *m*-, *o*-, *p*-xylene by **B**, and *p*-xylene by **A**. The shift of the methyl groups from the ortho to meta to para positions in the xylene

substrate does induce significant shifts of the product distribution toward the benzyl products (aryl vs benzyl products obtained from **2**: *o*-xylene = 14.6(4) : 1) > *m*-xylene = 9.3(7) : 1 > *p*-xylene = 6.2(4) : 1). Also, the aryl vs benzyl product distribution obtained from **2** in *p*-xylene favours the aryl product significantly more than that obtained from **1** (aryl vs benzyl = 1.14(7) : 1). The relevant equations from Chapter 2 are reproduced below.



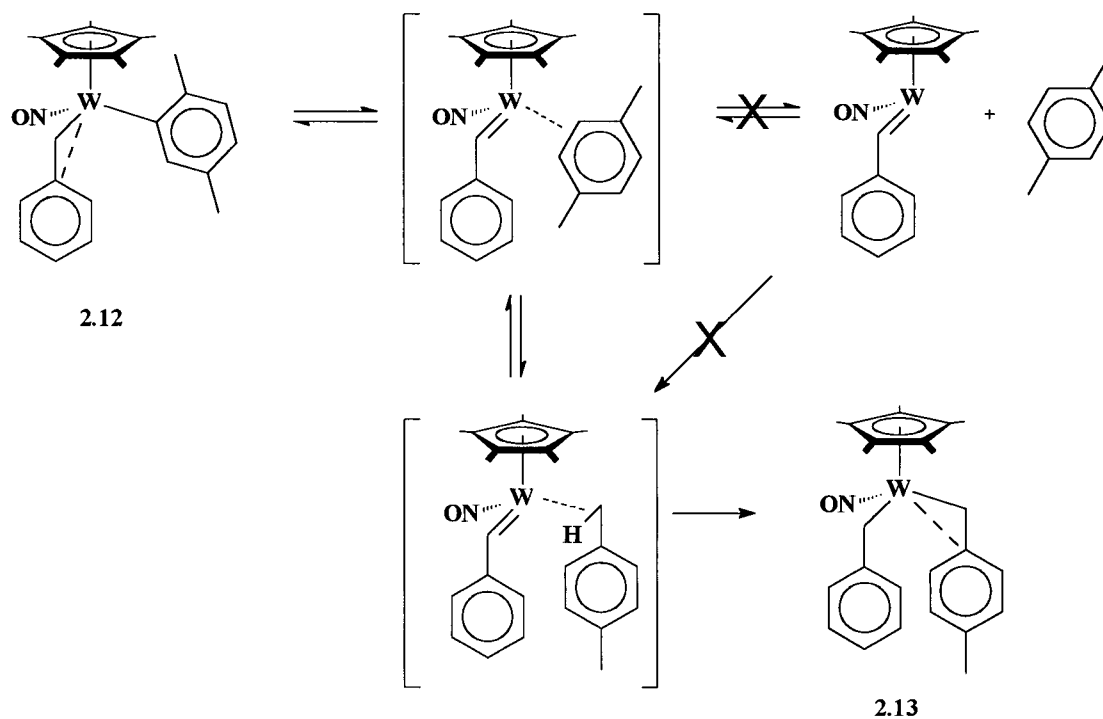


#### 4.2.2.1 The Nature of the Product Distributions

As with the case of toluene, the nature of the aryl vs benzyl product distributions needs to be determined. To that end, selected products of xylene C-H activation have been independently thermolysed in the parent solvent (i.e. *m*-, *o*- or *p*-xylene) and in benzene-*d*<sub>6</sub>. The benzyl complex derived from sp<sup>3</sup> C-H bond activation of *m*-xylene by **B**, namely Cp\*W(NO)(CH<sub>2</sub>C<sub>6</sub>H<sub>5</sub>)(CH<sub>2</sub>C<sub>6</sub>H<sub>4</sub>-3-Me) (**2.9**), is thermally robust, exhibiting no chemical transformations after 40 h of heating in either solvent. Thus, complex **2.9**, like the related bis(benzyl) complex **2.3**, does not undergo reversible sp<sup>3</sup> C-H bond cleavage at any appreciable rate under thermolysis conditions. In contrast, the aryl product of sp<sup>2</sup> C-H bond activation of *p*-xylene, namely Cp\*W(NO)(CH<sub>2</sub>C<sub>6</sub>H<sub>5</sub>)(C<sub>6</sub>H<sub>3</sub>-2,5-Me<sub>2</sub>) (**2.12**), does interconvert to the respective benzyl product of sp<sup>3</sup> C-H bond activation, Cp\*W(NO)(CH<sub>2</sub>C<sub>6</sub>H<sub>5</sub>)(CH<sub>2</sub>C<sub>6</sub>H<sub>4</sub>-4-Me) (**2.13**), when heated in *p*-xylene, albeit rather slowly. A ~ 95 : 5 ratio of **2.12** : **2.13** can be detected by <sup>1</sup>H NMR spectroscopy of the reaction mixture obtained after heating **2.12** in *p*-xylene for 40 h at 70

°C. Some decomposition is also observed (~ 10 %). Note that the distribution of **2.12** : **2.13** at 40 h is ~ 86 : 14, so the isomerization is not fast enough to attain equilibrium under these conditions. When the thermolysis is conducted in benzene- $d_6$ , only a trace amount (< 1 %) of the product of benzene- $d_6$  activation, namely  $\text{Cp}^*\text{W}(\text{NO})(\text{CHDC}_6\text{H}_5)(\text{C}_6\text{D}_5)$  (**2.5- $d_6$** ), is observed over the same time period. Thus, nearly all, of the isomerization of **2.12** to **2.13** occurs via an *intramolecular* interconversion of the respective  $\pi$ -arene and  $\sigma$ -arylmethane complexes, rather than dissociation of *p*-xylene (Scheme 4.5). Note that the term “ $\sigma$ -arylmethane complex” will henceforth be used as a generic term for the  $\text{sp}^3$  C-H bound  $\sigma$ -complex of substituted arenes.

Scheme 4.5



The thermolyses of two other aryl products, the benzyl *m*-xylyl complex  $\text{Cp}^*\text{W}(\text{NO})(\text{CH}_2\text{C}_6\text{H}_5)(\text{C}_6\text{H}_3\text{-3,5-Me}_2)$  (**2.8**) and the neopentyl *p*-xylyl complex  $\text{Cp}^*\text{W}(\text{NO})(\text{CH}_2\text{CMe}_3)(\text{C}_6\text{H}_3\text{-2,5-Me}_2)$  (**1.7**), in the respective parent solvents and benzene-*d*<sub>6</sub> also reveal a trace amount (< 2 %) of conversion to the respective benzyl products of  $\text{sp}^3$  C-H activation, namely  $\text{Cp}^*\text{W}(\text{NO})(\text{CH}_2\text{C}_6\text{H}_5)(\text{CH}_2\text{C}_6\text{H}_4\text{-3-Me})$  (**2.9**) and  $\text{Cp}^*\text{W}(\text{NO})(\text{CH}_2\text{CMe}_3)(\text{CH}_2\text{C}_6\text{H}_4\text{-4-Me})$  (**1.8**). Thus, it would appear that, unlike those derived from toluene, the aryl products derived from the xylenes can intramolecularly isomerize to the respective benzyl products, albeit very slowly.

#### 4.2.2.2 Interpretation of Aryl vs Benzyl Product Selectivity

Given the similarities between toluene and the xylenes, it can be safely assumed that the reaction coordinates for toluene and xylene activation are similar. Thus, Figure 4.8 depicts the likely reaction coordinate for activation of the xylenes by **A** and **B**. Since the aryl and benzyl C-H activation products interconvert very slowly once formed, if at all, the aryl vs benzyl product distributions are mostly kinetic in origin. The magnitudes of the selectivities thus chiefly arise from the relative energies of coordination of the xylene substrate in the  $\pi$ -arene and  $\sigma$ -arylmethane fashions (i.e.  $\Delta\Delta G^\ddagger$  in Figure 4.8). The subtle shift from aryl products towards the benzyl products when moving from *p*- to *m*- to *o*-xylene for **B** therefore arises from a decrease in the relative difference in energy barriers to formation of the  $\pi$ -arene and  $\sigma$ -arylmethane complexes, likely due to increased steric interactions in the  $\pi$ -arene complexes as more of the  $\pi$ -ring is shielded by the methyl substituents. The aryl to benzyl product isomerizations of **2.12** to **2.13**, **1.7** to **1.8**, and **2.8** to **2.9**, can be explained by an energy barrier for interconversion of the  $\pi$ -arene complex to the  $\sigma$ -arylmethane complex (i.e. the dashed line in Figure 4.8) that is lower

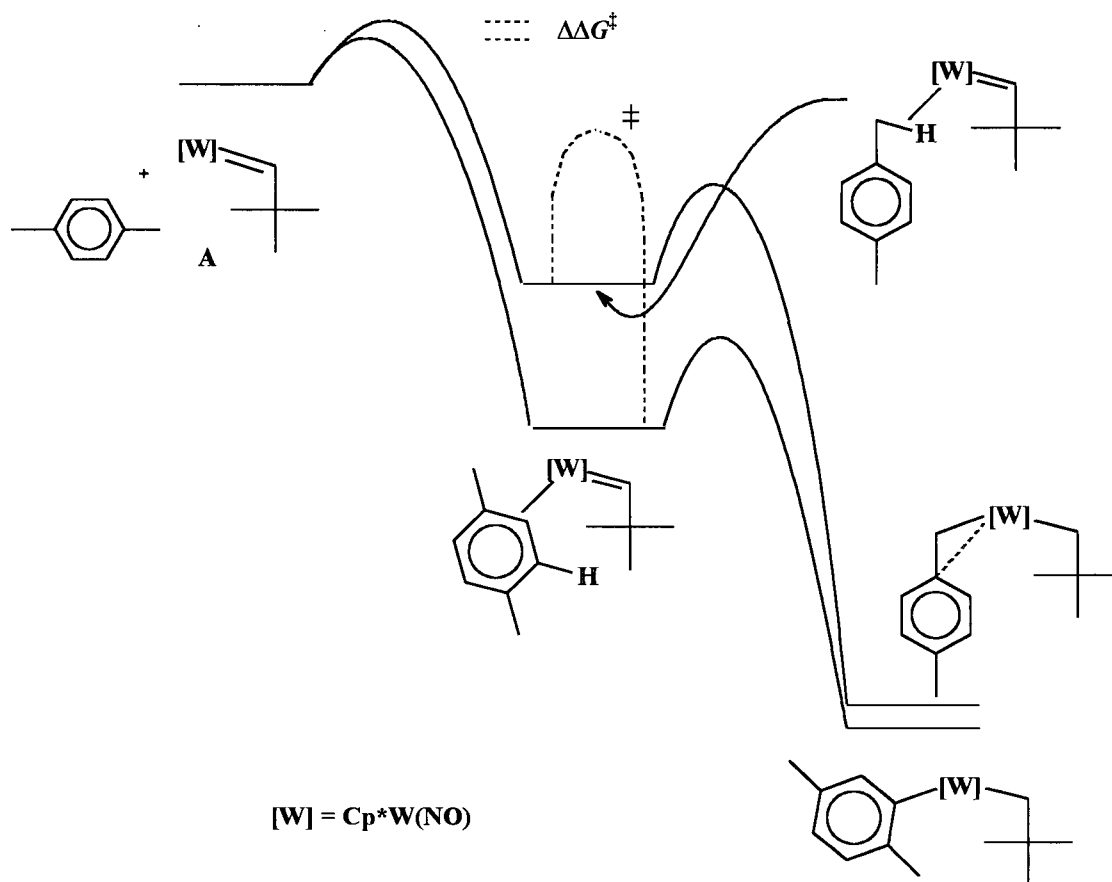


**Figure 4.8.** A qualitative representation of the free energy vs reaction coordinate diagram for the activation of xylenes by **A** and **B**, using **A** and *p*-xylene as an illustrative example.

than the respective barrier in the reaction coordinate for toluene activation. Note that the isomerization may also be statistically assisted by the increased number of methyl C-H bonds and corresponding  $\sigma$ -arylmethane complexes, compared to the fixed number of possible  $\pi$ -arene complexes. On the other hand, the reverse process, namely isomerization of **2.9** to **2.8** is not observed, likely due to the higher energy barrier for

reversion to the  $\sigma$ -arylmethane complex, as well as the existence of an additional  $\eta^2$ -benzyl conformation in the benzyl activation products, which have to convert to the less stable  $\eta^1$  form to undergo reversible C-H bond scission.

#### 4.2.2.3 Rationalizing The Differences between Aryl vs Benzyl Product

##### Distributions Derived From A and B

As with toluene, the fact that **B** leads to a higher relative amount of the aryl product in the activation of *p*-xylene (6.2(4):1) vs 1.14(7):1 for **A**) appears to be due to a greater difference in the relative transition state energies for  $\pi$ -arene vs  $\sigma$ -arylmethane coordination. The phenomenon is likely caused by weaker steric interactions between the phenyl substituent of **B** and the methyl substituents of the xylene substrate in the formation of the  $\pi$ -arene complex.

#### 4.2.3 Case 3. C-H Activation of Mesitylene.

Mesitylene is the one methyl-substituted arene that does not generate more than one type of product. The origin of this preference can now be rationalized based on the work conducted on the activations of toluene and the xylenes. As described in Sections 2.2.13 and 2.2.15.2, the benzyl product of  $sp^3$  C-H bond activation are formed exclusively over the corresponding aryl products for both **A** and **B**. Three factors may be responsible for the inversion in product selectivity. One factor is that the transition-state energies for formation of the  $\pi$ -arene complexes leading to  $sp^2$  C-H bond scission may be higher, rather than lower, in energy than those for formation of the  $\sigma$ -arylmethane complex, due to the presence of unfavourable steric interactions (i.e.  $\Delta\Delta G^\ddagger$  in Figure 4.9). Alternatively, the barrier for isomerization of the  $\pi$ -arene complex to the  $\sigma$ -arylmethane

complex may be lower than for scission of the  $sp^2$  C-H bond so that only the  $\sigma$ -arylmethane complex leads to substrate C-H bond scission. This feature is also illustrated in Figure 4.9. Finally, the statistical dominance of  $sp^3$  C-H bonds compared to  $sp^2$  C-H bonds means that, unlike toluene and the xylenes, there is a statistical dominance of  $\sigma$ -arylmethane complexes vs  $\pi$ -arene complexes. Either one or any combination of these factors could lead to the exclusive formation of the benzyl product of mesitylene C-H activation.

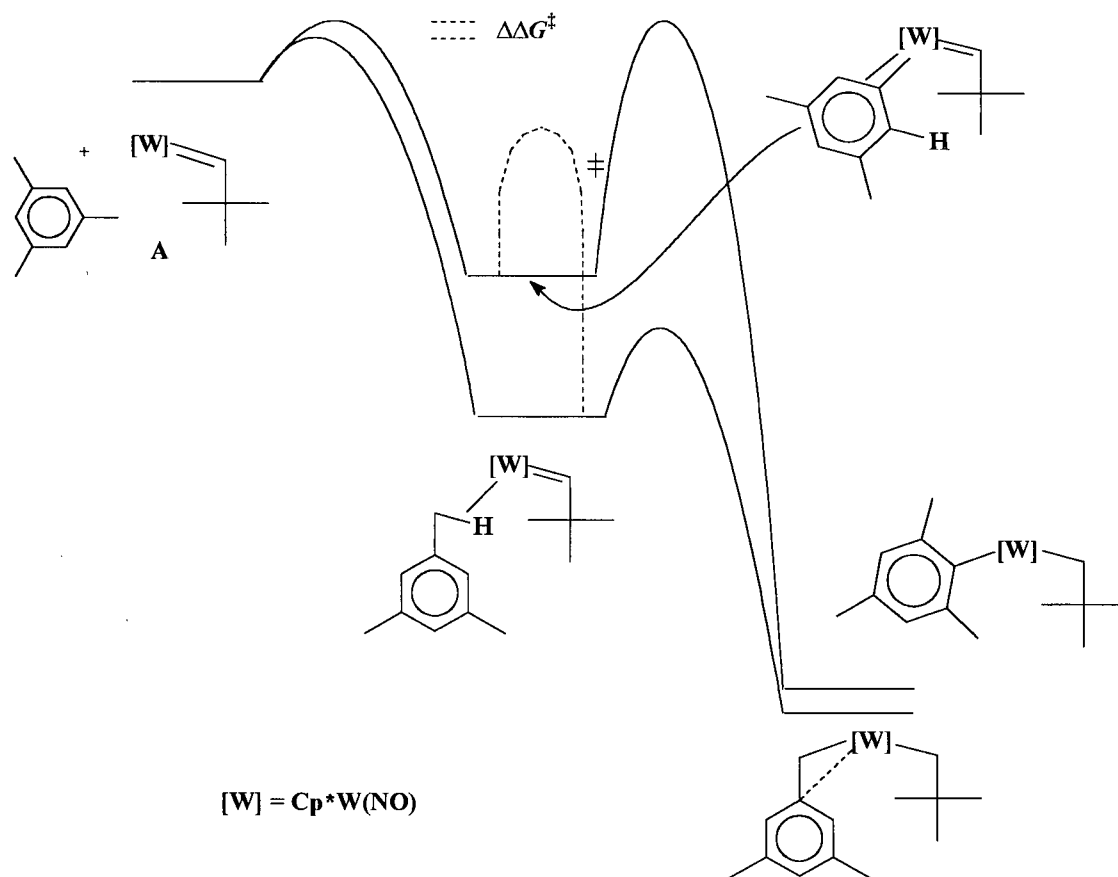


**Figure 4.9.** A qualitative representation of the free energy vs reaction coordinate diagram for the activation of mesitylene by **A** and **B**, using **A** as an illustrative example.

#### 4.2.4 Case 4. Activation of $\alpha,\alpha,\alpha$ -Trifluorotoluene By A.

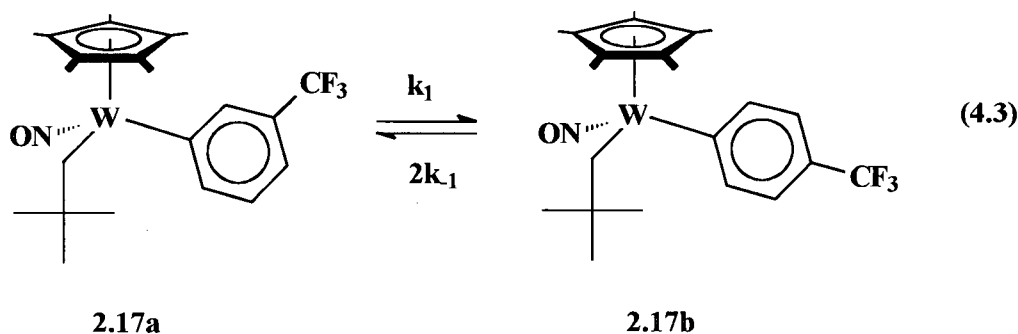
As detailed in Section 2.1.15.3, the thermolysis of **1** in  $\alpha,\alpha,\alpha$ -trifluorotoluene for 40 h at 70 °C yields the meta and para aryl products  $\text{Cp}^*\text{W}(\text{NO})(\text{CH}_2\text{CMe}_3)(\text{C}_6\text{H}_4\text{-3-CF}_3)$  (**2.17a**) and  $\text{Cp}^*\text{W}(\text{NO})(\text{CH}_2\text{CMe}_3)(\text{C}_6\text{H}_4\text{-4-CF}_3)$  (**2.17b**) in a 1.85(6):1 ratio.

Consequently, only the relationship between the aryl regioisomers needs to be considered in this instance.

##### 4.2.4.1.1 The Nature of the Product Distribution

$^1\text{H}$  NMR spectroscopic analysis of the reaction mixtures obtained from the partial thermolysis of **1** after only 15 h of heating in  $\alpha,\alpha,\alpha$ -trifluorotoluene (70 °C) reveals that the products exist in the same ratios at 15 h and 40 h. Thus, the isomers either do not interconvert (i.e.  $\text{sp}^2$  C-H bond cleavage is irreversible) or equilibrate by rapid isomerization under the thermolysis conditions (i.e.  $\text{sp}^2$  bond cleavage is reversible).

Fortuitously, these options can be tested since **2.17a** and **2.17b** co-crystallize in a mixture that significantly favours **2.17a** over **2.17b** (11.5:1). Monitoring the thermolysis of this mixture in benzene- $d_6$  by  $^{19}\text{F}$  NMR spectroscopy over 6 h reveals that **2.17a** does indeed isomerize to the mixture of **2.17a-b** observed in the thermolyses of **1** (eq 4.3).



A non-linear least-squares analysis of the data from the reaction (Figure 4.10) using an exponential approach to equilibrium kinetic model yields a calculated  $k_{\text{obs}}$  of  $1.2(1) \times 10^{-4} \text{ s}^{-1}$ . This corresponds to rate constants of  $4.1 \times 10^{-5} \text{ s}^{-1}$  for the isomerization of **2.17a** to **2.17b** and  $3.9 \times 10^{-5} \text{ s}^{-1}$  for the opposite reaction after statistical correction. The similarities in the rate constants are not surprising. The calculated  $K_{\text{eq}}$  is  $0.53(1)$ , which agrees with the experimental value of 0.54.

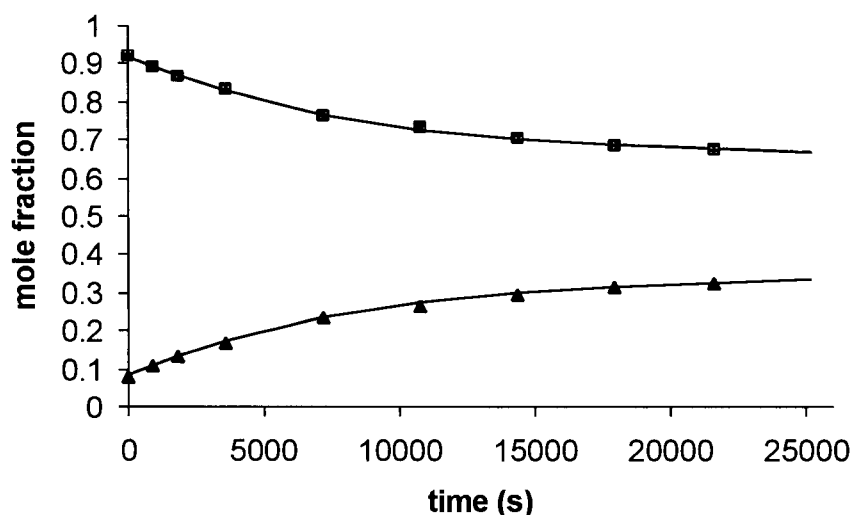


**Figure 4.10.** Plot of conversion of **2.17a** to **2.17b** versus time for the approach to equilibrium at  $70^\circ\text{C}$  (■ = **2.17a**, ▲ = **2.17b**). The solid lines indicate a non-linear least-squares fit to an exponential decay to equilibrium.

#### 4.2.4.1.2 The Origin of Meta vs Para Aryl Product Selectivity

The rapid equilibration of **2.17a-b** implies that the distribution of complexes **2.17a-b** is under thermodynamic control when formed from **A**. Thus, the product distribution arises from the relative energies of the meta and para isomers (i.e.  $\Delta\Delta G^\circ$  in

Figure 4.11). Moreover, the increase in meta isomer for the distribution obtained from  $\alpha,\alpha,\alpha$ -trifluorotoluene compared to that obtained from toluene (1.45(8):1) is due to a decrease in the relative difference in the energies of the meta and para complexes as a whole.

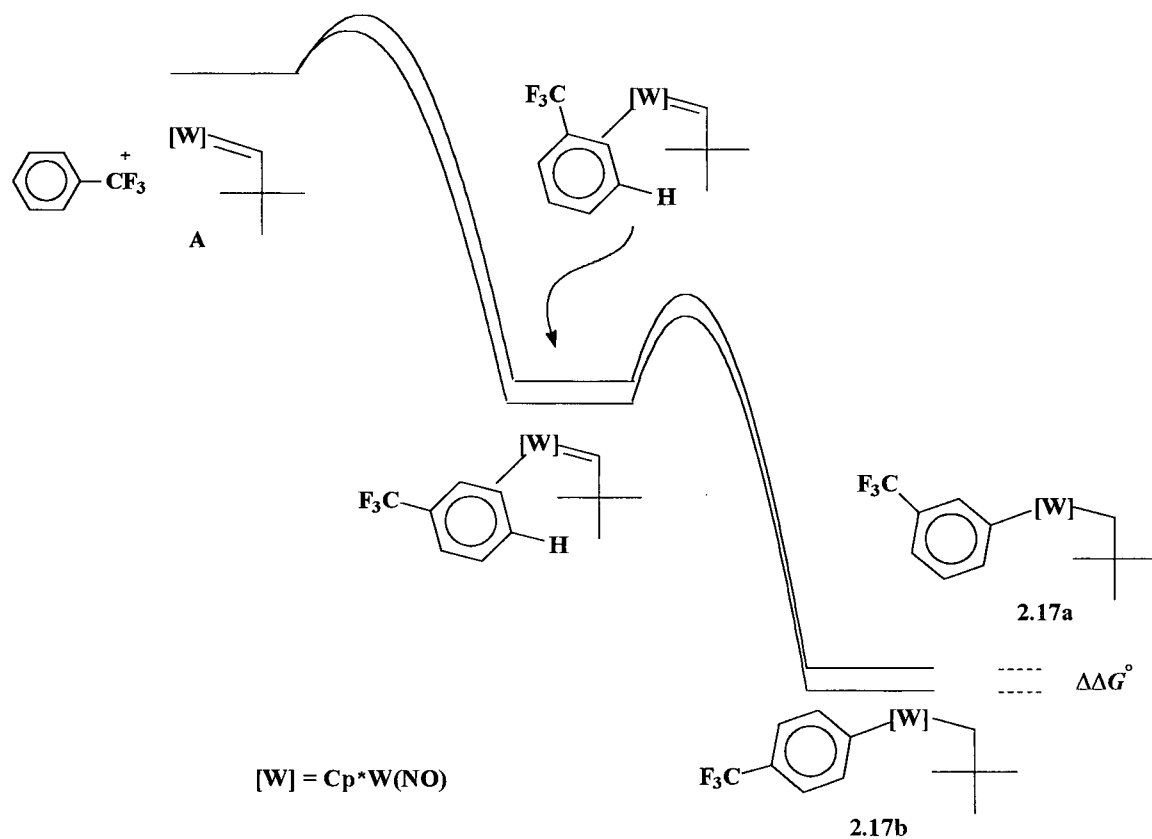


**Figure 4.11.** A qualitative representation of the free energy vs reaction coordinate diagram for the activation of  $\alpha,\alpha,\alpha$ -trifluorotoluene by A.

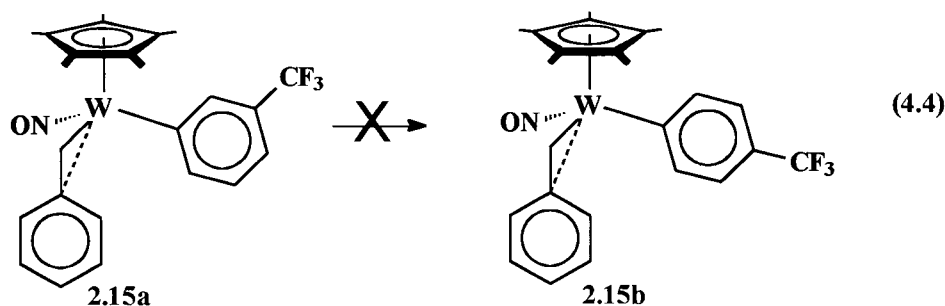
#### 4.2.5 Case 5: Activation of $\alpha,\alpha,\alpha$ -Trifluorotoluene By B

As detailed in Section 2.1.14, the thermolysis of **2** in  $\alpha,\alpha,\alpha$ -trifluorotoluene (40 h, 70 °C) results in the formation of the meta and para aryl products

$\text{Cp}^*\text{W}(\text{NO})(\text{CH}_2\text{C}_6\text{H}_5)(\text{C}_6\text{H}_4\text{-3-CF}_3)$  (**2.15a**) and  $\text{Cp}^*\text{W}(\text{NO})(\text{CH}_2\text{C}_6\text{H}_5)(\text{C}_6\text{H}_4\text{-4-CF}_3)$  (**2.15b**) in a 2.27(3):1 ratio.

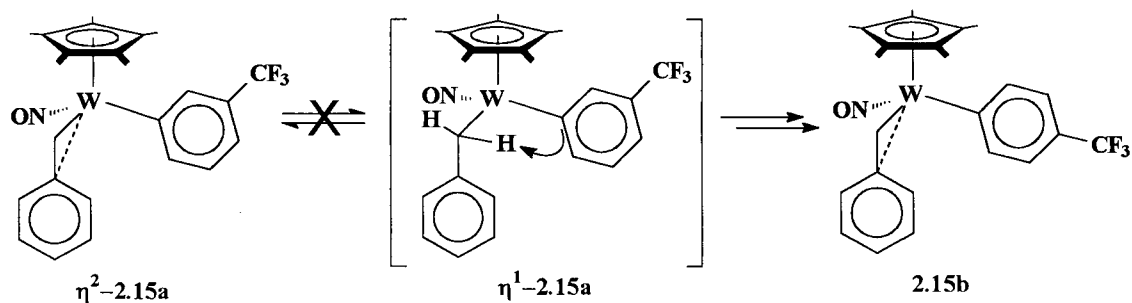
#### 4.2.5.1.1 Nature of Product Distribution

As with **2.17a-b**, the partial thermolysis of **2** for 15 h reveals that **2.15a-b** grow in over time in the same relative distribution as at 40 h. Also, **2.15a-b** co-crystallize in a mixture enriched in **2.15a** (8.3:1) thereby permitting an analysis of the nature of the distribution of **2.15a-b**. Thermolysis of the enriched mixture in benzene- $d_6$ , however, yields a very different result than **2.17a-b**, namely that complex **2.15a** *does not isomerize at all to 2.15b* even after 40 h at 70 °C (eq 4.4). So, unlike the activation effected by **A**, the meta and para products are formed irreversibly from **B**, and the observed meta vs para regioisomer distribution is a kinetic product distribution.



This result is also very different from that obtained for the meta and para aryl products derived from toluene and **B**, which are in thermodynamic equilibrium under the same conditions. The only logical explanation for the lack of isomerization of **2.15a-b** is that the electron-withdrawing nature of the  $\text{CF}_3$  group of the aryl ligand stabilizes the  $\eta^2$ -benzyl interaction in the products **2.15a-b** so much that the  $\eta^1$  conformation of **2.15a** is not formed in sufficient concentration to permit the reversible  $\text{sp}^2$  C-H bond activation under the thermolytic conditions (Scheme 4.6).

Scheme 4.6



#### 4.2.5.1.2 Interpretation of Product Selectivity

Given that **2.15a** and **2.15b** form under kinetically-controlled conditions, there are two possible points that could give the observed meta: para product ratio of 2.27(3):1 during the activation of  $\alpha,\alpha,\alpha$ -trifluorotoluene by **B** (Figure 4.12). If the  $\pi$ -arene complexes themselves are formed independently, then the discriminating point is at the formation of the  $\pi$ -arene complexes from **B**, and the product distribution arises from the relative rates of meta vs para  $\pi$ -arene complex formation ( $\Delta\Delta G_2$ ). Alternatively, if the respective  $\pi$ -arene complexes leading to meta and para aryl products can interconvert as they form, then discriminating point is the C-H bond scission step, and the observed ratio reflects the relative energies of meta vs para C-H bond scission from the  $\pi$ -arene complexes ( $\Delta\Delta G_1$ ). The latter case seems intuitively more likely, and is consistent with the fact that the  $\text{CF}_3$  group is known to direct the electrophilic C-H activation of arenium cations to the meta position of the aromatic ring.<sup>14</sup>

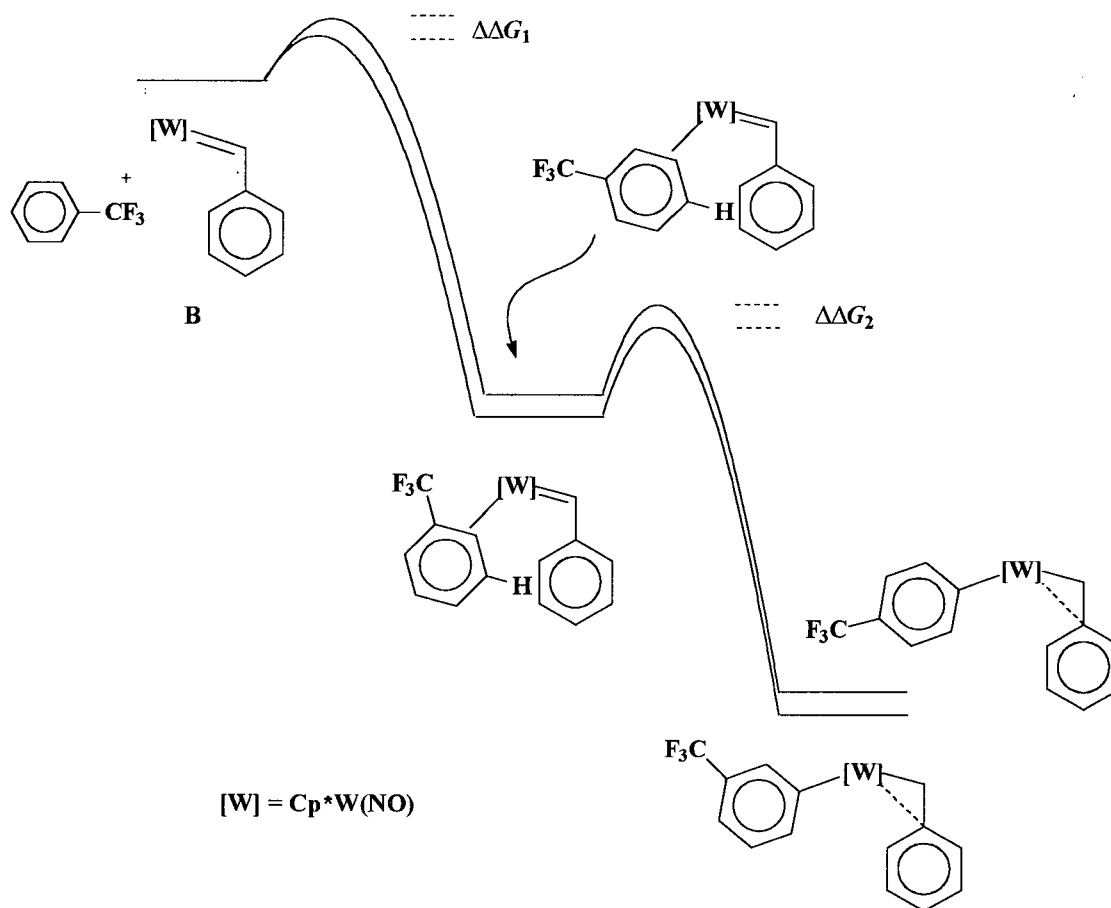


**Figure 4.12.** A qualitative representation of the free energy vs reaction coordinate diagram for the activation of  $\alpha,\alpha,\alpha$ -trifluorotoluene by **B**.

### 4.3 Epilogue

Through both experimental and theoretical work, the arene activation chemistry reported in Chapter 2 has been successfully rationalized. It is now apparent that the factors that control the product distributions can vary significantly with the particular properties of the substrate, the type of activation products and the alkylidene complex employed. In short, the observed product selectivities do not result from the simple correlation to the relative activated product energies like in the imido systems studied by Wolczanski et al.

Despite these complications, some general conclusions can be made regarding the activation of substituted arenes by the neopentylidene and benzylidene systems:

1. Aryl and benzyl products are mostly formed under kinetic control with a preference for the aryl products, but the aryl products can slowly isomerize to the corresponding benzyl products with increased methyl substitution and shielding of the  $sp^2$  C-H bonds, so that the aryl vs benzyl distribution shifts towards the benzyl products.
2. In the case of toluene, aryl vs benzyl product distributions are controlled by the relative energies of the  $\pi$ -arene vs  $\sigma$ -arylmethane coordination of toluene to the metal center (in **A** and **B**, or in  $\sigma$ -**A** and  $\sigma$ -**B**). In the case of xylenes and mesitylene, subtle changes in the energetics of the formation of these complexes lead to the observed shifts towards the benzyl products.
3. The rapid reversible scission of the  $sp^2$  C-H bonds of arenes appears to be a general phenomenon for aryl complexes, so that aryl regioisomer distributions formed from  $sp^2$  C-H activation by **A** and **B** are controlled by the thermodynamic stability of the respective complexes. An exception occurs for  $\alpha,\alpha,\alpha$ -trifluorotoluene when activated by **B**, where the requisite intermediate for isomerization apparently cannot form due to the strong  $\eta^2$ -benzyl interactions in the product. In this instance, the regioisomer distribution is strictly controlled by the rates of formation of the respective  $\pi$ -arene complexes.

4. The benzylidene and neopentylidene systems exhibit different product selectivities in the activation of substituted arenes, but the origin of the difference can vary with the substrate. For example, in the activation of methyl-substituted arenes, the alkylidene substituent primarily influences the aryl vs benzyl selectivity in the coordination step, while it is the alkyl ligand derived from the alkylidene linkage that influences the aryl regioisomeric distribution. In contrast, in the activation of  $\alpha,\alpha,\alpha$ -trifluorotoluene, the nature of the alkylidene substituent controls the product distribution by affecting the reversibility of the C-H bond scission step.

In addition to these conclusions regarding arene activation by the benzylidene and neopentylidene systems, some additional statements can be made regarding the activation of the other substrates explored in Chapter 2. For example, the activation of benzene likely proceeds via the formation of  $\pi$ -arene complex and reversible C-H bond scission, as outlined by the lower-energy pathway for  $sp^2$  C-H bond scission in Figure 4.2. Likewise, the activation of tetramethylsilane and cyclohexane should proceed via the formation of an intermediate  $\sigma$ -alkane complex prior to C-H bond scission, as outlined by the higher-energy pathway for benzylic  $sp^3$  C-H bond scission in Figure 4.2. Finally, in the case of the alkyl-substituted alkanes and acyclic alkanes, the exclusive formation of the terminal allyl hydride complexes, such as **1.5** and **2.7**, may arise from the exclusive formation of the  $1^\circ$   $\sigma$ -alkane complex over the other possible  $2^\circ$  and  $3^\circ$   $\sigma$ -alkane complexes during coordination of the metal center. This interpretation is consistent with those put forth for the activation of alkanes by other soluble metal complexes involving intermediate hydrocarbon complexes. It should be acknowledged, however, that it is

possible that the observed product distributions do not correlate with the intrinsic selectivity of **A** and **B** for 1° vs 2°  $\sigma$ -alkane complex formation, due to the fact that terminal allyl linkages in these complexes do not have to be formed by exclusive activation at the terminal methyl group.<sup>15</sup> Yet, as discussed in the next Chapter, how these particular products are formed is not as important compared to what we may be able to do with them once they are formed.

#### 4.4 Experimental Procedures

##### 4.4.1 General

All reactions and subsequent manipulations were performed under anaerobic and anhydrous conditions using procedures described in Section 2.4.1.

##### 4.4.2 Reagents

The  $R_2Mg \cdot x(\text{dioxane})$  ( $R = C_6H_4\text{-}2\text{-Me}$ ,  $C_6D_5$ ) alkylating reagents<sup>16</sup> and the complexes  $Cp^*W(NO)(CH_2CMe_3)(C_6H_4\text{-}2\text{-Me})$  (**2.1c**),<sup>17</sup>  $Cp^*W(NO)(CH_2C_6H_5)(C_6H_4\text{-}2\text{-Me})$  (**2.2c**),  $Cp^*W(NO)(CH_2CMe_3)(C_6D_5)$  (**4.1-d<sub>5</sub>**) and  $Cp^*W(NO)(CH_2C_6H_5)(C_6D_5)$  (**4.2-d<sub>5</sub>**) were prepared by metathetical routes from the corresponding neopentyl or benzyl chloro complex (see Section 2.4.4). Pertinent synthetic details for the new compounds are described below. Complexes  $Cp^*W(NO)(CH_2C_6H_5)(C_6H_3\text{-}3,4\text{-Me}_2)$  (**2.8**),  $Cp^*W(NO)(CH_2C_6H_5)(CH_2C_6H_4\text{-}3\text{-Me})$  (**2.9**) and  $Cp^*W(NO)(CH_2C_6H_5)(C_6H_3\text{-}2,5\text{-Me}_2)$  (**2.12**) were prepared as described in Sections 2.4.16, 2.4.17 and 2.4.19 respectively. A crystalline mixture of  $Cp^*W(NO)(CH_2C_6H_5)(C_6H_4\text{-}3\text{-CF}_3)$  (**2.15a**) and  $Cp^*W(NO)(CH_2C_6H_5)(C_6H_4\text{-}4\text{-CF}_3)$  (**2.15b**) was prepared as described in Section 2.4.21. A crystalline mixture of  $Cp^*W(NO)(CH_2CMe_3)(C_6H_4\text{-}3\text{-CF}_3)$  (**2.17a**) and

$\text{Cp}^*\text{W}(\text{NO})(\text{CH}_2\text{CMe}_3)(\text{C}_6\text{H}_4\text{-4-CF}_3)$  (**2.17b**), and complex

$\text{Cp}^*\text{W}(\text{NO})(\text{CH}_2\text{CMe}_3)(\text{C}_6\text{H}_3\text{-2,5-Me}_2)$  (**1.7**), were prepared and purified according to the methodology described by E. Tran.<sup>18</sup>

#### 4.4.3 Preparation of $\text{Cp}^*\text{W}(\text{NO})(\text{CH}_2\text{C}_6\text{H}_5)(\text{C}_6\text{H}_4\text{-2-Me})$ (**2.2c**)

Complex **2.2c** was prepared via the reaction of  $\text{Cp}^*\text{W}(\text{NO})(\text{CH}_2\text{C}_6\text{H}_5)\text{Cl}$  (0.160 g, 0.34 mmol) and  $(2\text{-Me-C}_6\text{H}_4)_2\text{Mg}\cdot x(\text{dioxane})$  (0.063 g, 0.34 mmol R<sup>-</sup>) in THF (10 mL). The crude residue was extracted with 4:1 Et<sub>2</sub>O/hexanes (3 x 5 mL), and the mixture was filtered through Celite (1 x 0.7 cm) supported on a frit. Concentration of the solution followed by storage at -30 °C overnight provided **2.2c** as red blocks (55 mg, 32 %). IR (cm<sup>-1</sup>) 1552 (s, ν<sub>NO</sub>). MS (LREI, m/z, probe temperature 150 °C) 531 [P<sup>+</sup>, <sup>184</sup>W]. <sup>1</sup>H NMR (400 MHz, C<sub>6</sub>D<sub>6</sub>) δ 1.92 (s, 15H, C<sub>5</sub>Me<sub>5</sub>), 2.62 (m, 4H, Tol Me, CH<sub>syn</sub>H), 3.46 (d, <sup>2</sup>J<sub>HH</sub> = 6.6, 1H, CH<sub>anti</sub>H), 5.77 (br d, 1H, Tol H), 6.59 (t, <sup>3</sup>J<sub>HH</sub> = 7.5, 1H, Bzl H<sub>para</sub>), 6.79 (t, <sup>3</sup>J<sub>HH</sub> = 7.9, 1H, Tol H), 6.90 (t, <sup>3</sup>J<sub>HH</sub> = 7.9, 2H, Bzl H<sub>meta</sub>), 7.07 (d, <sup>3</sup>J<sub>HH</sub> = 7.9, 1H, Tol H), 7.16 (t, <sup>3</sup>J<sub>HH</sub> = 7.9, 1H, Tol H), 7.21 (d, <sup>3</sup>J<sub>HH</sub> = 7.5, 2H, Bzl H<sub>ortho</sub>). <sup>13</sup>C{<sup>1</sup>H} NMR (75 MHz, CDCl<sub>3</sub>) δ 10.4 (C<sub>5</sub>Me<sub>5</sub>), 28.5 (Tol Me), 52.8 (br s, CH<sub>2</sub>), 109.6 (C<sub>5</sub>Me<sub>5</sub>), 119.9 (br, Bzl C<sub>ipso</sub>), 124.0, 124.8, 128.5, 129.1, 131.2, 134.3, 149.6 (Ar C<sub>aryl</sub>), 177.7 (Tol C<sub>ipso</sub>). Anal. Calcd. for C<sub>24</sub>H<sub>29</sub>NO: C, 54.25; H, 5.50; N, 2.64. Found: C, 54.16; H, 5.64; N, 2.74.

#### 4.4.4 Kinetic Studies of the Isomerization of **2.1c** and **2.2c**

Kinetic studies of the isomerization of **2.1c** and **2.2c** were conducted in a similar fashion. Two J. Young NMR tubes were charged with **2.1c** or **2.2c** (12 mg, 0.022 mmol) and 1.0 mL of benzene-*d*<sub>6</sub>, and placed in a VWR 1160A constant-temperature bath set a

70.0 °C. The tubes were removed from the bath at selected time intervals, and  $^1\text{H}$  NMR spectra were recorded. The relative conversions and rate constants were calculated using integrations of **2.1a-b** product signals to the combined  $\text{CMe}_3$  signals for **2.1a-c**, and integrations of **2.2c** signals versus the combined  $\text{Cp}^*$  signal for **2.2a-c**. See Appendix B for plots of the data.

#### 4.4.5 Preparation of $\text{Cp}^*\text{W}(\text{NO})(\text{CH}_2\text{CMe}_3)(\text{C}_6\text{D}_5)$ (**4.1-d<sub>5</sub>**).

Complex **4.1-d<sub>5</sub>** was prepared in a manner analogous to its protio analogue (**1.1**)<sup>17</sup> via the reaction of  $\text{Cp}^*\text{W}(\text{NO})(\text{CH}_2\text{CMe}_3)\text{Cl}$  (0.135 g, 0.30 mmol) and  $(\text{C}_6\text{D}_5)_2\text{Mg}\cdot x(\text{dioxane})$  (45 mg, 0.30 mmol  $\text{R}^-$ ) in  $\text{Et}_2\text{O}$  (10 mL). The crude residue was extracted with  $\text{Et}_2\text{O}$  (5 mL), and the mixture was filtered through Celite (1 x 0.7 cm) rather than Florisil. The solvent was removed in vacuo to obtain an orange residue that was then recrystallized from hexanes to obtain red rosettes (68 mg, 46%).

$^1\text{H}$  NMR (400 MHz,  $\text{C}_6\text{D}_6$ )  $\delta$  -2.05 (d,  $^2J_{\text{HH}} = 11.4$ , 1H,  $\text{CH}_{\text{syn}}\text{H}$ ), 1.26 (s, 9H,  $\text{CMe}_3$ ), 1.53 (s, 15H,  $\text{C}_5\text{Me}_5$ ), 4.50 (d,  $^2J_{\text{HH}} = 11.4$ , 1H,  $\text{CH}_{\text{anti}}\text{H}$ ).  $^2\text{H}\{^1\text{H}\}$  NMR (61 MHz,  $\text{C}_6\text{H}_6$ )  $\delta$  7.10 (m, Ph D), 7.70 (br s, Ph D). Anal. Calcd. for  $\text{C}_{21}\text{H}_{26}\text{D}_5\text{NOW}$ : C, 50.21; H/D,<sup>19</sup> 6.22; N, 2.79. Found: C, 50.24; H/D, 6.34; N, 2.87.

#### 4.4.6 Preparation of $\text{Cp}^*\text{W}(\text{NO})(\text{CH}_2\text{C}_6\text{H}_5)(\text{C}_6\text{D}_5)$ (**4.2-d<sub>5</sub>**).

The reaction of  $\text{Cp}^*\text{W}(\text{NO})(\text{CH}_2\text{C}_6\text{H}_5)\text{Cl}$  (0.145 g, 0.30 mmol) and  $(\text{C}_6\text{D}_5)_2\text{Mg}\cdot x(\text{dioxane})$  (45 mg, 0.30 mmol  $\text{R}^-$ ) in THF (10 mL) for 6 h yielded a yellow-orange solid after work-up. Repeated attempts to crystallize the resulting crude residue, including from neat  $\text{Et}_2\text{O}$  in the same manner as used for **2.5-d<sub>6</sub>**, afforded only a small

amount of semi-crystalline orange solid (10 mg, 7%). The sample was determined to be ~ 85 % pure by  $^1\text{H}$  NMR spectroscopy.

$^1\text{H}$  NMR (400 MHz,  $\text{C}_6\text{D}_6$ )  $\delta$  1.53 (s, 15H,  $\text{C}_5\text{Me}_5$ ), 2.12 (d,  $^2J_{\text{HH}} = 6.4$ , 1H,  $\text{CH}_{\text{syn}}\text{H}$ ), 3.41 (d,  $^2J_{\text{HH}} = 6.4$ , 1H,  $\text{CH}_{\text{anti}}\text{H}$ ), 6.50 (t,  $^3J_{\text{HH}} = 7.8$ , 2H, Bzl  $\text{H}_{\text{meta}}$ ), 6.84 (d,  $^3J_{\text{HH}} = 7.6$ , 2H, Bzl  $\text{H}_{\text{ortho}}$ ), 7.05 (t,  $^3J_{\text{HH}} = 7.5$ , 1H, Bzl  $\text{H}_{\text{para}}$ ).  $^2\text{H}\{^1\text{H}\}$  NMR (61 MHz,  $\text{C}_6\text{H}_6$ )  $\delta$  6.9-7.2 (Ph D).

#### 4.4.7 Thermolysis of Complexes **4.1-*d*<sub>5</sub>** and **4.2-*d*<sub>5</sub>**

The thermolyses were conducted in a fashion similar to those used for **2.1c** and **2.2c**. A J. Young NMR tube was charged with **4.1-*d*<sub>5</sub>** or **4.2-*d*<sub>5</sub>** (12-15 mg, 0.024-0.030 mmol) and either  $\text{C}_6\text{D}_6$  or  $\text{CD}_2\text{Cl}_2$  (1.0 mL). The thermolyses were conducted in the constant-temperature bath set to 70.0 °C, and the tubes were periodically removed to record  $^1\text{H}$  NMR spectra at ambient temperatures. For **4.1-*d*<sub>5</sub>**, the progress of the reaction was monitored for 5 h. New signals attributable to **4.1'-*d*<sub>5</sub>** were observed to grow in simultaneously for  $\text{H}_{\text{anti}}$  at  $\delta$  4.37 and Ph-H at  $\delta$  6.9-7.1 and 7.70. Average conversions of **4.1-*d*<sub>5</sub>** to **4.1'-*d*<sub>5</sub>** were determined from multiple integrations of the respective  $\text{H}_{\text{anti}}$  signals of **4.1-*d*<sub>5</sub>** and **4.1'-*d*<sub>5</sub>** at several time intervals. The observed rate constant for H/D exchange and the corresponding equilibrium constant were calculated from the experiment performed in  $\text{CD}_2\text{Cl}_2$  via non-linear least-squares analysis of the plot of percent conversion vs time using Origin 5.0 software and an approach-to-equilibrium kinetic model.<sup>20</sup> After 5 h, the solvent was removed in vacuo, and the residue was dissolved in  $\text{C}_6\text{H}_6$  to record a  $^2\text{H}\{^1\text{H}\}$  NMR spectrum which showed a new signal at  $-\delta$  1.98 corresponding to  $\text{D}_{\text{syn}}$  of **4.1'-*d*<sub>5</sub>**. For **4.2-*d*<sub>5</sub>**, the thermolysis was conducted under

the same conditions for 45 h. A new signal attributable to  $CH_{anti}D$  of **4.2'-d<sub>5</sub>** was observed at  $\delta$  3.38. After 45 h, the solvent was replaced with  $C_6H_6$  in order to record a  $^2H\{^1H\}$  NMR spectrum. A resonance for  $CHD_{syn}$  of **4.2'-d<sub>5</sub>** was evident at  $\delta$  2.17.

#### 4.4.8 Theoretical Calculations Using the DFT Approach.

All calculations were performed on Intel PII PC computers with Gaussian 98<sup>21</sup> employing the LANL2DZ basis set and a DFT approach using the three-parameter exchange functional of Becke<sup>22</sup> and the correlation functional of Lee, Yang and Parr (B3LYP).<sup>23</sup> The LANL2DZ basis set includes both Dunning and Hay's D95 sets for H, C, N and O<sup>24</sup> and the relativistic electron core potential (ECP) sets of Hay and Wadt for W.<sup>25</sup> It does not include polarization and diffuse functions on any of the atoms. The alkylidene fragment **C** has previously been optimized.<sup>10</sup> Frequency calculations on optimized species established that all the transition states possessed one and only one imaginary frequency and that the products and intermediates possessed no imaginary frequencies. The reported energies are calculated gas-phase free energies at standard temperature (298.15K) and pressure (1 atm). Spatial plots of the optimized geometries and frontier orbitals were obtained from Gaussian 98 output using Molden v3.6.<sup>26</sup>

#### 4.4.9 Thermolysis of Complexes 1.7, 2.8, 2.9 and 2.12

The thermolyses of these complexes in benzene-*d*<sub>6</sub> were conducted in the same fashion as **4.1-d<sub>5</sub>** and **4.2-d<sub>5</sub>**, with hexamethyldisilane (2 mg, 0.014 mmol) added as an integration standard. Over the course of 40 h, the samples were removed periodically from the heating bath to record  $^1H$  NMR spectra. Thermolyses in the parent xylene

solvent were conducted on a similar scale for 40 h whereupon the solvent was removed, and a  $^1\text{H}$  NMR spectrum was recorded for each sample.

#### 4.4.10 Kinetic Studies of the Isomerizations of 2.15a-b and 2.17a-b

The thermolysis 2.17a-b in benzene- $d_6$  and the ensuing kinetic analysis of the  $^{19}\text{F}$  NMR spectral data were conducted in the same fashion as for 4.1-d<sub>5</sub>, using a non-linear least-square analysis of an approach-to-equilibrium kinetic model. The thermolysis of 2.15a-b was monitored by both  $^1\text{H}$  and  $^{19}\text{F}$  NMR spectroscopies for a total of 40 h. See Appendix B for a plot of the data for 2.17a-b.

#### 4.5 References and Notes

- (1) (a) Feher, F. J.; Jones, W. D. *J. Am. Chem. Soc.* **1984**, *106*, 1650-1663. (b) Chin, R. M.; Dong, L.; Duckett, S. B.; Partridge, M. G.; Jones, W. D.; Perutz, R. N. *J. Am. Chem. Soc.* **1993**, *115*, 7685-7695. (c) Sweet, J. R.; Graham, W. A. G. *J. Am. Chem. Soc.* **1983**, *105*, 304-306.
- (2) (a) Erker, G. *J. Organomet. Chem.* **1977**, *134*, 189-202. (b) Debad, J. D.; Legzdins, P.; Lumb, S. A.; Rettig, S. J.; Batchelor, R. J.; Einstein, F. W. B. *Organometallics* **1999**, *18*, 3414-3428. (c) Price, R. T.; Andersen, R. A.; Muetterities, E. L. *J. Organomet. Chem.* **1989**, *376*, 407-417.
- (3) Jones, W. D.; Feher, F. J. *Acc. Chem. Res.* **1989**, *22*, 91-100.
- (4) Thompson, M. E.; Baxter, S. M.; Bulls, R.; Burger, B. J.; Nolan, M. C.; Santarsiero, B. D.; Schaefer, W. P.; Bercaw, J. E. *J. Am. Chem. Soc.* **1987**, *109*, 203-219.
- (5) Jones, W. D.; Feher, F. J. *J. Am. Chem. Soc.* **1986**, *108*, 4814-4819.
- (6) The corresponding incorporation of H into the phenyl ring is not detectable in the  $^1\text{H}$  NMR spectra due to the masking of these signals by those for the aryl protons of the benzyl ligand.

- (7) (a) Legzdins, P.; Jones, R. H.; Phillips, E. C.; Yee, V. C.; Trotter, J.; Einstein, F. W. B. *Organometallics* **1991**, *10*, 986-1002. (b) Dryden, N. H.; Legzdins, P.; Trotter, J.; Yee, V. C. *Organometallics* **1991**, *10*, 2857-2870.
- (8) Herein, the two types of  $\sigma$ -complexes for toluene will be distinguished as the  $\sigma$ -arene complex for the  $sp^2 \eta^2$ -(C,H) coordination mode, and the  $\sigma$ -phenylmethane complex for the  $sp^3 \eta^2$ -(C,H) coordination mode.
- (9) Bau, R.; Mason, S. A.; Patrick, B. O.; Adams, C. S.; Sharp, W. B.; Legzdins, P. *Organometallics* (in press).
- (10) Poli, R.; Smith, K. M. *Organometallics* **2000**, *19*, 2858-2867.
- (11) Levine, I. N.; *Quantum Chemistry*, 5<sup>th</sup> ed. Prentice-Hall: Upper Saddle River, NJ, 2000.
- (12) The difference may be due in part to the difference between gas-phase and solution-phase free energies, but the formation of methyldiene analogs of neopentylidene complexes has been found to be energetically less favourable in both theoretical and experimental studies. For example, see: (a) Wu, Y.-D.; Peng, Z. H.; Xue, Z. *J. Am. Chem. Soc.* **1996**, *118*, 9772-9777. (b) Warren, T. H.; Schrock, R. R.; Davis, W. M. *J. Organomet. Chem.* **1998**, *569*, 125-137.
- (13) Legzdins, P.; Veltheer, J. E. *Acc. Chem. Res.* **1993**, *26*, 41-48.

- (14) March, J. *Advanced Organic Chemistry: Reactions, Mechanisms and Structure*, 4<sup>th</sup> ed. Wiley and Sons, Inc.: Toronto, ON, 1992; Chapter 11.
- (15) For example, the formation of the terminal allyl linkage may occur via initial activation at one of the other allyl positions, followed by dehydrogenation at the methyl position. Alternatively, since the C-H activation steps are all post-rate-determining, other allyl hydride isomers could be derived from activation by **A** at endocyclic C-H bond positions but undergo rapid isomerization (e.g. by reversible  $\gamma$ -H activation by the metal center) to the more thermodynamically stable isomers.
- (16) Dryden, N. H.; Legzdins, P.; Rettig, S. J.; Veltheer, J. E. *Organometallics* **1992**, *11*, 2583-2590.
- (17) Debad, J. D.; Legzdins, P.; Batchelor, R. J.; Einstein, F. W. B. *Organometallics* **1993**, *12*, 2094-2102.
- (18) Tran, E.; Legzdins, P., unpublished observations.
- (19) Since the detection method used in the elemental analysis cannot distinguish between D<sub>2</sub>O and H<sub>2</sub>O, H/D abundances were calculated using 1 D = 1 H
- (20) Origin 5.0 Microcal Software Inc., 1991-1997.
- (21) Gaussian 98 (Revision A.9), Frisch, M. J.; Trucks, G. W.; Schlegel, H. B.; Scuseria, G. E.; Robb, M. A.; Cheeseman, J. R.; Zakrzewski, V. G.; Montgomery,

- J. A.; Stratmann, R. E.; Burant, J. C.; Dapprich, S.; Millam, J. M.; Daniels, A. D.; Kudin, K. N.; Strain, M. C.; Farkas, O.; Tomasi, J.; Barone, V.; Cossi, M.; Cammi, R.; Mennucci, B.; Pomelli, C.; Adamo, C.; Clifford, S.; Ochterski, J.; Petersson, G. A.; Ayala, P. Y.; Cui, Q.; Morokuma, K.; Malick, D. K.; Rabuck, A. D.; Raghavachari, K.; Foresman, J. B.; Cioslowski, J.; Ortiz, J. V.; Stefanov, B. B.; Liu, G.; Liashenko, A.; Piskorz, P.; Komaromi, I.; Gomperts, R.; Martin, R. L.; Fox, D. J.; Keith, T.; Al-Laham, M. A.; Peng, C. Y.; Nanayakkara, A.; Gonzalez, C.; Challacombe, M.; Gill, P. M. W.; Johnson, B. G.; Chen, W.; Wong, M. W.; Andres, J. L.; Head-Gordon, M.; Replogle, E. S.; Pople, J. A.: Gaussian, Inc., Pittsburgh PA, 1998.
- (22) Becke, A. D. *J. Chem. Phys.* **1993**, *98*, 5648-5652.
- (23) (a) Lee, C.; Yang, W.; Parr, R. G. *Phys. Rev.* **1988**, **B37**, 785-789. (b) Volko, S. H.; Wilk, L.; Nusair, N. *Can. J. Phys.* **1980**, *58*, 1200-1211.
- (24) Dunning, T. H., Jr.; Hay, P. J. *In Modern Theoretical Chemistry*; Schaefer, H. F., III, Ed.; Plenum Press: New York, 1976; pp 1-28.
- (25) (a) Hay, P. J.; Wadt, W. R. *J. Chem. Phys.* **1985**, *82*, 270-283. (b) Wadt, W. R.; Hay, P. J. *J. Chem. Phys.* **1985**, *82*, 284-298. (c) Hay, P. J.; Wadt, W. R. *J. Chem. Phys.* **1985**, *82*, 299-310.
- (26) Schaftenaar, G.; Nordik, J. H. *J. Comput.-Aided Mol. Design* **2000**, *14*, 123-134.

## CHAPTER 5

# Towards the Development of Alkylidene and Related Complexes as Reagents for The Conversion of Alkanes Into Functionalized Chemicals

---

<b>5.1</b>	<b>Introduction .....</b>	<b>188</b>
<b>5.2</b>	<b>Results and Discussion.....</b>	<b>191</b>
<b>5.3</b>	<b>Epilogue.....</b>	<b>211</b>
<b>5.4</b>	<b>Experimental Procedures.....</b>	<b>212</b>
<b>5.5</b>	<b>References and Notes.....</b>	<b>218</b>

---

## 5.1 Introduction

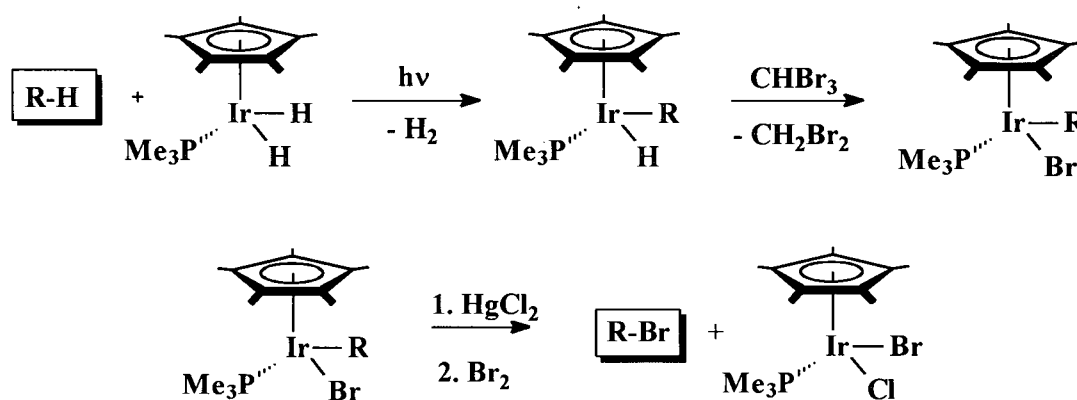
With the research described in Chapters 2-4, the chemistry of the benzylidene system has successfully been compared to that of its neopentylidene analogue, and the issues regarding the mechanism of activation of both systems and the origin of the product selectivities observed for arene and alkane substrates have been addressed. The level of understanding of the activation chemistry exhibited by these prototypical alkylidene systems is now on par with the level of understanding acquired for systems that belong to the other general classes of soluble metal complexes that activate hydrocarbons by organometallic pathways. What remains to be determined is whether or not these alkylidene systems can be exploited for the net conversion of hydrocarbons into functionalized organic chemicals.

As mentioned in Section 1.1.5, the formation of organometallic complexes from the C-H activation of hydrocarbon substrates is the first step in the transformation of the hydrocarbons into functionalized and more useful chemicals, such as alkenes and alcohols. To complete the transformation, the organic fragment that results from the C-H activation event needs to be functionalized and/or released from the metal's coordination sphere. Transformations of alkane substrates are of particular interest, and a few representative stoichiometric and catalytic processes that generate functionalized derivatives of alkanes via organometallic intermediates are described in Section 1.1.5. Catalytic processes are especially valuable since they may be viable for large-scale industrial use if the organic products can be produced efficiently with high selectivity. In fact, efficient and selective catalytic alkane functionalization processes are regarded as the "Holy Grails" of C-H activation research.<sup>1</sup>

Unfortunately, the majority of organometallic hydrocarbon C-H activations mediated by soluble metal complexes only provide routes to stoichiometric and “non-spontaneous” conversions of alkanes to functionalized organic derivatives.<sup>1</sup> Put simply, most activations form organometallic products that either do not lend themselves to spontaneous functionalization of the activated alkyl fragment, or, if they do induce a functionalization of the alkyl fragment, do not spontaneously release the organic species from the metal’s coordination sphere. The organometallic products must then be treated with other reagents to induce functionalization and/or release of the organic derivative.

In addition to these limitations, the majority of alkane C-H activations yield organometallic products that can only be converted into common organic reagents, such as the example shown in Scheme 5.1.<sup>2</sup> Likely for this reason, very few non-spontaneous conversions of the organometallic products of alkane C-H activations into organic molecules have been reported.<sup>2,3</sup>

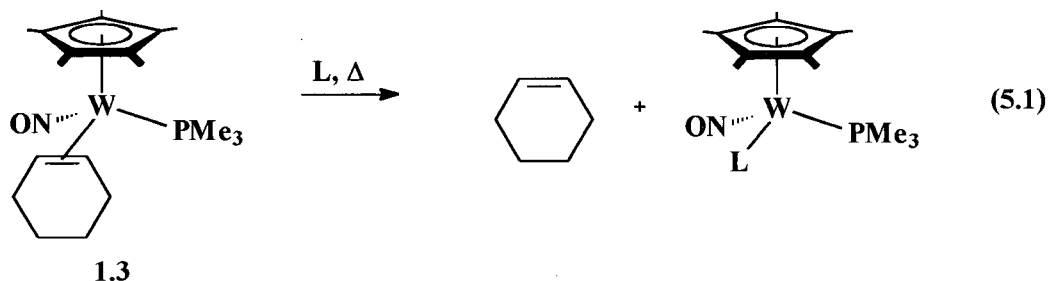
**Scheme 5.1**



> 98 % for R = neopentyl

At first glance, it would appear that the synthetic utility of the alkylidene-mediated C-H activation chemistry derived from **1** and **2** is similarly limited. The net

transformations of any alkane substrate into an organic derivative will be non-spontaneous and stoichiometric in metal complex. Moreover, while cycloalkanes are spontaneously dehydrogenated to cycloalkenes that might be released from the metal's coordination sphere by treatment with a strong Lewis base, L (eq. 5.1), a rather common type of organic compound is produced.



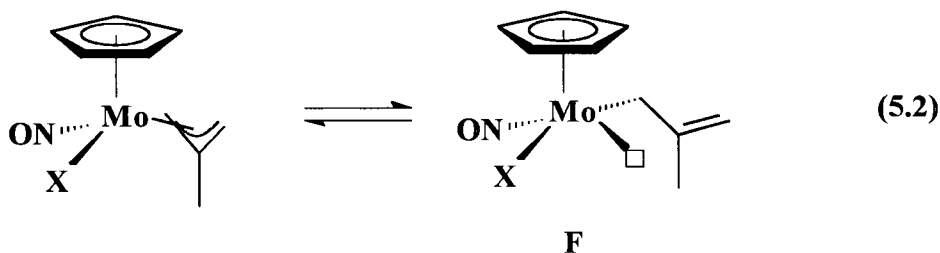
However, there is one stoichiometric process involving neopentylidene **A** that could potentially transform alkyl-substituted cycloalkanes and acyclic alkanes into novel organic products that are suitable starting materials for organic syntheses. The details of this proposed process are provided in the first part of this Chapter.

The remainder of the Chapter concerns the development of other alkylidene C-H activation systems related to the neopentylidene and benzylidene systems that may be used to effect the same chemistry as **A** and **B**, and may be more suitable for the proposed alkane functionalization procedure. In addition, there are other complexes similar to **1** and **2** that are known to, or may be able to, effect alkane activation and dehydrogenations to yield organometallic products that are different from those obtained from **A** and **B**. These systems may provide a means to generate other types of functionalized organic chemicals via the activation of alkane substrates.

## 5.2 Results and Discussion

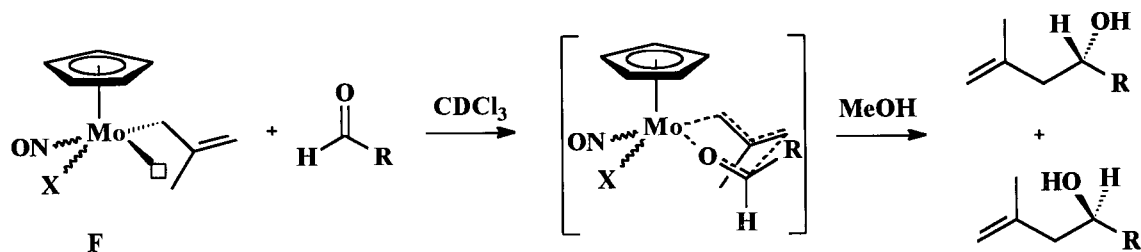
### 5.2.1 The Conversion of Allyl Ligands into Functionalized Organic Compounds

Molybdenum allyl complexes of the type  $\text{CpMo}(\text{NO})(\text{X})(\eta^3\text{-allyl})$  ( $\text{X} = \text{halide}$ ) have previously been used as reagents in the syntheses of organic compounds.<sup>4,5,6</sup> The synthetic utility of these complexes derives from the  $\sigma$ - $\pi$  distortion of the allyl ligand that is induced by the  $\pi$ -bonding influences of the NO ligand.<sup>7</sup> In solution, the allyl ligand can adopt a  $\eta^1$  conformation with an accessible double bond (eq 5.2).



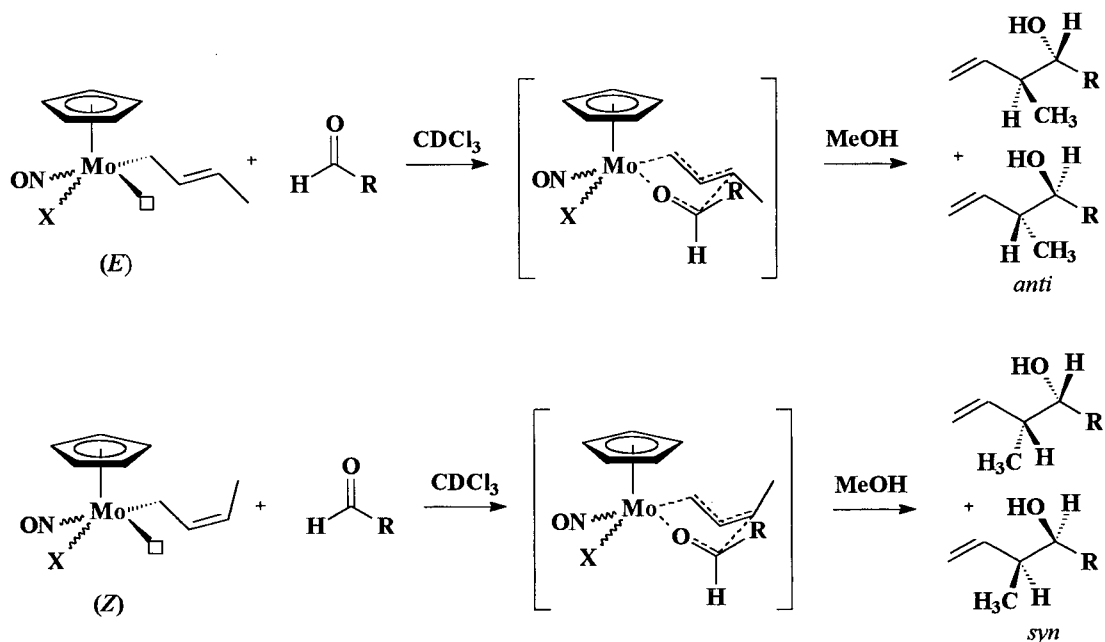
The  $\eta^1$ -allyl complex can thus bind an aldehyde and induce a regio- and stereoselective C-C bond-forming reaction. Protonolysis of the resulting complex with methanol ( $\sim 2$  equiv) generates a free “homoallylic” alcohol. The specific type of alcohol product depends on the nature of the allyl ligand. When the symmetric 2-methylallyl ligand is used (e.g. **F** in eq 5.2), a racemic mixture of the 2-methyl “homoallylic” alcohol enantiomers is generated (Scheme 5.2).<sup>4,5</sup> The conversion can be made to yield only one enantiomer either by separating the (R) and (S) isomers of the  $\text{CpMo}(\text{NO})(\text{X})(\text{allyl})$  complex, or the (R) and (S) isomers of complexes featuring a more elaborate alkyl-substituted Cp derivative.<sup>5</sup> Product yields can be quantitative with  $> 98\%$  enantiomeric excess depending on the halide ligand, aldehyde, and conditions used.

Scheme 5.2



When an asymmetric allyl ligand is employed, enantiomeric homoallylic alcohols with two chiral centers are formed after protonation by methanol. For example, use of the 1-methylallyl ligand leads to the homoallylic alcohols shown in Scheme 5.3.<sup>6</sup> Whether the syn or anti diastereomers are formed depends on the (*E*) or (*Z*)-type orientation of the  $\eta^1$ -allyl ligand in the organometallic reagent.

Scheme 5.3



The products in both Schemes 5.2 and 5.3 can then be converted by standard methods into complex acyclic alcohol derivatives or other organic compounds, such as

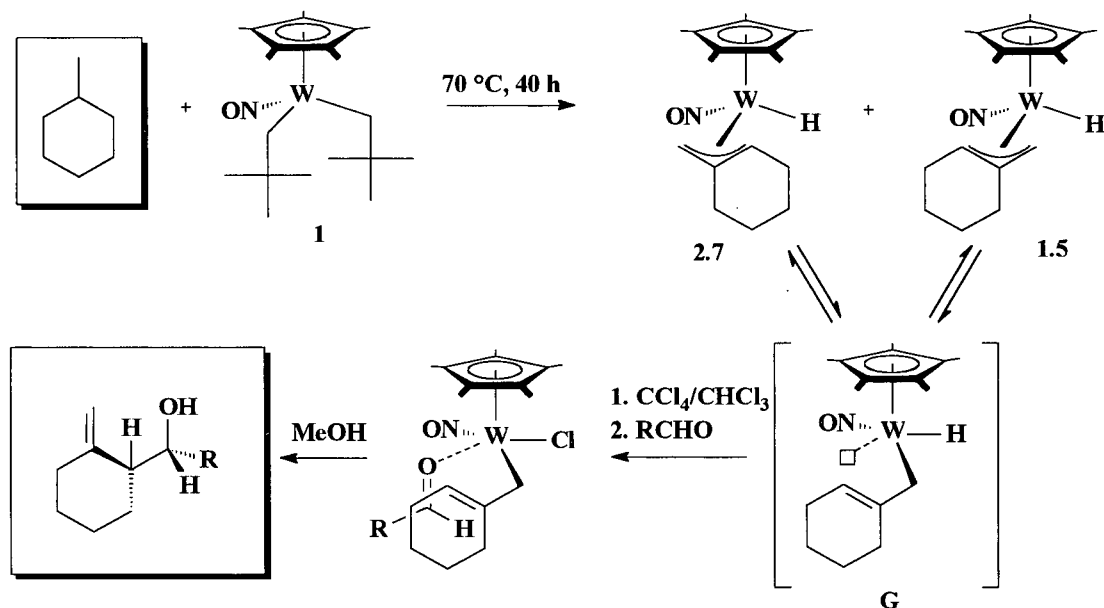
optically-active epoxides by the Sharpless asymmetric epoxidation of the double bond.<sup>8</sup>

It should be noted that although the overall reactions are stoichiometric in metal complex, a similar coupling process featuring the related  $\text{CpMo}(\text{NO})(\text{CO})^+$  fragment<sup>9</sup> has been used to create a key component in the synthesis of a complex natural product with over 50 synthetic steps.<sup>10</sup>

### **5.2.2 Proposed Method for the Conversion of Acyclic Alkanes and Alkyl-Substituted Cycloalkanes Into Homoallylic Alcohols Via Alkylidene-Mediated C-H Activation**

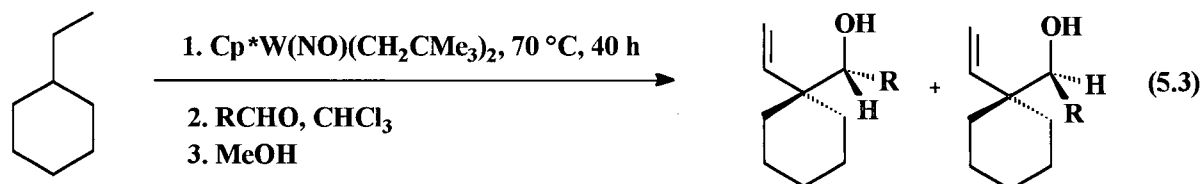
Given the electronic and structural similarities between the  $\text{Cp}^*\text{W}$  and  $\text{CpMo}$  fragments,<sup>11,12,13</sup> the related  $\text{Cp}^*\text{W}(\text{NO})(\text{allyl})\text{X}$  complexes should react with aldehydes in the same manner as their  $\text{CpMo}$  cousins. Furthermore, hydride complexes can usually be converted to the corresponding chloride or bromide complex simply by dissolution in halogenated organic solvents.<sup>14</sup> Thus, it may be possible to effect the conversion of alkyl-substituted cycloalkanes and acyclic alkanes into homoallylic alcohols using the general process illustrated in Scheme 5.4 for methylcyclohexane.

Scheme 5.4



As discussed in Section 2.2.8.3, the thermolysis of **1** in methylcyclohexane yields two allyl hydride complexes, **1.5** (major) and **2.7** (minor), which interconvert on the NMR timescale, most likely through an  $\eta^1$ -allyl intermediate. Based on the work of Faller et al., the  $\eta^1$  conformation should have a  $\sigma$ -bond to the least sterically hindered terminal allyl group.<sup>6</sup> Thus, only one type of  $\eta^1$ -allyl complex (**G**) should be present in solution. Note, however, that the  $\eta^1$ -allyl complex will exist in two enantiomeric forms, only one of which is shown in Scheme 5.4. The product obtained from the reaction of the halide derivative of the complex shown in the Scheme with an aldehyde in chloroform should yield, in principle, the (R),(S)-homoallylic alcohol diastereomer. The reaction of the other enantiomeric allyl complex with the aldehyde will generate the enantiomer of this diastereomer, with the opposite stereochemistries at the chiral centers.

With ethylcyclohexane as the substrate, the expected products are even more elaborate: the C-C coupling reaction from the two expected enantiomeric  $\eta^1$ -allyl halide complexes should yield the two enantiomers of the homoallylic alcohol shown in eq 5.3.



Similar reaction sequences with acyclic alkanes should also yield homoallylic alcohols, but these reactions may be complicated by the existence of one major and several minor allyl hydride complexes<sup>15</sup> that could lead to a variety of  $\eta^1$  allyl intermediates and thus, a variety of products with different regio- and stereochemistries. Yet, if any of the above processes prove to be successful, it would be, to our knowledge, the first time that an alkane has been transformed into an elaborate organic molecule suitable for organic syntheses applications by a C-H activation route utilizing an organometallic intermediate derived from a soluble metal complex. Clearly, given the demonstrated synthetic utility of the  $\text{CpMo}(\text{NO})(\text{X})(\text{allyl})$  complexes, this chemistry should be investigated immediately.

### 5.2.3 The Utilization of Other Alkylidene Complexes of the Type

#### $\text{Cp}'\text{M}(\text{NO})(=\text{CHR})$ for Alkane Activations and Functionalizations

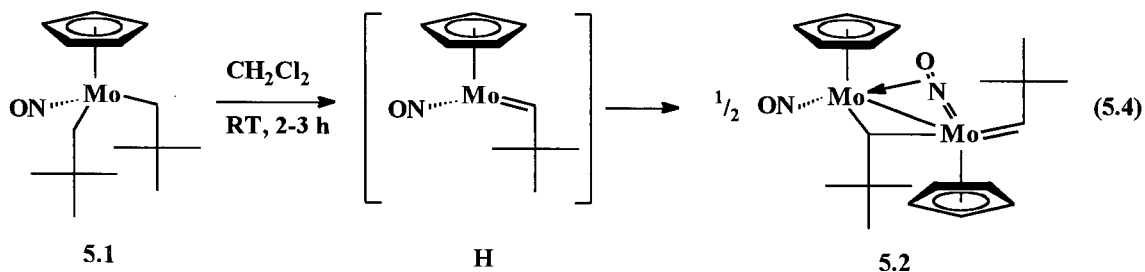
The alkane functionalization chemistry based on the C-H activations initiated by alkylidenes **A** could be enhanced by the development of other C-H activating alkylidene

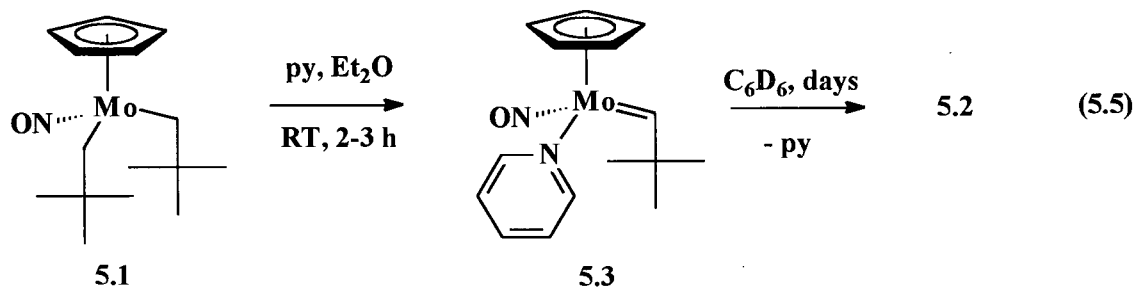
complexes of the type  $\text{Cp}'\text{M}(\text{NO})(=\text{CHR})$  ( $\text{Cp}' = \text{Cp}, \text{Cp}^*$ ;  $\text{M} = \text{Mo}, \text{W}$ ;  $\text{R} = \text{alkyl}, \text{aryl}$ ).

The goal of this work would be to discover alkylidene complexes that effect the same alkane activation chemistry as **A**, as well as permit subsequent dehydrogenation functionalizations, but do so at a lower temperature and/or shorter reaction time. To date, one possible candidate has been found, as discussed below.

### 5.2.3.1 The C-H Activation of Hydrocarbons by $\text{CpMo}(=\text{CHCMe}_3)$

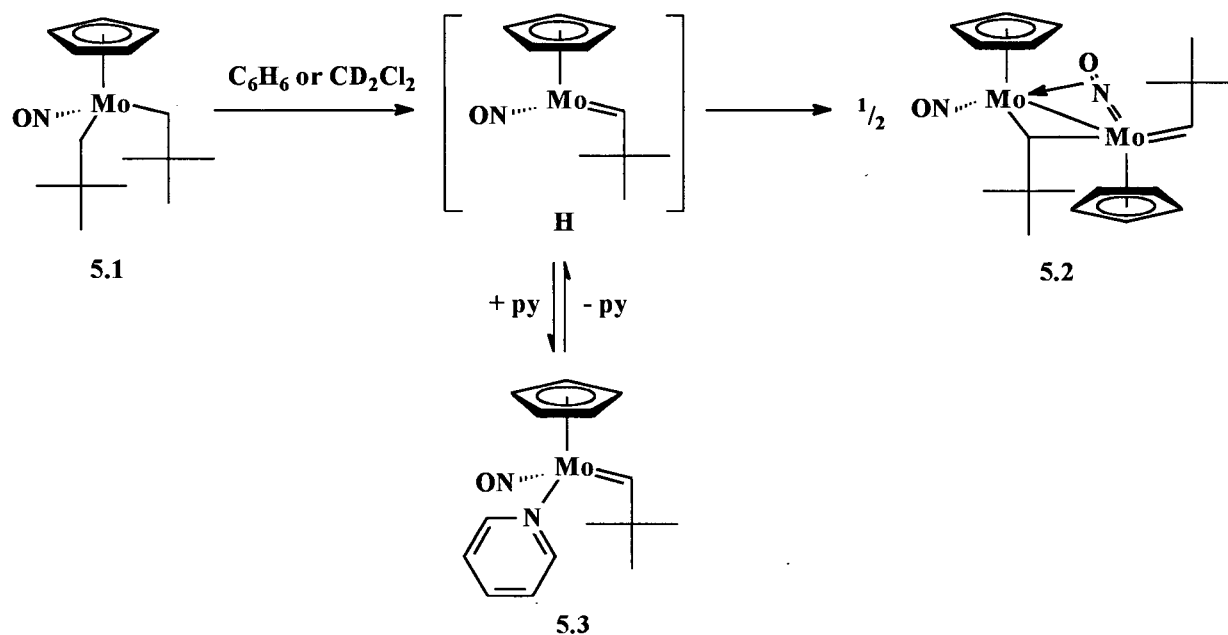
There is one  $\text{Cp}'\text{M}(\text{NO})(\text{R})(\text{R}')$  complex that has been previously reported by our research group to form an alkylidene intermediate and do so much more readily than **1** and **2**. However, the reports describing the chemistry of this particular system are ambiguous as to whether or not the alkylidene derivative can activate hydrocarbon C-H bonds. Specifically, the  $\text{CpMo}$  analogue of **1**, namely  $\text{CpMo}(\text{NO})(\text{CH}_2\text{CMe}_3)_2$  (**5.1**), cannot be isolated in the solid state because it undergoes  $\alpha$ -H abstraction at low temperatures ( $> -40^\circ\text{C}$ ) to form the respective neopentylidene fragment,  $\text{CpMo}(\text{NO})(=\text{CHCMe}_3)$  (**H**).<sup>16,17</sup> Dichloromethane solutions of **5.1** generate the dimeric alkylidene derivative  $[\text{CpMo}(\text{NO})(=\text{CHCMe}_3)]_2$  (**5.2**) after 2-3 h at room temperature (eq 5.4), while solutions of **5.1** containing pyridine yield the 18e adduct of neopentylidene **H**, namely complex **5.3**. Complex **5.3** itself is quite thermally sensitive in benzene- $d_6$  and forms the dimer **5.2** over time, along with free pyridine (eq 5.5).





At the time, these observations were interpreted to mean that the pyridine adduct was a stable source of the reactive alkylidene complex **H**. In other words, unlike its Cp\*W congener **A**, neopentylidene **H** was not evidently reactive towards the C-H bonds of benzene, but rather dimerized in benzene and dichloromethane solutions (Scheme 5.5).

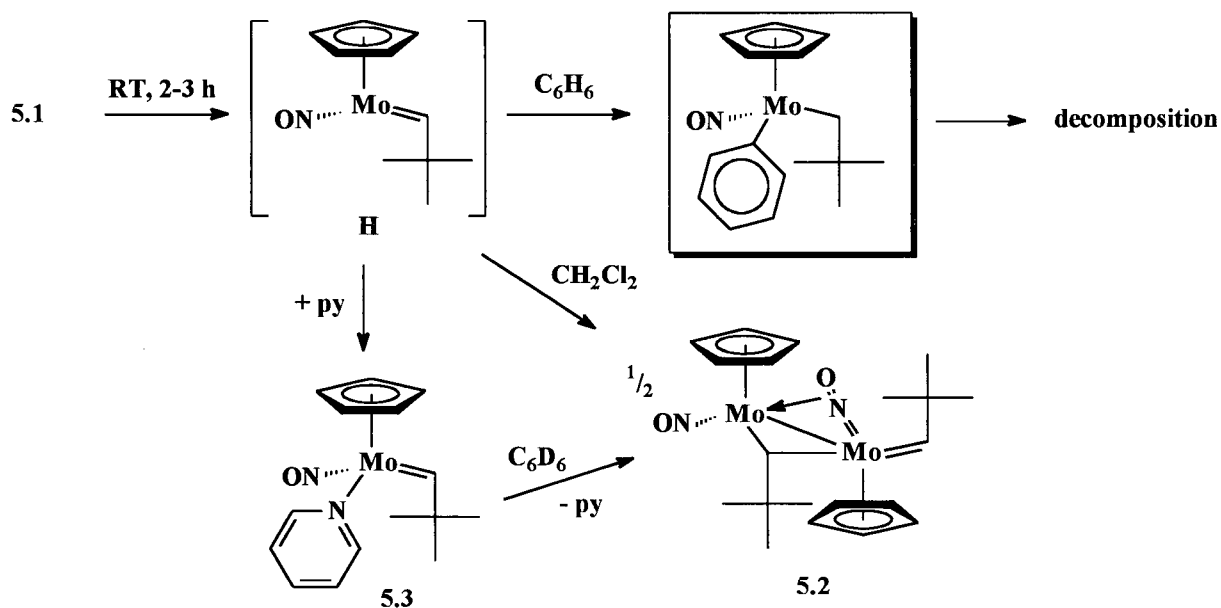
Scheme 5.5



Following these initial experiments, a study of the kinetics of decomposition was conducted by UV-vis spectroscopy using the more robust and isolable  $\alpha$ -deuterated

analog of **5.1**, namely  $\text{CpMo}(\text{NO})(\text{CD}_2\text{CMe}_3)_2$  (**5.1-d<sub>4</sub>**).<sup>17</sup> The study revealed that the decomposition of **5.1-d<sub>4</sub>** is clean and first-order in the complex in solvents such as dichloromethane, diethyl ether, hexanes, THF and mesitylene. Yet, the decomposition of **5.1-d<sub>4</sub>** is not clean in chloroform, benzene or toluene, as indicated by the non-first order changes in the UV-vis spectra utilized to monitor these thermolyses. Because of the method employed, the chemical origin for the discrepancies between solvents could not be ascertained, so all that could be stated at the time was that a derivative of **5.1-d<sub>4</sub>**, whatever it might be, is reactive towards these solvents. One interpretation of these facts is that the reactive derivative of **5.1-d<sub>4</sub>** in these three solvents is the dimeric complex **5.2**, meaning that **5.2** is reactive towards benzene, toluene and chloroform, but not dichloromethane. However, another interpretation of the kinetic data is that they reflect the formation of products of solvent C-H activation by **H**, at least in the case of benzene and toluene. The resulting aryl products are known to be very thermally sensitive themselves,<sup>18</sup> and non-linear kinetics would result if these products absorb light at the wavelength used for the kinetic analyses. This interpretation is consistent with the trapping and dimerization experiments in eq 5.4 and 5.5, providing that the pyridine adduct **5.3** is not a source of free **H** in solution as originally assumed. Instead, the formation of the dimeric product **5.2** from **5.3** in benzene-*d*<sub>6</sub> has to occur via an associative bimetallic pathway without forming free **H** (Scheme 5.6).

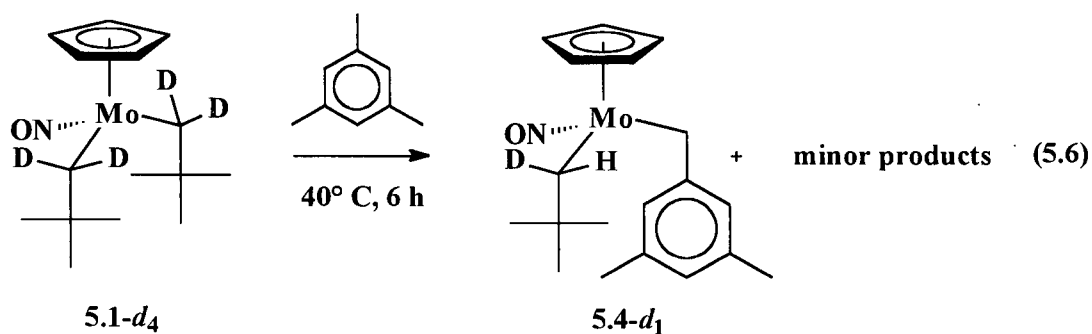
Scheme 5.6



To determine if the latter interpretation is correct, the thermolysis of **5.1-*d*<sub>4</sub>** has been conducted in mesitylene and the resulting mixture has been characterized by spectroscopic techniques. Mesitylene was selected as the solvent for two reasons. First, given the exclusive formation of the benzyl products of  $\text{sp}^3$  C-H bond activation for the activation of mesitylene by the related  $\text{Cp}^*\text{W}$  alkylidenes **A** and **B**, a similar preference for the benzyl product of  $\text{sp}^3$  C-H activation over the thermally-unstable aryl product of  $\text{sp}^2$  C-H activation should occur for **H-*d*<sub>1</sub>**. Second, the related benzyl molybdenum complexes  $\text{CpMo}(\text{NO})(\text{CH}_2\text{Ar})(\text{R})$  ( $\text{R} = \text{alkyl, aryl, benzyl}$ ) are thermally robust,<sup>19</sup> so the benzyl product of  $\text{sp}^3$  C-H bond activation of mesitylene by **H-*d*<sub>1</sub>** should be stable and characterizable if formed.

The thermolysis of **5.1-*d*<sub>4</sub>** in mesitylene for 6 h at 40 °C generates one major product in ~80% overall yield, along with several minor products as determined by  $^1\text{H}$

NMR spectroscopy (eq 5.6). The NMR and MS spectroscopic properties of the major product are fully consistent with those of the C-H activation product derived from **H-d<sub>1</sub>**, namely CpMo(NO)(CHD<sub>anti</sub>CMe<sub>3</sub>)(CH<sub>2</sub>C<sub>6</sub>H<sub>3</sub>-3,5-Me<sub>2</sub>) (**5.4-d<sub>1</sub>**). Diagnostic NMR spectroscopic features of **5.4-d<sub>1</sub>** are the singlet resonances for the neopentyl ligand's D<sub>anti</sub> and H<sub>syn</sub> methylene protons, and the triplet resonance ( $^2J_{\text{HD}} = 17.9$  Hz) for the deuterated  $\alpha$ -carbon of the neopentyl ligand. It is also important to note that no signals are observed that can be attributed to the robust dimeric product **5.2**. Thus, it would appear that the chemistry depicted in Scheme 5.6 is indeed the correct interpretation of the previously reported data, and that both neopentylidenes **H** and **H-d<sub>1</sub>** can activate hydrocarbon C-H bonds.



Interestingly, there is no spectroscopic evidence for H/D scrambling in the neopentyl ligand during the thermolysis of **5.1-d<sub>4</sub>** in mesitylene. This observation is in sharp contrast to the H/D scrambling observed for the related Cp\*W complex **1-d<sub>4</sub>** (see Sections 3.2.1 to 3.2.6). It is consistent, however, with the DFT calculations conducted by Poli and Smith on the  $\alpha$ -abstraction of methane from CpMo(NO)Me<sub>2</sub> vs CpW(NO)Me<sub>2</sub>.<sup>13</sup> Unlike the tungsten congener for which the energy barriers are similar in energy, the barrier to  $\alpha$ -C-H cleavage for CpMo(NO)Me<sub>2</sub> is significantly higher than that for dissociation of neopentane from the resulting  $\sigma$ -neopentane alkylidene complex.

These results suggest that, in contrast to the substrate C-H activations mediated by the tungsten alkylidene complexes **A** and **B**, the rate-determining step in the activations mediated by **H** and **H-d<sub>1</sub>** is substrate C-H bond addition, not coordination of the substrate to the metal center. In other words, the reaction coordinate for **H** is fundamentally different from those for **A** and **B**. The reaction coordinate for alkane activation derived from **5.1** in which **H** is a discrete intermediate is shown in Figure 5.1. An interchange-dissociative version without **H** as a discrete intermediate is also viable. A full study of the mechanism, scope, and selectivity of the activation chemistry derived from **5.1** or **5.1-d<sub>4</sub>** is clearly warranted to confirm, and expand upon, these initial findings.

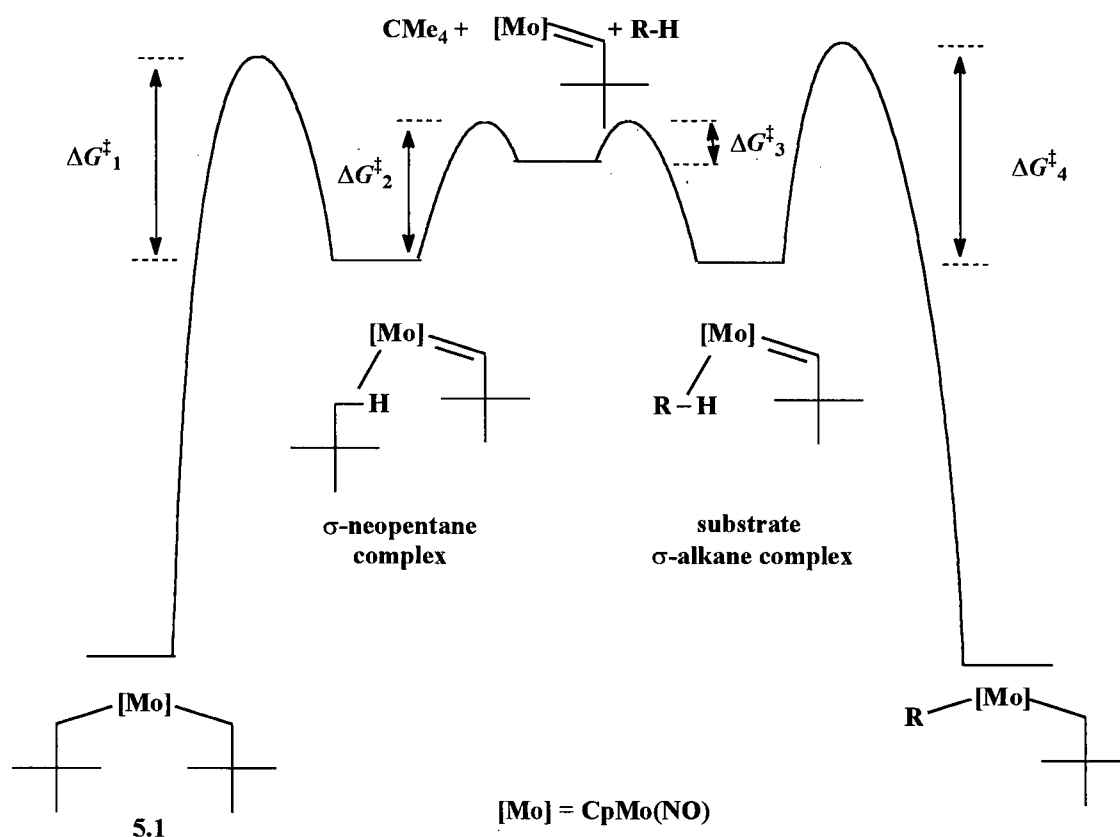


**Figure 5.1.** A qualitative representation of the general free energy vs reaction coordinate for alkane C-H activation derived from **5.1**.

### 5.2.3.2 Towards the Use of CpMo Alkylidene Complexes and Other

#### Cp'M(NO)(=CHR) Complexes for Alkane C-H Activation and Functionalization Reactions

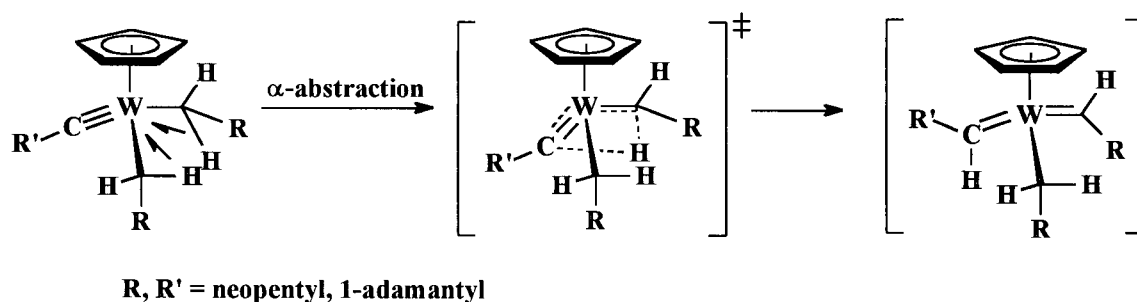
By the Principle of Microscopic Reversibility, neopentylidenes **H** and **H-d<sub>1</sub>** should activate alkane substrates. Furthermore, despite the different reaction coordinates, the thermodynamic products of alkane activation by **H** and **H-d<sub>1</sub>** should be alkene or allyl complexes since the 16e alkyl and alkene organometallic products should be susceptible to  $\beta$ -H and  $\gamma$ -H elimination reactions. If the desired terminal allyl hydride complexes can indeed be formed cleanly from thermolysis of **5.1** or **5.1-d<sub>4</sub>** in alkyl-substituted cycloalkanes and acyclic alkanes, then the milder conditions required for the formation of these alkylidene complexes might make them more suitable than **A** for the proposed alkane functionalization processes.

There are other alternatives to neopentylidenes **H** and **H-d<sub>1</sub>**. The Cp analog of **1**, namely CpW(NO)(CH<sub>2</sub>CMe<sub>3</sub>)<sub>2</sub> (**5.5**) also forms its neopentylidene derivative when thermolysed, but under milder conditions than **1** (i.e. 16 h, 65 °C).<sup>15</sup> This particular neopentylidene complex does appear to be capable of activating alkane and arene C-H bonds, but these reactions do not yield the activated products as cleanly as those effected by **A**.<sup>15</sup> Interestingly, the Cp\* analog of **5.1**, namely Cp\*Mo(NO)(CH<sub>2</sub>CMe<sub>3</sub>)<sub>2</sub> (**5.6**), can be isolated in crystalline form and has recently been demonstrated to form its alkylidene derivative under modest conditions (i.e. 2 d at room temperature).<sup>20</sup> Given the acute thermal sensitivity of **5.1**, the additional complexities of synthesizing the deuterated **5.1-d<sub>4</sub>**, and the fact that the substrate C-H activation reactions mediated by the Cp\*-containing **1** are cleaner than those mediated by the Cp-containing **5.5**, one can infer that

the activation system based on **5.6** will possess the best characteristics for alkane C-H activation and potential functionalization applications. Another available option is to see if the related benzyl neopentyl derivatives of **5.1** or **5.6** can effect the same chemistry.

Besides the complexes mentioned thus far, other bis(hydrocarbyl) precursors of the type  $\text{Cp}'\text{M}(\text{NO})(\text{R})(\text{R}')$  may generate alkylidene complexes. However, it should be noted that the search for these complexes must be conducted in a trial-and-error fashion, since the two literature-based guides for identifying bis(alkyl) complexes that may readily form alkylidene derivatives do not seem to apply to  $\text{Cp}'\text{M}(\text{NO})(\text{R})(\text{R}')$  complexes. Briefly, in other families of bis(alkyl) complexes, the formation of alkylidene intermediates from  $\alpha$ -C-H bond scission has been correlated with the presence of  $\alpha$ -agostic interactions<sup>21</sup> in the solution structures of the complexes. An example is shown in Scheme 5.7.<sup>22</sup> The  $\alpha$ -agostic linkages are thus thought to be incipient alkylidene linkages.<sup>22,23</sup>

**Scheme 5.7**



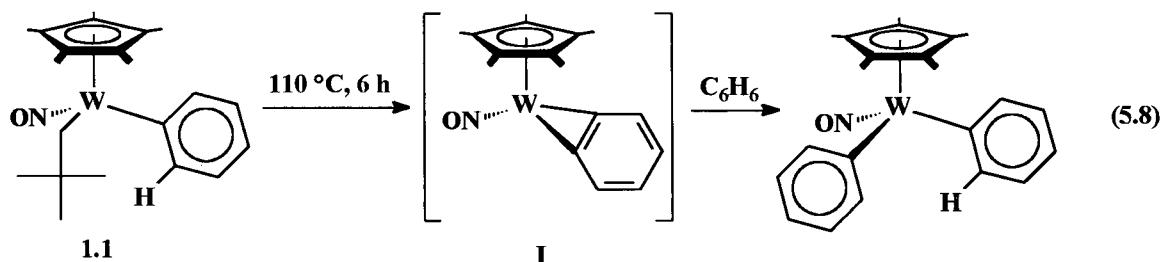
Similar  $\alpha$ -agostic interactions appear to exist in the solution structures of several  $\text{Cp}'\text{M}(\text{NO})(\text{R})(\text{R}')$  complexes ( $\text{Cp}' = \text{Cp}^*, \text{Cp}$ ;  $\text{M} = \text{Mo}, \text{W}$ ;  $\text{R} = \text{hydrocarbyl}$ ,  $\text{R}' = \text{hydrocarbyl}$ , halide), including complexes **1**,  $\text{Cp}^*\text{W}(\text{NO})(\text{CH}_2\text{CMe}_3)(\text{Ph})$  (**1.1**) (vide infra), and **2** (see Section 2.2.1.2).<sup>15,24</sup> However, the presence of these  $\alpha$ -agostic



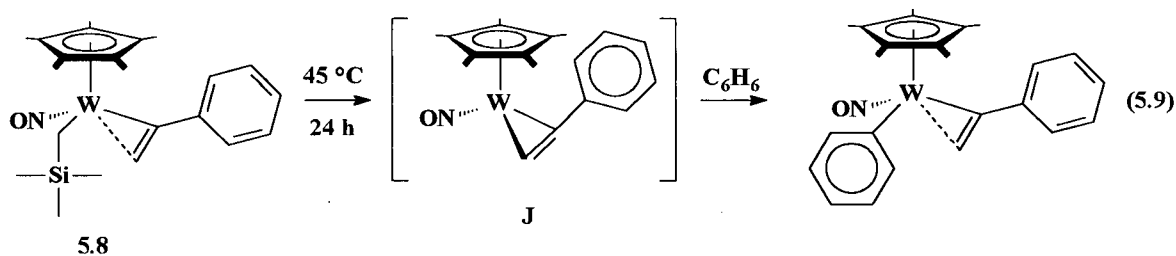
#### 5.2.4 Alternatives to Cp'M(NO) Alkylidene-Based C-H Activation and Functionalization of Alkanes

It should be noted that the characteristics of **A** and **B** that permit the C-H activation and spontaneous dehydrogenations of alkanes are not unique to the alkylidene-based systems. Quite simply, the following general requirements need to be met to have a Cp'M(NO)(R)(R') system that C-H activates hydrocarbon substrates: The bis(hydrocarbyl) complex must contain one hydrocarbyl ligand that can readily be eliminated as R-H (e.g. a neopentyl ligand) and a second hydrocarbyl ligand that can donate an H atom to the ligand being eliminated and then form an addition M-C bond to the metal center in the resulting organometallic intermediate (i.e.  $M-CH_2R \rightarrow M=CHR$ ). By the Principle of Microscopic Reversibility, the intermediate will activate the C-H bonds of alkanes and arenes, providing it does not react with itself first.

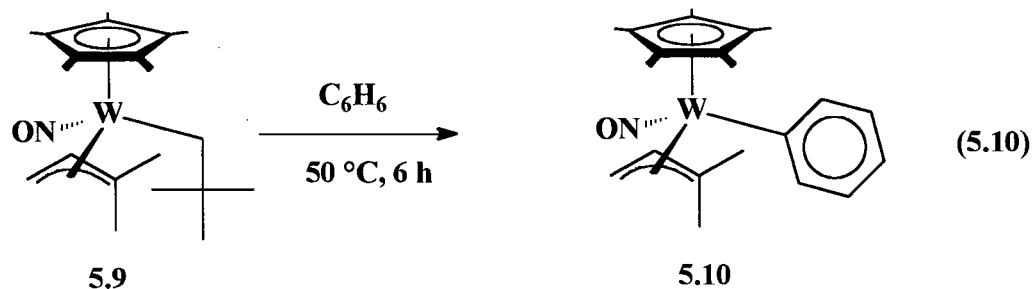
The validity of this argument is supported by the previously reported chemistry of two other complexes, namely Cp\*W(NO)(CH<sub>2</sub>CMe<sub>3</sub>)(Ph) (**1.1**) and Cp\*W(NO)(CH<sub>2</sub>=CPh)(CH<sub>2</sub>SiMe<sub>3</sub>) (**5.8**). In the first example, complex **1.1** is moderately thermally sensitive and undergoes β-H elimination of neopentane to generate a benzyne complex, **I**. Complex **I** has been shown to activate the sp<sup>2</sup> C-H bonds of benzene and *p*-xylene by σ-bond metathesis (eq 5.8).<sup>28</sup> Note that the benzyne ligand in **I** contains two M-C bonds to the metal center.



Similarly, complex **5.8** eliminates tetramethylsilane under mild conditions (24 h, 45 °C) to generate the corresponding reactive fragment,  $\text{Cp}^*\text{W}(\text{NO})(\eta^2\text{-CH=CPh})$  (**J**), which then activates alkanes and arenes by the microscopic reverse of the process (eq 5.9).<sup>29</sup> Note again that the derivative of the vinyl ligand in intermediate **J** is stabilized by bonding to the metal center.

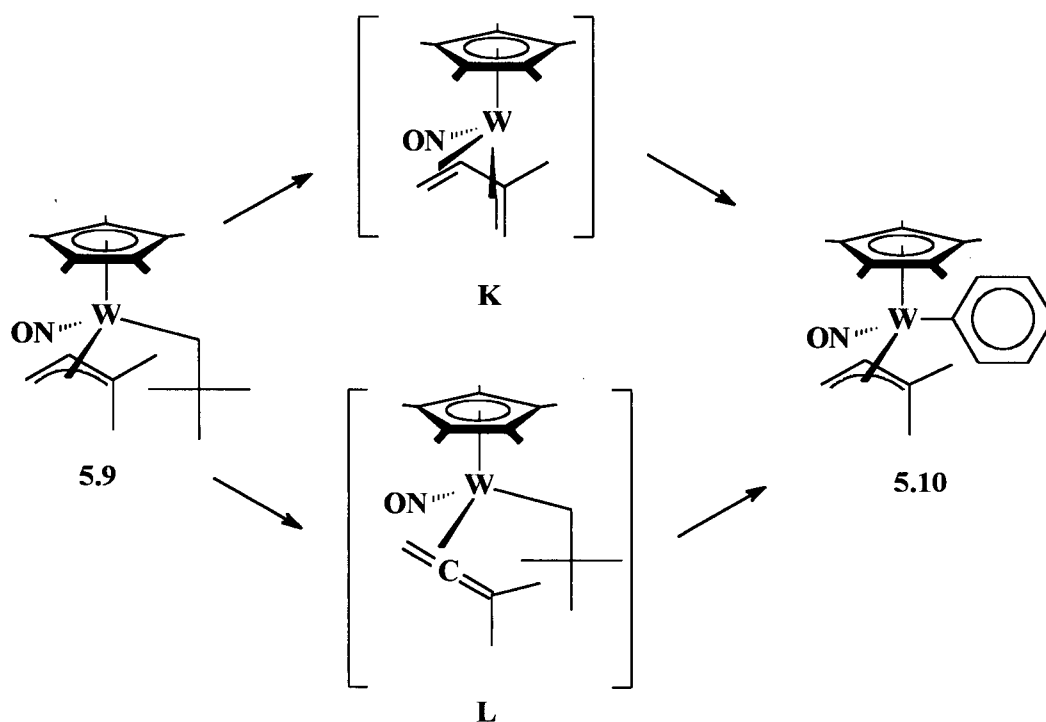


Additional support for the theory stated above lies in the thermal chemistry of the new neopentyl dimethylallyl complex,  $\text{Cp}^*\text{W}(\text{NO})(\text{CH}_2\text{CMe}_3)(\eta^3\text{-1,1-Me}_2\text{-C}_3\text{H}_3)$  (**5.9**).<sup>30</sup> Complex **5.9** readily eliminates neopentane and generates the corresponding benzene C-H activation product,  $\text{Cp}^*\text{W}(\text{NO})(\text{C}_6\text{H}_5)(\eta^3\text{-1,1-Me}_2\text{-C}_3\text{H}_3)$  (**5.10**), in >97 % yield as judged by <sup>1</sup>H NMR spectroscopy (eq 5.10). Complex **5.10** has been isolated in crystalline form (69 % yield) and fully characterized. The solid-state molecular structure has been established by X-ray diffraction (Figure 5.2),<sup>31</sup> and the spectroscopic data indicate that the general structure is unchanged in solutions.<sup>32</sup>



Preliminary mechanistic and labeling studies indicate that the activations proceed through *two* distinct intermediates, namely the *cis*-diene complex (**K**) and the allene complex (**L**), which are formed simultaneously from **5.9** by first-order processes (Scheme 5.8).<sup>33</sup> Both of these intermediates again contain at least two M-C bonding interactions to the metal center from the derivative of the allyl ligand.

**Scheme 5.8**



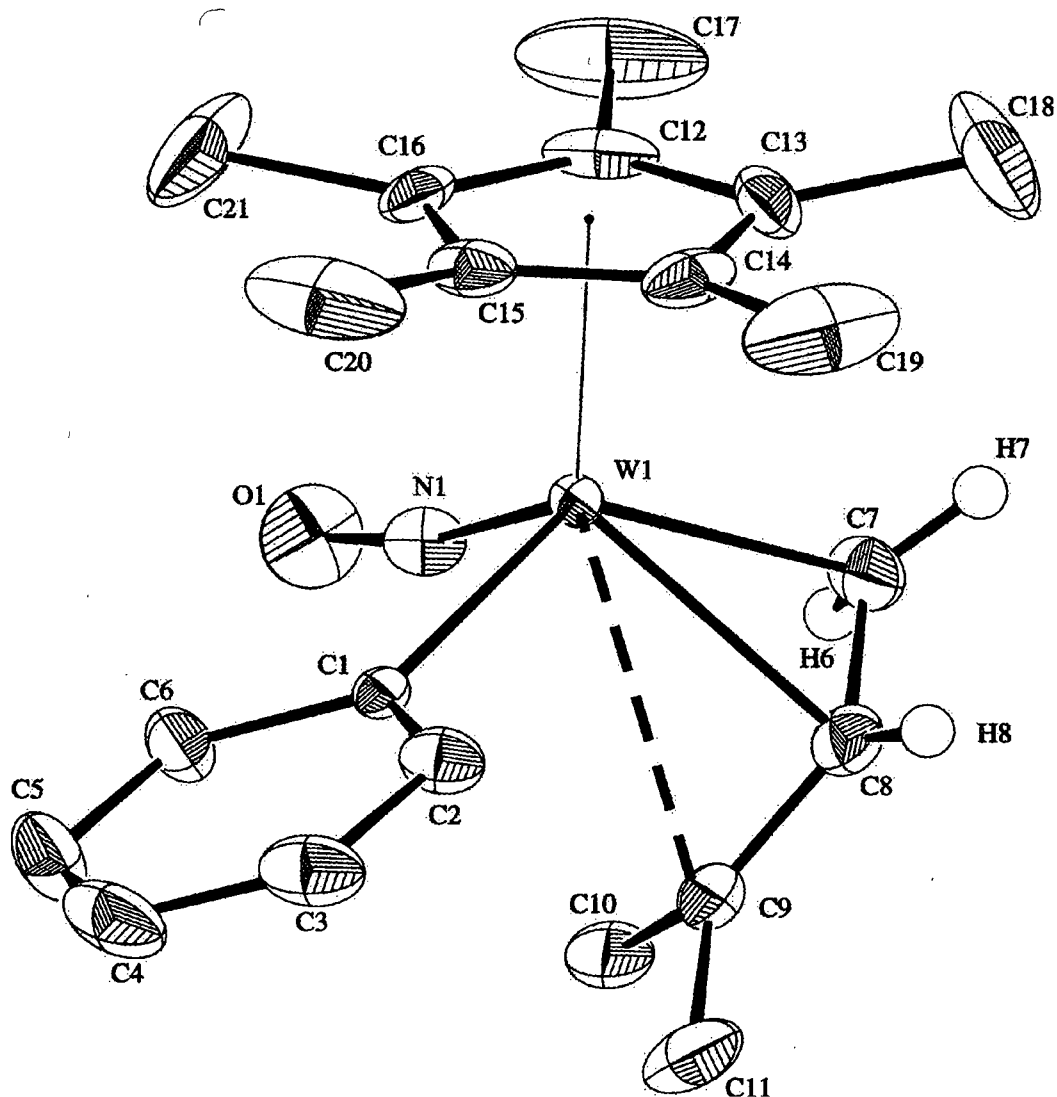
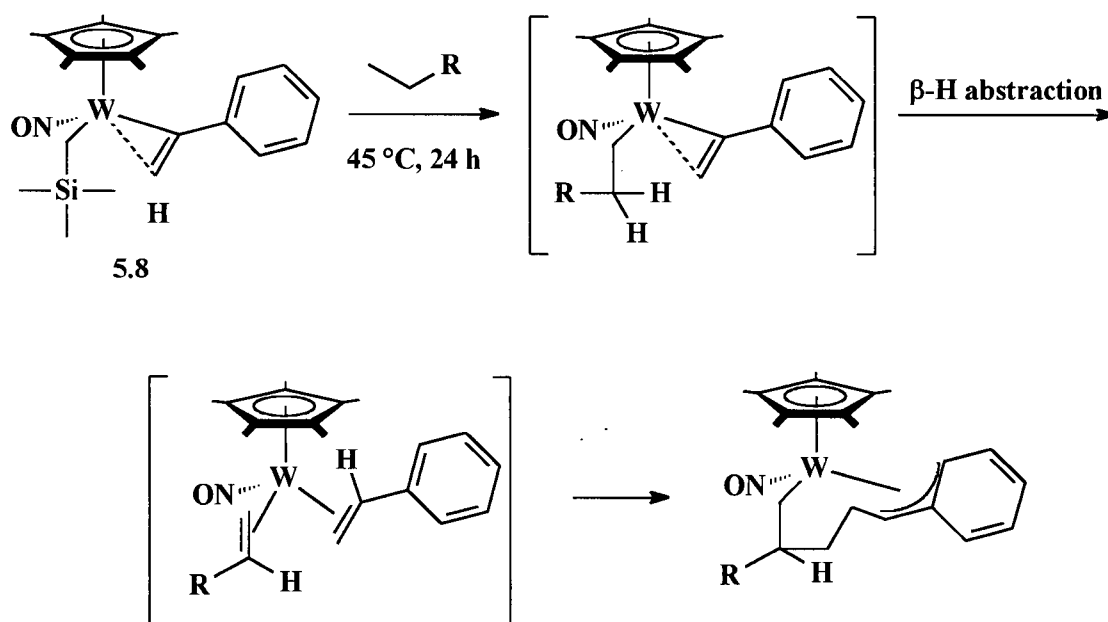


**Figure 5.2.** ORTEP plot of the solid-state molecular structure of  $\text{Cp}^*\text{W}(\text{NO})(\text{C}_6\text{H}_5)(1,1\text{-Me}_2\text{-C}_3\text{H}_3)$  (**5.10**) with 50% probability ellipsoids. Selected bond lengths ( $\text{\AA}$ ) and angles ( $^\circ$ );  $\text{W}(1)\text{-C}(1) = 2.186(3)$ ,  $\text{W}(1)\text{-C}(7) = 2.218(4)$ ;  $\text{W}(1)\text{-C}(8) = 2.363(4)$ ;  $\text{W}(1)\text{-C}(9) = 2.768(4)$ ;  $\text{C}(7)\text{-C}(8) = 1.439(6)$ ;  $\text{C}(8)\text{-C}(9) = 1.365(5)$ ;  $\text{N}(1)\text{-O}(1) = 1.224(4)$ ;  $\text{W}(1)\text{-N}(1)\text{-O}(1) = 169.5(3)$ ,  $\text{N}(1)\text{-W}(1)\text{-C}(7) = 92.1(2)$ ;  $\text{N}(1)\text{-W}(1)\text{-C}(8) = 104.6(1)$ ;  $\text{N}(1)\text{-W}(1)\text{-C}(9) = 86.6(1)$ ;  $\text{W}(1)\text{-C}(1)\text{-C}(2) = 123.0(2)$ ;  $\text{W}(1)\text{-C}(1)\text{-C}(6) = 121.4(2)$ ;  $\text{C}(7)\text{-C}(8)\text{-C}(9) = 124.8(4)$ ;  $\text{C}(7)\text{-C}(8)\text{-C}(9)\text{-C}(10) = 20.0(6)$ ;  $\text{H}(6)\text{-C}(7)\text{-C}(8)\text{-H}(8) = 157(4)$ .

### 5.2.5 Towards Alkane Functionalizations Using Complexes 1.1, 5.8 and 5.9

The  $\text{Cp}'\text{M}(\text{NO})(\text{R})(\text{R}')$  systems cited in Section 5.2.4, are either known to be, or should be, capable of activating alkanes as well as permit subsequent dehydrogenations and even further elaborations of the resulting alkyl ligands. For example, thermolysis of complex **5.8** in alkanes that have primary and secondary CH groups in sequence, such as n-pentane ( $\text{R} = \text{C}_3\text{H}_8$ ) and n-hexane ( $\text{R} = \text{C}_4\text{H}_{10}$ ), is known to produce metallacycles in moderate yields (50 -70 %) (Scheme 5.9).<sup>29</sup>

Scheme 5.9

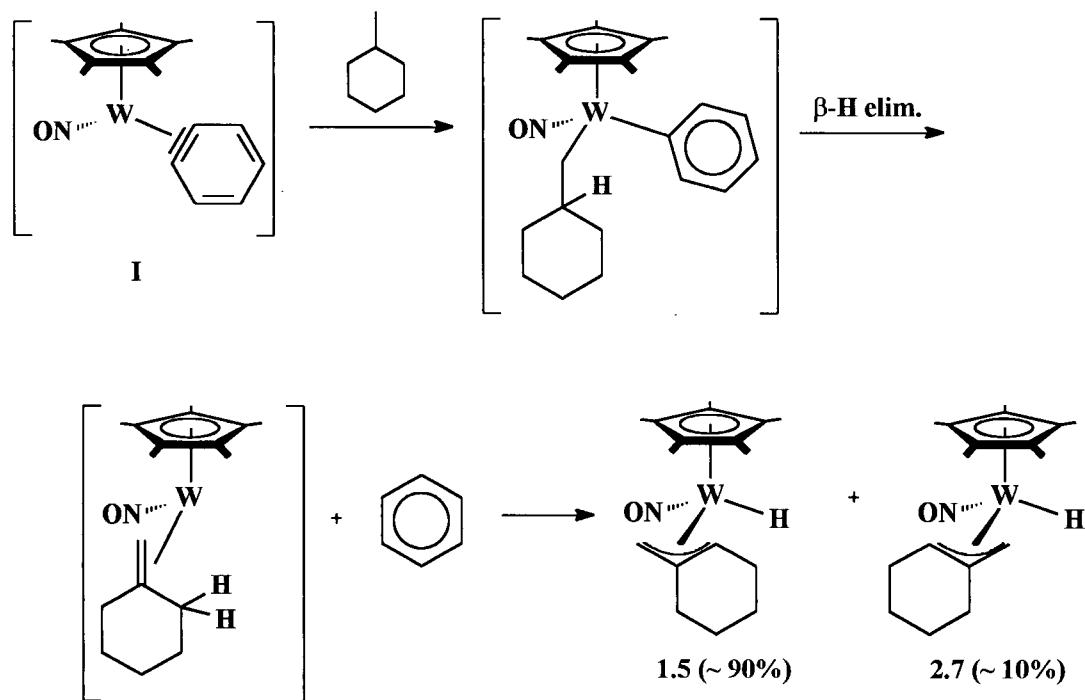


During the activation process, the alkane substrate is transformed into an alkene fragment, first via C-H activation by **J**, then  $\beta$ -H transfer to the regenerated vinyl ligand. However, unlike alkylidenes **A** and **B**, the resulting styrene alkene complex can undergo a C-C coupling reaction prior to elimination of either alkene ligand from the metal's coordination sphere. The net result is an elaboration of the alkane substrate into an allyl

metallacycle. To date, no attempts have been made to complete the functionalization process by releasing the organic fragment from the coordination sphere, but conceivably, treatment of the metallacycles with halogen sources, like  $\text{Br}_2$ , could release the organic fragments as functionalized organic compounds.

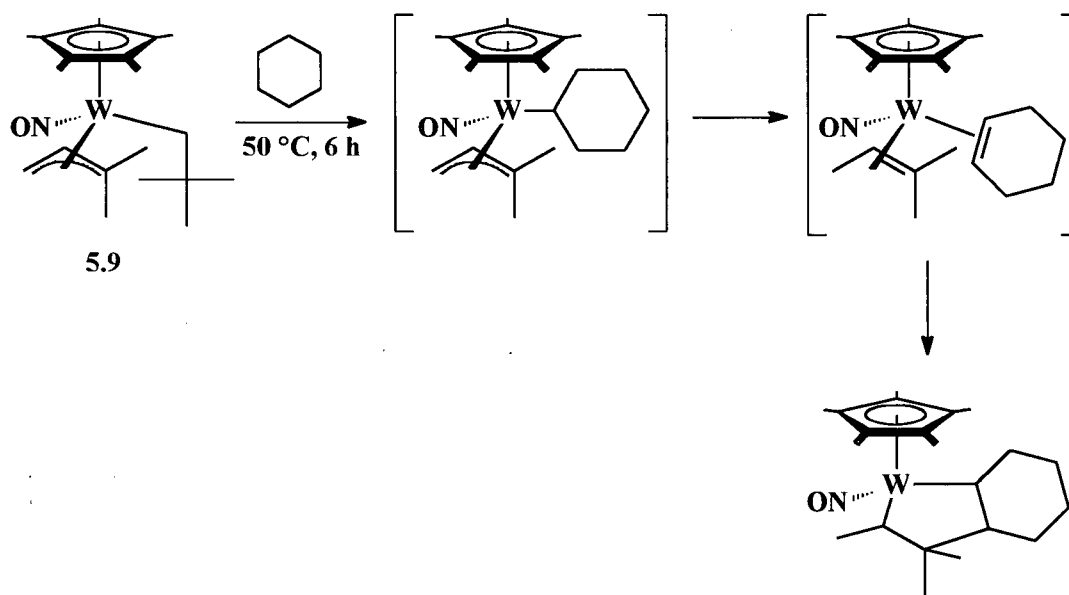
Attempts to activate alkane substrates with benzyne **I** by thermolysis of **1.1** in alkane solvent have not been attempted, but should be successful based on the Principle of Microscopic Reversibility. Interestingly, the final products will likely be the same ones that are obtained from activations mediated by **A** and **B**. As shown in Scheme 5.10, the activation of alkanes with  $\beta$ -Hs by **I** would generate an alkyl phenyl complex that should be susceptible to the elimination of benzene by  $\beta$ -H transfer. Given the harsher conditions required to generate **I** as compared to **A** and **B**, however, this chemistry is probably not worth exploring further if the same final products are indeed obtained.

**Scheme 5.10**



In contrast, the activation of alkanes by **K** and **L** should also facilitate subsequent alkyl ligand dehydrogenations, but ultimately should form novel types of organometallic products (Scheme 5.11). In this case,  $\beta$ -H elimination from the alkyl allyl product will generate a bis(olefin) complex that can couple much like the system based on **5.8**. The resulting metallacyclopentanes might then be converted into unique organic chemicals by treatment with other reagents, such as  $\text{Br}_2$ . The activation of alkanes by this system is currently being investigated by Stephen Ng of this research group.

**Scheme 5.12**



### 5.3 Epilogue

Unlike the majority of soluble metal complexes that mediate the organometallic C-H activation of alkanes, neopentylidene **A** and benzylidene **B** may have some synthetic utility for the stoichiometric conversions of alkanes into novel organic products. In addition, there are several other bis(hydrocarbyl)  $\text{Cp}'\text{M}(\text{NO})(\text{R})(\text{R}')$  complexes that are

known to activate hydrocarbons via alkylidene or other intermediate complexes, and these may be employed to activate and functionalize alkanes to generate organic compounds of various types. Given the number of possible combinations of Cp', M and hydrocarbyl ligands that have not yet been explored, it is clear that the C-H activation chemistry that can be effected by Cp'M(NO)(R)(R') complexes and their derivatives has only just begun to be harvested.

## 5.4 Experimental Procedures

### 5.4.1 General Methods

All reactions and subsequent manipulations were performed under anaerobic and anhydrous conditions using procedures described in Section 2.4.1.

### 5.4.2 Reagents

The  $(\text{CD}_2\text{CMe}_3)_2\text{Mg}\cdot x(\text{dioxane})$  alkylating reagent<sup>17</sup> and the complexes  $\text{CpMo}(\text{NO})(\text{CD}_2\text{CMe}_3)_2$  (**5.1-d<sub>4</sub>**)<sup>17</sup> and  $\text{Cp}^*\text{W}(\text{NO})(\text{CH}_2\text{CMe}_3)\text{Cl}$ <sup>35</sup> were prepared according to published procedures.

### 5.4.3 Preparation of $\text{CpMo}(\text{NO})(\text{CHD}_{\text{anti}}\text{CMe}_3)(\text{CH}_2\text{C}_6\text{H}_3\text{-3,5-Me}_2)$ (**5.4-d<sub>1</sub>**)

A bomb was charged with complex **5.1-d<sub>4</sub>** (80 mg, 0.24 mol), a magnetic stir-bar and mesitylene (4 mL), and it was placed in a constant-temperature oil-bath at 40 °C for 6 h. The volatiles were removed in vacuo, and the residue was analyzed spectroscopically. Complex **5.4-d<sub>1</sub>** was identified as the major product in the reaction mixture. Several attempts were made to isolate **5.4-d<sub>1</sub>** from this mixture in crystalline form, but all were unsuccessful.

IR ( $\text{cm}^{-1}$ ) 1614 (s,  $\nu_{\text{NO}}$ ). MS (LREI,  $m/z$ , probe temperature 120 °C) 382 [ $\text{P}^+$ ,  $^{96}\text{Mo}$ ], 352 [ $\text{P}^+$  - NO].  $^1\text{H}$  NMR (400 MHz,  $\text{C}_6\text{D}_6$ )  $\delta$  -3.32 (s, 1H, Npt  $\text{CH}_{\text{synD}}$ ), 1.11 (s, 9H, Npt  $\text{CMe}_3$ ), 1.91 (s, 6H, Mes Me), 2.67 (d,  $^2J_{\text{HH}} = 4.3$ , 1H, Mes  $\text{CH}_{\text{synH}}$ ), 3.16 (d,  $^2J_{\text{HH}} = 4.3$ , 1H, Mes  $\text{CH}_{\text{antiH}}$ ), 5.08 (s, 5H, Cp), 5.91 (v br s, Mes H).  $^2\text{H}\{^1\text{H}\}$  NMR (400 MHz,  $\text{C}_6\text{H}_6$ )  $\delta$  1.76 (s, Npt  $\text{CD}_{\text{antiH}}$ ).  $^{13}\text{C}\{^1\text{H}\}$  NMR (125 MHz,  $\text{CDCl}_3$ )  $\delta$  20.8 (Mes Me), 34.1 (Npt  $\text{CMe}_3$ ), 36.8 (Mes  $\text{CH}_2$ , Npt  $\text{CMe}_3$ ), 51.2 (t,  $^2J_{\text{HD}} = 17.9$ , Npt CHD), 99.6 ( $\text{C}_5\text{H}_5$ ), 113.5 (Mes  $\text{C}_{\text{ipso}}$ ), 131.9 (v br, Mes  $\text{C}_{\text{ortho}}$ ), 134.0 (Mes,  $\text{C}_{\text{meta}}$ ), 138.4 (br, Mes  $\text{C}_{\text{para}}$ ).

#### 5.4.4 Thermolysis of $\text{Cp}^*\text{W}(\text{NO})(\text{CH}_2\text{CMe}_3)(\text{CH}_2\text{SiMe}_3)$ (1.4) in Tetramethylsilane

Complex 1.4 was prepared by the thermolysis of **1** (40 mg, 0.082 mmol) in tetramethylsilane (3 mL) by the method described in Section 2.4.22. The complex was not isolated, but instead the solution was heated for an additional 40 h at 70 °C, whereupon the solvent was removed and a  $^1\text{H}$  NMR spectrum was recorded. Complex **5.7** was identified in the reaction mixture by comparison of this spectrum to its reported  $^1\text{H}$  NMR spectral features.<sup>36</sup>

#### 5.4.5 Synthesis of $(1,1\text{-Me}_2\text{-C}_3\text{H}_3)_2\text{Mg}\cdot x(\text{dioxane})$

This diallyl magnesium reagent was prepared by a modified version of the general synthetic method for dialkyl magnesium reagents.<sup>18,37</sup> 3,3-dimethylallyl bromide (Fluka, 10 mL, 0.085 mol) was distilled under Ar into a 200-mL two-neck, round-bottom flask and diluted with  $\text{Et}_2\text{O}$  (100 mL). In a glovebox, a 500-mL three-neck, round-bottom flask was charged with magnesium powder (20.6 g, 0.858 mol) and a magnetic stir-bar. On a vacuum-line, the 500-mL flask was charged with  $\text{Et}_2\text{O}$  (300 mL), and was fitted

with a reflux condenser. Sufficient dibromoethane (~ 1-2 mL) was added to the suspension via syringe to activate the magnesium powder. The suspension was then cooled in an ice bath to 0 °C, whereupon the ethereal bromide solution was added dropwise via a cannula over a period of 3 h. During this time, the contents of the flask were stirred rapidly, and the ethereal solution remained clear. After the addition was complete, the contents of the flask were warmed to room temperature, and the remainder of the preparation, namely the transformation of the Grignard reagent into the bis(alkyl)magnesium reagent, was conducted in the usual manner. A total of 3.6 g of  $(1,1\text{-Me}_2\text{-C}_3\text{H}_3)_2\text{Mg}\cdot x(\text{dioxane})$  was isolated as a snow white powder. Note that the reagent as prepared is extremely smelly with an obnoxious and persistent skunk-like odour. It is best stored in the freezer of a glovebox in a sealed vial, and it must be handled carefully at all times.

#### 5.4.6 Synthesis of $\text{Cp}^*\text{W}(\text{NO})(\text{CH}_2\text{CMe}_3)(\eta^3\text{-}1,1\text{-Me}_2\text{-C}_3\text{H}_3)$ (5.9)

In a glovebox, a 100-mL Schlenk tube was charged with  $\text{Cp}^*\text{W}(\text{NO})(\text{CH}_2\text{CMe}_3)\text{Cl}$  (165 mg, 0.36 mmol) and a magnetic stir bar. A second Schlenk tube was charged with  $(1,1\text{-Me}_2\text{-C}_3\text{H}_3)_2\text{Mg}\cdot x(\text{dioxane})$  (72 mg, 0.36 mmol  $\text{R}^-$ ) and a magnetic stir bar. On a vacuum-line, sufficient diethyl ether was added to the first Schlenk tube to dissolve the purple solid (~ 20 mL), while 50 mL was added to the second Schlenk. The first vessel was cooled to -78 °C in an acetone/Dry Ice bath, while the latter vessel was cooled in a liquid  $\text{N}_2$  bath to -196 °C to solidify the solution. The chilled solution of  $\text{Cp}^*\text{W}(\text{NO})(\text{CH}_2\text{CMe}_3)\text{Cl}$  was then added to the flask containing  $(1,1\text{-Me}_2\text{-C}_3\text{H}_3)_2\text{Mg}\cdot x(\text{dioxane})$  via cannula at a slow enough rate that it quickly froze. Additional diethyl ether was used as necessary to ensure complete transfer of the

$\text{Cp}^*\text{W}(\text{NO})(\text{CH}_2\text{CMe}_3)\text{Cl}$  reagent. After the addition was complete, the liquid  $\text{N}_2$  bath was removed and replaced with a Dry Ice/acetone bath at  $-78\text{ }^\circ\text{C}$  while the magnetic stirring was engaged. The contents of the flask changed from purple to red to yellow upon melting. The yellow solution was stirred at  $-78\text{ }^\circ\text{C}$  for 15 min to ensure completion of the reaction, whereupon the vessel was warmed to  $0\text{ }^\circ\text{C}$  and the volume of the solvent was reduced in vacuo to  $\sim 50\text{ mL}$ . The concentrated yellow-orange solution was then filtered through alumina (I) supported on a frit ( $2 \times 2\text{ cm}$ ). The alumina was washed with cold  $\text{Et}_2\text{O}$  ( $2 \times 10\text{ mL}$ ), and the combined filtrates were then dried in vacuo. The vacuum was maintained for an additional 30 min to ensure complete drying of the resulting yellow-orange solid. Analysis of this solid by  $^1\text{H}$  NMR spectroscopy revealed that complex **5.9** was the sole organometallic product. Recrystallization of the solid from 5:1  $\text{Et}_2\text{O}$ /hexanes yielded orange microcrystals (63 mg, 36 %).

IR ( $\text{cm}^{-1}$ ) 1584 (w,  $\nu_{\text{C}=\text{C}}$ ), 1546 (s,  $\nu_{\text{NO}}$ ). MS (LREI,  $m/z$ , probe temperature  $150\text{ }^\circ\text{C}$ ) 489 [ $\text{P}^+$ ,  $^{184}\text{W}$ ].  $^1\text{H}$  NMR (300 MHz,  $\text{C}_6\text{D}_6$ )  $\delta$  0.77 (s, 3H, allyl Me), 0.93 (d,  $^2J_{\text{HH}} = 14.0$ , 1H, Npt  $\text{CH}_2$ ), 1.05 (s, 3H, allyl Me), 1.38 ( $\text{CMe}_3$ ), 1.45 (d,  $^2J_{\text{HH}} = 14.0$ , 1H, Npt  $\text{CH}_2$ ), 1.54 (m, 1H, allyl  $\text{CH}_2$ ), 1.56 (s, 15H,  $\text{C}_5\text{Me}_5$ ), 2.66 (m, 1H, allyl  $\text{CH}_2$ ), 4.48 (m, 1H, allyl CH).  $^1\text{H}$  NMR (400 MHz,  $\text{CD}_2\text{Cl}_2$ )  $\delta$  0.88 (d,  $^2J_{\text{HH}} = 14.2$ , 1H, Npt  $\text{CH}_2$ ), 0.99 (s, 3H, allyl Me), 1.02 (d,  $^2J_{\text{HH}} = 14.2$ , 1H, Npt  $\text{CH}_2$ ), 1.06 (s, 9H, Npt  $\text{CMe}_3$ ), 1.24 (s, 3H, allyl Me), 1.61 (m, 1H, allyl  $\text{CH}_2$ ), 1.82 (s, 15H,  $\text{C}_5\text{Me}_5$ ), 2.55 (m, 1H, allyl  $\text{CH}_2$ ), 4.40 (m, 1H, allyl CH).  $^{13}\text{C}\{^1\text{H}\}$  NMR (75 MHz,  $\text{CD}_2\text{Cl}_2$ )  $\delta$  10.2 ( $\text{C}_5\text{Me}_5$ ), 19.5, 30.7 (allyl Me), 34.3 ( $\text{CMe}_3$ ), 37.6 (allyl  $\text{CH}_2$ ), 39.9 ( $\text{CMe}_3$ ), 40.7 (Npt  $\text{CH}_2$ ), 101.7 (allyl CH), 107.5 ( $\text{C}_5\text{Me}_5$ ), 147.8 (allyl C). Anal. Calcd. for  $\text{C}_{20}\text{H}_{35}\text{NOW}$ : C, 49.09; H, 7.21; N, 2.86. Found: C, 49.16; H 7.03; N.2.87.

#### 5.4.7 Preparation of Cp\*W(NO)(C<sub>6</sub>H<sub>5</sub>)( $\eta^3$ -1,1-Me<sub>2</sub>-C<sub>3</sub>H<sub>3</sub>) (5.10)

A bomb was charged with **5.9** (48 mg, 0.098 mmol) and benzene (3 mL), and it was placed in a constant-temperature bath set at 50 °C for 6 h. The bomb was then removed from the bath, and the solvent was removed in vacuo. Recrystallization of the residue from 3:1 Et<sub>2</sub>O/hexanes afforded **5.10** as yellow microcrystals (34 mg, 69 %).

IR (cm<sup>-1</sup>) 1562 (s,  $\nu_{\text{NO}}$ ). MS (LREI, m/z, probe temperature 150 °C) 495 [P<sup>+</sup>, <sup>184</sup>W]. <sup>1</sup>H NMR (300 MHz, C<sub>6</sub>D<sub>6</sub>)  $\delta$  0.82 (s, 3H, allyl Me), 1.51 (s, 15H, C<sub>5</sub>Me<sub>5</sub>), 1.62 (br s, allyl Me), 1.74 (br m, 1H, allyl CH<sub>2</sub>), 2.49 (br m, 1H, allyl CH<sub>2</sub>), 3.54 (br m, 1H, allyl CH), 6.64 (br d, 1H, Ph H<sub>ortho</sub>), 7.08 (t, <sup>3</sup>J<sub>HH</sub> = 7.1, 1H, Ph H<sub>para</sub>), 7.30 (m, 2H, Ph H<sub>meta</sub>), 8.39 (d, <sup>3</sup>J<sub>HH</sub> = 6.7, 1H, Ph H<sub>ortho</sub>). <sup>1</sup>H NMR (400 MHz, CDCl<sub>3</sub>)  $\delta$  0.87 (s, 3H, allyl Me), 1.51 (br s, allyl Me), 1.76 (s, 15H, C<sub>5</sub>Me<sub>5</sub>), 1.90 (br m, 1H, allyl CH<sub>2</sub>), 2.42 (br m, 1H, allyl CH<sub>2</sub>), 3.73 (br m, 1H, allyl CH), 6.68 (br d, 1H, Ph H<sub>ortho</sub>), 6.93 (t, <sup>3</sup>J<sub>HH</sub> = 7.1, 1H, Ph H<sub>para</sub>), 7.12 (q, <sup>3</sup>J<sub>HH</sub> = 7.0, 2H, Ph H<sub>meta</sub>), 7.86 (d, <sup>3</sup>J<sub>HH</sub> = 6.4, 1H, Ph H<sub>ortho</sub>). <sup>13</sup>C{<sup>1</sup>H} NMR (75 MHz, CD<sub>2</sub>Cl<sub>2</sub>)  $\delta$  10.4 (C<sub>5</sub>Me<sub>5</sub>), 21.8, 29.4 (allyl Me), 37.6 (allyl CH<sub>2</sub>), 95.3 (allyl CH), 107.6 (C<sub>5</sub>Me<sub>5</sub>), 123.4 (Ph C<sub>para</sub>), 126.8, 127.9 (Ph C<sub>meta</sub>), 139.6, 141.9 (Ph C<sub>ortho</sub>), 148.5 (allyl C), 168.8 (Ph C<sub>ipso</sub>). Anal. Calcd. for C<sub>21</sub>H<sub>29</sub>NO: C, 50.92; H, 5.90; N, 2.83. Found: C, 50.61; H, 5.95; N, 2.92.

#### 5.4.8 The Thermolysis of **5.9** in Benzene-*d*<sub>6</sub>: Kinetic Studies and the Preparation of Cp\*W(NO)(C<sub>6</sub>D<sub>5</sub>)( $\eta^3$ -1,1-Me<sub>2</sub>-allyl-*d*<sub>1</sub>) (5.10-*d*<sub>6</sub>).

A J. Young NMR tube was charged with **5.9** (10 mg, 0.020 mmol), benzene-*d*<sub>6</sub> (0.8 mL) and hexamethyldisilane (1 mg, 0.007 mmol), and the contents were mixed thoroughly. The thermolysis was conducted in-probe by variable-temperature <sup>1</sup>H NMR

spectroscopy at 323.0 K, with the number of scans set to one. The loss of starting material vs time was determined by the integration of the  $\text{CMe}_3$  signal vs the hexamethyldisilane signal, except for the  $t = 0$  value which was extrapolated from the plot of starting material loss vs time. The first-order rate constant for the decomposition of **5.9** was determined by the plot of  $\ln(A(t)/A(0))$  vs time. See Appendix B for a plot of the data. After 4 h, the sample was removed from the probe and the crystalline product **5.10-d<sub>6</sub>** was analyzed by NMR and MS spectroscopic techniques.

**5.10-d<sub>6</sub>**: MS (LREI,  $m/z$ , probe temperature 120 °C) 501 [ $\text{P}^+$ ,  $^{184}\text{W}$ ].  $^1\text{H}$  NMR (400 MHz,  $\text{C}_6\text{D}_6$ )  $\delta$  0.82 (s, 3H, allyl Me), 1.51 (s, 15H,  $\text{C}_5\text{Me}_5$ ), 1.62 (br s, allyl Me), 1.73 (br m, 1H, allyl  $\text{CH}_2$ ), 2.48 (br m, 1H, allyl  $\text{CH}_2$ ), 3.52 (br m, 1H, allyl CH).  $^2\text{H}\{^1\text{H}\}$  NMR (61 MHz,  $\text{C}_6\text{H}_6$ )  $\delta$  0.78 (allyl Me), 1.61 (br s, allyl Me), 3.52 (allyl CD), 6.60-8.4 (Ph D).

#### 5.4.9 X-ray Diffraction Analysis of 5.10

Data collection and structure solution were conducted at the University of British Columbia by Dr. B. O. Patrick. All measurements were recorded at  $-93(1)$  °C on a Rigaku/ADSC CCD area detector using graphite-monochromated Mo  $\text{K}_\alpha$  radiation. The data set was corrected for Lorentz and polarization effects. The solid-state molecule structure was solved by direct methods, expanded using Fourier techniques, and refined by the full-matrix least-squares method. The non-hydrogen atoms were refined anisotropically and some hydrogen atoms were refined isotropically. The rest were included in fixed positions. All calculations were performed using the *teXsan* crystallographic software package of Molecular Structure Corporation.<sup>38</sup>

## 5.5 References and Notes

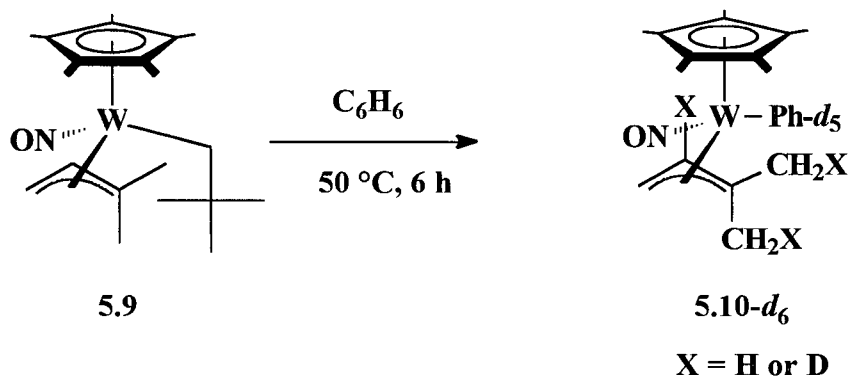
- (1) Arndtsen, B. A.; Bergman, R. G.; Mobley, T. A.; Peterson, T. H. *Acc. Chem. Res.* **1995**, *28*, 154-162.
- (2) (a) Periana, R. A.; Bergman, R. G. *Organometallics* **1984**, *3*, 508-510. (b) Janowicz, A. H.; Bergman, R. G. *J. Am. Chem. Soc.* **1983**, *105*, 3929-3939.
- (3) Baker, M. V.; Field, L. D. *J. Am. Chem. Soc.* **1987**, *109*, 2825-2826.
- (4) Faller, J. W.; Nguyen, J. T.; Ellis, W.; Mazzieri, M. R. *Organometallics* **1993**, *12*, 1434-1438.
- (5) Faller, J. W.; Linebarrier, D. L. *J. Am. Chem. Soc.* **1989**, *111*, 1937-1939.
- (6) Faller, J. W.; DiVerdi, M. J.; John, J. A. *Tetrahedron. Lett.* **1991**, *32*, 1271-1274.
- (7) Schilling, B. E. R.; Hoffman, R.; Faller, J. W. *J. Am. Chem. Soc.* **1979**, *101*, 592-598.
- (8) March, J. *Advanced Organic Chemistry: Reactions, Mechanism and Structure*, 4<sup>th</sup> ed.; Wiley Interscience: Toronto, ON, 1992.
- (9) For key references describing the use of  $\text{CpMo}(\text{NO})(\text{CO})(\text{allyl})^+$  and  $\text{CpM}(\text{CO})_2(\text{allyl})$  complexes in organic chemistry, see: (a) Adams, R. D.; Chodosh, D. F.; Faller, J. W.; Rosan, A. M. *J. Am. Chem. Soc.* **1979**, *101*, 2570-

2578. (b) Faller, J. W.; Chao, K.-H. *J. Am. Chem. Soc.* **1983**, *105*, 3893-3989. (c) Faller, J. W.; Lambert, C.; Mazzieri, M. R. *J. Organomet. Chem.* **1990**, *383*, 161-177. (d) Chen, C.-C.; Fan, J.-F.; Shieh, S.-U.; Lee, G.-H.; Peng, S.-M.; Wang, S.-L.; Liu, R.-S. *J. Am. Chem. Soc.* **1996**, *118*, 9279-9287.
- (10) Kocienski, P. J.; Brown, R. C. D.; Pommier, A.; Procter, M.; Schmidt, B. *J. Chem. Soc., Perkin Trans. 1*, **1998**, 8-40.
- (11) (a) Bursten, B. E.; Cayton, R. H. *Organometallics* **1987**, *6*, 2004-2005. (b) Legzdins, P.; Rettig, S. J.; Sánchez, L.; Bursten, B. E.; Gatter, M. G. *J. Am. Chem. Soc.* **1985**, *107*, 1411-1413.
- (12) Legzdins, P.; Veltheer, J. E. *Acc. Chem. Res.* **1993**, *26*, 41-48.
- (13) Poli, R.; Smith, K. M. *Organometallics* **2000**, *19*, 2858-2967.
- (14) Crabtree, R. H. *The Organometallic Chemistry of the Transition Metals*, 3<sup>rd</sup> ed.; Wiley & Sons: Toronto, ON, 2001; pg 70.
- (15) Tran, E.; Legzdins, P., unpublished results.
- (16) Legzdins, P.; Rettig, S. J.; Veltheer, J. E.; Batchelor, R. J.; Einstein, F. W. B. *Organometallics* **1993**, *12*, 3575-3585.
- (17) Legzdins, P.; Veltheer, J. E.; Young, M. A.; Batchelor, R. J.; Einstein, F. W. B. *Organometallics* **1995**, *14*, 407-417.

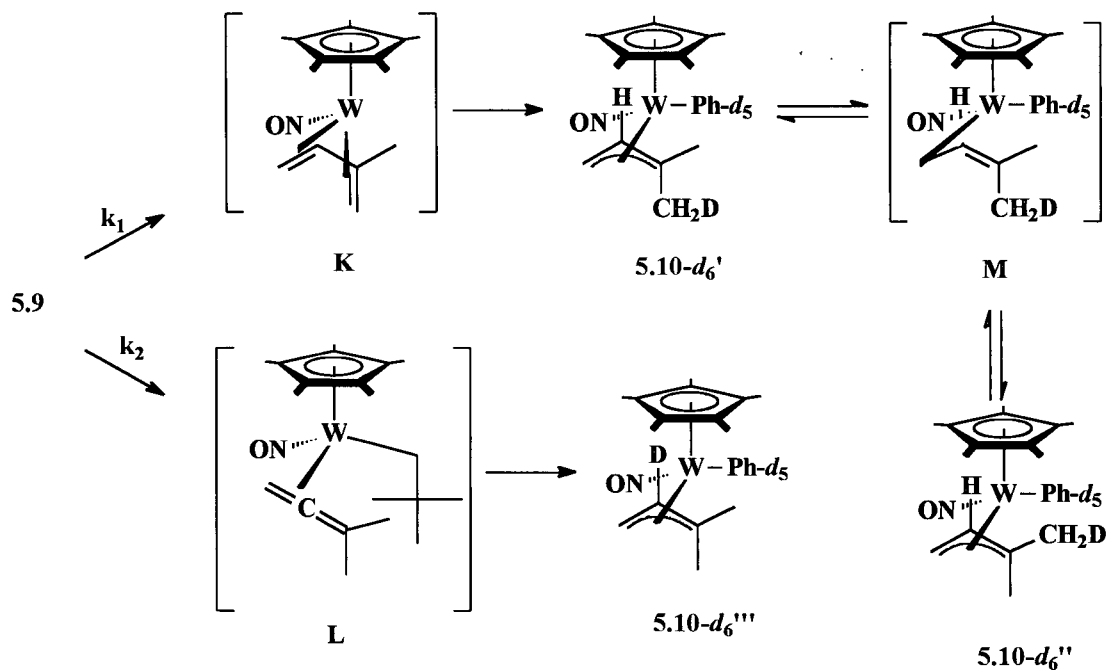
- (18) Dryden, N. H.; Legzdins, P.; Rettig, S. J.; Veltheer, J. E. *Organometallics* **1992**, *11*, 2583-2590.
- (19) Dryden, N. H.; Legzdins, P.; Trotter, J.; Yee, V. C. *Organometallics* **1991**, *10*, 2857-2870.
- (20) Hayton, T. W.; Chan, B.; Legzdins, P., unpublished results.
- (21) For a review of agostic interactions, see: Brookhart, M.; Green, M. L. H.; Wong, L.-L. *Prog. Inorg. Chem.* **1988**, *36*, 1-124.
- (22) Warren, T. H.; Schrock, R. R.; Davis, W. M. *J. Organomet. Chem.* **1998**, *569*, 125-137.
- (23) Fellmann, J. D.; Schrock, R. R.; Traficante, D. D. *Organometallics* **1982**, *1*, 481-482.
- (24) Bau, R.; Mason, S. A.; Patrick, B. O.; Adams, C. S.; Sharp, W. B.; Legzdins, P. *Organometallics* (in press).
- (25) (a) Reference 14, Chapter 11 (b) Schrock, R. R. *Acc. Chem. Res.* **1979**, *12*, 98-104.
- (26) Nugent, W. A.; Mayer, J. M. *Metal-Ligand Multiple Bonds*; Wiley: New York, 1988; Chapter 3.

- (27) A small amount of **5.7** (~ 3 %) is also generated when the thermolysis of **1** is conducted in tetramethylsilane at 70 °C for 40 h.
- (28) Debad, J. D. Ph.D. Dissertation, University of British Columbia, 1994.
- (29) Debad, J. D.; Legzdins, P.; Lumb, S. A.; Rettig, S. J.; Batchelor, R. J.; Einstein, F. W. B. *Organometallics* **1999**, *18*, 3414-3428.
- (30) Complex **5.9** is generated by the low temperature metathesis reaction of  $\text{Cp}^*\text{W}(\text{NO})(\text{CH}_2\text{CMe}_3)\text{Cl}$  and  $(1,1\text{-Me}_2\text{-C}_3\text{H}_3)_2\text{Mg}\cdot x(\text{dioxane})$ . It can be isolated in microcrystalline form in modest yield (36 %) from  $\text{Et}_2\text{O}$ /hexane mixtures, and it has been fully characterized. In benzene- $d_6$  and chloroform- $d_1$  solutions, only one isomer is observed, and its  $^1\text{H}$  and  $^{13}\text{C}\{^1\text{H}\}$ NMR spectral features are consistent with a  $\sigma$ - $\pi$  distortion of the allyl ligand as expected for this class of compound. In particular, the resonances attributable to the C-Me<sub>2</sub> ( $\delta$  147.8) and CH ( $\delta$  101.7) carbons of the allyl ligand are shifted downfield from the  $\text{sp}^3$ -like resonance attributable to the terminal CH<sub>2</sub> carbon ( $\delta$  37.6), thereby indicating that the more electron-rich dimethyl end of the allyl ligand is the  $\pi$ -distorted moiety, and is cis to the neopentyl ligand. The full stereochemistry of this complex in solution needs to be established by NOE difference spectroscopy. Complex **5.9** is moderately stable in solution at ambient temperatures, but rapidly decomposes at elevated temperatures ( $t_{1/2} \cong 10$  min at 70 °C).

- (31) Crystals of **5.10** are monoclinic of space group  $P2_1/c$ (#14),  $a = 12.8869(3) \text{ \AA}$ ,  $b = 9.0219(3) \text{ \AA}$ ,  $c = 16.7835(7) \text{ \AA}$ ,  $\alpha = 90^\circ$ ,  $\beta = 92.439(2)^\circ$ ,  $\gamma = 90^\circ$ . The structure was solved by direct methods. Full-matrix least-squares refinement procedures led to  $R1 = 0.022$  for 3649 observed reflections ( $I > 3\sigma(I)$ ). Full details of the crystallographic analysis are provided in Appendix A.
- (32) The  $^1\text{H}$ ,  $^{13}\text{C}\{^1\text{H}\}$  and  $^1\text{H}-^{13}\text{C}$  HMQC NMR data indicate that the allyl ligand is distorted in solution in a  $\sigma$ - $\pi$  fashion with the dimethyl portion of the allyl ligand being the  $\pi$ -distorted moiety cis to the phenyl ligand. Interestingly, all of the phenyl H and C atoms have unique resonances in both spectra, thus indicating that rotation about the W-C bond of the phenyl ligand is slow on the NMR timescale, in contrast to the aryl ligands in other  $\text{CpM}(\text{NO})(\text{R})(\text{aryl})$  complexes mentioned in this Thesis.
- (33) Monitoring the thermolysis for 4 h in benzene- $d_6$  at  $50^\circ\text{C}$  by  $^1\text{H}$  NMR spectroscopy reveals that 1 equiv of neopentane is formed, and that the loss of **5.9** is first-order with a rate constant of  $2.2(1) \times 10^{-4} \text{ s}^{-1}$  ( $R^2 = 0.9991$ ). Moreover, a single product is formed, and its spectroscopic properties are consistent with the general formulation  $\text{Cp}^*\text{W}(\text{NO})(\text{C}_6\text{D}_5)(1,1\text{-Me}_2\text{-allyl-}d_1)$  (**5.10- $d_6$** ). The  $^1\text{H}$  and  $^2\text{H}\{^1\text{H}\}$  NMR spectroscopic analyses of complex **5.10- $d_6$**  indicates that one equiv of deuterium label is partitioned between three different positions in the allyl ligand: at the two methyl positions ( $\sim 35\%$  combined), and at the central allyl position ( $\sim 65\%$ ).



The partitioning of deuterium between these positions suggests that complex **5.10- $d_6$**  is really a mixture of three different isotopomers formed by C-H activation of benzene- $d_6$  by two different types of reactive intermediates, as illustrated below. In other words, complex **5.9** decomposes intramolecularly (hence first-order kinetics) by two pathways to produce 1 equiv of neopentane and two different intermediates. One intermediate is the *cis*-diene complex, **K**, formed by  $\gamma$ -H abstraction of a methyl H atom. Complex **K** then activates benzene- $d_6$  by the microscopic reverse of the neopentane elimination process to generate the methyl-labeled complex, **5.10- $d_6'$** . The isomerization of **5.10- $d_6'$**  via rotation about the  $\pi$ -bond in the  $\eta^1$ -allyl intermediate **M**, yields the other methyl-labeled complex, **5.10- $d_6''$** . Note **5.10- $d_6''$**  is shown to be produced in this manner rather than from benzene- $d_6$  activation by the *trans*-diene analogue of **K**, since such *trans*-diene complexes are known to be thermally robust and unreactive towards benzene- $d_6$ .<sup>34</sup>



The second intermediate formed from **5.9** is the allene complex, **L**, which arises from abstraction of the  $\beta$ -allyl H atom. The activation of benzene- $d_6$  by **L** thus leads to the formation of **5.10- $d_6'''$**  which is labeled in the  $\beta$ -allyl position. If the rate of formation of **L** is approximately twice as fast as that of **K** (i.e.  $k_2 \cong 2k_1$ ) then approximately twice as much **5.10- $d_6'''$**  will be formed as **5.10- $d_6'$**  and **5.10- $d_6''$** . The combined mixture of **5.10- $d_6'$** , **5.10- $d_6''$**  and **5.10- $d_6'''$**  would exhibit the spectral features currently assigned to **5.10- $d_6$** . More detailed investigations to support this interpretation of the mechanism of thermolysis of **5.9** are currently being conducted by Stephen Ng of this research group.

(34) Sharp, W. B.; Legzdins, P., unpublished observations.

- (35) Debad, J. D.; Legzdins, P.; Rettig, S. J.; Veltheer, J. E. *Organometallics* **1993**, *12*, 2714-2725.
- (36) Legzdins, P.; Rettig, S. J.; Sánchez, L. *Organometallics* **1988**, *7*, 2394-2403.
- (37) Harvey, S.; Junk, P. C.; Raston, C. L.; Salem, G. *J. Org. Chem.* **1988**, *53*, 3134-3140.
- (38) *teXsan: Structure Analysis Package*. Molecular Structure Corp.: The Woodlands, TX, 1985 and 1992.

**Appendix A. Tables of Bond Distances, Angles and  
Fractional Atomic Coordinates for the Structurally  
Characterized Complexes Described in this Thesis**

Table A1. Crystal Data for Compounds 2.4a, 2.12, 2.14 and 5.10

Crystal Data	2.4a	2.14	2.12	5.10
Empirical formula	C <sub>20</sub> H <sub>30</sub> NOPW	C <sub>26</sub> H <sub>31</sub> NOW	C <sub>25</sub> H <sub>31</sub> NOW	C <sub>21</sub> H <sub>29</sub> NOW
Crystal Habit, color	block, yellow	orange, chip	red-brown block	yellow, prism
Crystal size (mm)	0.40 × 0.20 × 0.20	0.50 × 0.40 × 0.20	0.50 × 0.44 × 0.20	0.30 × 0.20 × 0.20
Crystal system	monoclinic	monoclinic	monoclinic	monoclinic
Space group	Pc (#7)	P2 <sub>1</sub> /a (#14)	P1 (#2)	P2 <sub>1</sub> /c (#14)
Volume (Å <sup>3</sup> )	1028.93(4)	2271.2(2)	1071.6(2)	1949.6(1)
a (Å)	9.5066(3)	8.7551(5)	8.5023(9)	12.8869(3)
b (Å)	8.8989(2)	27.187(1)	8.6298(9)	9.0219(3)
c (Å)	12.5831(3)	9.7641(5)	15.805(1)	16.7835(7)
α°	90	90	74.510(2)	90
β°	104.8540(5)	102.254(4)	79.936(2)	92.439
γ°	90	90	74.797(3)	90
Z	2	4	2	4
Density (calculated) (Mg/m <sup>3</sup> )	1.663	1.630	1.690	1.687
Absorption coefficient (cm <sup>-1</sup> )	57.04	51.08	54.11	59.39
F <sub>000</sub>	508	1104	540	976

**Table A2.** Data Refinement, and Structural Solution and Refinement Data for Compounds **2.4a**, **2.12**, **2.14** and **5.10**

Data Collection and Refinement	2.4a	2.14	2.12	5.10
Data Images	462 exposures at 12.0 s	464 exposures at 15.0 s	464 exposures at 12.0 s	462 exposures at 12.0 s
$\phi$ oscillation Range, ( $\chi = 0$ ) ( $^{\circ}$ )	0.0 - 190.0	0.0 - 190.0	0.0 - 190.0	0.0 - 190.0
$\omega$ oscillation Range, ( $\chi = 90$ ) ( $^{\circ}$ )	-18.0 - 23.0	-19.0 - 23.0	-19.0 - 23.0	-18.0 - 23.0
Detector Swing Angle ( $^{\circ}$ )	-5.00	-5.56	-5.50	-5.50
$2\theta_{\max}$ ( $^{\circ}$ )	55.8	55.8	55.8	55.8
Detector Position (mm)	40.13	40.58	40.69	39.76
Measured Reflections: Total	8241	14628	8915	13123
Unique	4072 ( $R_{\text{int}} = 0.040$ )	4763 ( $R_{\text{int}} = 0.043$ )	4030 ( $R_{\text{int}} = 0.031$ )	4484 ( $R_{\text{int}} = 0.031$ )
<b>Structure Solution and Refinement</b>				
Structure Solution method	Patterson	Direct	Patterson	Direct
Refinement	Full-matrix least-squares	Full-matrix least-squares	Full-matrix least-squares	Full-matrix least-squares
No. Observations	3850	4653	4030	4264
No. Variables	215	262	253	229
Final R indices <sup>a</sup>	R1 = 0.016, wR2 = 0.025	R1 = 0.027, wR2 = 0.049	R1 = 0.026, wR2 = 0.036	R1 = 0.022, wR2 = 0.031
Goodness-of-fit on $F^2$ <sup>b</sup>	0.89	1.06	1.31	1.07
Largest diff. peak and hole ( $e^{-\text{Å}^{-3}}$ )	1.29 and -1.125	0.98 and -1.43	1.73 and -2.53	1.08 and -1.64

<sup>a</sup> R1 on  $F = \Sigma (|F_o| - |F_c|) / \Sigma |F_o|$ ; wR2 =  $[\Sigma (w(|F_o|^2 - |F_c|^2)) / \Sigma wF_o^4]^{1/2}$ ; w =  $[\sigma^2 F_o^{-1}]$ ; <sup>b</sup> GOF =  $[\Sigma (w(|F_o| - |F_c|)^2) / (\text{degrees of freedom})]^{1/2}$ .

**Table A3.** Bond Distances (Å) in the Solid-State Molecular Structure Determined for 2.4a

atom	atom	distance	atom	atom	distance	atom	atom	distance	atom	atom	distance
W(1)	P(1)	2.4249(9)	C(3)	C(4)	1.393(6)	C(2)	C(7)	1.407(5)	C(13)	C(14)	1.435(6)
W(1)	N(1)	1.774(4)	C(4)	C(5)	1.378(8)	C(2)	C(3)	1.406(5)	C(12)	C(17)	1.502(6)
W(1)	C(1)	1.976(3)	C(5)	C(6)	1.380(7)	C(1)	C(2)	1.476(5)	C(13)	C(18)	1.513(5)
W(1)	C(11)	2.437(3)	C(6)	C(7)	1.391(5)	C(15)	C(20)	1.490(5)	O(1)	N(1)	1.244(6)
W(1)	C(12)	2.417(4)	C(11)	C(12)	1.416(6)	C(14)	C(19)	1.496(5)	C(11)	C(16)	1.497(5)
W(1)	C(13)	2.363(3)	C(11)	C(15)	1.432(5)	C(14)	C(15)	1.434(6)	C(12)	C(13)	1.424(5)
W(1)	C(14)	2.368(4)	P(1)	C(9)	1.814(4)	P(1)	C(10)	1.813(4)	P(1)	C(8)	1.827(4)
W(1)	C(15)	2.420(3)	C(1)	H(1)	0.985						

**Table A4.** Bond Angles (°) in the Solid-State Molecular Structure Determined for 2.4a

atom	atom	atom	angle	atom	atom	atom	angle	atom	atom	atom	angle
P(1)	W(1)	N(1)	86.6(1)	C(13)	W(1)	C(15)	57.9(1)	W(1)	C(12)	C(17)	125.2(3)
P(1)	W(1)	C(1)	91.5(1)	C(14)	W(1)	C(15)	34.8(1)	C(11)	C(12)	C(13)	107.8(3)
P(1)	W(1)	C(11)	92.15(9)	W(1)	P(1)	C(8)	118.6(1)	C(11)	C(12)	C(17)	125.4(4)
P(1)	W(1)	C(12)	111.9(1)	W(1)	P(1)	C(9)	112.1(1)	C(13)	C(12)	C(17)	126.5(4)
P(1)	W(1)	C(13)	146.28(9)	W(1)	P(1)	C(10)	114.6(1)	W(1)	C(13)	C(12)	74.7(2)
P(1)	W(1)	C(14)	140.1(1)	C(8)	P(1)	C(9)	103.2(2)	W(1)	C(13)	C(14)	72.5(2)
P(1)	W(1)	C(15)	105.53(9)	C(8)	P(1)	C(10)	103.8(2)	W(1)	C(13)	C(18)	124.2(3)
N(1)	W(1)	C(1)	101.1(1)	C(9)	P(1)	C(10)	102.7(2)	C(12)	C(13)	C(14)	108.3(3)
N(1)	W(1)	C(11)	140.4(1)	W(1)	N(1)	O(1)	178.1(3)	C(12)	C(13)	C(18)	125.9(4)
N(1)	W(1)	C(12)	158.5(2)	W(1)	C(1)	C(2)	137.2(2)	C(14)	C(13)	C(18)	125.4(4)
N(1)	W(1)	C(13)	125.4(1)	C(1)	C(2)	C(3)	119.6(3)	W(1)	C(14)	C(13)	72.2(2)
N(1)	W(1)	C(14)	100.9(2)	C(1)	C(2)	C(7)	122.9(3)	W(1)	C(14)	C(15)	74.5(2)
N(1)	W(1)	C(15)	108.5(1)	C(3)	C(2)	C(7)	117.5(3)	W(1)	C(14)	C(19)	122.1(3)
C(1)	W(1)	C(11)	118.5(1)	C(2)	C(3)	C(4)	121.0(4)	C(13)	C(14)	C(15)	107.6(3)
C(1)	W(1)	C(12)	89.7(1)	C(3)	C(4)	C(5)	120.6(4)	C(13)	C(14)	C(19)	127.2(4)
C(1)	W(1)	C(13)	92.1(1)	C(4)	C(5)	C(6)	119.4(4)	C(15)	C(14)	C(19)	125.0(4)
C(1)	W(1)	C(14)	124.5(1)	C(5)	C(6)	C(7)	121.0(4)	W(1)	C(15)	C(11)	73.5(2)
C(1)	W(1)	C(15)	146.4(1)	C(2)	C(7)	C(6)	120.6(4)	W(1)	C(15)	C(14)	70.6(2)
C(11)	W(1)	C(12)	33.9(1)	W(1)	C(11)	C(12)	72.3(2)	W(1)	C(15)	C(20)	128.8(3)
C(11)	W(1)	C(13)	57.1(1)	W(1)	C(11)	C(15)	72.2(2)	C(11)	C(15)	C(14)	107.3(4)
C(11)	W(1)	C(14)	57.4(1)	W(1)	C(11)	C(16)	130.5(2)	C(11)	C(15)	C(20)	125.2(3)
C(11)	W(1)	C(15)	34.3(1)	C(12)	C(11)	C(15)	108.9(3)	C(14)	C(15)	C(20)	126.8(4)
C(12)	W(1)	C(13)	34.6(1)	C(12)	C(11)	C(16)	126.8(3)	W(1)	C(12)	C(13)	70.6(2)
C(12)	W(1)	C(14)	57.9(1)	C(15)	C(11)	C(16)	123.3(3)	C(13)	W(1)	C(14)	35.3(1)
C(12)	W(1)	C(15)	57.3(1)	W(1)	C(12)	C(11)	73.8(2)	W(1)	C(1)	H(1)	111.51
P(1)	C(10)	H(15)	108.87	C(2)	C(1)	H(1)	111.23				

Table A5. Dihedral Angles (°) in the Solid-State Molecular Structure Determined for 2.4a

(1)	(2)	(3)	(4)	angle	(1)	(2)	(3)	(4)	angle	(1)	(2)	(3)	(4)	angle
W(1)	C(1)	C(2)	C(3)	-171.3(3)	P(1)	W(1)	C(11)	C(16)	4.1(3)	C(13)	C(12)	W(1)	C(15)	-79.6(2)
W(1)	C(1)	C(2)	C(7)	9.6(6)	P(1)	W(1)	C(12)	C(11)	-58.3(2)	C(13)	C(12)	C(11)	C(15)	-0.5(4)
W(1)	C(11)	C(12)	C(13)	62.8(3)	P(1)	W(1)	C(12)	C(13)	-174.5(2)	C(13)	C(12)	C(11)	C(16)	-169.4(3)
W(1)	C(11)	C(12)	C(17)	-122.0(4)	P(1)	W(1)	C(12)	C(17)	63.9(4)	C(13)	C(14)	W(1)	C(15)	114.8(3)
W(1)	C(11)	C(15)	C(14)	-62.9(2)	P(1)	W(1)	C(13)	C(12)	9.3(3)	C(13)	C(14)	C(15)	C(20)	170.4(4)
W(1)	C(11)	C(15)	C(20)	126.3(4)	P(1)	W(1)	C(13)	C(14)	-106.0(2)	C(14)	W(1)	C(11)	C(15)	37.7(2)
W(1)	C(12)	C(11)	C(15)	-63.3(2)	P(1)	W(1)	C(13)	C(18)	132.6(3)	C(14)	W(1)	C(11)	C(16)	156.7(4)
W(1)	C(12)	C(11)	C(16)	127.8(4)	P(1)	W(1)	C(14)	C(13)	123.7(2)	C(14)	W(1)	C(12)	C(17)	-159.7(4)
W(1)	C(12)	C(13)	C(14)	65.3(3)	P(1)	W(1)	C(14)	C(15)	8.9(3)	C(14)	W(1)	C(13)	C(18)	-121.4(4)
W(1)	C(12)	C(13)	C(18)	-121.4(4)	P(1)	W(1)	C(14)	C(19)	-113.1(3)	C(14)	W(1)	C(15)	C(20)	122.1(4)
W(1)	C(13)	C(12)	C(11)	-64.9(3)	P(1)	W(1)	C(15)	C(11)	70.2(2)	C(14)	C(13)	W(1)	C(15)	-37.8(2)
W(1)	C(13)	C(12)	C(17)	120.0(4)	P(1)	W(1)	C(15)	C(14)	-174.1(2)	C(14)	C(13)	C(12)	C(17)	-174.8(4)
W(1)	C(13)	C(14)	C(15)	66.7(2)	P(1)	W(1)	C(15)	C(20)	-52.0(3)	C(14)	C(15)	C(11)	C(16)	169.8(3)
W(1)	C(13)	C(14)	C(19)	-117.1(4)	O(1)	N(1)	W(1)	C(1)	-164(8)	C(15)	W(1)	C(11)	C(16)	119.0(4)
W(1)	C(14)	C(13)	C(12)	-66.7(3)	O(1)	N(1)	W(1)	C(11)	16(8)	C(15)	W(1)	C(12)	C(17)	158.8(4)
W(1)	C(14)	C(13)	C(18)	119.9(4)	O(1)	N(1)	W(1)	C(12)	-45(8)	C(15)	W(1)	C(13)	C(18)	-159.1(4)
W(1)	C(14)	C(15)	C(11)	64.8(2)	O(1)	N(1)	W(1)	C(13)	-64(8)	C(15)	W(1)	C(14)	C(19)	-122.0(5)
W(1)	C(14)	C(15)	C(20)	-124.5(4)	O(1)	N(1)	W(1)	C(14)	-36(8)	C(15)	C(11)	C(12)	C(17)	174.7(4)
W(1)	C(15)	C(11)	C(12)	63.4(2)	O(1)	N(1)	W(1)	C(15)	0(8)	C(15)	C(14)	C(13)	C(18)	-173.4(3)
W(1)	C(15)	C(11)	C(16)	-127.3(3)	N(1)	W(1)	P(1)	C(8)	162.3(2)	C(16)	C(11)	C(12)	C(17)	5.8(6)
W(1)	C(15)	C(14)	C(13)	-65.1(2)	N(1)	W(1)	P(1)	C(9)	42.1(2)	C(16)	C(11)	C(15)	C(20)	-1.0(6)
W(1)	C(15)	C(14)	C(19)	118.6(4)	N(1)	W(1)	P(1)	C(10)	-74.5(2)	C(17)	C(12)	C(13)	C(18)	-1.4(6)
P(1)	W(1)	N(1)	O(1)	105(8)	N(1)	W(1)	C(1)	C(2)	-8.3(4)	C(18)	C(13)	C(14)	C(19)	2.8(6)
P(1)	W(1)	C(1)	C(2)	78.5(4)	N(1)	W(1)	C(11)	C(12)	-145.0(2)	C(19)	C(14)	C(15)	C(20)	-5.9(6)
P(1)	W(1)	C(11)	C(12)	127.8(2)	N(1)	W(1)	C(11)	C(15)	-27.6(3)	C(13)	C(12)	W(1)	C(14)	-38.1(2)
P(1)	W(1)	C(11)	C(15)	-114.9(2)	N(1)	W(1)	C(11)	C(16)	91.4(4)	C(11)	C(15)	C(14)	C(19)	-176.6(4)
N(1)	W(1)	C(12)	C(11)	89.5(4)	C(1)	W(1)	C(14)	C(19)	96.5(3)	C(13)	W(1)	C(15)	C(20)	160.4(4)
N(1)	W(1)	C(12)	C(13)	-26.6(5)	C(1)	W(1)	C(15)	C(11)	-47.6(3)	C(11)	C(15)	C(14)	C(13)	-0.2(4)
N(1)	W(1)	C(12)	C(17)	-148.2(3)	C(1)	W(1)	C(15)	C(14)	68.1(3)	C(13)	W(1)	C(15)	C(14)	38.3(2)
N(1)	W(1)	C(13)	C(12)	168.4(2)	C(1)	W(1)	C(15)	C(20)	-169.7(3)	C(11)	C(15)	W(1)	C(14)	-115.7(3)
N(1)	W(1)	C(13)	C(14)	53.1(3)	C(1)	C(2)	C(3)	C(4)	179.2(4)	C(13)	W(1)	C(14)	C(19)	123.2(4)
N(1)	W(1)	C(13)	C(18)	-68.3(4)	C(1)	C(2)	C(7)	C(6)	-179.8(4)	C(11)	C(15)	W(1)	C(13)	-77.4(2)
N(1)	W(1)	C(14)	C(13)	-138.4(2)	C(2)	C(1)	W(1)	C(11)	171.7(3)	C(13)	W(1)	C(14)	C(15)	-114.8(3)
N(1)	W(1)	C(14)	C(15)	106.8(2)	C(2)	C(1)	W(1)	C(12)	-169.6(4)	C(11)	C(15)	W(1)	C(12)	-36.1(2)
N(1)	W(1)	C(14)	C(19)	-15.2(4)	C(2)	C(1)	W(1)	C(13)	-135.0(4)	C(13)	W(1)	C(12)	C(17)	-121.6(5)
N(1)	W(1)	C(15)	C(11)	161.8(2)	C(2)	C(1)	W(1)	C(14)	-120.0(4)	C(11)	C(12)	C(13)	C(18)	173.7(3)
N(1)	W(1)	C(15)	C(14)	-82.5(2)	C(2)	C(1)	W(1)	C(15)	-160.0(3)	C(13)	W(1)	C(11)	C(16)	-161.1(4)
N(1)	W(1)	C(15)	C(20)	39.7(3)	C(2)	C(3)	C(4)	C(5)	2.0(7)	C(11)	C(12)	C(13)	C(14)	0.4(4)
C(1)	W(1)	P(1)	C(8)	61.3(2)	C(2)	C(7)	C(6)	C(5)	-0.9(6)	C(13)	W(1)	C(11)	C(15)	79.9(2)
C(1)	W(1)	P(1)	C(9)	-58.9(2)	C(3)	C(2)	C(7)	C(6)	1.1(5)	C(11)	C(12)	W(1)	C(15)	36.5(2)
C(1)	W(1)	P(1)	C(10)	-175.5(2)	C(3)	C(4)	C(5)	C(6)	-1.8(7)	C(12)	C(13)	C(14)	C(19)	176.2(4)
C(1)	W(1)	C(11)	C(12)	34.9(3)	C(4)	C(3)	C(2)	C(7)	-1.6(5)	C(11)	C(12)	W(1)	C(14)	78.0(3)
C(1)	W(1)	C(11)	C(15)	152.3(2)	C(4)	C(5)	C(6)	C(7)	1.2(7)	C(12)	C(13)	C(14)	C(15)	-0.1(4)
C(1)	W(1)	C(11)	C(16)	-88.7(3)	C(8)	P(1)	W(1)	C(11)	-57.4(2)	C(11)	C(12)	W(1)	C(13)	116.1(3)
C(1)	W(1)	C(12)	C(11)	-149.8(2)	C(8)	P(1)	W(1)	C(12)	-29.0(2)	C(12)	C(13)	W(1)	C(15)	77.6(2)
C(1)	W(1)	C(12)	C(13)	94.1(2)	C(8)	P(1)	W(1)	C(13)	-34.7(3)	C(11)	W(1)	C(15)	C(20)	-122.2(4)
C(1)	W(1)	C(12)	C(17)	-27.5(4)	C(8)	P(1)	W(1)	C(14)	-94.7(2)	C(12)	C(13)	W(1)	C(14)	115.3(3)
C(1)	W(1)	C(13)	C(12)	-86.5(2)	C(8)	P(1)	W(1)	C(15)	-89.4(2)	C(11)	W(1)	C(15)	C(14)	115.7(3)
C(1)	W(1)	C(13)	C(14)	158.2(2)	C(9)	P(1)	W(1)	C(11)	-177.5(2)	C(12)	C(11)	C(15)	C(20)	-170.4(3)
C(1)	W(1)	C(13)	C(18)	36.9(3)	C(9)	P(1)	W(1)	C(12)	-149.1(2)	C(11)	W(1)	C(14)	C(19)	-159.0(4)

Table A5. continued

C(1) W(1) C(14)C(13) -26.7(3)	C(9) P(1) W(1) C(13) -154.8(2)	C(12)C(11)C(15)C(14) 0.5(4)
C(1) W(1) C(14)C(15) -141.5(2)	C(9) P(1) W(1) C(14) 145.1(2)	C(11)W(1) C(14)C(15) -37.1(2)
C(9) P(1) W(1) C(15) 150.4(2)	C(12)W(1) C(11)C(15) 117.4(3)	C(12)C(11)W(1) C(15) -117.4(3)
C(10)P(1) W(1) C(11) 65.9(2)	C(12)W(1) C(11)C(16) -123.6(4)	C(11)W(1) C(14)C(13) 77.7(2)
C(10)P(1) W(1) C(12) 94.3(2)	C(12)W(1) C(13)C(14) -115.3(3)	C(12)C(11)W(1) C(14) -79.7(3)
C(10)P(1) W(1) C(13) 88.6(2)	C(12)W(1) C(13)C(18) 123.3(4)	C(11)W(1) C(13)C(18) 160.0(4)
C(10)P(1) W(1) C(14) 28.6(2)	C(12)W(1) C(14)C(13) 37.3(2)	C(12)C(11)W(1) C(13) -37.4(2)
C(10)P(1) W(1) C(15) 33.8(2)	C(12)W(1) C(14)C(15) -77.4(2)	C(11)W(1) C(13)C(14) -78.7(2)
C(11)W(1) C(12)C(13) -116.1(3)	C(12)W(1) C(14)C(19) 160.6(4)	C(12)W(1) C(15)C(20) -158.3(4)
C(11)W(1) C(12)C(17) 122.3(5)	C(12)W(1) C(15)C(14) 79.6(3)	C(11)W(1) C(13)C(12) 36.6(2)

Table A6. Fractional Atomic Coordinates in the Solid-State Molecular Structure Determined for 2.4a

atom	x	y	z	B(eq)	atom	x	y	z	B(eq)
W(1)	-0.0018	0.223878(9)	0.4962	1.284(3)	H(1)	-0.1232	0.0464	0.5999	2.0440
P(1)	-0.1852(1)	0.4183(1)	0.47757(7)	1.71(2)	H(2)	-0.3242	-0.1100	0.5863	3.1817
O(1)	-0.0652(5)	0.2274(3)	0.2486(3)	2.75(8)	H(3)	-0.5245	-0.2473	0.4822	3.7132
N(1)	-0.0414(4)	0.2246(3)	0.3505(3)	1.56(8)	H(4)	-0.5752	-0.2542	0.2900	4.1976
C(1)	-0.1388(4)	0.0691(4)	0.5211(3)	1.71(6)	H(5)	-0.4367	-0.1058	0.1985	4.0918
C(2)	-0.2610(4)	-0.0191(4)	0.4538(3)	2.02(7)	H(7)	-0.1821	0.4792	0.6595	4.2215
C(3)	-0.3466(4)	-0.1072(4)	0.5058(3)	2.46(7)	H(8)	-0.3279	0.5417	0.5775	4.2215
C(4)	-0.4637(5)	-0.1903(6)	0.4445(5)	3.09(9)	H(9)	-0.3142	0.3672	0.6095	4.2215
C(5)	-0.4954(5)	-0.1918(6)	0.3314(5)	3.35(9)	H(10)	-0.4188	0.4565	0.3647	3.4370
C(6)	-0.4124(5)	-0.1065(5)	0.2787(3)	3.23(8)	H(11)	-0.3183	0.3779	0.2964	3.4370
C(7)	-0.2957(4)	-0.0216(4)	0.3382(3)	2.48(7)	H(12)	-0.3850	0.2804	0.3787	3.4370
C(8)	-0.2613(5)	0.4567(6)	0.5942(3)	3.38(9)	H(13)	-0.0432	0.6343	0.4966	3.9254
H(14)	-0.1081	0.5961	0.3692	3.9254	H(15)	-0.2091	0.6737	0.4375	3.9254
C(9)	-0.3451(4)	0.3790(5)	0.3667(3)	2.90(8)	H(16)	0.2277	0.5300	0.7532	3.4598
C(10)	-0.1293(5)	0.6017(4)	0.4408(4)	3.10(9)	H(17)	0.0763	0.5583	0.6643	3.4598
C(11)	0.1570(4)	0.3469(4)	0.6554(3)	1.70(7)	H(18)	0.0808	0.4595	0.7714	3.4598
C(12)	0.1391(5)	0.1957(5)	0.6845(3)	1.85(7)	H(19)	-0.0199	0.1845	0.7667	3.1817
C(13)	0.1985(4)	0.1018(4)	0.6152(3)	1.89(7)	H(20)	0.0782	0.0361	0.7815	3.1817
C(14)	0.2545(4)	0.1961(5)	0.5430(3)	1.77(7)	H(21)	0.1404	0.1857	0.8475	3.1817
C(15)	0.2289(4)	0.3492(4)	0.5683(3)	1.76(7)	H(22)	0.1198	-0.1132	0.6154	3.1754
C(16)	0.1333(4)	0.4845(4)	0.7171(3)	2.75(7)	H(23)	0.2606	-0.1047	0.5680	3.1754
C(17)	0.0796(4)	0.1456(5)	0.7784(3)	2.63(8)	H(24)	0.2778	-0.0932	0.6977	3.1754
C(18)	0.2161(5)	-0.0669(4)	0.6248(3)	2.68(8)	H(25)	0.3374	0.0373	0.4589	3.5098
C(19)	0.3344(4)	0.1473(5)	0.4608(3)	2.78(8)	H(26)	0.2849	0.1855	0.3878	3.5098
C(20)	0.2871(4)	0.4862(5)	0.5264(3)	2.84(8)	H(27)	0.4337	0.1870	0.4826	3.5098
H(28)	0.3595	0.5333	0.5865	3.2878	H(29)	0.3312	0.4583	0.4672	3.2878
H(30)	0.2067	0.5570	0.4983	3.2878					

**Table A7.** Bond Distances (Å) in the Solid-State Molecular Structure Determined for **2.12**

atom	atom	distance									
W(1)	O(1)	2.980(3)	C(4)	C(6)	2.400(9)	C(2)	C(5)	2.804(6)	C(10)	C(11)	1.424(6)
W(1)	N(1)	1.769(3)	C(4)	C(7)	2.785(7)	C(2)	C(6)	2.427(6)	C(10)	C(12)	2.298(6)
W(1)	C(1)	2.191(4)	C(5)	C(6)	1.36(1)	C(2)	C(7)	1.411(6)	C(10)	C(14)	2.626(6)
W(1)	C(2)	2.554(4)	C(5)	C(7)	2.396(8)	C(3)	C(4)	1.381(6)	C(10)	C(15)	1.507(6)
W(1)	C(8)	2.297(4)	C(6)	C(7)	1.388(7)	C(3)	C(5)	2.415(7)	C(10)	C(16)	2.610(6)
W(1)	C(9)	2.298(4)	C(8)	C(9)	1.435(5)	C(3)	C(6)	2.779(7)	C(10)	C(18)	2.958(5)
W(1)	C(10)	2.409(4)	C(8)	C(10)	2.310(5)	C(3)	C(7)	2.426(6)	C(11)	C(12)	1.428(5)
W(1)	C(11)	2.455(4)	C(8)	C(11)	2.319(5)	C(4)	C(5)	1.409(9)	C(11)	C(15)	2.615(6)
W(1)	C(12)	2.405(4)	C(8)	C(12)	1.426(5)	C(11)	C(16)	1.499(6)	C(11)	C(17)	2.607(7)
W(1)	C(18)	2.181(3)	C(8)	C(13)	1.507(5)	C(12)	C(13)	2.619(6)	C(12)	C(17)	1.504(6)
O(1)	N(1)	1.224(4)	C(8)	C(14)	2.599(6)	C(12)	C(16)	2.608(6)	C(18)	C(19)	1.420(6)
N(1)	C(1)	2.819(5)	C(8)	C(17)	2.603(6)	C(18)	C(21)	2.839(5)	C(18)	C(23)	1.408(5)
N(1)	C(8)	2.974(5)	C(9)	C(10)	1.427(5)	C(18)	C(20)	2.436(5)	C(18)	C(24)	2.564(6)
C(1)	C(2)	1.455(5)	C(9)	C(11)	2.317(5)	C(18)	C(22)	2.478(5)	C(19)	C(21)	2.442(5)
C(1)	C(3)	2.492(6)	C(9)	C(12)	2.308(6)	C(19)	C(20)	1.405(5)	C(19)	C(22)	2.830(5)
C(1)	C(7)	2.500(6)	C(9)	C(13)	2.618(6)	C(19)	C(23)	2.403(5)	C(19)	C(24)	1.493(6)
C(2)	C(3)	1.417(6)	C(9)	C(14)	1.502(5)	C(20)	C(21)	1.380(6)	C(20)	C(22)	2.403(6)
C(2)	C(4)	2.429(6)	C(9)	C(15)	2.597(6)	C(20)	C(23)	2.729(6)	C(21)	C(22)	1.398(6)
C(20)	C(24)	2.479(6)	C(21)	C(23)	2.385(6)	C(21)	C(25)	2.541(7)	C(22)	C(23)	1.390(5)
C(22)	C(25)	1.508(6)	C(23)	C(25)	2.517(5)						

**Table A8.** Bond Angles (°) in the Solid-State Molecular Structure Determined for **2.12**

atom	atom	atom	angle	atom	atom	atom	angle	atom	atom	atom	angle
O(1)	W(1)	N(1)	4.4(1)	C(2)	W(1)	C(10)	136.6(1)	N(1)	W(1)	C(1)	90.1(2)
O(1)	W(1)	C(1)	91.0(1)	C(2)	W(1)	C(11)	107.9(1)	C(9)	W(1)	C(10)	35.2(1)
O(1)	W(1)	C(2)	100.2(1)	C(2)	W(1)	C(12)	105.2(1)	N(1)	W(1)	C(2)	97.1(1)
O(1)	W(1)	C(8)	88.7(1)	C(2)	W(1)	C(18)	90.1(1)	C(9)	W(1)	C(11)	58.2(1)
O(1)	W(1)	C(9)	90.6(1)	C(8)	W(1)	C(9)	36.4(1)	N(1)	W(1)	C(8)	93.1(1)
O(1)	W(1)	C(10)	123.1(1)	C(8)	W(1)	C(10)	58.7(1)	C(9)	W(1)	C(12)	58.7(1)
O(1)	W(1)	C(11)	145.9(1)	C(8)	W(1)	C(11)	58.3(1)	N(1)	W(1)	C(9)	94.2(1)
O(1)	W(1)	C(12)	119.8(1)	C(8)	W(1)	C(12)	35.2(1)	C(9)	W(1)	C(18)	99.6(1)
O(1)	W(1)	C(18)	101.6(1)	C(8)	W(1)	C(18)	135.4(1)	C(10)	W(1)	C(11)	34.0(1)
N(1)	W(1)	C(10)	126.0(1)	N(1)	W(1)	C(11)	150.2(1)	C(10)	W(1)	C(12)	57.0(1)
N(1)	W(1)	C(12)	123.9(1)	C(10)	W(1)	C(18)	80.1(1)	C(2)	W(1)	C(8)	131.1(1)
N(1)	W(1)	C(18)	98.6(1)	C(11)	W(1)	C(12)	34.2(1)	O(1)	N(1)	C(8)	118.9(3)
C(1)	W(1)	C(2)	34.7(1)	C(11)	W(1)	C(18)	97.3(1)	C(2)	W(1)	C(9)	163.8(1)
C(1)	W(1)	C(8)	98.0(1)	C(12)	W(1)	C(18)	131.4(1)	C(1)	N(1)	C(8)	71.5(1)
C(1)	W(1)	C(9)	134.3(1)	W(1)	O(1)	N(1)	6.3(2)	W(1)	C(1)	N(1)	38.85(9)
C(1)	W(1)	C(10)	134.8(2)	W(1)	N(1)	O(1)	169.3(3)	C(4)	C(2)	C(6)	59.2(2)
C(1)	W(1)	C(11)	101.2(1)	W(1)	N(1)	C(1)	51.0(1)	W(1)	C(1)	C(2)	86.4(2)
C(1)	W(1)	C(12)	81.4(1)	W(1)	N(1)	C(8)	50.5(1)	C(4)	C(2)	C(7)	88.8(3)
C(1)	W(1)	C(18)	124.7(1)	O(1)	N(1)	C(1)	130.3(3)	W(1)	C(1)	C(3)	91.2(2)

Table A8. continued

C(5) C(2) C(6)	29.1(2)	W(1) C(1) C(7)	80.5(2)	C(5) C(2) C(7)	58.7(3)
N(1) C(1) C(2)	94.9(3)	C(6) C(2) C(7)	29.6(3)	C(1) C(2) C(3)	120.3(4)
N(1) C(1) C(3)	115.5(2)	C(1) C(3) C(2)	30.3(2)	C(1) C(2) C(4)	149.6(3)
N(1) C(1) C(7)	72.6(2)	C(1) C(3) C(4)	150.7(4)	C(4) C(3) C(7)	89.7(3)
C(2) C(1) C(3)	29.4(2)	C(1) C(3) C(5)	120.4(3)	C(5) C(3) C(6)	29.4(2)
C(2) C(1) C(7)	28.8(2)	C(1) C(3) C(6)	91.0(2)	C(1) C(2) C(5)	176.8(3)
C(3) C(1) C(7)	58.2(2)	C(1) C(3) C(7)	61.1(2)	C(5) C(3) C(7)	59.3(2)
W(1) C(2) C(1)	58.9(2)	C(2) C(3) C(4)	120.5(4)	C(1) C(2) C(6)	150.9(4)
W(1) C(2) C(3)	111.9(3)	C(2) C(3) C(5)	90.2(3)	C(6) C(3) C(7)	30.0(2)
W(1) C(2) C(4)	119.6(2)	C(2) C(3) C(6)	60.8(3)	C(1) C(2) C(7)	121.4(4)
W(1) C(2) C(5)	117.9(2)	C(2) C(3) C(7)	30.9(2)	C(2) C(4) C(3)	30.2(2)
W(1) C(2) C(6)	109.4(2)	C(4) C(3) C(5)	30.4(3)	C(3) C(2) C(4)	29.3(2)
W(1) C(2) C(7)	95.8(3)	C(4) C(3) C(6)	59.7(3)	C(2) C(4) C(5)	89.8(4)
C(3) C(2) C(5)	59.5(3)	C(2) C(4) C(6)	60.3(2)	C(3) C(5) C(4)	29.7(2)
C(3) C(2) C(6)	88.5(3)	C(2) C(4) C(7)	30.4(1)	C(3) C(7) C(5)	60.1(2)
C(3) C(2) C(7)	118.1(4)	C(3) C(4) C(5)	119.9(5)	C(3) C(5) C(6)	90.3(3)
C(4) C(2) C(5)	30.2(2)	C(3) C(4) C(6)	90.5(3)	C(3) C(7) C(6)	89.2(4)
C(3) C(4) C(7)	60.6(3)	C(1) C(7) C(4)	90.5(2)	C(3) C(5) C(7)	60.6(2)
C(5) C(4) C(6)	29.5(3)	C(1) C(7) C(5)	120.8(3)	C(4) C(7) C(5)	30.4(2)
C(5) C(4) C(7)	59.3(3)	C(1) C(7) C(6)	150.0(4)	C(4) C(5) C(6)	120.0(4)
C(6) C(4) C(7)	29.9(2)	C(2) C(7) C(3)	31.0(2)	C(4) C(7) C(6)	59.5(3)
C(2) C(5) C(3)	30.4(1)	C(2) C(7) C(4)	60.7(3)	C(4) C(5) C(7)	90.3(3)
C(2) C(5) C(4)	60.1(3)	C(2) C(7) C(5)	91.1(3)	C(5) C(7) C(6)	29.1(3)
C(2) C(5) C(6)	59.9(3)	C(2) C(7) C(6)	120.2(5)	C(6) C(5) C(7)	29.7(3)
C(2) C(5) C(7)	30.2(1)	C(3) C(7) C(4)	29.7(2)	W(1) C(8) N(1)	36.43(8)
C(2) C(6) C(3)	30.7(1)	W(1) C(8) C(9)	71.8(2)	N(1) C(8) C(14)	74.3(1)
C(2) C(6) C(4)	60.4(2)	W(1) C(8) C(10)	63.1(1)	W(1) C(9) C(12)	62.9(1)
C(2) C(6) C(5)	91.0(4)	W(1) C(8) C(11)	64.3(1)	C(1) C(7) C(3)	60.8(2)
C(2) C(6) C(7)	30.2(2)	W(1) C(8) C(12)	76.5(2)	N(1) C(8) C(17)	115.0(2)
C(3) C(6) C(4)	29.8(2)	W(1) C(8) C(13)	120.3(3)	W(1) C(9) C(13)	84.8(2)
C(3) C(6) C(5)	60.3(3)	W(1) C(8) C(14)	86.5(2)	N(1) C(8) C(13)	87.4(2)
C(3) C(6) C(7)	60.8(3)	W(1) C(8) C(17)	92.9(2)	C(1) C(7) C(2)	29.8(2)
C(4) C(6) C(5)	30.6(3)	N(1) C(8) C(9)	77.2(2)	N(1) C(8) C(12)	109.1(2)
C(4) C(6) C(7)	90.6(3)	N(1) C(8) C(10)	89.0(2)	C(12) C(8) C(13)	126.5(4)
C(5) C(6) C(7)	121.1(5)	N(1) C(8) C(11)	100.3(2)	C(11) C(9) C(14)	162.6(3)
C(9) C(8) C(10)	36.1(2)	W(1) C(9) C(14)	123.1(3)	C(12) C(8) C(14)	135.8(3)
C(9) C(8) C(11)	71.9(2)	W(1) C(9) C(15)	92.8(2)	C(11) C(9) C(15)	64.0(2)
C(9) C(8) C(12)	107.6(3)	C(8) C(9) C(10)	107.6(3)	C(12) C(8) C(17)	28.1(2)
C(9) C(8) C(13)	125.8(4)	C(8) C(9) C(11)	72.0(2)	C(12) C(9) C(13)	63.9(2)
C(9) C(8) C(14)	28.4(2)	C(8) C(9) C(12)	36.1(2)	C(13) C(8) C(14)	97.4(3)
C(9) C(8) C(17)	135.2(3)	C(8) C(9) C(13)	27.8(2)	C(12) C(9) C(14)	160.0(3)
C(10) C(8) C(11)	35.8(2)	C(8) C(9) C(14)	124.5(4)	C(13) C(8) C(17)	98.5(3)
C(10) C(8) C(12)	71.5(2)	C(8) C(9) C(15)	135.8(3)	C(12) C(9) C(15)	99.8(2)
C(10) C(8) C(13)	161.7(3)	C(10) C(9) C(11)	35.6(2)	C(14) C(8) C(17)	161.9(2)
C(10) C(8) C(14)	64.4(2)	C(10) C(9) C(12)	71.6(2)	C(13) C(9) C(14)	96.7(3)
C(10) C(8) C(17)	99.3(2)	C(10) C(9) C(13)	135.4(3)	W(1) C(9) C(8)	71.8(2)
C(11) C(8) C(12)	35.7(2)	C(10) C(9) C(14)	127.5(4)	C(13) C(9) C(15)	162.7(2)
C(11) C(8) C(13)	162.2(3)	C(10) C(9) C(15)	28.6(2)	W(1) C(9) C(10)	76.7(2)
C(11) C(8) C(14)	100.2(2)	C(11) C(9) C(12)	36.0(1)	C(14) C(9) C(15)	98.9(3)
C(11) C(8) C(17)	63.7(2)	C(11) C(9) C(13)	99.8(2)	W(1) C(9) C(11)	64.3(1)
W(1) C(10) C(9)	68.1(2)	C(12) C(10) C(15)	161.6(3)	W(1) C(10) C(8)	58.2(1)
W(1) C(10) C(11)	74.7(2)	C(12) C(10) C(16)	63.8(2)	C(11) C(10) C(12)	36.4(2)

Table A8. continued

W(1) C(10) C(12)	61.4(1)	C(12) C(10) C(18)	104.7(2)	C(8) C(11) C(16)	161.5(3)
W(1) C(10) C(14)	83.6(2)	C(14) C(10) C(15)	97.6(3)	C(11) C(10) C(14)	135.5(3)
W(1) C(10) C(15)	128.7(3)	C(14) C(10) C(16)	162.6(2)	C(8) C(11) C(17)	63.5(2)
W(1) C(10) C(16)	90.5(2)	C(14) C(10) C(18)	92.7(2)	C(9) C(11) C(10)	35.7(2)
W(1) C(10) C(18)	46.58(9)	C(15) C(10) C(16)	98.9(3)	C(11) C(10) C(15)	126.3(4)
C(8) C(10) C(9)	36.3(2)	C(15) C(10) C(18)	82.2(2)	C(11) C(10) C(16)	27.5(2)
C(8) C(10) C(11)	72.4(2)	C(16) C(10) C(18)	95.0(2)	(9) C(11) C(12)	71.7(2)
C(8) C(10) C(12)	36.0(1)	W(1) C(11) C(8)	57.5(1)	C(11) C(10) C(18)	99.4(2)
C(8) C(10) C(14)	63.2(2)	W(1) C(11) C(9)	57.5(1)	C(9) C(11) C(15)	63.2(2)
C(8) C(10) C(15)	159.9(3)	W(1) C(11) C(10)	71.2(2)	C(12) C(10) C(14)	99.1(2)
C(8) C(10) C(16)	99.9(2)	W(1) C(11) C(12)	71.0(2)	C(9) C(11) C(16)	162.1(3)
C(8) C(10) C(18)	103.0(2)	W(1) C(11) C(15)	88.9(2)	C(9) C(12) C(13)	63.8(2)
C(9) C(10) C(11)	108.7(3)	W(1) C(11) C(16)	127.1(3)	C(9) C(11) C(17)	99.4(2)
C(9) C(10) C(12)	72.3(2)	W(1) C(11) C(17)	89.3(2)	C(10) C(11) C(12)	107.4(3)
C(9) C(10) C(14)	27.0(2)	C(8) C(11) C(9)	36.1(1)	C(9) C(12) C(16)	100.0(2)
C(9) C(10) C(15)	124.5(4)	C(8) C(11) C(10)	71.7(2)	C(10) C(11) C(15)	27.7(2)
C(9) C(10) C(16)	136.2(3)	C(8) C(11) C(12)	35.6(2)	C(9) C(12) C(17)	160.5(3)
C(9) C(10) C(18)	96.2(2)	C(8) C(11) C(15)	99.1(2)	C(10) C(11) C(16)	126.5(4)
C(10) C(11) C(17)	134.8(3)	C(10) C(12) C(13)	99.9(2)	C(10) C(12) C(11)	36.3(2)
C(12) C(11) C(15)	134.5(3)	C(10) C(12) C(16)	63.9(2)	C(9) C(14) C(10)	25.6(2)
C(12) C(11) C(16)	125.9(4)	C(10) C(12) C(17)	160.3(3)	C(8) C(12) C(9)	36.3(2)
C(12) C(11) C(17)	28.0(2)	C(11) C(12) C(13)	136.2(3)	C(8) C(12) C(10)	72.4(2)
C(15) C(11) C(16)	98.9(3)	C(11) C(12) C(16)	27.7(2)	C(9) C(15) C(10)	26.9(2)
C(15) C(11) C(17)	160.1(2)	C(11) C(12) C(17)	125.4(4)	C(8) C(12) C(11)	108.7(3)
C(16) C(11) C(17)	98.0(3)	C(13) C(12) C(16)	163.7(2)	C(9) C(15) C(11)	52.8(1)
W(1) C(12) C(8)	68.3(2)	C(13) C(12) C(17)	97.9(3)	C(8) C(12) C(13)	27.5(2)
W(1) C(12) C(9)	58.3(1)	C(16) C(12) C(17)	97.8(3)	C(10) C(15) C(11)	26.0(2)
W(1) C(12) C(10)	61.6(1)	C(8) C(13) C(9)	26.4(2)	C(8) C(12) C(16)	136.3(3)
W(1) C(12) C(11)	74.8(2)	C(8) C(13) C(12)	25.9(2)	C(10) C(16) C(11)	26.0(2)
W(1) C(12) C(13)	82.7(2)	C(9) C(13) C(12)	52.3(1)	C(8) C(12) C(17)	125.3(4)
W(1) C(12) C(16)	90.6(2)	C(8) C(14) C(9)	27.1(2)	C(10) C(16) C(12)	52.3(1)
W(1) C(12) C(17)	129.6(3)	C(8) C(14) C(10)	52.5(1)	W(1) C(18) C(20)	158.4(2)
C(9) C(12) C(10)	36.1(1)	C(11) C(16) C(12)	26.3(2)	C(18) C(19) C(20)	119.1(3)
C(9) C(12) C(11)	72.3(2)	C(8) C(17) C(11)	52.9(1)	W(1) C(18) C(21)	172.5(2)
C(8) C(17) C(12)	26.5(2)	C(21) C(18) C(24)	88.4(2)	C(18) C(19) C(21)	90.7(3)
C(11) C(17) C(12)	26.5(2)	C(22) C(18) C(23)	27.5(2)	W(1) C(18) C(22)	143.0(2)
W(1) C(18) C(10)	53.3(1)	C(22) C(18) C(24)	117.9(2)	C(18) C(19) C(22)	61.1(2)
W(1) C(18) C(19)	128.2(3)	C(23) C(18) C(24)	145.4(3)	W(1) C(18) C(23)	115.5(3)
W(1) C(18) C(24)	99.1(2)	C(18) C(19) C(24)	123.3(3)	C(18) C(19) C(23)	31.7(2)
C(10) C(18) C(19)	120.0(3)	C(20) C(19) C(21)	28.5(2)	C(22) C(20) C(23)	30.6(1)
C(10) C(18) C(20)	128.2(2)	C(20) C(19) C(22)	58.1(2)	C(19) C(22) C(25)	178.5(3)
C(10) C(18) C(21)	125.1(2)	C(20) C(19) C(23)	87.5(3)	C(22) C(20) C(24)	124.5(2)
C(10) C(18) C(22)	111.9(2)	C(20) C(19) C(24)	117.5(4)	C(20) C(22) C(21)	29.9(2)
C(10) C(18) C(23)	95.3(2)	C(21) C(19) C(22)	29.6(1)	C(23) C(20) C(24)	93.9(2)
C(10) C(18) C(24)	104.9(2)	C(21) C(19) C(23)	59.0(2)	C(20) C(22) C(23)	87.8(3)
C(19) C(18) C(20)	30.3(2)	C(21) C(19) C(24)	146.0(3)	C(18) C(21) C(19)	30.0(1)
C(19) C(18) C(21)	59.3(2)	C(22) C(19) C(23)	29.4(1)	C(20) C(22) C(25)	151.8(3)
C(19) C(18) C(22)	88.8(2)	C(22) C(19) C(24)	175.6(3)	C(18) C(21) C(20)	59.1(2)
C(19) C(18) C(23)	116.3(3)	C(23) C(19) C(24)	155.0(3)	C(21) C(22) C(23)	117.6(4)
C(19) C(18) C(24)	29.1(2)	C(18) C(20) C(19)	30.6(2)	C(18) C(21) C(22)	60.8(2)
C(20) C(18) C(21)	29.1(1)	C(18) C(20) C(21)	91.9(3)	C(21) C(22) C(25)	121.9(4)
C(20) C(18) C(22)	58.6(2)	C(18) C(20) C(22)	61.6(2)	C(18) C(21) C(23)	29.7(1)
C(20) C(18) C(23)	86.1(2)	C(18) C(20) C(23)	31.0(1)	C(23) C(22) C(25)	120.5(4)

Table A8. continued

C(20) C(18) C(24)	59.4(2)	C(18) C(20) C(24)	62.9(2)	C(22) C(21) C(25)	30.2(2)
C(21) C(18) C(22)	29.5(1)	C(19) C(20) C(21)	122.5(4)	C(20) C(23) C(21)	30.4(1)
C(21) C(18) C(23)	57.0(2)	C(19) C(20) C(22)	92.2(3)	C(23) C(21) C(25)	61.3(2)
C(19) C(20) C(23)	61.6(2)	C(18) C(22) C(23)	27.9(2)	C(20) C(23) C(22)	61.6(2)
C(19) C(20) C(24)	32.3(2)	C(18) C(22) C(25)	148.4(3)	(18) C(22) C(19)	30.1(1)
C(21) C(20) C(22)	30.3(2)	C(19) C(22) C(20)	29.8(1)	C(20) C(23) C(25)	92.7(2)
C(21) C(20) C(23)	60.9(2)	C(19) C(22) C(21)	59.6(2)	C(18) C(22) C(20)	59.9(2)
C(21) C(20) C(24)	154.8(3)	C(19) C(22) C(23)	58.0(2)	C(21) C(23) C(22)	31.3(2)
C(18) C(21) C(25)	91.0(2)	C(18) C(23) C(19)	32.0(2)	C(18) C(22) C(21)	89.7(3)
C(19) C(21) C(20)	29.1(2)	C(18) C(23) C(20)	62.9(2)	C(21) C(23) C(25)	62.4(2)
C(19) C(21) C(22)	90.8(2)	C(18) C(23) C(21)	93.3(3)	C(22) C(23) C(25)	31.1(2)
C(19) C(21) C(23)	59.7(2)	C(18) C(23) C(22)	124.6(4)	C(18) C(24) C(19)	27.6(2)
C(19) C(21) C(25)	121.0(2)	C(18) C(23) C(25)	155.6(3)	C(18) C(24) C(20)	57.7(2)
C(20) C(21) C(22)	119.8(3)	C(19) C(23) C(20)	31.0(1)	C(19) C(24) C(20)	30.2(2)
C(20) C(21) C(23)	88.7(3)	C(19) C(23) C(21)	61.3(2)	C(21) C(25) C(22)	27.8(2)
C(20) C(21) C(25)	150.1(3)	C(19) C(23) C(22)	92.6(3)	C(21) C(25) C(23)	56.3(2)
C(22) C(21) C(23)	31.1(2)	C(19) C(23) C(25)	123.7(2)	C(22) C(25) C(23)	28.4(2)

Table A9. Select Dihedral Angles (°) in the Solid-State Molecular Structure Determined for 2.12

(1) (2) (3) (4)	angle	(1) (2) (3) (4)	angle
W(1) N(1) C(1) C(2)	78.1(2)	W(1) C(1) N(1) O(1)	166.3(4)
W(1) C(1) C(2) C(3)	-98.7(4)	W(1) C(8) N(1) O(1)	179.3(3)
W(1) C(12)C(11)C(8)	-60.2(3)	W(1) C(18)C(23)C(19)	179.0(5)
O(1) N(1) W(1) C(1)	-101(2)	O(1) N(1) W(1) C(18)	133(2)
N(1) C(1) C(2) C(4)	-134.3(5)	N(1) W(1) C(18)C(19)	-23.3(4)
N(1) W(1) C(18)C(21)	154(1)	N(1) W(1) C(18)C(22)	157.1(3)
N(1) W(1) C(18)C(23)	157.9(3)	C(1) W(1) C(8) C(9)	-176.5(2)
C(1) W(1) C(8) C(13)	62.2(3)	C(1) W(1) C(18)C(23)	61.7(3)
C(1) W(1) C(18)C(19)	-119.4(3)	C(1) C(2) C(3) C(4)	177.6(4)
C(1) W(1) C(18)C(20)	-119.2(5)	C(2) W(1) C(9) C(13)	70.4(5)
C(2) W(1) C(18)C(19)	-120.5(3)	C(2) W(1) C(10)C(8)	118.4(2)
C(2) W(1) C(18)C(22)	59.9(3)	C(2) W(1) C(10)C(9)	157.8(2)
C(2) W(1) C(18)C(23)	60.7(3)	C(6) C(2) C(3) C(7)	-0.6(3)
C(8) W(1) C(9) C(10)	-113.9(3)	C(8) W(1) C(18)C(19)	80.1(4)
C(8) C(9) C(12)C(10)	179.9(4)	C(18)C(19)C(20)C(21)	-0.5(6)

**Table A10.** Fractional Atomic Coordinates in the Solid-State Molecular Structure Determined for **2.12**

atom	x	y	z	B(eq)	atom	x	y	z	B(eq)
W(1)	0.18170(1)	0.27926(1)	0.177641(7)	0.851(4)	O(1)	0.1930(4)	0.5879(4)	0.0383(2)	2.42(7)
N(1)	0.1826(4)	0.4709(4)	0.1013(2)	1.27(6)	C(1)	-0.0835(5)	0.3216(5)	0.1758(3)	1.68(8)
C(2)	-0.1011(5)	0.3654(5)	0.2603(3)	1.54(8)	C(3)	-0.1275(5)	0.2484(6)	0.3403(3)	1.97(9)
C(4)	-0.1382(6)	0.2873(7)	0.4207(3)	3.1(1)	C(5)	-0.1161(6)	0.4419(9)	0.4235(4)	4.0(1)
C(6)	-0.0903(6)	0.5552(8)	0.3469(4)	3.6(1)	C(7)	-0.0810(5)	0.5198(6)	0.2653(3)	2.30(9)
C(8)	0.2659(5)	0.1326(5)	0.0697(2)	1.33(7)	C(9)	0.4087(5)	0.1380(5)	0.1047(2)	1.26(7)
C(10)	0.4060(5)	0.0394(5)	0.1930(2)	1.50(8)	C(11)	0.2615(5)	-0.0236(5)	0.2140(3)	1.49(7)
C(12)	0.1772(5)	0.0313(5)	0.1369(2)	1.41(8)	C(13)	0.2243(6)	0.2114(6)	-0.0233(3)	2.29(9)
C(14)	0.5441(5)	0.2166(6)	0.0518(3)	2.24(9)	C(15)	0.5448(6)	-0.0059(6)	0.2491(3)	2.5(1)
C(16)	0.2136(6)	-0.1387(5)	0.2984(3)	2.6(1)	C(17)	0.0336(6)	-0.0283(6)	0.1243(3)	2.7(1)
C(18)	0.2965(4)	0.3181(5)	0.2811(2)	1.13(7)	C(19)	0.4001(5)	0.4276(5)	0.2729(2)	1.41(7)
C(20)	0.4614(5)	0.4340(5)	0.3486(3)	1.74(8)	C(21)	0.4239(5)	0.3385(5)	0.4312(3)	1.86(9)
C(22)	0.3250(5)	0.2271(5)	0.4413(2)	1.48(7)	C(23)	0.2656(5)	0.2197(5)	0.3662(2)	1.32(7)
C(24)	0.4484(5)	0.5378(5)	0.1872(3)	1.99(9)	C(25)	0.2821(6)	0.1184(6)	0.5299(3)	2.34(9)
H(1)	-0.1300	0.4117	0.1276	1.9834	H(2)	-0.1233	0.2231	0.1779	1.9834
H(3)	-0.1383	0.1387	0.3397	2.4920	H(4)	-0.1631	0.2065	0.4755	3.6347
H(5)	-0.1174	0.4639	0.4818	5.0885	H(6)	-0.0761	0.6621	0.3500	4.2038
H(7)	-0.0612	0.6035	0.2108	2.9200	H(8)	0.3057	0.2735	-0.0557	2.8453
H(9)	0.2246	0.1244	-0.0532	2.8453	H(10)	0.1151	0.2852	-0.0221	2.8453
H(11)	0.6283	0.2051	0.0898	2.6796	H(12)	0.5937	0.1632	0.0030	2.6796
H(13)	0.4995	0.3347	0.0276	2.6796	H(14)	0.5116	-0.0734	0.3075	3.0232
H(15)	0.6415	-0.0707	0.2209	3.0232	H(16)	0.5682	0.0935	0.2568	3.0232
H(17)	0.2032	-0.0854	0.3482	3.3254	H(18)	0.1081	-0.1620	0.2964	3.3254
H(19)	0.2978	-0.2411	0.3082	3.3254	H(20)	-0.0552	0.0683	0.1042	3.2767
H(21)	0.0665	-0.0933	0.0794	3.2767	H(22)	-0.0061	-0.0949	0.1801	3.2767

**Table A11.** Bond Distances (Å) in the Solid-State Molecular Structure Determined for **2.14**

atom	atom	distance	atom	atom	distance	atom	atom	distance	atom	atom	distance
W(1)	N(1)	1.764(3)	C(6)	C(9)	1.525(7)	C(1)	C(2)	1.467(6)	C(17)	C(22)	1.499(6)
W(1)	C(1)	2.181(4)	C(10)	C(11)	1.500(6)	C(2)	C(3)	1.405(6)	C(18)	C(19)	1.432(6)
W(1)	C(2)	2.491(4)	C(11)	C(12)	1.389(6)	C(2)	C(7)	1.391(6)	C(18)	C(23)	1.494(6)
W(1)	C(10)	2.225(4)	C(11)	C(16)	1.392(6)	C(3)	C(4)	1.394(6)	C(19)	C(20)	1.410(6)
W(1)	C(17)	2.310(4)	C(12)	C(13)	1.385(7)	C(4)	C(5)	1.398(7)	C(19)	C(24)	1.517(6)
W(1)	C(18)	2.377(4)	C(13)	C(14)	1.382(8)	C(4)	C(8)	1.505(6)	C(20)	C(21)	1.434(6)
W(1)	C(19)	2.435(4)	C(14)	C(15)	1.380(8)	C(5)	C(6)	1.390(7)	C(20)	C(25)	1.489(6)
W(1)	C(20)	2.418(4)	C(15)	C(16)	1.385(7)	O(1)	N(1)	1.231(5)	C(17)	C(21)	1.426(6)
W(1)	C(21)	2.313(4)	C(17)	C(18)	1.418(6)	C(6)	C(7)	1.388(6)	C(21)	C(26)	1.508(6)

**Table A12.** Bond Angles (°) in the Solid-State Molecular Structure Determined for 2.14

atom	atom	atom	angle	atom	atom	atom	angle	atom	atom	atom	angle	°
N(1)	W(1)	C(1)	94.0(2)	C(17)	W(1)	C(18)	35.2(1)	N(1)	W(1)	C(17)	89.5(2)	
N(1)	W(1)	C(2)	94.0(1)	C(17)	W(1)	C(19)	57.9(1)	C(17)	W(1)	C(21)	35.9(1)	
N(1)	W(1)	C(10)	94.9(2)	C(17)	W(1)	C(20)	58.5(1)	N(1)	W(1)	C(18)	112.0(2)	
N(1)	W(1)	C(19)	145.7(2)	C(18)	W(1)	C(20)	57.6(1)	C(18)	W(1)	C(19)	34.6(1)	
N(1)	W(1)	C(20)	138.1(2)	C(18)	W(1)	C(21)	58.8(1)	N(1)	W(1)	C(21)	103.0(2)	
C(1)	W(1)	C(2)	35.8(1)	C(19)	W(1)	C(21)	57.8(1)	C(19)	W(1)	C(20)	33.8(1)	
C(1)	W(1)	C(10)	124.0(1)	C(20)	W(1)	C(21)	35.2(1)	C(1)	W(1)	C(18)	80.0(2)	
C(1)	W(1)	C(17)	108.6(2)	W(1)	N(1)	O(1)	170.4(3)	W(1)	C(1)	C(2)	83.7(2)	
C(1)	W(1)	C(19)	87.5(2)	W(1)	C(2)	C(1)	60.5(2)	C(1)	W(1)	C(21)	138.8(2)	
C(1)	W(1)	C(20)	120.2(2)	W(1)	C(2)	C(3)	95.6(2)	W(1)	C(2)	C(7)	107.1(3)	
C(2)	W(1)	C(10)	88.4(1)	C(1)	C(2)	C(3)	119.0(4)	C(2)	W(1)	C(18)	113.0(1)	
C(2)	W(1)	C(17)	144.4(1)	C(1)	C(2)	C(7)	121.9(4)	C(3)	C(2)	C(7)	118.6(4)	
C(2)	W(1)	C(19)	106.5(1)	C(2)	C(3)	C(4)	120.8(4)	C(2)	W(1)	C(21)	162.9(1)	
C(2)	W(1)	C(20)	127.9(1)	C(3)	C(4)	C(5)	118.8(4)	C(3)	C(4)	C(8)	120.8(4)	
C(10)	W(1)	C(17)	126.7(1)	C(5)	C(4)	C(8)	120.3(4)	C(18)	C(17)	C(22)	126.8(4)	
C(10)	W(1)	C(18)	143.3(1)	C(4)	C(5)	C(6)	121.2(4)	C(21)	C(17)	C(22)	124.9(4)	
C(10)	W(1)	C(19)	112.5(1)	C(5)	C(6)	C(7)	118.9(4)	W(1)	C(18)	C(17)	69.8(2)	
C(10)	W(1)	C(20)	85.7(1)	C(5)	C(6)	C(9)	120.4(4)	W(1)	C(18)	C(19)	74.9(2)	
C(10)	W(1)	C(21)	92.0(1)	C(7)	C(6)	C(9)	120.7(4)	W(1)	C(18)	C(23)	127.1(3)	
C(2)	C(7)	C(6)	121.6(4)	C(18)	C(19)	C(24)	124.5(4)	C(17)	C(18)	C(19)	107.6(4)	
W(1)	C(10)	C(11)	120.1(3)	C(20)	C(19)	C(24)	126.6(4)	C(19)	C(18)	C(23)	126.7(4)	
C(10)	C(11)	C(12)	122.0(4)	W(1)	C(20)	C(19)	73.8(2)	C(17)	C(18)	C(23)	125.2(4)	
C(10)	C(11)	C(16)	120.9(4)	W(1)	C(20)	C(21)	68.4(2)	W(1)	C(19)	C(18)	70.5(2)	
C(12)	C(11)	C(16)	117.0(4)	W(1)	C(20)	C(25)	127.9(3)	W(1)	C(19)	C(24)	126.8(3)	
C(11)	C(12)	C(13)	122.0(4)	C(19)	C(20)	C(21)	107.7(4)	W(1)	C(19)	C(20)	72.4(2)	
C(12)	C(13)	C(14)	119.2(4)	C(19)	C(20)	C(25)	125.5(4)	C(18)	C(19)	C(20)	108.7(4)	
C(13)	C(14)	C(15)	120.7(5)	C(21)	C(20)	C(25)	126.5(4)	C(18)	C(17)	C(21)	108.2(4)	
C(14)	C(15)	C(16)	118.9(5)	W(1)	C(21)	C(17)	71.9(2)	C(17)	C(21)	C(26)	124.2(4)	
C(11)	C(16)	C(15)	122.2(4)	W(1)	C(21)	C(20)	76.4(2)	C(20)	C(21)	C(26)	127.0(4)	
W(1)	C(17)	C(18)	75.0(2)	W(1)	C(21)	C(26)	125.9(3)	W(1)	C(17)	C(22)	121.3(3)	
W(1)	C(17)	C(21)	72.1(2)	C(17)	C(21)	C(20)	107.8(4)					

**Table A13.** Dihedral Angles (°) in the Solid-State Molecular Structure Determined for 2.14

(1)	(2)	(3)	(4)	angle	(1)	(2)	(3)	(4)	angle	(1)	(2)	(3)	(4)	angle
W(1)	C(1)	C(2)	C(3)	-79.3(3)	O(1)	N(1)	W(1)	C(1)	-110(2)	N(1)	W(1)	C(21)	C(20)	175.2(3)
W(1)	C(1)	C(2)	C(7)	92.6(4)	O(1)	N(1)	W(1)	C(2)	-146(2)	C(1)	C(2)	C(3)	C(4)	173.4(4)
W(1)	C(2)	C(3)	C(4)	114.2(4)	O(1)	N(1)	W(1)	C(10)	126(2)	N(1)	W(1)	C(21)	C(26)	49.1(4)
W(1)	C(2)	C(7)	C(6)	-107.4(4)	O(1)	N(1)	W(1)	C(17)	-1(2)	C(1)	C(2)	C(7)	C(6)	-172.9(4)
W(1)	C(10)	C(11)	C(12)	-123.4(4)	O(1)	N(1)	W(1)	C(18)	-29(2)	C(1)	W(1)	C(2)	C(3)	120.3(4)
W(1)	C(10)	C(11)	C(16)	60.1(5)	O(1)	N(1)	W(1)	C(19)	-18(2)	C(2)	W(1)	C(10)	C(11)	-142.9(3)
W(1)	C(17)	C(18)	C(19)	-66.0(3)	O(1)	N(1)	W(1)	C(20)	37(2)	C(1)	W(1)	C(2)	C(7)	-117.5(4)
W(1)	C(17)	C(18)	C(23)	121.9(4)	O(1)	N(1)	W(1)	C(21)	32(2)	C(2)	W(1)	C(17)	C(18)	-35.3(3)
W(1)	C(17)	C(21)	C(20)	68.6(3)	N(1)	W(1)	C(1)	C(2)	-91.3(3)	C(1)	W(1)	C(10)	C(11)	-147.2(3)
W(1)	C(17)	C(21)	C(26)	-121.5(4)	N(1)	W(1)	C(2)	C(1)	91.3(3)	C(2)	W(1)	C(17)	C(21)	-150.5(3)
W(1)	C(18)	C(17)	C(21)	65.0(3)	N(1)	W(1)	C(2)	C(3)	-148.4(3)	C(1)	W(1)	C(17)	C(18)	-37.4(3)
W(1)	C(18)	C(17)	C(22)	-118.2(4)	N(1)	W(1)	C(2)	C(7)	-26.2(3)	C(2)	W(1)	C(17)	C(22)	89.0(4)

Table A13. continued

W(1) C(18)C(19)C(20) -62.7(3)	N(1) W(1) C(10)C(11) -49.1(3)	C(1) W(1) C(17)C(21) -152.6(2)
W(1) C(18)C(19)C(24) 121.8(4)	N(1) W(1) C(17)C(18) -131.5(2)	C(2) W(1) C(18)C(17) 158.6(2)
W(1) C(19)C(18)C(17) 62.6(3)	N(1) W(1) C(17)C(21) 113.3(3)	C(1) W(1) C(17)C(22) 86.8(4)
W(1) C(19)C(18)C(23) -125.4(4)	N(1) W(1) C(17)C(22) -7.2(4)	C(2) W(1) C(18)C(19) -85.9(3)
W(1) C(19)C(20)C(21) -60.4(3)	N(1) W(1) C(18)C(17) 53.9(3)	C(1) W(1) C(18)C(17) 144.2(3)
W(1) C(19)C(20)C(25) 125.4(4)	N(1) W(1) C(18)C(19) 169.5(2)	C(2) W(1) C(18)C(23) 39.1(4)
W(1) C(20)C(19)C(18) 61.5(3)	N(1) W(1) C(18)C(23) -65.5(4)	C(1) W(1) C(18)C(19) -100.2(3)
W(1) C(20)C(19)C(24) -123.2(4)	N(1) W(1) C(19)C(18) -17.4(4)	C(2) W(1) C(19)C(18) 106.7(3)
W(1) C(20)C(21)C(17) -65.6(3)	N(1) W(1) C(19)C(20) 100.5(3)	C(1) W(1) C(18)C(23) 24.8(4)
W(1) C(20)C(21)C(26) 124.9(4)	N(1) W(1) C(19)C(24) -136.5(4)	C(2) W(1) C(19)C(20) -135.3(2)
W(1) C(21)C(17)C(18) -66.9(3)	N(1) W(1) C(20)C(19) -124.0(3)	C(1) W(1) C(19)C(18) 76.0(3)
W(1) C(21)C(17)C(22) 116.2(4)	N(1) W(1) C(20)C(21) -6.9(4)	C(2) W(1) C(19)C(24) -12.4(4)
W(1) C(21)C(20)C(19) 63.8(3)	N(1) W(1) C(20)C(25) 113.3(4)	C(1) W(1) C(19)C(20) -166.1(3)
W(1) C(21)C(20)C(25) -122.0(4)	N(1) W(1) C(21)C(17) -70.5(3)	C(2) W(1) C(20)C(19) 58.8(3)
C(1) W(1) C(19)C(24) -43.1(4)	C(2) W(1) C(20)C(21) 175.8(2)	C(2) C(7) C(6) C(5) 0.4(7)
C(1) W(1) C(20)C(19) 16.2(3)	C(2) W(1) C(20)C(25) -64.0(5)	C(10)W(1) C(19)C(18) -158.0(2)
C(1) W(1) C(20)C(21) 133.2(3)	C(2) W(1) C(21)C(17) 103.0(5)	C(2) C(7) C(6) C(9) 177.7(4)
C(1) W(1) C(20)C(25) -106.6(4)	C(2) W(1) C(21)C(20) -11.2(6)	C(10)W(1) C(19)C(20) -40.1(3)
C(1) W(1) C(21)C(17) 41.4(4)	C(2) W(1) C(21)C(26) -137.4(5)	C(3) C(2) W(1) C(10) -53.6(3)
C(1) W(1) C(21)C(20) -72.9(3)	C(2) C(1) W(1) C(10) 7.4(3)	C(10)W(1) C(19)C(24) 82.9(4)
C(1) W(1) C(21)C(26) 161.0(3)	C(2) C(1) W(1) C(17) 177.9(2)	C(3) C(2) W(1) C(17) 116.9(3)
C(1) C(2) W(1) C(10) -173.9(3)	C(2) C(1) W(1) C(18) 157.1(3)	C(10)W(1) C(20)C(19) 143.4(3)
C(1) C(2) W(1) C(17) -3.4(4)	C(2) C(1) W(1) C(19) 123.1(3)	C(3) C(2) W(1) C(18) 95.7(3)
C(1) C(2) W(1) C(18) -24.6(3)	C(2) C(1) W(1) C(20) 114.1(2)	C(10)W(1) C(20)C(21) -99.5(3)
C(1) C(2) W(1) C(19) -60.8(3)	C(2) C(1) W(1) C(21) 153.7(2)	C(3) C(2) W(1) C(19) 59.5(3)
C(1) C(2) W(1) C(20) -90.5(3)	C(2) C(3) C(4) C(5) -1.0(6)	C(10)W(1) C(20)C(25) 20.7(4)
C(1) C(2) W(1) C(21) -82.4(5)	C(2) C(3) C(4) C(8) -178.1(4)	C(3) C(2) W(1) C(20) 29.8(3)
C(3) C(2) W(1) C(21) 37.9(6)	C(10)W(1) C(21)C(20) 79.7(3)	C(10)W(1) C(21)C(17) -166.0(2)
C(3) C(2) C(7) C(6) -1.0(6)	C(10)W(1) C(21)C(26) -46.4(4)	C(7) C(2) W(1) C(10) 68.6(3)
C(3) C(4) C(5) C(6) 0.5(6)	C(10)C(11)C(12)C(13) -176.9(5)	C(11)C(10)W(1) C(20) 88.9(3)
C(4) C(3) C(2) C(7) 1.3(6)	C(10)C(11)C(16)C(15) 177.7(4)	C(11)C(10)W(1) C(21) 54.2(3)
C(4) C(5) C(6) C(7) -0.1(7)	C(11)C(10)W(1) C(17) 44.0(4)	C(7) C(2) W(1) C(17) -120.9(3)
C(4) C(5) C(6) C(9) -177.4(4)	C(11)C(10)W(1) C(18) 89.1(4)	C(7) C(2) W(1) C(18) -142.1(3)
C(6) C(5) C(4) C(8) 177.6(4)	C(11)C(10)W(1) C(19) 109.9(3)	C(11)C(12)C(13)C(14) -0.9(9)
C(7) C(2) W(1) C(19) -178.3(3)	C(11)C(16)C(15)C(14) -0.5(8)	C(7) C(2) W(1) C(21) 160.2(4)
C(7) C(2) W(1) C(20) 152.0(3)	C(12)C(11)C(16)C(15) 1.0(7)	C(12)C(13)C(14)C(15) 1.5(9)
C(10)W(1) C(17)C(18) 132.8(2)	C(13)C(12)C(11)C(16) -0.3(7)	C(18)W(1) C(17)C(21) -115.2(3)
C(10)W(1) C(17)C(21) 17.5(3)	C(13)C(14)C(15)C(16) -0.8(9)	C(19)C(18)W(1) C(21) 77.2(3)
C(10)W(1) C(17)C(22) -103.0(4)	C(17)W(1) C(18)C(19) 115.6(3)	C(18)W(1) C(17)C(22) 124.2(4)
C(10)W(1) C(18)C(17) -80.3(3)	C(17)W(1) C(18)C(23) -119.5(5)	C(18)W(1) C(19)C(20) 118.0(4)
C(10)W(1) C(18)C(19) 35.3(4)	C(17)W(1) C(19)C(18) -37.9(2)	C(19)C(18)C(17)C(21) -1.0(5)
C(10)W(1) C(18)C(23) 160.3(3)	C(17)W(1) C(19)C(20) 80.1(3)	C(19)C(18)C(17)C(22) 175.8(4)
C(17)W(1) C(19)C(24) -156.9(5)	C(18)C(17)W(1) C(20) 77.2(3)	C(18)W(1) C(19)C(24) -119.1(5)
C(17)W(1) C(20)C(19) -78.2(3)	C(18)C(17)W(1) C(21) 115.2(3)	C(19)C(20)W(1) C(21) -117.1(4)
C(17)W(1) C(20)C(21) 38.9(2)	C(18)C(17)C(21)C(20) 1.7(5)	C(20)C(19)W(1) C(21) 37.4(2)
C(17)W(1) C(20)C(25) 159.1(5)	C(18)C(17)C(21)C(26) 171.6(4)	C(20)C(19)C(18)C(23) 171.9(4)
C(17)W(1) C(21)C(20) -114.3(4)	C(18)C(19)W(1) C(20) -118.0(4)	C(20)C(21)C(17)C(22) -175.2(4)
C(17)W(1) C(21)C(26) 119.6(5)	C(18)C(19)W(1) C(21) -80.6(3)	C(21)W(1) C(17)C(22) -120.5(5)
C(17)C(18)W(1) C(19) -115.6(3)	C(18)C(19)C(20)C(21) 1.1(5)	C(21)W(1) C(18)C(23) -157.8(4)
C(17)C(18)W(1) C(20) -80.0(3)	C(18)C(19)C(20)C(25) -173.1(4)	C(21)W(1) C(19)C(24) 160.3(4)
C(17)C(18)W(1) C(21) -38.4(2)	C(19)W(1) C(17)C(21) -78.0(3)	C(21)W(1) C(20)C(25) 120.2(5)
C(17)C(18)C(19)C(20) -0.1(5)	C(19)W(1) C(17)C(22) 161.4(4)	C(21)C(17)C(18)C(23) -173.1(4)
C(17)C(18)C(19)C(24) -175.6(4)	C(19)W(1) C(18)C(23) 125.0(5)	C(21)C(20)C(19)C(24) 176.5(4)

Table A13. continued

C(17)C(21)W(1) C(18)	37.5(2)	C(19)W(1) C(20)C(21)	117.1(4)	C(22)C(17)C(18)C(23)	3.7(7)
C(17)C(21)W(1) C(19)	78.4(3)	C(19)W(1) C(20)C(25)	-122.7(5)	C(22)C(17)C(21)C(26)	-5.3(7)
C(17)C(21)W(1) C(20)	114.3(4)	C(19)W(1) C(21)C(20)	-35.8(2)	C(23)C(18)C(19)C(24)	-3.6(7)
C(17)C(21)C(20)C(19)	-1.7(5)	C(19)W(1) C(21)C(26)	-162.0(4)	C(24)C(19)C(20)C(25)	2.2(7)
C(17)C(21)C(20)C(25)	172.5(4)	C(19)C(18)W(1) C(20)	35.6(2)	C(25)C(20)C(21)C(26)	3.0(7)
C(18)W(1) C(20)C(19)	-36.4(2)	C(19)C(20)C(21)C(26)	-171.3(4)	C(20)W(1) C(21)C(26)	-126.1(5)
C(18)W(1) C(20)C(21)	80.6(3)	C(20)W(1) C(17)C(21)	-38.0(2)	C(18)C(17)W(1) C(19)	37.2(2)
C(18)W(1) C(20)C(25)	-159.2(5)	C(20)W(1) C(17)C(22)	-158.6(4)	C(20)W(1) C(19)C(24)	122.9(5)
C(18)W(1) C(21)C(20)	-76.7(3)	C(20)W(1) C(18)C(23)	160.5(5)	C(18)W(1) C(21)C(26)	157.1(4)

Table A14. Fractional Atomic Coordinates in the Solid-State Molecular Structure Determined for 2.14

atom	x	y	z	B(eq)	atom	x	y	z	B(eq)
W(1)	0.69108(2)	0.374242(5)	0.17644(1)	0.809(4)	H(1)	0.7341	0.4106	-0.0754	1.6577
O(1)	1.0037(4)	0.3335(1)	0.1614(4)	2.53(8)	H(2)	0.5609	0.4255	-0.0626	1.6577
N(1)	0.8812(4)	0.3542(1)	0.1708(4)	1.18(7)	H(3)	0.5197	0.4753	0.1420	1.8079
C(1)	0.6683(5)	0.4200(2)	-0.0103(4)	1.40(8)	H(4)	0.8939	0.5472	0.3819	2.1934
C(2)	0.7321(5)	0.4585(1)	0.0908(4)	1.21(8)	H(5)	0.9623	0.4513	0.0778	1.6964
C(3)	0.6323(5)	0.4822(1)	0.1651(5)	1.47(8)	H(6)	0.5934	0.5754	0.3475	2.9202
C(4)	0.6911(6)	0.5154(2)	0.2721(5)	1.75(9)	H(7)	0.4768	0.5295	0.3168	2.9202
C(5)	0.8520(6)	0.5242(2)	0.3060(5)	1.81(9)	H(8)	0.6157	0.5296	0.4530	2.9202
C(6)	0.9529(5)	0.5009(2)	0.2346(5)	1.72(8)	H(9)	1.1668	0.4992	0.3742	3.3592
C(7)	0.8916(5)	0.4682(2)	0.1280(4)	1.39(8)	H(10)	1.1817	0.4907	0.2154	3.3592
C(8)	0.5847(6)	0.5395(2)	0.3546(5)	2.4(1)	H(11)	1.1504	0.5447	0.2681	3.3592
C(9)	1.1287(6)	0.5094(2)	0.2774(6)	2.8(1)	H(12)	0.8171	0.4331	0.3902	1.3378
C(10)	0.7563(5)	0.4030(1)	0.3944(4)	1.12(7)	H(13)	0.6587	0.4113	0.4226	1.3378
C(11)	0.8498(5)	0.3717(1)	0.5087(4)	1.19(8)	H(14)	0.6933	0.3718	0.6384	2.3509
C(12)	0.7972(6)	0.3604(2)	0.6295(5)	1.97(9)	H(15)	0.8478	0.3262	0.8225	3.2982
C(13)	0.8868(6)	0.3335(2)	0.7378(5)	2.8(1)	H(16)	1.0954	0.2973	0.8001	3.6602
C(14)	1.0322(7)	0.3168(2)	0.7249(6)	3.0(1)	H(17)	1.1935	0.3162	0.5992	3.1782
C(15)	1.0896(6)	0.3277(2)	0.6073(5)	2.7(1)	H(18)	1.0391	0.3631	0.4175	1.8464
C(16)	0.9982(5)	0.3551(2)	0.5011(5)	1.58(8)	H(19)	0.6658	0.2255	0.0910	2.0772
C(17)	0.5968(5)	0.2966(1)	0.1090(4)	1.15(7)	H(20)	0.6923	0.2599	-0.0349	2.0772
C(18)	0.4961(5)	0.3294(2)	0.0191(4)	1.21(8)	H(21)	0.8080	0.2637	0.1155	2.0772
C(19)	0.4125(5)	0.3572(2)	0.1038(5)	1.40(8)	H(22)	0.3931	0.3550	-0.1752	2.6244
C(20)	0.4607(5)	0.3419(2)	0.2443(5)	1.43(8)	H(23)	0.5664	0.3347	-0.1666	2.6244
C(21)	0.5779(5)	0.3047(1)	0.2488(4)	1.37(8)	H(24)	0.4248	0.2970	-0.1724	2.6244
C(22)	0.6995(5)	0.2580(2)	0.0664(5)	1.72(9)	H(25)	0.2458	0.4084	0.1258	2.8700
C(23)	0.4677(6)	0.3291(2)	-0.1372(5)	2.2(1)	H(26)	0.3265	0.4201	-0.0031	2.8700
C(24)	0.2844(5)	0.3940(2)	0.0471(6)	2.4(1)	H(27)	0.1987	0.3773	-0.0162	2.8700
C(25)	0.3901(6)	0.3580(2)	0.3628(6)	2.6(1)	H(28)	0.3995	0.3936	0.3737	3.0709
C(26)	0.6486(6)	0.2727(2)	0.3720(5)	2.1(1)	H(29)	0.2796	0.3485	0.3437	3.0709
H(30)	0.4451	0.3418	0.4493	3.0709	H(32)	0.6110	0.2390	0.3543	2.5166
H(31)	0.6183	0.2854	0.4565	2.5166	H(33)	0.7627	0.2735	0.3852	2.5166

**Table A15.** Bond Distances (Å) in the Solid-State Molecular Structure Determined for **5.10**

atom	atom	distance	atom	atom	distance	atom	atom	distance	atom	atom	distance
W(1)	N(1)	1.762(3)	C(5)	C(6)	1.401(6)	O(1)	N(1)	1.224(4)	C(13)	C(18)	1.510(6)
W(1)	C(1)	2.186(3)	C(7)	C(8)	1.439(6)	C(1)	C(2)	1.406(5)	C(14)	C(15)	1.403(6)
W(1)	C(7)	2.218(4)	C(8)	C(9)	1.365(5)	C(1)	C(6)	1.397(4)	C(14)	C(19)	1.501(5)
W(1)	C(8)	2.363(4)	C(9)	C(10)	1.495(5)	C(2)	C(3)	1.383(5)	C(15)	C(16)	1.405(5)
W(1)	C(12)	2.306(3)	C(9)	C(11)	1.500(5)	C(3)	C(4)	1.375(6)	C(15)	C(20)	1.489(6)
W(1)	C(13)	2.398(3)	C(12)	C(13)	1.411(6)	W(1)	C(14)	2.430(3)	C(12)	C(16)	1.408(6)
W(1)	C(15)	2.389(3)	C(12)	C(17)	1.513(6)	C(4)	C(5)	1.368(7)	C(16)	C(21)	1.502(5)
W(1)	C(16)	2.306(3)	C(13)	C(14)	1.409(7)	C(7)	H(7)	0.91(4)	C(19)	H(22)	0.984
C(7)	H(6)	1.06(4)	C(19)	H(21)	0.981	C(8)	H(8)	1.00(5)			

**Table A16.** Bond Angles (°) in the Solid-State Molecular Structure Determined for **5.10**

atom	atom	atom	angle	atom	atom	atom	angle	atom	atom	atom	angle
N(1)	W(1)	C(1)	93.3(1)	C(12)	W(1)	C(13)	34.8(2)	N(1)	W(1)	C(16)	92.3(1)
N(1)	W(1)	C(7)	92.1(2)	C(12)	W(1)	C(14)	57.8(1)	C(14)	W(1)	C(15)	33.8(1)
N(1)	W(1)	C(8)	104.6(1)	C(12)	W(1)	C(15)	57.8(1)	N(1)	W(1)	C(15)	121.7(1)
N(1)	W(1)	C(12)	95.4(1)	C(12)	W(1)	C(16)	35.6(1)	C(13)	W(1)	C(16)	57.8(1)
N(1)	W(1)	C(13)	127.7(1)	C(13)	W(1)	C(14)	33.9(2)	C(13)	W(1)	C(15)	56.4(1)
C(1)	W(1)	C(7)	130.1(1)	C(14)	W(1)	C(16)	57.6(1)	W(1)	C(16)	C(15)	75.9(2)
C(1)	W(1)	C(8)	94.7(1)	C(15)	W(1)	C(16)	34.8(1)	W(1)	C(16)	C(12)	72.2(2)
C(1)	W(1)	C(12)	133.1(1)	W(1)	N(1)	O(1)	169.5(3)	C(16)	C(15)	C(20)	124.6(5)
C(1)	W(1)	C(13)	129.6(1)	W(1)	C(1)	C(2)	123.0(2)	C(14)	C(15)	C(20)	125.7(5)
C(1)	W(1)	C(14)	95.8(1)	W(1)	C(1)	C(6)	121.4(2)	C(14)	C(15)	C(16)	109.0(3)
C(1)	W(1)	C(15)	78.5(1)	C(2)	C(1)	C(6)	115.5(3)	W(1)	C(15)	C(20)	129.5(3)
C(1)	W(1)	C(16)	98.2(1)	C(1)	C(2)	C(3)	122.5(3)	W(1)	C(15)	C(16)	69.4(2)
C(7)	W(1)	C(8)	36.4(2)	C(2)	C(3)	C(4)	120.3(4)	W(1)	C(15)	C(14)	74.7(2)
C(7)	W(1)	C(12)	95.5(1)	C(3)	C(4)	C(5)	119.3(4)	C(15)	C(14)	C(19)	128.7(5)
C(7)	W(1)	C(13)	81.8(1)	C(4)	C(5)	C(6)	120.4(4)	C(13)	C(14)	C(19)	123.8(5)
C(7)	W(1)	C(14)	103.8(2)	C(1)	C(6)	C(5)	121.9(4)	C(13)	C(14)	C(15)	107.1(3)
C(7)	W(1)	C(15)	136.5(1)	W(1)	C(7)	C(8)	77.3(2)	W(1)	C(14)	C(19)	128.1(3)
C(7)	W(1)	C(16)	131.1(1)	W(1)	C(8)	C(7)	66.3(2)	W(1)	C(14)	C(15)	71.5(2)
C(8)	W(1)	C(12)	127.0(1)	W(1)	C(8)	C(9)	92.0(2)	W(1)	C(14)	C(13)	71.8(2)
C(8)	W(1)	C(13)	100.5(1)	C(7)	C(8)	C(9)	124.8(4)	C(14)	C(13)	C(18)	124.3(5)
C(8)	W(1)	C(14)	103.6(1)	C(8)	C(9)	C(10)	124.3(4)	C(12)	C(13)	C(18)	126.7(5)
C(8)	W(1)	C(15)	133.4(1)	C(8)	C(9)	C(11)	120.6(4)	C(12)	C(13)	C(14)	108.6(3)
C(8)	W(1)	C(16)	158.1(1)	C(10)	C(9)	C(11)	113.5(3)	W(1)	C(13)	C(18)	128.8(3)
W(1)	C(12)	C(13)	76.1(2)	W(1)	C(16)	C(21)	121.7(2)	W(1)	C(13)	C(14)	74.3(2)
W(1)	C(12)	C(16)	72.2(2)	C(12)	C(16)	C(15)	107.7(3)	W(1)	C(13)	C(12)	69.0(2)
W(1)	C(12)	C(17)	121.1(3)	C(12)	C(16)	C(21)	126.9(5)	C(16)	C(12)	C(17)	125.2(5)
C(13)	C(12)	C(16)	107.6(3)	C(15)	C(16)	C(21)	125.2(5)	C(13)	C(12)	C(17)	127.1(5)
N(1)	W(1)	C(14)	149.5(1)	W(1)	C(7)	H(6)	110(2)	W(1)	C(7)	H(7)	120(3)
C(8)	C(7)	H(6)	113(2)	C(8)	C(7)	H(7)	116(3)	H(6)	C(7)	H(7)	115(4)
W(1)	C(8)	H(8)	106(3)	C(7)	C(8)	H(8)	117(3)	C(9)	C(8)	H(8)	118(3)

**Table A17.** Dihedral Angles (°) in the Solid-State Molecular Structure Determined for **5.10**

(1) (2) (3) (4) angle	(1) (2) (3) (4) angle	(1) (2) (3) (4) angle
W(1) C(1) C(2) C(3) 175.6(3)	O(1) N(1) W(1) C(7) -116(2)	W(1) C(14)C(13)C(12) 60.9(2)
W(1) C(1) C(6) C(5) -175.9(3)	O(1) N(1) W(1) C(8) -150(2)	N(1) W(1) C(12)C(16) 86.4(2)
W(1) C(7) C(8) C(9) 75.0(4)	O(1) N(1) W(1) C(12) -20(2)	W(1) C(14)C(13)C(18) -126.5(4)
W(1) C(8) C(9) C(10) 82.3(4)	O(1) N(1) W(1) C(13) -35(2)	N(1) W(1) C(12)C(17) -34.5(5)
W(1) C(8) C(9) C(11) -113.3(3)	O(1) N(1) W(1) C(14) 6(2)	W(1) C(14)C(15)C(16) -61.3(2)
W(1) C(12)C(13)C(14) -64.2(3)	O(1) N(1) W(1) C(15) 35(2)	N(1) W(1) C(13)C(12) 25.9(3)
W(1) C(12)C(13)C(18) 123.4(4)	O(1) N(1) W(1) C(16) 15(2)	W(1) C(14)C(15)C(20) 128.0(4)
W(1) C(12)C(16)C(15) 68.2(2)	N(1) W(1) C(1) C(2) 166.4(3)	N(1) W(1) C(13)C(14) 143.4(2)
W(1) C(12)C(16)C(21) -116.7(3)	N(1) W(1) C(1) C(6) -17.7(3)	W(1) C(15)C(14)C(13) 63.4(2)
W(1) C(13)C(12)C(16) 65.9(2)	N(1) W(1) C(7) C(8) -112.0(2)	N(1) W(1) C(13)C(18) -95.0(6)
W(1) C(13)C(12)C(17) -118.8(4)	N(1) W(1) C(8) C(7) 73.3(2)	W(1) C(15)C(14)C(19) -124.5(4)
W(1) C(13)C(14)C(15) -63.2(2)	N(1) W(1) C(8) C(9) -54.2(3)	N(1) W(1) C(14)C(13) -68.5(4)
W(1) C(13)C(14)C(19) 124.2(4)	N(1) W(1) C(12)C(13) -159.7(2)	W(1) C(15)C(16)C(12) -65.7(2)
W(1) C(15)C(16)C(21) 119.0(3)	N(1) W(1) C(14)C(19) 172.5(4)	N(1) W(1) C(14)C(15) 47.4(4)
W(1) C(16)C(12)C(13) -68.5(2)	N(1) W(1) C(15)C(14) -154.0(2)	C(1) W(1) C(15)C(14) 119.2(2)
W(1) C(16)C(12)C(17) 116.0(4)	N(1) W(1) C(15)C(16) -36.4(3)	C(7) W(1) C(8) C(9) -127.5(4)
W(1) C(16)C(15)C(14) 64.7(2)	N(1) W(1) C(15)C(20) 82.1(5)	C(7) W(1) C(12)C(13) -67.0(3)
W(1) C(16)C(15)C(20) -124.5(3)	N(1) W(1) C(16)C(12) -96.1(2)	C(1) W(1) C(15)C(16) -123.2(2)
O(1) N(1) W(1) C(1) 114(2)	N(1) W(1) C(16)C(15) 149.7(2)	C(1) W(1) C(15)C(20) -4.7(5)
N(1) W(1) C(16)C(21) 26.8(5)	C(2) C(1) W(1) C(15) -72.0(3)	C(7) W(1) C(12)C(16) 179.0(2)
C(1) W(1) C(7) C(8) -15.8(3)	C(2) C(1) W(1) C(16) -100.8(3)	C(1) W(1) C(16)C(12) 170.2(2)
C(1) W(1) C(8) C(7) 167.9(2)	C(2) C(1) C(6) C(5) 0.3(5)	C(7) W(1) C(12)C(17) 58.2(5)
C(1) W(1) C(8) C(9) 40.5(3)	C(2) C(3) C(4) C(5) -0.1(6)	C(1) W(1) C(16)C(15) 55.9(2)
C(1) W(1) C(12)C(13) 100.6(3)	C(3) C(2) C(1) C(6) -0.5(5)	C(7) W(1) C(13)C(12) 112.2(3)
C(1) W(1) C(12)C(16) -13.4(3)	C(3) C(4) C(5) C(6) -0.1(7)	C(1) W(1) C(16)C(21) -66.9(5)
C(1) W(1) C(12)C(17) -134.2(4)	C(6) C(1) W(1) C(7) -113.3(3)	C(1) C(2) C(3) C(4) 0.4(6)
C(1) W(1) C(13)C(12) -111.3(3)	C(6) C(1) W(1) C(8) -122.6(3)	C(7) W(1) C(13)C(14) -130.2(3)
C(1) W(1) C(13)C(14) 6.3(3)	C(6) C(1) W(1) C(12) 82.9(3)	C(7) W(1) C(13)C(18) -8.6(6)
C(1) W(1) C(13)C(18) 127.9(5)	C(6) C(1) W(1) C(13) 129.7(3)	C(7) W(1) C(14)C(13) 51.1(3)
C(1) W(1) C(14)C(13) -175.2(2)	C(6) C(1) W(1) C(14) 133.2(3)	C(1) C(6) C(5) C(4) 0.0(7)
C(1) W(1) C(14)C(15) -59.3(2)	C(6) C(1) W(1) C(15) 104.0(3)	C(2) C(1) W(1) C(7) 70.7(3)
C(1) W(1) C(14)C(19) 65.8(5)	C(6) C(1) W(1) C(16) 75.1(3)	C(7) W(1) C(14)C(15) 167.0(2)
C(2) C(1) W(1) C(8) 61.4(3)	C(7) W(1) C(14)C(19) -68.0(5)	C(8) C(7) W(1) C(16) 153.1(2)
C(2) C(1) W(1) C(12) -93.0(3)	C(7) W(1) C(15)C(14) -18.5(3)	C(7) C(8) W(1) C(12) -35.3(3)
C(2) C(1) W(1) C(13) -46.3(3)	C(7) W(1) C(15)C(16) 99.1(3)	C(7) C(8) W(1) C(13) -60.4(3)
C(2) C(1) W(1) C(14) -42.8(3)	C(7) W(1) C(15)C(20) -142.5(5)	C(9) C(8) W(1) C(12) -162.8(2)
C(7) W(1) C(16)C(12) -1.3(3)	C(8) C(7) W(1) C(13) 120.3(2)	C(7) C(8) W(1) C(14) -95.0(3)
C(7) W(1) C(16)C(15) -115.5(3)	C(8) C(7) W(1) C(14) 94.2(2)	C(9) C(8) W(1) C(13) 172.2(3)
C(7) W(1) C(16)C(21) 121.6(5)	C(8) C(7) W(1) C(15) 104.7(2)	C(7) C(8) W(1) C(15) -113.5(3)
C(7) C(8) W(1) C(16) -66.3(5)	C(9) C(8) W(1) C(15) 119.0(2)	C(9) C(8) W(1) C(14) 137.6(2)
C(7) C(8) C(9) C(10) 20.0(6)	C(9) C(8) W(1) C(16) 166.3(3)	C(12)C(16)W(1) C(15) 114.2(3)
C(7) C(8) C(9) C(11) -175.5(4)	C(12)W(1) C(13)C(14) 117.5(3)	C(14)W(1) C(16)C(15) -35.7(2)
C(8) W(1) C(12)C(13) -46.8(3)	C(12)W(1) C(13)C(18) -120.8(7)	C(12)C(16)C(15)C(14) -1.1(4)
C(8) W(1) C(12)C(16) -160.8(2)	C(12)W(1) C(14)C(13) -36.8(2)	C(14)W(1) C(16)C(21) -158.6(5)
C(8) W(1) C(12)C(17) 78.4(5)	C(12)W(1) C(14)C(15) 79.1(2)	C(12)C(16)C(15)C(20) 169.7(3)
C(8) W(1) C(13)C(12) 143.7(2)	C(12)W(1) C(14)C(19) -155.8(6)	C(14)C(13)W(1) C(15) 37.0(2)
C(8) W(1) C(13)C(14) -98.8(2)	C(12)W(1) C(15)C(14) -78.8(3)	C(13)W(1) C(12)C(16) -113.9(3)
C(8) W(1) C(13)C(18) 22.8(6)	C(12)W(1) C(15)C(16) 38.8(2)	C(14)C(13)W(1) C(16) 78.6(3)
C(8) W(1) C(14)C(13) 88.6(2)	C(12)W(1) C(15)C(20) 157.2(6)	C(13)W(1) C(12)C(17) 125.2(6)

Table A17. continued

C(8) W(1) C(14)C(15) -155.5(2)	C(12)W(1) C(16)C(15) -114.2(3)	C(14)C(13)C(12)C(16) 1.7(4)
C(8) W(1) C(14)C(19) -30.4(5)	C(12)W(1) C(16)C(21) 122.9(5)	C(13)W(1) C(14)C(15) 115.9(3)
C(8) W(1) C(15)C(14) 33.7(3)	C(12)C(13)W(1) C(14) -117.5(3)	C(13)W(1) C(14)C(19) -119.0(6)
C(8) W(1) C(15)C(16) 151.3(2)	C(12)C(13)W(1) C(15) -80.6(3)	C(14)C(13)C(12)C(17) 177.0(4)
C(8) W(1) C(15)C(20) -90.2(5)	C(12)C(13)W(1) C(16) -38.9(2)	C(13)W(1) C(15)C(14) -37.1(2)
C(8) W(1) C(16)C(12) 44.9(5)	C(12)C(13)C(14)C(15) -2.3(4)	C(14)C(15)W(1) C(16) -117.6(3)
C(8) W(1) C(16)C(15) -69.3(5)	C(12)C(13)C(14)C(19) -175.0(3)	C(14)C(15)C(16)C(21) -176.3(3)
C(8) W(1) C(16)C(21) 167.8(5)	C(12)C(16)W(1) C(13) 38.1(2)	C(13)W(1) C(15)C(16) 80.5(2)
C(8) C(7) W(1) C(12) 152.4(2)	C(12)C(16)W(1) C(14) 78.5(2)	C(15)W(1) C(12)C(16) -37.9(2)
C(13)W(1) C(15)C(20) -161.0(6)	C(15)W(1) C(12)C(17) -158.8(5)	C(13)C(14)W(1) C(16) -79.1(3)
C(13)W(1) C(16)C(15) -76.1(2)	C(15)W(1) C(13)C(18) 158.6(6)	C(16)W(1) C(14)C(19) 161.8(6)
C(13)W(1) C(16)C(21) 161.0(5)	C(15)W(1) C(14)C(19) 125.1(6)	C(13)C(14)C(15)C(16) 2.1(4)
C(13)C(12)W(1) C(14) 35.8(2)	C(15)W(1) C(16)C(21) -122.9(6)	C(16)W(1) C(15)C(20) 118.5(6)
C(13)C(12)W(1) C(15) 76.0(3)	C(15)C(14)W(1) C(16) 36.7(2)	C(13)C(14)C(15)C(20) -168.6(3)
C(13)C(12)W(1) C(16) 113.9(3)	C(15)C(14)C(13)C(18) 170.3(4)	C(16)C(12)C(13)C(18) -170.7(4)
C(13)C(12)C(16)C(15) -0.4(4)	C(15)C(16)C(12)C(17) -175.8(3)	C(14)W(1) C(12)C(16) -78.1(2)
C(13)C(12)C(16)C(21) 174.8(3)	C(16)W(1) C(12)C(17) -120.9(5)	C(16)C(15)C(14)C(19) 174.3(3)
C(13)C(14)W(1) C(15) -115.9(3)	C(16)W(1) C(13)C(18) -159.7(6)	C(20)C(15)C(16)C(21) -5.5(5)
C(14)W(1) C(12)C(17) 161.0(5)	C(17)C(12)C(13)C(18) 4.6(6)	C(14)W(1) C(15)C(20) -123.9(6)
C(14)W(1) C(13)C(18) 121.6(6)	C(17)C(12)C(16)C(21) -0.7(6)	C(19)C(14)C(15)C(20) 3.6(6)
C(14)W(1) C(15)C(16) 117.6(3)	C(18)C(13)C(14)C(19) -2.4(6)	

Table A18. Fractional Atomic Coordinates in the Solid-State Molecular Structure Determined for 5.10

atom	x	y	z	B(eq)	atom	x	y	z	B(eq)
W(1)	0.220191(8)	0.87001(1)	0.856033(7)	0.996(3)	C(11)	0.5013(3)	1.0023(5)	0.8605(3)	2.87(9)
O(1)	0.1084(2)	1.1493(3)	0.8912(2)	3.09(7)	C(10)	0.3722(3)	1.1414(4)	0.9393(3)	2.59(9)
N(1)	0.1631(2)	1.0416(3)	0.8786(2)	1.70(6)	C(9)	0.4069(3)	0.9939(4)	0.9097(2)	1.89(7)
C(1)	0.2966(2)	0.9582(3)	0.7523(2)	1.22(6)	C(8)	0.3738(3)	0.8610(4)	0.9379(3)	2.04(8)
C(2)	0.3756(3)	0.8819(3)	0.7140(2)	1.91(7)	C(7)	0.2805(3)	0.8399(5)	0.9807(2)	2.47(8)
C(3)	0.4186(3)	0.9343(5)	0.6454(2)	2.58(8)	C(12)	0.0714(3)	0.7322(4)	0.8701(2)	2.44(8)
C(4)	0.3852(4)	1.0660(5)	0.6119(3)	3.12(9)	C(13)	0.1521(4)	0.6269(3)	0.8782(3)	2.46(8)
C(5)	0.3088(4)	1.1446(4)	0.6473(3)	2.85(9)	C(14)	0.2026(3)	0.6184(3)	0.8055(3)	2.23(8)
C(6)	0.2649(3)	1.0916(4)	0.7167(2)	2.10(7)	C(15)	0.1500(3)	0.7144(4)	0.7519(2)	2.02(7)
C(16)	0.0701(3)	0.7860(3)	0.7913(3)	2.11(7)	C(20)	0.1643(5)	0.7217(7)	0.6644(3)	5.6(1)
C(17)	-0.0063(4)	0.7726(7)	0.9316(4)	6.0(2)	C(21)	-0.0076(4)	0.8909(4)	0.7530(4)	5.5(2)
C(18)	0.1734(6)	0.5242(6)	0.9481(4)	6.7(2)	H(1)	0.4011	0.7882	0.7368	2.2738
C(19)	0.2871(4)	0.5093(5)	0.7896(5)	5.4(1)	H(2)	0.4728	0.8770	0.6202	3.1180
H(3)	0.4164	1.1029	0.5633	3.7031	H(15)	-0.0042	0.8801	0.9409	7.3304
H(4)	0.2847	1.2387	0.6238	3.4746	H(16)	-0.0760	0.7437	0.9124	7.3304
H(5)	0.2105	1.1495	0.7408	2.5032	H(18)	0.1288	0.5521	0.9918	8.1366
H(6)	0.261(3)	0.934(5)	1.015(3)	2.7(8)	H(17)	0.0118	0.7210	0.9817	7.3304
H(7)	0.273(3)	0.750(5)	1.005(3)	2.6(8)	H(19)	0.1579	0.4222	0.9318	8.1366
H(8)	0.412(4)	0.770(5)	0.922(3)	3.7(8)	H(20)	0.2462	0.5327	0.9661	8.1366
H(9)	0.3064	1.1295	0.9658	3.1228	H(21)	0.2601	0.4082	0.7945	6.5712

**Table A18. continued**

H(10)	0.4251	1.1804	0.9775	3.1228	H(22)	0.3103	0.5239	0.7350	6.5712
H(11)	0.3628	1.2098	0.8945	3.1228	H(23)	0.3454	0.5242	0.8276	6.5712
H(12)	0.4877	1.0697	0.8152	3.4718	H(24)	0.2245	0.6619	0.6511	6.8006
H(13)	0.5172	0.9032	0.8401	3.4718	H(26)	0.1757	0.8250	0.6489	6.8006
H(14)	0.5603	1.0390	0.8933	3.4718	H(25)	0.1020	0.6835	0.6359	6.8006
H(27)	0.0286	0.9761	0.7309	6.6209	H(29)	-0.0553	0.9258	0.7932	6.6209
H(28)	-0.0473	0.8397	0.7103	6.6209					

---

**Appendix B. Plots of Kinetic Data and Corresponding  
Regression Analyses for Systems Studied Kinetically in  
this Thesis**

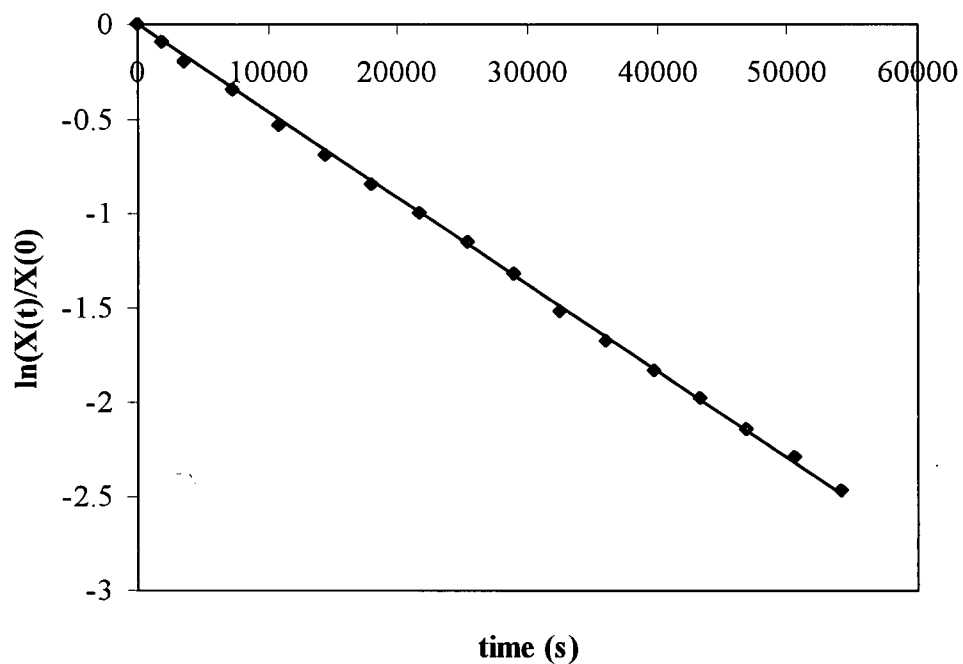


**Figure B1.** First-Order Plot of Loss of Starting Material vs Time for the Thermolysis of  $\text{Cp}^*\text{W}(\text{NO})(\text{CH}_2\text{CMe}_3)_2$  (**1**) in Benzene- $d_6$ . Note that the slope of the regression line is  $-4.6(1) \times 10^{-5} \text{ s}^{-1}$  and  $R^2 = 0.9995$ .

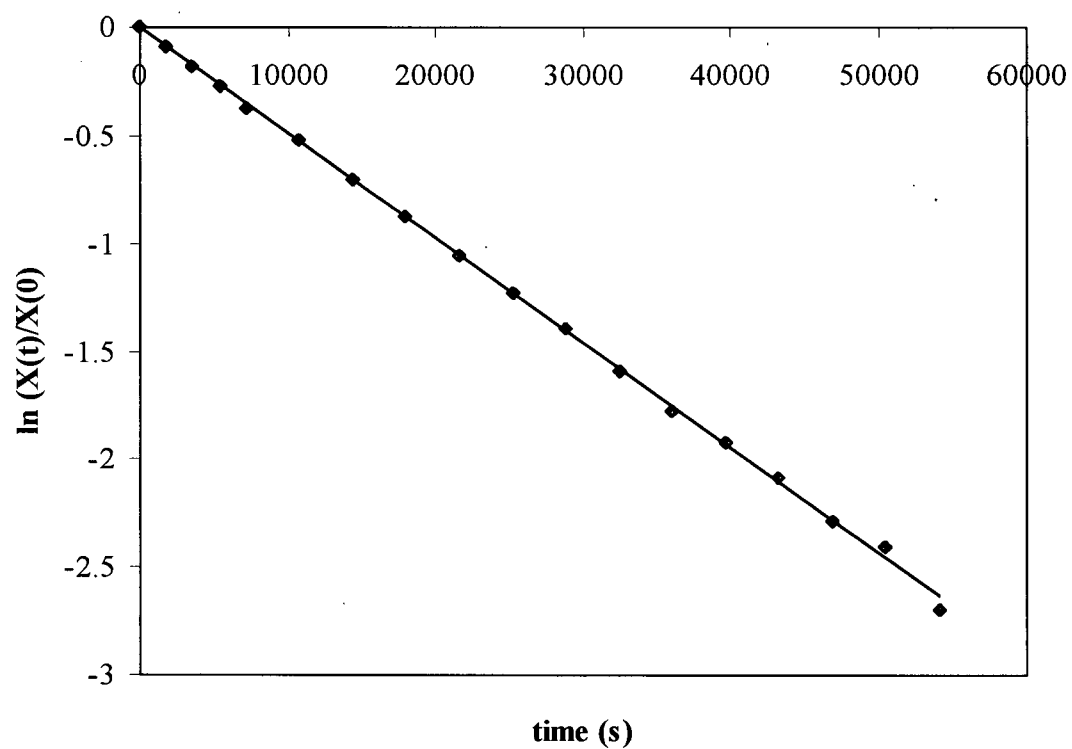


**Figure B2.** First-Order Plot of Loss of Starting Material vs Time for the Thermolysis of  $\text{Cp}^*\text{W}(\text{NO})(\text{CH}_2\text{C}_6\text{H}_5)(\text{CH}_2\text{CMe}_3)$  (**2**) in Benzene- $d_6$ . Note that the slope of the regression line is  $-4.9(1) \times 10^{-5} \text{ s}^{-1}$  and  $R^2 = 0.9996$ .

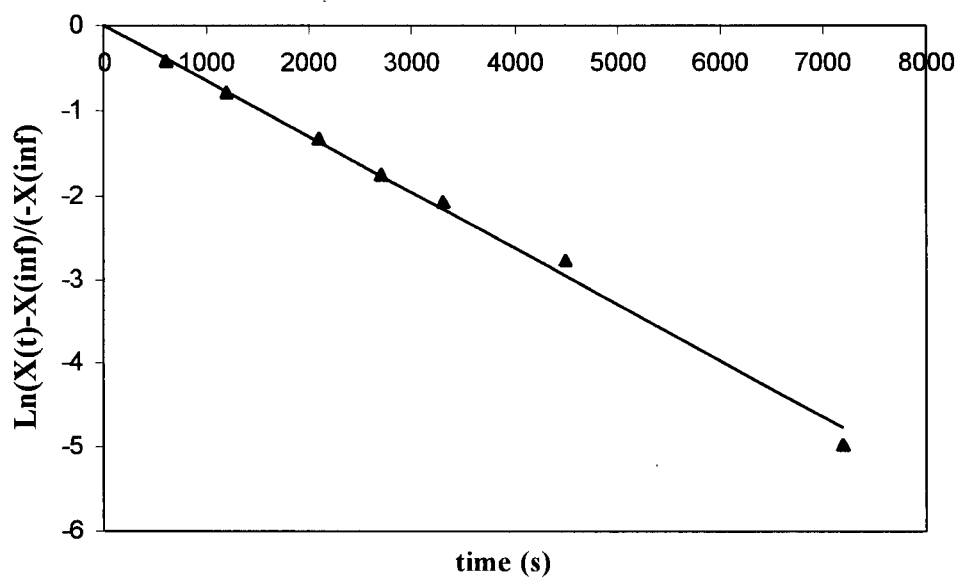


**Figure B3.** First-Order Plot of Loss of Starting Material vs Time for the Thermolysis of  $\text{Cp}^*\text{W}(\text{NO})(\text{CH}_2\text{CMe}_3)(\text{C}_6\text{H}_4\text{-2-Me})$  (**2.1c**) in Benzene- $d_6$ . Note that the slope of the regression line is  $-6.6(3) \times 10^{-4} \text{ s}^{-1}$  and  $R^2 = 0.9929$ .

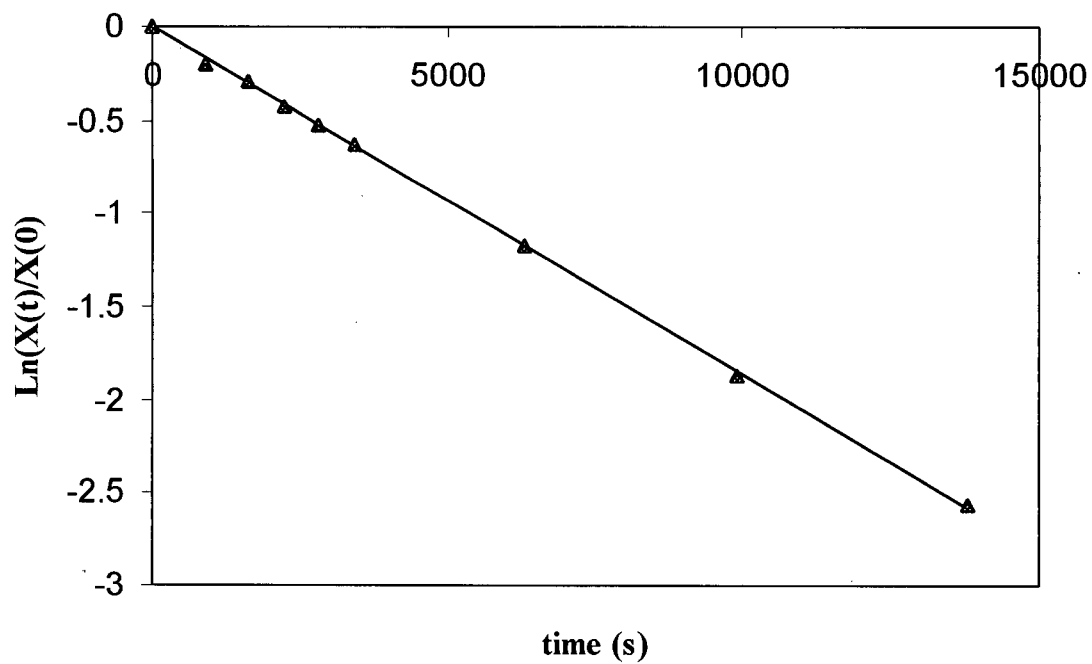


**Figure B4.** First-Order Plot of Loss of Starting Material vs Time for the Thermolysis of  $\text{Cp}^*\text{W}(\text{NO})(\text{CH}_2\text{C}_6\text{H}_5)(\text{C}_6\text{H}_4\text{-2-Me})$  (**2.2c**) in Benzene- $d_6$ . Note that the slope of the regression line is  $-1.9(1) \times 10^{-4} \text{ s}^{-1}$  and  $R^2 = 0.9997$ .

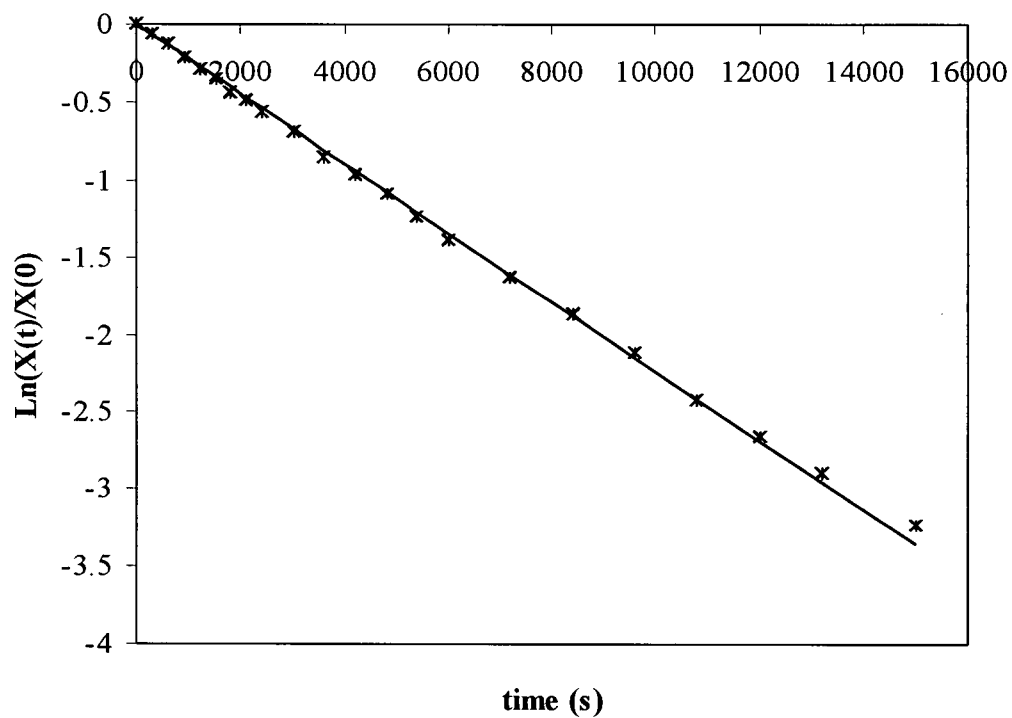


**Figure B5.** First-Order Plot of Loss of Starting Material vs Time for the Thermolysis of  $\text{Cp}^*\text{W}(\text{NO})(\text{CH}_2\text{CMe}_3)(\eta^3\text{-}1,1\text{-Me}_2\text{-C}_3\text{H}_3)$  (**5.9**) in Benzene- $d_6$ . Note that the slope of the regression line is  $-2.2(1) \times 10^{-4} \text{ s}^{-1}$  and  $R^2 = 0.9992$ .

**Appendix C. Optimized Geometries, Z-Matrices and  
Energies Calculated by DFT Methods for Toluene  
Activation by Methylidene C**

Data for  $\text{CpW(NO)}(=\text{CH}_2)(\text{H-CH}_2\text{C}_6\text{H}_5)$  (**D**)

## Selected Bond Distances and Angles

$$\text{W(1)-C(28)} = 2.7056$$

$$\text{W(1)-C(14)} = 1.9474$$

$$\text{W-H(31)} = 2.0645$$

$$\text{W(1)-H(30)} = 2.5844$$

$$\text{W(1)-H(29)} = 3.3156$$

$$\text{C(28)-H(31)} = 1.1420$$

$$\text{C(28)-H(30)} = 1.0979$$

$$\text{C(28)-H(29)} = 1.0936$$

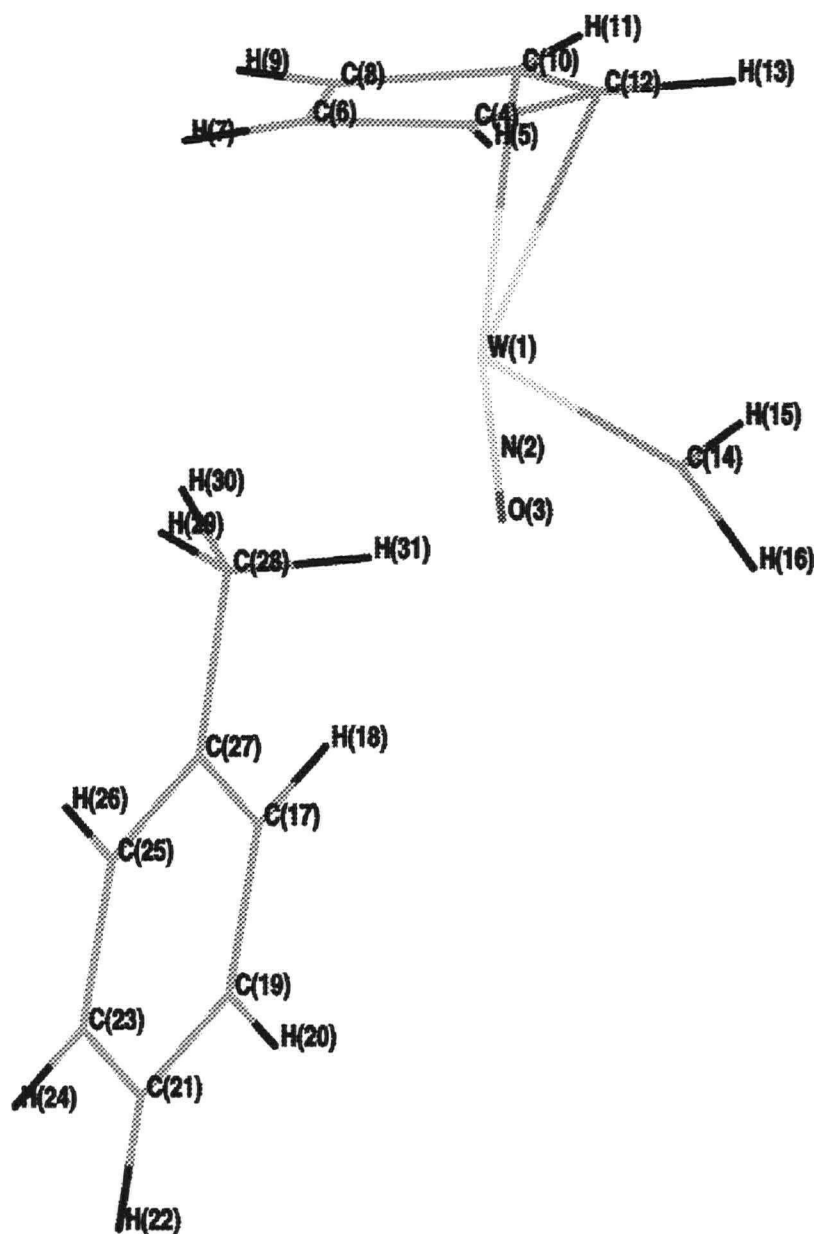
$$\text{C(28)-W(1)-C(14)} = 102.4$$

$$\text{W(1)-C(28)-C(27)} = 130.5$$

$$\text{W(1)-C(28)-H(31)} = 44.3$$

$$\text{C(14)-W(1)-C(28)-C(27)} = -60.7$$

$$\text{H(31)-C(14)-W(1)-C(28)} = 9.2$$



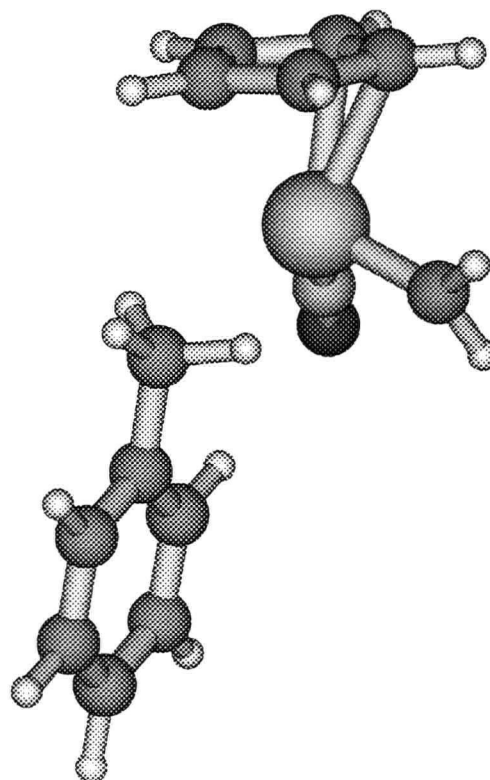
Data for CpW(NO)(=CH<sub>2</sub>)(H-CH<sub>2</sub>C<sub>6</sub>H<sub>5</sub>) (**D**) cont'd

31

scf done: -702.044530

Thermal corr. to free energy: 0.199358

W	0.666802	0.735765	-0.335071
N	0.666802	0.735765	1.446438
O	0.725678	0.735765	2.697692
C	1.562466	0.881085	-2.656192
H	0.936777	1.004927	-3.529048
C	2.055370	-0.369833	-2.132831
H	1.835761	-1.349988	-2.537480
C	2.904698	-0.100929	-1.015785
H	3.435928	-0.830653	-0.419830
C	2.901831	1.329467	-0.795968
H	3.486159	1.858697	-0.056833
C	2.098257	1.933963	-1.838867
H	1.951955	2.993755	-1.984809
C	-0.641328	2.163371	-0.542583
H	-0.819029	2.664696	-1.506444
H	-1.215020	2.628595	0.268035
C	-2.021907	-1.526258	1.940350
H	-1.225066	-0.900322	2.334076
C	-3.063069	-1.940366	2.789981
H	-3.058327	-1.631424	3.832425
C	-4.107485	-2.748625	2.298470
H	-4.910604	-3.066345	2.959127
C	-4.105442	-3.140840	0.946957
H	-4.907237	-3.764183	0.557970
C	-3.064066	-2.726404	0.094716
H	-3.069205	-3.033044	-0.949951
C	-2.013999	-1.920232	0.583595
C	-0.892439	-1.493593	-0.350259
H	-0.966302	-1.972610	-1.330611
H	0.084401	-1.747383	0.081932
H	-1.053906	-0.382606	-0.559441



Data For  $\text{CpW(NO)}(\text{H}_2\text{C}\cdots\text{H}\cdots\text{C}_6\text{H}_4\text{-CH}_3)$ 

## Selected Bond Distances and Angles

$$\text{W(1)-C(28)} = 2.3960$$

$$\text{W(1)-C(14)} = 1.9705$$

$$\text{W-H(31)} = 1.8018$$

$$\text{C(14)-H(31)} = 1.7156$$

$$\text{C(28)-H(31)} = 1.4747$$

$$\text{C(28)-W(1)-C(14)} = 91.8$$

$$\text{W(1)-C(28)-C(27)} = 127.0$$

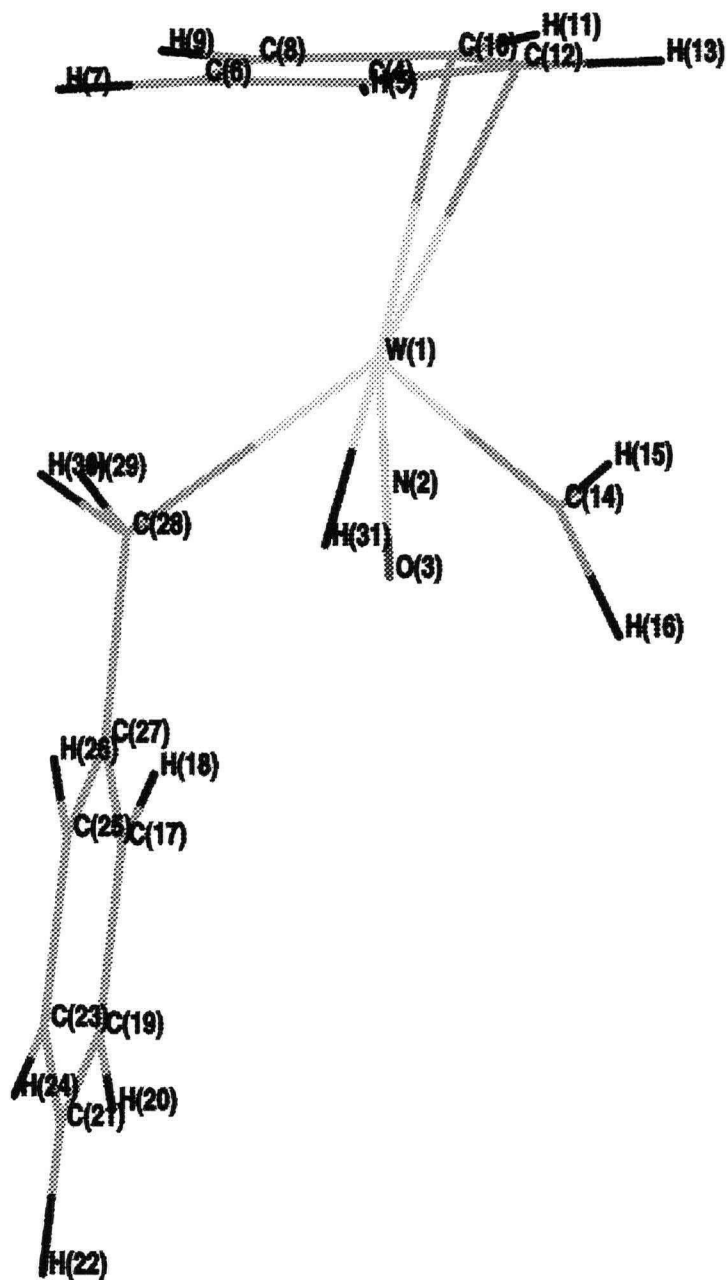
$$\text{W(1)-C(28)-H(31)} = 48.6$$

$$\text{H(31)-W(1)-C(28)} = 37.9$$

$$\text{H(31)-W(1)-C(14)} = 53.9$$

$$\text{C(14)-W(1)-C(28)-C(27)} = -52.1$$

$$\text{H-(31)-C(14)-W(1)-C(28)} = -1.3$$



Data For CpW(NO)(H<sub>2</sub>C•••H•••C<sub>6</sub>H<sub>4</sub>-CH<sub>3</sub>) con'td

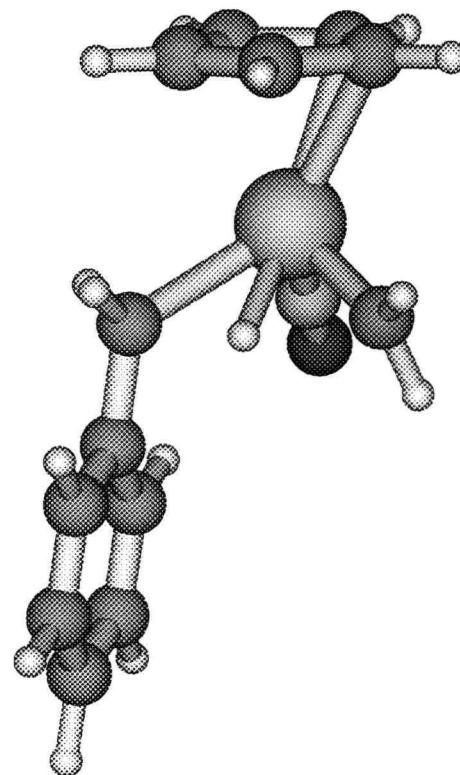
31

scf done: -702.027569

Thermal corr. to free energy: 0.197909

One imaginary frequency: 1169.25i cm<sup>-1</sup>

W	0.602960	0.688568	-0.254987
N	0.602960	0.688568	1.523056
O	0.674625	0.688568	2.771969
C	1.483569	0.832172	-2.595430
H	0.844082	0.747807	-3.463779
C	2.189081	-0.249119	-1.951910
H	2.161145	-1.288212	-2.253202
C	2.962970	0.289173	-0.874387
H	3.617554	-0.263845	-0.214400
C	2.705351	1.708891	-0.813424
H	3.168254	2.408599	-0.131699
C	1.809043	2.040363	-1.896807
H	1.451747	3.031892	-2.136791
C	-1.094429	1.661174	-0.490942
H	-1.450601	1.990816	-1.478232
H	-1.793326	1.934998	0.306883
C	-1.704460	-1.791028	1.872788
H	-0.841174	-1.380472	2.389999
C	-2.816711	-2.224528	2.615413
H	-2.795848	-2.155146	3.700453
C	-3.955308	-2.740023	1.963902
H	-4.814076	-3.073135	2.541855
C	-3.972376	-2.817683	0.558725
H	-4.845231	-3.213775	0.044470
C	-2.857882	-2.386541	-0.185681
H	-2.877666	-2.456548	-1.272396
C	-1.709999	-1.874170	0.460681
C	-0.511054	-1.430221	-0.358465
H	-0.604526	-1.746370	-1.402610
H	0.399378	-1.876970	0.057652
H	-1.023278	-0.052953	-0.483109



Data For CpW(NO)(CH<sub>3</sub>)(CH<sub>2</sub>C<sub>6</sub>H<sub>5</sub>)

## Selected Bond Distances and Angles

$$W(1)-C(28) = 2.1761$$

$$W(1)-C(14) = 2.1723$$

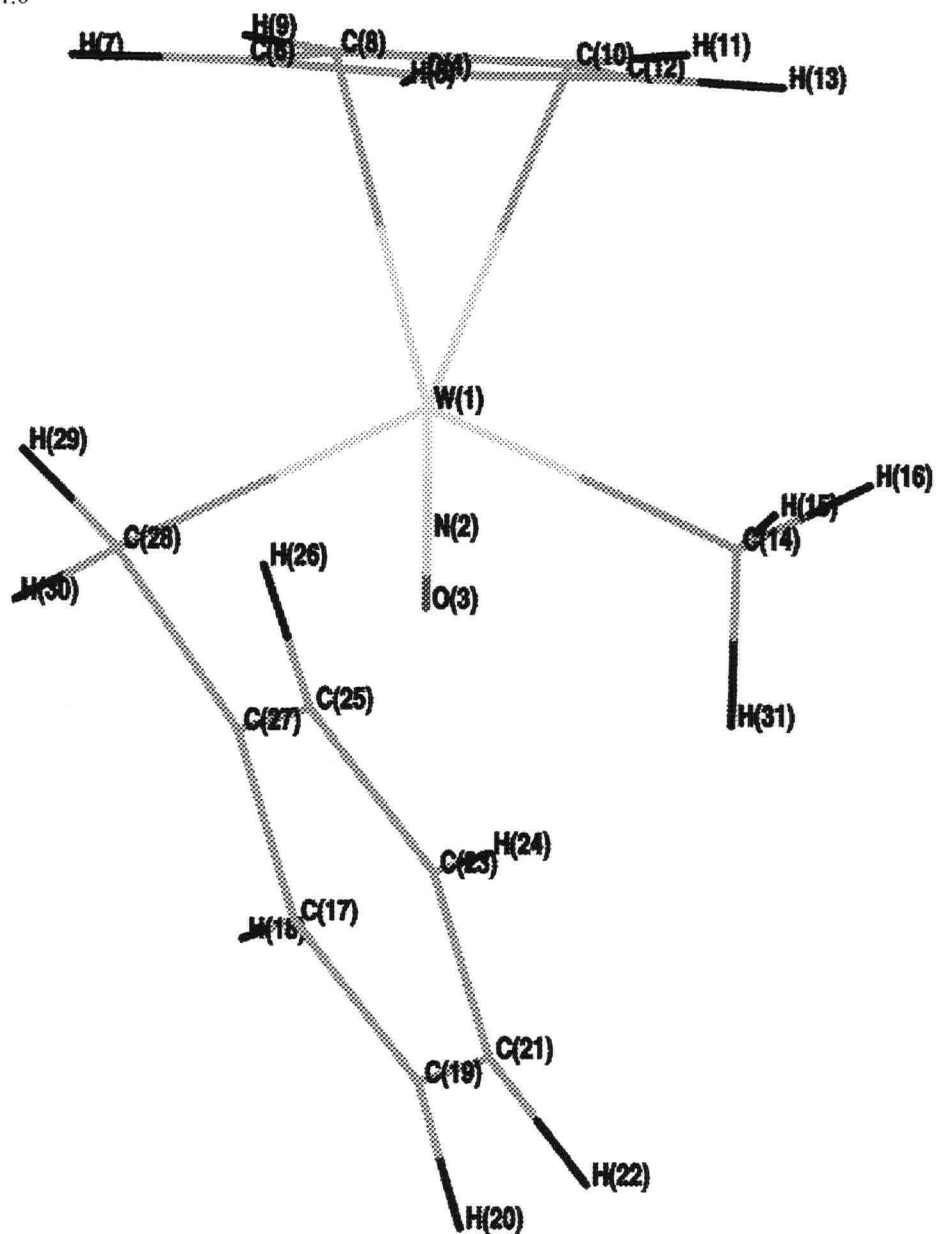
$$C(28)-W(1)-C(14) = 121.5$$

$$W(1)-C(28)-C(27) = 89.2$$

$$C(14)-W(1)-C(28)-C(27) = -4.0$$

$$H(31)-C(14)-W(1)-C(28)$$

$$= 46.0$$



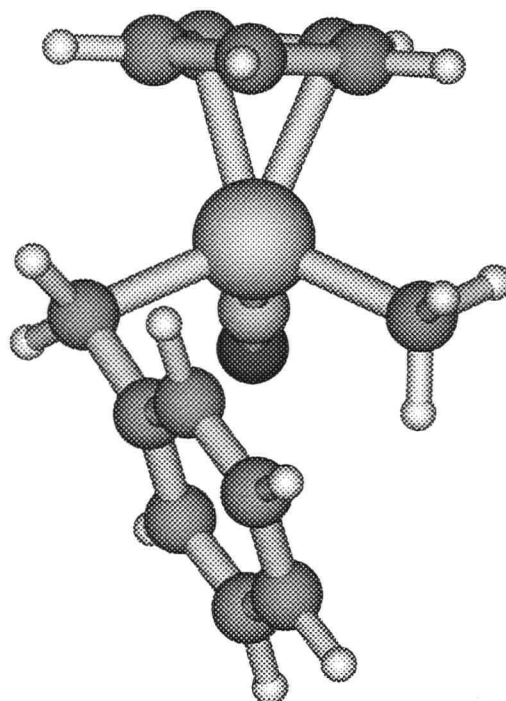
Data For CpW(NO)(CH<sub>3</sub>)(CH<sub>2</sub>C<sub>6</sub>H<sub>5</sub>) con'td

31

scf done: -702.094021

Thermal corr. to free energy: 0.203558

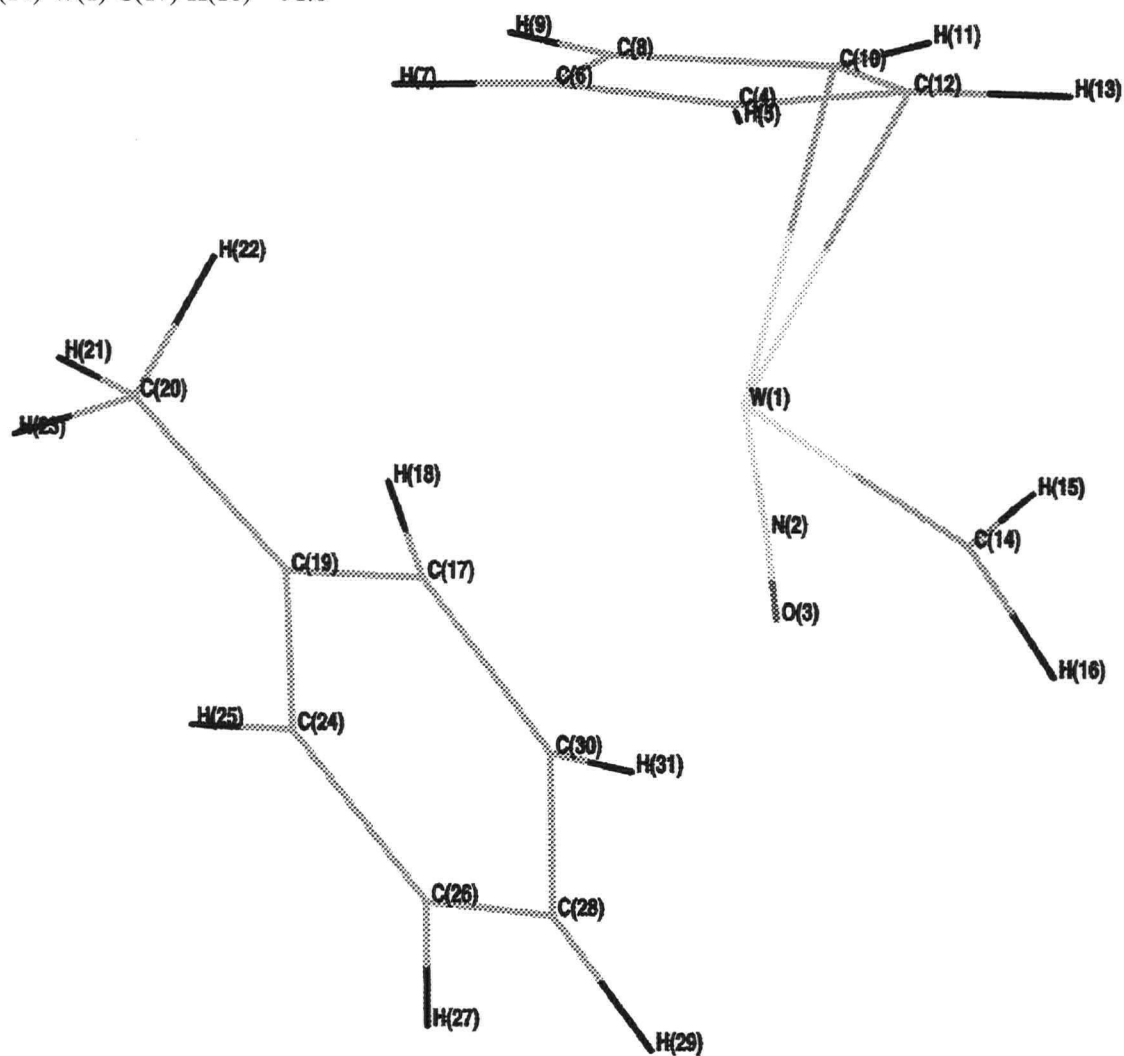
W	0.561877	0.099848	0.133479
N	0.561877	0.099848	1.904079
O	0.682978	0.099848	3.150155
C	1.705850	0.129013	-2.160179
H	1.193871	-0.003919	-3.103482
C	2.284424	-0.911282	-1.355318
H	2.282974	-1.967431	-1.584612
C	2.875865	-0.312066	-0.192792
H	3.419574	-0.824474	0.588495
C	2.653639	1.116786	-0.274719
H	3.012983	1.854829	0.428534
C	1.939134	1.376126	-1.497359
H	1.617776	2.348069	-1.843207
C	-0.625547	1.910749	-0.038164
H	-0.921201	2.124483	-1.075417
H	-0.059412	2.771196	0.348525
C	-2.454832	-0.924142	1.037657
H	-2.073276	-1.223208	2.010743
C	-3.680771	-0.251137	0.937333
H	-4.252475	-0.033135	1.835857
C	-4.169187	0.150592	-0.324686
H	-5.117764	0.677144	-0.398734
C	-3.429481	-0.138781	-1.488199
H	-3.808234	0.160393	-2.462491
C	-2.203323	-0.816547	-1.389742
H	-1.643753	-1.060943	-2.290978
C	-1.688742	-1.223614	-0.125499
C	-0.342440	-1.873163	-0.024186
H	-0.070922	-2.431497	-0.924018
H	-0.210072	-2.490306	0.867301
H	-1.533498	1.817129	0.571375



Data For CpW(NO)(=CH<sub>2</sub>)(H-C<sub>6</sub>H<sub>4</sub>CH<sub>3</sub>) (**E**), (ortho, anti)

## Selected Bond Distances and Angles

W(1)-C(30) = 2.7562
W(1)-C(17) = 2.4741
W(1)-C(14) = 1.9516
W(1)-H(31) = 3.1117
C(14)-H(31) = 2.7885
C(30)-H(31) = 1.0829
C(17)-H(18) = 1.0886
W(1)-H(18) = 2.8235
C(14)-H(18) = 3.8367
C(30)-W(1)-C(14) = 77.9
H(31)-W(1)-C(14) = 61.9
W(1)-C(17)-C(30) = 85.4
C(14)-W(1)-C(17)-C(30) = -26.4
H(31)-C(30)-W(1)-C(14) = 35.3
C(17)-W(1)-C(14) = 106.0
H(18)-W(1)-C(14) = 105.5
W(1)-C(17)-C(18) = 106.3
C(14)-W(1)-C(17)-H(18) = 91.8



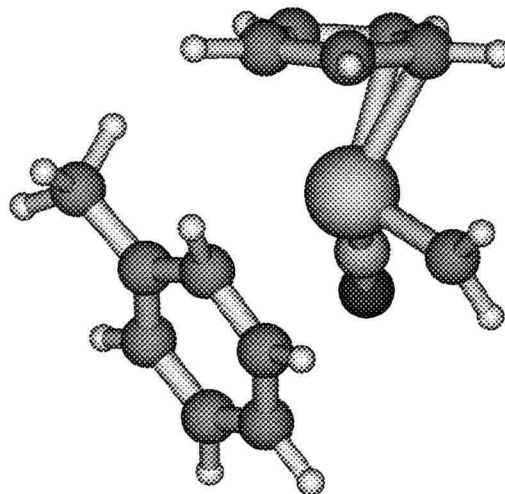
Data For CpW(NO)(=CH<sub>2</sub>)(H-C<sub>6</sub>H<sub>4</sub>CH<sub>3</sub>) (E), (ortho, anti) con'td

31

scf done: -702.057827

Thermal corr. to free energy: 0.200872

W	-0.420106	0.472311	-0.188084
N	-0.420106	0.472311	1.587729
O	-0.376718	0.472311	2.840594
C	0.040374	1.314056	-2.528128
H	-0.399497	0.884006	-3.417372
C	1.338599	1.003947	-1.985298
H	2.029325	0.274268	-2.387214
C	1.572286	1.833107	-0.847808
H	2.458928	1.848911	-0.228831
C	0.393143	2.644442	-0.643938
H	0.273071	3.415084	0.104220
C	-0.535441	2.343676	-1.711120
H	-1.488483	2.826426	-1.867844
C	-2.351390	0.323789	-0.426040
H	-2.843068	0.493882	-1.396786
H	-3.081217	0.151527	0.375120
C	0.476066	-1.821905	-0.421715
H	0.674664	-1.780539	-1.491284
C	1.597280	-1.913219	0.485569
C	2.996348	-1.585549	0.004991
H	3.189606	-2.011981	-0.988332
H	3.147892	-0.500904	-0.069372
H	3.752001	-1.976629	0.694641
C	1.370386	-2.337108	1.798118
H	2.203587	-2.393351	2.494227
C	0.070562	-2.701679	2.237027
H	-0.073573	-3.023833	3.264849
C	-1.013141	-2.674619	1.356086
H	-2.001668	-2.980618	1.685143
C	-0.818436	-2.247181	0.017608
H	-1.619022	-2.352439	-0.703902



Data For CpW(NO)(=CH<sub>2</sub>)(H-C<sub>6</sub>H<sub>4</sub>CH<sub>3</sub>) (**E**), (meta, anti)

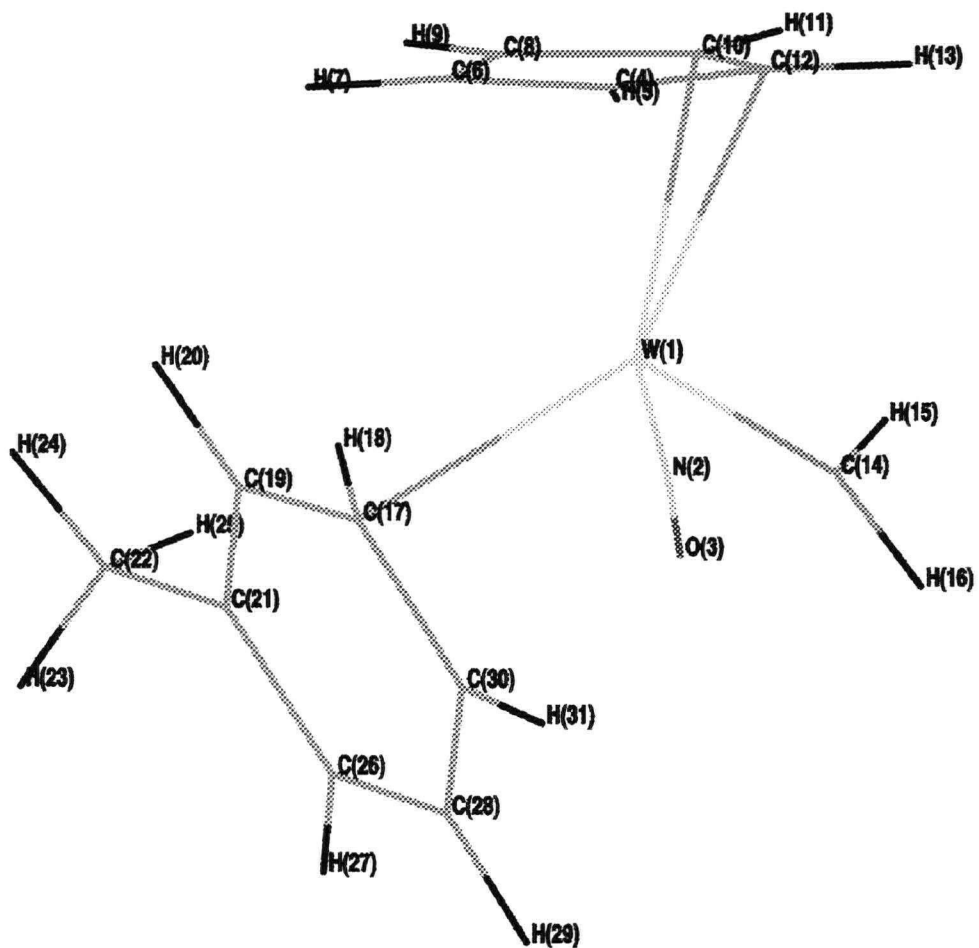
## Selected Bond Distances and Angles

W(1)-C(30) = 2.8191  
 W(1)-C(17) = 2.4547  
 W(1)-C(14) = 1.9474  
 W(1)-H(31) = 3.1862  
 C(14)-H(31) = 2.8732  
 C(30)-H(31) = 1.0835

C(17)-H(18) = 1.0881  
 W(1)-H(18) = 2.7963  
 C(14)-H(18) = 3.6839

C(30)-W(1)-C(14) = 80.4  
 H(31)-W(1)-C(14) = 62.7  
 W(1)-C(17)-C(30) = 89.0  
 C(14)-W(1)-C(17)-C(30) = -37.9  
 H-(31)-C(30)-W(1)-C(14) = 24.10

C(17)-W(1)-C(14) = 104.8  
 H(18)-W(1)-C(14) = 100.4  
 W(1)-C(17)-C(18) = 96.6  
 C(14)-W(1)-C(17)-H(18) = 81.5



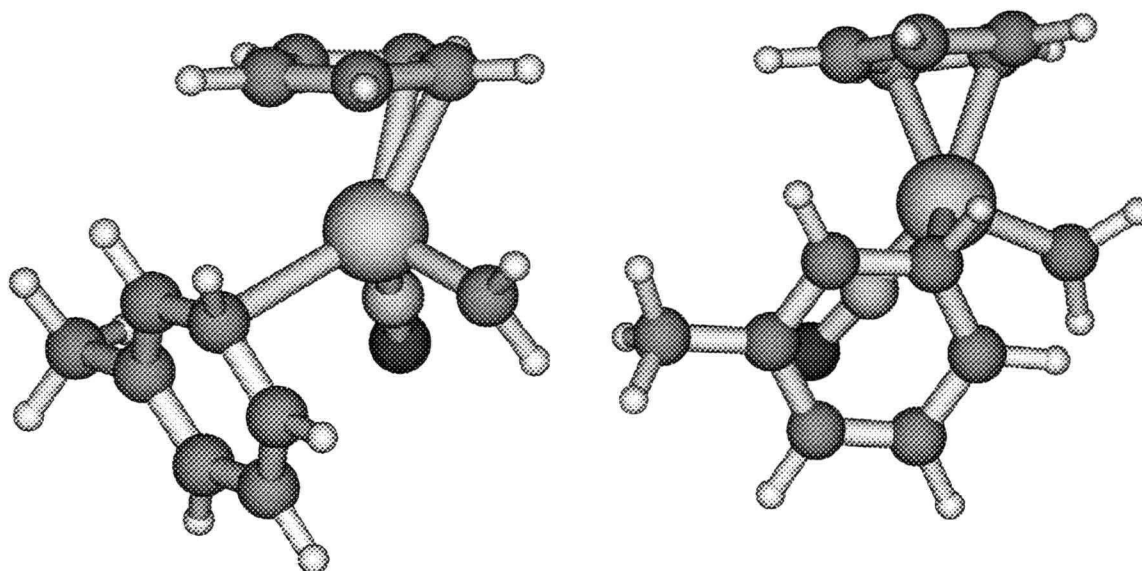
Data For CpW(NO)(=CH<sub>2</sub>)(H-C<sub>6</sub>H<sub>4</sub>CH<sub>3</sub>) (E), (meta, anti) con'td

31

scf done: -702.059438

Thermal corr. to free energy: 0.201754

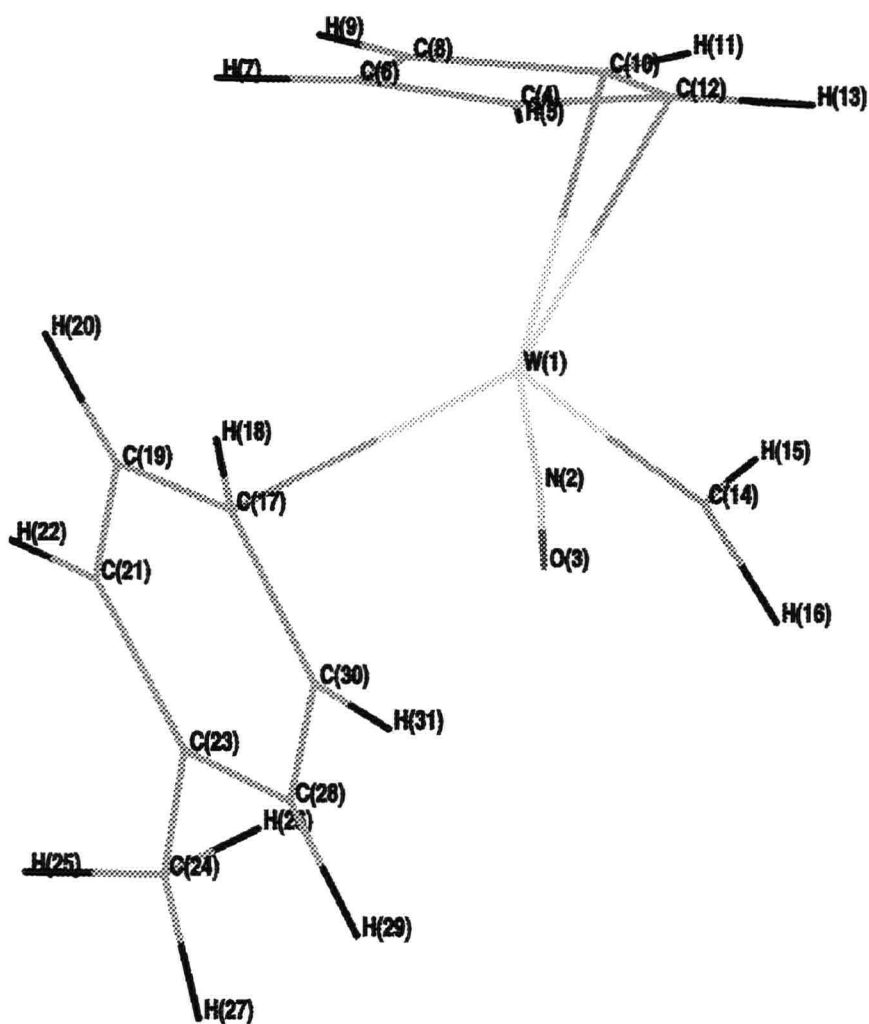
W	-0.571597	0.357309	-0.294731
N	-0.571597	0.357309	1.481375
O	-0.493742	0.357309	2.734227
C	-0.317385	1.291348	-2.633475
H	-0.688527	0.791287	-3.517414
C	1.026362	1.229128	-2.120749
H	1.833872	0.646173	-2.545504
C	1.123924	2.076148	-0.976247
H	2.005126	2.246380	-0.372734
C	-0.182959	2.645901	-0.738158
H	-0.430695	3.372495	0.022732
C	-1.062583	2.182664	-1.789284
H	-2.091393	2.480560	-1.925240
C	-2.416289	-0.210936	-0.552989
H	-2.916952	-0.157001	-1.532322
H	-3.105896	-0.525007	0.240477
C	0.759776	-1.684086	-0.587077
H	0.776244	-1.666935	-1.674880
C	1.948295	-1.342099	0.143698
H	2.748929	-0.818081	-0.373537
C	2.102397	-1.673863	1.495451
C	3.332240	-1.258930	2.277702
H	3.740245	-2.096111	2.858756
H	4.124988	-0.886444	1.618788
H	3.082275	-0.459367	2.988729
C	1.055616	-2.395788	2.136331
H	1.163586	-2.662601	3.185337
C	-0.101752	-2.768343	1.446045
H	-0.886072	-3.321127	1.954656
C	-0.264730	-2.419310	0.083846
H	-1.123905	-2.775702	-0.471763



Data For CpW(NO)(=CH<sub>2</sub>)(H-C<sub>6</sub>H<sub>4</sub>CH<sub>3</sub>) (E), (para)

## Selected Bond Distances and Angles

W(1)-C(30) = 2.8479
W(1)-C(17) = 2.4474
W(1)-C(14) = 1.9474
W(1)-H(31) = 3.2139
C(14)-H(31) = 2.8971
C(30)-H(31) = 1.0839
C(17)-H(18) = 1.0883
W(1)-H(18) = 2.7831
C(14)-H(18) = 3.6571
C(30)-W(1)-C(14) = 80.4
H(31)-W(1)-C(14) = 62.8
W(1)-C(17)-C(30) = 90.6
C(14)-W(1)-C(17)-C(30) = -38.6
H(31)-C(30)-W(1)-C(14) = 23.7
C(17)-W(1)-C(14) = 104.3
H(18)-W(1)-C(14) = 99.8
W(1)-C(17)-C(18) = 100.8
C(14)-W(1)-C(17)-H(18) = 81.1



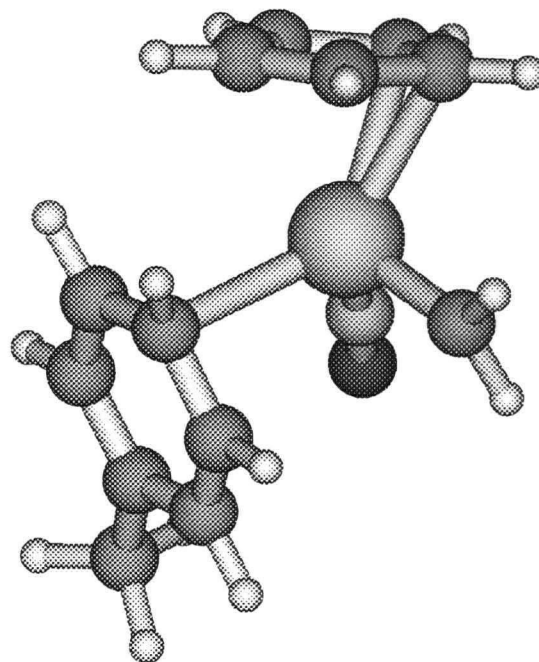
Data For CpW(NO)(=CH<sub>2</sub>)(H-C<sub>6</sub>H<sub>4</sub>CH<sub>3</sub>) (E), (para) cont'd

31

scf done: -702.060912

Thermal corr. to free energy: 0.201210

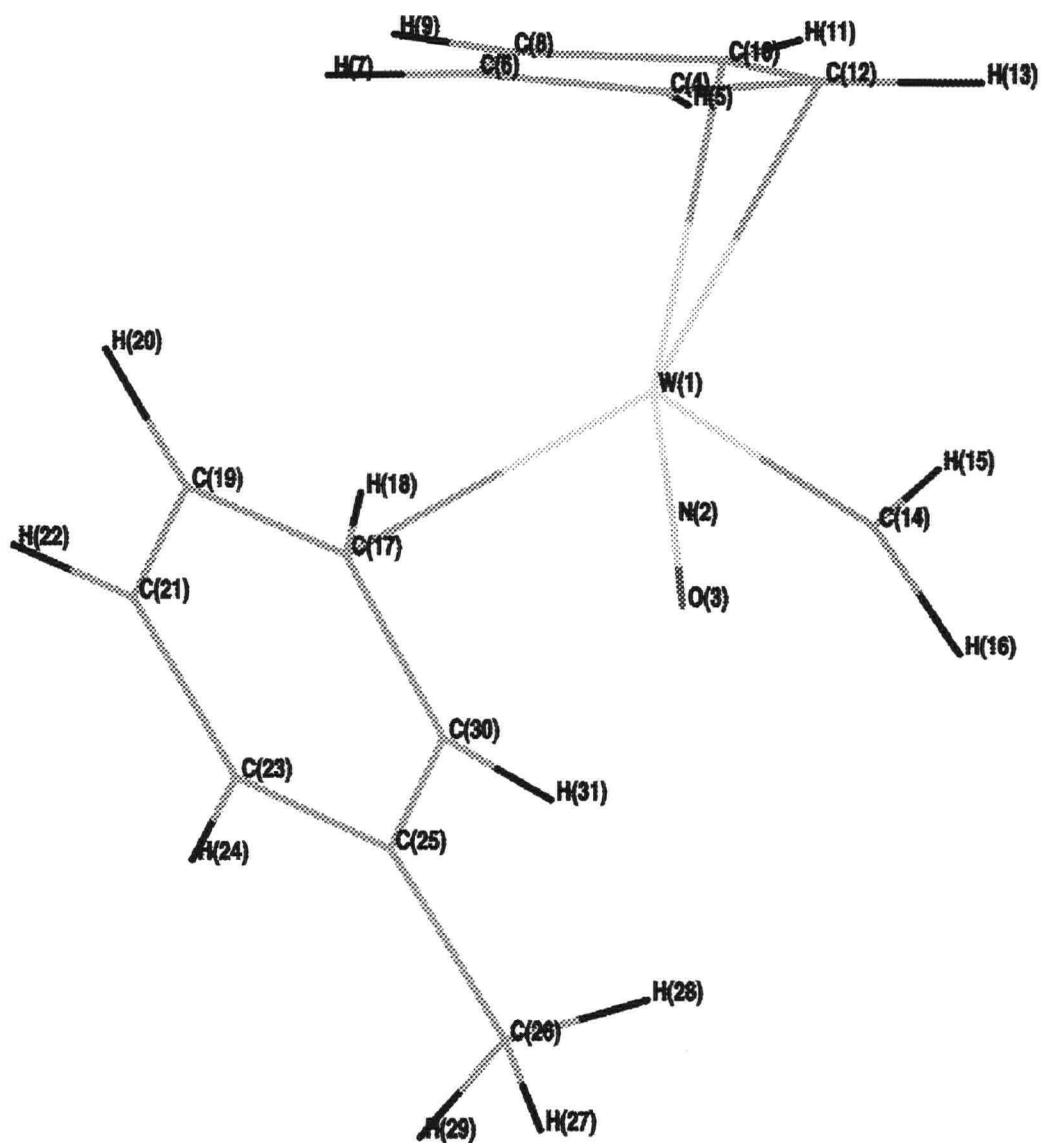
W	-0.558078	0.306070	-0.370055
N	-0.558078	0.306070	1.404956
O	-0.478139	0.306070	2.658847
C	-0.533177	1.242825	-2.718387
H	-0.782857	0.657889	-3.592730
C	0.790661	1.494198	-2.212670
H	1.708286	1.104132	-2.634911
C	0.696548	2.358422	-1.080008
H	1.518186	2.733509	-0.484732
C	-0.704687	2.619773	-0.842229
H	-1.108596	3.282168	-0.089659
C	-1.459360	1.952846	-1.881121
H	-2.529472	2.006133	-2.013951
C	-2.213649	-0.687803	-0.622109
H	-2.716469	-0.756286	-1.599402
H	-2.805692	-1.156989	0.173563
C	1.201189	-1.376875	-0.619804
H	1.210008	-1.375988	-1.708059
C	2.275079	-0.754127	0.102974
H	2.931974	-0.061231	-0.416892
C	2.492917	-1.039680	1.450852
H	3.297110	-0.540112	1.985947
C	1.665879	-1.966986	2.147050
C	1.886036	-2.227183	3.620472
H	2.953430	-2.256429	3.872798
H	1.424994	-1.419453	4.204366
H	1.428135	-3.170540	3.938065
C	0.640433	-2.618890	1.439052
H	0.009618	-3.340539	1.950986
C	0.402064	-2.337679	0.076044
H	-0.348800	-2.899515	-0.467506



Data For  $\text{CpW}(\text{NO})(=\text{CH}_2)(\text{H}-\text{C}_6\text{H}_4\text{CH}_3)$  (**E**), (meta, syn)

## Selected Bond Distances and Angles

W(1)-C(30) = 2.7651  
W(1)-C(17) = 2.4697  
W(1)-C(14) = 1.9474  
W(1)-H(31) = 3.0924  
C(14)-H(31) = 2.8973  
C(30)-H(31) = 1.0842  
C(30)-W(1)-C(14) = 83.7  
H(31)-W(1)-C(14) = 63.9  
W(1)-C(17)-C(30) = 86.0  
C(14)-W(1)-C(17)-C(30) = -50.0  
H(31)-C(30)-W(1)-C(14) = 12.3  
C(17)-W(1)-C(14) = 104.3  
C(14)-W(1)-C(17)-H(18) = 69.1





Data For  $\text{CpW}(\text{NO})(=\text{CH}_2)(\text{H}-\text{C}_6\text{H}_4\text{CH}_3)$  (**E'**), (ortho, syn)

## Selected Bond Distances and Angles

W(1)-C(14) = 1.9527

W(1)-C(30) = 2.5756

W(1)-C(17) = 2.6843

W(1)-C(25) = 3.3975

W(1)-H(31) = 2.8179

C(14)-H(31) = 2.8331

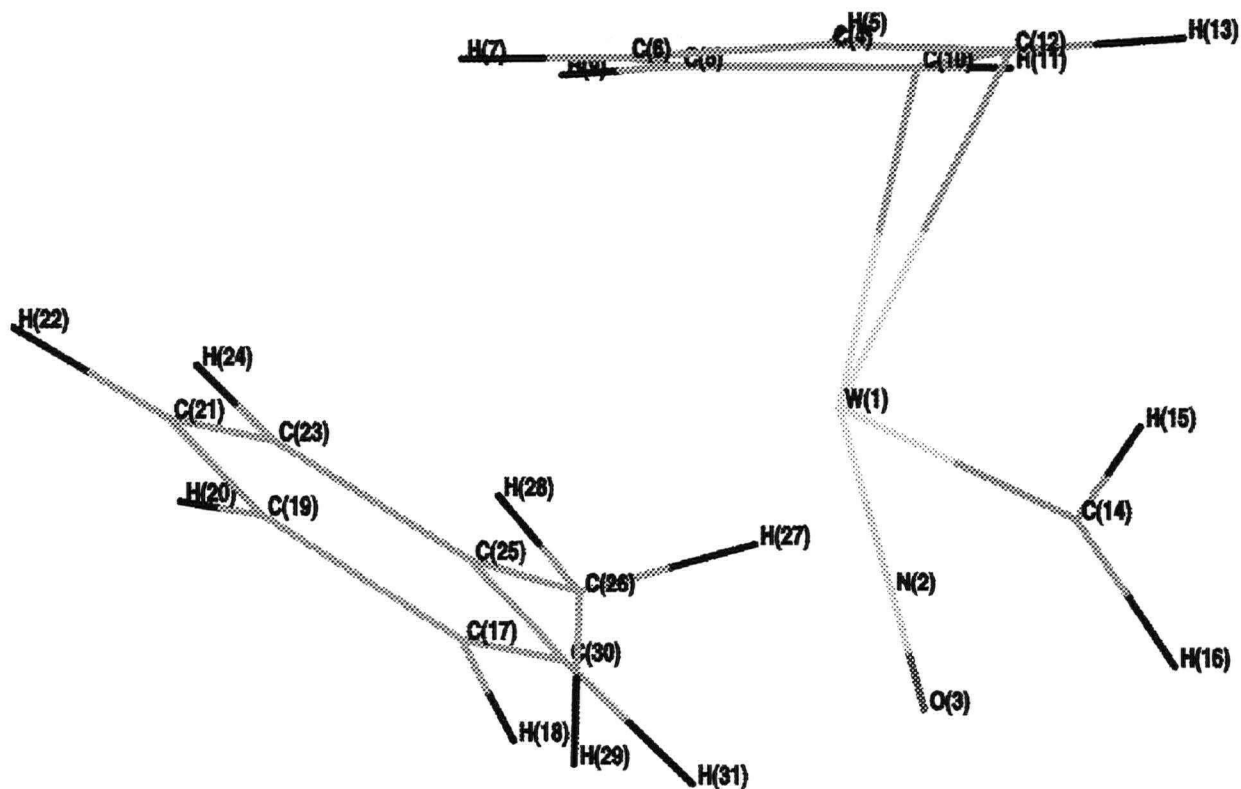
C(30)-H(31) = 1.0846

C(30)-W(1)-C(14) = 88.9

W(1)-C(30)-C(21) = 100.8

H(31)-C(14)-W(1)-C(30) = -33.3

H(31)-C(30)-C(17)-C(19) = 166.0



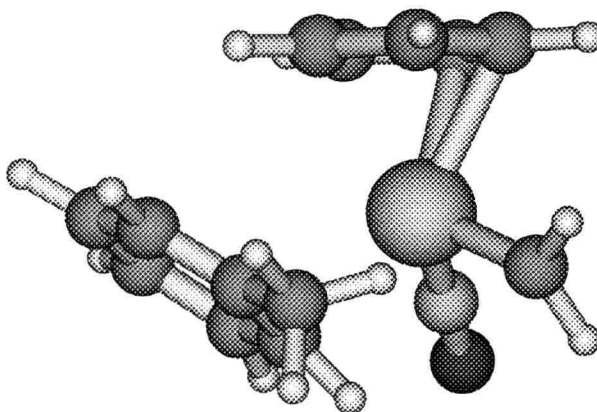
Data For CpW(NO)(=CH<sub>2</sub>)(H-C<sub>6</sub>H<sub>4</sub>CH<sub>3</sub>) (E'), (ortho, syn) cont'd

31

scf done: -702.058520

Thermal corr. to free energy: 0.200707

W	-0.024922	0.626555	0.369503
N	-0.024922	0.626555	2.150421
O	0.044494	0.626555	3.402400
C	0.743746	1.277384	-1.919114
H	0.082876	1.290008	-2.774493
C	1.586710	0.186136	-1.515827
H	1.645903	-0.775324	-2.004864
C	2.339662	0.584241	-0.364297
H	3.065649	-0.015454	0.167339
C	1.925272	1.920540	-0.011476
H	2.324863	2.519829	0.794434
C	0.952512	2.355417	-0.990288
H	0.491756	3.331138	-1.027443
C	-1.709586	1.594809	0.175752
H	-2.010718	2.086450	-0.762381
H	-2.404297	1.829269	0.992521
C	-0.199745	-2.002912	0.880052
H	-0.203697	-1.867920	1.956209
C	0.804424	-2.819763	0.278992
H	1.646949	-3.156100	0.877224
C	0.666277	-3.224393	-1.048985
H	1.409950	-3.879186	-1.497767
C	-0.452363	-2.803110	-1.822380
H	-0.547110	-3.138934	-2.852796
C	-1.445696	-1.988560	-1.269334
C	-2.668959	-1.570733	-2.054847
H	-2.799509	-0.481172	-2.013614
H	-2.602786	-1.876231	-3.104778
H	-3.578900	-2.017530	-1.630523
C	-1.320693	-1.583655	0.105263
H	-2.187553	-1.164598	0.604537



Data For  $\text{CpW}(\text{NO})(=\text{CH}_2)(\text{H}-\text{C}_6\text{H}_4\text{CH}_3)$  ( $\mathbf{E}'$ ), (meta, syn)

## Selected Bond Distances and Angles

$$\text{W}(1)-\text{C}(14) = 1.9480$$

$$\text{W}(1)-\text{C}(30) = 2.5027$$

$$\text{W}(1)-\text{C}(17) = 3.1300$$

$$\text{W}(1)-\text{C}(28) = 3.2439$$

$$\text{W}(1)-\text{H}(31) = 2.3620$$

$$\text{C}(14)-\text{H}(31) = 2.8086$$

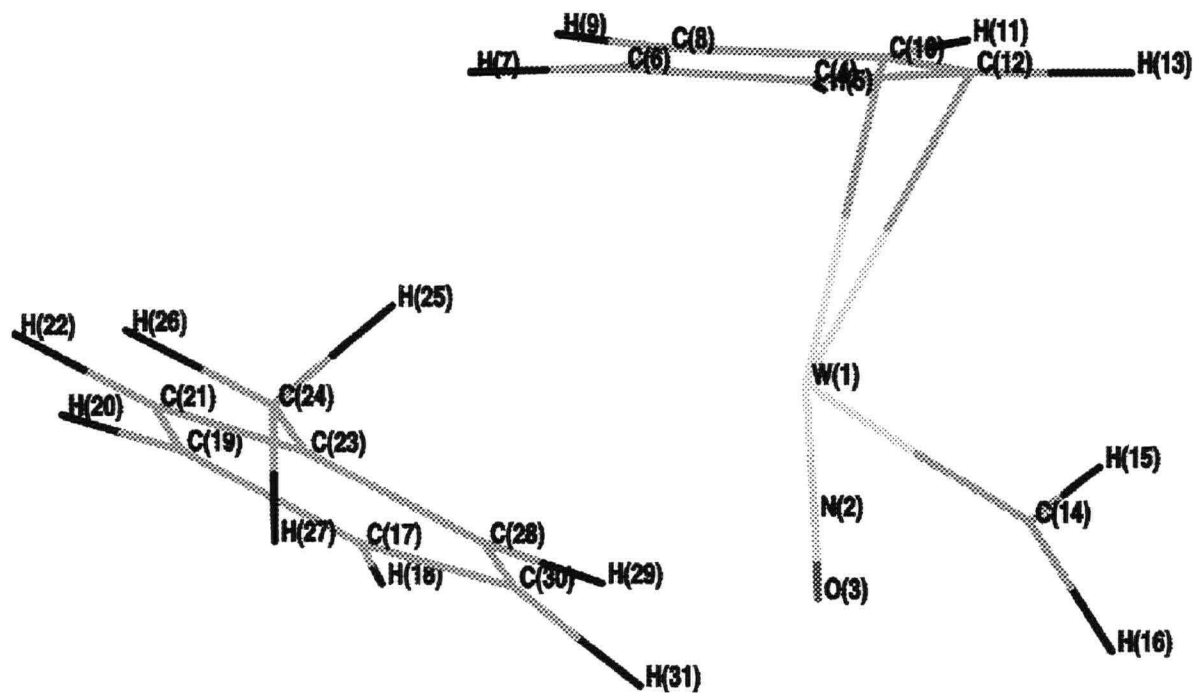
$$\text{C}(30)-\text{H}(31) = 1.1001$$

$$\text{C}(30)-\text{W}(1)-\text{C}(14) = 100.2$$

$$\text{W}(1)-\text{C}(30)-\text{C}(21) = 121.1$$

$$\text{H}(31)-\text{C}(14)-\text{W}(1)-\text{C}(30) = -42.0$$

$$\text{H}(31)-\text{C}(30)-\text{C}(17)-\text{C}(19) = 168.0$$



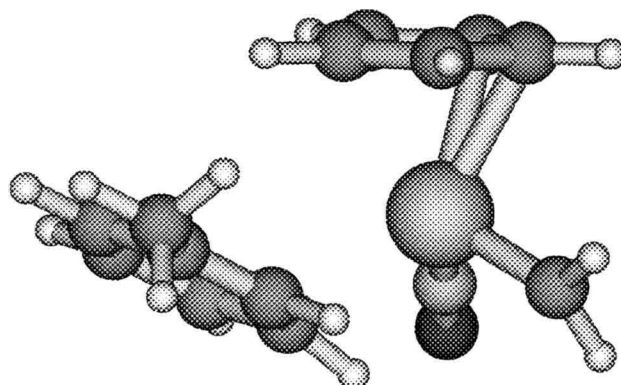
Data For CpW(NO)(=CH<sub>2</sub>)(H-C<sub>6</sub>H<sub>4</sub>CH<sub>3</sub>) (E'), (meta, syn) cont'd

31

scf done: -702.056457

Thermal corr. to free energy: 0.1986640

W	-0.054534	0.813443	0.419168
N	-0.054534	0.813443	2.199166
O	0.034989	0.813443	3.452134
C	0.891511	1.129794	-1.883795
H	0.286690	1.130590	-2.779910
C	1.600757	0.000002	-1.335697
H	1.579981	-1.007472	-1.729437
C	2.331862	0.427091	-0.187152
H	2.963749	-0.188114	0.438806
C	2.036036	1.826688	0.026772
H	2.468473	2.458727	0.789394
C	1.172593	2.263951	-1.050849
H	0.823759	3.274002	-1.204859
C	-1.587219	1.992090	0.184289
H	-1.832074	2.445331	-0.789533
H	-2.231493	2.379914	0.983155
C	-0.250936	-2.265549	0.946636
H	0.006192	-2.098801	1.988317
C	0.319373	-3.324066	0.217247
H	1.045205	-3.981792	0.687864
C	-0.062964	-3.542984	-1.122228
H	0.376538	-4.374253	-1.670884
C	-1.014839	-2.719584	-1.769577
C	-1.434335	-2.979810	-3.205048
H	-1.246597	-2.105145	-3.842106
H	-0.891389	-3.829112	-3.634276
H	-2.507620	-3.202696	-3.269968
C	-1.576934	-1.655973	-1.032483
H	-2.324809	-1.009307	-1.486565
C	-1.190063	-1.414086	0.308594
H	-1.788279	-0.713652	0.910081

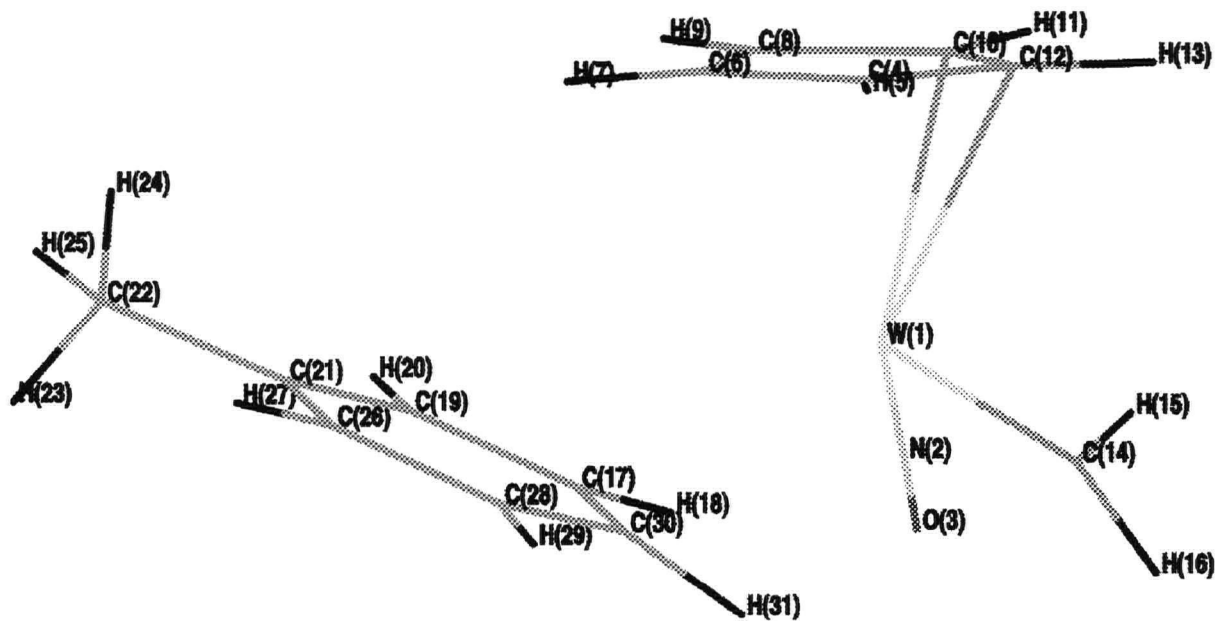
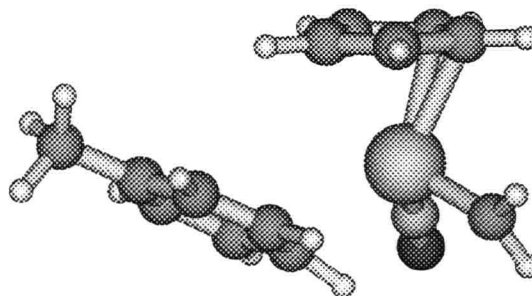


Data For CpW(NO)(=CH<sub>2</sub>)(H-C<sub>6</sub>H<sub>4</sub>CH<sub>3</sub>) (E'), (para)

## Selected Bond Distances and Angles

W(1)-C(14) = 1.9473  
 W(1)-C(30) = 2.4918  
 W(1)-C(17) = 3.2462  
 W(1)-C(28) = 3.1194  
 W(1)-H(31) = 2.3663  
 C(14)-H(31) = 2.7835  
 C(30)-H(31) = 1.0996

C(30)-W(1)-C(14) = 100.4  
 W(1)-C(30)-C(21) = 121.0  
 H(31)-C(14)-W(1)-C(30) = -37.8  
 H(31)-C(30)-C(17)-C(19) = 12.7

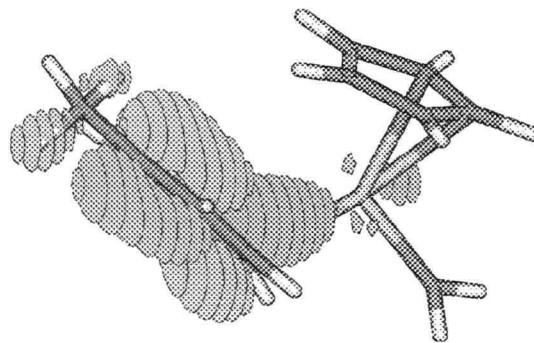
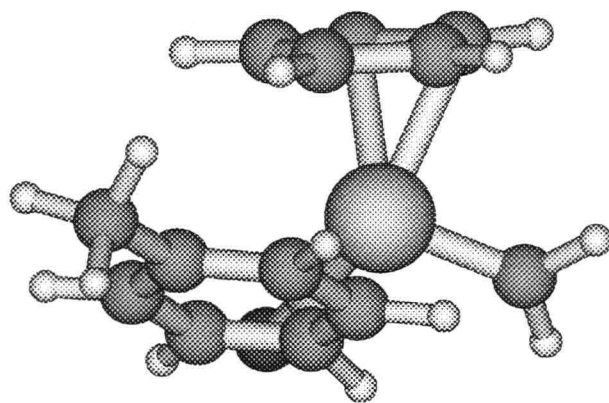


31

scf done: -702.057786

Thermal corr. to free energy: 0.199214

W	-0.220293	0.896293	0.330005
N	-0.220293	0.896293	2.110129
O	-0.131632	0.896293	3.363476
C	0.703062	1.244010	-1.977191
H	0.096497	1.196857	-2.870980
C	1.478584	0.164381	-1.417073
H	1.516522	-0.845989	-1.801157
C	2.184210	0.646942	-0.275171
H	2.850056	0.076606	0.358011
C	1.805615	2.028865	-0.076073
H	2.201799	2.694341	0.677792
C	0.918368	2.402415	-1.158586
H	0.508863	3.387824	-1.323085
C	-1.814444	1.990181	0.097840
H	-2.088600	2.429944	-0.874437
H	-2.476224	2.341444	0.899421
C	-1.496081	-1.702465	-1.138559
H	-2.243839	-1.124514	-1.675182
C	-0.814367	-2.752281	-1.769675
H	-1.029212	-2.991005	-2.809116
C	0.148610	-3.518631	-1.063772
C	0.856076	-4.672884	-1.746100
H	0.188478	-5.542515	-1.826322
H	1.165750	-4.408720	-2.764854
H	1.744622	-4.988594	-1.188949
C	0.411449	-3.206910	0.290048
H	1.144174	-3.791263	0.841498
C	-0.275652	-2.163131	0.936196
H	-0.097782	-1.952655	1.986912
C	-1.219142	-1.383710	0.217067
H	-1.902053	-0.712530	0.757683



Data For  $\text{CpW}(\text{NO})(=\text{CH}_2)(\text{H}-\text{C}_6\text{H}_4\text{CH}_3)$  ( $\text{E}'$ ), (ortho, anti)

## Selected Bond Distances and Angles

$$\text{W}(1)-\text{C}(14) = 1.9453$$

$$\text{W}(1)-\text{C}(30) = 2.5875$$

$$\text{W}(1)-\text{C}(17) = 3.3895$$

$$\text{W}(1)-\text{C}(28) = 2.6960$$

$$\text{W}(1)-\text{H}(31) = 2.8146$$

$$\text{C}(14)-\text{H}(31) = 3.3932$$

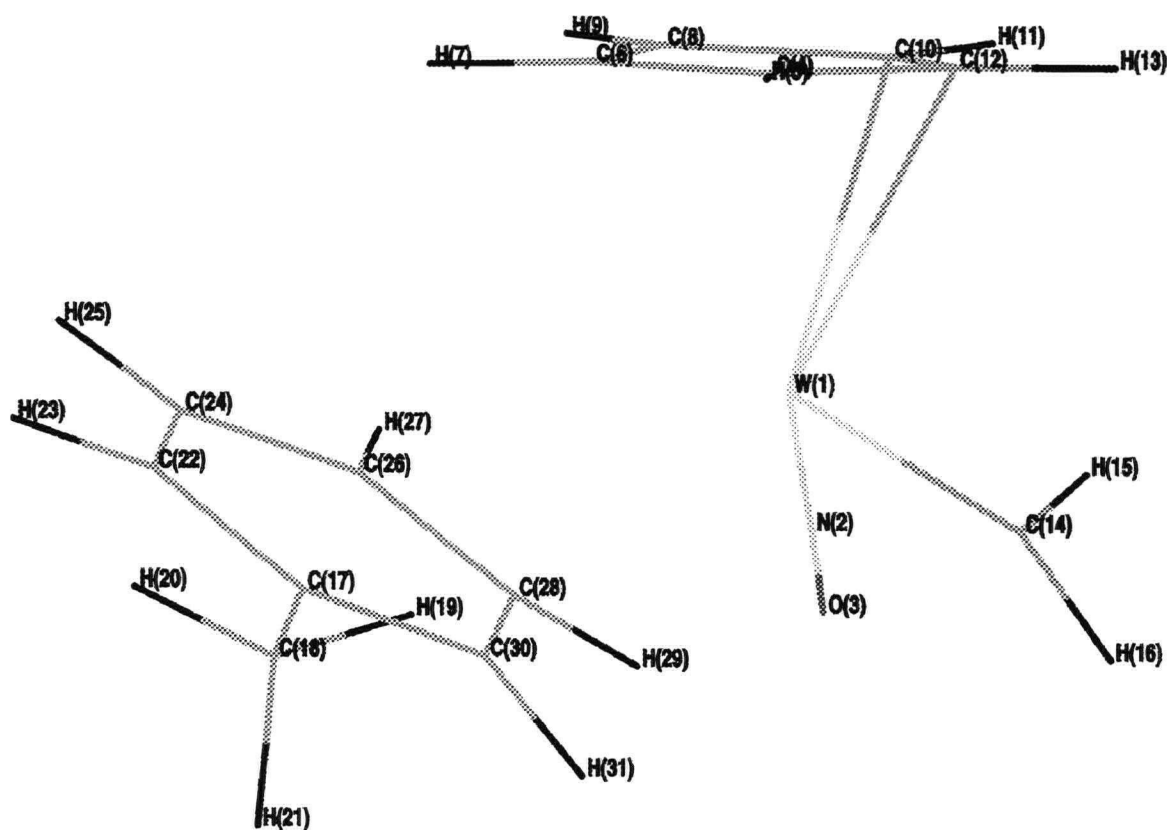
$$\text{C}(30)-\text{H}(31) = 1.0858$$

$$\text{C}(30)-\text{W}(1)-\text{C}(14) = 103.1$$

$$\text{W}(1)-\text{C}(30)-\text{C}(24) = 100.8$$

$$\text{H}(31)-\text{C}(14)-\text{W}(1)-\text{C}(30) = -52.8$$

$$\text{H}(31)-\text{C}(30)-\text{C}(17)-\text{C}(22) = 166.3$$



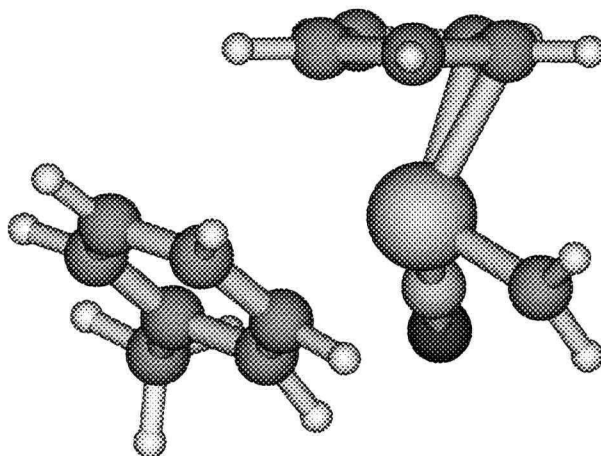
Data For CpW(NO)(=CH<sub>2</sub>)(H-C<sub>6</sub>H<sub>4</sub>CH<sub>3</sub>) (E'), (ortho, anti) cont'd

31

scf done: -702.059541

Thermal corr. to free energy: 0.201471

W	-0.191383	0.723892	0.066925
N	-0.191383	0.723892	1.847972
O	-0.092272	0.723892	3.099697
C	0.801423	1.093894	-2.207322
H	0.242079	0.979561	-3.125393
C	1.620605	0.081823	-1.577821
H	1.745484	-0.932254	-1.928742
C	2.245168	0.646612	-0.428652
H	2.919487	0.142297	0.250010
C	1.763810	2.004161	-0.289611
H	2.074035	2.714832	0.463400
C	0.906942	2.285951	-1.421823
H	0.436389	3.235326	-1.629300
C	-1.788681	1.813640	-0.145688
H	-2.074953	2.255519	-1.113655
H	-2.437870	2.163025	0.666482
C	-0.104068	-2.565811	0.878706
C	0.300166	-2.759894	2.324119
H	0.573905	-1.803795	2.787069
H	1.145541	-3.450501	2.416615
H	-0.534516	-3.166433	2.912399
C	0.478206	-3.299961	-0.161534
H	1.253028	-4.028180	0.067815
C	0.054798	-3.130910	-1.509458
H	0.503824	-3.740823	-2.290397
C	-0.937230	-2.204713	-1.831166
H	-1.272367	-2.083338	-2.857947
C	-1.551102	-1.438577	-0.795104
H	-2.441398	-0.859289	-1.009977
C	-1.146347	-1.630447	0.556310
H	-1.754646	-1.226932	1.360094



Data For  $\text{CpW}(\text{NO})(\text{H}_2\text{C}\cdots\text{H}\cdots\text{C}_6\text{H}_4\text{-CH}_3)$ , (ortho, anti)

Selected Bond Distances and Angles

$\text{W}(1)\text{-C}(30) = 2.2673$

$\text{W}(1)\text{-C}(14) = 1.9827$

$\text{W}(1)\text{-H}(31) = 1.8493$

$\text{C}(14)\text{-H}(31) = 1.6961$

$\text{C}(30)\text{-H}(31) = 1.4472$

$\text{C}(30)\text{-W}(1)\text{-C}(14) = 91.8$

$\text{H}(31)\text{-W}(1)\text{-C}(14) = 52.4$

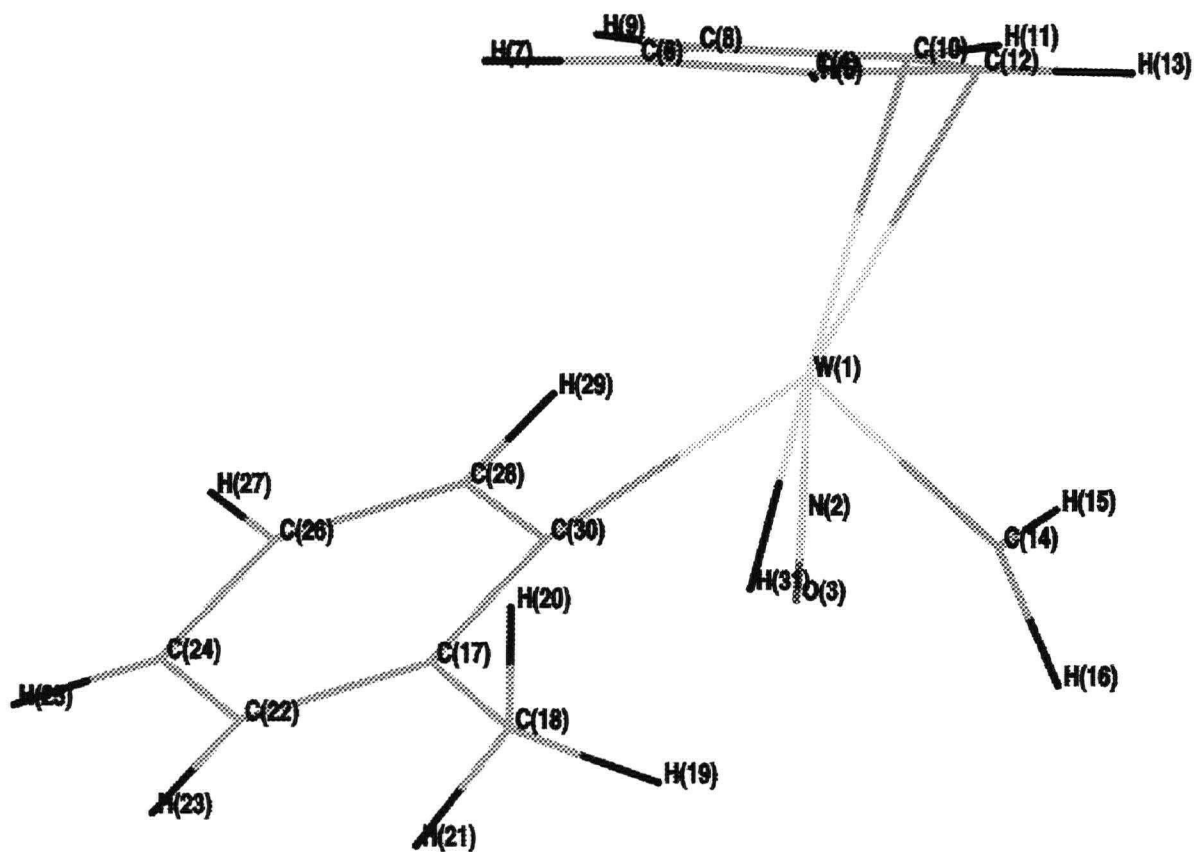
$\text{H}(31)\text{-W}(1)\text{-C}(30) = 39.5$

$\text{W}(1)\text{-C}(30)\text{-H}(31) = 54.4$

$\text{W}(1)\text{-C}(30)\text{-C}(28) = 120.6$

$\text{C}(14)\text{-W}(1)\text{-C}(30)\text{-C}(28) = 87.4$

$\text{H}(31)\text{-C}(14)\text{-W}(1)\text{-C}(30) = 3.1$



Data For CpW(NO)(H<sub>2</sub>C•••H•••C<sub>6</sub>H<sub>4</sub>-CH<sub>3</sub>), (ortho, anti) cont'd

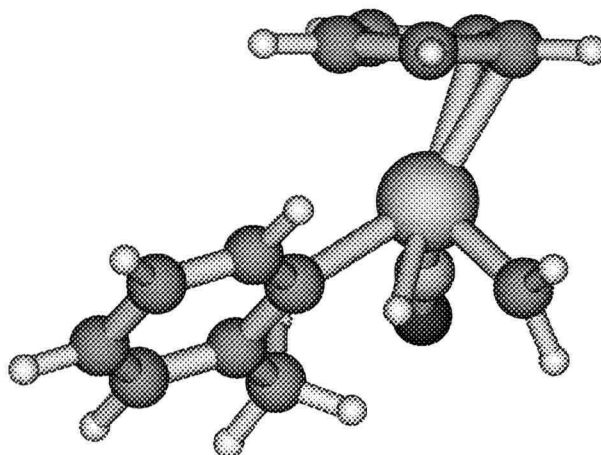
31

scf done: -702.008563

Thermal corr. to free energy: 0.198850

One Imaginary Frequency: 1190.23i cm<sup>-1</sup>

W	0.089585	0.781718	0.003536
N	0.089585	0.781718	1.779433
O	0.175931	0.781718	3.026753
C	1.050907	0.974158	-2.311631
H	0.460510	0.850636	-3.209510
C	1.805886	-0.054648	-1.639339
H	1.845934	-1.096952	-1.923533
C	2.491567	0.534002	-0.532310
H	3.147554	0.024369	0.160047
C	2.134141	1.932967	-0.483618
H	2.518883	2.662046	0.215692
C	1.263667	2.202554	-1.604129
H	0.851185	3.167712	-1.862577
C	-1.655982	1.694317	-0.222558
H	-2.041489	1.991485	-1.209224
H	-2.346955	1.969667	0.582069
C	-0.982189	-2.062755	1.052697
C	-0.825505	-1.456533	2.360536
H	-1.431164	-0.553246	2.416854
H	0.221345	-1.202167	2.519671
H	-1.149020	-2.158891	3.127316
C	-1.225786	-3.444211	0.949980
H	-1.288581	-4.046762	1.853352
C	-1.391636	-4.049460	-0.308720
H	-1.583488	-5.119342	-0.374446
C	-1.327332	-3.278934	-1.493254
H	-1.457230	-3.758338	-2.462388
C	-1.084285	-1.896465	-1.375962
H	-1.062767	-1.293588	-2.283539
C	-0.881187	-1.263645	-0.117020
H	-1.582189	0.002335	-0.129587



Data For CpW(NO)(H<sub>2</sub>C•••H•••C<sub>6</sub>H<sub>4</sub>-CH<sub>3</sub>), (meta, anti)

## Selected Bond Distances and Angles

W(1)-C(30) = 2.2673

W(1)-C(14) = 1.9824

W(1)-H(31) = 1.8499

C(14)-H(31) = 1.6954

C(30)-H(31) = 1.4469

C(30)-W(1)-C(14) = 91.8

H(31)-W(1)-C(14) = 52.4

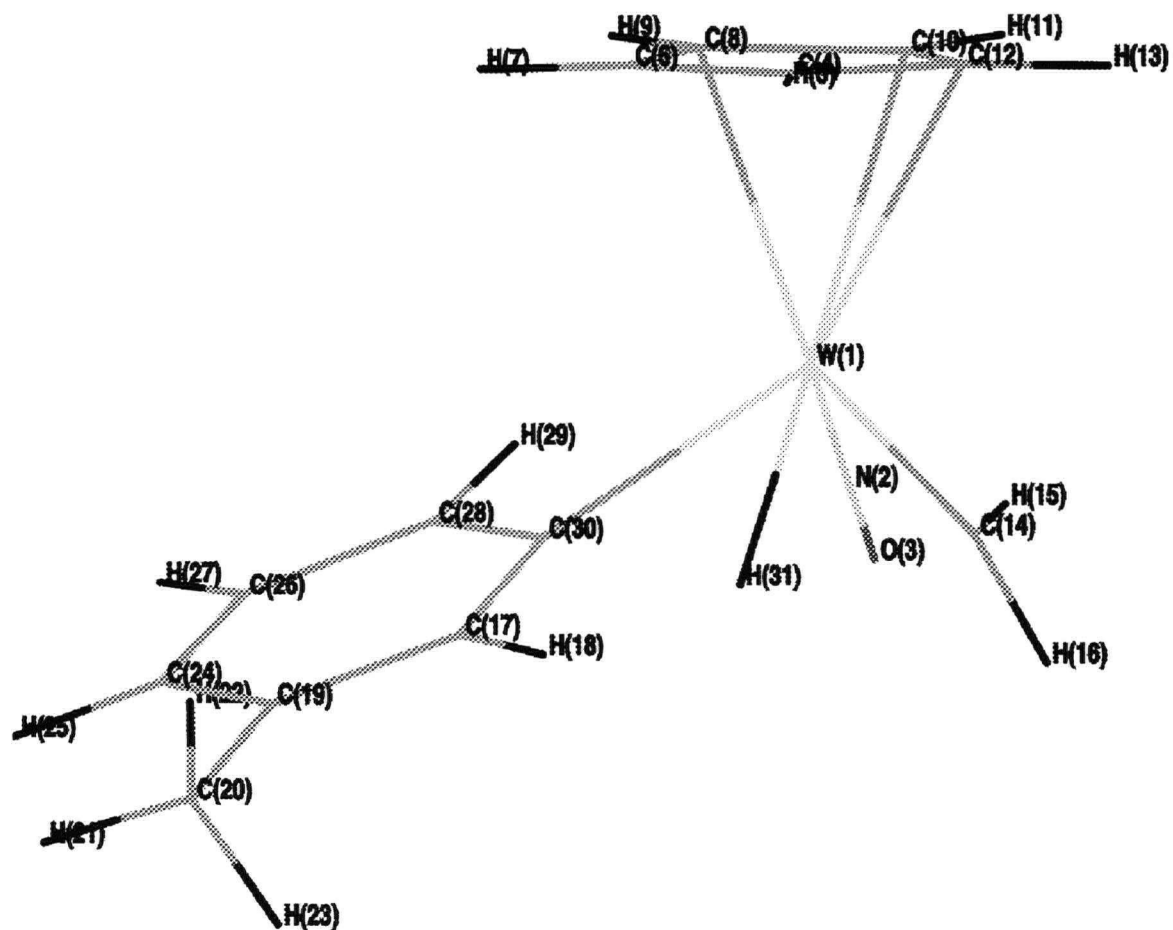
H(31)-W(1)-C(30) = 39.5

W(1)-C(30)-H(31) = 54.5

W(1)-C(30)-C(28) = 120.8

C(14)-W(1)-C(30)-C(28) = 87.5

H-(31)-C(14)-W(1)-C(30) = 2.9



Data For CpW(NO)(H<sub>2</sub>C•••H•••C<sub>6</sub>H<sub>4</sub>-CH<sub>3</sub>), (meta, anti) cont'd

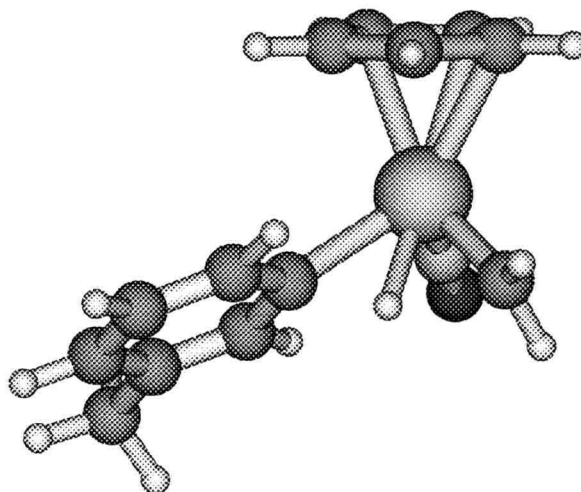
31

scf done: -702.039770

Thermal corr. to free energy: 0.196342

Imaginary Frequency: 1131.98i cm<sup>-1</sup>

W	0.140883	0.910876	0.004828
N	0.205762	0.892969	1.779263
O	0.336080	0.874645	3.022881
C	1.020424	1.092366	-2.343292
H	0.392260	0.995430	-3.218562
C	1.766067	0.033579	-1.708158
H	1.761078	-1.007005	-2.001427
C	2.511861	0.589770	-0.623387
H	3.174975	0.052458	0.040696
C	2.202729	1.999167	-0.550312
H	2.637413	2.709152	0.139285
C	1.299135	2.306563	-1.634363
H	0.908134	3.286535	-1.869181
C	-1.582534	1.878222	-0.150638
H	-1.993442	2.197070	-1.120142
H	-2.236449	2.165840	0.680225
C	-0.983978	-1.903148	1.074802
H	-0.816414	-1.444289	2.046114
C	-1.273332	-3.282705	1.016012
C	-1.310305	-4.120276	2.282210
H	-2.066497	-4.912369	2.218536
H	-0.340216	-4.606130	2.460515
H	-1.533645	-3.505056	3.161113
C	-1.510501	-3.869762	-0.247638
H	-1.746153	-4.930764	-0.311693
C	-1.461270	-3.092975	-1.420628
H	-1.663473	-3.553392	-2.385296
C	-1.166608	-1.721364	-1.347892
H	-1.160930	-1.127410	-2.260103
C	-0.897119	-1.102328	-0.096157
H	-1.558402	0.184530	-0.078609



Data For CpW(NO)(H<sub>2</sub>C•••H•••C<sub>6</sub>H<sub>4</sub>-CH<sub>3</sub>), (para)

## Selected Bond Distances and Angles

W(1)-C(30) = 2.2625

W(1)-C(14) = 1.9827

W(1)-H(31) = 1.8508

C(14)-H(31) = 1.6910

C(30)-H(31) = 1.4494

C(30)-W(1)-C(14) = 91.8

H(31)-W(1)-C(14) = 52.1

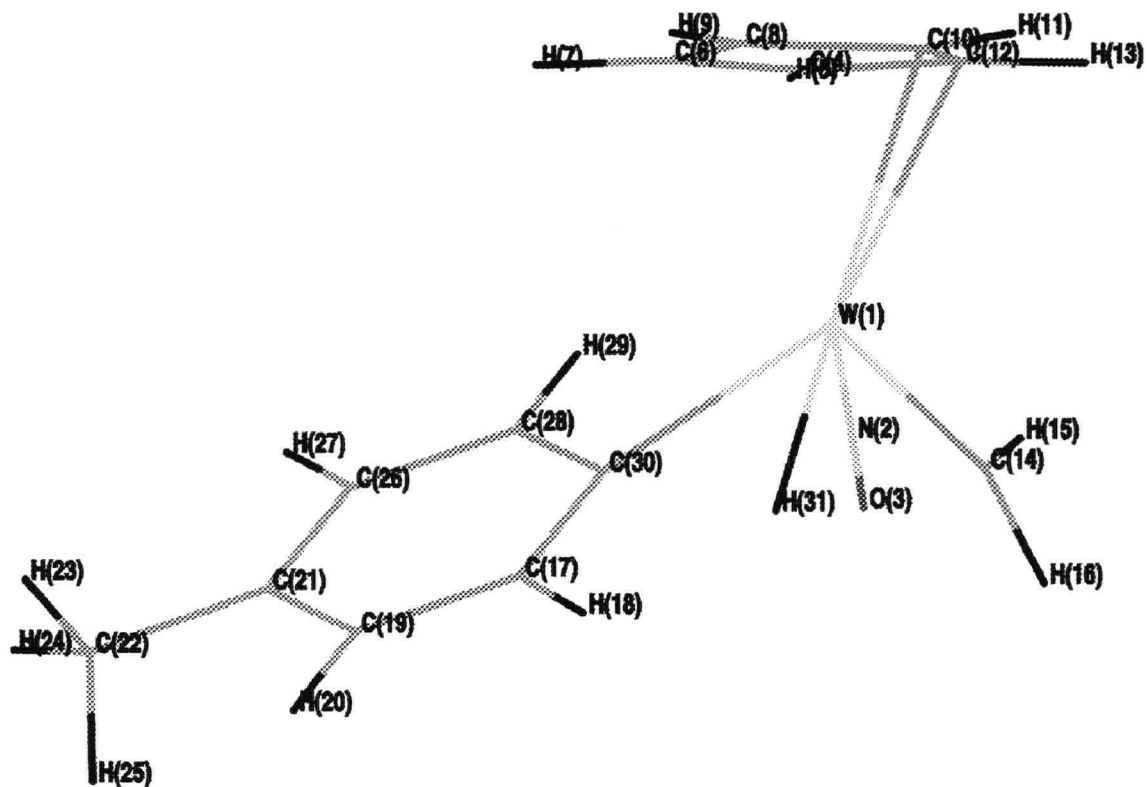
H(31)-W(1)-C(30) = 39.7

W(1)-C(30)-H(31) = 54.7

W(1)-C(30)-C(28) = 121.1

C(14)-W(1)-C(30)-C(28) = 87.5

H(31)-C(14)-W(1)-C(30) = 3.0



Data For CpW(NO)(H<sub>2</sub>C•••H•••C<sub>6</sub>H<sub>4</sub>-CH<sub>3</sub>), (para) cont'd

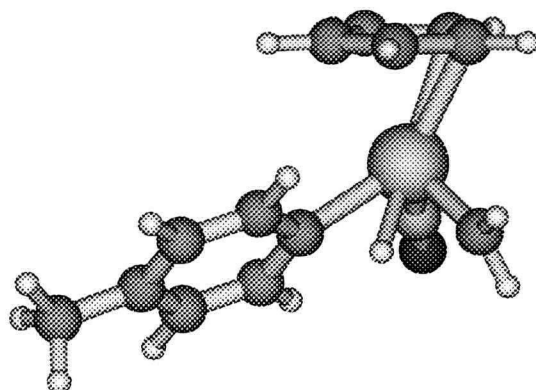
31

scf done: -702.040158

Thermal corr. to free energy:0.195989

One imaginary frequency: 1154.27i cm<sup>-1</sup>

W	0.117599	0.977454	0.127987
N	0.117599	0.977454	1.903909
O	0.201104	0.977454	3.151590
C	1.074869	1.160196	-2.189575
H	0.489093	1.004400	-3.085534
C	1.859545	0.165021	-1.500341
H	1.930879	-0.880077	-1.767939
C	2.526468	0.791812	-0.403063
H	3.195506	0.312392	0.298364
C	2.127773	2.180387	-0.377264
H	2.490132	2.931636	0.310477
C	1.250111	2.405469	-1.502220
H	0.809165	3.353422	-1.776562
C	-1.642954	1.861671	-0.095276
H	-2.034411	2.155007	-1.080745
H	-2.336419	2.125808	0.710920
C	-0.904077	-1.885057	1.178526
H	-0.783383	-1.427702	2.156445
C	-1.130032	-3.267778	1.090108
H	-1.174144	-3.859423	2.003078
C	-1.303141	-3.906440	-0.159872
C	-1.577161	-5.396149	-0.241048
H	-1.372233	-5.789666	-1.243316
H	-0.964068	-5.954788	0.477052
H	-2.629447	-5.615312	-0.009013
C	-1.245515	-3.108581	-1.324623
H	-1.386389	-3.572329	-2.299376
C	-1.019172	-1.724552	-1.241572
H	-1.007449	-1.137546	-2.158724
C	-0.819370	-1.078526	0.009464
H	-1.545247	0.175907	-0.005732



Data For CpW(NO)(H<sub>2</sub>C•••H•••C<sub>6</sub>H<sub>4</sub>-CH<sub>3</sub>), (meta, syn)

## Selected Bond Distances and Angles

W(1)-C(30) = 2.2672

W(1)-C(14) = 1.9827

W(1)-H(31) = 1.8493

C(14)-H(31) = 1.6962

C(30)-H(31) = 1.4471

C(30)-W(1)-C(14) = 91.8

H(31)-W(1)-C(14) = 52.4

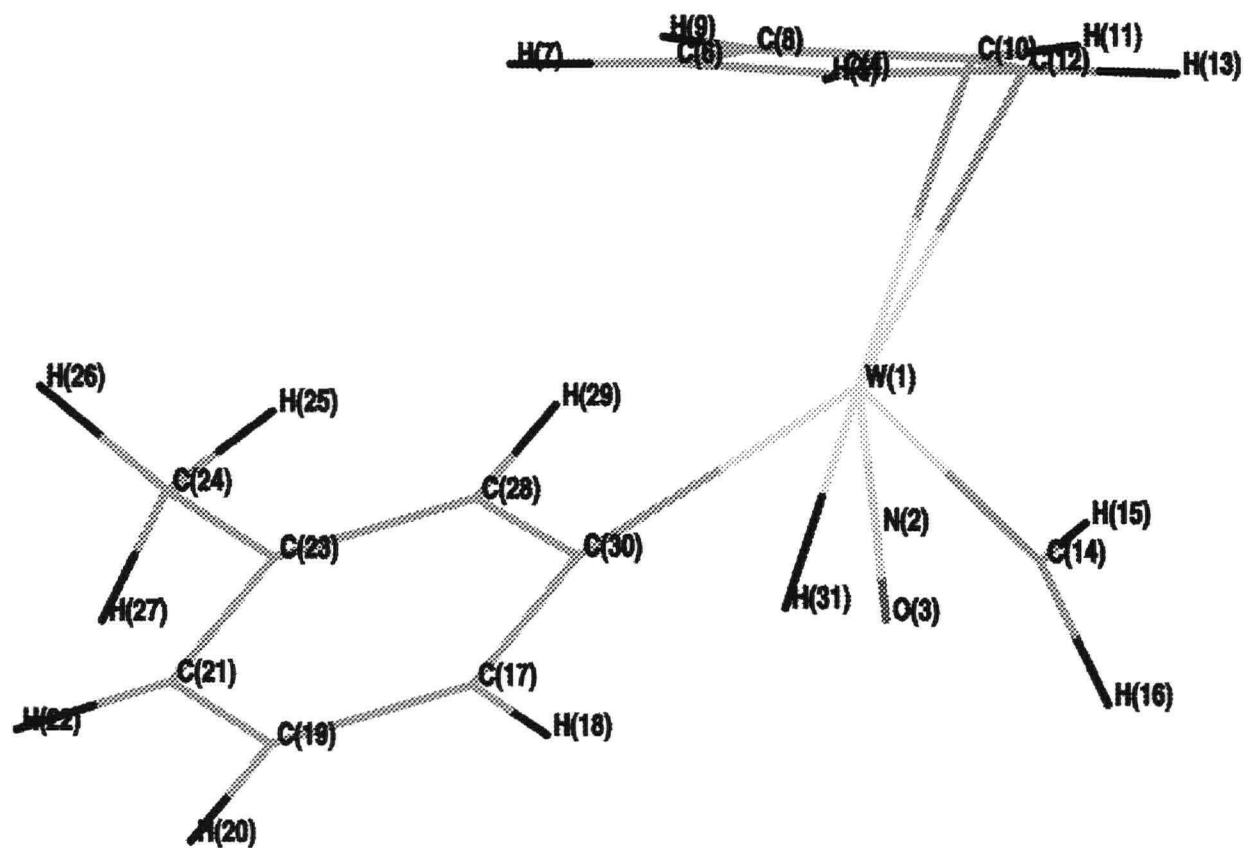
H(31)-W(1)-C(30) = 39.5

W(1)-C(30)-H(31) = 54.4

W(1)-C(30)-C(28) = 120.7

C(14)-W(1)-C(30)-C(28) = 87.4

H(31)-C(14)-W(1)-C(30) = 3.1



Data For CpW(NO)(H<sub>2</sub>C•••H•••C<sub>6</sub>H<sub>4</sub>-CH<sub>3</sub>), (meta, syn) cont'd

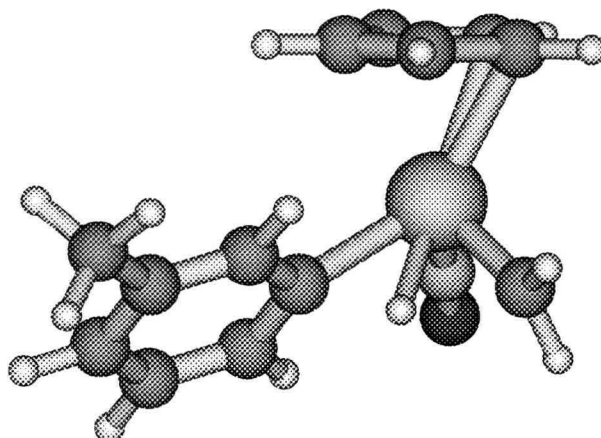
31

scf done: -702.039402

Thermal corr. to free energy: 0.196508

One imaginary frequency: 1134.49i cm<sup>-1</sup>

W	0.121910	0.897702	0.247861
N	0.121910	0.897702	2.023758
O	0.208257	0.897702	3.271078
C	1.083217	1.090138	-2.067312
H	0.492811	0.966622	-2.965186
C	1.838211	0.061338	-1.395030
H	1.878267	-0.980965	-1.679228
C	2.523899	0.650000	-0.288012
H	3.179905	0.140377	0.404336
C	2.166477	2.048938	-0.239283
H	2.551224	2.778006	0.460033
C	1.295999	2.318533	-1.359804
H	0.883527	3.283696	-1.618250
C	-1.623651	1.810313	0.021765
H	-2.009147	2.107484	-0.964904
H	-2.314626	2.085665	0.826388
C	-0.949876	-1.946768	1.297025
H	-0.832511	-1.492709	2.276578
C	-1.193478	-3.328223	1.194313
H	-1.256281	-3.930769	2.097687
C	-1.359313	-3.933486	-0.064383
H	-1.551162	-5.003368	-0.130108
C	-1.294990	-3.162983	-1.248930
C	-1.483590	-3.815702	-2.607656
H	-1.536648	-3.068717	-3.407978
H	-0.652103	-4.495534	-2.840824
H	-2.406461	-4.409480	-2.640721
C	-1.051937	-1.780514	-1.131649
H	-1.030394	-1.177640	-2.039227
C	-0.848857	-1.147662	0.127287
H	-1.549857	0.118306	0.114726



Data For  $\text{CpW}(\text{NO})(\text{H}_2\text{C}\cdots\text{H}\cdots\text{C}_6\text{H}_4\text{-CH}_3)$ , (ortho, syn)

## Selected Bond Distances and Angles

$$\text{W}(1)\text{-C}(30) = 2.2767$$

$$\text{W}(1)\text{-C}(14) = 1.9839$$

$$\text{W}(1)\text{-H}(31) = 1.8488$$

$$\text{C}(14)\text{-H}(31) = 1.6816$$

$$\text{C}(30)\text{-H}(31) = 1.4758$$

$$\text{C}(30)\text{-W}(1)\text{-C}(14) = 92.0$$

$$\text{H}(31)\text{-W}(1)\text{-C}(14) = 51.9$$

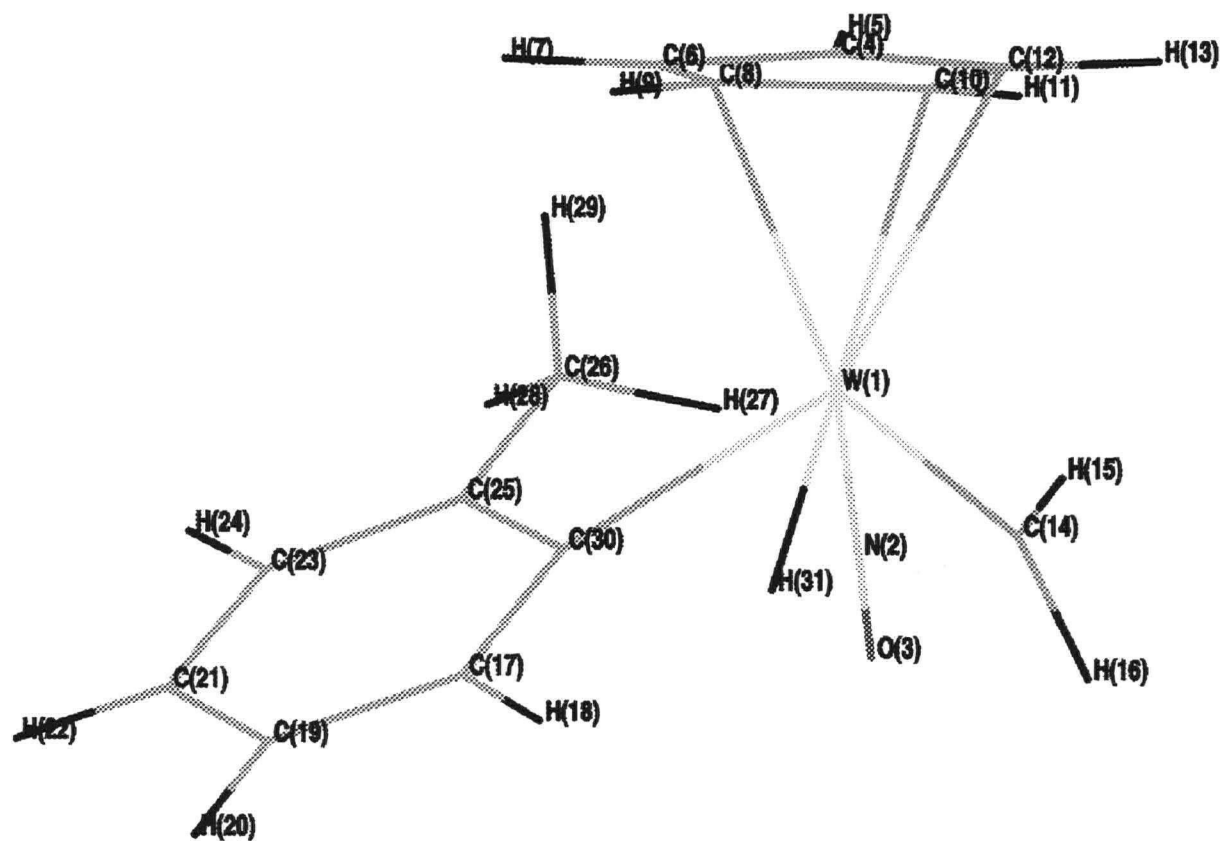
$$\text{H}(31)\text{-W}(1)\text{-C}(30) = 40.3$$

$$\text{W}(1)\text{-C}(30)\text{-H}(31) = 54.1$$

$$\text{W}(1)\text{-C}(30)\text{-C}(25) = 125.1$$

$$\text{C}(14)\text{-W}(1)\text{-C}(30)\text{-C}(25) = 80.4$$

$$\text{H}(31)\text{-C}(14)\text{-W}(1)\text{-C}(30) = 3.9$$



Data For CpW(NO)(H<sub>2</sub>C•••H•••C<sub>6</sub>H<sub>4</sub>-CH<sub>3</sub>), (ortho, syn) cont'd

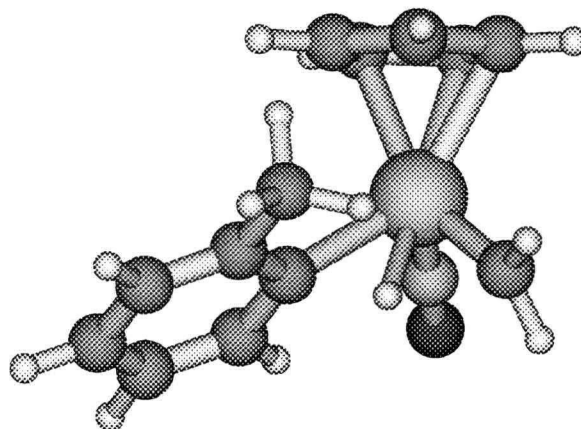
31

scf done: -702.035440

Thermal corr. to free energy: 0.198789

One Imaginary Frequency: 1207.4i cm<sup>-1</sup>

W	0.142683	0.760497	0.203100
N	0.142683	0.760497	1.976919
O	0.245065	0.760497	3.223387
C	1.163187	1.102882	-2.079790
H	0.577955	1.136362	-2.987846
C	1.795329	-0.060244	-1.513315
H	1.751071	-1.065643	-1.909014
C	2.514017	0.338981	-0.341000
H	3.103915	-0.303173	0.298655
C	2.298760	1.753538	-0.151319
H	2.734361	2.362914	0.628053
C	1.478127	2.222205	-1.241658
H	1.162752	3.244345	-1.398729
C	-1.567428	1.741843	-0.016328
H	-1.940111	2.067303	-0.998927
H	-2.242503	2.045530	0.791358
C	-0.873189	-2.030144	1.290748
H	-0.616304	-1.551040	2.229975
C	-1.159841	-3.403793	1.290004
H	-1.107275	-3.967295	2.218413
C	-1.522945	-4.041248	0.088438
H	-1.752743	-5.104302	0.076441
C	-1.612448	-3.288278	-1.094205
H	-1.924885	-3.774471	-2.016870
C	-1.317613	-1.906264	-1.116880
C	-1.478268	-1.161698	-2.431740
H	-1.874765	-0.149960	-2.283584
H	-2.161278	-1.698456	-3.099972
H	-0.520035	-1.059683	-2.957972
C	-0.907875	-1.256274	0.093018
H	-1.566863	0.064242	0.099222



Data For CpW(NO)(CH<sub>3</sub>)(C<sub>6</sub>H<sub>4</sub>-CH<sub>3</sub>), (ortho, anti)

## Selected Bond Distances and Angles

$$W(1)-C(30) = 2.1095$$

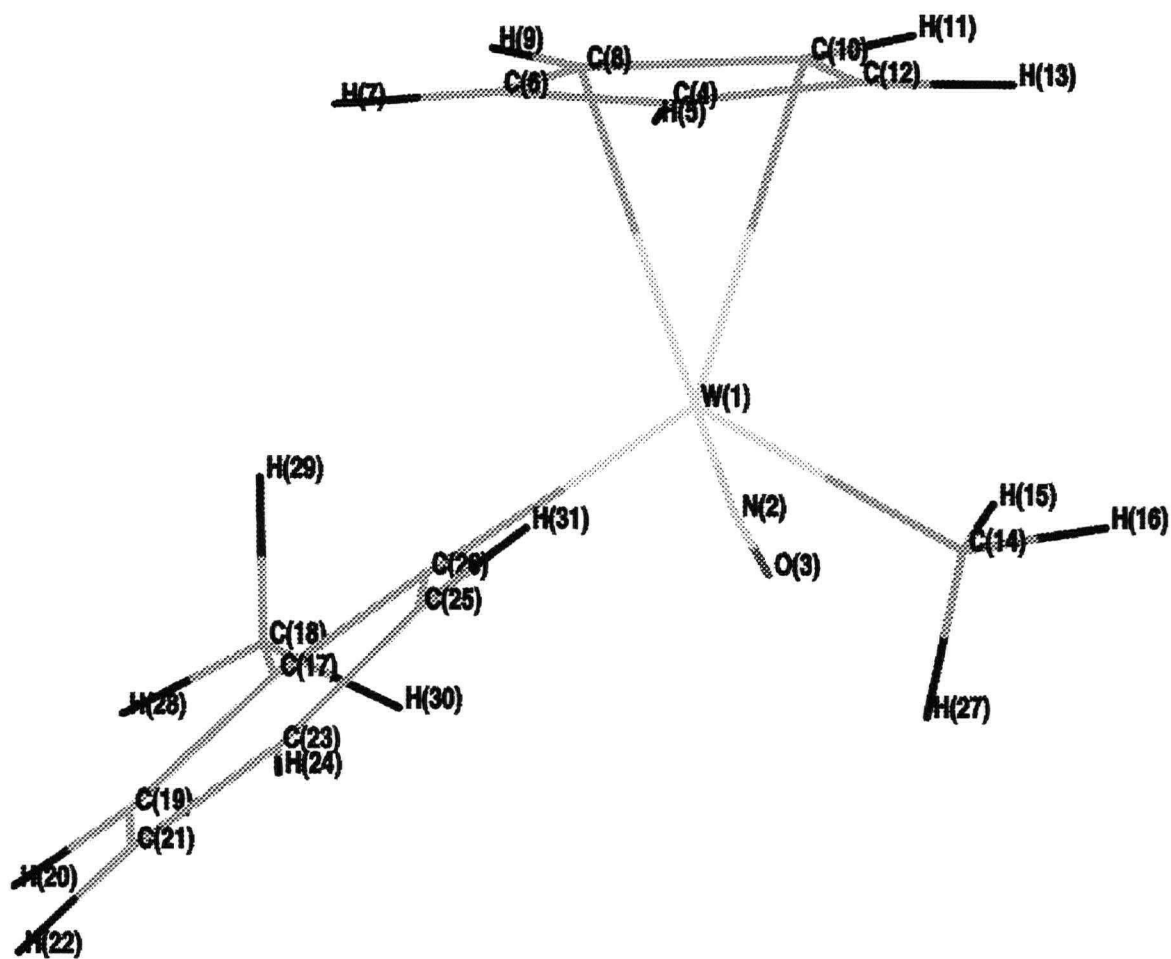
$$W(1)-C(14) = 2.1415$$

$$C(30)-W(1)-C(14) = 109.9$$

$$W(1)-C(30)-C(25) = 110.4$$

$$C(14)-W(1)-C(30)-C(25) = 50.2$$

$$H(31)-C(14)-W(1)-C(30) = 56.3$$



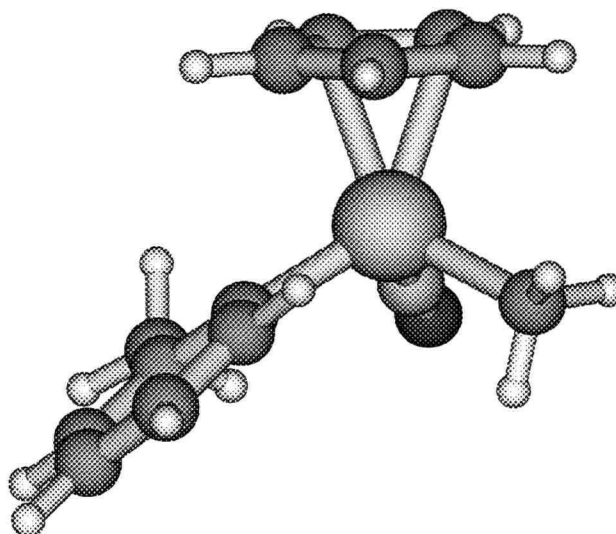
Data For CpW(NO)(CH<sub>3</sub>)(C<sub>6</sub>H<sub>4</sub>-CH<sub>3</sub>), (ortho, anti) cont'd

31

scf done: -702.091840

Thermal corr. to free energy: 0.201020

W	0.083544	0.682488	0.039265
N	0.138575	0.842825	1.799320
O	0.296372	1.014807	3.028937
C	1.042863	0.937947	-2.332834
H	0.474287	0.766643	-3.236861
C	1.813008	-0.038036	-1.622257
H	1.917144	-1.080859	-1.886125
C	2.410720	0.603403	-0.480394
H	3.084246	0.149260	0.232953
C	2.016237	1.995043	-0.498883
H	2.331885	2.750866	0.206552
C	1.164882	2.189679	-1.638720
H	0.697076	3.121345	-1.924107
C	-1.564682	2.030140	-0.191639
H	-1.835353	2.232063	-1.237034
H	-1.419015	2.985650	0.330336
C	-0.528351	-2.374696	0.903649
C	0.354296	-2.289587	2.135772
C	-1.299556	-3.538771	0.695851
H	-1.243536	-4.345935	1.423976
C	-2.144433	-3.678646	-0.423434
H	-2.730751	-4.586304	-0.549651
C	-2.212006	-2.652699	-1.381535
H	-2.847129	-2.754344	-2.258299
C	-1.423952	-1.500461	-1.203559
C	-0.602356	-1.310288	-0.052504
H	-2.406355	1.521120	0.310280
H	0.391452	-3.252314	2.658847
H	1.381385	-2.002066	1.878482
H	-0.014539	-1.533783	2.839067
H	-1.464056	-0.731862	-1.977838



Data For CpW(NO)(CH<sub>3</sub>)(C<sub>6</sub>H<sub>4</sub>-CH<sub>3</sub>), (para)

## Selected Bond Distances and Angles

W(1)-C(30) = 2.1069

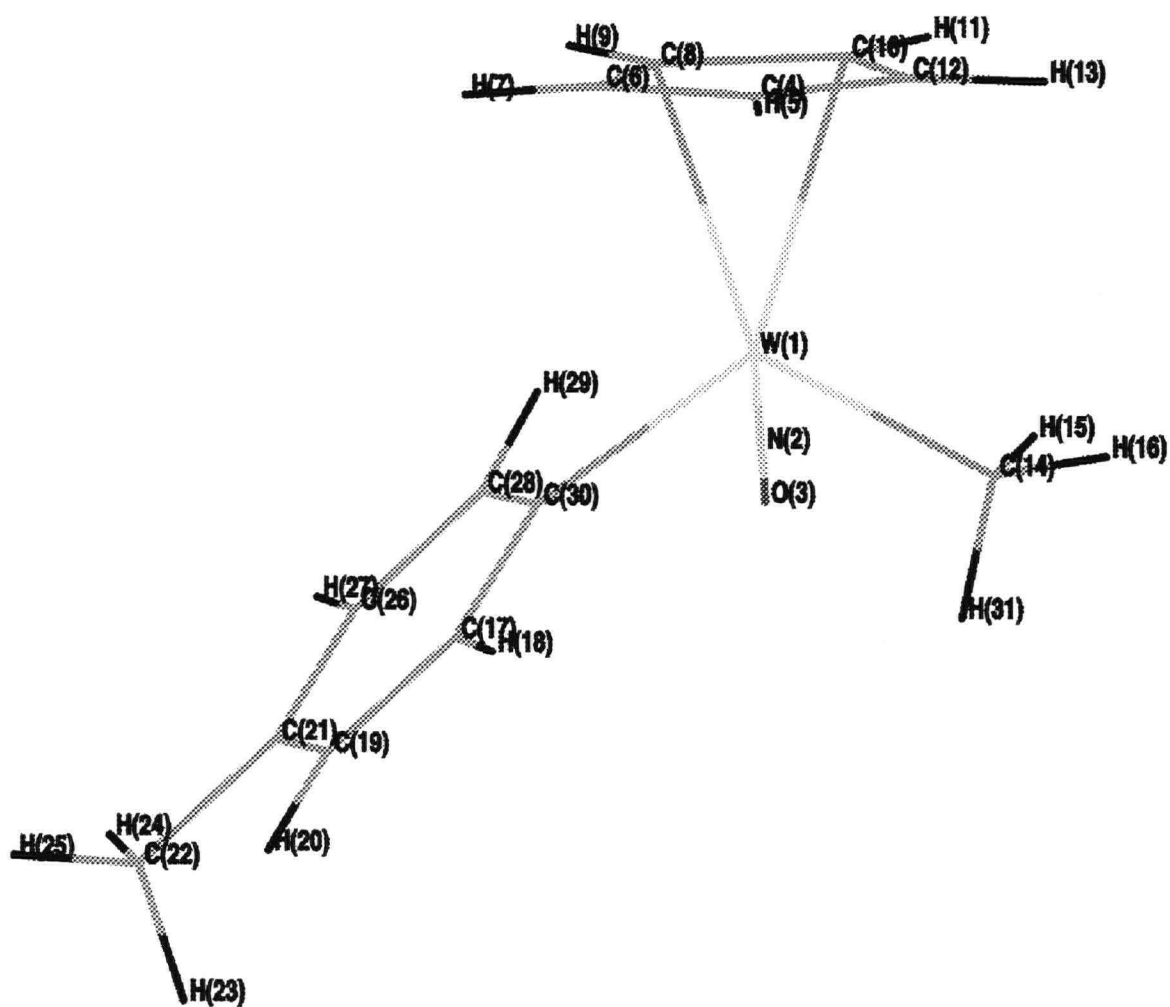
W(1)-C(14) = 2.1394

C(30)-W(1)-C(14) = 108.9

W(1)-C(30)-C(28) = 120.2

C(14)-W(1)-C(30)-C(28) = 77.4

H-(31)-C(14)-W(1)-C(30) = 33.0

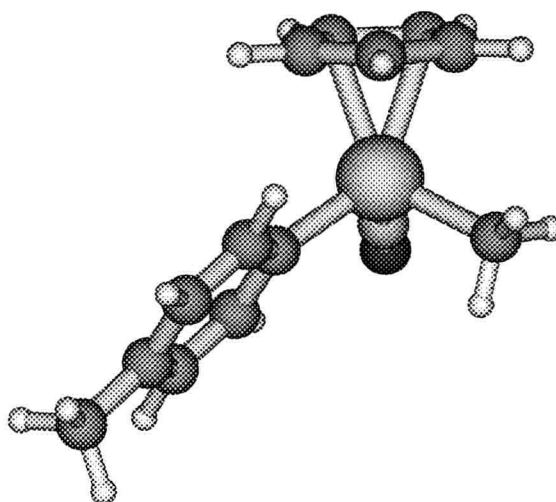


Data For CpW(NO)(CH<sub>3</sub>)(C<sub>6</sub>H<sub>4</sub>-CH<sub>3</sub>), (para) cont'd

scf done: -702.095728

Thermal corr. to free energy: 0.199403

W	0.405126	0.747698	0.168553
N	0.405126	0.747698	1.937264
O	0.520095	0.747698	3.183172
C	1.496051	0.925416	-2.146535
H	0.942203	0.934262	-3.075583
C	1.998371	-0.232647	-1.469706
H	1.882542	-1.259013	-1.787530
C	2.679341	0.201204	-0.276618
H	3.204038	-0.429230	0.427540
C	2.613187	1.645209	-0.233056
H	3.055897	2.275442	0.525569
C	1.871923	2.081908	-1.379756
H	1.633481	3.107599	-1.623130
C	-0.861029	2.463650	-0.002585
H	-1.035345	2.787473	-1.037650
H	-0.524766	3.325280	0.590133
C	-1.309959	-1.699861	1.084986
H	-1.000719	-1.423658	2.089593
C	-2.238933	-2.738066	0.920968
H	-2.630868	-3.251971	1.797600
C	-2.680459	-3.127303	-0.366486
C	-3.689351	-4.247468	-0.532529
H	-4.638904	-3.999082	-0.038671
H	-3.901897	-4.445824	-1.588811
H	-3.325010	-5.179504	-0.079559
C	-2.152280	-2.444966	-1.484957
H	-2.473259	-2.730002	-2.485379
C	-1.210404	-1.414058	-1.321967
H	-0.822721	-0.928791	-2.216927
C	-0.770395	-0.989412	-0.030964
H	-1.817026	2.130221	0.438901



Data For  $\text{CpW}(\text{NO})(\text{CH}_3)(\text{C}_6\text{H}_4\text{-CH}_3)$ , (meta, syn)

## Selected Bond Distances and Angles

$$\text{W}(1)\text{-C}(30) = 2.1254$$

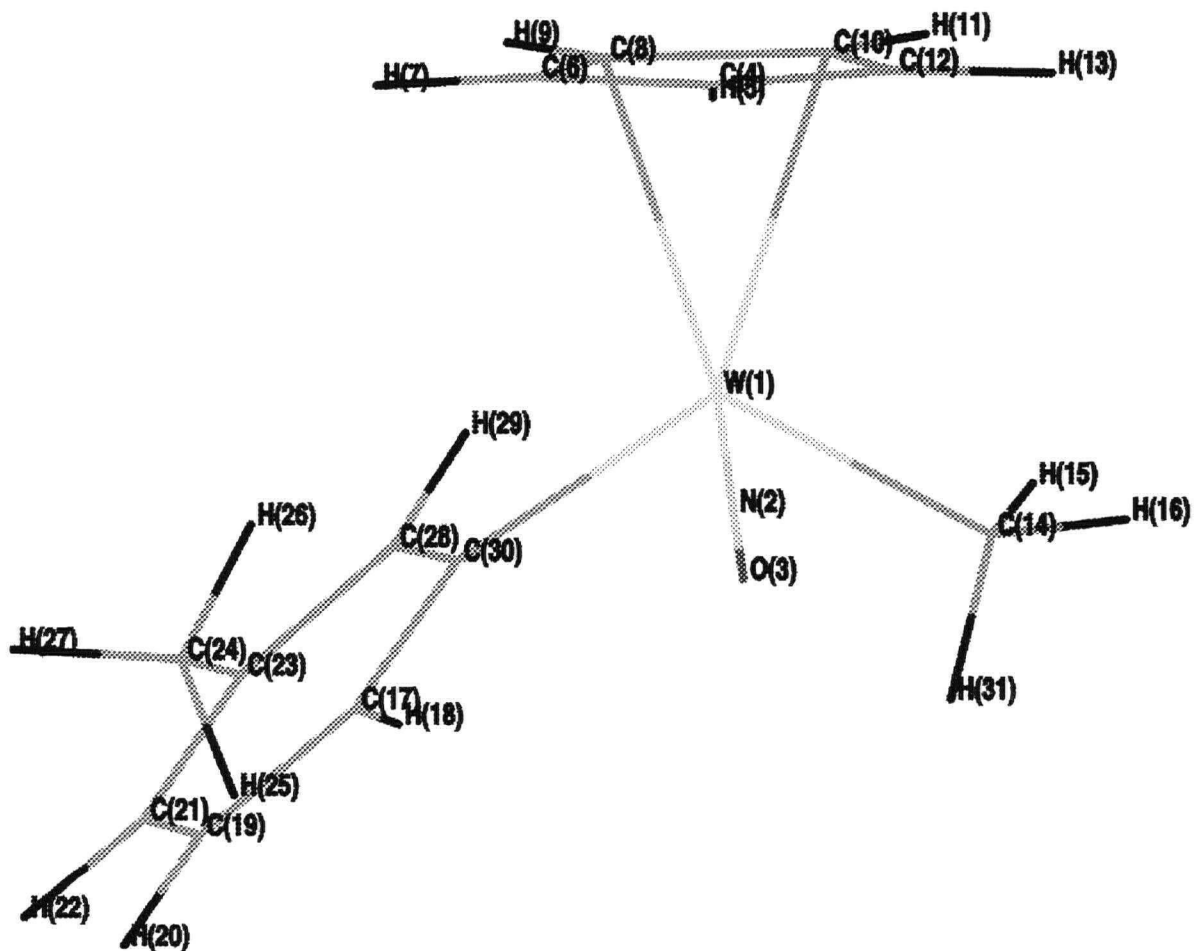
$$\text{W}(1)\text{-C}(14) = 2.1317$$

$$\text{C}(30)\text{-W}(1)\text{-C}(14) = 112.5$$

$$\text{W}(1)\text{-C}(30)\text{-C}(28) = 122.5$$

$$\text{C}(14)\text{-W}(1)\text{-C}(30)\text{-C}(28) = 49.9$$

$$\text{H}(31)\text{-C}(14)\text{-W}(1)\text{-C}(30) = 25.9$$



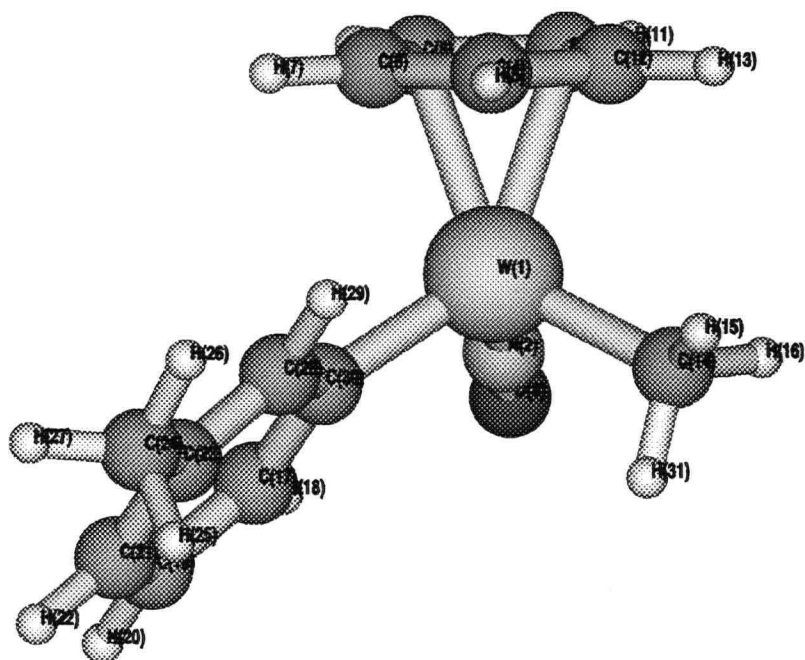
Data For CpW(NO)(CH<sub>3</sub>)(C<sub>6</sub>H<sub>4</sub>-CH<sub>3</sub>), (meta, syn) cont'd

31

scf done: -702.094580

Thermal corr. to free energy: 0.199477

W	0.346358	0.687192	0.281002
N	0.346358	0.687192	2.049474
O	0.463956	0.687192	3.294753
C	1.441689	0.873181	-2.034148
H	0.889861	0.889312	-2.964286
C	1.942309	-0.290187	-1.364946
H	1.825079	-1.313907	-1.690651
C	2.619890	0.133922	-0.167154
H	3.140922	-0.502599	0.534261
C	2.551674	1.577349	-0.110449
H	2.994069	2.201098	0.653620
C	1.814329	2.023638	-1.257071
H	1.577410	3.051379	-1.493362
C	-0.940716	2.384541	0.101945
H	-1.109540	2.706333	-0.934566
H	-0.625971	3.250806	0.699519
C	-1.259483	-1.837154	1.196032
H	-0.912011	-1.590294	2.195579
C	-2.166678	-2.897590	1.023265
H	-2.505291	-3.466747	1.886330
C	-2.643839	-3.221517	-0.260355
H	-3.348109	-4.043247	-0.384270
C	-2.217222	-2.495015	-1.396206
C	-2.747991	-2.838342	-2.777741
H	-3.809093	-2.568183	-2.873348
H	-2.199175	-2.304003	-3.561925
H	-2.667160	-3.913870	-2.983283
C	-1.288999	-1.450954	-1.206956
H	-0.948990	-0.908839	-2.090132
C	-0.800592	-1.075199	0.082767
H	-1.894833	2.032651	0.534097



Data For CpW(NO)(CH<sub>3</sub>)(C<sub>6</sub>H<sub>4</sub>-CH<sub>3</sub>), (ortho, syn)

## Selected Bond Distances and Angles

W(1)-C(30) = 2.1069

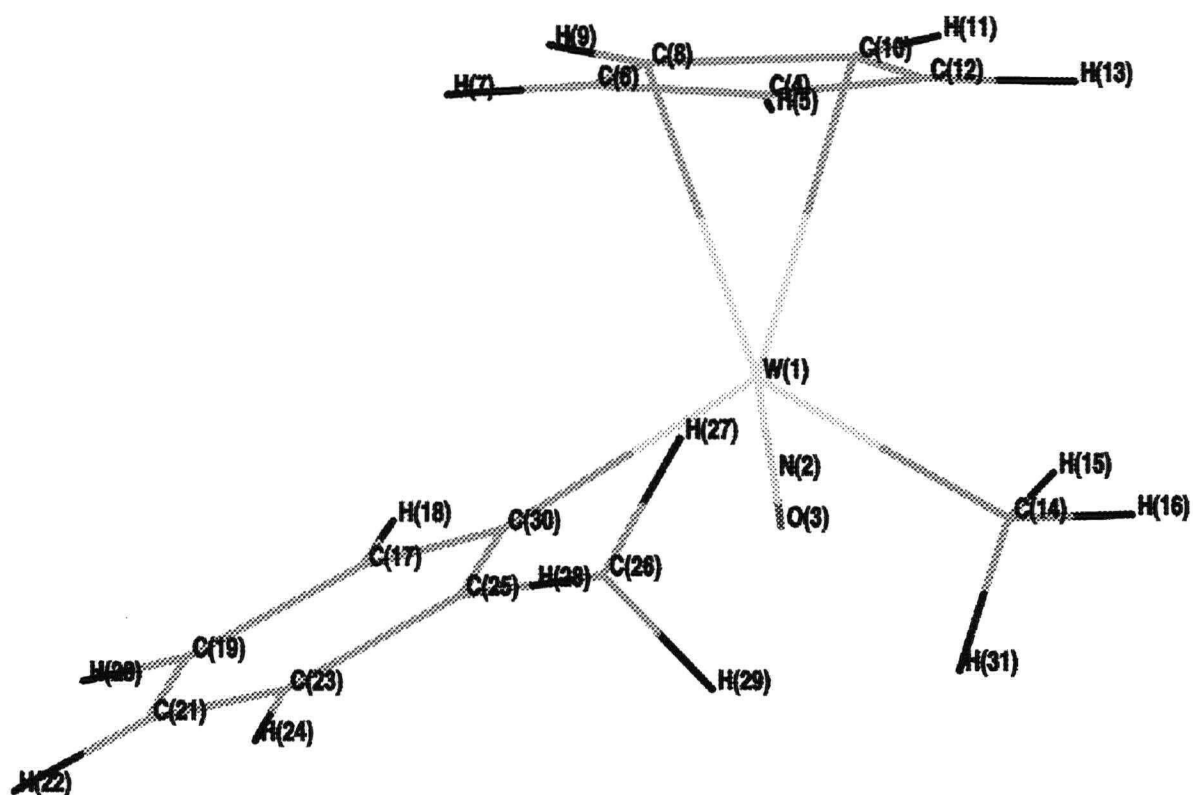
W(1)-C(14) = 2.1394

C(30)-W(1)-C(14) = 108.9

W(1)-C(30)-C(25) = 120.2

C(14)-W(1)-C(30)-C(25) = 77.4

H(31)-C(14)-W(1)-C(30) = 33.0



Data For CpW(NO)(CH<sub>3</sub>)(C<sub>6</sub>H<sub>4</sub>-CH<sub>3</sub>), (ortho, syn) cont'd

31

scf done: -702.089244

Thermal corr. to free energy: 0.200402

W	0.155645	0.654281	0.207205
N	0.155645	0.654281	1.974795
O	0.285000	0.654281	3.217063
C	1.286029	1.032937	-2.099507
H	0.767009	1.063338	-3.047809
C	1.840627	-0.130760	-1.478271
H	1.798928	-1.140435	-1.861738
C	2.457534	0.271955	-0.240104
H	3.006228	-0.364766	0.440029
C	2.290005	1.703510	-0.108564
H	2.676821	2.312824	0.696173
C	1.555668	2.161411	-1.252052
H	1.256583	3.182722	-1.441776
C	-1.296807	2.203223	0.019587
H	-1.444413	2.566525	-1.005701
H	-1.152476	3.060174	0.689820
C	-0.380667	-2.281323	1.028389
H	0.258973	-2.019141	1.867914
C	-0.871362	-3.594475	0.940208
H	-0.599216	-4.330264	1.693525
C	-1.732134	-3.944520	-0.118032
H	-2.125811	-4.955723	-0.195567
C	-2.090103	-2.975231	-1.071448
H	-2.768033	-3.244736	-1.880139
C	-1.586671	-1.656362	-1.007402
C	-2.063479	-0.654097	-2.047794
H	-1.267313	0.038705	-2.350008
H	-2.430467	-1.160137	-2.948620
H	-2.886879	-0.039135	-1.657024
C	-0.701879	-1.284783	0.059450
H	-2.217781	1.690149	0.360933

